

# INVESTIGATION OF THE PATHOGENESIS OF INFLUENZA INFECTION IN ASTHMA AND COPD; POTENTIAL THERAPEUTIC INTERVENTIONS

**Kamal Dua**

*BPharm, MPharm, PhD (Pharm. Sci.)*

Priority Research Centre for Healthy Lungs,  
School of Biomedical Sciences and Pharmacy,  
Faculty of Health,  
Hunter Medical Research Institute and the University of Newcastle,  
Newcastle, NSW, Australia

Submitted in fulfilment of the requirements for the degree of  
Doctor of Philosophy

January 2018



## **STATEMENT OF ORIGINALITY**

This thesis contains no material which has been accepted for the award of any other degree or diploma in any university or other tertiary institution and to the best of my knowledge and belief, contains no material previously published or written by another person, except where due reference has been made in the text. I give consent to the final version of my thesis being made available worldwide when deposited in the University's Digital Repository\*\*, subject to the provisions of the Copyright Act 1968 and any approved embargo.

\*\*Unless an Embargo has been approved for a determined period

**Kamal Dua**

January 2018

## STATEMENT OF COLLABORATION

I hereby certify that the work embodied in this thesis has been done in collaboration with other researchers, or carried out in other institutions. I have included as part of the thesis a statement clearly outlining the extent of collaboration, with whom and under what auspices.

For many of the results included in Chapters 2, 3 and 4, I would like to acknowledge Dr. Malcolm Starkey, Dr Alan Hsu, Dr Prema Mono Nair and Dr Tatt Jhong Haw as collaborators. In the study, I was majorly involved in experimental design; implementation of experimental procedures; collection, processing and analysis of samples; and interpretation of data. Dr. Starkey was significantly involved in experimental design, analysis of samples and interpretation of data. Dr Nair and Dr Haw provided important contributions in collection, processing and analysis of samples.

Kamal Dua

August 2017

## ACKNOWLEDGEMENT

Firstly, I wish to express my sense of gratitude and indebtedness to my primary and associate supervisors, Professor Philip Michael Hansbro, Dr. Malcolm Starkey, Dr. Jay Horvat, Laureate Professor Paul Foster, Professor Peter Wark and Dr. Simon Keely. I deeply acknowledge their constructive guidance and unwavering support throughout my tenure of doctoral studies, along with their devotion in providing me with many personal hours to guide and mentor me in reviewing my numerous drafts of thesis.

I would like to convey my special thanks to Professor Phil Hansbro and Dr. Alan Hsu, for their enormous contribution, continuous support, guidance and immense patience right from my candidature confirmation through to the thesis-writing phase.

A big thank you to past and present members of the Hansbro Laboratory for the constant support, encouragement and sharing the abundance of knowledge with me, along with inspiring involvements in making my journey gratifying.

I would like to extend my thanks to the University of Newcastle for providing me this wonderful opportunity to study and carry out my Higher Degree Research (HDR) by awarding me with the University of Newcastle International Postgraduate Research Scholarship (UNIPRS) and University of Newcastle Research Scholarship Central (UNRSC50:50).

On a personal level, this achievement would not have been ever possible without the immense support, constant encouragement and sacrifice from my loving seven year old daughter Tannishtha, ever loving parents, spouse Dr Kavita Pabreja, in-laws and extended family Mrs. Upward, Stuart and Arvids. I owe sincere thanks to my dear friends Nicole, Krishna, Prema, Tatt Jhong, Duc, Andi, Anne, Marcia, Assunta and Charlie whose contributions during my journey would be cherished for a lifetime. I thank Gaurav for providing his graphical skills in amending figures for my thesis along with Shakti for his help. I am eternally grateful to you all for standing by my side in good or trying scenarios

by continuously infusing me with motivation and strength. I would also like to express my sincere gratitude to my professional mentors; Prof. Michael John Rathbone (ULTI Pharmaceuticals, NZ), Assoc. Prof. Mary Bebawy (UTS, Aus), Prof. Kylie Williams (UTS, Aus) and Prof. Charlie Benrimoj (UTS, Aus) for their continuous support and encouragement especially during the writing phase of my thesis.

Lastly but not least, I acknowledge all those who knowingly and unknowingly contributed in my doctoral studies and making me to reach this step of my research journey.

To these people and four legged friends, I dedicate my thesis.

# CONTENTS

<b>STATEMENT OF ORIGINALITY</b> .....	ii
<b>STATEMENT OF COLLABORATION</b> .....	iii
<b>ACKNOWLEDGEMENT</b> .....	iv
<b>CONTENTS</b> .....	vi
<b>SYNOPSIS</b> .....	xv
<b>PUBLICATIONS</b> .....	xix
Publications from this thesis .....	xix
Other publications .....	xix
<b>CONFERENCE PRESENTATIONS</b> .....	xx
<b>LIST OF FIGURES</b> .....	xxii
<b>LIST OF SUPPLEMENTARY FIGURES</b> .....	xxix
<b>LIST OF TABLES</b> .....	xxx
<b>ABBREVIATIONS</b> .....	xxxi
<b>CHAPTER 1 INTRODUCTION</b> .....	1
1.1. ASTHMA .....	2
1.1.1. Epidemiology of asthma .....	2
1.1.2. Pathophysiology of asthma .....	3
1.1.3. Immunology of asthma .....	4
1.1.4. Role of IL-13 in Asthma .....	9
1.2. CHRONIC OBSTRUCTIVE PULMONARY DISEASE (COPD) .....	12
1.2.1. Epidemiology of COPD .....	14
1.2.2. Pathophysiology of COPD .....	16
1.2.3. Immunology of COPD .....	20
1.2.4. Adaptive Immune Response .....	22
1.3. INFLUENZA .....	23

1.3.1 Epidemiology of influenza A virus (IAV).....	23
1.3.2. Preventive measures & treatment options.....	25
1.3.3. Pathogenesis of IAV infection.....	25
1.3.4. Host immune responses to IAV infection.....	30
1.3.5. Association between asthma and IAV infection: Potential Mechanisms and Therapeutic Interventions.....	35
1.3.6. Associations between COPD and IAV infection .....	38
1.4. MOUSE MODELS OF ASTHMA, COPD AND INFLUENZA.....	39
1.4.1. Asthma .....	39
1.4.2. COPD .....	40
1.4.3. Influenza.....	40
1.5. MICRORNAS (miRs): POTENTIAL THERAPEUTIC TARGETS IN CHRONIC LUNG DISEASES.....	41
1.5.1. Biogenesis of miRs.....	42
1.5.2. miRs in lung diseases.....	42
1.5.3. miR-21 in Chronic Respiratory Diseases.....	49
1.5.4. miR-125 a and b in chronic respiratory diseases.....	50
1.6. HYPOTHESES AND AIMS.....	52
1.6.1. Hypothesis.....	53
1.6.2. Aims .....	55
<b>CHAPTER 2 IAV INFECTION EXACERBATES HOUSE DUST MITE (HDM)- INDUCED ALLERGIC AIRWAYS DISEASE (AAD).....</b>	<b>56</b>
2.1. ABSTRACT .....	57
2.2. INTRODUCTION .....	57
2.3. METHODS.....	59
2.3.1. Ethics statement.....	59
2.3.2. Mice.....	60
2.3.3. Induction of AAD.....	60

2.3.4. IAV infection .....	60
2.3.5. Plaque assay .....	62
2.3.6. Histopathology .....	62
2.3.7. Protein isolation .....	62
2.3.8. Cytokine concentrations in lungs .....	63
2.3.9. Total RNA extraction .....	63
2.3.10. Reverse transcription.....	64
2.3.11. Quantitative real-time Polymerase Chain Reaction (qPCR) .....	65
2.3.13. Airway remodelling .....	66
2.3.14. Soluble collagen .....	66
2.3.14. Lung function .....	67
2.3.15. Statistical analyses .....	67
2.4. RESULTS .....	67
2.4.1. HDM-induced AAD predisposes to severe IAV infection .....	67
2.4.2. IAV infection leads to severe tissue inflammation, increase in mucus secreting cells (MSCs) and lung eosinophils in AAD.....	68
2.4.3. IAV infection induces IL-13R $\alpha$ 1 expression and levels of Th2- associated cytokines following HDM-induced AAD .....	74
2.4.4. HDM-induced AAD impairs antiviral responses to IAV infection.....	75
2.4.5. IAV infection leads to airway remodelling following HDM-induced AAD.....	78
2.4.6. IAV infection leads to increased AHR following AAD .....	78
2.4.7. Remodelling studies and effect of corticosteroids on HDM-induced AAD and IAV infection.....	79
2.5. DISCUSSION .....	92
2.6. CONCLUSION.....	101
<b>CHAPTER 3 TARGETING THE IL-13/ miR-21 AXIS FOR RESPIRATORY VIRAL INFECTIONS .....</b>	<b>102</b>

3.1. ABSTRACT .....	103
3.2. INTRODUCTION .....	104
3.3. METHODS.....	109
3.3.1. Ethics Statement .....	109
3.3.2. Mice.....	110
3.3.3. Induction of AAD using Ova .....	110
3.3.4. Experimental COPD .....	110
3.3.5. IAV infection .....	112
3.3.6. Administration of rIL-13 .....	112
3.3.7. IAV infection in IL-13 deficient ( $^{-/-}$ ) mice.....	112
3.3.8. Treatment with dexamethasone (Dex) in AAD .....	112
3.3.9. miR inhibition with antagomirs.....	115
3.3.10. PI3K inhibition .....	115
3.3.11. Neutralisation of IL-13 in experimental AAD and COPD.....	115
3.3.12. Plaque assay.....	118
3.3.13. Histopathology.....	118
3.3.14. Cytokine concentrations in lungs.....	120
3.3.15. Total RNA extraction .....	120
3.3.16. Reverse transcription.....	121
3.3.17. Quantitative real-time Polymerase Chain Reaction (qPCR) .....	121
3.3.18. Lung function.....	122
3.3.19. Airway remodelling .....	122
3.3.20. Immunohistochemistry.....	123
3.3.21. miR <i>in situ</i> hybridization (ISH) .....	123
3.3.22. Flow cytometry .....	124
3.3.23. Statistical analyses .....	124
3.4. RESULTS .....	125

3.4.1. Allergic airway inflammation increases the severity of IAV infection consequently exacerbating the underlying AAD.....	125
3.4.2. IL-13 drives susceptibility to IAV infection in mice .....	129
3.4.3. IAV infection increases IL-13 <sup>+</sup> CD4 <sup>+</sup> T-cells and IL-13 <sup>+</sup> NKT cells but not IL-13 <sup>+</sup> ILC2s in experimental AAD.....	135
3.4.4. IAV infection increases miR-21 expression in Ova-induced AAD... ..	138
3.4.5. miR-21 increases in the luminal epithelium associated with small airways in IAV infection in Ova-induced AAD.....	138
3.4.6. miR-21 expression increases in mice administered with rIL-13 and infected with IAV .....	138
3.4.7. miR-21 expression increases in HDM-induced AAD with IAV infection .....	138
3.4.8. IL-13 <sup>-/-</sup> mice have lower viral titres in IAV infection .....	144
3.4.9. IL-13 <sup>-/-</sup> mice have reduced tissue inflammation in IAV infection .....	144
3.4.10. IL-13 <sup>-/-</sup> mice have reduced AHR in IAV infection .....	144
3.4.11. IAV infection in IL-13 <sup>-/-</sup> mice have decreased miR-21 expression .....	144
3.4.12. Treatment with anti-IL-13 reduces IAV infection and exacerbation of experimental AAD .....	149
3.4.13. Treatment with anti-IL-13 reduces levels of IL-13 protein and IL-13Rα1 mRNA expression in IAV infection in experimental AAD .....	150
3.4.14. Treatment with anti-IL-13 reduces miR-21 expression in IAV infection but not in IAV infection in experimental AAD .....	154
3.4.15. Treatment with intranasal dexamethasone did not reduce viral titre in IAV infection .....	154
3.4.16. Treatment with intranasal dexamethasone did not resolve tissue inflammation in IAV infection.....	157
3.4.17. Treatment with intranasal dexamethasone did not reduce tissue eosinophils in IAV infection following Ova-induced AAD.....	160

3.4.18. Treatment with intranasal dexamethasone reduces number of MSCs in IAV infection following Ova-induced AAD.....	160
3.4.19. Treatment with intranasal dexamethasone worsens AHR substantially in IAV infection following Ova-induced AAD .....	164
3.4.20. Treatment with intranasal dexamethasone had no effect on miR-21 expression in IAV infection following Ova-induced AAD .....	164
3.4.21. Treatment with intranasal Ant-21 reduces viral titre in IAV infection following Ova-induced AAD .....	167
3.4.22. Treatment with intranasal Ant-21 suppresses tissue inflammation in IAV infection following Ova-induced AAD .....	168
3.4.23. Treatment with intranasal Ant-21 suppresses number of MSCs in IAV infection following Ova-induced AAD .....	168
3.4.24. Treatment with intranasal Ant-21 suppresses number of tissue eosinophils in IAV infection following Ova-induced AAD.....	173
3.4.25. Treatment with intranasal Ant-21 does not suppress AHR in IAV infection following Ova-induced AAD .....	173
3.4.26. Treatment with intranasal Ant-21 suppresses miR-21 expression in IAV infection following Ova-induced AAD .....	176
3.4.27. Treatment with intranasal LY29 reduces viral titre in IAV infection following Ova-induced AAD .....	176
3.4.28. Treatment with intranasal LY29 suppresses tissue inflammation in IAV infection following Ova-induced AAD .....	178
3.4.29. Treatment with intranasal LY29 suppresses number of MSCs in IAV infection following Ova-induced AAD .....	178
3.4.30. Treatment with intranasal LY29 suppresses number of tissue eosinophils in IAV infection following Ova-induced AAD.....	179
3.4.31. Treatment with intranasal LY29 does not suppress AHR in IAV infection following Ova-induced AAD .....	179
3.4.32. Treatment with intranasal LY29 does not suppress miR-21 expression in IAV infection following Ova-induced AAD .....	186

3.4.33. IAV infection influences IL-13R $\alpha$ 1 expression in experimental COPD .....	188
3.4.34. IAV infection increases localization of miR-21 expression in experimental COPD .....	188
3.4.35. IAV infection increases number of MSCs in experimental COPD.	192
3.4.36. Treatment with Anti-IL-13 reduces viral titre in experimental COPD with IAV infection.....	192
3.4.37. Treatment with Anti-IL-13 decreases tissue inflammation in experimental COPD with IAV infection.....	196
3.4.38. Treatment with Anti-IL-13 reduces number of MSCs in experimental COPD with IAV infection .....	196
3.4.39. Treatment with Anti-IL-13 did not inhibit miR-21 expression in experimental COPD with IAV infection.....	196
3.4.40. Inhibition of miR-21 reduces viral titre in experimental COPD with IAV infection.....	196
3.4.41. Treatment with intranasal Ant-21 suppresses tissue inflammation in experimental COPD with IAV infection.....	201
3.4.42. Treatment with intranasal Ant-21 reduces number of MSCs back to base line in experimental COPD with IAV infection.....	205
3.4.43. Treatment with intranasal Ant-21 suppresses miR-21 expression back to base line in experimental COPD with IAV infection .....	205
3.5. DISCUSSION .....	208
3.6. CONCLUSIONS .....	223
<b>CHAPTER 4 miR-125a/b INHIBITS A20 AND MAVS TO PROMOTE INFLAMMATION AND IMPAIR ANTIVIRAL RESPONSE IN CHRONIC OBSTRUCTIVE PULMONARY DISEASE .....</b>	<b>224</b>
4.1. ABSTRACT .....	225
4.2. INTRODUCTION .....	225
4.3. METHODS.....	228

4.3.1. <i>Ex vivo</i> methods .....	228
4.3.2. In vivo methods .....	233
4.3.3. Statistical analysis .....	235
4.3.4. Study Approvals .....	235
4.4. RESULTS .....	235
4.4.1. IAV infection induces increased inflammatory but reduced antiviral responses <i>ex vivo</i> in human COPD pulmonary bronchial epithelial cells (pBECs) .....	235
4.4.2. IAV infection also induces increased inflammatory but reduced antiviral responses in vivo in experimental COPD .....	239
4.4.3. A20 is an important negative regulatory of NF- $\kappa$ B-mediated inflammatory but not antiviral responses, and its expression is reduced in human COPD and experimental COPD .....	241
4.4.4. Elevated miR-125a and b levels decrease A20 levels, increase inflammation and impair antiviral responses in COPD pBEC and experimental COPD .....	244
4.4.5. miR-125a and b target MAVS.....	247
4.4.6. miR-125a and b targeting of MAVS regulates antiviral responses in COPD pBEC and experimental COPD.....	250
4.5. DISCUSSION .....	253
4.6. CONCLUSION.....	257
4.7. SUPPLEMENATRY FIGURES .....	258
<b>CHAPTER 5 GENERAL DISCUSSION AND CONCLUSIONS</b> .....	269
5.1. IAV INFECTION IN EXPERIMENTAL AAD .....	271
5.2. IAV INFECTION IN EXPERIMENTAL COPD .....	274
5.3. FUTURE DIRECTIONS .....	280
5.3.1. IAV infection in AAD .....	280
5.3.2. IAV infection in COPD .....	285
5.4. CONCLUSIONS .....	285

<b>BIBLIOGRAPHY .....</b>	<b>287</b>
<b>APPENDIX: PUBLICATIONS.....</b>	<b>338</b>

## SYNOPSIS

People with chronic lung diseases, such as asthma and chronic obstructive pulmonary disease (COPD) are more susceptible to influenza A virus (IAV) infections that subsequently exacerbate these diseases, leading to more severe symptoms with increased risk of mortality. However, the immune mechanisms driving the increased susceptibility of these patients to IAV infection and consequent exacerbations are largely unknown. Current prevention options are primarily vaccinations that have serious limitations including long manufacturing processes, vaccine mismatches and inability to target all virus strains that also undergo frequent mutations and recombination. Current anti-IAV treatments are only effective if given within the first 48 h of infection. This is normally before symptoms appear and are severe enough to present to a clinic or hospital. Thus, there is an urgent need to develop novel effective therapies for the management of IAV infections, particularly in patients with underlying respiratory diseases. The primary objective of this PhD was to determine the mechanisms responsible for increased susceptibility to IAV infection in asthma and COPD, and understand how infection causes exacerbations. To accomplish the aims of the study, we used established and developed novel mouse models of IAV infection in experimental asthma (Ovalbumin (Ova)- and house dust mite (HDM)-induced) and COPD.

Firstly, we found that Ova- and HDM-induced allergic airways disease (AAD) increased susceptibility to IAV infection as evident by increased viral titre. In addition, the infection exacerbated AAD with severe histopathology, increased eosinophils, mucus hypersecretion, impaired antiviral responses, increased collagen deposition around small airways, small airways epithelial thickening and airway hyper-responsiveness (AHR). Also, an allergen rechallenge in infected mice with AAD demonstrated an ongoing remodelling characterised by excessive mucus and collagen production that are resistant to dexamethasone treatment.

Secondly, to confirm whether production of IL-13, an important Th2 cytokine, is a likely mechanism driving infection and exacerbating disease, we assessed the

levels of IL-13 and its receptor, IL-13R $\alpha$ 1, in Ova-induced AAD lung tissues. Non-infected allergic mice had AAD features that were associated with increased protein levels of IL-13 compared to non-allergic controls. IAV infection did not induce IL-13 in non-AAD mice, but further increased IL-13 levels in AAD. IHC determined the localisation of IL-13R $\alpha$ 1 in lung tissues and showed its increased expression in airway epithelium. We then used IL-13-reporter mice to show that AAD with or without IAV infection induced IL-13 production predominantly from IL-13+CD4+ T-cells and to a lesser extent from IL-13+ ILC2 cells but IAV infection alone induced high level of IL-13 production by IL-13+ NKT cells. Treatment of IAV infected mice with recombinant (r)IL-13 induced severe histopathology, increased eosinophils, mucus hypersecretion and AHR. Further, we identified the involvement of microRNA (miR)-21 in IL-13/IL-13R $\alpha$ 1-induced susceptibility to IAV infection in experimental AAD. We found significantly increased miR-21 expression in allergic mice, which was further increased after IAV infection. ISH determined an increased localisation of miR-21 expression to the airway epithelium. Also, rIL-13 treatment showed increased miR-21 expression which was further increased after IAV infection. Similar observations were found in HDM-induced AAD. To further assess the role of IL-13 in susceptibility to IAV in AAD, we used mice deficient in IL-13 (IL-13 $^{-/-}$  mice). A significant decrease in viral titre, lung tissue inflammation and transpulmonary resistance was observed in infected IL-13 $^{-/-}$  compared to infected WT mice. Infected IL-13 $^{-/-}$  mice also demonstrated reduced miR-21 expression compared with infected WT mice. These observations clearly indicate that the absence of IL-13 during IAV infection improved disease features. Using IL-13-specific monoclonal antibody (Anti-IL-13), we showed that inhibition of IL-13 signalling protected mice against infection and reduced the severity of IAV infection-induced exacerbations of AAD. This was shown by reduced viral titres, tissue inflammation, eosinophil counts, mucus secreting cells (MSCs) and transpulmonary resistance, IL-13 and IL-13R $\alpha$ 1 mRNA expression in Anti-IL-13-treated groups compared to isotype-treated controls. Further, anti-IL13-treated infected non-allergic mice also had significantly reduced miR-21 expression compared to controls, whilst similar levels of expression were observed in both anti-IL-13-treated and isotype-treated

infected mice with AAD. We also assessed the effects of corticosteroid (dexamethasone) on IAV infection and exacerbations of AAD. We found that the disease features in Ova-induced AAD mice with IAV infection were steroid-insensitive. miR-21 may promote PI3K activity and we found that anti-miR-21 (Ant-21) significantly reduced viral titres, tissue inflammation, numbers of MSCs and tissue eosinophils in AAD with IAV infection. However, Ant-21 treatment did not suppress AHR in Ova-induced AAD with IAV infection. PI3K inhibition using a pan-inhibitor (LY294002) had similar effects and reduced viral titres and features of asthma.

The association of IL-13 with COPD is not well understood. We demonstrated that IAV infection in experimental COPD increased the expression of IL-13R $\alpha$ 1 in the airway epithelium of COPD mice compared to non-infected normal air-exposed mice. Surprisingly, infected normal air-exposed mice and infected mice with had further substantial increases in IL-13R $\alpha$ 1 levels in the airway epithelium. To further identify the mechanisms involved downstream of IL-13R $\alpha$ 1, miR-21 expression was measured in the lung sections and observed to be increased in response to IAV infection in experimental COPD. We also observed a significant increase in the numbers of MSCs in infected mice with COPD compared to COPD alone. We found that inhibiting IL-13 using Anti-IL-13 reduced viral replication and severity of IAV infection in experimental COPD. This reduction was accompanied by significantly reduced tissue inflammation, numbers of MSCs and miR-21 expression in infected mice with COPD. We next demonstrated that treatment with Ant-21 protected mice against IAV infection in experimental COPD as assessed by significant reductions in viral titre, tissue inflammation, numbers of MSCs and miR-21 expression.

Thirdly, we demonstrated that targeting miR125 a and b with specific antagomirs reduced IAV-mediated inflammation and reversed immune signalling abnormalities in COPD. We also observed that COPD pBECs and mice with experimental COPD infected with IAV had higher levels of inflammatory cytokines, reduced antiviral responses and increased levels of miR-125 a and b. The study discovered that the mechanism underlying

excessive inflammation and increased susceptibility to IAV infection in COPD was facilitated by a miR-125-mediated pathway that reduced A20 (negative regulator of NF- $\kappa$ B) and MAVS proteins.

In conclusion, this is the first study to define the functional relevance of IAV infection-induced activation and maintenance of novel IL-13/IL-13R $\alpha$ 1/miR-21 and IL-13R $\alpha$ 1/miR-21 axes in AAD and COPD, respectively. Our data identified promising therapeutic interventions for increased susceptibility to IAV infection in AAD (anti-IL-13, Ant-21 and PI3K inhibitors) and COPD (anti-IL-13, Ant-21, Ant-125 a and b) which suppressed various key features of the respective airway disease. While we show promising findings experimentally, we have yet to explore some of these findings in clinical settings. This would be the next critical step to translate these promising findings from bench to bedside. The models used and developed in this study have clear utility in identifying new and effective therapeutic interventions and are well suited for *in vivo* studies investigating modulation of immune responses in exacerbation-induced expression of various cytokines and corticosteroid insensitivity.

## PUBLICATIONS

### Publications from this thesis

- Hsu AC-Y, **Dua K**, Starkey MR, et al. MicroRNA-125a and -b inhibit A20 and MAVS to promote inflammation and impair antiviral response in COPD. JCI Insight. 2017;2(7):e90443.
- **Dua K**, Hansbro, N.G and Hansbro, P.M. Steroid resistance and concomitant respiratory Infections: a challenging battle in pulmonary clinic, EXCLI Journal 2017; 16: 981-985.
- **Dua K**, Hansbro NG, Foster PS, Hansbro PM, MicroRNAs (miRNAs) as therapeutics for future drug delivery systems in treatment of lung diseases, Drug Delivery and Translational Research, 2017, 7(1), 179-187.
- Hansbro P.M., Kim R.Y., Starkey M.R., Donovan C., **Dua K**, Mayall J., Liu G., Hansbro N.G., Simpson J.L., Wood L.G., Hirota J.A., Knight D.A., Foster P.S. and Horvat J.C. Mechanisms and treatments for severe, steroid-resistant allergic airways disease and asthma. Immunological Reviews. (2017) Immunological Reviews 278(1):41-62.

### Other publications

- **Dua K**, Shukla SD, Tekade RK, Hansbro PM. Whether a novel drug delivery system can overcome the problem of biofilms in respiratory diseases? Drug Delivery and Translational Research, 2017, 7 (1), 179–187.
- **Dua K**, Shukla SD, Hansbro PM. Aspiration techniques for bronchoalveolar lavage in translational respiratory research: Paving the way to develop novel therapeutic moieties. J Biol Methods 2017;4(3):e73.
- **Dua K**, Shukla SD, Pinto TJA, Hansbro PM, Nanotechnology: Advancing the translational respiratory research, Interventional Medicine & Applied Science, 2017, 9 (1), 39–41.

## CONFERENCE PRESENTATIONS

1. Hsu A, Dua K, Starkey MR, Haw TJ, Nair PM, Nichol K, Zammit N, Grey ST, Baines KJ, Foster PS, Hansbro PM, Wark PA. MicroRNA-125a and -b inhibit A20 and MAVS to promote inflammation and impair antiviral response in COPD. The Australia and New Zealand Society for Cell and Developmental Biology Meeting, Apr 3<sup>rd</sup> 2017, Sydney, NSW, Australia. (***Awarded travel fellowship by the Australia and New Zealand Society for Cell and Developmental Biology***).
2. Starkey MR, Dua K, Hsu A, Nair PM, Haw TJ, Duc HN, Kim RY, Horvat JC, Godfrey DI, McKenzie AN, Lukacs NW, Wark PA, Hansbro PM, Interleukin-13 predisposes to more severe influenza infection in mice and human epithelial cells by suppressing interferon responses and activating the microRNA-21/PI3K signalling pathway. American Thoracic Society International Conference, May 19-24, 2017 - Washington, DC.
3. Jones B, Harrison CL, Waters DW, Dua K, Starkey MR, *et al.*, Bromodomain inhibitors reverse disease features in experimental chronic obstructive pulmonary disease. Thoracic Society of Australia and New Zealand Annual Meeting, Perth, Australia 2016.
4. Dua K, Starkey MR, Hanish I, Hsu A, Monogar P, Foster PS, Knight DA, Hovart JC, Wark PA, Hansbro PM, Interleukin-13 predisposes to more severe influenza infection in mice, and human epithelial cells, by activating microRNA-21/PI3K signaling pathway, EMBL Australia PhD Course, 22 July- 3 July, 2015, Harry Perkins Medical Institute, Perth, WA, Australia. (***Selected to attend 3<sup>rd</sup> weeks residential EMBL Australia PhD course by The European Molecular Biology Laboratory***).
5. Starkey MR, Dua K, Hanish I, Hsu A, Monogar P, Foster PS, Knight DA, Hovart JC, Wark PA, Hansbro PM Interleukin-13 predisposes to more severe influenza infection in mice, and human epithelial cells, by activating microRNA-21/PI3K signaling pathway. Australian Respiratory Virology meeting, Canberra, Australia 2015.
6. Starkey MR, Dua K, Hanish I, Hsu A, Monogar P, Foster PS, Knight DA, Hovart JC, Wark PA, Hansbro PM, IL-13 predisposes to more severe

influenza infection in mice and human epithelial cells by suppressing interferon responses and activating the miRNA-21/PI3K signalling pathway at Newcastle Asthma Meeting (NAME11), 22-23<sup>rd</sup> October 2015, Newcastle, Australia.

7. Nair PM, Starkey MR, Haw TJ, **Dua K**, Deane A, Liu G, Ammit A, Clark A, Hansbro PM. Tristetraprolin is protective against influenza virus infection in mice at the Australasian Society for Immunology (ASI) 2015, Canberra, Australia.
8. Nair PM, Starkey MR, Haw TJ, **Dua K**, Deane A, Liu G, Ammit A, Clark A, Hansbro PM. Tristetraprolin is protective against influenza virus infection in mice at the Australian Respiratory Virology meeting, Canberra 2015.
9. Starkey MR, **Dua K**, Hanish I, Hsu A, Monogar P, Foster PS, Knight DA, Hovart JC, Wark PA, Hansbro PM, Interlukin-13 predisposes mice to more severe influenza infection and exacerbated allergic airway disease at American Thoracic Society International Conference; May 16- 21, 2014, San Diego, USA.
10. Starkey MR, **Dua K**, Hanish I, Hsu A, Monogar P, Foster PS, Knight DA, Hovart JC, Wark PA, Hansbro PM, Interlukin-13 predisposes mice to more severe influenza infection by supressing interferon responses and activation of microRNA-21/PI3K pathway presented at International Cytokine and Interferon (ICIS) Annual Meeting, Oct 26-29 2014, Melbourne, Australia.
11. Starkey MR, **Dua K**, Hanish I, Hsu A, Monogar P, Foster PS, Knight DA, Hovart JC, Wark PA, Hansbro PM, Interleukin-13 predisposes mice to more severe influenza infection and exacerbated allergic airways disease. *Am J Respir Crit Care Med* 2014; 189: A5353.

## LIST OF FIGURES

Figure 1.1. Clinical features of asthma.....	5
Figure 1.2. The role of Th2 cells and cytokines in the pathogenesis of asthma. ....	7
Figure 1.3. The role of dendritic cells in the pathogenesis of asthma. ....	8
Figure 1.4. Role of IL-13 in asthma.....	11
Figure 1.5. Airway features of a healthy individual and a patient with COPD.....	18
Figure 1.6. The protease/anti-protease hypothesis in COPD.....	19
Figure 1.7. Inflammatory factors and cells involved in the immunopathology of COPD.....	21
Figure 1.8. The structure of influenza virus that consists of 8 single stranded, negative sense RNA segments. ....	27
Figure 1.9. Innate sensing of influenza viruses.....	32
Figure 1.10. miR Biogenesis.....	43
Figure 2.1. Experimental protocol of HDM-induced AAD and IAV infection.....	61
Figure 2.2. Viral titre at 3 dpi.....	69
Figure 2.3. IAV infection exacerbates lung tissue inflammation in HDM-induced AAD.....	70
Figure 2.4. IAV infection increased the numbers of MSCs in HDM-induced AAD. ....	72
Figure 2.5. IAV infection leads to increased numbers of tissue eosinophils in HDM-induced AAD. ....	73
Figure 2.6. IAV infection induces IL-13R $\alpha$ 1 expression and levels of Th2-associated cytokines following HDM-induced AAD .....	76
Figure 2.7. HDM-induced AAD impairs antiviral IFN responses to IAV infection. ....	77
Figure 2.8. IAV infection leads to remodelling in AAD.....	81

Figure 2.9. IAV infection increases AHR in AAD.....	83
Figure 2.10. Remodeling studies and effect of corticosteroids on HDM-induced AAD and IAV infection.....	84
Figure 2.11. Allergen re-challenge increased pulmonary inflammation in AAD with IAV infection, which could be attenuated by intranasal dexamethasone treatment. ....	85
Figure 2.12. Allergen re-challenge increased the numbers of MSCs in AAD with IAV infection, which was not affected by intranasal dexamethasone treatment. ....	87
Figure 2.13. IAV infection influences collagen deposition around small airways following AAD.....	89
Figure 2.14. IAV infection influences small airway epithelial thickness following AAD. ....	91
Figure 2.15. The two phases of AAD development in mice. ....	93
Figure 2.16. Hypothesis attributed corticosteroid resistant remodelling.....	100
Figure 3.1. Schematic representation of IAV entry process. ....	107
Figure 3.2. Virus induces inflammatory cascades in airway epithelium. ....	108
Figure 3.3. Experimental protocol of Ova-induced AAD and IAV infection. ....	111
Figure 3.4. Experimental protocol of cigarette smoke-induced COPD and IAV infection. ....	113
Figure 3.5. Experimental protocol of rIL-13 treatment and IAV infection. ....	113
Figure 3.6. Experimental protocol of IAV infection. ....	114
Figure 3.7. Treatment with dexamethasone in Experimental AAD and IAV infection. ....	114
Figure 3.8. Treatment with anti-miR-21 (Ant-21) in Experimental AAD and IAV infection. ....	116

Figure 3.9. Treatment with anti-miR-21 (Ant-21) in Experimental COPD and IAV infection.....	116
Figure 3.10. Treatment with LY29 in experimental AAD and IAV infection.....	117
Figure 3.11. Treatment with anti-IL-13 in experimental AAD and IAV infection.....	119
Figure 3.12. Treatment with anti-IL-13 treatment in experimental COPD and IAV infection.....	119
Figure 3.13. Ova-induced AAD promotes severe IAV infection. ....	127
Figure 3.14. Administration of recombinant IL-13 (rIL-13) promotes severe IAV infection and AAD. ....	130
Figure 3.15. IAV infection increases IL-13 and IL-13R $\alpha$ 1 expression in lungs in Ova-induced AAD.....	133
Figure 3.16. IAV infection increases IL-13 and IL-13R $\alpha$ 1 expression in rIL-13 treated mice. ....	134
Figure 3.17. Cellular source of IL-13 in IAV infection and Ova-induced experimental AAD.....	136
Figure 3.18. miR-21 expression increases in Ova-induced AAD with IAV infection. ....	139
Figure 3.19. miR-21 is localised to the luminal epithelium associated with small airways in IAV infection in Ova-induced AAD. ....	140
Figure 3.20. miR-21 expression increases in mice with rIL-13 treatment and IAV infection. ....	142
Figure 3.21. miR-21 expression increases in HDM-induced AAD with IAV infection. ....	143
Figure 3.22. IL-13 <sup>-/-</sup> mice have lower viral titres in IAV infection. ....	145
Figure 3.23. IL-13 <sup>-/-</sup> mice have reduced tissue inflammation in IAV infection.....	146
Figure 3.24. IAV infection in IL-13 <sup>-/-</sup> mice have decreased AHR. ....	147

Figure 3.25. IAV infection in IL-13 <sup>-/-</sup> mice have decreased miR-21 expression.....	148
Figure 3.26. Treatment with anti-IL-13 reduces IAV infection and exacerbation of experimental AAD.....	151
Figure 3.27. IAV infection decreases IL-13 and IL-13R $\alpha$ 1 expression in Ova-induced AAD mice administered with anti-IL-13. ....	153
Figure 3.28. Treatment with anti-IL-13 reduces miR-21 expression in IAV infection but not in IAV infection in experimental AAD.....	155
Figure 3.29. Viral titre at 3 dpi.....	156
Figure 3.30. Treatment with intranasal dexamethasone did not reduce tissue inflammation in IAV infection.....	158
Figure 3.31. Treatment with intranasal dexamethasone did not reduce tissue eosinophils.....	161
Figure 3.32. Treatment with intranasal dexamethasone reduces the number of MSCs.....	162
Figure 3.33. Treatment with intranasal dexamethasone worsens AHR substantially.....	165
Figure 3.34. Treatment with intranasal dexamethasone had no effect on miR-21 expression.....	166
Figure 3.35. Viral titre at 3 dpi.....	169
Figure 3.36. Treatment with intranasal Ant-21 suppresses tissue inflammation in IAV infection following Ova-induced AAD.....	170
Figure 3.37. Treatment with intranasal Ant-21 suppresses number of MSCs in IAV infection following Ova-induced AAD.....	172
Figure 3.38. Treatment with intranasal Ant-21 suppresses number of tissue eosinophils in IAV infection following Ova-induced AAD.....	174
Figure 3.39. Treatment with intranasal Ant-21 does not suppress AHR in IAV infection following Ova-induced AAD.....	175

Figure 3.40. Treatment with intranasal Ant-21 suppresses miR-21 expression in IAV infection following Ova-induced AAD.....	177
Figure 3.41. Viral titre at 3 dpi.....	180
Figure 3.42. Treatment with intranasal LY29 suppresses tissue inflammation in IAV infection following Ova-induced AAD.....	181
Figure 3.43. Treatment with intranasal LY29 suppresses number of MSCs in IAV infection following Ova-induced AAD. ....	183
Figure 3.44. Treatment with intranasal LY29 suppresses number of tissue eosinophils in IAV infection following Ova-induced AAD.....	184
Figure 3.45. Treatment with intranasal LY29 does not suppress AHR in IAV infection following Ova-induced AAD.....	185
Figure 3.46. Treatment with intranasal LY29 does not suppress miR-21 expression in IAV infection following Ova-induced AAD.....	187
Figure 3.47. IAV infection influences IL-13R $\alpha$ 1 expression in experimental COPD. ....	189
Figure 3.48. miR-21 is localised to the luminal epithelium associated with small airways in IAV infection in experimental COPD.....	190
Figure 3.49. IAV infection increases number of MSCs in chronically cigarette smoke-exposed mice.....	193
Figure 3.50. Viral titre at 7 dpi.....	195
Figure 3.51. Treatment with Anti-IL-13 decreases tissue inflammation in experimental COPD with IAV infection. ....	197
Figure 3.52. Treatment with Anti-IL-13 reduces number of MSCs in experimental COPD with IAV infection. ....	199
Figure 3.53. Treatment with Anti-IL-13 did not inhibit miR-21 expression in experimental COPD with IAV infection.....	200
Figure 3.54. Viral titre at 7 dpi.....	202

Figure 3.55. Treatment with intranasal Ant-21 suppresses tissue inflammation in experimental COPD with IAV infection. ....	203
Figure 3.56. Treatment with intranasal Ant-21 reduces number of MSCs back to base line in experimental COPD with IAV infection. ....	206
Figure 3.57. Treatment with intranasal Ant-21 suppresses miR-21 expression back to base line in experimental COPD with IAV infection. ....	207
Figure 3.58. Roles of IL-13 and miR-21 in increased susceptibility to IAV in AAD and COPD. ....	221
Figure 4.1. IAV infection is more severe and results in exaggerated inflammatory but impaired antiviral responses in pBECs from patients with COPD. ....	237
Figure 4.2. IAV infection is more severe and results in exaggerated inflammatory and impaired antiviral responses in experimental COPD. ....	240
Figure 4.3. A20 expression is reduced and it negatively regulates inflammatory but not antiviral responses in pBECs from patients with COPD. ....	242
Figure 4.4. IAV infection increases the levels of miR-125 and b. ....	245
Figure 4.5. miR-125a and b target a functional binding site of the 3'-UTR of the mRNA of MAVS to suppress its expression. ....	248
Figure 4.6. miR-125a and b suppresses the induction of MAVS. ....	251
Figure 4.7. Roles of miR-125a and b in the regulation of inflammatory and antiviral responses in IAV infection. ....	254
Figure 5.1. Roles of IL-13, IL-13R $\alpha$ 1 and miR-21 in increased susceptibility to IAV infection in AAD. ....	275
Figure 5.2. Roles of IL-13R $\alpha$ 1 and miR-21 in increased susceptibility to IAV infection in COPD. ....	279

Figure 5.3. Roles of miR-125a and b in the regulation of inflammatory and antiviral responses in IAV infection.....	281
Figure 5.4. Roles of IL-13, IL-13R $\alpha$ 1 and miR-21, miR-125 and b in increased susceptibility to IAV infection in AAD and COPD.....	282

## LIST OF SUPPLEMENTARY FIGURES

Supplementary Figure S4.1. Protein levels of phospho-p65 in IAV infected pBECs from human COPD patients and histopathology and phospho-p65 and antiviral responses in experimental COPD.....	258
Supplementary Figure S4.2. Protein levels of A20 in IAV infected human COPD pBECs and experimental COPD, and the effect of A20 inhibition on inflammatory and antiviral responses in pBECs.....	260
Supplementary Figure S4.3. miR-125a and b levels and the effects of their inhibition or ectopic-expression on A20, and phospho-p65, inflammatory cytokine/chemokine and IFN- $\beta$ production during IAV infection in human COPD pBECs.....	262
Supplementary Figure S4.4. miR-125a and b levels and the effects of their inhibition on histopathology, lung function, A20, and phospho-p65, inflammatory cytokine/chemokine and IFN- $\beta$ production during IAV infection in experimental COPD.....	264
Supplementary Figure S4.5. Protein levels of MAVS during IAV infection in human COPD pBECs and experimental COPD.....	266
Supplementary Figure S4.6. The effect of miR-125a and b inhibition or over-expression on the protein levels of MAVS and IFN- $\beta$ in IAV infection of human COPD pBECs and experimental COPD. ....	267

## LIST OF TABLES

Table 1.1. Role of IL-13 and IL-13R $\alpha$ 1 in the pathogenesis of asthma. ....	13
Table 1.2. GOLD staging of COPD .....	17
Table 1.3. miRs involved in inflammatory airway diseases .....	44
Table 1.4. miRs, their therapeutic indications and clinical trial status .....	49
Table 2.1. Histopathological scoring system for mouse lungs. ....	63
Table 2.2. Custom designed primers used in qPCR analysis .....	66
Table 3.1. Custom designed primers used in qPCR analysis .....	122
Table 3.2. Surface antigens used to characterise mouse lung cell subsets by flow cytometry .....	125
Table 3.3. Antibody used in flow analysis .....	125
Table 4.1. Subject characteristics .....	229

## ABBREVIATIONS

AAID: Allergic airway disease  
AHR: Airway hyper-responsiveness  
APC: Antigen presenting cell  
BAL: Bronchoalveolar lavage  
BM: Basement membrane  
BOLD: Burden of Obstructive Lung Disease  
CARD: Caspase activation and recruitment domain  
COPD: Chronic Obstructive Pulmonary Disease  
COX-2: Cyclooxygenase-2  
cRNA: Complementary ribonucleic acid  
cRNAs: Complementary RNAs  
CS: Cigarette smoke  
CXC: Chemokine (C-X-C motif) ligand  
DCs: Dendritic cells  
Dex: Dexamethasone  
DLBCL: Diffuse large B-cell lymphoma  
DNA: Deoxyribonucleic acid  
dpi: Days post infection  
dsRBD: Double stranded RNA-binding domain  
ELISA: Enzyme-linked immunosorbent assay  
ERK: Extracellular signal-regulated kinase  
FACS: Fluorescence activated cell sorting  
FcεRI: High affinity IgE receptor  
FEV1: Forced expiratory volume in 1 second  
FVC: Forced vital capacity  
GM-CSF: Granulocyte macrophage colony-stimulating factor  
GOLD: Global Initiative for Chronic Obstructive Pulmonary Disease  
H&E: Haematoxylin and eosin  
HA: Haemagglutinin  
HDAC: Histone deacetylase  
HDM: House dust mite  
HPRT: Hypoxanthine-guanine phosphoribosyltransferase

i.n: Intranasal  
i.p: Intraperitoneal  
IAV: Influenza A virus  
ICAM-1: Intracellular adhesion molecule 1  
IFN: Interferon  
Ig: Immunoglobulin  
IKK: IκB kinase  
IKK-i: IκB kinase-i  
IL: Interleukin  
ILC2: Type 2 innate lymphoid cells  
IL-13Rα1: Interleukin-13 receptor alpha-1  
IPS-1: IFN-β promoter stimulator 1  
IRF7: IFN regulatory factor 7  
IκB: Inhibitor of κB  
KC: Keratinocyte-derived protein chemokine  
KLF: Krüppel-like factor  
LNA: Locked nucleic acid  
LPS: Lipopolysaccharide  
MACS: Magnetic-activated cell sorting  
MAPK: Mitogen-activated protein kinase  
MCP: Monocyte chemoattractant protein  
mDCs: Myeloid dendritic cells  
MHC: Major histocompatibility complex  
MHC: Myosin heavy chain  
MIP: Macrophage inflammatory protein  
miR: Micro RNA  
MK2: MAPK-activated protein kinase 2  
MMP: Matrix metalloproteinase  
mRNA: Messenger ribonucleic acid  
MSCs: Mucus secreting cells  
Muc5AC: Mucin 5AC  
NA: Neuraminidase  
NCDs: Non-communicable diseases

NEP: Nuclear export protein  
NF- $\kappa$ B: Nuclear factor kappa-light-chain-enhancer of activated B cells  
NIK: NF-  $\kappa$ B inducing kinase  
NK: Natural killer  
NLRP3: NOD-like receptor family pyrin domain containing 3  
NOS: nitric oxide synthase  
NP: Neucleoprotein  
NS: Non structural  
Ova: Ovalbumin  
PA: Polymerase acidic  
PAMP: Pathogen-associated molecular pattern  
PAS: Periodic acid-Shiff  
PB: Polymerase basic  
pBEC: Primary bronchial epithelial cell  
PBMC: Peripheral blood mononuclear cell  
pfu: Plaque forming units  
PI3K: Phosphoinositide 3-kinase  
PIP2: Phosphatidylinositol 4,5-bisphosphate  
PIP3: Phosphatidylinositol (3,4,5)-trisphosphate  
PKC: Protein kinase C  
PP2A: Protein phosphatase 2A  
PPP: Phosphoprotein phosphatase  
PRR: Pattern recognition receptor  
PTEN: Phosphatase and tensin homolog  
PTP: Protein tyrosine phosphatase  
qPCR: Quantitative polymerase chain reaction  
RAGE: receptor for advanced glycation end-products  
RIG-I: Retinoic acid-inducible gene I  
RISC: RNA-induced silencing complex  
RNA: Ribonucleic acid  
RNP: Ribonucleoprotein  
ROS: Reactive oxidant species  
RSV: Respiratory syncytial virus

RV: Rhinovirus  
S.E.M: Standard error of the mean  
SIPR1: Sphingosine-1-phosphate receptor  
siRNA: Small interfering RNA  
SNP: Single nucleotide polymorphism  
SPP: Secreted phosphoprotein  
Spred: Sprouty-related protein with an EVH1 domain  
STAT6: Signal transducer and activator of transcription-6  
TANK: TRAF family member-associated NF- $\kappa$ B activator  
TBK1: TANK binding kinase-1  
TDI: Toluene diisocyanate  
TGF- $\beta$ : Transforming growth factor beta  
Th: T helper lymphocyte  
TIS11: TPA-induced sequence 11  
TLR: Toll-like receptor  
TNF: Tumour necrosis factor  
TRAF: TNF receptor associated factor  
TRAIL: Tumour necrosis factor-related apoptosis-inducing ligand  
Tregs: Regulatory T cells  
TSLP: Thymic stromal lymphopietin  
TTP: Tristetraprolin  
UCHL-1: Ubiquitin carboxyl-terminal hydrolase L1  
US: United States  
VEHF: Vascular endothelial growth factor  
WHO: World Health Organisation  
WT: Wild-type  
ZFP36: Zinc finger protein 36  
 $\gamma\delta$  T cell: Gamma delta T cell

# CHAPTER 1

## INTRODUCTION

The sub-sections of this chapter have been included in the below listed publications:

- **Dua, K.**, N. G. Hansbro, P. S. Foster and P. M. Hansbro (2017). "MicroRNAs as therapeutics for future drug delivery systems in treatment of lung diseases." Drug delivery and translational research: 1-11.
- **Dua, K.**, Hansbro, N.G, Hansbro, P.M. (2017). "Steroid resistance and concomitant respiratory Infections: a challenging battle in pulmonary clinic." EXCLI Journal **16**: 981-985.
- Hansbro, P. M., R. Y. Kim, M. R. Starkey, C. Donovan, **K. Dua**, J. R. Mayall, G. Liu, N. G. Hansbro, J. L. Simpson and L. G. Wood (2017). "Mechanisms and treatments for severe, steroid-resistant allergic airway disease and asthma." Immunological Reviews **278**(1): 41-62.

## 1.1. ASTHMA

Asthma is a chronic inflammatory disease of the airways characterised by cellular infiltration and by accompanying increases in the sensitivity and response to contractile agents termed airway hyper-responsiveness (AHR) and to allergen exposure[1, 2]. The global prevalence of asthma is increasing[3, 4] and the symptoms are often inadequately controlled[5]. The main clinical features include breathlessness and chest congestion. These symptoms commence due to airway inflammation, mucus over production and increased contraction of airway smooth muscle, a phenomenon termed AHR. Allergic asthma is considered to be a T-helper 2 cell (Th2)-mediated inflammatory disease that develops due to abnormal immune responses to otherwise innocuous allergens. The disease features are exacerbated acutely that are typically induced by respiratory viral infections[6]. Influenza A virus (IAV) is an important respiratory virus that induces severe exacerbations of asthma[7].

### 1.1.1. Epidemiology of asthma

Recent reports from the World Health Organisation (WHO) suggest that greater than three hundred million people worldwide suffer from asthma, which has a significant impact on healthcare expenditure. It is prevalent across all age groups, however the highest rates are in children. By 2025, an additional 100 million people are predicted to be diagnosed with this disease [3]. In the United States the annual expenditure on asthma ranges between USD \$3.6 and \$8 billion (approx. AUD \$3.8 and \$8.5 billion) respectively, where half of these costs are due to hospitalisations[8].

In 2014-15, 10.8% of Australians (2.5 million people) had clinical diagnosis of asthma. The prevalence of asthma has increased about 9.9% since 2007-08. The rate of asthma among Indigenous Australians is almost twice as high as that of non-Indigenous Australians. This is even more marked in the older adult age group[9, 10]. Overall, females had higher rates of asthma than males in 2014-15 (11.8% compared with 9.8%). However, asthma was more common amongst boys aged 0-14 years (12.4%) than girls (9.6%), with this pattern being consistent since 2001. The total number of reported deaths due to asthma was

378 in 2011 where the highest proportion of cases comprised of elderly people[11].

The annual global economic cost of asthma including direct medical costs from hospital stays and indirect costs, such as lost school and work days amounts to more than \$56 billion dollars annually[12]. In Australia, asthma results in 54,000 hospitalisations annually, and has healthcare costs over \$693 million, which accounts for approximately 1.4% of the total national healthcare expenditure[3, 13, 14]. Based on current worldwide trends, by 2025 there will be an additional 100 million asthma patients causing further healthcare and economic burdens[15].

### **1.1.2. Pathophysiology of asthma**

Asthma had been typically considered an allergic condition demonstrating increased eosinophil counts, however not all patients have allergic asthma. However, it is now recognised to be a heterogeneous complex inflammatory airway disease involving a combination of genetic and environmental interactions that culminate with various inflammatory subtypes identified on the basis of differential cell counts in induced or spontaneous sputum samples[16]. A simple classification of asthma includes eosinophilic asthma (EA) and non-eosinophilic asthma (NEA). However, Simpson et al., reported that four distinct inflammatory subtypes of asthma occur namely eosinophilic, neutrophilic, paucigranulocytic and mixed granulocytic identified on the basis of differential cell count in the airways[16]. The heterogeneity of the disease is one of the prime reasons attributed to why all patients respond differently to treatment. In clinical practice, identifying these phenotypes may be of significance particularly for individualised asthma management especially in steroid-resistant severe asthma[17].

The major clinical symptoms of asthma include wheezing, breathlessness, dyspnea and cough. These symptoms result from airway inflammation due to the influx of T-lymphocytes, neutrophils, macrophages, eosinophils and mast cells. This continuous process of inflammatory cells influx leads to process of

tissue damage and repair that result in AHR, dysfunctional neuroregulation and airway remodelling. Airway remodelling is characterised by various structural changes including thickening of airways, collagen deposition around the airways, airway smooth muscle cell hypertrophy, blood vessel proliferation and mucus secreting cells (MSCs) metaplasia[18-20] (Figure 1.1). Collectively these events lead to progressive loss of lung function[21] which is not fully reversible by current therapies[22]. Collectively, these symptoms may result in hospitalisation and in severe cases death due to asphyxiation[23].

The development and progression of mild to moderate allergic asthma is primarily considered to be due to the actions of activated mast cells, eosinophils and Th2 lymphocytes upon exposure to allergens[24, 25]. Multiple genes have been identified that have been linked to increased susceptibility to asthma including ADAM metallopeptidase domain 33 (ADAM33), PHD finger protein 11 (PHF11) and dipeptidyl peptidase like 10 (DPP10)[26-28].

Environmental factors, such as exposure to air pollutants and allergens are important triggers of asthma exacerbations[29].

### **1.1.3. Immunology of asthma**

In asthma, various immunological mechanisms occur as a consequence of exposure to common aero-allergens, like house dust mite (HDM), plant pollens, animal and fungal antigens, air pollutants and animal dander. Mild to moderate allergic asthma is strongly linked to CD4+ Th2 cells, eosinophils and mast cells and when these cells are activated they release range of a pro-inflammatory and pro-fibrotic mediators which induce AHR, airway re-modelling and MSC metaplasia[30, 31] (Figure 1.2). Neutrophils are also recruited into the airways after either allergen exposure or injury, and are prominent in more severe, steroid-resistant form of asthma and in COPD. These cells can produce a wide range of products including lipids (LTB<sub>4</sub>, PAF, TXA<sub>2</sub>, LTA<sub>4</sub>), cytokines (IL-1 $\beta$ , IL-6, IL-8, TNF $\alpha$ , TGF $\beta$ ), proteases (elastase, collagenase, MMP-9), microbicidal products (lactoferrin, MPO, lysozyme), reactive oxygen intermediates (superoxide, H<sub>2</sub>O<sub>2</sub>, OH<sup>-</sup>) and nitric oxide [32].

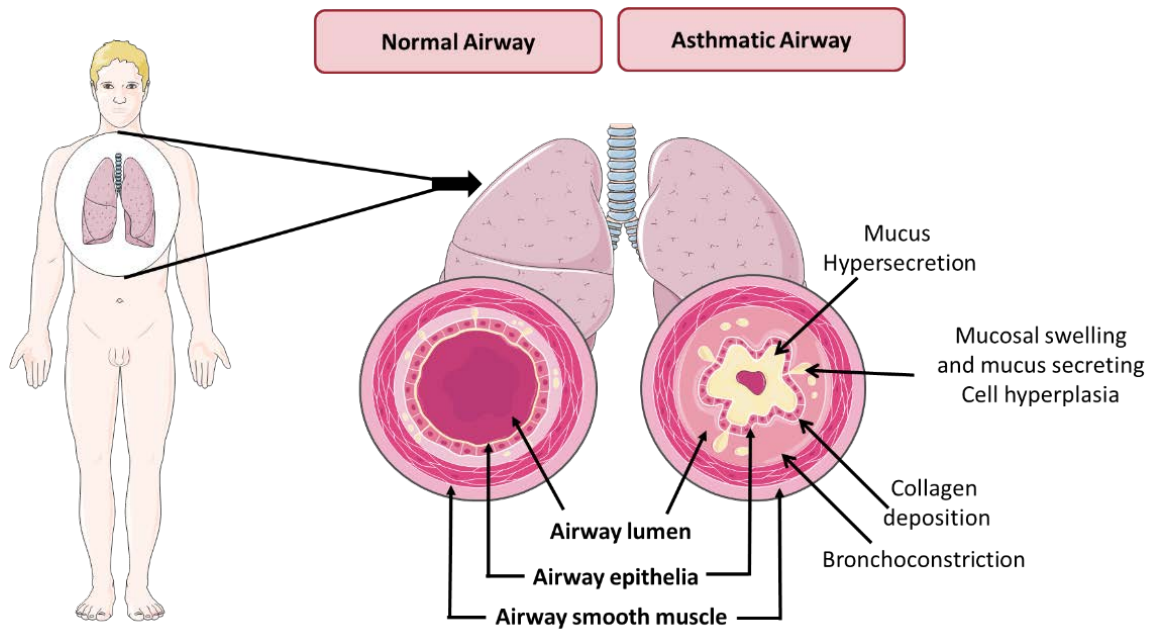


**Figure 1.1. Clinical features of asthma.**

Asthma is an allergic airway disease characterised by allergic airway inflammation, thickening of airways along with the hypersecretion of mucus that lead to narrowing of the airways which cause and interference with the airflow. Response to exposure to factors such as allergens, viruses and irritants cause exacerbations of the existing disease. Adapted from [30, 33, 34].

The airway epithelium constitutes the first physical, chemical, and immunologic barrier to inhaled agents. Epithelial cells express pattern recognition receptors, integrate information from many receptors simultaneously, and bridge the innate and adaptive immune system through the release of chemokines and cytokines. Evidence is accumulating that epithelial-derived type-2 alarmins, IL-25, IL-33, and TSLP, orchestrate many of the pathologic responses to inhaled noxious agents, particularly allergens, observed in asthma. TSLP, in particular, has been shown to be necessary for the persistence of eosinophilic inflammation and elevated levels of exhaled nitric oxide in subjects with mild allergic asthma, and allergen-induced increases in these inflammatory biomarkers (Figure 1.2) [35].

The immunological mechanisms of how asthma is initiated after an exposure to allergens such as plant pollens, animal and fungal antigens, house dust mite (HDM), and air pollutants involves hypersensitivity reactions and increases in the levels of immunoglobulin (Ig)E antibodies in serum. Prior to the initiation of IgE synthesis, antigens are recognised by DCs which act as antigen presenting cells (APCs) in the airways. They migrate to the draining lymph nodes of the lungs where the processed antigens are presented to T and B cells[36]. B-cells are activated resulting in the production of cytokines which promotes switching of antibody release from IgG to IgE. IgE antibodies encounter Fc epsilon receptor I (FcεRI) forming cross-linked IgE-FcεRI complexes that leads to activation of mast cells. This results in the production of mediators, such as histamine and prostaglandins, which play important roles in vascular leakage and subsequent pulmonary infiltration of inflammatory cells and oedema. Also, naïve CD4 T cells polarise to become Th2 effector cells[36-38]. Th2 cells produce various Th2 cytokines such as IL-4, IL-5 and IL-13 that lead to goblet cell hyperplasia/metaplasia, recruitment and infiltration of eosinophils in airways, increase matrix metalloproteinase activity and AHR [39-41] (Figure 1.3).

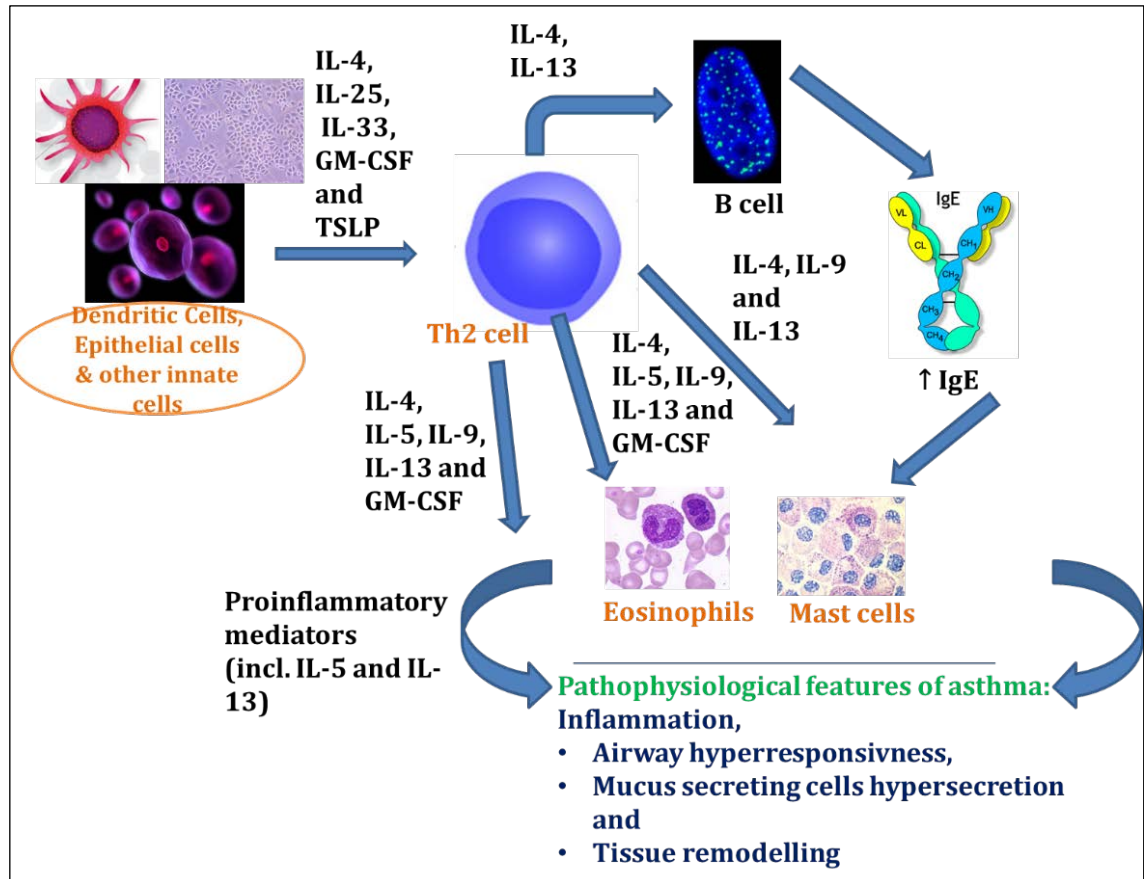


**Figure 1.2. The role of Th2 cells and cytokines in the pathogenesis of asthma.**

Dendritic cells, epithelial cells and other innate immune cells present in the extra cellular environment produce various Th2 inducing cytokines (IL-4, IL-25, IL-33, GM-CSF and thymic stromal lymphopoietin (TSLP)) which induce Th2 cell differentiation, recruitment and activation. Activated Th-2 cells secrete Th-2 cytokines (IL-4, IL-5, IL-9, IL-13 and GM-CSF) which promote IgE production and eosinophil and mast cells recruitment. Th-2 cytokines and other pro-inflammatory mediators lead to the pathological features of asthma. Adapted from reference[42].

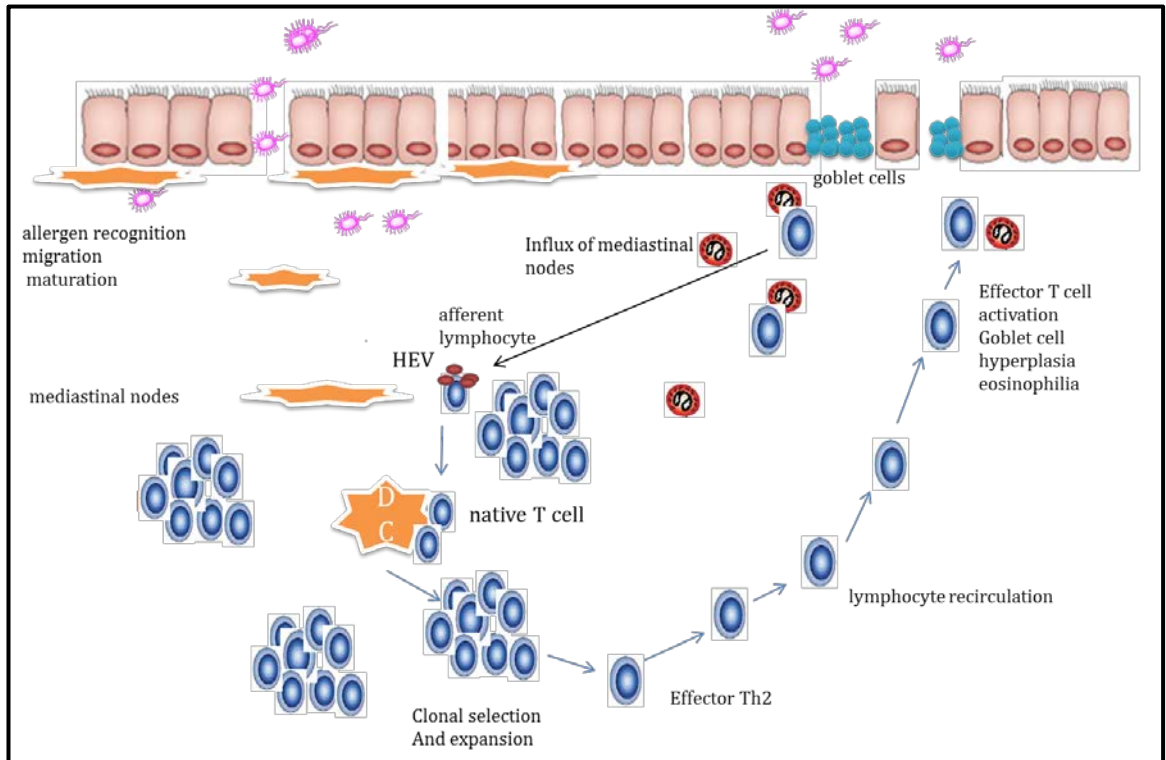


**Figure 1.3. The role of dendritic cells in the pathogenesis of asthma.**

Allergens and other foreign matter in the airways are taken up by dendritic cells (DCs), which act as antigen presenting cells (APCs). Subsequently, the APCs migrate to the draining lymph nodes where they interact with the naïve T-cells. DCs regulate the differentiation of T cells into unresponsive T cells or responsive (Th1/Th2) effector cells. The activation of DCs takes place when they receive danger signals provided by inhaled pathogens like viruses, bacteria or fungi or derived indirectly from pathogens (LPS, peptidoglycan etc.). Activated effector T-cells migrate back to the site of allergen entrance and in case of second encounter with allergens, local DCs activates the effector cells to secrete their cytokines. Th2 cells mainly produce IL-4, IL-5 and IL-13 which are important in regulating various pathological features that lead to goblet cell hyperplasia, recruitment of eosinophils, increase matrix metalloproteinase activity and bronchial hyperactivity. Adapted from reference[41].

Another player that has recently been shown to exist in the lungs and have a role in the pathophysiology of asthma and allergic inflammation are group 2 innate lymphoid cells (ILC2s). ILC2s are rapid and potent producers of the type 2 cytokines IL-5 and IL-13 upon stimulation by epithelial cell-derived cytokines. These cells require the transcription factor retinoic acid receptor–related orphan receptor (ROR)- $\alpha$  and the transcription factor Gata3. ILC2s have been shown to mediate eosinophilia and goblet cell hyperplasia, which are critical for allergic diseases and asthma. ILC2 were shown to accumulate in the lungs of mice after infection with IAV, via an IL-33 dependent mechanism. These ILC2 induced AHR through IL-13 secretion and also restored airway epithelial integrity and lung function and contributed to airway remodeling by the production of amphiregulin[43]. In addition to asthma, ILC2s were found in nasal polyps of patients with chronic rhinitis, another classical Th2-driven disease[44].

#### **1.1.4. Role of IL-13 in Asthma**

IL-13 is a Th2-associated cytokine which is produced mainly by Th2-polarised CD4+ T cells and it regulates allergic inflammatory immune responses in asthma[45, 46]. Recent investigations have also shown that natural killer T cells, mast cells, basophils, eosinophils and innate lymphoid cells are important sources of IL-13 during allergic responses[89-92]. It has been shown *in-vitro* that IL-13 regulates the differentiation of epithelial cells, production of mucus and extra cellular matrix proteins as well as the contractility of airway smooth muscle[46].

Asthmatics lung specimens and broncho-alveolar lavage (BAL) cells have been shown to increase the expression of IL-13 compared to non-asthmatics[47, 48]. IL-13 levels are reduced in the patients that receive allergen desensitisation treatment[49] or steroid treatment[50]. Besides, various studies have reported an increase in IL-13 levels upon allergen challenge. Baumann and his colleagues found pronounced levels of IL-13 in nasal secretions 5h after allergen-challenge in allergic rhinitis patients compared with a challenge control cohort[51]. Huang *et al.*, also demonstrated significant increases in both IL-13 transcripts and secreted proteins in the allergen-challenged BAL compared with

the saline-challenged control sites of asthmatic and rhinitic patients. However, this study did not detect the expression of IL-13 transcripts in the BAL of normal subjects challenged with the same dose of allergen[52]. Furthermore, Kroegel and colleagues demonstrated active secretion of IL-13 during the late asthmatic response in mild asthmatic subjects following local allergen exposure [53].

IL-13 binds to the IL-13 receptor, comprising of IL-13R $\alpha$ 1 and IL-4R $\alpha$ [54]. Receptor engagement leads to the phosphorylation of JAK, and the phosphorylation and dimerization of STAT6. pSTAT6 then translocates to the nucleus where, genes encoding IgE, eotaxin and vascular cell adhesion molecules are transcribed. This leads to inflammation of the airways, increased production of mucus and AHR. Alternatively, IL-13 may also interact with IL-13R $\alpha$ 2 which may function as a decoy receptor or as an active membrane receptor (Figure 1.4)[55-61].

IL-13R $\alpha$ 1, previously called NR4, IL-13R $\alpha$  and IL-13R $\alpha'$ , is a member of haemopoietin receptor family and was cloned based on its conserved WSXWS motif[62-65]. Wills-Karp *et al.*, found that administration of IL-13 was sufficient to induce AHR, which is found in allergic asthma[66]. Munitz *et al.*, reported that IL-13R $\alpha$ 1 is essential for baseline IgE production, but Th2 and IgE responses to T cell-dependent antigens are IL-13R $\alpha$ 1-independent. Furthermore, they also demonstrated that increased airway resistance, mucus, TGF- $\beta$ , and eotaxin(s) production, but not cellular infiltration, were critically dependent on IL-13R $\alpha$ 1[67]. Similarly, Myrtek and colleagues showed that the expression of the IL-13R $\alpha$ 1-subunit on peripheral blood eosinophils is regulated by a network of cytokines[68].

IL-13R $\alpha$ 1 had been identified to be required for aeroallergen-induced airway resistance. Also, allergen-induced chemokine production and consequent eosinophilia is dictated by the balance between IL-4 and IL-13 production *in situ*[69]. IL-13R $\alpha$ 1 has also been reported to mediate protective effects in lung injury and subsequent repair in response to bleomycin[70].

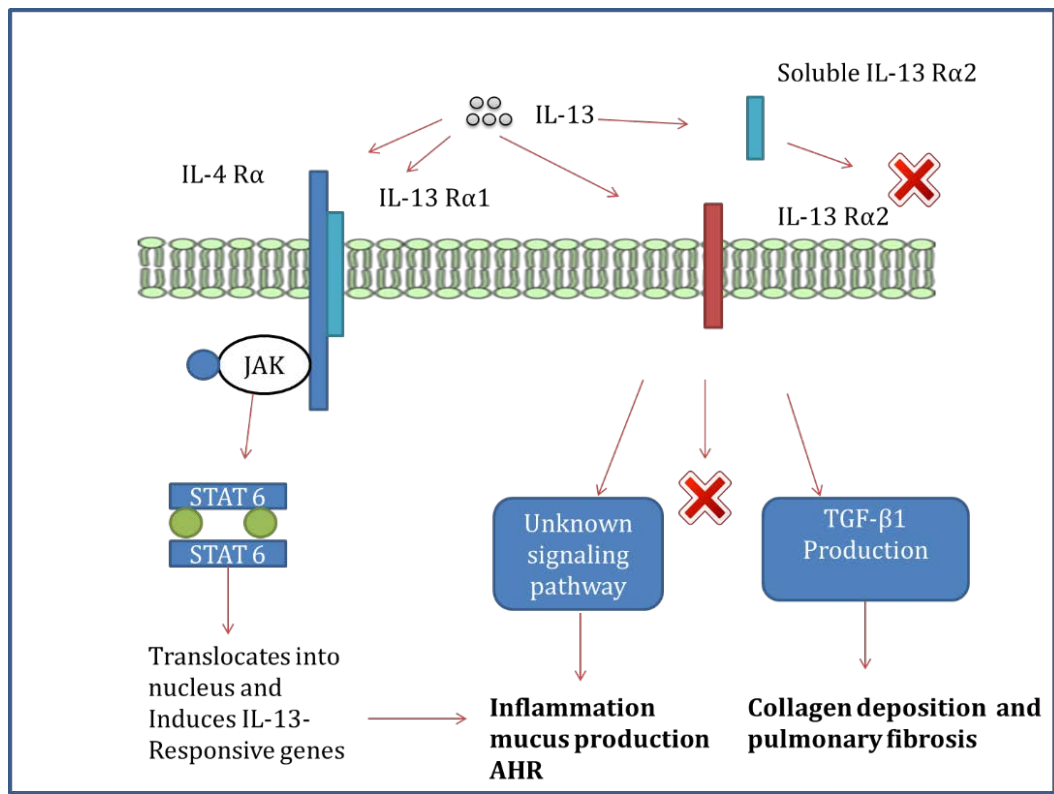


**Figure 1.4. Role of IL-13 in asthma.**

IL-13 binds to the IL-13 receptor, comprising of IL-13Rα1 and IL-4Rα. Receptor engagement leads to the phosphorylation of JAK, and the phosphorylation and dimerization of STAT6. pSTAT6 then translocates to the nucleus where genes encoding IgE, eotaxin and vascular cell adhesion molecules are transcribed. This leads to inflammation of the airways, increased production of mucus and AHR. Alternatively, IL-13 may also interact with IL-13Rα2 which may function as a decoy receptor or as an active membrane receptor.

An in-depth study demonstrated that IL-13R $\alpha$ 1 subunit gene -281T>G and 1365A>G polymorphisms do not contribute to asthma susceptibility or severity, although the IL-13R $\alpha$ 1 subunit gene locus might be involved in the control of IgE production[54].

A recent study using IL-13R $\alpha$ 1<sup>-/-</sup> mice showed that these mice are protected from *Schistosoma mansoni* egg antigen-induced mucus hypersecretion and AHR[71]. IL-13R $\alpha$ 1 expression has been observed on human CD4<sup>+</sup> Th17 cells and demonstrated to attenuate IL-17A production[72]. A study conducted in India highlighted the importance of IL13R $\alpha$ 1 + 1398A/G polymorphism in posing a significant risk toward asthma in the north Indian population[73].

Both the human and mouse IL-13R $\alpha$ 1 and IL-13R $\alpha$ 2 genes are located on the X chromosome[57], possibly suggesting a role in X-linked immune diseases. The role of IL-13 and IL-13R $\alpha$ 1 is being investigated in asthma and its pathogenesis using mouse models as well as specific inhibitors that block the receptor function. Some of the findings are summarized in Table 1.1[42]. Research focusing on IL-13 and the IL-13R complex could have significant impacts onto the understanding and treatment of X-linked immune diseases and allergen-induced asthma.

## **1.2. CHRONIC OBSTRUCTIVE PULMONARY DISEASE (COPD)**

Chronic Obstructive Pulmonary Disease (COPD) is a heterogeneous disease characterised by chronic airway inflammation mucus hypersecretion and airway remodelling with fibrosis, emphysema and lung function changes and impaired gas exchange. The widely used functional definition of COPD by the Global Initiative for Chronic Obstructive Lung Disease (GOLD) defines COPD as a disease state characterised by airflow limitation that is not fully reversible[74]. These changes are associated with increased risk of acute exacerbations of COPD, decreased quality of life and accelerated decline of lung function.

**Table 1.1. Role of IL-13 and IL-13R $\alpha$ 1 in the pathogenesis of asthma.**

<b>Cytokine</b>	<b>Role</b>	<b>Deficient Mice</b>	<b>Over-expressing mice/ recombinant treatment</b>	<b>Neutralizing antibody/ inhibitor in AAD</b>	<b>Summary of importance of cytokines found in mouse models</b>
IL-13	Induces all hallmarks of asthma (eosinophilic airway inflammation, mucus hypersecretion, airway remodelling, and AHR)	Decreased MSCs, may or may not have AHR in acute AAD Pulmonary eosinophilic inflammation	Increased baseline mucus secretion, airway remodelling, and AHR (all further enhanced after allergen challenge)	Reduced airway inflammation, mucus production, and AHR	Antagonizing IL-13 may have a therapeutic potential in chronic asthma[42]
IL-4R $\alpha$ /IL-13R $\alpha$ 1	Common receptor for both IL-4 and IL-13 signalling	Reduced eosinophilic inflammation, mucus hypersecretion, IgE production, and AHR	Increased serum IgE and mucus production		Targeting IL-4R $\alpha$ /IL-13R $\alpha$ 1 is beneficial in asthma; more effective than antagonizing IL-4 alone[42]

### **1.2.1. Epidemiology of COPD**

It is currently the third leading cause of mortality and morbidity worldwide and affects approximately 65 million people[75]. COPD accounted for almost 5% of deaths or 3 million people globally in 2005[76]. In Australia, COPD is one of the leading causes of death and hospitalisation and accounted for 4.2% of all deaths in the year 2003[77].

COPD has also been listed as an associated cause of death and is often linked to other comorbidities such as cardiovascular disease, diabetes and recurrent respiratory tract infections[77]. COPD also causes significant economic burden. The health expenditure for COPD in Australia in 2008/2009 was estimated to be \$929 million with the greatest proportion of expenditure attributed to hospital admissions[78].

In Australia, the death rates due to COPD have approximately halved between 1979 and 2011 among males, although it increased between 1979 and 1997 among females before starting to decline. Moreover, deaths due to COPD are higher among people of indigenous origin compared to non-indigenous Australians[79]. Data from The Sax Institute's 45 and Up Study (n= 204,953; aged  $\geq 45$  years) showed that two-thirds of deaths in current smokers can be directly attributed to smoking, which is much higher than the earlier international estimates of 50%. In addition, current smokers are estimated to die an average of 10 years earlier than non-smokers[80].

The Burden of Obstructive Lung Disease (BOLD) initiative was designed to be somewhat more accurate and develop standardised methods for estimating COPD prevalence world-wide that would be practical for use in countries with differing economic development profiles and also to estimate the economic burden of COPD[81]. BOLD study data from 12 sites (n=9425; in China, Turkey, South Africa, Austria, Iceland, Germany, Poland, Norway, Canada, USA, Philippines and Australia), up to 2006, reported the estimated population prevalence of COPD GOLD Stage II and higher as  $10.1 \pm 4.8\%$  (SE) overall ( $11.8 \pm 7.9\%$  for men and  $8.5 \pm 5.8\%$  for women). Australian BOLD study

estimates that approximately 14.5% (one in seven) Australians >40 years have airflow limitation of their lungs, which increases to 29.2% in Australians >75 years. Moreover, around 7.5% Australians (>40 years) have subjective symptoms and it is estimated that about half of them are under-diagnosed [82].

The prevalence of COPD increased with age and pack-years of smoking, although other risk factors, such as biomass use for heating and cooking, occupational exposures and tuberculosis, could also contribute to location-specific variations in disease prevalence[83]. Though smoking has been identified as an important risk factor in pathogenesis of COPD, only 10%–20% of all heavy cigarette smokers develop the disease[84]. Epidemiological data show that genetic predisposition plays a role in COPD. Moreover, COPD has been known to aggregate in families with a stronger correlation between parents and children or siblings than between spouses[85]. Also, mutations in the anti-proteinases and antioxidants have been found to be currently the best candidates to explain part of the genetic risk of COPD [86].

Rycroft *et al.*, reviewed 133 studies published between 2000-2010 on the trends in COPD prevalence (80 articles), incidence (15 articles), and mortality (58 articles) in Australia, Canada, France, Germany, Italy, Japan, The Netherlands, Spain, Sweden, the United Kingdom, and the USA[87]. COPD prevalence ranged from 0.2% (Japan) to 37% (USA), but varied widely across countries and populations, COPD diagnosis and classification methods and age groups reported. The burden of COPD was more commonly reported in older populations (>75 years). Moreover, the prevalence of COPD has increased over time, although the rate of increase has declined in recent years, particularly among men.

Similar to prevalence, the overall mortality rate varied between countries, ranging from 3–9 deaths per 100,000 in Japan to 7–111 deaths per 100,000 in the USA. Respiratory diseases, including asthma and COPD, were the third leading non-communicable diseases (NCDs) causing 4.2 million deaths globally in 2008 and are expected to become more prevalent in the near future[88].

Globally, COPD affects approximately 329 million people, which accounts for nearly 5 percent of the total population[89]. In terms of mortality, COPD resulted in 2.9 million deaths in 2013 alone, which increased from 2.4 million deaths in 1990, which was published as an international collaborative global burden of disease project[90].

Understanding the economic implications associated with COPD and its treatments is as important as understanding their clinical impact. In terms of global expenditure on COPD, the cost is expected to rise from US\$2.1 trillion in 2010 to US\$4.8 trillion in 2030, half of which is expected to arise in developing countries[91]. Of the US\$2.1 trillion expenditure in 2010, approximately US\$1.9 trillion was accounted for by direct costs such as medical care, while US\$0.2 trillion was spent as indirect productivity losses, such as absence from work[92].

### **1.2.2. Pathophysiology of COPD**

Depending on the severity of airflow limitation, COPD is categorised into four stages based on the Global Initiative for Chronic Obstructive Lung Disease (GOLD) [93]. GOLD classification is based on forced expiratory volume in one second (FEV<sub>1</sub>) and FEV<sub>1</sub>/FVC (functional vital capacity) values. Decreased forced expiratory volume (FEV<sub>1</sub>) in one second is a characteristic feature of COPD [93, 94]. Patients with FEV<sub>1</sub> more than 80% predicted values are classified as GOLD A or mild in terms of severity. Reduced values of FEV<sub>1</sub>% indicates increase in COPD severity which declines with disease progression as shown in (Table 1.2)[94].

Smoke exposure results in the infiltration of inflammatory cells into the mucosa, submucosa, and glandular tissue which in turn induces the excess production of mucus, causes epithelial-cell hyperplasia and interrupts tissue repair, thickens the small airway walls, induces emphysema and impairs lung function and gas exchange which are the main features of COPD[37, 95] (Figure 1.5). However, these symptoms do not develop in all smokers, but only those who develop COPD.

A current concept namely the “protease-anti-protease hypothesis” aims to explain the mechanisms of physical destruction of the lung tissue resulting in emphysema as a result of disproportionate proteolytic activity.

**Table 1.2. GOLD staging of COPD**

GOLD Stage	FEV <sub>1</sub> % predicted	Disease severity
A	FEV <sub>1</sub> ≥ 80% predicted	Mild
B	FEV <sub>1</sub> = 50-80% predicted	Moderate
C	FEV <sub>1</sub> = 30-50% predicted	Severe
D	FEV <sub>1</sub> < 30% predicted	Very Severe

FEV<sub>1</sub>: forced expiratory volume in 1 second

Various factors contribute to the imbalance between proteases and anti-proteases. An important one is cigarette smoke, which induces inflammation by recruiting neutrophils and CD8+ T lymphocytes into the airways and causes increases in protease levels and deficient anti-protease responses that upsets the normal equilibrium resulting in pulmonary destruction/emphysema[38, 96-99] (Figure 1.6).

Cigarette smoke (CS) also causes the release of various mediators that activate the epidermal growth factor receptor (EGFR)[100-103]. This leads to the metaplasia of normal pseudostratified epithelium into goblet cells because of the altered expression of mucins where the COPD patient experiences abnormal sputum production and chronic cough[104, 105].

Extensive evidence of oxidative stress in COPD patients has been demonstrated in the lungs, blood and skeletal muscle. This likely occurs because of mitochondrial dysfunction resulting in excessive production of reactive oxygen species (ROS) that has harmful effects, including damage to lipids, proteins and DNA[106]. ROS in patients with COPD are also produced by

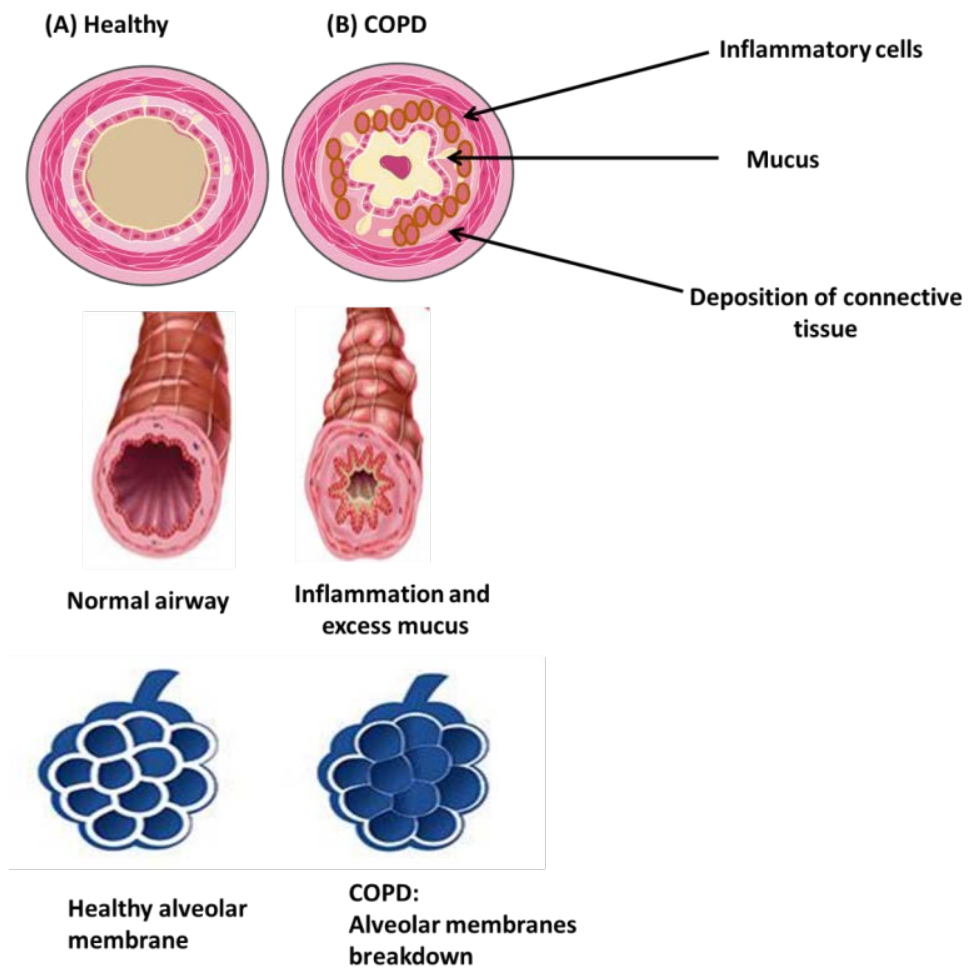


**Figure 1.5. Airway features of a healthy individual and a patient with COPD.**

(A) Normal airway. (B) In COPD the airways become narrowed by infiltration of inflammatory cells, mucosal hyperplasia, and deposition of connective tissue in the peribronchiolar space, and tissue damage results in the breakdown of alveolar tissue and emphysema. In combination these features impair lung function and gas exchange. Adapted from reference[36].

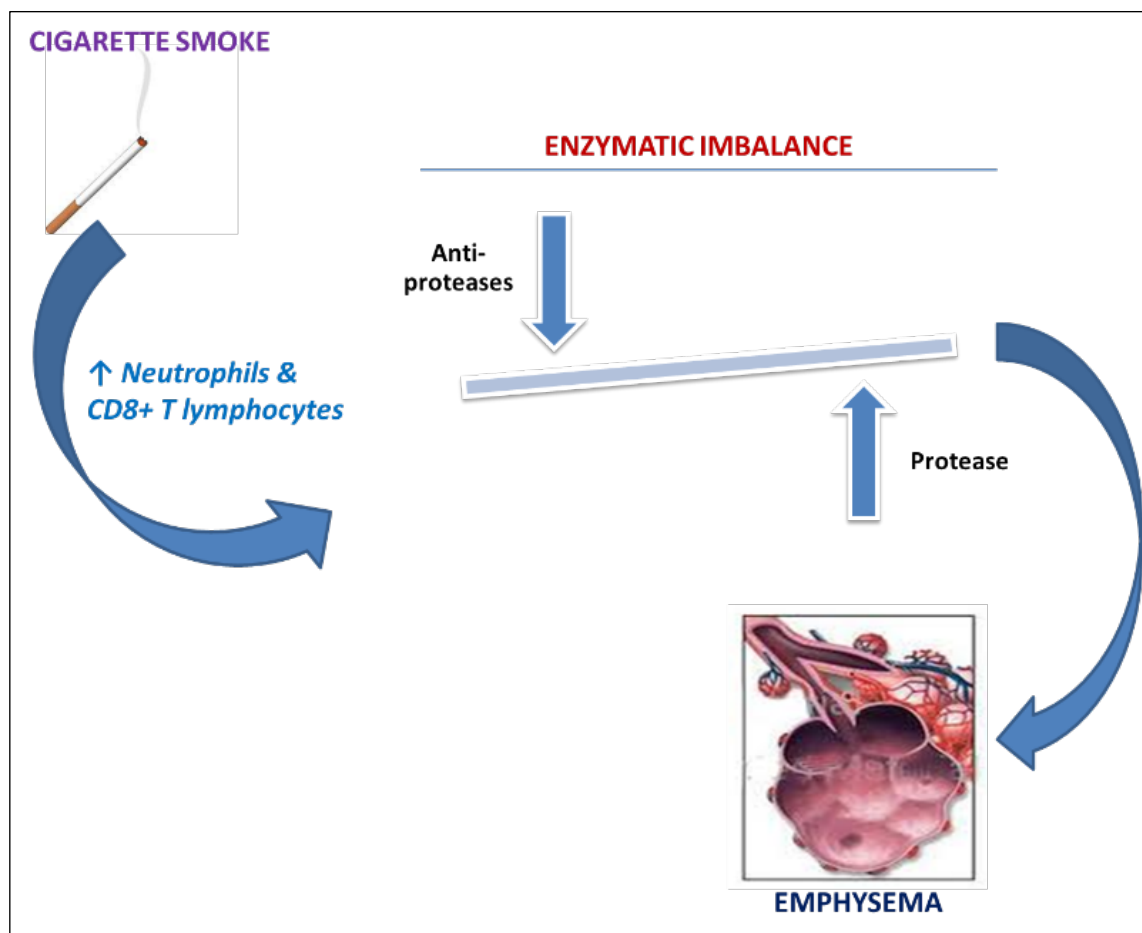


**Figure 1.6. The protease/anti-protease hypothesis in COPD.**

CS induces inflammation by recruiting neutrophils and CD8+ T lymphocytes into the airways and causes increases in protease levels and deficient anti-proteases responses that upsets the normal equilibrium resulting in pulmonary destruction/emphysema.

inflammatory (i.e. neutrophils, macrophages) and structural cells, (i.e. epithelial cells) activated in the airways. Under physiological conditions, a balance exists between the amount of reactive oxygen species (ROS) produced in normal cellular metabolism and the endogenous oxidative defence. An imbalance between the oxidants and antioxidant capacity leads to oxidative stress which has also been proposed to be important in the pathogenesis of COPD. There is considerable evidence that indicate an increased oxidative burden in the lungs of patients with COPD mediated by NF- $\kappa$ B and histone acetyltransferase activation. This subsequently promotes the expression of multiple inflammatory genes and drives many pathogenic processes, such as direct injury to lung cells, mucus hypersecretion, inactivation of anti-proteases, and enhancing lung inflammation through activation of redox-sensitive transcription factors[106, 107].

### **1.2.3. Immunology of COPD**

Inflammation and injury to the pulmonary epithelia is induced when inhaled particulates (eg CS) are exposed to the airways. This leads to the activation of transforming growth factor- $\beta$  (TGF- $\beta$ ) in airway epithelium[108]. During this process, CS also interrupts the TGF- $\beta$  signalling which causes alveolar macrophages to release pro-inflammatory mediators, facilitating inflammation and fibroblast proliferation and fibrosis in the airway. CS exposure also activates and produces various inflammatory mediators such as interleukin (IL)-8 (IL-8), TNF- $\alpha$ , IFN- $\gamma$  and IL-1 $\beta$  from the infiltrating immune cells. CS and these cytokines also induce the release of reactive oxygen (ROS) and reactive nitrogen species (RNS), which further amplifies inflammation, leading to mucus hyper-secretion and alveolar wall destruction[109-113] (Figure 1.7).

CS-induced injury to airway epithelial cells also causes the release of various danger-associated molecular patterns[114]. The signals associated with these patterns are recognised by PRRs, such as Toll-like receptors 4 and 2 on epithelial cells which trigger non-specific, inflammatory responses including the release of TNF- $\alpha$ , IL-1 $\beta$ , IL-8, and the influx and activation of macrophages, neutrophils, and dendritic cells at the inflammation site to commence the innate

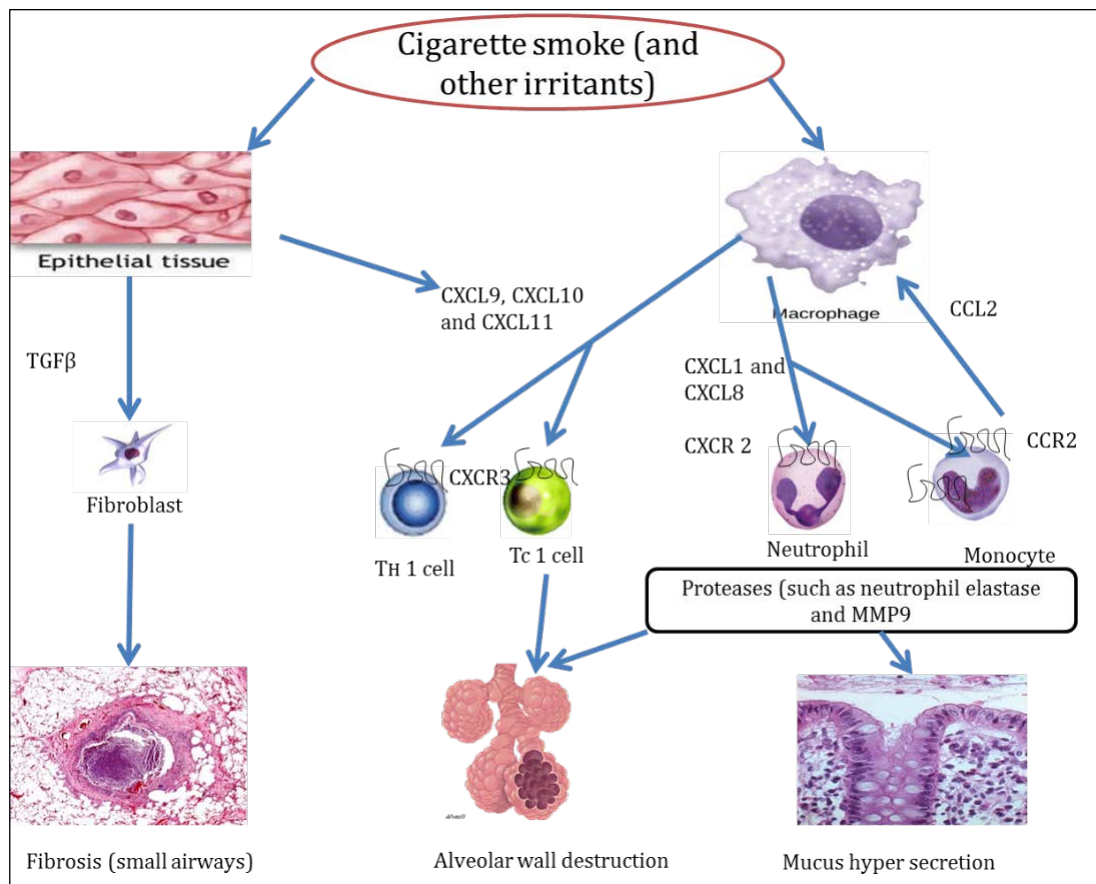


**Figure 1.7. Inflammatory factors and cells involved in the immunopathology of COPD.**

Exposure of epithelial cells to CS leads to the activation of transforming growth factor- $\beta$  (TGF- $\beta$ ) in airway epithelium. During this process, CS also interrupts the TGF- $\beta$  signalling which causes alveolar macrophages to release pro-inflammatory mediators, facilitating inflammation and fibroblast proliferation and fibrosis in the airway. CS exposure also activates and produces various inflammatory mediators such as IL-8, TNF- $\alpha$ , IFN- $\gamma$  and IL-1 $\beta$  from the infiltrating immune cells. CS and these cytokines also induce the release of reactive oxygen (ROS) and reactive nitrogen species (RNS), which further amplifies inflammation, leading to mucus hyper-secretion and alveolar wall destruction. Adapted from reference[113].

immune response[115, 116]. The various reactive oxygen species along with the proteolytic enzymes also leads to further damage[116, 117].

#### **1.2.4. Adaptive Immune Response**

In healthy lungs, alveolar macrophages along with epithelial cells and DCs act as reconnaissance units, continuously scanning for foreign protein signatures and microorganisms through their PRRs[118]. Activation and terminal differentiation of DCs is significantly enhanced by IFN- $\beta$ , which assist DCs in executing their role as antigen presenting cells (APCs)[119]. Upon recognition, DCs integrate influenza viral antigens as part of their surface major histocompatibility (MHC) structures, prior to maturation and migration to lymph nodes. Once they arrive in the lymph nodes, the DCs present the antigen to T cells with receptors uniquely specific to that antigen. This, along with accessory signals delivered through co-stimulatory molecules, initiates T cell priming. During this process, influenza-specific CD8+ T cells undergo significant proliferation in the lymph nodes, and are subsequently redeployed to the site of infection, such as the lung[120].

In the lung, influenza virus antigens, in association with MHC class 1 molecules, are presented on the surface of infected airway epithelial cells. They are utilised as recognition elements by CD8+ T cells that are recruited from the lymph nodes. This allows the CD8+ T cells to bind to infected epithelial cells, consequently deliver cytotoxic factors such as granzymes and perforins into the target epithelial cells, and ultimately destroy those cells and the virus in them[121]. B cells have also been reported to be an important part of the adaptive immune response against influenza viruses, and their absence significantly increases susceptibility to lethal IAV infection[122]. This is achieved by the production of influenza virus-specific IgM, which is an important intermediate factor that affects virus clearance[122].

## 1.3. INFLUENZA

The term 'influenza' was first used in Italy during the 15th Century. It is believed that the first influenza epidemic occurred in 1580. However, it was in 1918, when scientists studied the virus responsible for the Spanish flu and termed it H1N1. As reverse engineering and molecular virology improved overtime, it was found that there were actually 5 influenza pandemics in the 19<sup>th</sup> century, and the first and only one properly recorded in 19th century was the 1889 Russian flu, caused by H2N2 (it was designated H2 because this virus was only studied after 1918 H1N1). A thorough knowledge of influenza and its causes were studied during late 1920s through the discovery of swine influenza in pigs[123]. The discoveries of human influenza type A, type B and type C followed in 1933[124], 1940[125], and 1950[126], respectively.

Influenza viruses are major and potentially lethal infectious pathogens that infect everyone on the planet. The viral particles are spread by droplets, which are highly contagious and infect the epithelia of the respiratory tract[127-129].

### 1.3.1 Epidemiology of influenza A virus (IAV)

IAV infection results in influenza that is a massive global clinical problem causing substantial annual morbidity and mortality that have enormous socioeconomic consequences[130]. The main reason attributed to this is the tendency of the virus to mutate into new strains leading to seasonal infections. Each year, seasonal IAV infects 100 million people worldwide causing 3-5 million severe infections and ~250,000-500,000 deaths[131]. In Australia seasonal influenza impacts the national health system enormously with >18,000 hospital admissions and >1,000 deaths per year[132]. Similarly, in various other countries like India ~43 million episodes of airway respiratory infections occur annually, around 4–12% of which are due to IAV infection[133-136].

The last century had 3 pandemics; Spanish flu (1918, H1N1), Asian flu (1957, H2N2), and the Hong Kong flu (1968, H3N2). The 1918 Spanish flu killed ~50–100 million people worldwide, while the Asian flu and the Hong Kong flu pandemics claiming ~500,000–2 million human lives[137]. The beginning of the

21st century had another global flu pandemic in 2009, due to novel swine-origin IAV (H1N1) that caused 500,000–1 million deaths[138]. Another outbreak of H7N9 has just recently occurred. In each seasonal and pandemic outbreak specific subsets of people are particularly at risk, which differ with each outbreak, and include, the healthy young, pregnant, elderly and those with underlying respiratory conditions such as asthma and COPD.

The influenza virus mutates rapidly which causes variations in its virulence from year to year. Due to the population having limited immunity to these new strains, there are further increases in complications and disease severity. In the last ten years, two novel viruses have arisen. The avian H5N1 in 2003 is highly pathogenic and causes severe disease in humans with 70% mortality rate. The swine-origin H1N1 (H1N1/09) in 2009 also led to a pandemic that was responsible for approximately 18,000 deaths, representing a 7-fold increase in mortality rates[139]. In the United States, the economic losses caused by the IAVs, without effective medical intervention, is estimated to cost \$187USD (approx. \$202AUD) per capita[140]. The impacts of these factors have contributed to placing IAV infection as a high priority concern in global healthcare and medical research.

People with chronic lung diseases, particularly asthma[141] and COPD are known to be more susceptible to viral infections[142], including IAV[143]. These infections are major causes of exacerbations and worsening of the underlying respiratory diseases[144]. However, the immunological mechanisms that underpin these associations in asthma and COPD are largely unknown. Approximately 35% of deaths in asthmatics are directly due to IAV infection[145]. Infection-induced exacerbations of COPD, often by caused by IAV, are the 2<sup>nd</sup> commonest cause of hospitalisations in Australia[146], and in 2006 influenza and its complications caused 2,715 deaths in these patients[132]. Furthermore, those with COPD are consistently over-represented in those hospitalised or who died during pandemics[147]. The mechanisms that promote susceptibility to IAV infection in asthma and in COPD are unclear.

Identification of these factors in chronic airways diseases could be targeted against infection in healthy and disease states.

### **1.3.2. Preventive measures & treatment options**

Due to high frequency of mutations in IAVs, there are various limitations associated with the current prevention and treatment strategies that include vaccinations. Current vaccines do not vaccinate against all strains and have to be administered every year[148, 149]. Also the present anti-viral treatments such as Neuraminidase inhibitors (e.g. oseltamivir) are only efficacious if given within the first 48 h of infection[150]. This is normally before symptoms are severe enough to present to hospital. Anti-viral therapies may also need to be given in combination to be efficacious, something that is currently under investigation.

In addition IAVs are rapidly becoming resistant to these treatments[151]. There is therefore an urgent need to develop novel and effective preventions and treatments for IAV infection, especially for those most susceptible to infection. For these reasons, IAV infection has attracted much attention from the pharmaceutical industry. The most effective approach may be to improve host immunity rather than targeting the virus and treatments directed against both IAV invasion and proliferation would be ideal[152].

### **1.3.3. Pathogenesis of IAV infection**

Influenza viruses have a unique ability to cause recurrent epidemics and global pandemics by transmitting to humans across all age groups[153]. The unique characteristics of the virus include its segmented genome, recombination in a single host, and its ability to acquire genetic mutations, which changes its virulence from year to year. Another unique aspect of IAV is that the transcription and replication of the viral genome takes place in the nucleus of the infected cells.

Influenza viruses belong to the Orthomyxoviridae family, having 8 single stranded, negative sense RNA segments which is a part of their viral

genome[154, 155]. Influenza viral RNAs are called negative strand RNAs because they are duplicated by enzymes called polymerases to generate complementary strands which serve as intermediates for the replication process to generate ribonucleoprotein complexes. These eight single strands of viral RNA in the IAV carry all the information needed to make new virus particles[156]. These segments encode for 11 proteins including glycoproteins [Haemagglutinin (HA); neuraminidase (NA)]; polymerase proteins PA, PB1, PB2, PB1-F2; nucleoprotein (NP); matrix proteins M1 and M2; and non-structural proteins NS1 and NS2, which are also known as nuclear export protein (NEP), which neutralises the suppression of interferons[128]. IAVs are subtyped based on two proteins; hemagglutinin (H1-H15) and neuraminidase (N1-N9). Viruses with HA types H1, H2 and H3 and NA types N1 and N2 cause seasonal epidemics in humans (Figure 1.8 A).

HA and NA are the two membrane glycoproteins and major surface antigen of the virus against which neutralizing antibodies are produced by the host and as a consequence undergoes antigenic variation leading to recurrent epidemics of respiratory disease[157]. HA contains various important locations of influenza antigenic sites while NA is the primary target for various anti-viral drugs such as Zanamivir and Oseltamivir. Viral particle formation is assisted by the matrix protein M1 which lies inside the viral membrane. However, the matrix protein M2 is a multifunctional protein that is expressed on the infected-cell surface[158]. M2 protein has been reported to play an essential role in the uncoating process of IAV in infected cells and in maintaining the HA in its pH neutral form during transport through the trans Golgi network[128, 159]. M2 transmembrane domain has a critical role in ion channel activity while its cytoplasmic domain is required for formation of viral ribonucleoprotein complexes and virion morphogenesis[160].

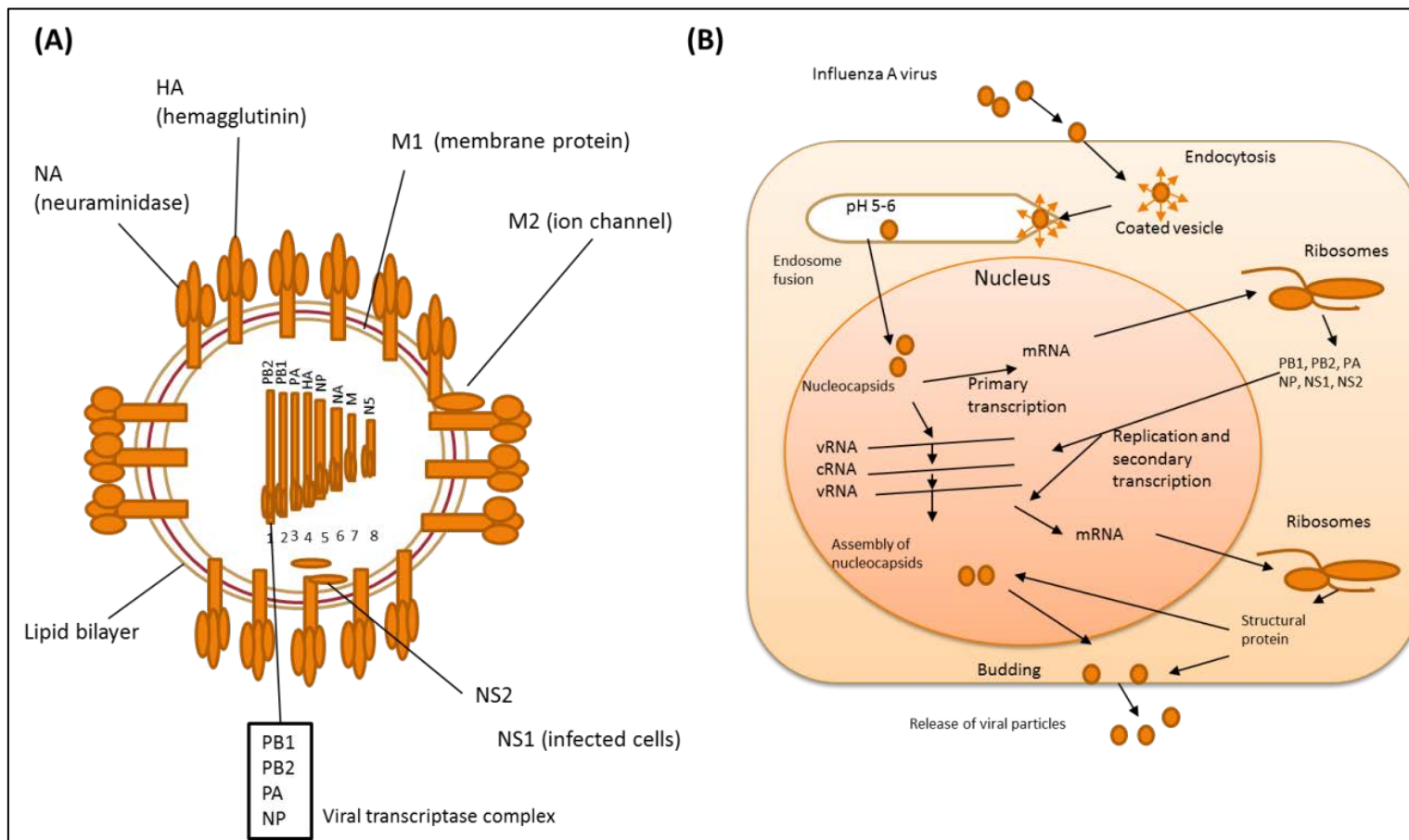


**Figure 1.8. The structure of influenza virus that consists of 8 single stranded, negative sense RNA segments.**

**(A)** The RNA segments are conserved with ribonucleoprotein complexes that are contained in the viral membrane. The various viral proteins include Haemagglutinin (HA); neuraminidase (NA); polymerase proteins PA, PB1, PB2, PB1-F2; nucleoprotein (NP);

matrix proteins M1 and M2; and non-structural proteins NS1 and NS2, which are also known as nuclear export protein (NEP). The HA and NA are distributed on the outer surface of the membrane. Viral formation is assisted by the matrix protein M1 that lies inside the viral membrane. M2 protein is responsible for forming a gated ion channel along the transmembrane region which maintains a low pH and is responsible for proton conductance. **(B)** Influenza virus binds through its HA to sialic acid residues on the epithelial lining of the respiratory mucosa, which allows the entry of virus into the host cell by the endocytic pathway followed by fusion of viral endosome membranes. The viral ribonucleoprotein complexes are then transported to the nucleus and are transcribed. The viral mRNAs are transported into the cytoplasm where the synthesis of viral proteins takes place and the newly synthesised polymerases, NP, NS1 and NS2 are transported to nucleus where viral RNA replicate into complimentary RNA. The secondary viral RNAs are transcribed to viral mRNAs leading to synthesis of structured protein. Finally, the assembly of viral nucleocapsids occurs in the nucleus which are transported the cytoplasm and plasma membrane where the budding and release of virus particles take place. Figure adapted from reference[161].

The ability of influenza virus to evade the host immune system mainly relies upon two phenomena referred to as “antigenic drift” and “antigenic shift”. In “antigenic drift”, the antigenic glycoprotein called hemagglutinin (HA) that exists on the surface of influenza virus is often the primary target for the host immune system to neutralise the infection. However, cumulative minor modifications that occur in HA allow the antigenic site to “drift” in configuration until it is no longer susceptible to the previous viral recognition molecules developed by the host [162]. The segmented nature of the influenza virus genome also allows for more dramatic changes to its antigenic sites, known as “antigenic shift”. This typically occurs during viral replication within host cells infected with multiple viruses from different species. Modifications of this nature are more significant as they may alter the genomic profile of the virus into a totally new configuration.

IAV infection is initiated when the viral HA binds to glycoproteins with specific terminal sialic residues on the surface of broncho-epithelial cells. The HA protein undergoes conformational changes leading to lowering of pH in the host cell endosome. These changes release multiple complexes of viral ribonucleoproteins into the cytoplasm, which then translocate into the nucleus[163, 164]. Inside the nucleus, viral messenger RNAs (mRNAs) and complementary RNAs (cRNAs) are synthesised from viral ribonucleoprotein templates. Transcription of viral mRNAs with positive polarity is achieved by the utilisation of 5'-methylated cap structures of the host cell[165]. This is then delivered to the cytoplasmic region of the host cell and translated into viral proteins. Concurrently, cRNAs remain in the nucleus and are utilised as templates for creating new viral negative sense RNAs. These daughter RNAs get associated with M1 proteins before being exported into the cytoplasmic region. Viral components including RNA segments, HA, NA and M2 move towards the apex of the host membrane, where eventually the NA cleaves the host sialic acid residues, liberating newly formed virions from the infected cell[166] (Figure 1.8 B).

IAV infection results in severe alveolar inflammation in the lower respiratory tract due to the loss of ciliated cells and epithelial cell damage, subsequently

contributing to the recruitment of neutrophils and mononuclear cells[167-171]. As a result, large amounts of cytokines and chemokines such as IL-6, tumor necrosis factor-alpha (TNF- $\alpha$ ), IL-1beta (IL-1 $\beta$ ) and IL-8 are produced by infected cells. The over-activation of immune cells results in an uncontrolled immune response and the excessive production of cytokines and chemokines[172, 173]. This 'cytokine storm' is strongly associated with influenza-induced mortality and was thought to be responsible for the death of young adults in the 1918 Spanish flu and the 2009 swine flu outbreaks[173]. The common clinical symptoms observed with IAV infection include headache, fever, AHR, broncho-constriction of the airways[174, 175], secondary bacterial pneumonia[176, 177] and obstruction in the small airways[174] leading to impaired diffusion capacity[178, 179].

#### **1.3.4. Host immune responses to IAV infection**

##### ***1.3.4.1. Innate immune response: Intracellular innate sensing of IAV infection***

In the initial stages of IAV infection, viral cRNA and mRNA are made during viral replication. These are vital pathogen-associated molecular patterns (PAMP) of IAV, which are recognised by specific pattern recognition receptors (PRRs) such as toll like receptors (TLRs), retinoic acid inducible gene-I (RIG-I)-like receptors (RLRs) and the NOD-like receptor family pyrin domain containing 3 (NLRP3) protein[180]. Once PRR activation takes place, signalling cascades are activated resulting in the production of pro-inflammatory chemokines that recruit inflammatory leukocytes to the site of infection[181-183].

Detection of influenza virus by RIG-I initiates its conformational changes and a cascade of downstream signals, which leads to the production of IFN- $\alpha/\beta$  (type I IFNs) and IFN- $\lambda 1/\lambda 2/\lambda 3$  (type III IFNs)[184, 185] through the JAK/STAT signalling pathway. The structure of RIG-I contains two caspase-recruitment domains (CARDs) as well as a DExD/H-box helicase domain which play a vital interfacing role and interacts with target viral RNA [186]. RIG-I recognises the uncapped 5'-triphosphate end of viral RNA, which is distinctly different from host RNA[187, 188]. Binding of influenza RNA to RIG-I results in structural changes

in the receptor, leading to exposure of the CARD domain. This subsequently allows the CARD domain to interact with the IFN- $\beta$  promoter stimulator 1 (IPS-1, also known as VISA, Cardif or MAVS)[189]. IPS-1 interacts with tumour necrosis factor (TNF) receptor associated factor -3 (TRAF-3) activates TRAF family member – associated nuclear factor- $\kappa$ B (NF- $\kappa$ B) activator (TANK) – binding kinase-1 (TBK1) and I  $\kappa$ B kinase-i (IKKi). The TBK1/IKKi complex phosphorylates interferon regulatory factor -7 and IRF-3 which are transported to the nucleus and lead to the production of type 1 and type 3 IFNs[190] . The host also generates IFN- $\gamma$  (a type II IFN), in order to begin the initiation of the adaptive immune response against influenza infection[191]. These antiviral responses are reinforced by the release of other cytokines, such as TNF- $\alpha$ , and chemokines, including IFN- $\gamma$ -induced protein (IP)-10 (CXCL10), macrophage inflammatory protein (MIP)-1 $\alpha$  (CCL3), as well as KC [192, 193]. Type 1 IFNs have strong antiviral activity that prevents viral replication[194-196]. Type 1 IFNs also stimulate dendritic cells (DCs), which induce adaptive immune response and the activation of CD4+ and CD8+ T cells[197-199].

IAV infection is detected by multiple host sensors and one of these is Toll-like receptors (TLRs). IAV infected cells are phagocytosed by macrophages and the recognition of double stranded viral RNA by TLR-3 leads to the induction of NF- $\kappa$ B dependent pro-inflammatory cytokines, type 1 IFNs and IFN-stimulated genes (ISGs) downstream of IFN regulatory factor 3 (IRF3). The single stranded RNA from the virion is released with the rupture of viral membrane and capsid within acidified endosomes and are detected by TLR7 in plasmacytoid p(DCs). TLR7 signalling induces NF- $\kappa$ B-dependent genes from the NF- $\kappa$ B endosomes and IRF7 activation from IRF7 endosomes[200, 201] (Figure 1.9 A).

In the infected cell the viral RNA in the cytosol is identified by RIG-I which via the activation of mitochondrial antiviral signalling protein (MAVS) results in the recruitment of pro-inflammatory cytokines and type 1 IFN.

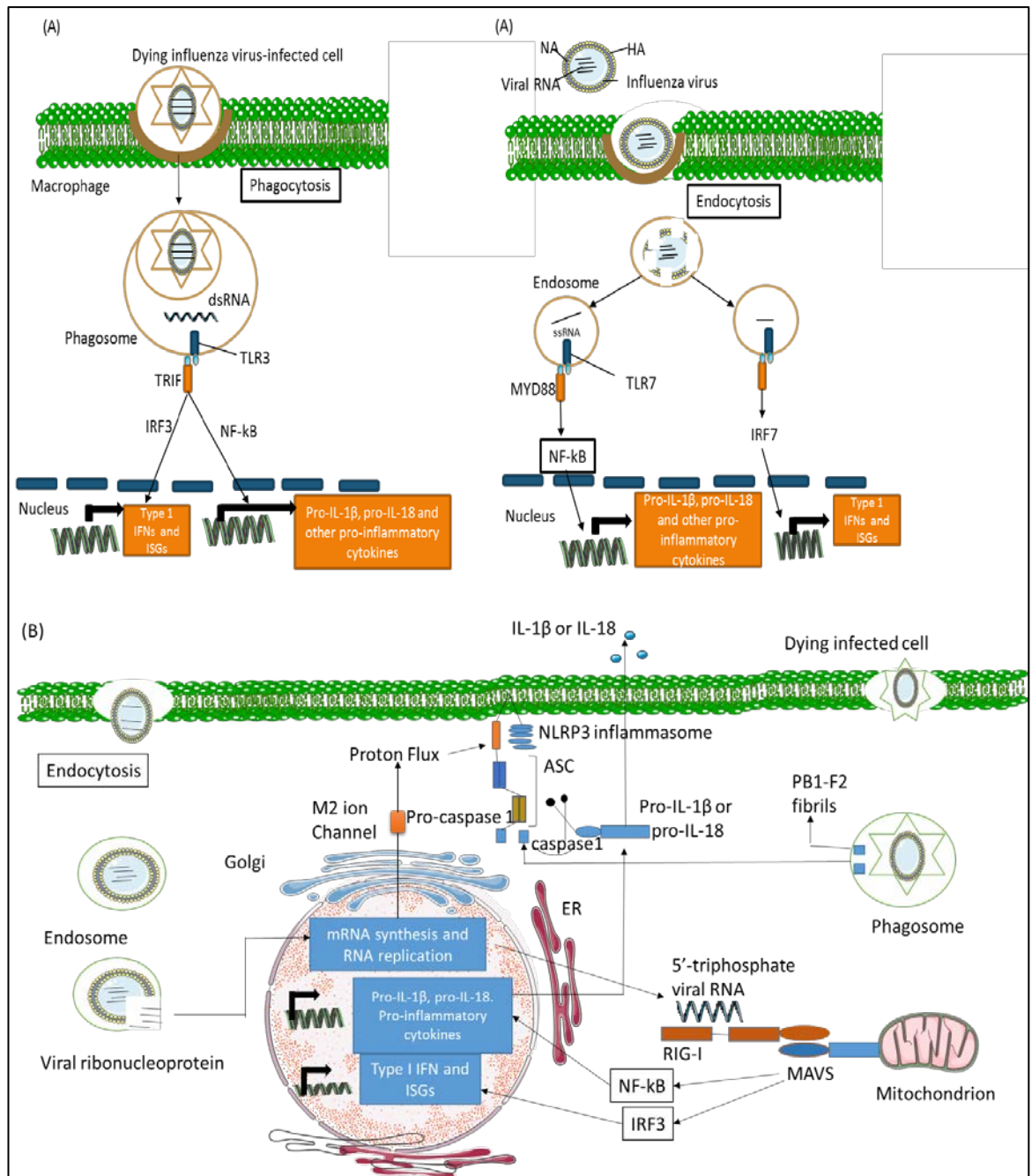


**Figure 1.9. Innate sensing of influenza viruses.**

Infected cells are phagocytosed by macrophages and the recognition of double stranded RNA by intracellular TLR-3 leads to the induction of NF- $\kappa$ B and IFN regulatory factor 3 (IRF3) dependent pro-inflammatory cytokines, type 1 IFNs and IFN-stimulated genes (ISGs). Single stranded RNA from the virion is released with the rupture of viral membrane and capsid within acidified endosomes which are detected by TLR7 in plasmacytoid dendritic cells (pDCs).

TLR7 signalling induces NF- $\kappa$ B–dependant genes from the NK- $\kappa$ B endosomes, and IRF7 activation from IRF7 endosomes. In the infected cell the viral RNA in the cytosol is identified by RIG1 which via the activation of mitochondrial antiviral signalling protein (MAVS) results in production of pro-inflammatory cytokines and type 1 IFN. In the golgi matrix 2 (M2) ion channel activity initiates the formation of nod-LRR and pyrin domain-containing 3 (NLRP3) inflammasome resulting in the activation of caspase 1 and release of cytokines. PB1-F2 fibrils accumulates in the phagosomes resulting in activation of NLRP3 and release of IL-1  $\beta$  and IL-18. Figure adapted from reference[201].

In the Golgi the M2 ion channel activity initiates the formation of nod-LRR and pyrin domain-containing 3 (NLRP3) inflammasomes resulting in the activation of caspase 1 and release of cytokines. PB1-F2 fibrils accumulate in the phagosomes resulting in activation of NLRP3 and release of IL-1  $\beta$  and IL-18[201, 202] (Figure 1.9 B).

#### **1.3.4.2. Alveolar macrophages in IAV infection**

On the initiation of infection alveolar macrophages are activated and limit viral spread[201]. The activation of these macrophages also produces nitric oxide synthase 2 (NOS2) & TNF $\alpha$  that contributes to the pathological features associated with IAV infection[203-205]. Anti-viral responses are reinforced by the production of various other cytokines like TNF $\alpha$ , and chemokines (IFN- $\gamma$ ) induced protein-10 (CXCL-10), macrophage inflammatory protein (MIP)-1 $\alpha$  (CCL3), CXCL1 and CXCL8.

#### **1.3.4.3. Adaptive immune system**

Alveolar macrophages, epithelial cells and DCs survey for foreign antigens and viruses using their PRRs. IFN- $\beta$  supports the activation and terminal differentiation of DCs which promotes their function as antigen presenting cells (APCs). Upon recognition, DCs interact with IAV antigens prior to maturation and migration to lymph nodes. On arrival at the lymph nodes, DCs present the antigen to T cells which initiates T cell priming. During this process influenza specific CD8+ T lymphocytes proliferate in lymph nodes and subsequently mobilise to the site of infection[203]. In the airways, influenza antigens are presented via major histocompatibility complex (MHC) class I molecules, which are on the surface of infected epithelial cells and are used as recognition elements by CD8+ T lymphocytes. This enables CD8+ lymphocytes to bind with infected cells and release cytotoxic factors like granzymes and perforins, which destroy the infected cell[204]. B cells also perform important roles in the adaptive immune response against IAV by the production of virus-specific, IgM which is a major antibody involved in viral clearance[205].

### **1.3.5. Association between asthma and IAV infection: Potential Mechanisms and Therapeutic Interventions**

Globally, viral respiratory infections are one of the major health problems. Investigations in this area are becoming more challenging because of the complexity of the relationship between the host's defences and the different influences of different microbes[206]. Infections can have pleiotropic roles in asthma and can cause wheezing as an "inducer" and can also acts as a "protector" against the allergic airway disease[207]. Sigurs *et al.*, have shown that the family history of asthma along with severe respiratory syncytial virus (RSV) infections increases the development of asthma in children at the age of seven[208]. Moreover, viral respiratory infections are also one of the major causes of asthma exacerbations in all groups, which further deteriorate the quality of life in these patients.

Various studies have provided mechanistic insights showing an association of respiratory viral (RSV, rhinovirus) infections with asthma [209]. Using mouse models, it has been well demonstrated that respiratory infections during early life modifies lung physiology and increases the severity of AAD by promoting IL-13[210] and TNF-related apoptosis-inducing ligand (TRAIL)[211] responses. Various other factors that have been shown to play roles in susceptibility to respiratory viral infections in AAD include monocyte chemoattractant protein-1 (MCP-1), keratinocyte-derived protein chemokine (KC)[212] and receptor for advanced glycation end-products (RAGE)[213].

There are increasing numbers of asthma patients with more severe disease that is resistant to steroid therapy. Often these patients have coexisting respiratory infections. Because they do not respond to steroids this group have substantially increased the cost of treating asthma patients[214]. miR-21/PI3K/histone deacetylase (HDAC) 2 axis has recently been reported to drive severe, steroid-insensitive experimental asthma[215]. Furthermore, in a dual T-helper 2/T-helper 17 (Th2/Th17) model of steroid-resistant asthma, IL-13-mediated and signal transducer and activator of transcription 6 (STAT6)-dependent mucus metaplasia and AHR was observed. However, IL-13 was not

identified to be directly contributing to airway/tissue inflammation. Similarly, in the same mixed model, IL-17A was identified as an independent contributor to AHR with only partial mediation of inflammation and mucus metaplasia[216].

Chambers *et al.*, investigated the immunological differences between steroid-sensitive and steroid-resistant asthma and demonstrated that patients with steroid resistance asthma produced significantly higher levels of IL-17A and IFN- $\gamma$ . Calcitriol treatment in both an *in-vitro* (peripheral blood mononuclear cell, PBMCs) and *in-vivo* (steroid resistance asthma patients) settings improved clinical responses to oral glucocorticoids. This probably occurred by directing the cytokine profile of steroid-resistance asthma patients towards the steroid-sensitive immune phenotype[217]. With an aim of increasing patient compliance in steroid-refractory asthma, Stuart and his co-workers designed and optimised various chemical compounds that could produce sustained action post-inhalation[218]. Further, microRNA-9 (miR-9) was investigated as another potential therapeutic target by Li *et.al.*, where it was hypothesised to regulate glucocorticoid receptor (GR) signalling and steroid-resistant AHR in steroid-resistant asthma[219]. Tian *et al.*, studied the apoptosis of inflammatory cells which is an important prerequisite feature in clearing airway inflammation induced by insults such as allergens. They demonstrated the potential of Bcl-2 inhibitors ABT-737 or ABT-199 as promising therapeutic tools in the treatment of corticosteroid-insensitive neutrophilic airway inflammation[220].

Another potential therapeutic intervention included an anti-RSV neutralizing antibody (palivizumab), which has recently been approved for the prevention of severe RSV infection in high-risk patients. This antibody was tested in a mouse model where the antibody was administered once either 24 h prior to infection as prophylaxis or 48 h post-infection (inoculation with RSV). Treatment attenuated RSV replication in the lower respiratory tract as well as significantly reduced the cytopathic effect of virus particularly in the respiratory epithelial cells[221-223].

Hines and colleagues investigated the molecular processes involved in structural remodelling as a consequence of repeated respiratory viral infections during early childhood. They demonstrated distinct responses from macrophages and mast cells along with abnormal re-epithelisation resulting in various structural defects using a Sendai virus infection model in weanling rats (an atopic asthma susceptible strain, Brown Norway, and a non-atopic asthma resistant strain, Fischer 344)[224]. A translational investigation using a blend of genetic animal models and *in-vitro* human studies identified an innate immune scavenger receptor MARCO to be associated with increased susceptibility of children to RSV infection[225]. Also a clinical trial investigating the efficacy and safety of long-term treatment with anti-IgE antibody, omalizumab, in children with uncontrolled severe allergic asthma demonstrated it to be well tolerated with improvements in asthma control[226].

A multicentre, randomised, double-blind, placebo-controlled, parallel-group study assessed the safety and efficacy of inhaled Zanamivir in preventing infection in adult and adolescent subjects susceptible to IAV particularly against the circulating strains of the 2000-2001 influenza season in the Northern Hemisphere (influenza A/New Calendonia/20/99-like and influenza B/Sichuan/379/99-like). Zanamivir was demonstrated to be well-tolerated with a placebo comparable safety profile[227]. Likewise, a randomised, double-blind, placebo-controlled, crossover phase 1 study evaluated the safety of an inhaled antiviral DAS181 (Fludase®) in adult subjects with well-controlled asthma[228, 229] which was a part of a clinical trial where DAS181 was shown to reduce viral load[230].

Though, there are many translational and clinical studies performed worldwide to investigate the molecular mechanisms interlinking IAV infection and AADs along with the ongoing search for potential therapeutic interventions, there are still many questions that remain unaddressed. Some of these impediments include patterns of inflammation involved due to various respiratory viruses and multiple genes and their products, which underpin the regulatory mechanisms driving disease pathology.

### **1.3.6. Associations between COPD and IAV infection**

The risk of mortality and morbidity in COPD patients increases with infectious exacerbations that worsen disease features[231-233]. This is very distressing for the patients who usually take weeks to recover[234]. Infectious exacerbations also increases both local and systemic inflammation, exaggerates the decline in lung function and reduces quality of life[235-238].

Acute exacerbations of COPD are often due to the respiratory viral infections. IAV is associated with 16-25% of all virus-induced COPD exacerbations[239]. RIG-I and IFN-initiated (type 1 and type 3) antiviral responses are well described to suppressing viral replication and limit the severity of IAV infection. CS inhibits RIG-I which also reduces the anti-viral response and predisposes to exacerbations induced by IAV. The main mechanism involved is oxidative stress induced by cigarette smoke, which reduces HDAC-1 expression in macrophages that regulates type 1 IFN responses[240-242]. Overall, the inflammation and impaired anti-viral responses alone or in combination contribute to the pathogenesis of the COPD and exacerbations induced by IAV infection. Various studies have reported that around 40-60% of episodes are due to viral infections primarily rhinovirus (RV) which play a major role[243, 244]. In addition, bacteria cause 50% of exacerbations, which is even higher (72%) in severe exacerbations requiring ventilatory support. A combination of viral and bacterial infections causes around 25% of exacerbations[245-247].

Virus-induced COPD exacerbations have been found to be associated with increased plasma levels of IL-10, IL-12 and IL-15[248], whereas all COPD exacerbations (with or without respiratory virus isolation) are characterised by increased plasma levels of IL-2, IL-13 and vascular endothelial growth factor[248]. Jian-Qing and colleagues showed an association of IL-13, IL-13R $\alpha$ 1 and IL-4R $\alpha$  polymorphisms with the rate of decline of lung function in COPD[249]. A meta-analysis study suggested that an IL-13 -1112 C/T promoter polymorphism is associated with the risk of COPD in Arabians[250]. Nada *et.al.*, demonstrated that the interaction between multiple genes and environmental influences in the presence of smoking and latent adenovirus C

infection, TNF- $\alpha$  -308A, SPB +1580 T and IL-13 -1055 T polymorphisms predispose to the development of COPD[251].

Tao and colleagues hypothesised that Th2 cytokines can also activate proteolytic pathways that could contribute to the pathogenesis of COPD[252]. To test this hypothesis, they used an inducible overexpression transgenic modelling system to target IL-13 in the adult murine lung. Their studies demonstrated that IL-13 caused a phenotype that mirrored human COPD including emphysema with macrophage-, lymphocyte- and eosinophil-rich inflammation, mucus metaplasia and enhanced lung volumes and pulmonary compliance. They also demonstrated that IL-13 caused emphysema via a MMP- and cathepsin-dependent mechanism(s) along with other mechanisms that may underlie COPD and asthma[252].

Holtzman *et.al.*, detected an increased level of IL-13 mRNA in COPD lungs with chronic mucous cell metaplasia. The increased IL-13 mRNA levels were observed to be associated with an increase number of cells stained positive for IL-13 protein in COPD lungs[253]. Another recent study also investigated the role of IL-13 in radiation lung injury where it was highlighted as a potential biomarker and target for therapeutic intervention[254].

## **1.4. MOUSE MODELS OF ASTHMA, COPD AND INFLUENZA**

### **1.4.1. Asthma**

Typically, animals models of asthma that are employed to understand AAD involve the use of various allergens like ovalbumin (Ova, protein from chicken egg) with a Th2-inducing adjuvant (aluminium hydroxide, alum) or HDM extract. In acute Ova-induced AAD model, mice are systemically sensitised to Ova in alum followed by airway Ova challenges while in case of HDM-induced AAD, mice are first locally sensitised to HDM followed by airway challenges. All these models show hallmark features of asthma with airway inflammation and increased numbers of eosinophils, elevated circulating levels of IgE, Th2 cytokine responses (IL-4, IL-5, IL-13), goblet cell hyperplasia, mast cell degranulation and pulmonary neutrophil responses, mucus hypersecretion and

AHR[255-258]. In chronic models, allergen exposures are at low levels for a prolonged period of time usually up to 12 weeks. Such chronic models are employed to understand airway remodelling and other chronic aspects of the diseases[259-261].

### **1.4.2. COPD**

In COPD, various experimental models have been developed over the years. Some models involve acute exposure (nose-only or whole body) to CS[262, 263]. The limitations of these models include no induction of airway remodelling, emphysema or lung function changes. In addition, whole body exposures do not realistically reflect the typical mode of exposure in humans. There are various studies that have shown the induction of all the hallmark features of COPD but the long duration of these models of up to 6 months is labour intensive and costly[263]. Our laboratory have developed a short-term mouse model of nose-only CS-induced COPD that recapitulates key features of human COPD including chronic bronchitis, airway remodelling, emphysema and lung function impairment after 8 weeks of CS exposure which we have employed in our present investigations[264].

### **1.4.3. Influenza**

The investigations in the area of IAV infection have become more challenging because of the complexity of relationship between the host's defences and microbial virulence[206]. Animal models are important to identify and understand the role of the factors which are involved in the development and progression of disease features, transmission of the virus in humans along with the discovery of new therapeutic interventions[265]. These models also enable pre-clinical testing of antiviral drugs and vaccines. Various animal models such as mice, ferrets, guinea pigs, cotton rats, hamsters and macaques have been employed to understand the pathogenesis of IAV infection and its therapeutic targeting[266, 267].

Mice are commonly employed to understanding the immune responses to IAV. The advantages of using mice over other animals include, small size, low cost,

and the availability of transgenic strains to facilitate the in-depth understanding of the host response[268]. The degree of susceptibility to IAV infection in mice depends on the mouse strain[266]. Various clinical signs in mice usually develop after 2-3 days of infection, which vary from strain to strain, and depends upon the challenge dose. Symptoms include lethargy, loss of bodyweight, huddling, ruffled fur, and death[269]. Various studies have shown the importance and relevance of using mouse model to understand infection and its association with various respiratory diseases such as asthma[270-272] and COPD[273, 274]. The most commonly employed IAV strains in mice include intranasal delivery of H1N1 A/Puerto-Rico/8/1934 (A/PR/8/34)[275] or A/WSN/1933 (WSN)[7] viruses. Various mouse models can also be modified to understand the role of IAV infections and immune responses in various other diseases like asthma, COPD, secondary bacterial pneumonia and pulmonary fibrosis.

## **1.5. MICRORNAS (miRs): POTENTIAL THERAPEUTIC TARGETS IN CHRONIC LUNG DISEASES**

miRs are short non-coding RNAs which control gene expression post-transcriptionally by directly blocking translation of their target mRNAs or by repressing protein production via mRNA destabilisation[276]. In the human genome, transcripts of approximately 60% of all mRNAs are estimated to be targeted by miRs[277]. miRs are important in the post-transcriptional regulation of gene expression. They regulate various biological processes (cell differentiation and growth, metabolism, cell signalling, apoptosis) related to cancer and inflammation[278]. miRs have been identified as novel candidates for targeted therapeutic approaches and also employed as biomarkers for various diseases like cancer and chronic inflammatory diseases including asthma and COPD[279-283].

There are two strategies that are being pursued to target miRs so as to harness their therapeutic potential. These include (i) miR replacement therapy involving the miR-mimics to restore a loss of the function. miR mimics are synthetic RNA

duplexes designed to mimic the endogenous functions of miRs with chemical modifications for stability and cellular uptake[284]. This approach is quite commonly employed for lung cancer and (ii) the second strategy is directed towards a gain of function and aims to inhibit oncomiRs by using anti-miRs. Chemical modifications, such as 2'-O-methyl-group and locked nucleic acid (LNA), would increase oligo stability against nucleases. Antisense oligonucleotides contained in these modifications are termed antagomirs or “LNA-antimiRs”[285, 286].

### **1.5.1. Biogenesis of miRs**

miR biogenesis commences with the transcription of the miRs by RNA polymerase II to generate Pri-miRs. Stem loop structures are fragmented by the RNase III enzyme Drosha and double stranded RNA-binding domain (dsRBD) protein DGCR8/Pasha to generate hairpin precursor pre-miR. The excised pre-miR is transported to the cytoplasm by Exportin-5 via Ran-GTP-dependant mechanisms where its cleavage occurs by the Dicer protein, which generates miR duplexes containing mature miR strands and various accessory protein assemblies. This duplex is incorporated into the RNA-induced silencing complex (RISC) to engage the post-transcriptional repression of target mRNA translation[287-297] (Figure 1.10).

### **1.5.2. miRs in lung diseases**

Various signalling pathways are activated during the generation of inflammation in the lungs involve miRs and their roles in inducing innate and adaptive immunity that underpin their potential function in promoting inflammatory diseases such as asthma and COPD[298]. Various miRs have been identified to be associated with specific airway inflammatory diseases, some of which are tabulated in Table 1.3. This evidence implies miRs are a promising technology for current and future therapeutic development.

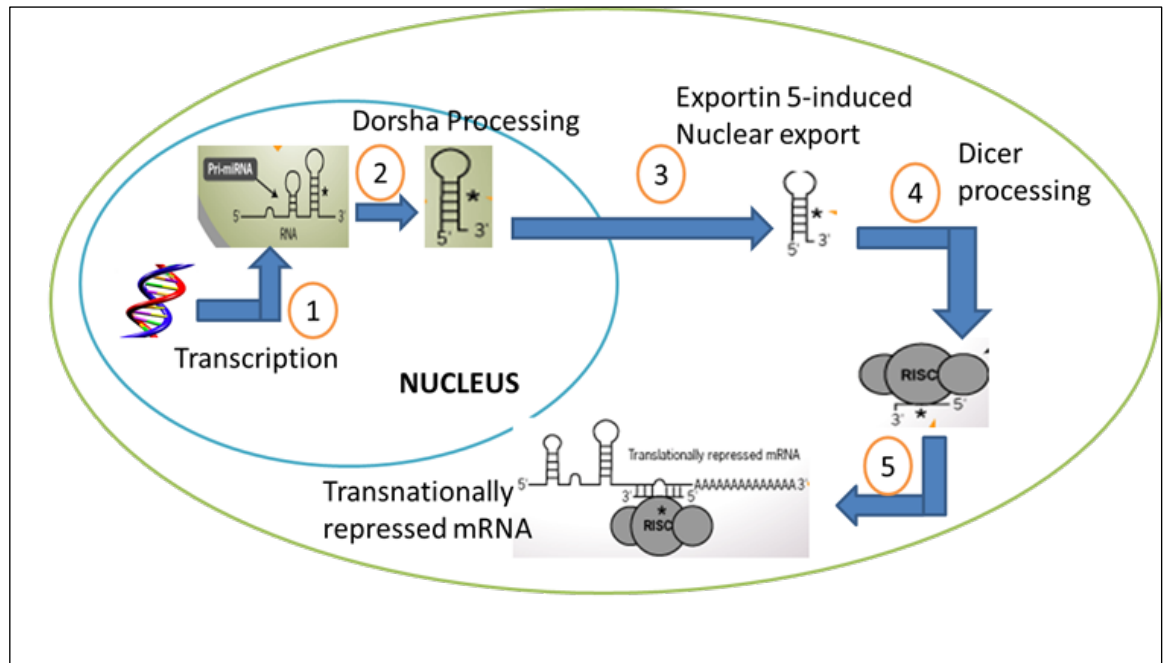


**Figure 1.10. miR Biogenesis.**

The miR biogenesis commences with the (1) transcription of the miRs by RNA polymerase II to generate (2) Pri-miRs. The stem loop structures which are fragmented by the RNase III enzyme Drosha and double stranded RNA-binding domain (dsRBD) protein DGCR8/Pasha to generate hairpin precursor pre-miR. (3) The excised pre miR is transported to the cytoplasm by Exportin -5 via Ran-GTP-dependant mechanisms where its (4) cleavage occurs by the Dicer protein which generates miR duplexes containing mature miR strands and various accessory protein assemblies. This duplex is incorporated into the RNA-induced silencing complex (RISC) (2) to engage the post-transcriptional repression of target mRNA translation; Adapted from reference[298].

**Table 1.3. miRs involved in inflammatory airway diseases**

miR	Cell type/tissue involved	Target	Reference
let-7	Lung	IL-13	[282, 299]
miR-21	Fibroblasts, Lung	IL-12p35, TGF- $\beta$ 1/Smad7, IL-12/IFN- $\gamma$	[300-302]
miR-25	Airway Smooth Muscle (ASM)	Krüppel-like factor 4 (KLF4)	[303]
miR-26a	ASM	glycogen synthase kinase-3 $\beta$	[304]
miR-106a	Lung	IL-10	[305]
miR-126	Epithelial cells & Lung	POU domain class 2 associating factor 1/ GATA3; TOM1 (target of Myb1) in TLR2/4 signalling pathways	[306-308]
miR-127	Macrophages	IgG Fc $\gamma$ receptor I	[309]
miR-133a	ASM	RhoA	[310]
miR-145	Lung	Th2 cytokines	[311]
miR-146a	ASM, Fibroblasts	Prostaglandin E2, NF- $\kappa$ B/MEK-1/2 /JNK-1/2	[312, 313]
miR-192	Human peripheral blood mononuclear cells (PBMC)	ChREBP , IFN $\alpha$ / $\beta$	[314]
miR-199a	Lung	Hypoxia-inducible factor-1 $\alpha$	[315]
miR-221	Lung	Sprouty-related protein with an EVH1 domain-2 (Spred-2)	[316, 317]
miR-485	Lung	Sprouty-related protein with an EVH1 domain-2 (Spred-2)	[316]

**1.5.2.1 miRs in asthma**

Various *in vitro* studies and mouse models have suggested the causative role of miRs in asthma. A recent study showed the role of miR-23b in controlling TGF- $\beta$ 1 induced airway smooth muscle cell proliferation by regulating Smad3 and thus suppressing airway remodelling[318]. Rodriguez *et. al.* reported that a total knockout of miR-155 causes spontaneous development of an asthma-like phenotype including inflammatory infiltration into the lung and airway remodelling[319].

Zhou and colleagues have briefly described the involvement, mechanisms and role of miR-155 in the allergic asthma[320]. Along similar lines, it has also been shown that miR-155 via IL-13 suppressed chemokine expression (CCL5, CCL11, CCL26, CXCL8, and CXCL10) in human epithelial cells[321]. Another important miR namely, miR-181b-5p was identified as a potential biomarker for airway eosinophilia in asthma where it was demonstrated to participate in eosinophilic airway inflammation by regulating proinflammatory cytokines expression by targeting secreted phosphoprotein-1 (SPP1)[322]. Moreover, miR-181b has also been demonstrated to increase inflammation by regulating the NF- $\kappa$ B signalling pathway[323].

An interesting study involving toluene diisocyanate (TDI), which is a major inducer of occupational asthma, demonstrated the involvement of miR-210 in controlling chemical induced allergic asthma by having inhibitory effects in Treg function particularly during the sensitisation phase of TDI. This particular study highlighted the immunological mechanisms that may contribute to chemical-induced allergic asthma.

Fan and his co-workers have investigated the role of miR-145 in asthma patients where it was believed to be involved in maintaining the balance between Th1 and Th2 responses by targeting RUNX3 and can also be used as a diagnostic biomarker and therapeutic target[324]. miR-196a2 polymorphisms also have been shown to be involved in regulating asthma in children and adolescents[325].

Tang *et al.*, identified mmu-miR-21a, mmu-miR-449c, and mmu-miR-496a in a mouse model of asthma using quantitative real-time PCR. They emphasised on the importance of miR-21/Acyr2a axis as one of the important immune mechanism involved in regulating inflammation associated with asthma[326]. Elbehidy *et al.*, further confirmed miR-21 as a potential and novel biomarker for the diagnosis of asthma in a paediatric population[327]. Likewise, miR-10a has been also identified as a potential therapeutic target in lung diseases where it

was demonstrated to regulate the proliferation of airway smooth muscle cells via the PI3K pathway[328].

The increased susceptibility of individuals with COPD to influenza likely results from impaired antiviral responses, which have been reported to be mediated by increased PI3K -p110 $\alpha$  activity. This pathway thus has a potential to be targeted therapeutically in COPD, or in healthy individuals during seasonal or pandemic outbreaks so as to prevent and/or treat influenza. The main factor that promoted the progression of asthma was identified to be over expression of IL-13 and several miRs such as miR-133a[329], miR-145[330], miR-126[331], miR-155[321] and miR-146[276] that have been reported to have important roles in regulating this mechanism. Also, the treatment of human bronchial smooth muscle cells with IL-13 caused a decrease in the expression of miR-133a. Artificial inhibition of miR-133a function in smooth muscle cells through the use of antagomirs was shown to increase the expression of RhoA, a known procontractile protein[329]. Ho *et al.*, have shown that diallyl sulphide has protective effects due to its induction of miR-144, -34a and -34b/c modulated Nrf2 activation in Ova-induced allergic asthma in BALB/c mice[332]. miR-19a also been identified as a potential new target to manage severe phenotypes of asthma where its downregulation has been reported to control epithelium repair during the disease[333].

miR-124 has been demonstrated to play an integral role along with IL-4/IL-13 in allergic inflammation by inducing an M2 phenotype in macrophages[334]. Inhibition of mmu-miR-106a has been shown to suppress airway inflammation, goblet cell metaplasia, subepithelial fibrosis and AHR in experimental asthma[335]. Apart from miRs, long non-coding RNAs (lncRNAs) such as lncRNAs BCYRN1[336], 846[337] or 4176[337] have also been described to play a role in airway allergic inflammation[337].

However, the role of miRs in corticosteroid-resistant asthma is not well illustrated. One study demonstrated that the expression of miR-146a is reduced in CD8<sup>+</sup> and CD4<sup>+</sup> T-cells from severe asthma patients who were

recommended continuous oral corticosteroid treatment[331]. Also with LPS-induced inflammation, a rapid change in the miR levels was observed in the mouse lungs but no influence or changes were observed in response to glucocorticoids treatment[338].

### **1.5.2.2 miRs in COPD**

Polymorphisms in multiple genes have been reported to be associated with COPD which includes various transcription factors such as nuclear factor-kappa B (NF $\kappa$ B)[339], extracellular matrix proteases (e.g., matrix metalloproteinase-12 (MMP-12)[340], TNF- $\alpha$ [341], IL-8, IL-8 receptor and chemokine receptor (CCR)1[342, 343], caspase-3 and vascular endothelial growth factor (VEGF)[344, 345]. Many of these have been identified as possible targets for therapeutic intervention using molecule inhibitors and/or antagonists.

In the lungs of rats exposed to the CS, expression of 24 miRs (especially let-7 family, miR-10, -26, -30, -34, -99, -122, -123, -124, -125, -140, -145, -146, -191, -192, -219, -222, and -223) were demonstrated to be down-regulated in comparison to air-exposed controls[346]. Likewise, in a different study, bronchial airway epithelial cells from smokers were found to have reduced levels of miRs especially miR-218, miR-15a, miR-199b, miR-125a/b, miR-294 compared to non-smokers. Similar results were also observed (down regulation of miR-218) with lung squamous cells carcinoma[347]. In another study, miR-294, an inhibitor of transcriptional repressor genes, was reported to be upregulated in smoke-exposed rats[348]. Moreover, miR profiling in lung tissue of patients with COPD revealed the role of miR-218 in the pathogenesis of COPD[349]. miR-146a-5p has also emerged as a regulator of inflammation in COPD via regulating various inflammatory pathways such as Toll-like receptor (TLR) or IL-1R signalling[350, 351]. The investigations completed so far, suggest that miRs contributes significantly to the pathogenesis of asthma and COPD.

### **1.5.2.3 miRs in other diseases**

Many pre-clinical and clinical trials have been performed and are underway to investigate the potential of targeting miRs to improve disease pathophysiology. These attempts have thus produced mechanistic data showing that miRs play a critical role in regulating disease-related pathways.

For tumors with reduced expression of miRs, restoration of their basal levels is the key strategy, which can be achieved through miR-mimetics or by regenerating “miRNAome” (full spectrum of expressed miRs in a cell at a specific time) functionality[285]. The most widely used approach is using miR-mimetics which have led to the progression of various miRs in the developmental phase (pre-clinical). Some of the therapeutic targets include let-7 for lung cancer, miR-34 for lung cancer and prostate cancer, miR-29 for cardiac fibrosis, miR-122 for hepatitis C virus[352-356]. miR-mimetics including Let-7[299] and miR-34[354] have been demonstrated efficacious in wide variety of solid tumours in mice. There are various miRs which are already being targeted therapeutically[357]. Some of them are miR-122 for Hepatitis C virus which is in Phase 2 clinical trials along with miR-208/499 and miR-34 for chronic heart failure and cancer, respectively that are in the pre-clinical development phase. To achieve the delivery of a stable molecule, miR's are delivered as perfectly complementary duplexes, similar in architecture to siRNAs[285]. Therapeutic efficacy of these miR-mimetics is being assessed based on their inhibitory effects on proliferation and apoptosis of tumour cells, as well as the specific repression of oncogenes.

In contrast, antagonist approaches that use antisense miRs termed antagomirs for miR-208, miR-499 and miR-195 have been shown to be beneficial in chronic heart disease where treatment ameliorated disease features such as cardiomyocyte hypertrophy, fibrosis and stress-induced expression of  $\beta$ -myosin heavy chain ( $\beta$ -MHC) and hypothyroidism in mouse models[358]. The various identified miRs with their therapeutic indication and clinical trial status is shown in Table 1.4[359]. Although targeting miRs is in clinical trials for several

diseases, the role of miRs in inflammatory airway disease still largely remains unknown and under investigation.

**Table 1.4. miRs, their therapeutic indications and clinical trial status**

<b>Identified miR</b>	<b>Therapeutic Indication</b>	<b>Status</b>
miR-208	Heart failure	Preclinical
miR-15/195	Post-myocardial infarction remodelling	Preclinical
miR-145	Vascular disease	Preclinical
miR-451	Myeloproliferative disease	Preclinical
miR-29	Pathological fibrosis	Preclinical
miR34, let 7	Cancer	Phase I
miR122	Liver transplant (HCV)	Phase III

### **1.5.3. miR-21 in Chronic Respiratory Diseases**

#### **1.5.3.1. miR-21 in asthma**

Various miRs such as Let-7, miR-25, miR-26a, miR-199a, miR-221, miR485, miR-146a have been identified and suggested to play roles in asthma pathogenesis where miR-21 (miR-21) is being investigated as an important regulatory factor in murine AAD[306, 360-362]. Reduced eosinophilic inflammation has been observed in mice deficient in miR-21 with Ova-induced AAD[301]. Furthermore, miR-21 has been also shown to promote steroid insensitivity in experimental severe, steroid-resistant asthma through the regulation of miR-21/PI3K/HDAC2 axis. The study demonstrated that the infection-induced miR-21 expression promoted PI3K-mediated phosphorylation and nuclear translocation of pAKT that suppressed HDAC2 levels subsequently leading to steroid insensitivity[363]. Li *et al.*, suggested that miR-21 could represent an important target in mediating protection of bronchial epithelial cells from hypoxic injury that triggers allergic airway inflammation[364].

Similarly, Lee and colleagues demonstrated that miR-21 suppression attenuated the development of allergic airway inflammation in a mouse model of acute bronchial asthma[365]. Moreover, miR-21 has been identified to be

significantly upregulated in smooth muscle cells of asthma compared to non-asthma patients. miR-21 overexpression has also been demonstrated to be associated with decreased levels of phosphatase and tensin homolog (PTEN) and activation of phosphoinositide 3-kinase (PI3K)/AKT pathway[366]. miR-21 has also been suggested to be associated with recurrent childhood wheezing and asthma risk[367]. Moreover, the levels of miR-21 were observed to be significantly increased in the serum of children and adults with asthma including patients with steroid resistance. This highlights its importance as a promising potential biomarker for the diagnosis of asthma and assessment of treatment responsiveness in paediatric asthma[327]. miR-21 has also been defined as a major regulator of Th1 versus Th2 responses that is mediated by the IL-12/IFN-gamma pathway[368]. Also, it has been presented as a potential regulator of L-12p35 expression in allergic airway inflammation[360].

#### **1.5.3.2. miR-21 in COPD**

A recent study in COPD patients demonstrated that the upregulation of miR-21 in serum and peripheral blood mononuclear cells was a contributor to the pathogenesis of this disease[369]. A similar study also showed that the ratio of miR-21 to miR-181a levels can be useful in evaluating the development of COPD in heavy smokers[370]. Specifically with PI3K, increased PI3K-p110 $\alpha$  activity has been demonstrated to increase susceptibility of individuals with COPD to influenza infections[371]. Efficacy of PI3K/Akt inhibitors are being investigated as potential therapeutic interventions in the management of COPD probably by regulating the PI3K/Akt pathway and miR-21 expression involved in regulating the growth, differentiation and survival of cells[372].

#### **1.5.4. miR-125 a and b in chronic respiratory diseases**

##### **1.5.4.1. miR-125 a and b in asthma**

miR-125b has been reported to inhibit SAM pointed domain-containing ETS transcription factor (SPDEF) at post-transcriptional levels thereby modulating goblet cell differentiation and mucus secretion in asthma[373]. Li and his colleagues revealed that miR-125a and IL-6R are perturbed in asthma patients, which provides the basis for development of new therapeutic strategies against

asthma. Furthermore, they identified a novel signal regulatory pathway, GATA3/miR-125a/IL-6R and STAT3/FOXP3 which determines the response of Treg cells to inflammatory IL-6-rich conditions[374].

A clinical study carried out in infants with acute RSV disease revealed that miR-125a has important functions within NF- $\kappa$ B signaling and macrophage function. The lack of downregulation of miR-125a in severe disease may help explain differences in disease manifestations on infection with RSV[375]. Ronaldo *et.al.*, identified that miR-125b levels were most predictive in allergic and asthmatic status revealing its potential for use as a non-invasive biomarkers to diagnose and characterize these diseases[376]. A recent study reported that the levels of miR-21 and miR-125b were inversely related to measures of lung function in asthmatic subjects and were repressed by dexamethasone treatment[377]. miR-125b also prove in enhancing type I IFN expression through suppressing 4E-BP1 protein expression in airway epithelial cells, which potentially contributes to mucosal eosinophilia in eosinophilic chronic rhinosinusitis without nasal polyps[378].

#### **1.5.4.2. miR-125 a and b in COPD**

Wang *et al.*, demonstrated the central role of miR-125a-5p in the development of COPD along with various other miRs such as miR-106b-5p, miR-183-5p, and miR-100-5p[379]. To the best of our knowledge, this is the only published study highlighting the involvement of miR-125a-5p in COPD. The involvement of miR-125a-5p has also been identified in GATA3/IL-6R and STAT3/FOXP3 regulatory pathways which control IL-6 and STAT 3 expression *via* Treg cells in asthma[380]. Overall, little is known regarding the role of miRs in COPD. This area is gaining massive attention and rapidly expanding to understand their roles in driving disease pathology in chronic inflammatory lung diseases.

#### **1.5.4.3. miR-125 a and b in lung cancer**

miR-125 family has been identified as either repressors or promoters in a variety of carcinomas and other diseases. This family has been revealed to be composed of three homologs hsa-miR-125a, hsa-miR-125b-1 and hsa-miR-

125-2[381]. All the members of this family have been reported to be involved in various cellular processes like cell-differentiation, proliferation and apoptosis[382]. All these processes normally occur by targeting transcription factors[382], matrix-metalloprotease[383] and growth factors[384]. miR-125b was found in the serum of non-small cell lung cancer patients where it was considered a promising biomarker for supplementing future screening studies[385, 386]. miR-125a and miR-125b are also identified to be involved with the regulation of tumor necrosis factor-alpha-induced protein 3 (TNFAIP3) expression and consequently NF- $\kappa$ B activity. This pathway has been reported to be involved in diffuse large B-cell lymphoma (DLBCL)[387]. Additionally, miR-125b expression has been shown to be involved in NF- $\kappa$ B signalling and its overexpression is related to an overall shorter survival of patients treated with Temozolomide for the treatment of neoplasia[388].

## 1.6. HYPOTHESES AND AIMS

IAV is a severe and potentially life-threatening respiratory viral infection that has caused three global pandemics in the 20<sup>th</sup> century[389]. IAV infection causes enormous morbidity and mortality with high socio-economic consequences worldwide. People with chronic lung diseases, such as asthma[141] and COPD[143] are more susceptible to viral and IAV infections that subsequently results in exacerbations of these diseases, leading to more severe symptoms with increased risk of death[144, 390]. However, the immune mechanisms driving susceptibility of these patients to IAV infection and consequent exacerbations are largely unknown. Current management options including vaccinations suffer from limitations including treatment unresponsiveness and resistance as well as inability of vaccines to target all virus strains, which have the tendency to alter their genetic makeup and undergo mutations. In addition, current anti-IAV treatments are only efficacious if given within the first 48 h of infection. This is normally before symptoms appear and are severe enough to present to a clinic or hospital.

Thus, there is an urgent need to develop effective novel therapies for the management of IAV infections, particularly in patients with underlying

respiratory diseases such as asthma and COPD. The primary objective of this project was to determine the mechanisms responsible for increased susceptibility to IAV infection in asthma and COPD, and understand how infection causes exacerbations. These studies would potentially aid the identification of novel therapeutic approaches.

### **1.6.1. Hypothesis**

Chronic lung diseases, particularly asthma and COPD, predispose to more severe IAV infection that subsequently exacerbates the underlying disease.

#### **1.6.1.1. Asthma**

To investigate the mechanisms *in vivo*, we established murine models of AAD induced by either Ova or HDM[215, 391-393] and cigarette smoked-induced experimental COPD[264, 274, 371] with subsequent IAV infection that mimicked the pathological features of the human diseases.

Preliminary data from our laboratory using both Ova-induced and recombinant IL-13 (rIL-13) induced-AAD mice models challenged with IAV infection demonstrated that infection worsened the underlying disease by augmenting viral load, lung eosinophils, MSC hyperplasia and AHR with concomitant reduction in anti-viral cytokines. Our laboratory also investigated the therapeutic potential of anti-IL-13 antibody in Ova-induced AAD mice infected with IAV. Moreover, our laboratory also demonstrated increase in the levels of miR-21 in the lungs of infection-induced severe steroid-insensitive AAD mice, which reduced expression of PTEN (a miR-21 target). PTEN is an inhibitor of PI3K and so miR-21 inhibition of PTEN subsequently potentiated PI3K activity. This emphasised the role of miR-21 and PI3K as potential therapeutic targets in the management of IAV infections in asthma.

Based on these preliminary data and studies performed in our laboratory, we hypothesised that these effects were driven by IL-13 responses along with the involvement of miR-21. This subsequently would increase viral entry, airway

inflammation, mucus hypersecretion, and remodelling and reduce the levels of protective anti-viral interferons leading to more severe infection.

We also proposed that inhibiting miR-21 would result in the improvement of infection outcomes including reduced viral titre, inflammation and mucus hypersecretion.

#### **1.6.1.2. COPD**

Our laboratory has previously demonstrated that the increased susceptibility to IAV infection in COPD involved increased virus entry and deficient antiviral responses that allowed increased virus replication thereby amplifying inflammation and impairing lung function. These effects were identified to be mediated by increased PI3K-p110 $\alpha$  activity involving miR-21[371]. Moreover, our laboratory has demonstrated increases in miR-21 expression using miRNA microarray analysis across the 8-weeks of a smoke exposure time course (weeks 2, 4, 6 and 8) in our well-established smoking mouse model. This was further validated by qPCR, thus identifying miR-21 as a potential target involved in COPD pathogenesis.

Our laboratory has also demonstrated increased expression of miR-125a and miR-125b in pBECs isolated from COPD patients. We have also shown that A20, (also known as TNF- $\alpha$ -inducing protein 3, TNFAIP3), a negative regulator of NF- $\kappa$ B-mediated inflammation, functions by targeting Receptor Interacting Protein 1 (RIP1) for degradation, and therefore suppresses NF- $\kappa$ B activation. miR-125a and b have been shown to directly inhibit A20, leading to increased NF- $\kappa$ B activation. It is currently unknown if A20 or miR-125a/b regulates type I and III IFNs during IAV infections.

Thus, we hypothesised that miR-21, miR-125a and 125b regulated the inflammatory responses and the pathogenesis of disease using various cells signalling pathways, which we investigated in our CS-induced mouse model of experimental COPD.

### 1.6.2. Aims

The objectives of this study were to:

1. assess the role of immune system activation against IAV infection in asthma and COPD with subsequent identification of the underlying immune mechanisms involved.
2. elucidate the role of key factors (such as cytokines and miRs) involved in immune mechanisms which can be targeted as potential therapies for the management of IAV infections in patients with asthma, COPD and IAV-induced asthma and COPD exacerbations.

The studies that were performed to accomplish these aims were:

- a) establishing and characterising a clinically relevant HDM-induced AAD murine model to investigate the IAV-induced exacerbations in asthma.
- b) elucidating the involvement of IL-13/IL-13R $\alpha$ 1 and miR-21 in AAD mice following IAV infection.
- c) investigating the potential of anti-IL-13 antibody, PI3K inhibitor (LY294002) and specific antagomirs against miR-21 as novel therapeutic interventions using Ova-induced experimental AAD.
- d) elucidating the involvement of IL-13/IL-13R $\alpha$ 1, miR-21 and miR-125 a and b in CS-induced experimental COPD following IAV infection.
- e) investigating the potential of anti-IL-13 antibody and specific antagomirs against miR-21, miR-125a and miR-125b as novel therapeutic interventions using CS-induced experimental COPD.

# **CHAPTER 2**

## **IAV INFECTION EXACERBATES HOUSE DUST MITE (HDM)- INDUCED ALLERGIC AIRWAYS DISEASE (AAD)**

## 2.1. ABSTRACT

IAV infections trigger severe exacerbations of asthma, which worsen the disease symptoms and impair lung function. The immune mechanisms that underpin these associations are incompletely understood. This study aimed to establish and utilise a murine model HDM-induced AAD to investigate IAV infection-induced exacerbations. Mice with experimental HDM-induced asthma and infected with IAV had more severe infection with increased viral titre and pulmonary tissue inflammation and elevated AHR, compared to non-allergic controls. These processes were associated with increased Th2 cytokines, impaired anti-viral immunity (reduced retinoic acid-inducible gene [RIG-I] and IFN responses) along with remodelling features. Since this murine HDM model of viral-induced asthma exacerbations replicates various human aspects of HDM-induced asthma exacerbations, it has translational potential. It can be used to understand the mechanisms involved in asthma exacerbations and corticosteroid insensitivity that have clear utility in identifying newer therapeutic interventions.

## 2.2. INTRODUCTION

Asthma is a complex, chronic inflammatory lung disease characterised by airflow obstruction, AHR, shortness of breath, coughing, chest tightness and wheezing[394]. Asthma exacerbations are typically caused by infection and result in significant worsening of underlying symptoms[395]. These events are common in patients with asthma regardless of disease severity but are most frequent in patients with severe disease[396]. Exacerbations negatively impact the quality of life[397] and are a major cause of hospitalisations leading to significant healthcare costs[398]. Conventional approaches to controlling mild to moderate asthma include inhalational corticosteroids (ICS), long-acting  $\beta_2$  agonist (LABA) and oral corticosteroids (OCS)[399, 400] however, these therapies are not effective in managing asthma exacerbations, leading to the urgent need for novel therapeutic interventions.

Globally, IAV infections are a major health problem because of the rapidity with which it can spread, the brevity of immunity it confers and its genetic variability[206]. IAV infections are a common cause of asthma exacerbations that further worsen the symptoms and increases mortality. IAVs mutate rapidly which causes variation in their virulence from year to year. Limited immunity of the population against these new strains and subtypes further augments the complications and disease severity.

Seasonal influenza causes 250,000-500,000 deaths annually and influenza pandemics are a major and frequent additional problem[131]. There has been an emergence of novel or re-emergence of ancient IAVs in the last decade, including pandemics caused by highly pathogenic avian influenza H5N1 in 2003, the swine-origin influenza H1N1 (H1N1/09) in 2009 and H7N9 in 2013. These viruses induce higher mortality rates than the seasonal IAVs, with a mortality rate to up to 70% in human infections of H5N1. In Australia, H1N1/09 resulted in approximately 18,000 deaths, representing a 7-fold increase in mortality rates[139]. In the United States, the economic loss caused by IAVs, without effective medical intervention, was estimated to \$187USD (approx. \$202AUD) per capita per year[140, 401]. Current prevention and treatments have serious limitations. Vaccinations and antiviral drugs have reduced efficacy in chronic respiratory diseases like asthma and COPD[402-404]. The impact of these factors contributes to placing influenza as a high priority concern in global healthcare and medical research.

Numerous studies have been performed to investigate the mechanisms of increased susceptibility and disease features induced by respiratory infections in allergic airway diseases (AAD) and that have aimed to develop potential therapeutic interventions[405-409]. Typically, the models used to understand the pathological processes and their influence on airway immune responses use systemic sensitisation to Ova-albumin (protein from chicken egg) with a Th2-inducing adjuvant (aluminium hydroxide, Al(OH)<sub>3</sub>). This does not simulate the levels of sensitisation as observed with aeroallergens such as pollen, moulds and HDM. The Ova model also needs prior i.p. sensitization, in contrast

to the HDM model. Another limitation associated with the use of Ova is that human subjects not frequently allergic to chicken egg protein unless it is a food allergy[410]. HDM (*Dermatophagoides pteronyssius* and *D. farinae*) are frequent human aeroallergens, and are associated with the induction of asthma, rhinitis, dermatitis and other allergic diseases. HDM has been shown to induce allergic reactions via allergen-specific CD4+ Th2 lymphocytes[410-413].

The kinetics of various hallmark features including viral titre, airway inflammation and AHR was performed at 3, 7 and 10 dpi in experimental AAD model (OVA) established in our laboratory. The pathological features were first detected in the lungs at 3 dpi, peaked at 7dpi and resolved by 10 dpi. Thus, we focused our studies at 3 dpi when viral titre, airway inflammation and AHR were first detectable in the model. This formed the basis of selection of 3 dpi as a time point in HDM model. The HDM model is expected to mimic the OVA model and thus we assume it to wane over time. Since, we did not perform the kinetics of pathological features in HDM-model it is difficult to comment on efficient/comparable IAV clearance. However, it is likely to be similar to the Ova model.

Thus, this study aimed to establish and characterise a murine model of HDM-induced AAD and to investigate IAV-induced exacerbations. We used this model to investigate the complex relationship between viral infection and host's immune responses in AAD.

## **2.3. METHODS**

### **2.3.1. Ethics statement**

This study was performed in strict accordance with the recommendations in the Australian code of practice for the care and use of animals for scientific purposes issued by the National Health and Medical Research Council of Australia. All protocols were approved by the Animal Ethics Committees of The University of Newcastle.

### **2.3.2. Mice**

Six to eight-week old specific pathogen-free (SPF) female BALB/c mice were used in all the experiments. Animals were obtained from The University of Newcastle Animal Services Unit, the Animal Resources Centre (Perth, Australia) or Australian Bio Resources (Moss Vale, Australia) and were given access to food and water *ad libitum*. Animals were housed in individually ventilated cages in a specific pathogen-free facility with controlled environment of 12 h light and dark cycles.

### **2.3.3. Induction of AAD**

Mice were sensitised intranasally (i.n.) with 50 µg HDM extract (*Dermatophagoides pteronyssinus*, Greer Labs, Lenoir, North Carolina, USA) in 200 µl sterile phosphate buffered saline (PBS). Mice were then challenged with HDM (5 µg in 50 µl sterile PBS) under isoflurane anaesthesia 12-15 days later by i.n. administration. Control mice were sham sensitised with PBS (Figure 2.1).

### **2.3.4. IAV infection**

On the last day of HDM challenge, groups of mice were anaesthetised with isoflurane and infected i.n. with 7.5 plaque forming units (PFUs) of mouse-adapted H1N1 IAV A/PR/8/34 (WHO Collaborating Centre for Reference and Research of Influenza, Victoria, Australia) in 50µl of media vehicle (Ultra MDCK, Lonza, NJ, USA). Controls were sham-inoculated with media. Mice were sacrificed at 3 days post infection (dpi, Figure 2.1).

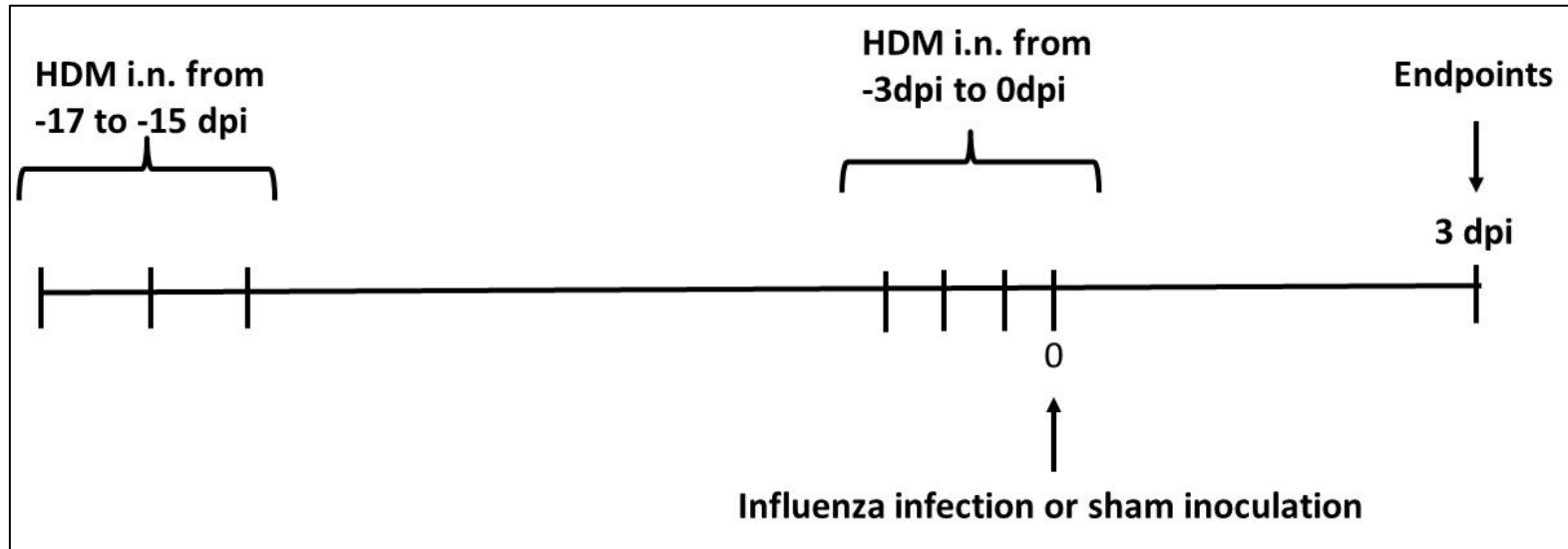


**Figure 2.1. Experimental protocol of HDM-induced AAD and IAV infection.**

BALB/c mice were sensitised with HDM or PBS (Sham), challenged with HDM, and inoculated with IAV A/PR/8/34 (7.5 pfu) or media (Sham) on the last day of HDM challenge. Mice were sacrificed 3 dpi.

### **2.3.5. Plaque assay**

Madin-Darby Canine Kidney (MDCK) cells were grown until approximately 70% confluence was achieved. The cells were then washed with Dulbecco's Phosphate Buffered Saline (DPBS; Sigma Aldrich) three times. The cells were submerged in Leibovitz's L-15 (L-15) medium (Invitrogen) supplemented with 2-[4-(2-hydroxyethyl) piperazin-1-yl] ethanesulphonic acid (HEPES; Invitrogen) and N-p-tosyl-L-phenylalanine chloromethyl ketone treated trypsin (trypsin-TPCK; Invitrogen). Bronchoalveolar lavage fluid (BALF) samples were serially diluted in L-15 medium, which had been supplemented with HEPES and were added to the cells. After 60 minutes of incubation (37°C, 5% CO<sub>2</sub>), the inocula were removed. A thin overlay of 1.8% agarose in L-15 medium containing trypsin-TPCK (Invitrogen) was placed on to the cell monolayers. After 48 h of incubation, plaques were stained with 0.1% crystal violet and counted[190, 371, 414, 415].

### **2.3.6. Histopathology**

Lungs were formalin fixed, embedded and sectioned. Longitudinal sections were stained with H&E (for histopathology), periodic acid-Schiff (PAS-for MSC numbers) or Lendrum's Carbolchromotrope (for eosinophils). Histopathology (tissue-inflammation) was scored in a blinded fashion according to a set of custom-designed criteria (Table 2.1). Eosinophils and MSC numbers were enumerated in inflamed airways as previously described[416].

### **2.3.7. Protein isolation**

Proteins were extracted from whole lungs. Briefly, tissues were homogenised in 500 µl of sterile Dulbecco's phosphate-buffered saline (Life Technologies, Mulgrave, Victoria, Australia) supplemented with PhoSTOP phosphatase and Complete ULTRA protease inhibitors cocktails (Roche Diagnostics, Mannheim, Germany) using a Tissue Tearor stick homogeniser (BioSpec Products, Bartlesville, Oklahoma, USA) on ice. Homogenates were then centrifuged (8000xg, 10 minutes, 4°C)[274]. Supernatants were collected and stored at -20°C for assessment by enzyme-linked immunosorbent assay (ELISA) or multi-analyte flow assay kits.

**Table 2.1. Histopathological scoring system for mouse lungs.**

<b>Score 1: Airway inflammation Score (/4)</b>
0 = Lack of inflammatory cells around airways - Absent 1 = Some airways have small numbers of cells - Mild 2 = Some airways have significant inflammation - Moderate 3 = Majority of airways have some inflammation - Marked 4 = Majority of airways are significantly inflamed – Severe
<b>Score 2: Vascular inflammation Score (/4)</b>
0 = Lack of inflammatory cells around vessels - Absent 1 = Some vessels have small numbers of cells - Mild 2 = Some vessels have significant inflammation - Moderate 3 = Majority of vessels have some inflammation - Marked 4 = Majority of vessels are significantly inflamed – Severe
<b>Score 3: Parenchymal inflammation (at 10X magnification) Score (/5)</b>
0 = <1% affected 1 = 1-9% affected 2 = 10-29% affected 3 = 30-49% affected 4 = 50-69% affected 5 = >70% affected
<b>Total score = Score 1 + Score 2 + Score 3 = /13</b>

### **2.3.8. Cytokine concentrations in lungs**

Protein concentrations in BALF supernatants were determined for various cytokines (IL-5, IL-13, IL-25, IL-33, TSLP and IFN- $\beta$  and IFN- $\lambda$  using mouse DuoSet ELISA kits (R&D systems, Minneapolis, USA) according to the manufacturer's instructions. Th2-type cytokine IL-4 was not measured as it is produced at low levels in mice, it can be considered for future investigations.

### **2.3.9. Total RNA extraction**

Total RNA was extracted from whole lungs by guanidinium thiocyanate phenol chloroform (TRIzol) extraction[417]. Lung tissues harvested from mice were

stored in RNA Stabilisation Reagent, RNAlater (Qiagen, Chadstone Centre, Australia) prior to extraction. Tissues were transferred into 5 ml tubes containing 1 ml of TRIzol solution (Ambion, Thermo Fisher Scientific), carefully ensuring minimal RNAlater carry over. Tissues were then homogenised at 4°C, transferred to 1.5 ml microcentrifuge tubes and centrifuged (12,000xg, 10 minutes, 4°C). The clear homogenates were then transferred into fresh microcentrifuge tubes and supplemented with 250 µl chloroform to separate RNAs from proteins. The microcentrifuge tubes were then pulse-vortexed for approximately 5 seconds, until the solutions were homogenous. Solutions were incubated at room temperature for 10 minutes before being centrifuged (12,000xg, 15 minutes, 4°C). The resulting aqueous phase was then transferred into fresh 1.5 ml microcentrifuge tubes and supplemented with 500 µl of cold isopropyl alcohol to precipitate the RNA. The solutions were again pulse-vortexed, incubated (room temperature, 10 minutes), and centrifuged at (12 000xg, 10 minutes, 4°C). Supernatants were discarded and the RNA pellets were washed with 1 ml of 75% (v/v) ethanol. The solutions were then pulse-vortexed to dislodge the pellets and to wash out trapped contaminants and centrifuged (7,500xg, 5 minutes, 4°C). A second wash was performed to remove any carbohydrate/phenol-based contaminants. Pellets were then allowed to air dry (15 minutes, 4°C). Pellets were eventually resuspended with 75-100 µl nuclease free water (Ambion, Thermo Fisher Scientific). The concentration of mRNA was measured using a NanoDrop Spectrophotometer (ND-1000, v3.8.0 Bio Lab, NanoDrop Technologies, DE, USA).

### **2.3.10. Reverse transcription**

1000 ng of RNA in 8 µl of nuclease free water (Ambion) was prepared to generate complementary DNA (cDNA). mRNA samples were mixed with 1 µl of 10X reaction buffer (Bioline, Alexandria, Australia) and 1 µl of amplification grade DNase I (Sigma Aldrich) and were incubated (room temperature, 15 minutes). 1 µl of DNase Stop Solution (Sigma Aldrich) was added into the mixture, and the samples were heated at 65°C for 10 minutes to inactivate and denature the DNase I. The samples were then added with 2 µl of 50 ng/ml random hexamer primers (Invitrogen) and 1 µl of 2.5mM dNTPs (Invitrogen),

and incubated (5 minutes, 65°C). The samples were allowed to cool to 25°C, and 4 µl of 5X reaction buffer, 1 µl of DTT (Bioline), 1 µl of nuclease free water, and 1 µl of Bioscript (Bioline) were added. The samples were then heated at 25°C for 20 minutes, 42°C for 50 minutes and 70°C for 15 minutes. The samples were finally resuspended with 500 µl of nuclease free water.

### **2.3.11. Quantitative real-time Polymerase Chain Reaction (qPCR)**

qPCR was performed to determine the relative abundance of cDNA in samples compared to the reference gene HPRT. qPCR cycles were performed using a Mastercycler Eppendorf RealPlex 2 System (Eppendorf South Pacific, North Ryde, Australia) or ViiA 7 Real-Time PCR System (Life Technologies, Thermo Fisher Scientific). Sample cDNA (2 µl) was added to a mixture containing 3 µl SYBR Green and ROX as a passive reference dye (SYBR Green ERTM reagent system, Invitrogen), 0.5 µl (10 µM) of each forward and reverse primers (Integrated DNA Technologies, Baulkham Hills, Australia, Table 2.2) and 4 µl of nuclease free water (Ambion), to make a total of 10 µl reaction volume.

Cycling conditions used for Mastercycler Eppendorf RealPlex 2 System were: holding stages at 50 °C for 2 minutes and 95 °C for 2 minutes; cycling stages at 95 °C for 15 seconds and 60 °C (variable) for 30 seconds (cycling stages were repeated for 40 cycles); melt curve/dissociation stages at 95 °C for 15 seconds, 60 °C (variable) for 15 seconds, 95 °C for 8 minutes and 95 °C for 15 seconds. Cycling conditions used for ViiA 7 Real-Time PCR System were: holding stage at 95 °C for 30 seconds; cycling stages at 95 °C for 15 seconds and 60 °C (variable) for 30 seconds (cycling stages were repeated for 40 cycles); melt curve/dissociation stages at 95 °C for 15 seconds, 60 °C (variable) for 15 seconds and 95 °C for 15 seconds. The threshold value (Ct value) for each sample was measured as the number of cycles needed for the specific fluorescent signals to cross “threshold”, which is a value that is set above the background levels of fluorescence (background “noise”). The Ct value from each gene was normalised against the constant housekeeping gene, the HPRT gene.

**Table 2.2. Custom designed primers used in qPCR analysis**

Primer	Forward (5'→3')	Reverse (5'→3')
HPRT	AGG CCA GAC TTT GTT GGA TTT GAA	CAA CTT GCG CTC ATC TTA GGC TTT
RIG-I (Ddx58)	ACA AAC CAC AAC CTG TTC CTG ACA	TGG CGC AGA ATA TCT TTG CTT TCT
IL-13R $\alpha$ 1	CAC AGT CAG AGT AAG AGT CAA AAC A	ATG GTG GTG TAG AAG GTG GA
Fibronectin	TGTGGTTGCCTTGCACGAT	GCTATCCACTGGGCAGTAAA GC
Col1a1	CTTCACCTACAGCACCCCTT GTG	TGACTGTCTTGCCCCAAGTT C

**2.3.13. Airway remodelling**

Lungs were formalin fixed, embedded and sectioned. Longitudinal sections were stained with H&E, Verhoff's-Van Gieson (VVG) stain (Australian Biostain) or Masson's Trichrome. Airway epithelial area ( $\mu\text{m}^2$ ) and area of collagen deposition ( $\mu\text{m}^2$ ) was assessed in a minimum of four small airways (basement membrane (BM) perimeter <1000  $\mu\text{m}$ ) per section[264, 274, 418]. Data were normalised to BM perimeter ( $\mu\text{m}$ ) and quantified using ImageJ software (Version 1.49h, NIH, New York City, USA).

**2.3.14. Soluble collagen**

Soluble collagen in mouse lungs was determined using a Sircol Collagen Assay kit (Biocolor) according to the manufacturer's instructions. Briefly, lungs were weighed and homogenised in pepsin (Sigma-Aldrich, 0.1 mg/ml in 0.5 M acetic acid) for 24 h at 4°C. Supernatants were collected after centrifugation (150xg, 10 minutes). Sircol dye reagent was added with shaking for (room temperature, 30 minutes) and was again centrifuged. Pellets were suspended in alkali reagent from the kit. Optical density was measured at 550 nm, and the concentrations of soluble collagen were compared with standard solutions and a standard curve provided by the manufacturers[419].

### **2.3.14. Lung function**

AHR was measured in anaesthetised mice using whole body invasive plethysmography (Buxco electronics, Sharon, Connecticut, USA) by determination of the peak of transpulmonary resistance in response to increasing doses of nebulised methacholine (Sigma-Aldrich) as previously described [210, 211].

### **2.3.15. Statistical analyses**

Data were expressed as mean  $\pm$  standard error of the mean (SEM) from 6-8 mice in each group and are representative of at least two or more independent experiments. Non-normally distributed data were analysed using non-parametric equivalents and summarised using the median and inter-quartile range. Comparisons between two groups were made using a two-tailed Mann-Whitney Test. Multiple comparisons were made using one-way ANOVA with Tukey's post-test, or Kruskal-Wallis with Dunn's post-test, where non-parametric analyses were appropriate. Analyses were performed using GraphPad Prism Software version 6 (GraphPad Software, CA, USA). A p-value of  $< 0.05$  was considered significant.

## **2.4. RESULTS**

### **2.4.1. HDM-induced AAD predisposes to severe IAV infection**

To investigate whether AAD predisposes to IAV infection, specific pathogen-free BALB/c mice were sensitised i.n. to HDM, and subsequently challenged i.n. with HDM 12-15 days after sensitisation. On the last day of HDM challenge, mice were infected i.n. with 7.5 pfu of mouse-adapted IAV H1N1 A/PR/8/34 strain (HDM+PR8). Controls were sham-inoculated (with media) and HDM-sensitised (HDM), or were infected and PBS-sensitised (PR8), or sham-inoculated and PBS-sensitised (Control). Mice were sacrificed 3 dpi (Figure 2.1) and viral titres assessed by plaque assay. A significant increase in viral titre was observed in infected mice with AAD (HDM+PR8) at 3 dpi compared to infected non-allergic controls (PR8) (Figure 2.2). This indicates that AAD following IAV infection leads to increased viral titre in the lung.

#### **2.4.2. IAV infection leads to severe tissue inflammation, increase in mucus secreting cells (MSCs) and lung eosinophils in AAD**

At 3dpi, non-infected allergic mice (HDM) had significantly increased histopathological score indicative of increased lung tissue inflammation compared to sham-inoculated non-allergic controls (Sham, Figure 2.3). Infected non-allergic mice (PR8) also had significantly increased histopathological scores compared to sham-inoculated non-allergic controls. Infected mice with AAD (HDM+PR8) had significantly increased histopathological scores compared with sham-inoculated non-infected non-allergic control, sham-inoculated allergic (HDM) and infected non-allergic (PR8) controls Figure 2.3.

At 3dpi, non-infected allergic mice had increased numbers of MSCs around the airways compared to non-infected non-allergic controls. The infected mice with AAD had even significantly greater number of MSCs compared with sham-inoculated non-infected non-allergic control, sham-inoculated allergic and infected non-allergic controls (Figure 2.4).

At 3dpi, sham-inoculated allergic mice also had higher numbers of lung eosinophils compared with sham-inoculated non-allergic controls. Infected mice with AAD had even significantly higher numbers of lung eosinophils compared to sham-inoculated non-infected non-allergic control, sham-inoculated allergic and infected non-allergic controls (Figure 2.5).

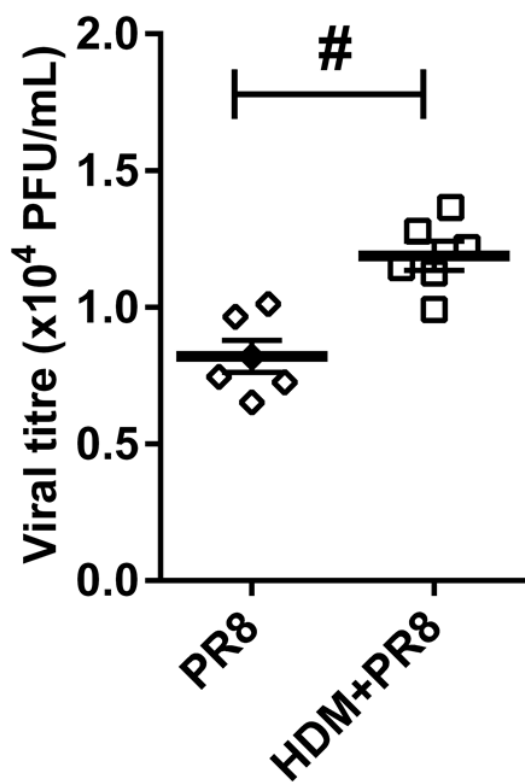


**Figure 2.2. Viral titre at 3 dpi.**

BALB/c mice were sensitised with HDM or PBS (Sham), challenged with HDM, and inoculated with IAV A/PR/8/34 (7.5 pfu) or media (Sham) on the last day of HDM challenge. Mice were sacrificed 3 dpi. Data are presented as mean  $\pm$  SEM (n=6); # represents  $P \leq 0.05$  versus PR8 control groups.

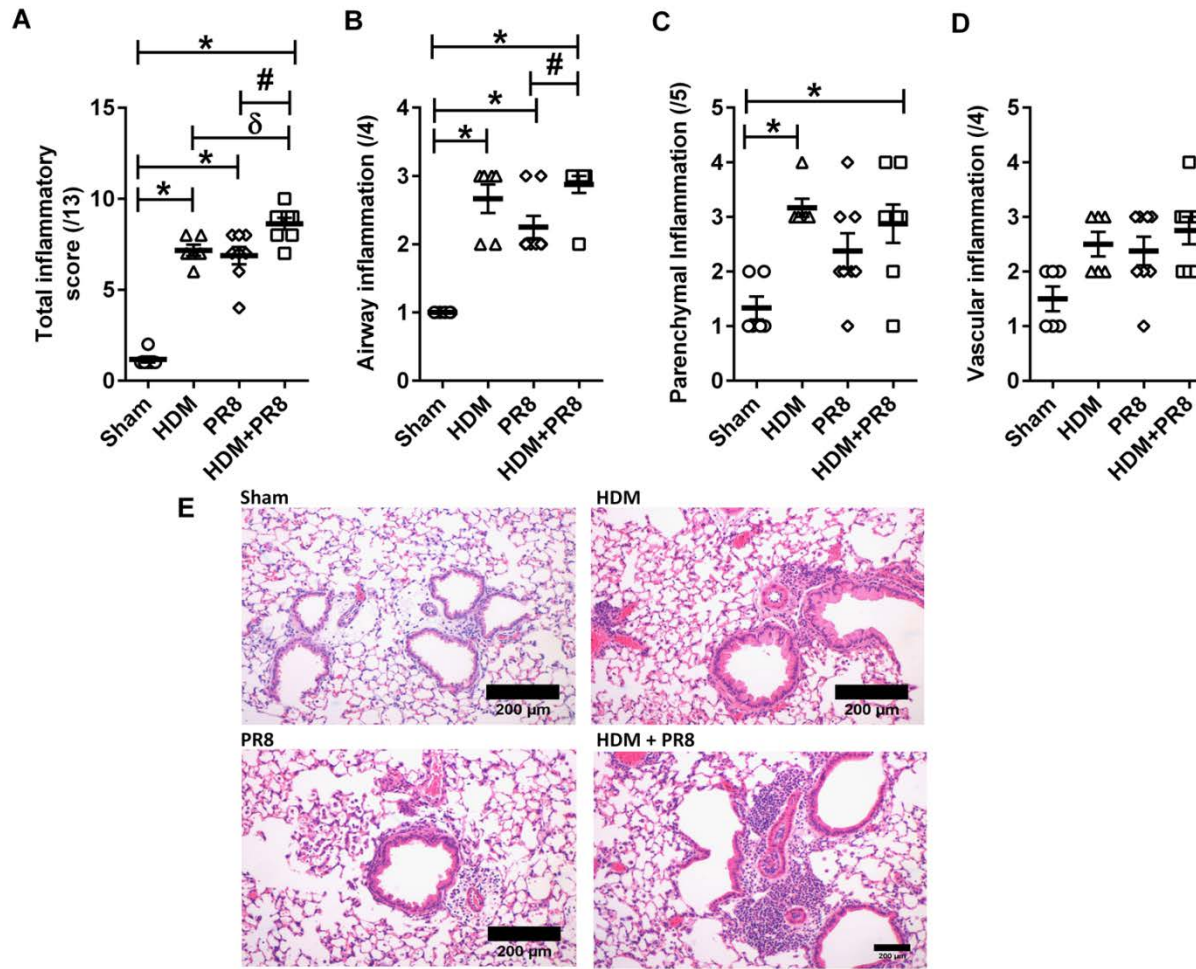
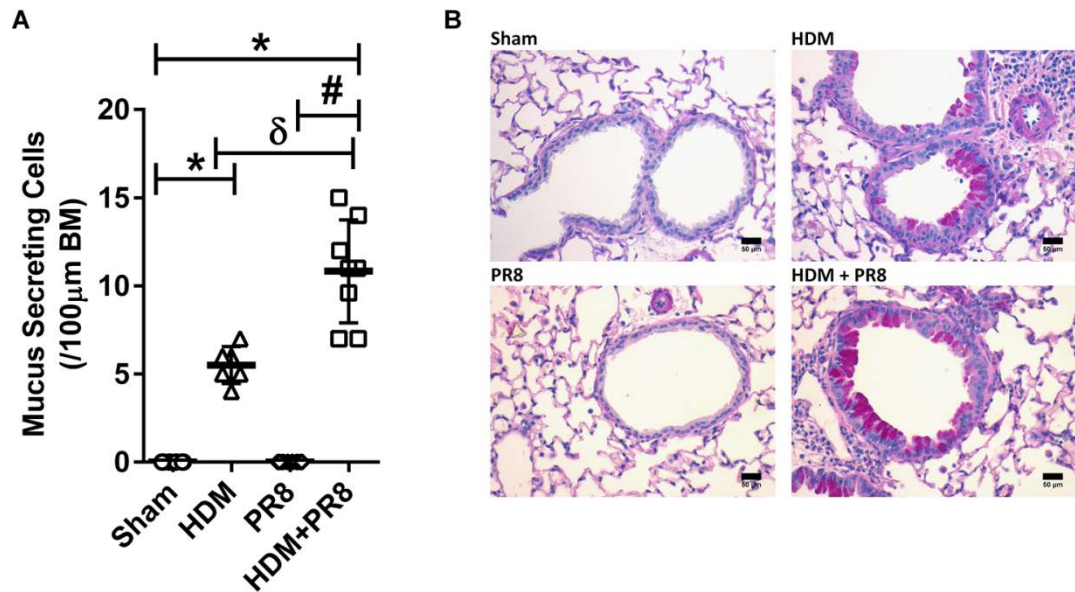


Figure 2.3. IAV infection exacerbates lung tissue inflammation in HDM-induced AAD.

BALB/c mice were sensitised with HDM (HDM) or PBS (sham), challenged with HDM and inoculated with IAV A/PR/8/34 (7.5 pfu, PR8, HDM+PR8) or media (control, HDM) on the last day of HDM challenge. Mice were sacrificed 3 dpi. **(A)** Total, **(B)** airway, **(C)** parenchymal and **(D)** vascular inflammation score in haematoxylin and eosin (H&E) stained lung sections. **(E)** Representative images (10X) of lung sections; Scale bar = 200  $\mu$ m. Data are presented as mean  $\pm$  SEM (n=6-8); \*, # and  $\delta$  represents  $P \leq 0.05$  versus sham, PR8 and HDM groups, respectively.



**Figure 2.4. IA V infection increased the numbers of MSCs in HDM-induced AAD.**

BALB/c mice were sensitised with HDM (HDM) or PBS (sham), challenged with HDM and inoculated with IA V A/PR/8/34 (7.5 pfu, PR8, HDM+PR8) or media (HDM) on the last day of HDM challenge. Mice were sacrificed 3 dpi. **(A)** MSC numbers per 100 μm basement membrane (BM) in periodic acid-Schiff (PAS) stained lung sections. **(B)** Representative images (20X) of lung sections; Scale bar = 50 μm. Data are presented as mean ± SEM (n=6-8); \*, # and δ represents  $P \leq 0.05$  versus sham, PR8 and HDM groups respectively.

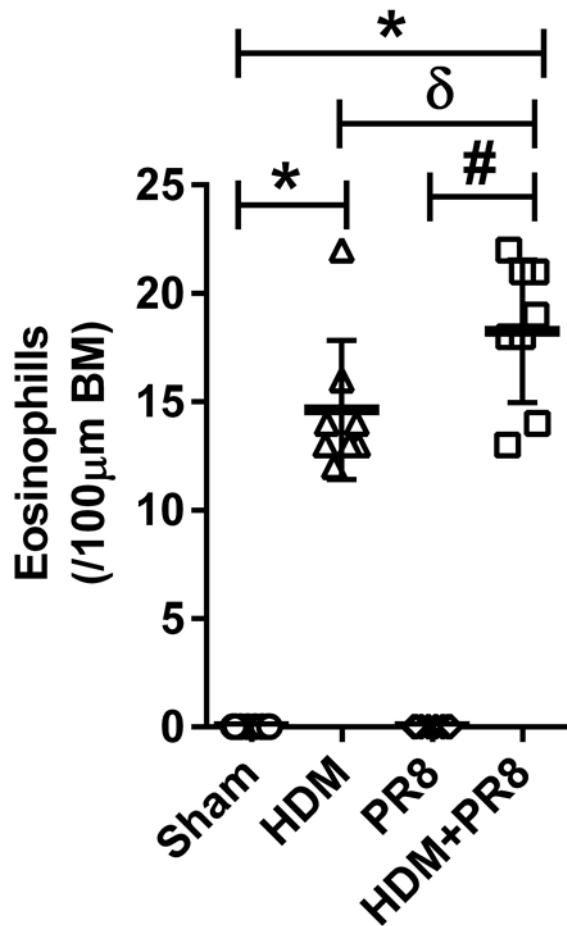


**Figure 2.5. IAV infection leads to increased numbers of tissue eosinophils in HDM-induced AAD.**

BALB/c mice were sensitised with HDM (HDM) or PBS (sham), challenged with HDM and inoculated with IAV A/PR/8/34 (7.5 pfu, PR8, HDM+PR8) or media (control, HDM) on the last day of HDM challenge. Mice were sacrificed 3 dpi. Data are presented as mean  $\pm$  SEM (n=6); \*, # and  $\delta$  represents  $P \leq 0.05$  versus sham, PR8 and HDM groups respectively.

### **2.4.3. IAV infection induces IL-13R $\alpha$ 1 expression and levels of Th2-associated cytokines following HDM-induced AAD**

We have demonstrated that IAV infection in AAD leads to severe tissue inflammation and increased numbers of MSCs and lung eosinophils. We then assessed if increases in IL-13 responses is a likely mechanism of increased MSCs and eosinophils.

To do this we assessed the protein levels of IL-13, its receptor IL-13R $\alpha$ 1 and other Th2-associated cytokines such as IL-5, IL-33 and TSLP. At 3dpi, in sham-inoculated allergic controls, AAD leads to a non-significant trend towards increases in IL-13 compared with the sham-inoculated non-allergic controls (Figure 2.6A). In infected non-allergic mice (PR8), there was a decrease in IL-13 compared to sham-inoculated non-allergic controls. Infected mice with AAD (HDM+PR8) also had significantly increased levels of IL-13 compared with infected non-allergic, but not sham-inoculated allergic controls and sham-inoculated non-allergic controls (Figure 2.6A).

At 3dpi, AAD leads to a non-significant trend towards increases in IL-13R $\alpha$ 1 compared with the sham-inoculated non-allergic controls (Figure 2.6B). In infected non-allergic mice (PR8), there was a statistical increase in IL-13R $\alpha$ 1 compared to sham-inoculated non-allergic controls. No change was observed in levels of IL-13R $\alpha$ 1 in the infected mice with AAD (HDM+PR8) compared with sham-inoculated non-allergic controls and sham-inoculated allergic controls. However a non-significant decrease in IL-13R $\alpha$ 1 was observed in infected mice with AAD compared with infected non-allergic mice (Figure 2.6B).

Moreover, other Th2-associated cytokines assessed in the study include IL-5, IL-33 and TSLP. At 3dpi, in sham-inoculated allergic controls, AAD leads to a significant increase in IL-5 compared with the sham-inoculated non-allergic controls (Figure 2.6C). In infected non-allergic mice (PR8), there was a decrease in IL-5 compared to sham-inoculated non-allergic controls. Infected mice AAD (HDM+PR8) also had increased levels of IL-5 compared with infected

non-allergic, but not sham-inoculated allergic controls and sham-inoculated non-allergic controls (Figure 2.6C).

At 3dpi, a statistically significant increase in IL-33 levels was observed in sham-inoculated allergic and infected non-allergic (PR8) mice, compared with the sham-inoculated non-allergic controls. Infected mice with AAD (HDM+PR8) had significantly increased levels of IL-33 compared with sham-inoculated non-allergic controls, infected non-allergic and sham-inoculated allergic controls (Figure 2.6D).

At 3dpi, no change in the levels of TSLP was observed among sham-inoculated non-allergic controls, sham-inoculated allergic controls and infected mice with AAD (HDM+PR8) (Figure 2.6E). In infected non-allergic mice (PR8), there was a significant decrease in TSLP compared to sham-inoculated non-allergic controls. Infected mice with AAD (HDM+PR8) had significantly increased levels of TSLP compared with infected non-allergic mice (Figure 2.6E).

#### **2.4.4. HDM-induced AAD impairs antiviral responses to IAV infection**

We then assessed the impact of AAD on antiviral responses. At 3dpi, infected non-allergic but not sham-inoculated allergic mice had significantly increased expression of RIG-I compared with sham-inoculated non-allergic controls. Similarly, increased expression of RIG-I was observed infected mice with AAD compared to sham-inoculated non-allergic control and sham-inoculated allergic mice (Figure 2.7A).

At 3dpi, infected non-allergic mice had significantly increased expression of antiviral IFN responses (IFN- $\alpha$ 4, IFN- $\beta$  and IFN- $\lambda$ ) to IAV infection compared with sham-inoculated non-allergic controls. However, antiviral IFN responses IFN- $\alpha$ 4 and IFN- $\lambda$  but not IFN- $\beta$  was observed to be significantly reduced in infected mice with AAD compared to infected non-allergic mice (Figure 2.7B-E).

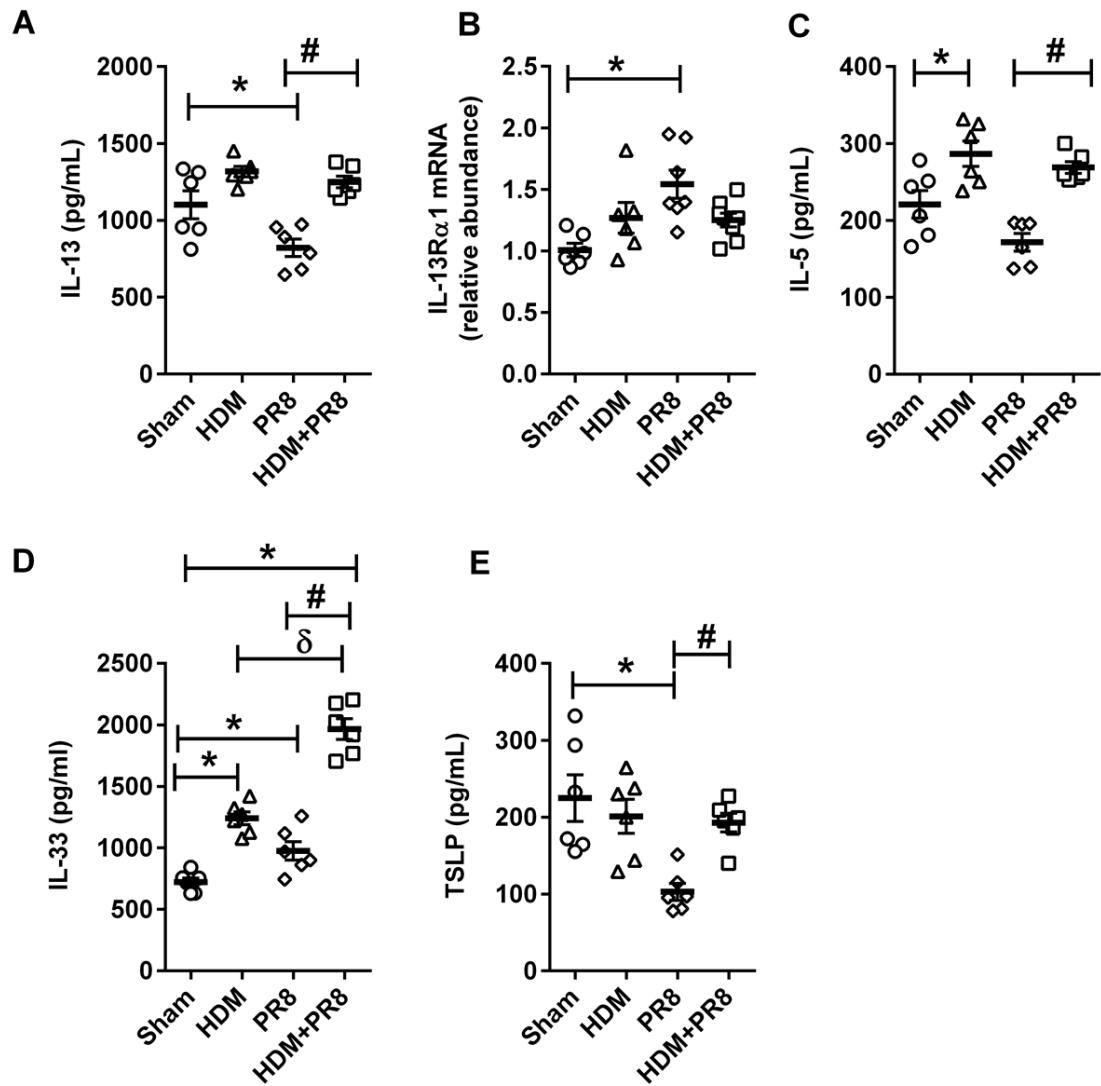


**Figure 2.6. IAV infection induces IL-13R $\alpha$ 1 expression and levels of Th2-associated cytokines following HDM-induced AAD .**

BALB/c mice were sensitised with HDM (HDM) or PBS (sham), challenged with HDM and inoculated with IAV A/PR/8/34 (7.5 pfu, PR8, HDM+PR8) or media (control, HDM) on the last day of HDM challenge. Mice were sacrificed 3 dpi. **(A)** IL-13 in lung homogenates; **(B)** IL-13 $\alpha$ 1 mRNA; **(C)** IL-5, **(D)** IL-33 and **(E)** TSLP in lung homogenates. Data are presented as mean  $\pm$  SEM (n=6); \*, # and  $\delta$  represents  $P \leq 0.05$  versus sham, PR8 and HDM groups, respectively.

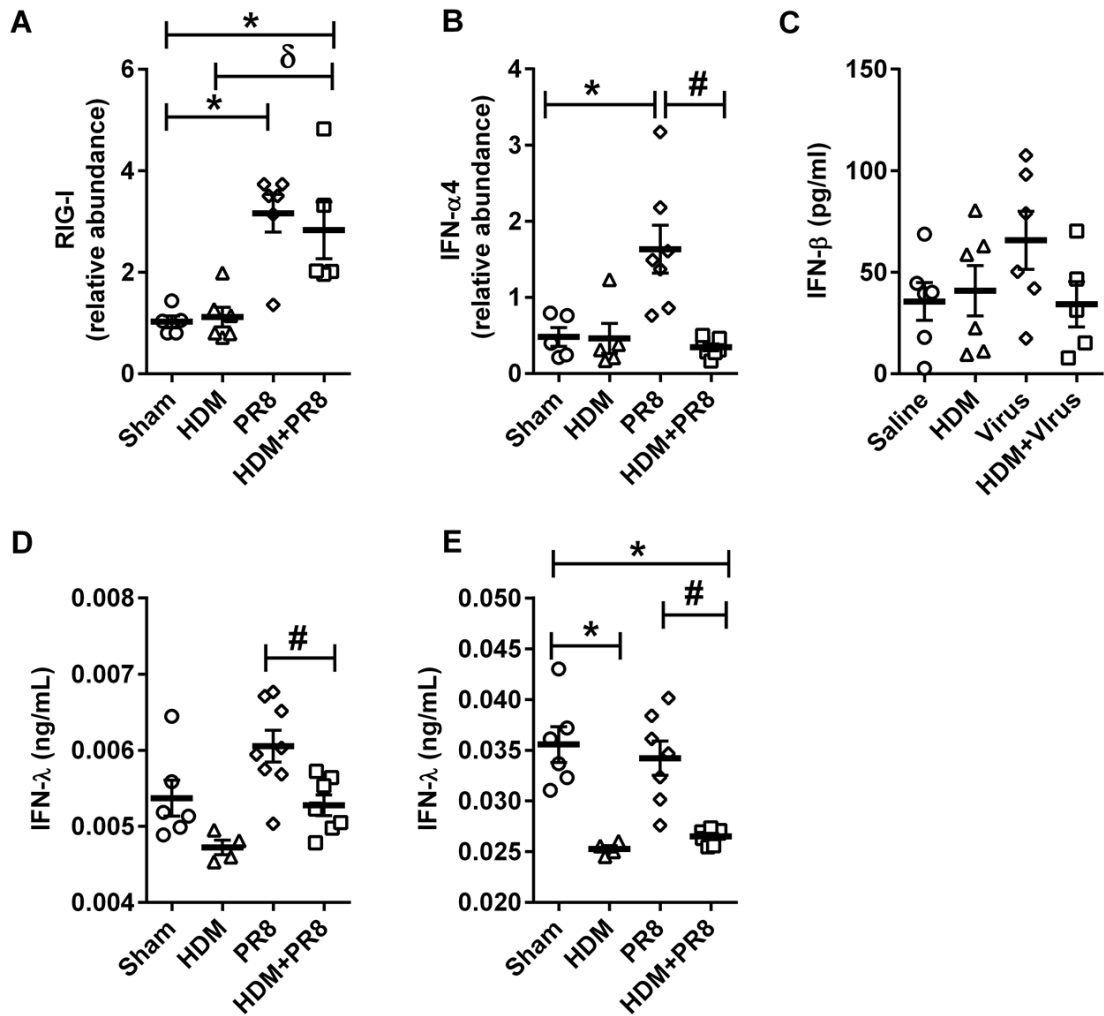


**Figure 2.7. HDM-induced AAD impairs antiviral IFN responses to IAV infection.**

BALB/c mice were sensitised with HDM (HDM) or PBS (sham), challenged with HDM and inoculated with IAV A/PR/8/34 (7.5 pfu, PR8, HDM+PR8) or media (control, HDM) on the last day of HDM challenge. Mice were sacrificed 3 dpi. **(A)** RIG-I; **(B)** IFN-α4; **(C)** IFN-β in lung homogenates; **(D)** IFN-λ in lung homogenates; **(E)** IFN-λ in BALF. Data are presented as mean ± SEM (n=6-8); \*, # and δ represents P≤0.05 versus sham, PR8 and HDM groups, respectively.

#### **2.4.5. IAV infection leads to airway remodelling following HDM-induced AAD**

Infection in allergic mice increased tissue inflammation (Figure 2.2). This may have damaging consequences on the lung tissue and may increase airway remodelling in AAD. Thus, we assessed various remodelling features such as the area of epithelial cells, collagen and fibronectin levels and deposition in whole lungs and around the small airways.

Sham-inoculated allergic controls had significantly increased soluble collagen levels compared to sham-inoculated non-allergic controls. Soluble collagen levels were observed to be increased significantly in infected mice with AAD compared to sham-inoculated non-allergic mice (sham) and infected non-allergic but not with sham-inoculated allergic control (Figure 2.8 A). Also, similar trend was detected with the qPCR validating the mRNA levels of type I collagen-1 (Col-1), the most abundant collagen (Figure 2.8 B) and fibronectin (Figure 2.8C).

Sham-inoculated allergic controls had significantly increased small airway epithelial cell area, indicating increases in airway epithelial cell thickness compared to sham-inoculated non-allergic controls. Infected mice with AAD had even greater small airway epithelial cell area compared with infected non-allergic controls and sham-inoculated allergic mice, however the later did not reach statistical significance (Figure 2.8 D).

Sham-inoculated allergic and infected non-allergic mice had increased collagen deposition compared with sham-inoculated non-allergic controls. Infected mice with AAD had even greater collagen deposition compared with sham-inoculated allergic and infected non allergic controls (Figure 2.8 E and F).

#### **2.4.6. IAV infection leads to increased AHR following AAD**

We then assessed the cumulative impact of disease features on AHR. At 3dpi, in sham-inoculated allergic mice, HDM challenge induced increases in

transpulmonary resistance compared to sham-inoculated non-allergic controls (Figure 2.9 A). In the infected non allergic group, PR8 infection also induced increases in transpulmonary resistance compared to sham-inoculated non allergic control. Infection in allergic mice induced significant further increases in transpulmonary resistance compared with sham-inoculated non-infected non-allergic control and sham-inoculated allergic, but not infected only controls.

At 3dpi, in sham-inoculated allergic mice, HDM challenge induced decrease in dynamic compliance compared to sham-inoculated non-allergic controls (Figure 2.9 B). In the infected non allergic group, PR8 infection also induced decrease in dynamic compliance compared to sham-inoculated non allergic control. The infected mice with AAD demonstrated significantly reduced dynamic compliance compared to sham-inoculated non-infected non-allergic control, sham-inoculated allergic controls and infected non-allergic controls (Figure 2.9 B).

#### **2.4.7. Remodelling studies and effect of corticosteroids on HDM-induced AAD and IAV infection**

Our investigations of HDM-induced AAD and secondary IAV infection have shown that infection following HDM challenge results in significant airway remodelling. This is characterised by numbers of MSCs around the airways (Figure 2.4) and increased collagen deposition (Figure 2.8). This suggests that airway remodelling is primarily occurring due to HDM, and the infection only increased MSCs and collagen deposition around the small airways.

This phenotype is a characteristic of severe human asthma that is not responsive to the current mainstay therapy of inhaled corticosteroids. Since, AAD wains over time, so to recapitulate additional re-challenges and assess the impact of ICS after infection we performed a study to investigate whether an IAV infection in AAD followed by additional allergen exposures causes severe asthma with airway remodelling that is not responsive to steroids. This mirrors an allergen-induced exacerbation.

HDM-induced AAD and IAV infection was extended. HDM-induced mice were infected with IAV A/PR8/8/34 (7.5 pfu; day 0) and 11-14 days later were re-challenged with (HDM 5 µg in 50 µl sterile PBS) and concurrently treated with dexamethasone (Dex; 2mg/kg) i.n (Figure 2.10). Mice were sacrificed after 24h and assessed.

We found that an additional challenge of the allergen (HDM) following HDM-induced AAD and IAV infection (HDM+PR8+HDM+vehicle) induced greater histopathology score (Figure 2.11) compared to Sham (PBS+Sham+HDM+Vehicle). However, a non-statistical trend towards increase in inflammatory score was observed in allergen rechallenge following HDM-induced AAD and IAV infection (HDM+PR8+HDM+Vehicle) compared with allergen (HDM+Sham+HDM+Vehicle) and infection (PBS+PR8+HDM+Vehicle) alone (Figures 2.11).

We demonstrated an increase in number of MSCs in mice rechallenged with allergen (HDM) following HDM-induced AAD and IAV infection (HDM+PR8+HDM+vehicle) compared to Sham (PBS+Sham+HDM+Vehicle) and infection (PBS+PR8+HDM+Vehicle) alone groups. However, there were no differences compared to the allergen (HDM+Sham+HDM+Vehicle) alone group (Figures 2.12).

No difference was observed in any of the investigated groups for collagen deposition or small airway epithelial thickening (Figures 2.13 and 2.14).

Co-administration of additional allergen challenge along with i.n. dexamethasone attenuated pulmonary inflammation (Figure 2.11). In contrast, dexamethasone treatment failed to suppress remodelling features in re-challenged non-infected allergic and infected non-allergic mice as well as allergic and infected groups (Figure 2.12-14).

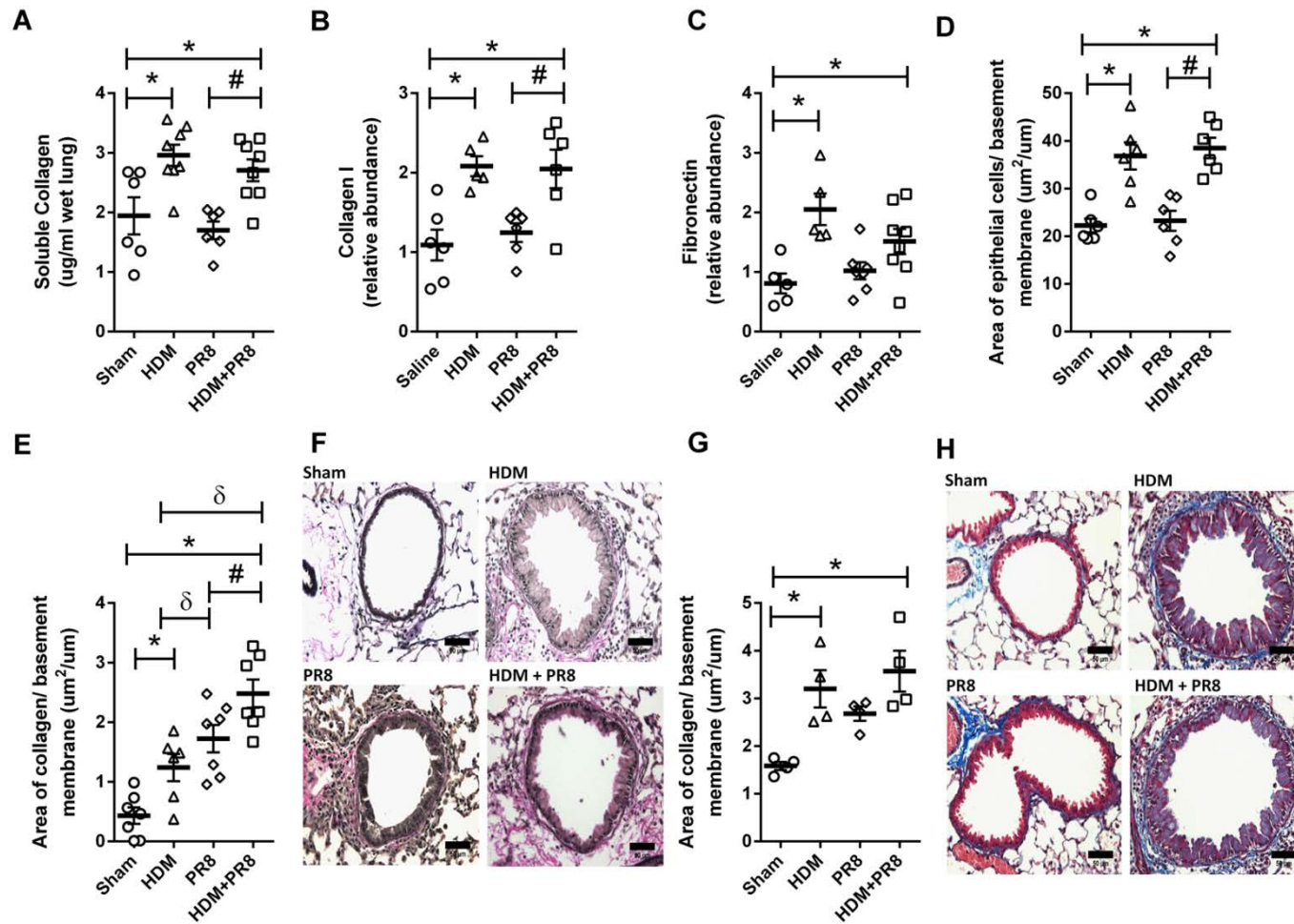
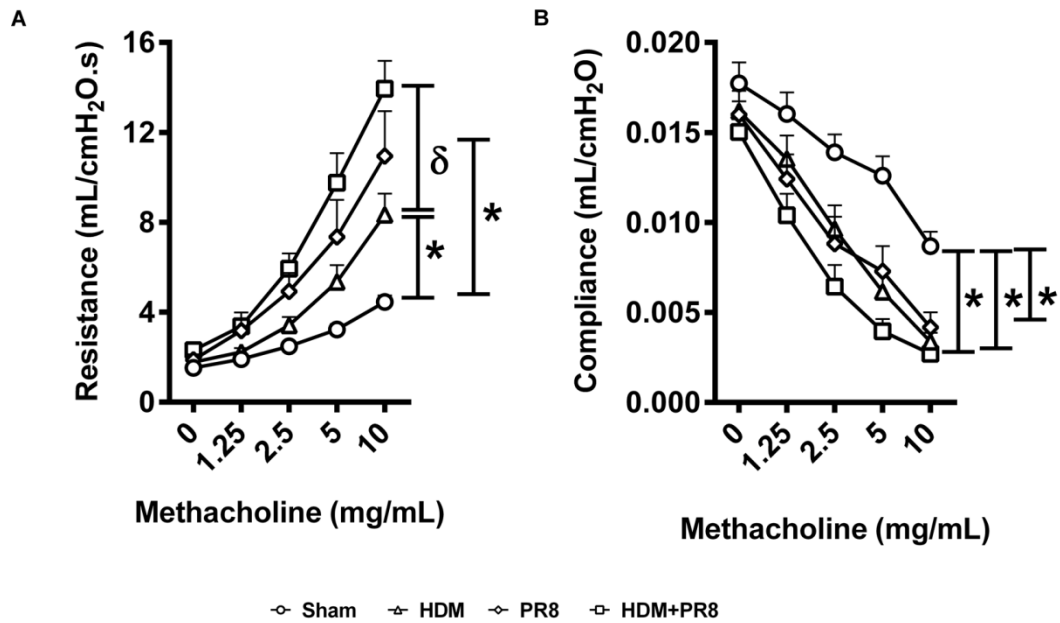


Figure 2.8. IAV infection leads to remodelling in AAD.

BALB/c mice were sensitised with HDM (HDM) or PBS (sham), challenged with HDM and inoculated with IAV A/PR/8/34 (7.5 pfu, PR8, HDM+PR8) or media (control, HDM) on the last day of HDM challenge. Mice were sacrificed 3 dpi. **(A)** Soluble collagen in whole lung; **(B)** Col-1 mRNA expression in lung homogenate; **(C)** Fibronectin mRNA expression in lung homogenates; **(D)** Small airway epithelial thickness in terms of epithelial cell area ( $\mu\text{m}^2$ )/basement (BM) perimeter in haematoxylin and eosin stained lung sections; **(E)** Area of collagen deposition ( $\mu\text{m}^2$ /BM perimeter) in Verhoeff-van Gieson stained lung sections; **(F)** Representative images (40X) of Verhoeff-van Gieson stained lung sections; Scale bar = 50 $\mu\text{m}$ ; **(G)** Area of collagen deposition ( $\mu\text{m}^2$ /BM perimeter) in Masson's Trichome stained lung sections; **(H)** Representative images of Masson's Trichome stained lung sections; Scale bar = 200 $\mu\text{m}$ . Data are presented as mean  $\pm$  SEM (n=6); \*, # and  $\delta$  represents  $P \leq 0.05$  versus sham, PR8 and HDM groups, respectively.

;



**Figure 2.9. IAV infection increases AHR in AAD.**

BALB/c mice were sensitised with HDM (HDM) or PBS (sham), challenged with HDM and inoculated with IAV A/PR/8/34 (7.5 pfu, PR8, HDM+PR8) or media (control, HDM) on the last day of HDM challenge. Mice were sacrificed 3 dpi. **(A)** transpulmonary resistance and **(B)** dynamic compliance. Data are presented as mean  $\pm$  SEM (n=6); \*, # and  $\delta$  represents  $P \leq 0.05$  versus sham, PR8 and HDM groups respectively.

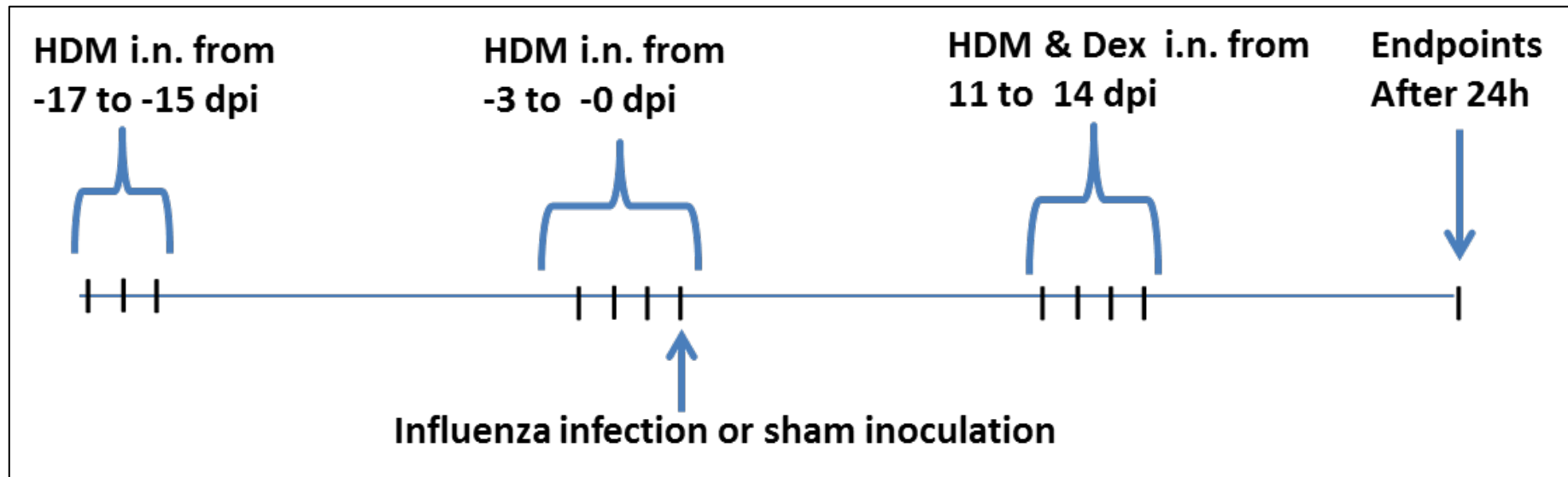


**Figure 2.10. Remodeling studies and effect of corticosteroids on HDM-induced AAD and IAV infection.**

BALB/c mice were sensitised to HDM and subsequently challenged with HDM. On the last day of HDM challenge, mice were infected with IAV A/PR8/8/34 (7.5 pfu; day 0). BALB/c mice were rested for 10 days. Subsequently, from day 11 until day 14 after infection, mice were re-challenged with (HDM 5 µg in 50 µl sterile PBS) and concurrently treated with dexamethasone (Dex; 2mg/kg) intra-nasally. Mice were sacrificed and assessed after 24h.

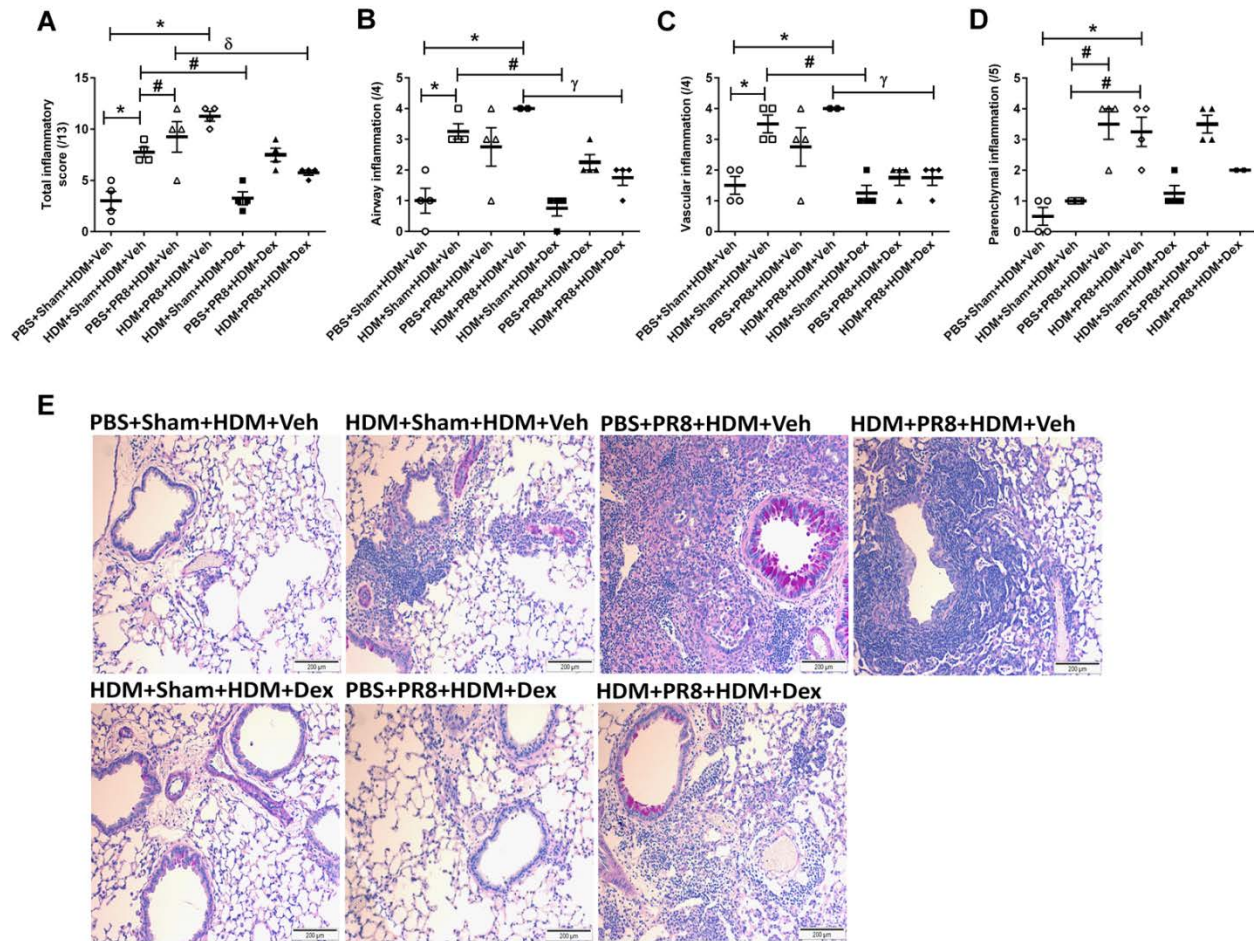


**Figure 2.11. Allergen re-challenge increased pulmonary inflammation in AAD with IAV infection, which could be attenuated by intranasal dexamethasone treatment.**

BALB/c mice were sensitised to HDM and subsequently challenged with HDM. On the last day of HDM challenge, mice were infected with IAV A/PR8/8/34 (7.5 pfu; day 0). Subsequently, from day 11 until day 14 after infection, mice were re-challenged with (HDM 5 µg in 50 µl sterile PBS) and concurrently treated with dexamethasone (Dex; 2mg/kg) intra-nasally. Mice were sacrificed after 24h. **(A)** Total, **(B)** airway, **(C)** parenchymal and **(D)** vascular inflammation score in Periodic acid-Schiff (PAS) stained lung sections; **(E)** Representative images (10X) of PAS stained lung sections; Scale Bar= 200µm. Data are presented as mean±SEM (n=4); \*, # and δ represents  $P \leq 0.05$  versus PBS+Sham+HDM+Veh and HDM+Sham+HDM+Veh, PBS+PR8+HDM+Veh groups respectively.

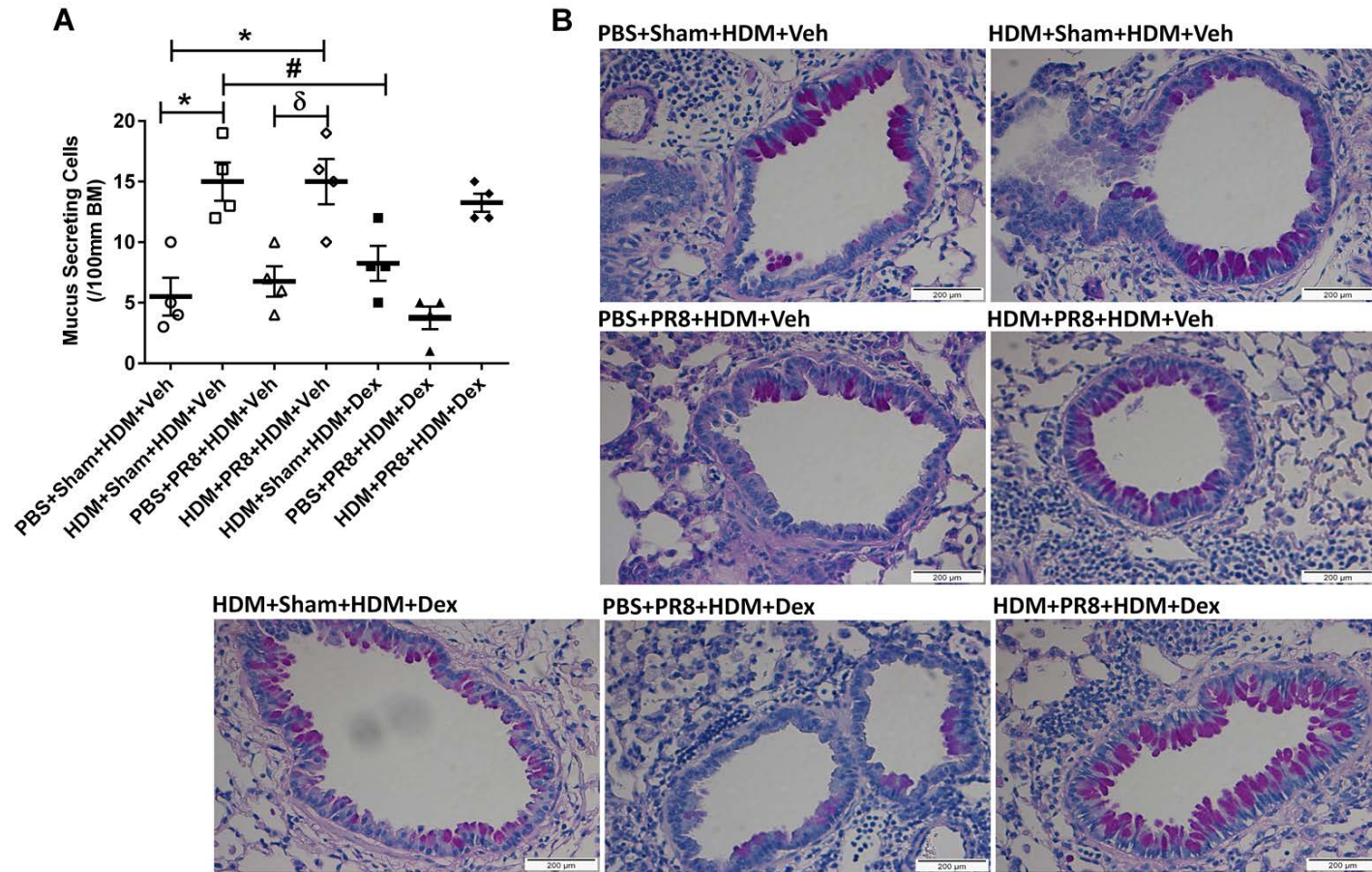


Figure 2.12. Allergen re-challenge increased the numbers of MSCs in AAD with IAV infection, which was not affected by intranasal dexamethasone treatment.

BALB/c mice were sensitised to HDM and subsequently challenged with HDM. On the last day of HDM challenge, mice were infected with IAV A/PR8/8/34 (7.5 pfu; day 0). Subsequently, from day 11 until day 14 after infection, mice were re-challenged with (HDM 5 µg in 50 µl sterile PBS) and concurrently treated with dexamethasone (Dex; 2mg/kg) intra-nasally. Mice were sacrificed after 24h and assessed. **(A)** MSCs number per 100 µm basement membrane (BM) in Periodic acid-Schiff stained lung sections **(B)** Representative images (40X) of stained lung sections; Scale Bar= 200µm. Data are presented as mean ± SEM (n=4); \*, #, δ and γ represents  $P \leq 0.05$  versus PBS+Sham+HDM+Veh, HDM+Sham+HDM+Veh, PBS+PR8+HDM+Veh and HDM+PR8+HDM+Veh groups, respectively.

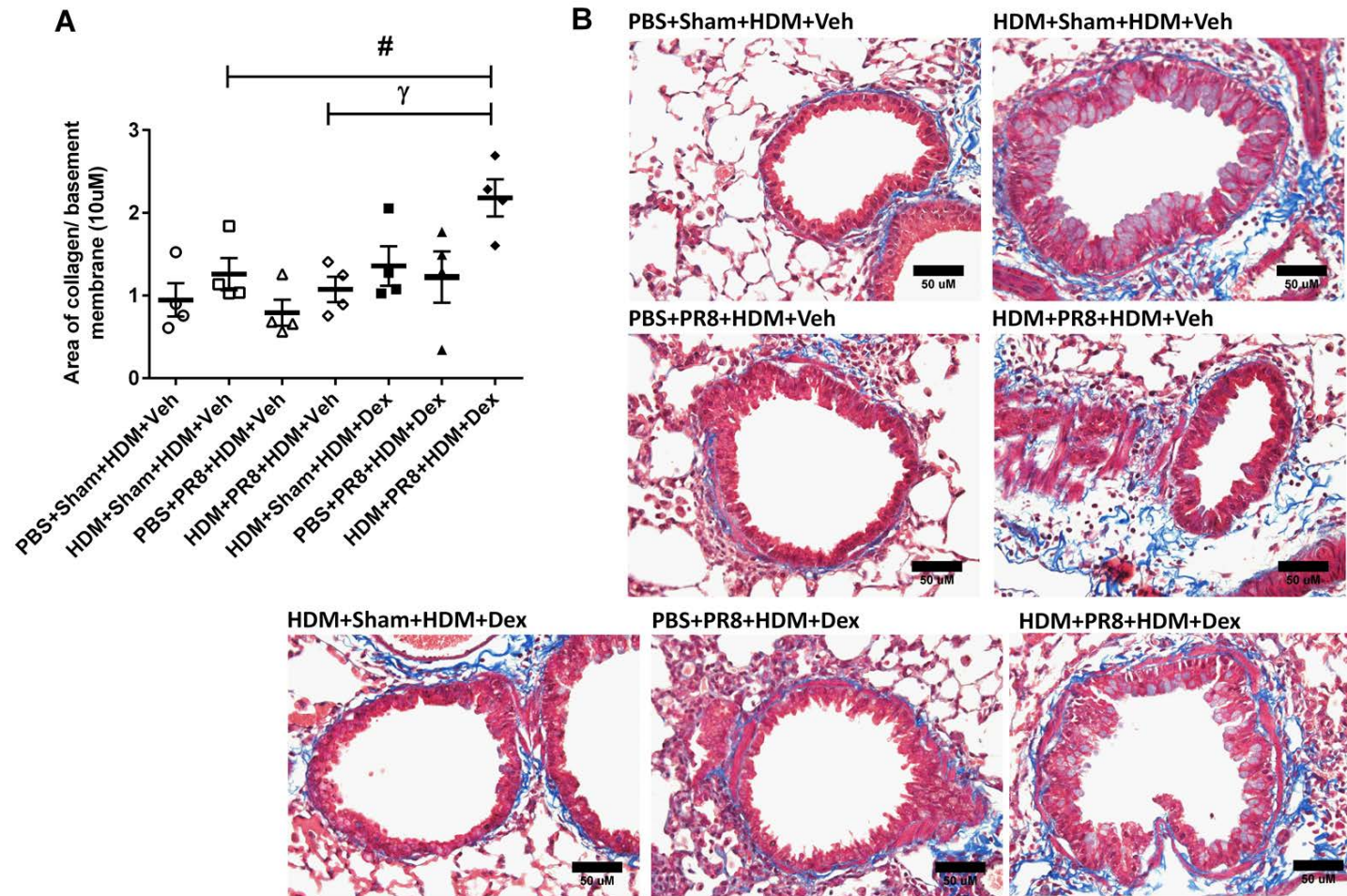
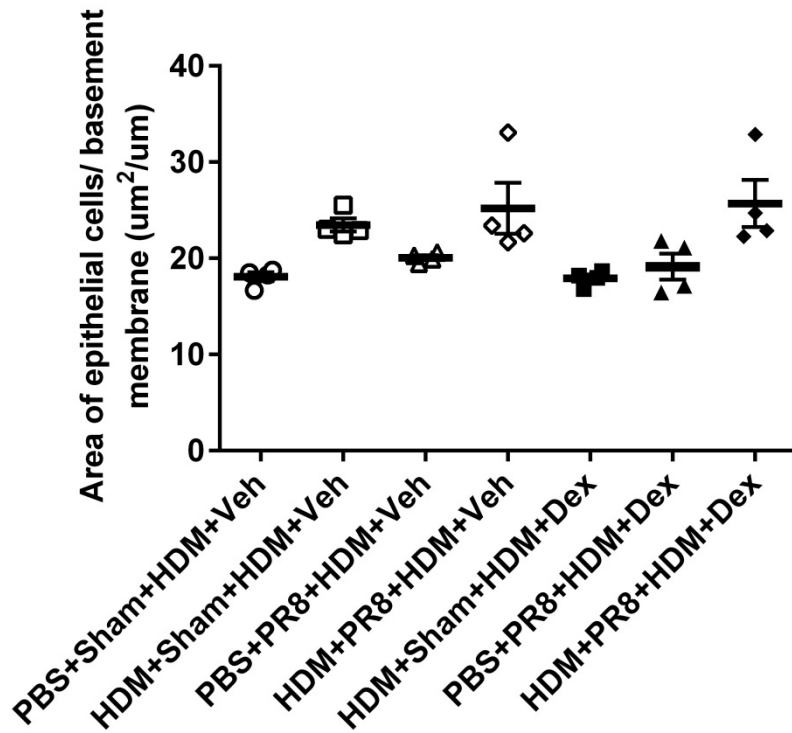


Figure 2.13. IAV infection influences collagen deposition around small airways following AAD.

BALB/c mice were sensitised to HDM and subsequently challenged with HDM. On the last day of HDM challenge, mice were infected with IAV A/PR8/8/34 (7.5 pfu; day 0). Subsequently, from day 11 until day 14 after infection, mice were re-challenged with (HDM 5 µg in 50 µl sterile PBS) and concurrently treated with dexamethasone (Dex; 2mg/kg) intra-nasally. Mice were sacrificed after 24h and assessed. **(A)** Area of collagen deposition ( $\mu\text{m}^2$ ) per BM perimeter in Masson's trichome stained lung sections; **(B)** Representative images (40X) of Masson's trichome stained lung sections; Scale Bar= 50µm. Data are presented as mean  $\pm$  SEM (n=4); \* , #,  $\delta$  and  $\gamma$  represents  $P \leq 0.05$  versus PBS+Sham+HDM+Veh, HDM+Sham+HDM+Veh, PBS+PR8+HDM+Veh and HDM+PR8+HDM+Veh groups respectively.



**Figure 2.14. IAV infection influences small airway epithelial thickness following AAD.**

BALB/c mice were sensitised to HDM and subsequently challenged with HDM. On the last day of HDM challenge, mice were infected with IAV A/PR8/8/34 (7.5 pfu; day 0). Subsequently, from day 11 until day 14 after infection, mice were re-challenged with (HDM 5 µg in 50 µl sterile PBS) and concurrently treated with dexamethasone (Dex; 2mg/kg) intra-nasally. Mice were sacrificed after 24h and assessed. Small airway epithelial thickness in terms of epithelial cell area (µm<sup>2</sup>) per basement BM perimeter in Periodic acid-Schiff (PAS) stained lung sections. Data are presented as mean ± SEM (n=4)

## 2.5. DISCUSSION

One of the most commonly employed mouse model of asthma is the Ova-induced model[420] where sensitisation is achieved either by concurrent administration of alum as an adjuvant. The main use of adjuvant is to induce mast cell independently from airway inflammation that is primarily driven by the Th2 inflammation and eosinophilia. However, a limitation of the Ova model is the use of a non-antigenic protein, and the development of an immune response to this protein through the use of adjuvant. Thus, in our present study we used HDM, which drives a disease-relevant natural antigenic protein response without adjuvant, which is a clinically relevant and significant source of indoor allergens.

IAV is a common trigger of asthma exacerbations[421, 422]. Various studies have been performed to elucidate the mechanisms involved but have produced conflicting results, which might be due to the lack of a reproducible and robust AAD model. To understand and explore AAD and the effects of IAV infection, we have developed and utilised an experimental model of HDM-induced AAD with IAV infection in established disease. This model recapitulates the hallmark features of virus-induced exacerbations and can be employed to investigate the predisposing mechanisms involved.

Like other models, our HDM-induced AAD comprises two phases, an induction and a maintenance phase[423]. The induction phase takes place with initial sensitisation of the airways with allergen while the maintenance phase involves airway allergen challenge. This establishes responses in the airway leading to the development of AHR in an IL-13 dependent manner[423, 424] (Figure 2.15). Investigation of our well established AAD model showed that as expected in the maintenance phase, the HDM challenge induced AHR with increased transpulmonary resistance compared to non-infected non allergic mice. Notably the combination of infection and allergen challenge induced significantly higher transpulmonary resistance compared to infection or allergen challenge alone (Figure 2.9).

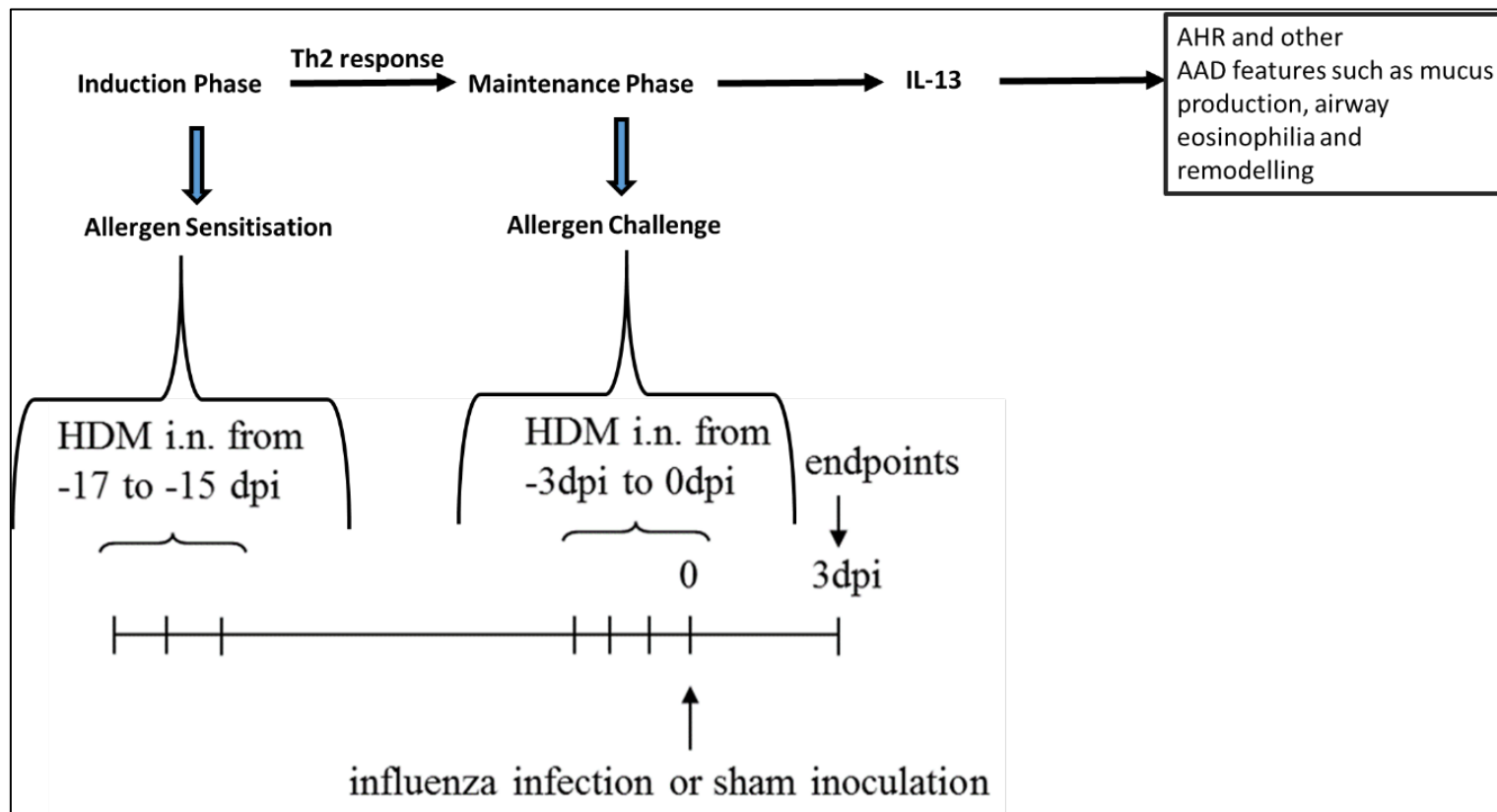


**Figure 2.15. The two phases of AAD development in mice.**

HDM-induced AAD comprises of two phases, the induction phase (initial sensitisation with the allergen) and the maintenance phase (allergen challenge), which establishes responses in the airway leading to the development of AHR in an IL-13-dependent manner.

A recent study using Ova-induced AAD with RSV infection showed similar findings where Ova-sensitised/challenged mice exhibited increased airway resistance compared with PBS-sensitised controls and RSV infection dramatically increased airway resistance in mice with AAD[212]. Our observations indicate that hosts with AAD are more susceptible to severe IAV infection. Increased IAV viral titres have previously been shown in mice exposed to asthma-exacerbating inducers such as diesel exhaust particles (a potent oxidant air pollutant)[425]. Our finding is also consistent with clinical observations that similarly show increased susceptibility of asthmatic patients to viral infection in general, including by IAV[426-430].

Administration of HDM extract in mice without adjuvant leads to a robust inflammatory response with significant histopathological abnormalities that are exacerbated by infection or further HDM challenge. Moreover, infected mice with AAD had the highest score compared with sham-inoculated allergic or infected non-allergic controls. This replicates the association of IAV infection with AAD and its involvement in disease exacerbations. Indeed, our findings are consistent with observations that typify the infection-induced exacerbations in asthmatic patients, which involve enhanced lung inflammation that worsens their symptoms[431, 432].

Abnormal metaplasia and hyperplasia of MSCs have been linked with asthma exacerbations, which can lead to excessive sputum production and compromised pulmonary gas exchange[433-436]. Our results indicate that the simultaneous concurrence of AAD and IAV infection may contribute to increases in mucus hypersecretion. Other viral infections such as rhinovirus have also been implicated in causing mucus hypersecretion in asthma[437-440]. The secretion of the mucus helps in the trapping and clearance of viruses but its overproduction leads to airway obstruction and exacerbation of the pre-existing AAD, which turns the powerful innate clearing defence system into a detrimental disease-promoting mechanism[441, 442].

In our model we observed that IAV infection led to increased numbers of eosinophils in AAD. Eosinophil recruitment and accumulation contributes to tissue damage, bronchoconstriction and respiratory dysfunction via degranulation of their cationic secretory proteins and enzymes which is typically associated with the production of Th2 cytokines[443-445]. A clinical trial with a formalin-inactivated RSV vaccine induced mortality in children that was associated with the deposition of antibody-virus complexes and a pronounced tissue eosinophilia in their lung histology[446].

Cytokines are important in allergic intercellular communication networks, which contributes to disease pathology by promoting the recruitment of pro-inflammatory leukocytes and activating various remodelling events[447]. Increases in Th2 cytokines are observed upon allergen challenge in the airways of allergic asthmatics, which correlates with the disease severity. Consistent with this the majority of the murine Ova models also have increased Th2 responses in the airways, where the disease phenotype is characterised by elevated levels of IL-5 and IL-13 in BALF[448]. Many researchers have already shown the profound role of IL-5 and IL-13 in the AADs[449]. Recruitment of immune cells to the site of infection is important in the clearance of virus. During IAV infection, infected airway epithelial cells produce pro-inflammatory cytokines such as IL-6, IL-8, MCP1 that attract neutrophils and macrophages to the site of infection, and also IL25/33/TSLP that are alarmins which recruit innate lymphoid cells[450, 451]. DCs with captured antigens/allergens polarise native CD4+ T cells to Th2 lymphocytes through the release of IL-4, and these cells also produce several cytokines including IL-4, IL-5 and IL-13 that further promotes the development Th2 cells and other immune cells such as eosinophils[452, 453]. In our model, we focussed our analysis on the expression of various cytokines in the lung, and clearly showed increased levels of IL-5, IL-13, IL-33 and TSLP in sham-inoculated allergic controls compared with non-allergic, non-infected controls. However, IL-13 and IL-5 levels did not increase further in infected mice with AAD even though we observed increases in eosinophil influx in the same group. This eosinophilia may be attributable to the production of chemokines such as eotaxin and RANTES, that have been

suggested to be key regulatory factors in the induction of eosinophil trafficking to the inflammatory site[454-456]. This warrants further investigations to assess the mechanisms that promote eosinophil influx in response to antigen-driven inflammation.

Persson and his co-workers have also shown increased expression of upstream type 2 cytokines in a mouse model of viral-induced asthma exacerbation[457]. Indeed the role of IL-33 and TSLP in the induction of disease is receiving considerable attention as they are considered as the upstream epithelial cytokines driving the production of potent type 2 cytokines such as IL-5 and IL-13 causing severe and difficult to treat eosinophilic asthma[458, 459].

Our data showed that sham-inoculated allergic controls have impaired antiviral IFN responses to IAV infection such as RIG-I, IFN- $\alpha$ 4, IFN- $\beta$  and IFN- $\lambda$ . RIG-I initiates a signalling cascade that begins with its relocalisation to mitochondria, where the exposed, ubiquitinated RIG-I associates with caspase activation and recruitment domain (CARD) of mitochondrial antiviral signalling adaptor (MAVS; also known as IPS-1/VISA/Cardif)[460]. Subsequently, RIG-I interacts with MAVS, which indirectly activates interferon regulatory factor 3 (IRF3) by phosphorylation. Activated IRF3 then translocates into the nucleus where it initiates the production of type I and III IFNs[461, 462]. The defective IFN response promotes susceptibility to infection by loss of the ability of the infected host cell to undergo early apoptosis, which leads to increased viral replication and finally cytolysis of the infected cells. Other published reports have also shown reduced levels of IFN- $\beta$  and IFN- $\lambda$  in response to infection with HRV-A16 that was associated with increased viral replication in human bronchial epithelial cells isolated from the asthmatic patients[463, 464]. These observations have led to various clinical trials with IFN treatments in order to prevent or reduce the effects of viral infections in asthma[465-469].

Airway remodelling is involved in various degrees of asthma severity, in both the large and small airways[470] and mainly refers to structural changes. In our model, we also observed various remodelling features such as airway wall

thickening, increased mucus and collagen production. The increased epithelial wall thickening leads to epithelial cell alterations, subepithelial fibrosis, submucosal gland hyperplasia, and increased airway smooth muscle mass and vascularisation[471-473]. Inflammation is the initiating event for remodelling[474] where overexpression of cytokines leads to altered pathognomic of asthmatic airway remodelling[475]. We observed association between the increased levels of IL-13 and remodelling events particularly increased sub-epithelial fibrosis, mucus metaplasia and eosinophils inflammation which was in agreement with previous studies[476, 477]. The increase in mucus production is the result of Th2 interleukins, in particular IL-13 that is induced through the STAT-6 signalling pathway[478, 479].

We also observed increases in the levels of IL-33 in sham-inoculated allergic control and infected mice with AAD. IL-33 has been shown to be involved in airway remodelling in asthma by activating the expression of fibronectin-1 and type 1 collagen in human lung fibroblasts[480]. Our model also shows increased fibronectin and collagen in non-infected allergic group and infected mice with AAD. IL-33 has also been shown to remain elevated in HDM-exposed ST2(-/-) mice lacking the IL-33 receptor where IL-33 has been demonstrated to mediate the persistent airway remodelling. Furthermore, the therapeutic inhibition of IL-13 in neonatal HDM-induced AAD does not reduce airway remodelling or IL-33 levels and only partly abrogates AHR. This indicates that inhibition of IL-33 expression or activity may represent a more effective therapeutic approach than IL-13 inhibition [481]. There may be various other factors also contributing to remodelling such as changes in mucin glycoproteins[482], epithelial growth factor (EGF)[479] which via TGF- $\beta$ [483, 484] activates matrix metalloproteinase (MMP) molecules such as MMP-9[485]. Moreover, there is strong evidence that clearly shows the roles of IL-33/IL-13 axis in respiratory virus infections in pre-clinical settings (mice models) and in samples from asthmatics and COPD. Intraperitoneal injection of IL-33 in mice increased the production of various Th2 cytokines such as IL-5 and IL-13 along with eosinophilic lung inflammation[486-488], which is consistent with our findings. Targeting the IL-33/IL-13 axis may

provide beneficial effects in the treatment of chronic respiratory diseases, such as asthma and COPD[489].

Similar findings have also been shown in HDM-challenged sheep that have significant eosinophilia during challenge and increased airway collagen and airway smooth muscle at the end of challenges along with hyperplasia of goblet cells[490]. Another similar study which support our current findings involves a non-human primate model of allergic asthma where all the hallmark features such as increased airway inflammation, release of cytokines like IL-5 along with various remodelling features such as goblet cell hyperplasia, basement membrane thickening, and smooth muscle hypertrophy and decreased dynamic compliance occurs by sensitizing cynomolgus monkeys to HDM antigen[491].

We also carried out an experiment where we showed that infected mice with AAD after rechallenging with an allergen have ongoing remodelling characterised by excessive mucus and collagen production that are resistant to dexamethasone treatment. This is supported by published literature showing that in patients with severe asthma, treatments like corticosteroids, long acting inhaled  $\beta_2$  agonists usually fail[399, 400, 492]. Our observations are consistent with published studies showing no reduction in the airway inflammation with inhaled steroids[493-495]. The probable mechanisms that might be driving this steroid insensitivity, disease exacerbations and tissue remodelling include altered glucocorticoid signalling, altered Th-cell polarization, innate immune activation and chronic inflammation[496]. To elucidate the mechanisms and kinetics involved in dexamethasone resistance and remodelling events further in-depth investigation is required as part of future ongoing studies.

We hypothesise that dexamethasone-resistant remodelling features/events observed after an additional allergen challenge may be due to (1) a persisting remodelling state that either has plateaued or is progressing or (2) a resolved remodelling during the rest period which is re-established and intensified after an additional allergen challenge. This study requires further in depth investigation

and validation to reveal corticosteroid unresponsive remodelling events (Figure 2.16).

Around 5-10% of the asthmatic patients do not respond well to glucocorticoid treatment, and because there are no effective treatments these patients account for almost 50% of the total health care costs of asthma[497, 498].

The various postulated mechanisms involved for the corticosteroid resistance include reduced number of glucocorticoid receptors (GRs), altered affinity of the ligand for GRs, reduced ability of the GRs to bind to DNA, or increased expression of inflammatory transcription factors, such as activator protein (AP-1), that compete for DNA binding[499, 500]. Various other factors involved in glucocorticoid resistance include viral infections, immunomodulation[501, 502] and genetic predisposition[503, 504].

Recent studies have shown that RSV infection reduces GR nuclear translocation, which in turn reduces corticosteroid effects[505]. There is evidence, which shows that collagen remodelling by airway smooth muscle is resistant to steroids and  $\beta$ 2-agonists[506]. Also, an association between the steroid resistance and airway remodelling has been demonstrated where the resistance to the steroid therapy leads to airway remodelling[507], resulting in permanent biomechanical and pathologic alteration of asthmatic airways[508-510].

In summary, we have made some important observations, which demonstrate that in AAD, IAV infection led to various allergic outcomes; namely increased viral titre, impaired antiviral responses, exaggerated airway inflammation, severe histopathology along with increased mucus hypersecretion, collagen deposition around small airways, small airways epithelial thickness, IL-13R $\alpha$ 1, and AHR.

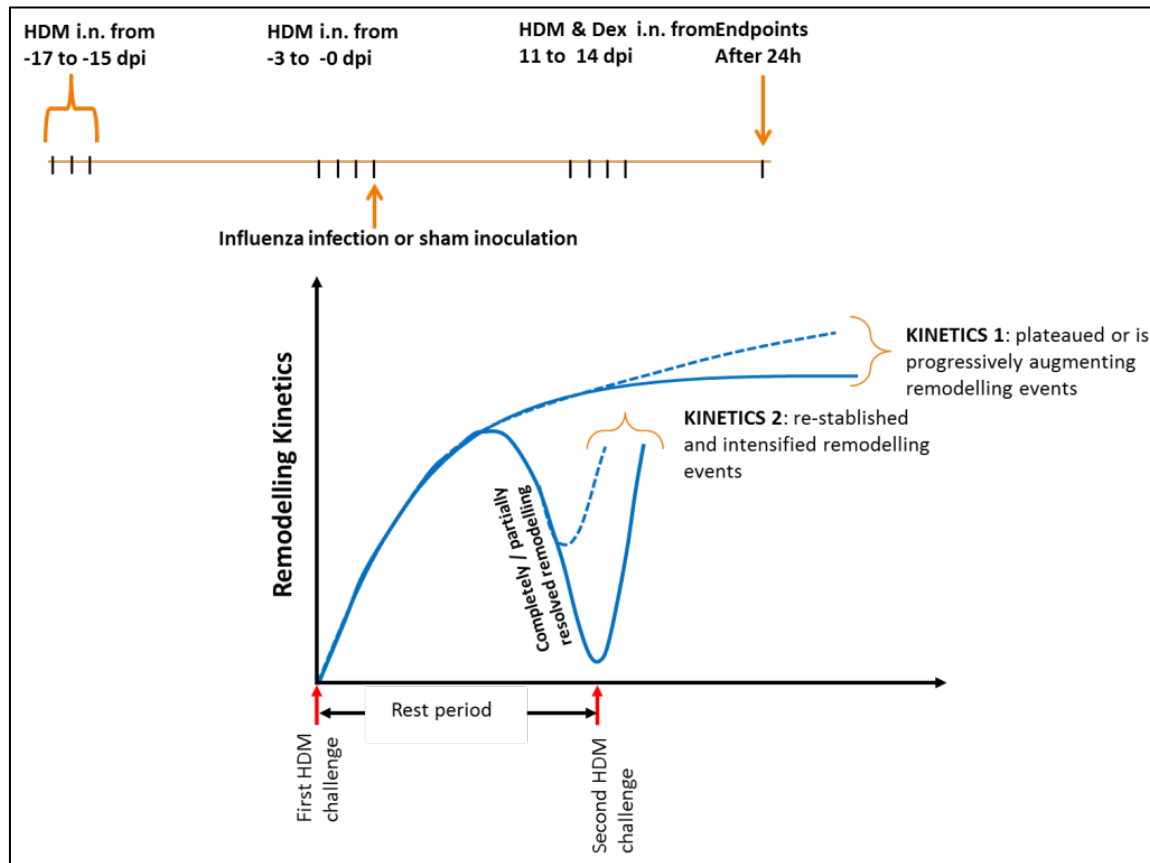


**Figure 2.16. Hypothesis attributed corticosteroid resistant remodelling.**

We believe that dexamethasone-resistant remodelling features/events observed after an additional allergen challenge may be due to either Kinetics 1 which presents a persistent remodelling state that either has plateaued or is progressing or Kinetics 2 where a resolved remodelling during the rest period is re-established and intensified after an additional allergen challenge.

## 2.6. CONCLUSION

IAV infection exacerbates HDM-induced AAD by inducing Th2 associated cytokines. Infection may be influencing AAD through several mechanisms such as pulmonary inflammation, mucus hypersecretion, remodelling and AHR. We suggest that this novel HDM model of viral-induced asthma exacerbation has translational value, which mimics aspects of HDM-induced exacerbations of asthma in humans. Our model has clear utility in identifying new and effective therapeutic interventions and is well suited for *in vivo* studies involving pharmacological effects on exacerbation-induced expression of various cytokines such as IL-13, IL-33 and TSLP and corticosteroid insensitivity.

# **CHAPTER 3**

## **TARGETING THE IL-13/ miR-21 AXIS FOR RESPIRATORY VIRAL INFECTIONS**

### 3.1. ABSTRACT

People with chronic lung diseases, such as asthma and COPD are more susceptible to IAV infections, which lead to exacerbations and worsening of disease with increased mortality and decreased quality of life. There are numerous limitations associated with current prevention and treatment strategies targeting virus-induced lung diseases. Influenza vaccinations are a major prevention strategy. However, current vaccines do not provide cross-serotype protection and new ones of varying efficacy have to be manufactured every year. Current anti-viral treatments are only partially effective and only if administered within the first 48 h after infection. They may also need to be given in combination to be efficacious, which is currently under investigation. Importantly, the immunological mechanisms that underpin these issues are incompletely understood.

To address these issues we have explored the underlying mechanisms by subjecting BALB/c mice to Ovalbumin (Ova)-, house dust mite (HDM)- and recombinant IL-13 (rIL-13)-induced models of AAD and subsequent infection with the mouse-adapted H1N1 (A/PR/8/34) IAV intranasally during the challenge phase of each model. In separate experiments mice with Ova-induced AAD were treated with anti-IL-13 neutralising antibody prior to and during IAV infection. The cellular source of IL-13 in the lung was also determined using novel IL-13-reporter mice. Furthermore, in separate experiments, mice were subjected to cigarette smoke-induced experimental COPD with subsequent intranasal infection with IAV. The effects of infection on hallmark features of AAD and COPD were assessed. Our data implicate IL-13/IL-13R $\alpha$ 1/miR-21 axis in IAV-induced exacerbations that lead to increases in severity of various hallmark features of disease. These include viral titre, lung tissue inflammation and airway remodelling resulting in more severe IAV infection that exacerbates the underlying AAD and COPD.

Our data implicate IL-13/IL-13R $\alpha$ 1/miR-21 axis in IAV-induced exacerbations that lead to increases in severity of various hallmark features of disease. These include viral titre, lung tissue inflammation and airway remodelling resulting in

more severe IAV infection that exacerbates the underlying AAD and COPD. These studies have identified potential new therapies for IAV infections and IAV-induced exacerbations of asthma and COPD by targeting the IL-13/ IL-13R $\alpha$ 1/miR-21 axis.

### 3.2. INTRODUCTION

Viral infections are a major cause of morbidity and mortality throughout the world, which includes IAV, RSV and RV. IAV infections induce massive global clinical problems that cause substantial socioeconomic consequences. A major issue is the capacity of the virus to mutate into new strains that result in seasonal infections to which the community has little immunity. The genetic variation in IAVs occurs through two different mechanisms involving a genetic drift and shift. Genetic drift in IAV HA and NA antigens occur due to the host immune response, while, genetic shift happens through the replacement of a whole gene from one subtype to another usually as a consequence of reassortment and recombination of different IAVs. Each year, seasonal IAV infects 100 million people worldwide causing 3-5 million severe infections and ~500,000 deaths[131]. In Australia seasonal influenza impacts the national health system enormously with >18,000 hospital admissions and >1,000 deaths per year[132]. In each seasonal epidemic, typically the very young and elderly and those with underlying respiratory conditions such as asthma[511] and COPD[143] are more susceptible. This indicates that factors are present in vulnerable individuals that promote susceptibility to infection.

IAV infections are major causes of exacerbations and worsening of the underlying respiratory diseases[144]. Approximately 34.97% deaths in asthmatics was directly due to IAV infection[145]. Infection-induced exacerbations, often by IAV, are the 2<sup>nd</sup> commonest cause of hospitalisations in Australia[146], and in 2006 influenza and its complications caused 2,715 deaths in COPD patients[132]. Furthermore, those with COPD are consistently over-represented in those hospitalised or who died during IAV-induced pandemics[147]. However, the immune mechanisms that underpin these associations are largely unknown.

Entry of IAV into target cells is the very first step of the viral life cycle and as such is crucial for the establishment of infection. IAV entry is a dynamic process that requires the completion of six individual steps: (i) attachment to target cells; (ii) internalization into cellular compartments; (iii) endosomal trafficking to the perinuclear region; (iv) fusion of viral and endosomal membranes; (v) uncoating and (vi) import of the viral genome into the nucleus (Figure 3.1)[512].

IAV attaches to host cells by binding of HA to sialic acids (SIA) present on the host cell surface. The entry of the virus into the host cells then occurs when neuraminidase breakdowns the mucosal material surrounding the epithelial cells. The virus then hijacks the cellular machinery leading to viral replication. Following attachment, viral entry is mediated via various endocytic routes including receptor-mediated endocytosis (receptor binding proteins HA and SIA; clathrin-mediated endocytosis) and macropinocytosis delivering the virus to the acidic environment of the late endosome that triggers HA-mediated fusion[512, 513]. Host innate immune responses recognise viral RNAs and initiate the production of numerous cytokines and chemokines such as IFN-  $\alpha$ ,  $\beta$ ,  $\gamma$  and  $\lambda$ , TNF- $\alpha$ , TSLP, IL-6, IL-12, IL-25, and IL-33[201, 514] and CC-chemokine genes such as CCL2/MCP-1, CCL3/ MIP-1 $\alpha$ , CCL4/MIP-1 $\beta$ , and CCL5[515-517]. When cytokines are produced they recruit alveolar macrophages and dendritic cells to clear the viral protein from infected and dying cells. Recruitment of dendritic cells has been reported to release IL-13 that subsequently results in AHR, progression of allergic airway inflammation together with induction and accumulation of mucus thereby altering normal lung environment and causing airway congestion (Figure 3.2)[515, 516].

IL-13 is known to be a crucial cytokine in asthma and may be important in increased susceptibility to viral infection and asthma exacerbations. Tekkanat *et al.*, showed that severe RSV infection in mice is related to the level of IL-13 that promotes mucus hypersecretion and AHR in the airway during severe infection[518]. Lukacs and colleagues subsequently demonstrated that initial RSV infection promotes a more severe asthmatic response, even when the

allergic response is initiated after clearance of the RSV-induced reactions[519]. IL-13 is released from different cells such as alveolar macrophages, mast cells, eosinophils, T cells such as CD4+, CD8+ and NKT cells[520, 521] and ILC2s[522, 523]. It is considered as a central regulator of IgE synthesis, responsible for various main features of airway diseases such as increased eosinophils, mucus cells production, goblet cell metaplasia and changes in the airway smooth muscles leading to AHR and wheezing[66, 523, 524]. Increased levels of IL-13 are observed in patients with asthma and very severe COPD when compared with non-asthmatics and non-COPD control subjects[525, 526].

The high frequency of mutations in IAVs has made it challenging to develop effective therapeutics, and current preventions and treatments have serious limitations. Vaccination is the mainstay of efforts to protect against infection, however efficacy is limited to known strains, varies from year to year and new vaccines need to be developed every year. In COPD, while vaccination reduces exacerbations, it has no effect on hospitalisations or mortality[149].

NA inhibitors (e.g. oseltamivir) are the only specific anti-influenza treatments available, however, they are poorly effective[150]. Also, treatments only have beneficial effects if given within the first 48 h of the appearance of clinical signs, which has proven difficult for both patients and physicians. In addition IAVs are rapidly becoming resistant to these treatments[151]. There is therefore an urgent need to develop novel and effective preventions and treatments for influenza, especially for those most susceptible to infection. For these reasons, influenza has attracted much attention from the pharmaceutical industry. The most effective approach may be to improve host immunity rather than targeting the virus. Treatments directed against both IAV attachment to the cell surface and replication within the host cell may also be effective[152].

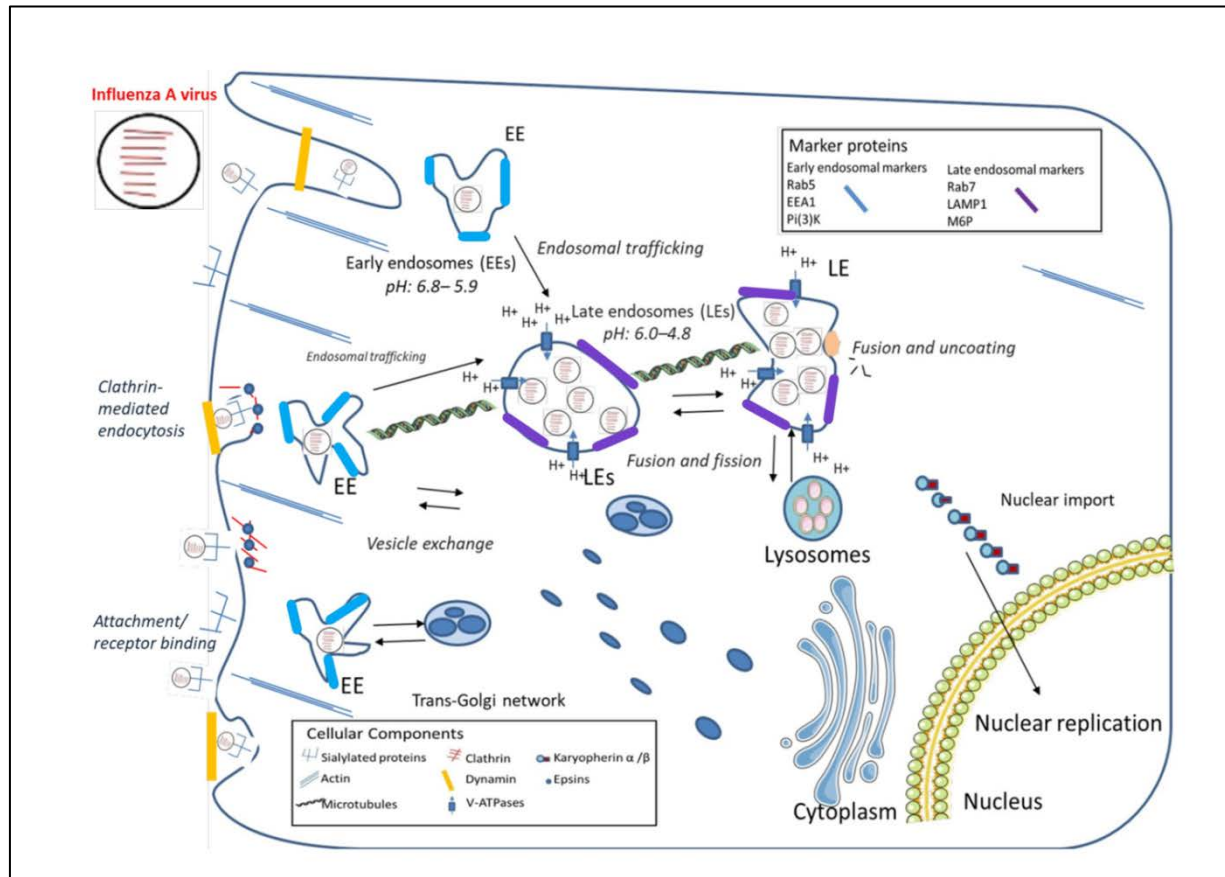


**Figure 3.1. Schematic representation of IAV entry process.**

IAV entry is a dynamic process that requires the completion of six individual steps: (i) attachment to target cells; (ii) internalization into cellular compartments; (iii) endosomal trafficking to the perinuclear region; (iv) fusion of viral and endosomal membranes; (v) uncoating and (vi) import of the viral genome into the nucleus

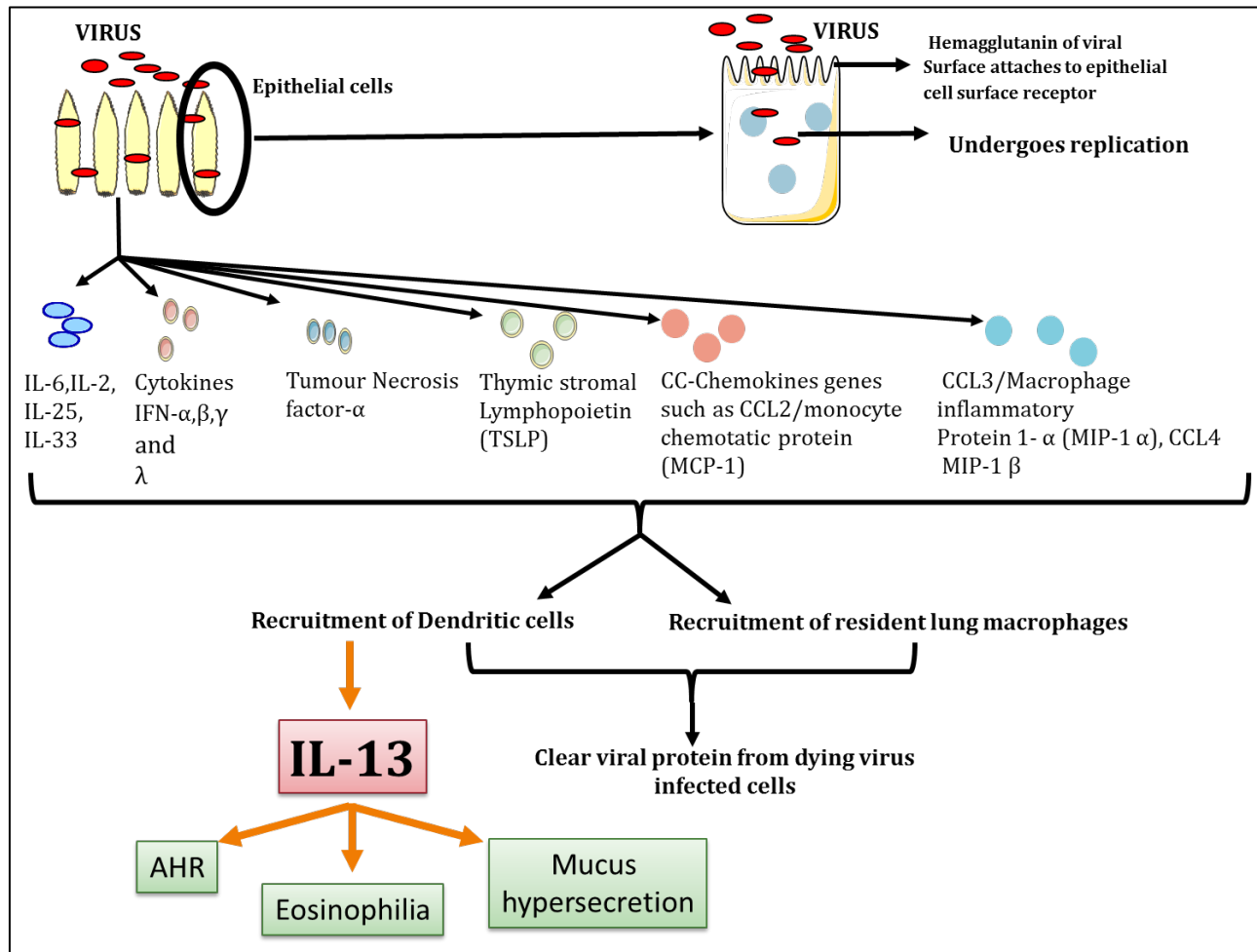


**Figure 3.2. Virus induces inflammatory cascades in airway epithelium.**

Adapted from reference <sup>[489]</sup>.

miRs are non-coding RNAs that regulate many biological processes including growth, apoptosis and immunity[527]. They exert their function at the post-transcriptional level by fine-tuning the expression of multiple target genes[527]. miR-21 is one of the best characterised and is implicated in a variety of inflammatory diseases and cancers[360, 528]. The role of miR-21 has been studied in murine AAD models[300, 306, 361, 529]. In severe asthma models, respiratory infection-induced miR-21 promotes steroid-insensitive airway inflammation and AHR. This occurs through the miR-21 downregulation of phosphatase and tensin homolog (PTEN), which increases phosphoinositide-3-kinase (PI3K) activity and leads to reduced histone deacetylase-2 levels that are necessary for steroid responsiveness[530]. Also, miR-21 expression is increased in serum of patients with mild to moderate COPD and asymptomatic smokers, compared to healthy controls, implicating its involvement in early pathogenesis[370]. miR-21 has been reported to be down-regulated in other pathological conditions such as cancer and myocardial infarction[531-533].

So far no investigations have assessed the role of IL-13/miR-21 signalling in predisposing to IAV infection in AAD and COPD. In the present investigation, we assessed the roles of IL-13 and miR-21 in the pathogenesis of IAV-induced exacerbations in AAD and COPD using mouse models that recapitulate the hallmark features of the respective disease. We identify a pathogenic role for the IL-13/miR-21 axis in IAV infections in AAD and COPD and define potential therapeutic interventions.

### **3.3. METHODS**

#### **3.3.1. Ethics Statement**

This study was performed in strict accordance with the recommendations in the Australian code of practice for the care and use of animals for scientific purposes issued by the National Health and Medical Research Council of Australia. All protocols were approved by the Animal Ethics Committees of The University of Newcastle.

### **3.3.2. Mice**

Six to eight-week old specific pathogen-free (SPF) female BALB/c mice were used in all the experiments. Animals were obtained from The University of Newcastle Animal Services Unit, the Animal Resources Centre (Perth, Australia) or Australian Bio Resources (Moss Vale, Australia) and were given access to food and water *ad libitum*. Animals were housed in individually ventilated cages in a specific pathogen-free facility with controlled environment of 12 h light and dark cycles.

### **3.3.3. Induction of AAD using Ova**

Existing data from our laboratory demonstrates that Ova-induced AAD increases susceptibility to influenza infection and that infection exacerbates the underlying AAD. Thus, the Ova-induced AAD model was used to investigate underlying mechanisms and potential therapeutic interventions. These studies can be further extended to additional models of AAD including HDM-induced AAD (Chapter 2), to determine if the effects are consistent in different models.

Mice were sensitised with 50 µg Ova (Sigma Aldrich) and 1 mg Rehydrogel (Reheis) in 200 µl sterile phosphate buffered saline (PBS) by intraperitoneal (i.p.) injection [534, 535]. Mice were then challenged i.n. with Ova (10 µg in 50 µl sterile PBS) under isofluorane anaesthesia 12-15 days later. Control mice received PBS sensitisation and Ova challenges [534, 535] (Figure.3.3).

### **3.3.4. Experimental COPD**

Six to eight-week old specific pathogen-free (SPF) female BALB/c mice were exposed to normal air or CS through the nose only for 8 weeks as previously described [264, 274, 418] (Figure 3.4)

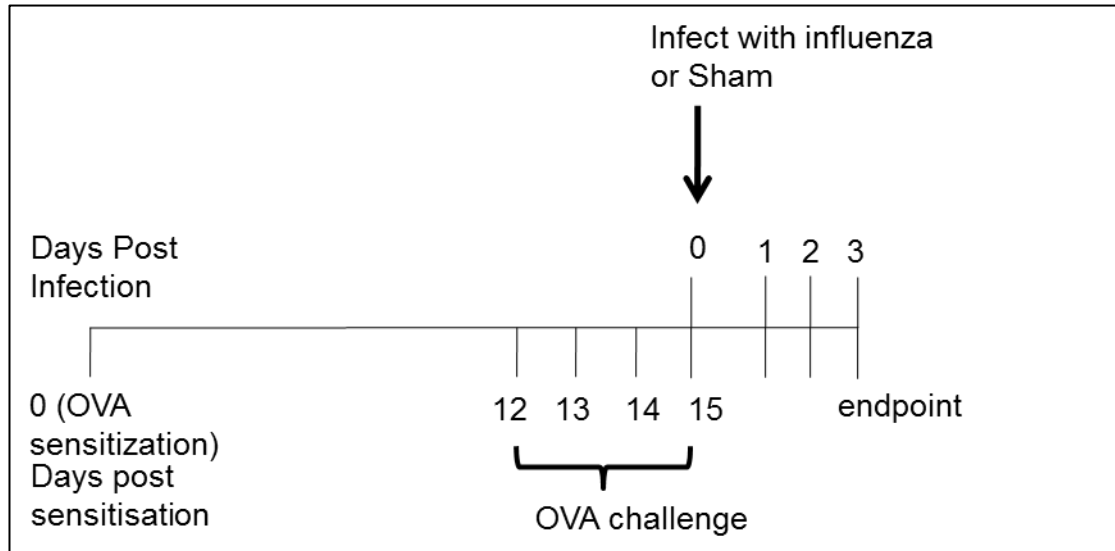


**Figure 3.3. Experimental protocol of Ova-induced AAD and IAV infection.**

BALB/c mice were sensitised with Ova or PBS, challenged with Ova and inoculated with IAV A/PR/8/34 (7.5 pfu) or media on the last day of Ova challenge. Mice were sacrificed 3 dpi.

### **3.3.5. IAV infection**

On the last day of Ova challenge or smoke-exposure, mice were anaesthetised with isofluorane and infected i.n. with 7.5 plaque forming unit (PFU) of the mouse-adapted IAV A/PR/8/34 (WHO Collaborating Centre for Reference and Research of Influenza, Victoria, Australia) in 50µl of media vehicle (UltraMDCK, Lonza, NJ, USA). Controls were sham-inoculated with media. Mice were sacrificed 3 dpi in AAD and 7 dpi in experimental COPD respectively (Figure 3.3-3.11).

### **3.3.6. Administration of rIL-13**

Mice were treated with 100 ng of murine rIL-13 (R&D systems, Gynea, Australia) in 30 µl sterile PBS i.n., once every 24 h, from the day before IAV infection (-1 dpi) through to 2 dpi. Mice were sacrificed 3 dpi. Controls were vehicle-treated with PBS [392] (Figure 3.5)

### **3.3.7. IAV infection in IL-13 deficient (<sup>-/-</sup>) mice**

To further investigate the effect of IL-13 in susceptibility to IAV infection we assessed infection in IL-13<sup>-/-</sup> mice. Wild-type (WT) and IL-13<sup>-/-</sup> mice were inoculated with IAV A/PR/8/34 (7.5 pfu) or media on day 0. Mice were sacrificed 3 dpi (Figure 3.6).

### **3.3.8. Treatment with dexamethasone (Dex) in AAD**

Some groups were treated with i.n. Dex (2 mg/kg, Sigma-Aldrich) on days 0, 1 and 2 dpi. Mice were sacrificed 3 dpi[536-538] (Figure 3.7).

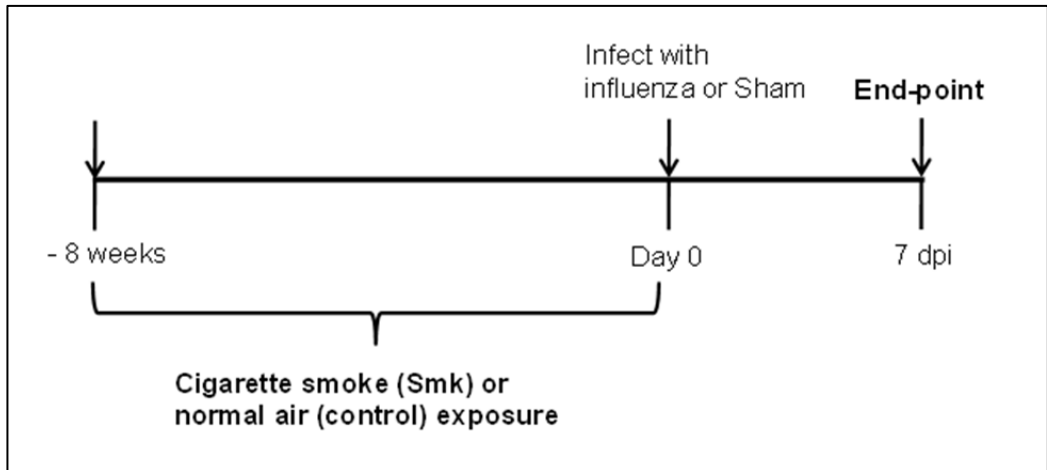


**Figure 3.4. Experimental protocol of cigarette smoke-induced COPD and IAV infection.**

BALB/c mice were exposed to CS or normal air for 8 weeks and inoculated with IAV A/PR/8/34 (7.5 pfu) or media on the last day of smoke exposure. Mice were sacrificed 7 dpi.

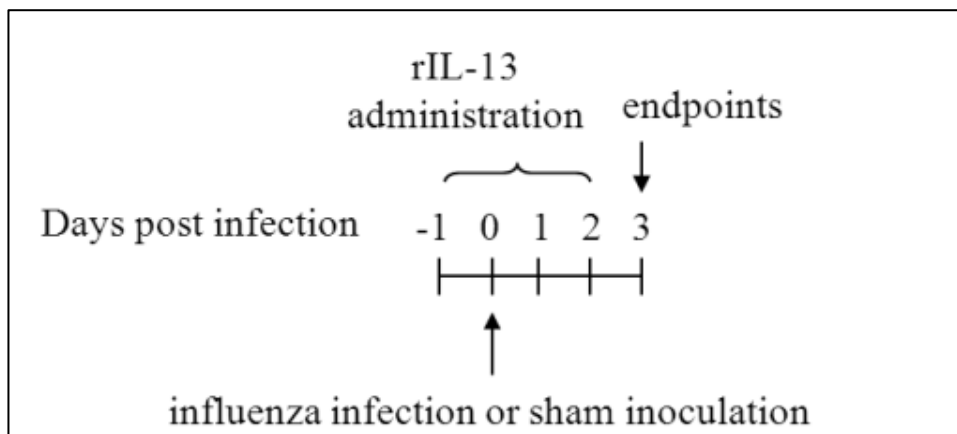


**Figure 3.5. Experimental protocol of rIL-13 treatment and IAV infection.**

BALB/c mice were administered rIL-13 one day prior to inoculation with IAV A/PR/8/34 (7.5 pfu) or media (at 0 dpi). rIL-13 administration was continued daily 2 dpi. Mice were sacrificed 3 dpi.

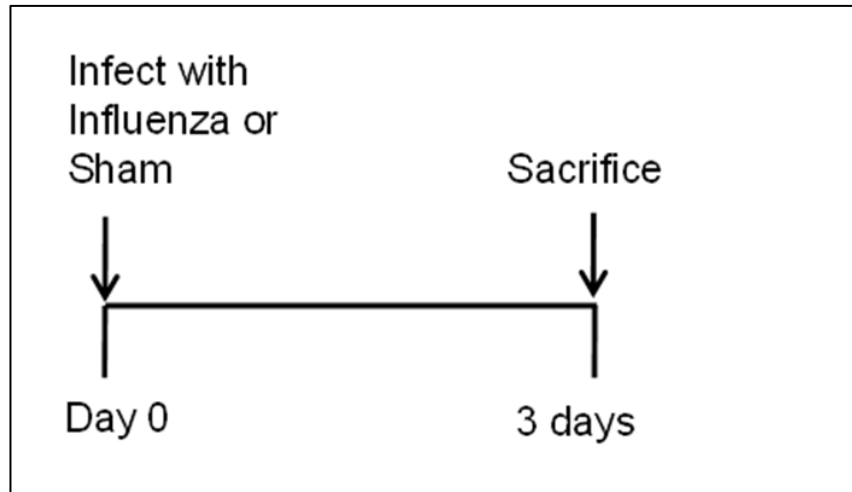


**Figure 3.6. Experimental protocol of IAV infection.**

Wild-type (WT) and IL-13<sup>-/-</sup> mice were inoculated with IAV A/PR/8/34 (7.5 pfu) or media on day 0. Mice were sacrificed 3 dpi.

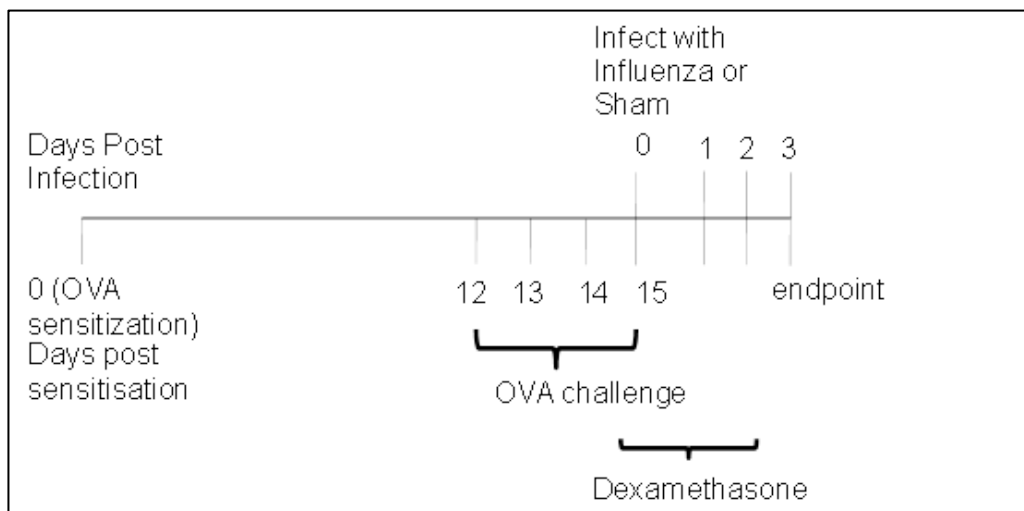


**Figure 3.7. Treatment with dexamethasone in Experimental AAD and IAV infection.**

BALB/c mice were sensitised with Ova or PBS, challenged with Ova and inoculated with IAV A/PR/8/34 (7.5 pfu) or media on the last day of Ova challenge. Mice were treated with dexamethasone (Dex) from 0 dpi till 2 dpi. Mice were sacrificed 3 dpi.

### 3.3.9. miR inhibition with antagomirs

The miR-21 sequence was downloaded from miRBase University of Manchester, UK (<http://www.mirbase.org/>). Ant-21 and scrambled antagomir control (Scram, nonspecific RNA VIII, BLAST searched against the mouse genome) were designed and purchased (Sigma-Aldrich). The sequence of Ant-21 was:

5'mU.\*.mC.\*.mA.mA.mC.mA.mU.mC.mA.mG.mU.mC.mU.mG.mA.mU.mA.mA.mG.\*.mC.\*.m U.\*.mA.\*.3'-Chl, where (m) denotes 2'-O-methyl-modified nucleotides, (\*) denotes phosphorothioate linkages, and (-Chl) denotes hydroxyprolinol-linked cholesterol. Groups of mice were treated with Ant-21 (50µg delivered in 50µL sterile saline i.n.) or an equivalent amount of Scram on day 0 in Ova-induced AAD and once a week from week 6 to week 8 in experimental COPD [362] (Figure 3.8 and 3.9)

### 3.3.10. PI3K inhibition

Groups were treated i.n. with the class I pan-PI3K inhibitor LY294002 (LY29, 2mg/kg, Selleck, 68 Houston, USA, in 3% dimethyl sulfoxide [DMSO] vehicle) from 0 to 2 dpi in Ova-induced AAD. Controls were treated with vehicle [143] (Figure 3.10).

### 3.3.11. Neutralisation of IL-13 in experimental AAD and COPD

Rabbit anti-murine IL-13 antibodies were kindly prepared and supplied by Professor Nick Lukacs, University of Michigan, USA [539]. These antibodies were produced by multiple-site immunisation of New Zealand White rabbits with murine rIL-13 (R&D Systems) and titred by direct ELISA. The antibodies were specifically verified by the failure to cross-react to these murine (m) and human (h) proteins: mL-3, mL-1α, mTNF, hTNF, mL-4, hIL-13, mL-10, mL-12, mMIP-1α, hMIP-1α, hMIP-1β mMIP-1β IL-6, mMCP-1, hMCP-1, hIL-8, and hRANTES. The *in vivo* half-life of the antibody was 30 h.

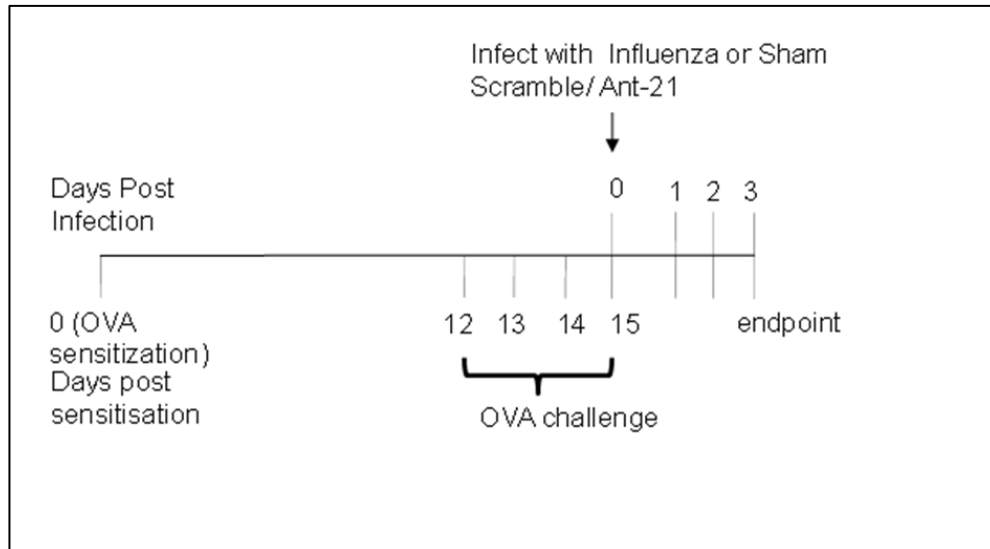


**Figure 3.8. Treatment with anti-miR-21 (Ant-21) in Experimental AAD and IAV infection.**

BALB/c mice were sensitised with Ova or PBS, challenged with Ova and inoculated with IAV A/PR/8/34 (7.5 pfu) or media on the last day of Ova challenge. Mice were treated with Ant-21 or scrambled control on 0 dpi. Mice were sacrificed 3 dpi.

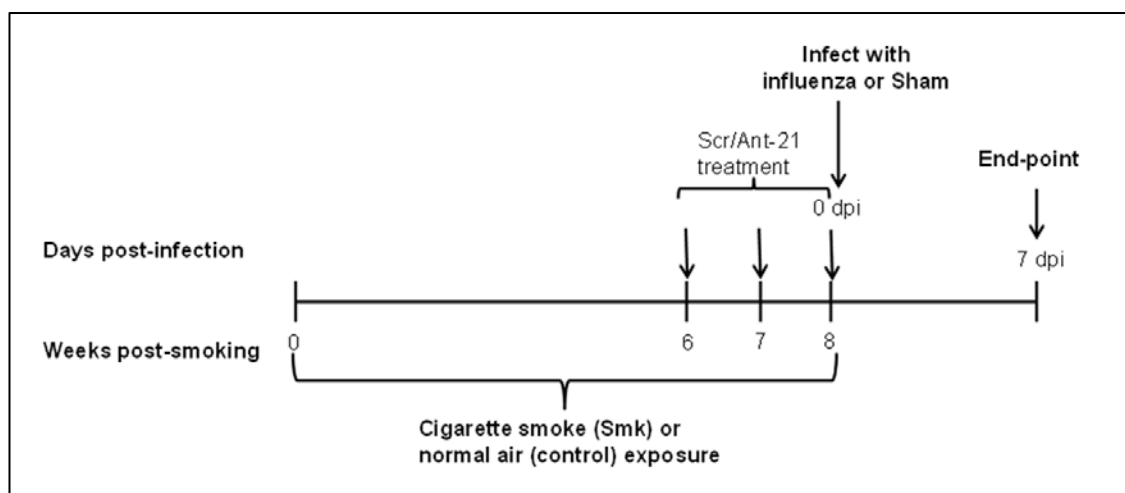


**Figure 3.9. Treatment with anti-miR-21 (Ant-21) in Experimental COPD and IAV infection.**

BALB/c mice were exposed to CS or normal air for 8 weeks and inoculated with IAV A/PR/8/34 (7.5 pfu) or media on the last day of smoke exposure. Mice were treated with Ant-21 or scrambled control once a week from week 6 till week 8. Mice were sacrificed 7 dpi.

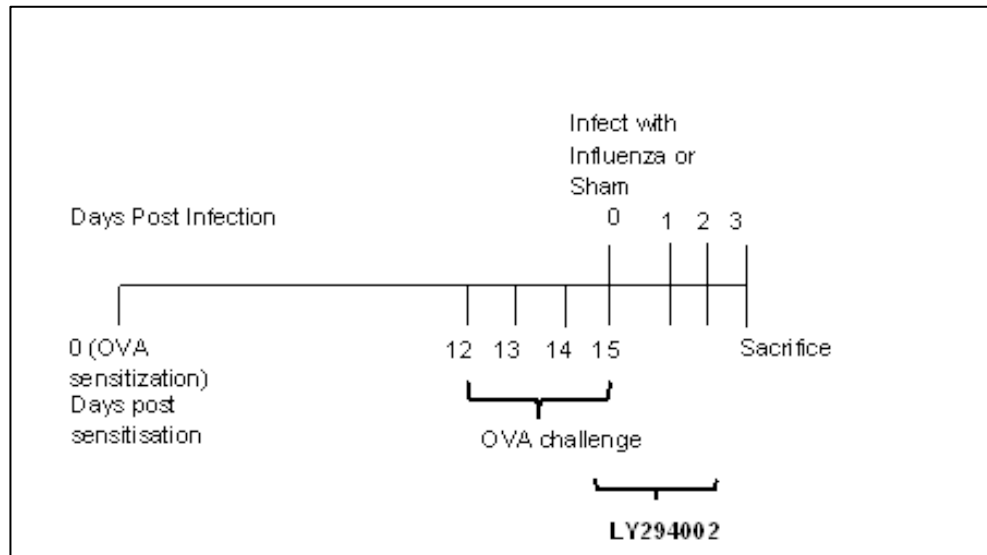


**Figure 3.10. Treatment with LY29 in experimental AAD and IAV infection.**

BALB/c mice were sensitised with Ova or PBS, challenged with Ova and inoculated with IAV A/PR/8/34 (7.5 pfu) or media on the last day of Ova challenge. Mice were treated with LY29 or vehicle from 0 dpi till 2 dpi. Mice were sacrificed 3 dpi.

Mice were administered intra-peritoneal (i.p) anti-IL-13 antibody or an equivalent amount of isotype (controls) from 0 dpi till 2 dpi. Mice were sacrificed 3 dpi in experimental AAD (Figure 3.11).

While in experimental COPD, mice were administered intra-peritoneal (i.p) anti-IL-13 antibody or an equivalent amount of isotype (controls) on day 0, 2, 4 and 6 dpi. Mice were sacrificed at 7 dpi (Figure 3.12).

### **3.3.12. Plaque assay**

Madin-Darby Canine Kidney (MDCK) cells were grown until approximately 70% confluent. The cells were then washed three times with Dulbecco's phosphate buffered saline (DPBS; Sigma Aldrich). The cells were submerged in Leibovitz's L-15 (L-15) medium (Invitrogen) supplemented with 2- [4-(2-hydroxyethyl) piperazin-1-yl] ethanesulphonic acid (HEPES, Invitrogen) and N-p-tosyl-L-phenylalanine chloromethyl ketone-treated trypsin (trypsin-TPCK, Invitrogen). BALF was collected, serially diluted in L-15 medium, which had been supplemented with HEPES, and added to MDCK cells. After 60 minutes of incubation (37°C, 5% CO<sub>2</sub>), the inocula were removed. A thin overlay of 1.8% agarose in L-15 medium containing trypsin-TPCK was placed onto the cell monolayers. After 48 h of incubation (37°C, 5% CO<sub>2</sub>), plaques were stained with 0.1% crystal violet and counted [190, 371, 414, 415].

### **3.3.13. Histopathology**

Lungs were formalin fixed, embedded and sectioned. Longitudinal sections were stained with H&E (for histopathology), periodic acid-Schiff (PAS-for MSC numbers) or Lendrum's carbolchromotrope (for eosinophils). Histopathology (tissue-inflammation) was scored in a blinded fashion according to a set of custom-designed criteria (Table 2.1). Eosinophils and MSC numbers were enumerated in inflamed airways as previously described [416].

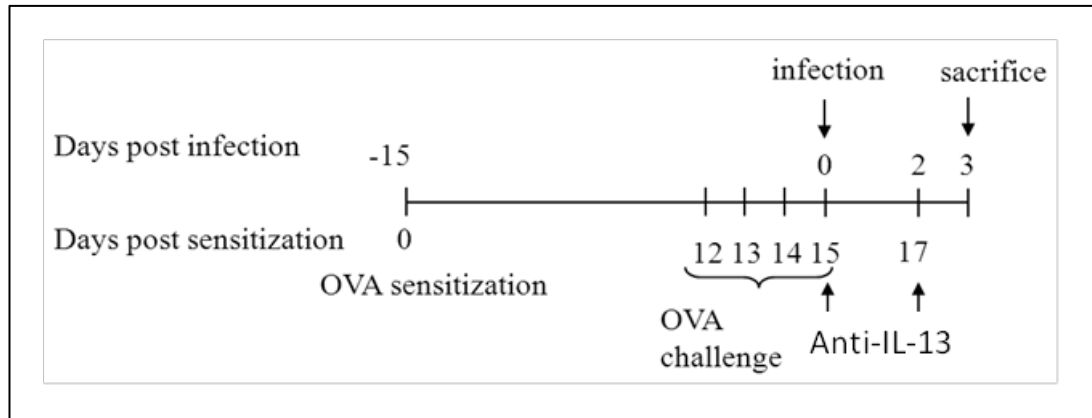


**Figure 3.11. Treatment with anti-IL-13 in experimental AAD and IAV infection.**

BALB/c mice were sensitised with Ova or PBS, challenged with Ova and inoculated with IAV A/PR/8/34 (7.5 pfu) or media on the last day of Ova challenge. Mice were treated with anti-IL-13 antibody or isotype from 0 dpi till 2 dpi. Mice were sacrificed 3 dpi.

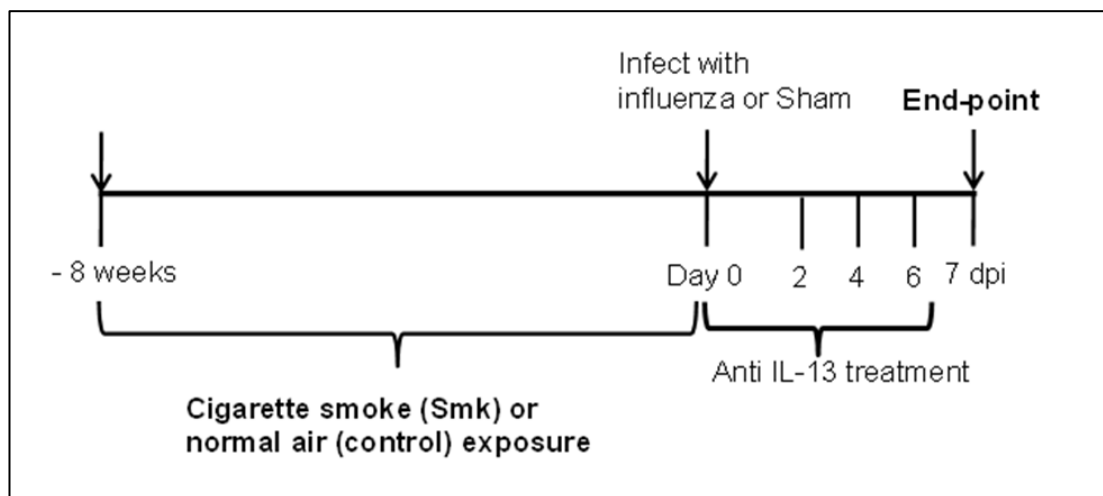


**Figure 3.12. Treatment with anti-IL-13 treatment in experimental COPD and IAV infection.**

BALB/c mice were exposed to CS or normal air for 8 weeks and inoculated with IAV A/PR/8/34 (7.5 pfu) or media on the last day of smoke exposure. Mice were treated anti-IL-13 antibody or isotype on day 0, 2, 4 and 6 dpi. Mice were sacrificed 7 dpi.

### **3.3.14. Cytokine concentrations in lungs**

Protein concentrations in BALF supernatants were determined for IL-13 using mouse DuoSet ELISA kits (R&D systems, Minneapolis, USA) according to the manufacturer's instructions.

### **3.3.15. Total RNA extraction**

Total RNA was extracted from whole lungs by guanidinium thiocyanate phenol chloroform (TRIzol) extraction[417]. Lung tissues harvested from mice were stored in RNA Stabilisation Reagent, RNAlater (Qiagen, Chadstone Centre, Australia) prior to extraction. Tissues were transferred into 5 ml tubes containing 1 ml of TRIzol solution (Ambion, Thermo Fisher Scientific), carefully ensuring minimal RNAlater carry over. Tissues were then homogenised at 4°C, transferred to 1.5 ml microcentrifuge tubes and centrifuged (12,000xg, 10 minutes, 4°C). The clear homogenates were then transferred into fresh microcentrifuge tubes and supplemented with 250 µl chloroform to separate RNAs from proteins. The microcentrifuge tubes were then pulse-vortexed for approximately 5 seconds, until the solutions were homogenous. Solutions were incubated at room temperature for 10 minutes before being centrifuged (12,000xg, 15 minutes, 4°C). The resulting aqueous phase was then transferred into fresh 1.5 ml microcentrifuge tubes and supplemented with 500 µl of cold isopropyl alcohol to precipitate the RNA. The solutions were again pulse-vortexed, incubated (room temperature, 10 minutes), and centrifuged at (12 000xg, 10 minutes, 4°C). Supernatants were discarded and the RNA pellets were washed with 1 ml of 75% (v/v) ethanol. The solutions were then pulse-vortexed to dislodge the pellets and to wash out trapped contaminants and centrifuged (7,500xg, 5 minutes, 4°C). A second wash was performed to remove any carbohydrate/phenol-based contaminants. Pellets were then allowed to air dry (15 minutes, 4°C). Pellets were eventually resuspended with 75-100 µl nuclease free water (Ambion, Thermo Fisher Scientific). The concentration of mRNA was measured using a NanoDrop Spectrophotometer (ND-1000, v3.8.0 Bio Lab, NanoDrop Technologies, DE, USA).

### **3.3.16. Reverse transcription**

1000 ng of RNA in 8 µl of nuclease free water (Ambion) was prepared to generate complementary DNA (cDNA). mRNA samples were mixed with 1 µl of 10X reaction buffer (Bioline, Alexandria, Australia) and 1 µl of amplification grade DNase I (Sigma Aldrich) and were incubated (room temperature, 15 minutes). 1 µl of DNase Stop Solution (Sigma Aldrich) was added into the mixture, and the samples were heated at 65°C for 10 minutes to inactivate and denature the DNase I. The samples were then added with 2 µl of 50 ng/ml random hexamer primers (Invitrogen) and 1 µl of 2.5mM dNTPs (Invitrogen), and incubated (5 minutes, 65°C). The samples were allowed to cool to 25°C, and 4 µl of 5X reaction buffer, 1 µl of DTT (Bioline), 1 µl of nuclease free water, and 1 µl of Bioscript (Bioline) were added. The samples were then heated at 25°C for 20 minutes, 42°C for 50 minutes and 70°C for 15 minutes. The samples were finally resuspended with 500 µl of nuclease free water.

### **3.3.17. Quantitative real-time Polymerase Chain Reaction (qPCR)**

qPCR was performed to determine the relative abundance of cDNA in samples compared to the reference gene HPRT. qPCR cycles were performed using a Mastercycler Eppendorf RealPlex 2 System (Eppendorf South Pacific, North Ryde, Australia) or ViiA 7 Real-Time PCR System (Life Technologies, Thermo Fisher Scientific). Sample cDNA (2 µl) was added to a mixture containing 3 µl SYBR Green and ROX as a passive reference dye (SYBR Green ERTM reagent system, Invitrogen), 0.5 µl (10 µM) of each forward and reverse primers (Integrated DNA Technologies, Baulkham Hills, Australia, Table 3.1) and 4 µl of nuclease free water (Ambion), to make a total of 10 µl reaction volume.

Cycling conditions used for Mastercycler Eppendorf RealPlex 2 System were: holding stages at 50 °C for 2 minutes and 95 °C for 2 minutes; cycling stages at 95 °C for 15 seconds and 60 °C (variable) for 30 seconds (cycling stages were repeated for 40 cycles); melt curve/dissociation stages at 95 °C for 15 seconds, 60 °C (variable) for 15 seconds, 95 °C for 8 minutes and 95 °C for 15 seconds. Cycling conditions used for ViiA 7 Real-Time PCR System were: holding stage at 95 °C for 30 seconds; cycling stages at 95 °C for 15 seconds and 60 °C

(variable) for 30 seconds (cycling stages were repeated for 40 cycles); melt curve/dissociation stages at 95 °C for 15 seconds, 60 °C (variable) for 15 seconds and 95 °C for 15 seconds. The threshold value (Ct value) for each sample was measured as the number of cycles needed for the specific fluorescent signals to cross “threshold”, which is a value that is set above the background levels of fluorescence (background “noise”). The Ct value from each gene was normalised against the constant housekeeping gene: the HPRT gene.

**Table 3.1. Custom designed primers used in qPCR analysis**

Primer	Forward (5'→3')	Reverse (5'→3')
HPRT	AGG CCA GAC TTT GTT GGA TTT GAA	CAA CTT GCG CTC ATC TTA GGC TTT
U6	CGGCAGCACATATACTAAAATT GG	GCCATGCTAATCTTCTCTGTAT C
U49	ATCACTAATAGGAAGTGCCGT C-	ACAGGAGTAGTCTTCGTCAGT
miR-21	T+AGCTTATCAGACTG <sup>1</sup>	GTAAAACGACGGCCAGTTCAA CAT
IL-13R $\alpha$ 1	CAC AGT CAG AGT AAG AGT CAA AAC A	ATG GTG GTG TAG AAG GTG GA

<sup>1</sup> LNATM-modified bases are preceded by a [+] symbol

### 3.3.18. Lung function

AHR was measured in anaesthetised mice using whole body invasive plethysmography (Buxco electronics, Sharon, Connecticut, USA) by determination of the peak of transpulmonary resistance in response to increasing doses of nebulised methacholine (Sigma-Aldrich) as previously described[210, 211].

### 3.3.19. Airway remodelling

Lungs were formalin fixed, embedded and sectioned. Longitudinal sections were stained with H&E, Verhoff's-Van Gieson (VVG) stain (Australian Biostain)

or Masson's Trichrome. Airway epithelial area ( $\mu\text{m}^2$ ) and area of collagen deposition ( $\mu\text{m}^2$ ) was assessed in a minimum of four small airways (basement membrane (BM) perimeter  $<1000 \mu\text{m}$ ) per section[264, 274, 418]. Data were normalised to BM perimeter ( $\mu\text{m}$ ) and quantified using ImageJ software (Version 1.49h, NIH, New York City, USA).

### **3.3.20. Immunohistochemistry**

Lungs were perfused, inflated, formalin-fixed, paraffin-embedded and sectioned (4-6 $\mu\text{m}$ ). Longitudinal sections of the left lung were incubated with primary antibody (anti-IL13R $\alpha$ 1, Abcam, Melbourne, Victoria, Australia) overnight at 4°C, followed by anti-rabbit horseradish peroxidase-conjugated secondary antibody (R&D Systems) as per the manufacturer's instructions. 3,3'-diaminobenzidine chromogen-substrate buffer (DAKO, North Sydney, New South Wales, Australia) was applied to sections and incubated. Sections were counterstained with haematoxylin, mounted and analysed with a BX51 microscope (Olympus, Tokyo, Shinjuku, Japan) and Image-Pro Plus software (Media Cybernetics, Rockville, MD).

### **3.3.21. miR *in situ* hybridization (ISH)**

miR-21 was localised in histological sections of formalin-fixed, paraffin-embedded lungs using a miRCURY LNATM miR ISH optimisation kits (miR-21, Exiqon, Vedbæk, Denmark) in accordance with the manufacturer's protocol. Briefly, lung sections were de-paraffinised, rehydrated in an ethanol:RNase free water gradient, protease-treated (15 $\mu\text{g}/\text{mL}$  of Proteinase K, 10 minutes, proteinase K buffer), washed in PBS, dehydrated in ethanol, air dried, and pre-hybridised in 1xISH buffer (55°C, 1 hr) in a humidifying chamber. miR-21-specific, and scrambled (negative control), double-digoxigenin (DIG) LNATM probes (40 nM) were then applied to the lung sections and hybridised at 55°C overnight in a humidifying chamber. Hybridised sections were then washed (5x-0.2x saline-sodium citrate [SSC] buffer gradient) and blocked (2% lamb serum in PBS-Tween [PBS-T, 0.1% Tween20, Ajax, Finechem, NSW, Australia]) at room temperature (RT) for 15 min. Sheep-anti-DIG antibody conjugated with alkaline phosphatase (AP, Roche, Life Science, Australia, 1:800 in 2% lamb

serum in PBS-T) was then applied to the sections and probe;target complexes were detected with an AP substrate solution (containing BM Purple [1:3, Roche, Life Science] and Levamisole [endogenous AP activity inhibitor, 0.2 mM, Sigma-Aldrich]) that produces a dark blue precipitate in the presence of AP activity. Nuclear Fast Red™ (Vector laboratories, CA, USA) was used as a counterstain [215].

### **3.3.22. Flow cytometry**

Numbers of NKT cells, CD4<sup>+</sup> T cells and CD8<sup>+</sup> T cells in lung homogenates were determined based on surface marker expression using flow cytometry (Table 3.2) (126, 128, 131, 430). Flow cytometric analysis was performed using a FACSAriaIII with FACSDiva software (BD Biosciences, North Ryde, Australia). Flow cytometry antibodies were from Biolegend (Karrinyup, Western Australia, Australia) (Table 3.3). OneComp compensation beads (eBioscience) were used to set up assays.

### **3.3.23. Statistical analyses**

Data were expressed as mean  $\pm$  standard error of mean (SEM) with 6-8 mice in each group and are representative of at least two or more independent experiments. Non-normally distributed data were analysed using non-parametric equivalents and summarised using the median and inter-quartile range. Comparisons between two groups were made using a two-tailed Mann-Whitney Test. Multiple comparisons were made using one-way ANOVA with Tukey's post-test, or Kruskal-Wallis with Dunn's post-test, where non-parametric analyses were appropriate. Analyses were performed using GraphPad Prism Software version 6 (GraphPad Software, CA, USA). A p-value of  $< 0.05$  was considered significant.

**Table 3.2. Surface antigens used to characterise mouse lung cell subsets by flow cytometry**

Cell subset	Cell surface antigens
ILC2	CD45 <sup>+</sup> Lin <sup>-</sup> CD90.2 <sup>+</sup> CD2 <sup>-</sup> IL-7R $\alpha$ <sup>+</sup> CD25 <sup>+</sup> IL-33R $\alpha$ <sup>+</sup>
NKT cell	CD45 <sup>+</sup> CD3 <sup>+</sup> $\alpha$ GalCer tetramer <sup>+</sup>
CD4 <sup>+</sup> T cell	CD45 <sup>+</sup> CD3 <sup>+</sup> CD4 <sup>+</sup> CD8 <sup>-</sup> $\gamma\delta$ TCR <sup>-</sup>
CD8 <sup>+</sup> T cell	CD45 <sup>+</sup> CD3 <sup>+</sup> CD4 <sup>+</sup> CD8 <sup>-</sup> $\gamma\delta$ TCR <sup>-</sup>

ILC2: type 2 innate lymphoid cell;  $\gamma\delta$  T-cells: gamma delta T cells; NKT cell: natural killer T-cell

**Table 3.3. Antibody used in flow analysis**

Cell Surface Antigen	Clone	Fluorophore	Company
CD45	30-F11	PerCPCy5.5	Biolegend
CD4	RM4-5	APC-Cy7	Biolegend
CD8a	53-6.7	BV510	Biolegend
$\gamma\delta$ TCR	GL3	BV421	Biolegend
CD3	17A2	AF700	Biolegend
CD90.2	30-H12	APC/Cy7	Biolegend
IL-33R $\alpha$	DIH9	APC	Biolegend
IL-7R $\alpha$	A7R34	BV605	Biolegend

$\gamma\delta$ TCR: gamma delta T cells receptor; IL-33R $\alpha$ : IL-33 receptor alpha; IL-7R $\alpha$ : IL-7 receptor alpha

## 3.4. RESULTS

### 3.4.1. Allergic airway inflammation increases the severity of IAV infection consequently exacerbating the underlying AAD

We investigated whether AAD predisposes to severe IAV infection, using an Ova-induce AAD disease model. In this model, specific pathogen-free BALB/c mice were sensitised by i.p. administration of Ova or PBS and subsequently

challenged i.n. with Ova 12-15 days later. On the last day of Ova challenge, mice were infected i.n. with IAV A/PR/8/34 (7.5 pfu) or media. Mice were sacrificed 3 dpi (Figure 3.3).

Preliminary studies showed a significant increase in viral titre in infected mice with AAD (Ova+PR8) at 3 dpi compared with infected non-allergic controls (PR8) (Figure 3.13A). This indicates that the presence of AAD predisposes to more severe IAV infection. Also at 3dpi, non-infected allergic mice (Ova) had increased histopathological score indicative of increased lung tissue inflammation compared to sham-inoculated non-allergic controls (Sham). Infected non-allergic mice (PR8) also had increased histopathological scores compared to sham-inoculated non-allergic controls. Infected mice with AAD (Ova+PR8) had increased histopathological scores compared to both sham-inoculated allergic and infected non-allergic controls (Figure 3.13B and C).

Sham-inoculated allergic mice (Ova) also had higher numbers of lung eosinophils compared with sham-inoculated non-allergic controls (Sham). Infected mice with AAD had the highest number of lung eosinophils compared to sham-inoculated allergic controls and infected non-allergic mice (Figure 3.13D). Non-infected allergic mice had increased numbers of MSCs around the airways compared with non-infected non-allergic controls. Infected mice with AAD also had the highest number of MSCs compared with both sham-inoculated allergic controls and infected non-allergic mice (Figure 3.13E and F).

In sham-inoculated allergic controls Ova challenge induced AHR with increased transpulmonary resistance compared to sham-inoculated non-allergic controls. In infected non-allergic groups, IAV infection also induced an increase in the transpulmonary resistance compared to sham-inoculated non-allergic controls. Again infected mice with AAD had significantly higher transpulmonary resistance compared with infected non-allergic or sham-inoculated allergic controls (Figure 3.13G).

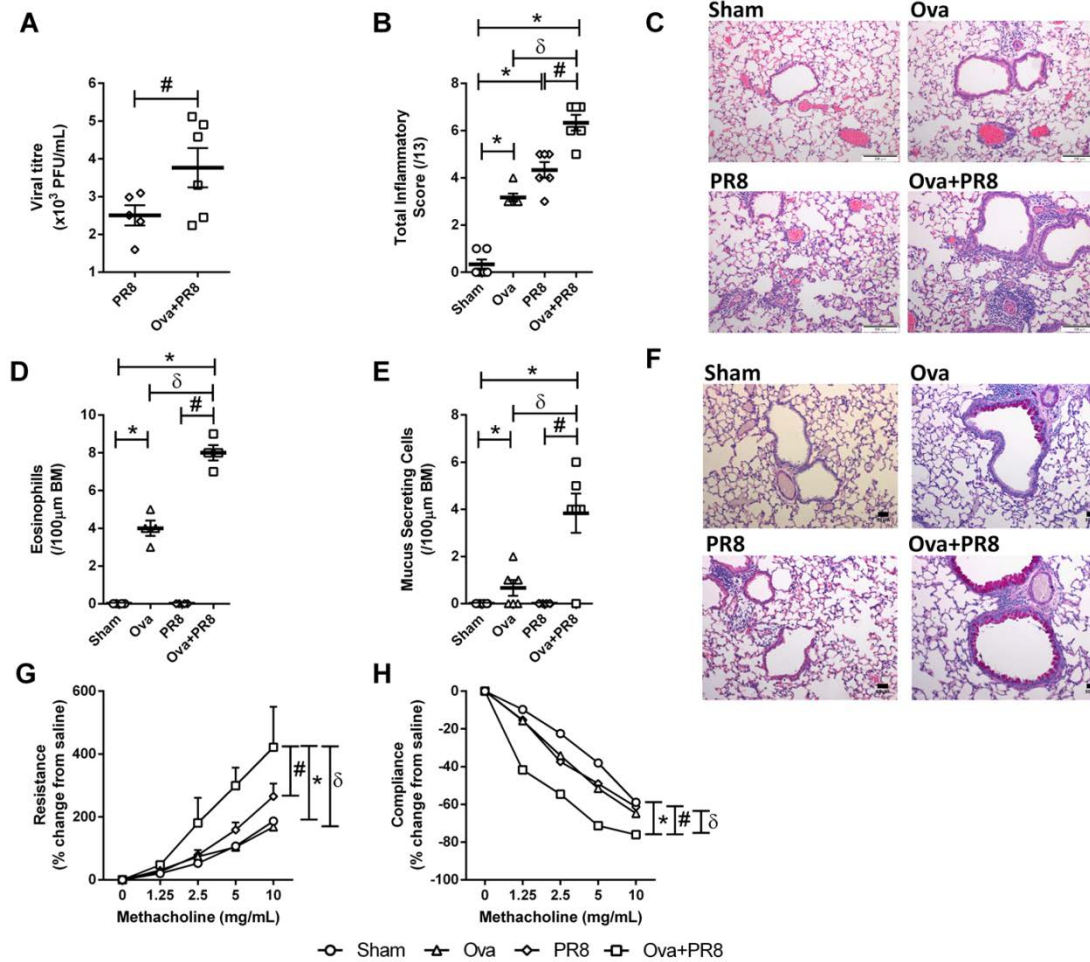


Figure 3.13. Ova-induced AAD promotes severe IAV infection.

BALB/c mice were sensitised with Ova or PBS, challenged with Ova and inoculated with IAV A/PR/8/34 (7.5 pfu) or media on the last day of Ova challenge. Mice were sacrificed 3 dpi. **(A)** Viral titre at 3 dpi; **(B)** Total inflammatory score in haematoxylin and eosin (H&E) stained lung sections; **(C)** Representative images (10X) of H&E stained lung sections; Scale bar = 200  $\mu$ m; **(D)** Numbers of tissue eosinophils; **(E)** MSCs per 100 $\mu$ m basement membrane (BM) in periodic acid-Schiff (PAS) stained lung sections; **(F)** Representative images (20X) of PAS stained lung sections; Scale bar = 50  $\mu$ m; **(G)** Transpulmonary resistance and **(H)** dynamic compliance. Data are presented as mean  $\pm$  SEM (n=6-8); \*, # and  $\bar{\delta}$  represents  $P \leq 0.05$  versus Sham, PR8 and Ova groups, respectively.

Moreover, in sham-inoculated allergic controls, Ova challenge reduced dynamic compliance compared to sham-inoculated non-allergic controls. In the infected non-allergic group, IAV infection also reduced dynamic compliance compared to sham-inoculated non-allergic controls. Infected mice with AAD had significantly reduced dynamic compliance compared to infected non allergic or sham-inoculated allergic controls (Figure 3.13H).

These results matched those made in HDM-induced AAD with IAV infection including increased viral titre (Figure 2.2), lung tissue inflammation (Figure 2.3A-E), number of mucus secreting cells (Figure 2.4) and eosinophils (Figure 2.5) and AHR (Figure 2.9) in infected allergic groups compared to infected non-allergic controls.

### **3.4.2. IL-13 drives susceptibility to IAV infection in mice**

To determine if IL-13 contributes to AAD and increases susceptibility to IAV infection, we performed further investigations where BALB/c mice were administered rIL-13 i.n. one day prior to inoculation with IAV A/PR/8/34 (7.5 pfu) or media (at 0 dpi). rIL-13 administration was continued daily until 2 dpi. Mice were sacrificed 3 dpi (Figure 3.5).

We found a significant increase in viral titre in rIL-13 administered IAV infected mice (rIL-13+PR8) at 3 dpi compared to untreated infected controls (PR8) (Figure 3.14A), indicating that rIL-13 predisposes to severe IAV infection in the lung. rIL-13 treated mice (rIL-13) mice exhibited increased lung tissue inflammation compared with sham-treated controls (Sham). Infected non-treated mice (PR8) had increased histopathological scores compared to sham-inoculated controls. rIL-13 treated infected mice (rIL-13+PR8) had increased histopathological scores compared with both rIL-13 treated or infected controls (Figure 3.14B and C).

Additionally, rIL-13 treated mice had higher numbers of lung eosinophils compared to sham-treated or infected controls. Numbers were even greater in the rIL-13 treated and infected group (Figure 3.14D). Furthermore, rIL-13

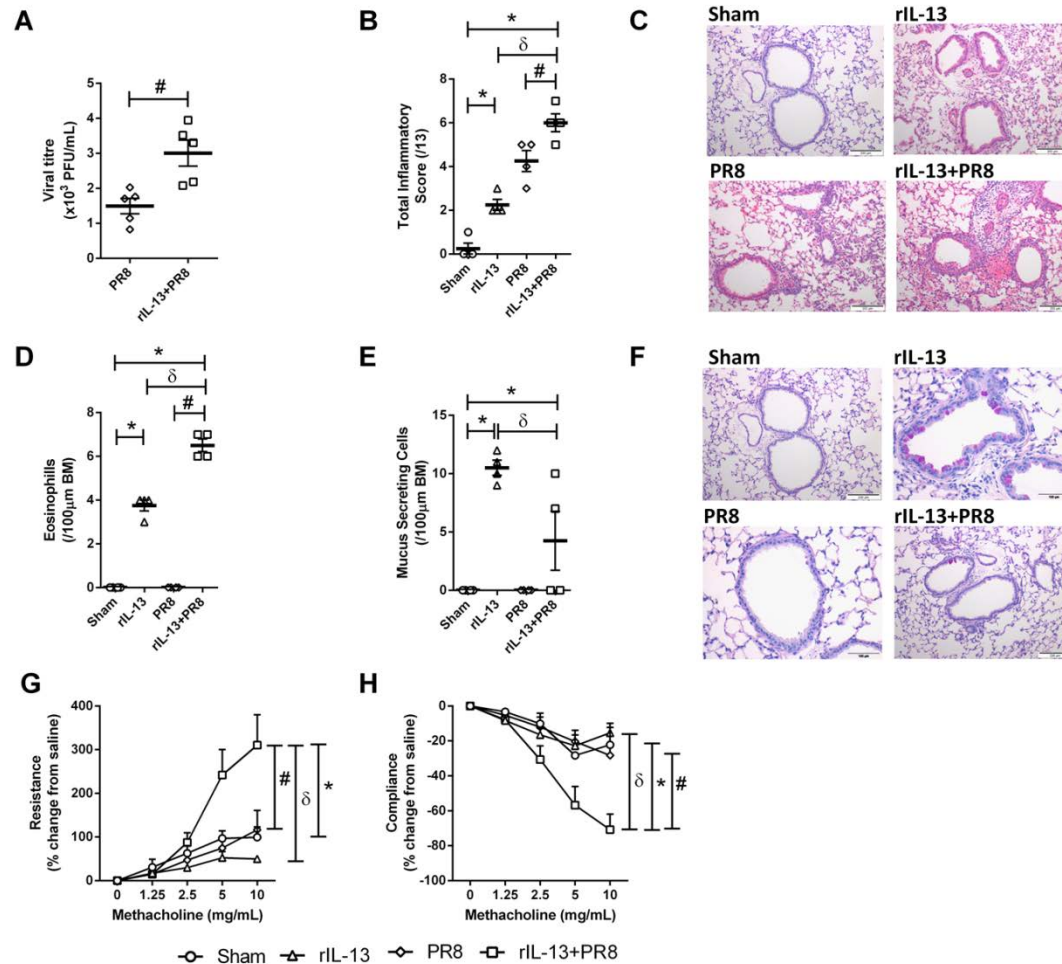


Figure 3.14. Administration of recombinant IL-13 (rIL-13) promotes severe IAV infection and AAD.

BALB/c mice were administered with rIL-13 one day prior to inoculation with IAV A/PR/8/34 (7.5 pfu) or media (at 0 dpi). rIL-13 administration was continued till 2 dpi. Mice were sacrificed 3 dpi. **(A)** Viral titre at 3 dpi; **(B)** Total inflammatory score in haematoxylin and eosin (H&E) stained lung sections; **(C)** Representative images (10X) of H&E stained lung sections; Scale bar = 200  $\mu$ m; **(D)** Numbers of tissue eosinophils; **(E)** MSCs per 100 $\mu$ m basement membrane (BM) in periodic acid-Schiff (PAS) stained lung sections; **(F)** Representative images (20X) of PAS stained lung sections; Scale bar = 200  $\mu$ m; **(G)** Transpulmonary resistance and **(H)** dynamic compliance. Data are presented as mean  $\pm$  SEM (n=4-8); \*, # and  $\delta$  represents  $P \leq 0.05$  versus Sham, PR8 and rIL-13 groups, respectively.

treated mice had increased numbers of MSCs around the airways compared to other controls. Infected mice treated with rIL-13 had lesser number of MSCs compared with rIL-13 treated controls (Figure 3.14E and F). Importantly, rIL-13 treated and infected mice demonstrated an increased transpulmonary resistance and decreased dynamic compliance compared to all control groups (Figure 3.2G and H). To confirm that IL-13 is a likely mechanism driving more severe infection and AAD (increased viral titre, MSCs, eosinophils and AHR), we assessed the levels of IL-13 and its receptor (IL-13R $\alpha$ 1) in Ova-induced AAD mice lung tissues.

At 3dpi, in sham-inoculated allergic (Ova) controls, AAD lead to increases in IL-13 protein levels in BALF compared to sham-inoculated non-allergic controls (Sham, Figure 3.15A). In infected non-allergic mice (PR8), no increase in IL-13 protein was detected. Importantly, infected mice with AAD (Ova+PR8) had increased levels of IL-13 compared with infected non-allergic, but not sham-inoculated allergic controls. These results show that IAV infection does not induce IL-13 in non-allergic mice, but increases IL-13 levels in AAD.

IL-13R $\alpha$ 1 mRNA expression was also increased in sham-inoculated allergic controls compared with sham-inoculated non-allergic controls. Both infected non-allergic and infected mice with AAD had more substantial increases in IL-13R $\alpha$ 1 mRNA levels (Figure 3.15B and C). Localization of IL-13R $\alpha$ 1 in lung tissues was observed using IHC where IL-13R $\alpha$ 1 expression was observed to be increased in the airway epithelium of infected mice with AAD compared to controls. Also, sham-inoculated allergic controls showed an increased trend in IL-13R $\alpha$ 1 expression in airway epithelium as compared with sham-inoculated non-allergic controls (Figure 3.15D). Similarly, mice with HDM-induced AAD also had increased IL-13 levels (Figure 2.6A) and IL-13R $\alpha$ 1 expression (Figure 2.6B) in their lungs.

Increased IL-13 (Figure 3.16A) and IL-13R $\alpha$ 1 (Figure 3.16B) expression was also observed in rIL-13 treated mice when compared to sham-inoculated controls and also in the rIL-13 infected mice compared to infected controls.

These results show that IAV infection in AAD increased IL-13 protein levels, and the expression of its receptor, IL-13R $\alpha$ 1.

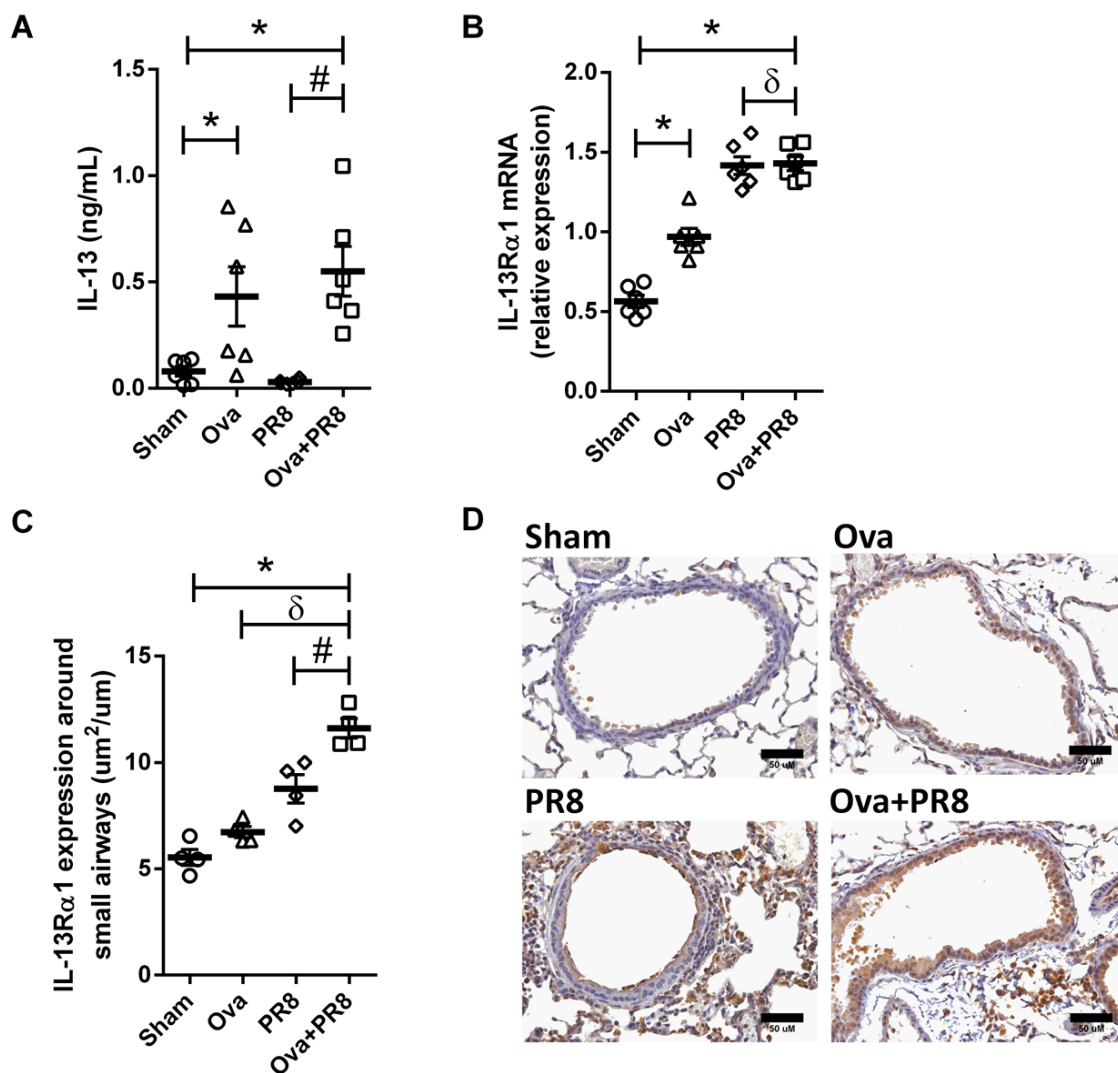


**Figure 3.15. IAV infection increases IL-13 and IL-13R $\alpha$ 1 expression in lungs in Ova-induced AAD.**

BALB/c mice were sensitised with Ova or PBS, challenged with Ova and inoculated with IAV A/PR/8/34 (7.5 pfu) or media on the last day of Ova challenge. Mice were sacrificed 3 dpi. **(A)** IL-13 protein expression in lung homogenate; **(B)** IL-13R $\alpha$ 1 mRNA; **(C)** IHC of IL-13R $\alpha$ 1 expression around small airways and **(D)** Representative images (40X) of IL-13R $\alpha$ 1 stained lung tissue sections. Data are presented as mean $\pm$ SEM (n=6); \*, # and  $\delta$  represents  $P \leq 0.05$  versus Sham, PR8 and Ova groups respectively.

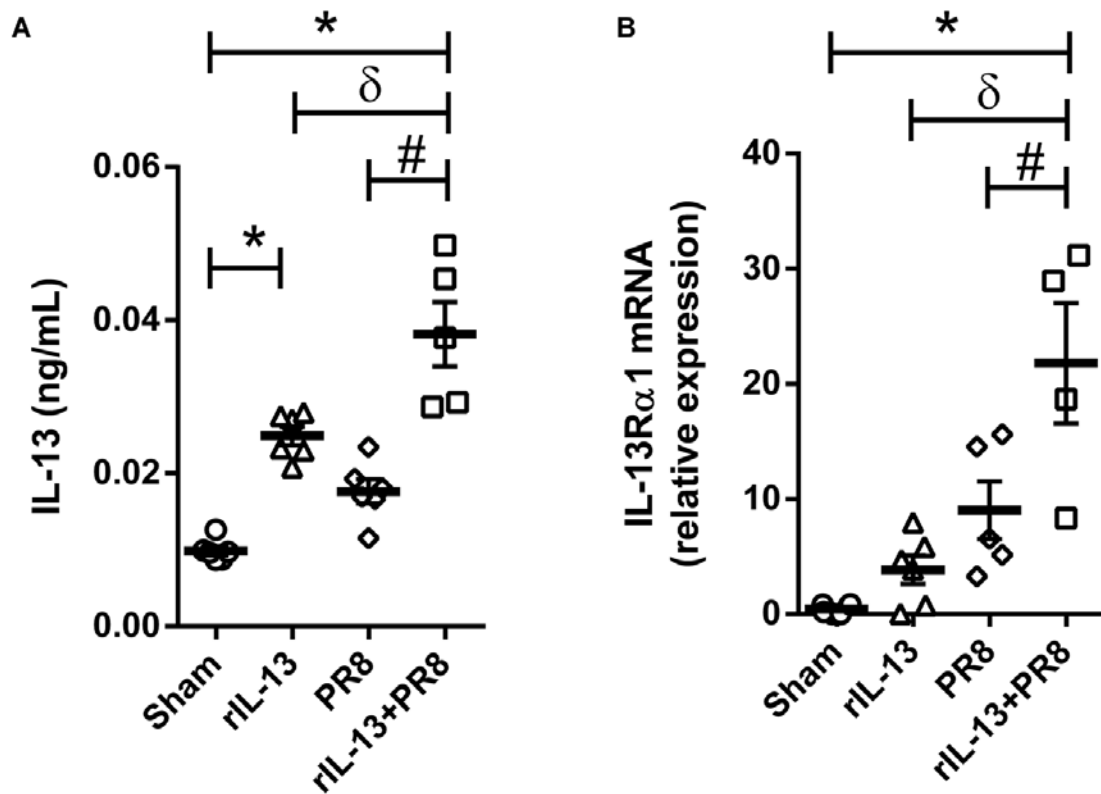


**Figure 3.16. IAV infection increases IL-13 and IL-13R $\alpha$ 1 expression in rIL-13 treated mice.**

BALB/c mice were administered with rIL-13 one day prior to inoculation with IAV A/PR/8/34 (7.5 pfu) or media (at 0 dpi). rIL-13 administration was continued till 2 dpi. Mice were sacrificed 3 dpi. **(A)** IL-13 in lung homogenates and **(B)** IL-13R $\alpha$ 1 mRNA expression in lungs. Data are presented as mean  $\pm$  SEM (n=6-8); \*, # and  $\delta$  represents  $P \leq 0.05$  versus Sham, PR8 and rIL-13 groups, respectively.

### **3.4.3. IAV infection increases IL-13<sup>+</sup>CD4<sup>+</sup> T-cells and IL-13<sup>+</sup> NKT cells but not IL-13<sup>+</sup> ILC2s in experimental AAD**

We then investigated the cellular source of IL-13. Flow cytometry was performed on cells isolated from the lung homogenates of IL-13<sup>td-tom</sup> mice. Increased numbers of IL-13<sup>+</sup>CD4<sup>+</sup> T-cells were observed in sham-inoculated allergic mice compared to sham-inoculated non-allergic controls. Infected mice with AAD had the highest number of IL-13<sup>+</sup>CD4<sup>+</sup> T-cells compared to sham-inoculated non-allergic, sham-inoculated allergic and infected non-allergic controls (Figure 3.17A).

No significant changes in the numbers of IL-13<sup>+</sup> NKT cells were observed in sham-inoculated allergic mice compared to sham-inoculated non-allergic controls. Infected non-allergic controls had the highest number of IL-13<sup>+</sup> NKT cells compared to sham-inoculated non-allergic control, sham-inoculated allergic controls and infected mice with AAD (Figure 3.17B).

Increased numbers of IL-13<sup>+</sup> ILC2 cells were observed in sham-inoculated allergic mice compared to sham-inoculated non-allergic controls. Infected mice with AAD had significantly increased number of IL-13<sup>+</sup> ILC2 cells compared to infected non-allergic controls. However, a non-significant trend towards decrease in number of IL-13<sup>+</sup> ILC2 cells was observed in infected mice with AAD compared to sham-inoculated allergic controls (Figure 3.17C).

These results shows that AAD with or without infection induces IL-13 production predominantly from IL-13<sup>+</sup>CD4<sup>+</sup> T-cells and to a lesser extent from IL-13<sup>+</sup> ILC2 cells but IAV infection alone induces high level of IL-13 production by IL-13<sup>+</sup> NKT cells.

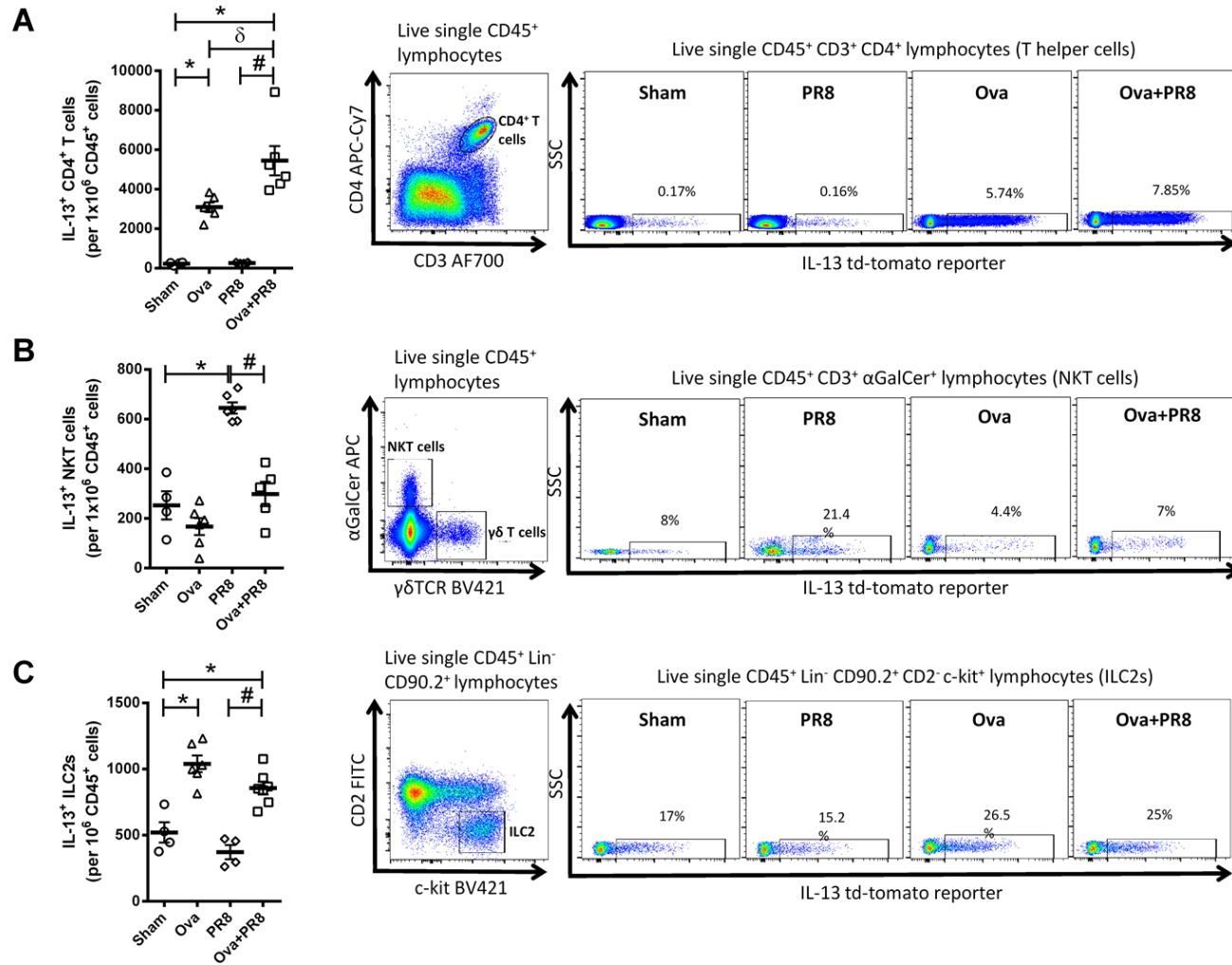


Figure 3.17. Cellular source of IL-13 in IAV infection and Ova-induced experimental AAD.

BALB/c mice were sensitised with Ova or PBS, challenged with Ova and inoculated with IAV A/PR/8/34 (7.5 pfu) or media on the last day of Ova challenge. Mice were sacrificed 3 dpi. **(A)** IL-13<sup>+</sup>CD4<sup>+</sup> T-cells gated as CD45<sup>+</sup>CD3<sup>+</sup>CD4<sup>+</sup> and represented as per million CD45<sup>+</sup> cells; **(B)** IL-13<sup>+</sup>NKT cells gated as CD45<sup>+</sup>CD3<sup>+</sup>αGalCer<sup>+</sup> and represented as per million CD45<sup>+</sup> cells; **(C)** IL-13<sup>+</sup>NKT cells gated as CD45<sup>+</sup>Lin<sup>-</sup>CD90.2<sup>+</sup>CD2<sup>-</sup>c-kit<sup>+</sup> and represented as per million CD45<sup>+</sup> cells. Data are presented as mean ± SEM (n=4-6); \*, # and γ represents P≤0.05 versus Sham, PR8 and Ova+PR8 groups, respectively.

#### **3.4.4. IAV infection increases miR-21 expression in Ova-induced AAD**

We then assessed the role of miR-21 in IAV and AAD. Non-infected allergic mice (Ova) had significantly increased miR-21 expression compared with sham-inoculated non-allergic controls (Sham). Infected non-allergic mice (PR8) also had increased miR-21 expression compared with Sham. Infected mice with AAD (Ova+PR8) had increased miR-21 expression compared to all other groups except infected non-allergic mice, where a non-statistical trend towards an increase in miR21 expression was observed (Figure 3.18).

#### **3.4.5. miR-21 increases in the luminal epithelium associated with small airways in IAV infection in Ova-induced AAD**

To identify the localization of miR-21, in situ hybridization (ISH) was performed in histological sections of formalin fixed, paraffin embedded lungs. Representative images of the stained lung sections showed increase in miR-21 localization to the airway epithelium of sham-inoculated allergic controls compared with sham-inoculated non-allergic controls. miR-21 localization was increased to the airway epithelium of infected mice with AAD compared with sham-inoculated allergic controls and infected non-allergic mice (Figure 3.19).

#### **3.4.6. miR-21 expression increases in mice administered with rIL-13 and infected with IAV**

At 3dpi, miR-21 expression showed a non-statistical trend to an increase in the lung tissues of rIL-13 treated mice (rIL-13) and infected non-allergic mice compared with sham-inoculated controls (Sham). Infected rIL-13 treated mice (rIL-13+PR8) had a significant increase in miR-21 expression compared with all controls (Figure 3.20).

#### **3.4.7. miR-21 expression increases in HDM-induced AAD with IAV infection**

At 3dpi, miR-21 expression showed a non-statistical trend to an increase in the non-infected allergic mice (HDM) and infected non-allergic mice (PR8) compared with sham-inoculated non-allergic controls (Sham). Infected mice with AAD (HDM+PR8) had significantly increased miR-21 expression compared with all controls (Figure 3.21).

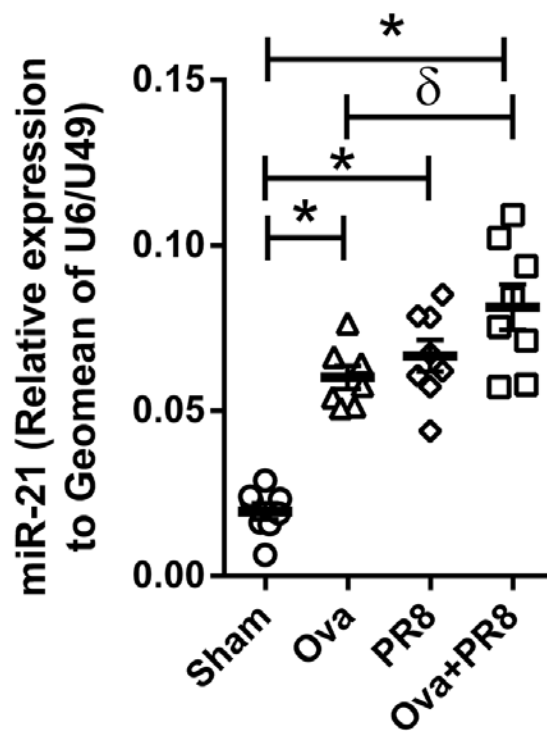


**Figure 3.18. miR-21 expression increases in Ova-induced AAD with IAV infection.**

BALB/c mice were sensitised with Ova or PBS, challenged with Ova and inoculated with IAV A/PR/8/34 (7.5 pfu) or media on the last day of Ova challenge. Mice were sacrificed 3 dpi. Data are presented as mean  $\pm$  SEM (n=6-8); \* and  $\delta$  represents  $P \leq 0.05$  versus Sham and Ova groups, respectively.

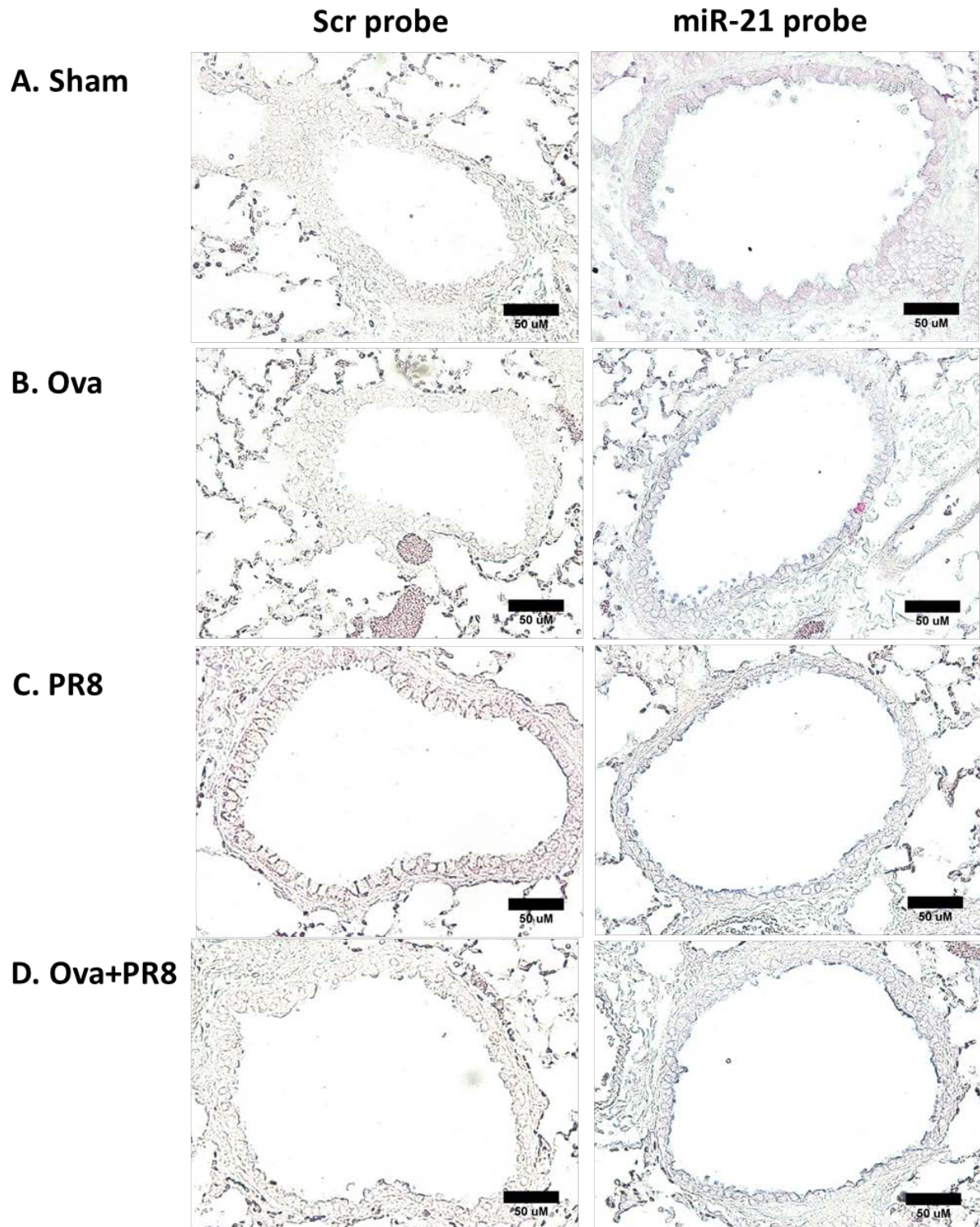


**Figure 3.19. miR-21 is localised to the luminal epithelium associated with small airways in IAV infection in Ova-induced AAD.**

BALB/c mice were sensitised with Ova or PBS, challenged with Ova and inoculated with IAV A/PR/8/34 (7.5 pfu) or media on the last day of Ova challenge. Mice were sacrificed 3 dpi. Representative photomicrographs (40X) showing tissue localization of miR-21 in histological sections of mouse lung collected on 3 dpi of the study

protocol. Localisation of miR-21 in lung sections was characterised using *in-situ* hybridisation analysis with a miR-21-specific locked nucleic acid (LNA<sup>TM</sup>). miR-21-positive signal (blue colour) is visible in epithelial cells associated with small airways. miR-21-positive signal is not evident when a scrambled (Scr) LNA<sup>TM</sup> miR probe was employed. Nuclear Fast Red<sup>TM</sup> was used as counterstain.

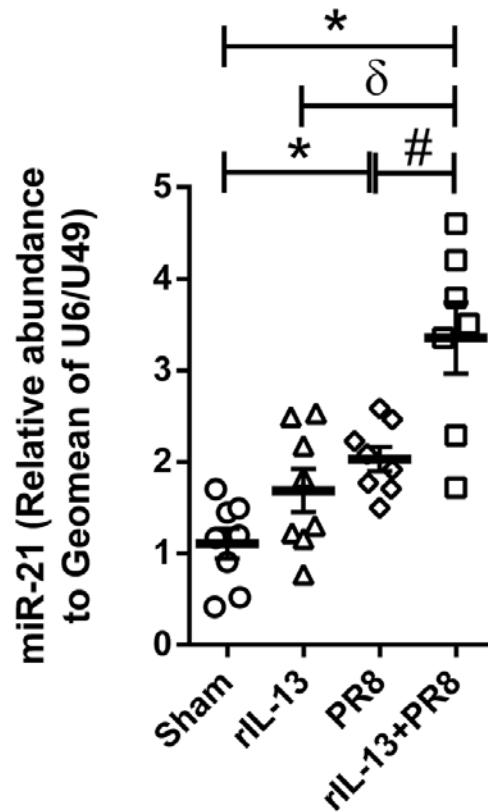


**Figure 3.20. miR-21 expression increases in mice with rIL-13 treatment and IAV infection.**

BALB/c mice were administered rIL-13 one day prior to inoculation with IAV A/PR/8/34 (7.5 pfu) or media (at 0 dpi). rIL-13 administration continued daily until 2 dpi. Mice were sacrificed 3 dpi. Data are presented as mean  $\pm$  SEM (n=6-8); \*, # and  $\delta$  represents  $P \leq 0.05$  versus Sham, PR8 and rIL-13 groups, respectively.

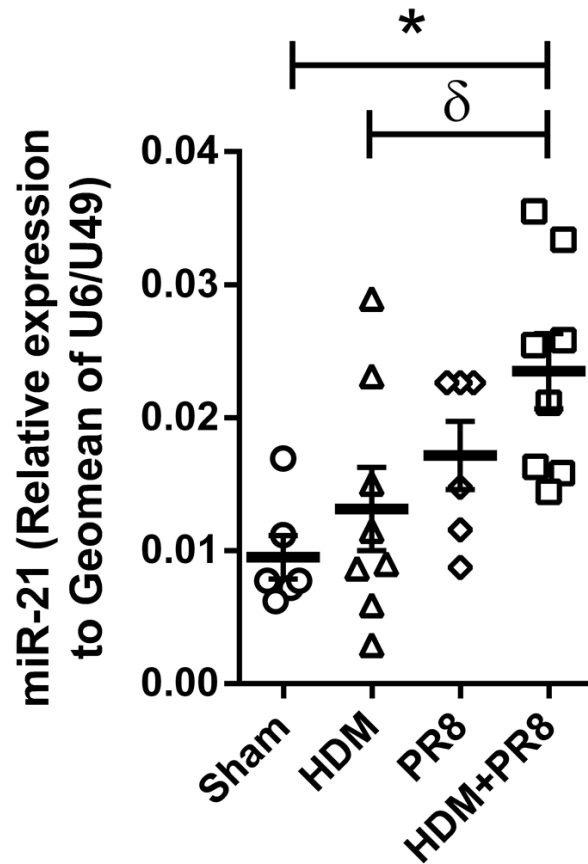


**Figure 3.21. miR-21 expression increases in HDM-induced AAD with IAV infection.**

BALB/c mice were sensitised with HDM or PBS (sham), challenged with HDM and inoculated with IAV A/PR/8/34 (7.5 pfu, PR8, HDM+PR8) or media (control, HDM) on the last day of HDM challenge. Mice were sacrificed 3 dpi. Data are presented as mean  $\pm$  SEM (n=6-8); \*,  $\delta$  represents  $P \leq 0.05$  versus Sham, HDM group.

#### **3.4.8. IL-13<sup>-/-</sup> mice have lower viral titres in IAV infection**

To further investigate the roles of IL-13 in susceptibility to IAV we assessed infection in IL-13<sup>-/-</sup> mice. Wild-type (WT) and IL-13<sup>-/-</sup> mice were inoculated with IAV A/PR/8/34 (7.5 pfu) or media on day 0. Mice were sacrificed at 3 dpi (Figure 3.6). We observed significant decreases in viral titre in infected IL-13<sup>-/-</sup> (IL-13<sup>-/-</sup>+PR8) mice at 3 dpi compared to infected WT mice (PR8). This demonstrates that the absence of IL-13 during IAV infection leads to decreased viral titre in the lung (Figure 3.22).

#### **3.4.9. IL-13<sup>-/-</sup> mice have reduced tissue inflammation in IAV infection**

At 3dpi, no inflammation was recorded in sham-inoculated WT controls (Sham) or sham-inoculated IL-13<sup>-/-</sup> control compared with infected WT mice. Infected IL-13<sup>-/-</sup> mice had decreased histopathological score (indicative of reduced lung tissue inflammation) compared to infected WT mice (Figure 3.23)

#### **3.4.10. IL-13<sup>-/-</sup> mice have reduced AHR in IAV infection**

At 3dpi, infected IL-13<sup>-/-</sup> mice had decreased transpulmonary resistance as compared with infected WT mice. A basal transpulmonary resistance was observed in sham-inoculated WT controls and sham-inoculated IL-13<sup>-/-</sup> control (Figure 3.24A). Furthermore, infected IL-13<sup>-/-</sup> mice demonstrated increased dynamic compliance as compared with infected WT mice. Likewise an increased dynamic compliance was observed in sham-inoculated WT controls when compared with sham-inoculated IL-13<sup>-/-</sup> control (Figure 3.24B) which did not attain statistical significance.

#### **3.4.11. IAV infection in IL-13<sup>-/-</sup> mice have decreased miR-21 expression**

At 3dpi, miR-21 expression was observed to be significantly increased in infected WT mice when compared with sham-inoculated WT control. Infected IL-13<sup>-/-</sup> mice had significantly decreased miR-21 expression compared with sham infected WT mice. However, in contrast to sham-inoculated IL-13<sup>-/-</sup> mice, an increased expression of miR-21 was detected in infected IL-13<sup>-/-</sup> mice (Figure 3.25).

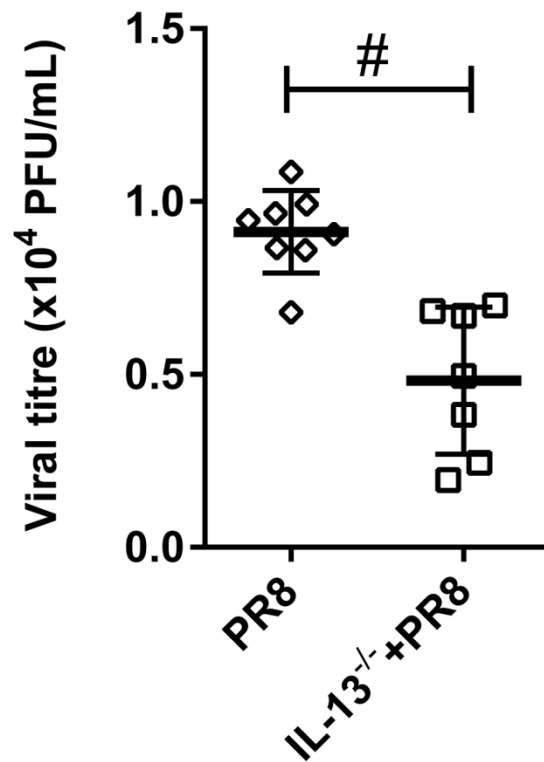


**Figure 3.22. IL-13<sup>-/-</sup> mice have lower viral titres in IAV infection.**

Wild-type (WT) and IL-13<sup>-/-</sup> mice were inoculated with IAV A/PR/8/34 (7.5 pfu) or media on day 0. Mice were sacrificed 3 dpi. Data are presented as mean ± SEM (n=6-8); # represents P ≤ 0.05 versus PR8.

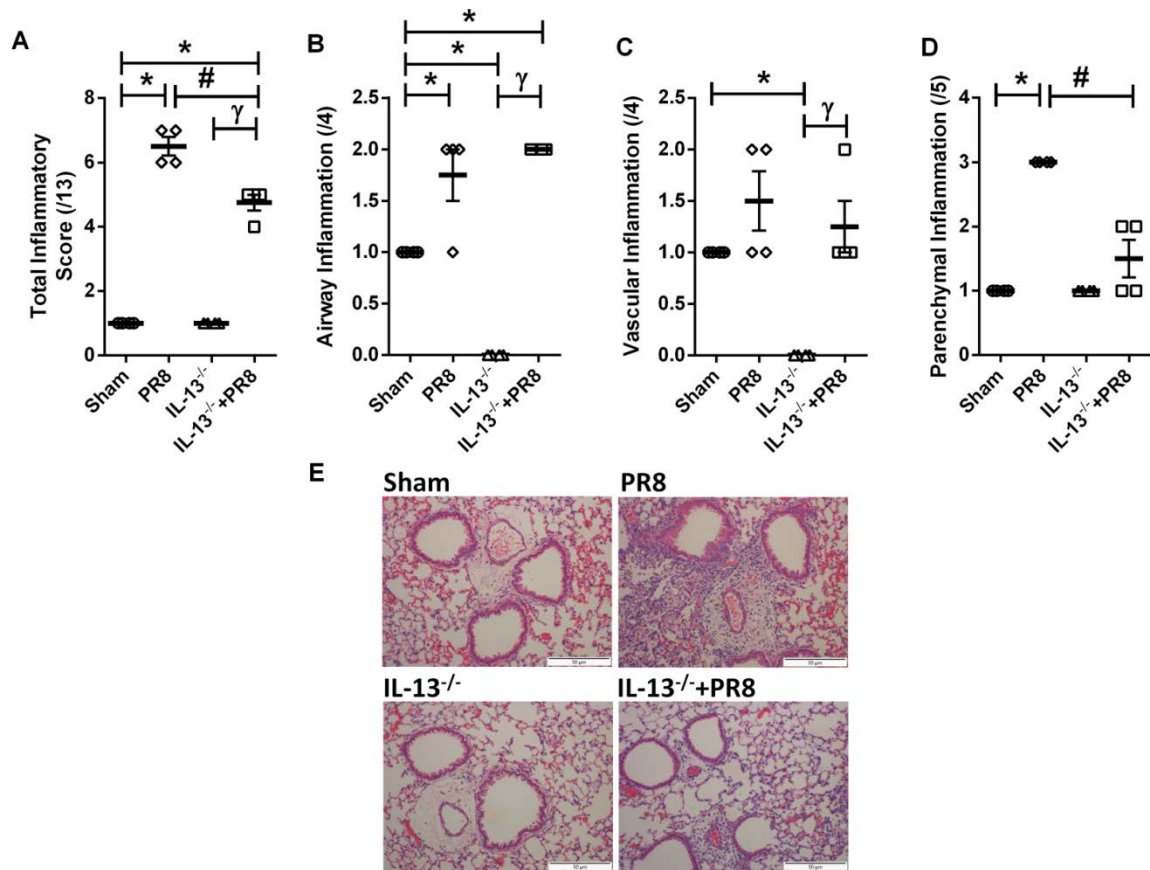


**Figure 3.23. IL-13<sup>-/-</sup> mice have reduced tissue inflammation in IAV infection.**

Wild-type (WT) and IL-13<sup>-/-</sup> mice were inoculated with IAV A/PR/8/34 (7.5 pfu) or media on day 0. Mice were sacrificed 3 dpi. **(A)** Total; **(B)** airway; **(C)** vascular and **(D)** parenchymal inflammation score in haematoxylin and eosin (H&E) stained lung sections; **(E)** Representative images of lung sections; Scale bar = 50µm. Data are presented as mean ± SEM (n=6-8); \*, # and γ represents P≤0.05 versus Sham, PR8 and IL-13<sup>-/-</sup> groups, respectively.

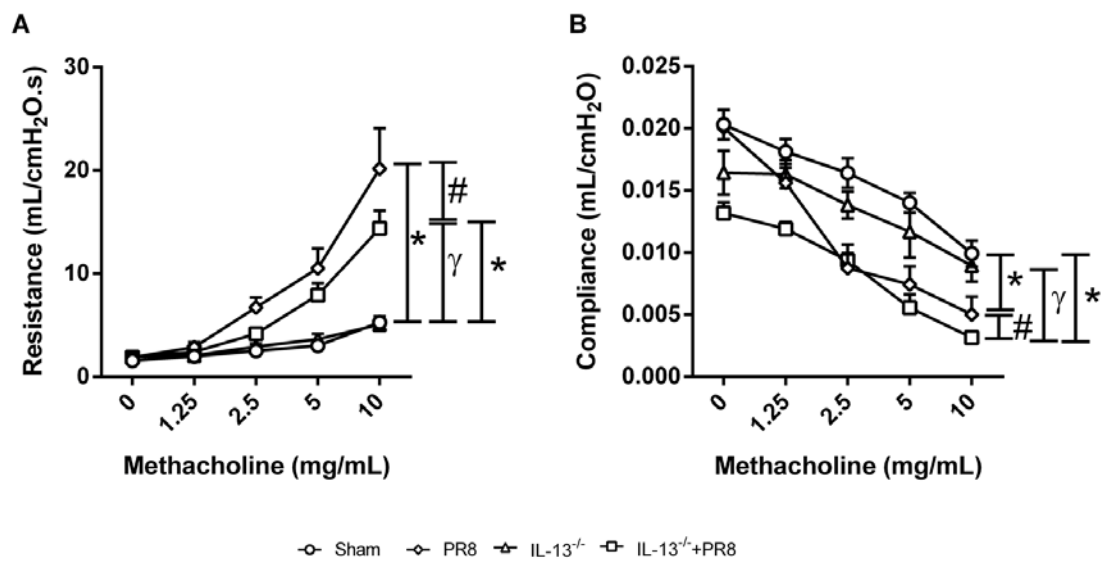


**Figure 3.24. IAV infection in IL-13<sup>-/-</sup> mice have decreased AHR.**

Wild-type (WT) and IL-13<sup>-/-</sup> mice were inoculated with IAV A/PR/8/34 (7.5 pfu) or media on day 0. Mice were sacrificed 3 dpi. **(A)** Transpulmonary resistance and **(B)** dynamic compliance. Data are presented as mean ± SEM (n=6-8); \*, # and γ represents P≤0.05 versus Sham, PR8 and IL-13<sup>-/-</sup> groups, respectively.

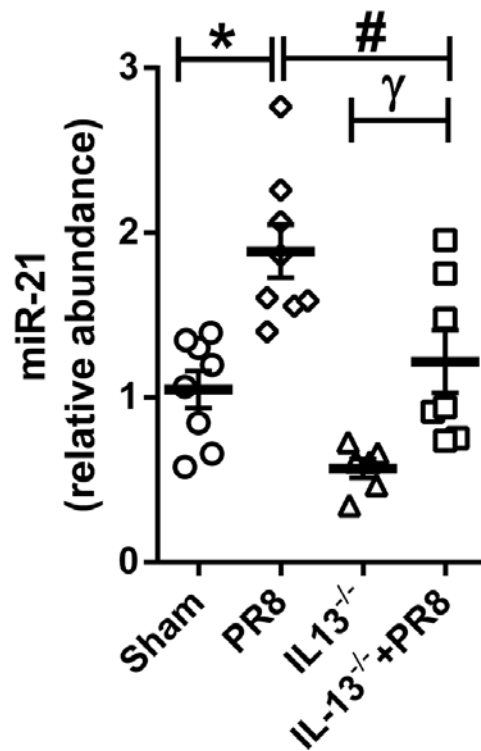


**Figure 3.25. IAV infection in IL-13<sup>-/-</sup> mice have decreased miR-21 expression.**

Wild-type (WT) and IL-13<sup>-/-</sup> mice were inoculated with IAV A/PR/8/34 (7.5 pfu) or media on day 0. Mice were sacrificed 3 dpi. Data are presented as mean ± SEM (n=6-8); \*, # and γ represents P≤0.05 versus Sham, PR8 and IL-13<sup>-/-</sup> groups, respectively.

### **3.4.12. Treatment with anti-IL-13 reduces IAV infection and exacerbation of experimental AAD**

Our previous observations indicated that IL-13 plays a critical role in driving infection-induced exacerbation of AAD. We next assessed whether inhibition of IL-13 could protect against infection and reduce the severity of AAD following IAV infection and be a potential human treatment. BALB/c mice were sensitized i.p. with Ova or PBS, challenged i.n. with Ova and inoculated with IAV A/PR/8/34 (7.5 pfu) or media intranasally on the last day of Ova challenge. Mice were treated i.p. with IL-13 specific monoclonal antibody (Anti-IL-13) or isotype from 0 dpi till 2 dpi. Mice were sacrificed 3 dpi (Figure 3.11).

A non-significant trend towards increase in viral titre was observed in infected mice with AAD compared to infected non-allergic control. Anti-IL-13 treated infected non-allergic mice (PR8+Anti-IL-13) had substantially reduced (2 log) viral titre compared to isotype treated infected non-allergic control (PR8). Importantly, anti-IL-13 treated infected mice with AAD (Ova+PR8+Anti-IL-13) had substantially reduced (2 log) viral titre compared to isotype-treated infected allergic control (Ova+PR8) (Figure 3.26A).

A significant increase in lung tissue inflammation was observed in infected mice with AAD compared to infected non-allergic control. Anti-IL-13 treated infected non-allergic mice had reduced tissue inflammation compared to isotype treated infected non-allergic controls (PR8). Importantly, anti-IL-13 treated infected mice with AAD (Ova+PR8+Anti-IL-13) had significantly reduced tissue inflammation compared to isotype-treated infected allergic control (Ova+PR8) (Figure 3.26B and C).

A significant increase in eosinophil count (Figure 3.26D) and MSCs (Figure 3.26E and F) was observed in infected mice with AAD compared to infected non-allergic control. Anti-IL-13 treated infected mice with AAD (Ova+PR8+Anti-IL-13) demonstrated significantly reduced eosinophil count (Figure 3.26D) and MSCs compared to isotype-treated infected allergic control (Ova+PR8, Figure 3.26E and F).

Isotype treated infected mice with AAD (Ova+PR8) but not anti-IL-13 treated or untreated infected non-allergic controls (PR8+Anti-IL-13), had AHR with increased transpulmonary resistance and decreased dynamic compliance compared with isotype treated infected non-allergic controls (PR8). Importantly, anti-IL-13 treated infected mice with AAD (Ova+PR8+Anti-IL-13) had significantly reduced AHR with decreased transpulmonary resistance but still had decreased dynamic compliance compared to isotype treated infected allergic controls (Figure 3.26G and H).

These results indicate that inhibition of IL-13 in AAD reduced viral titre, tissue inflammation, number of eosinophils and MSCs and suppressed AHR during IAV infection.

#### **3.4.13. Treatment with anti-IL-13 reduces levels of IL-13 protein and IL-13R $\alpha$ 1 mRNA expression in IAV infection in experimental AAD**

Anti-IL13-treated infected non-allergic mice (PR8+Anti-IL-13) demonstrated a non-significant trend towards reduced IL-13 compared to isotype-treated infected non-allergic controls (PR8). Isotype-treated infected mice with AAD (Ova+PR8) had significantly increased IL-13 compared to isotype-treated infected non-allergic controls. Importantly, anti-IL13-treated infected mice with AAD (Ova+PR8+Anti-IL-13) had significantly reduced IL-13 compared to isotype-treated infected allergic controls (Figure 3.27A).

Anti-IL13-treated infected non-allergic mice, but not isotype-treated infected mice with AAD had reduced IL-13R $\alpha$ 1 mRNA expression compared to isotype-treated infected non-allergic controls (Figure 3.27B). Figure 3.27B demonstrates a decrease in IL-13R $\alpha$ 1 expression in response to anti-IL-13 treatment in anti-IL13-treated infected mice with AAD compared to isotype-treated infected mice with AAD, however a non-statistical trend was observed. It can be further clarified by increasing the power of the experiment. Additionally, anti-IL-13 suppresses IL-13 but does not directly target the receptor and so has less of an effect.

These results show that inhibition of IL-13 reduces the IL-13 protein levels, and also the expression of its receptor, IL-13R $\alpha$ 1.

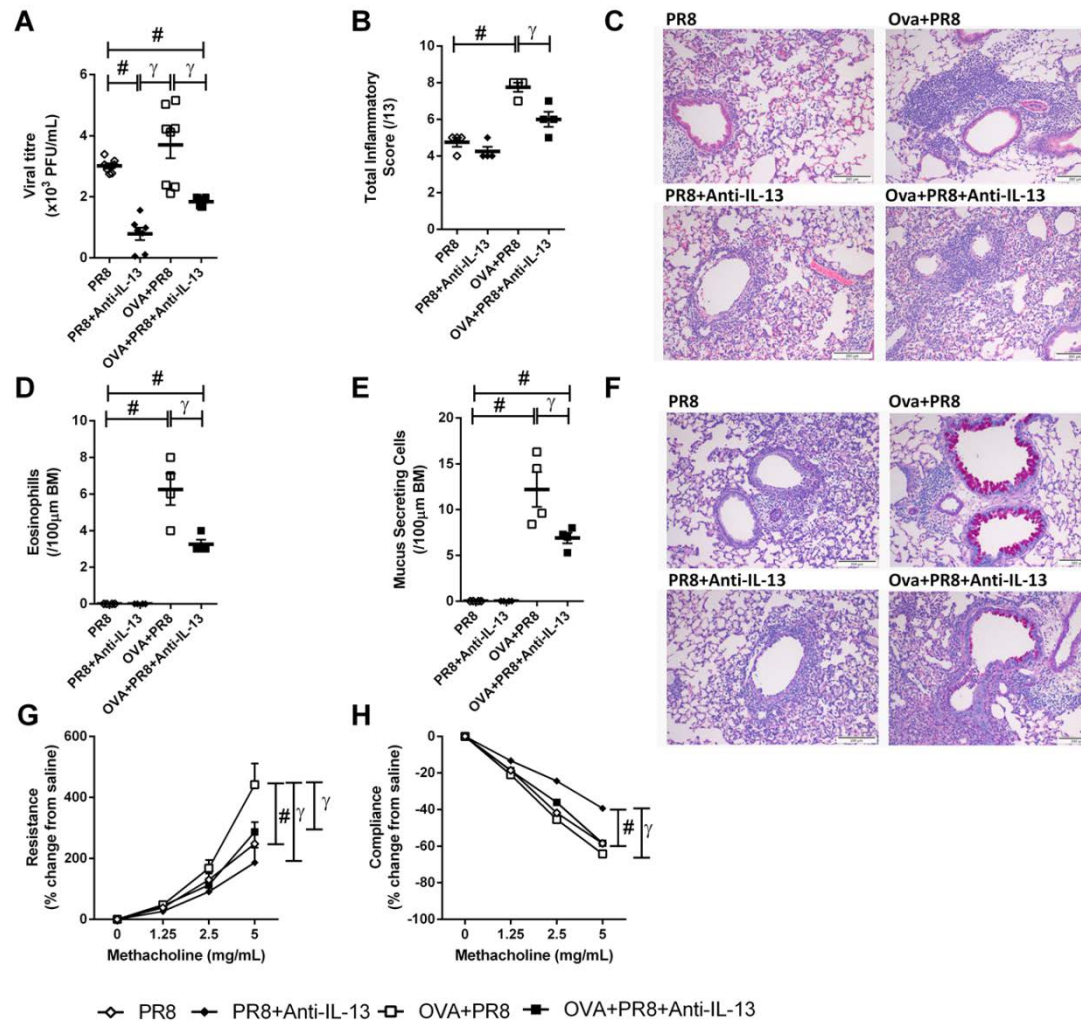
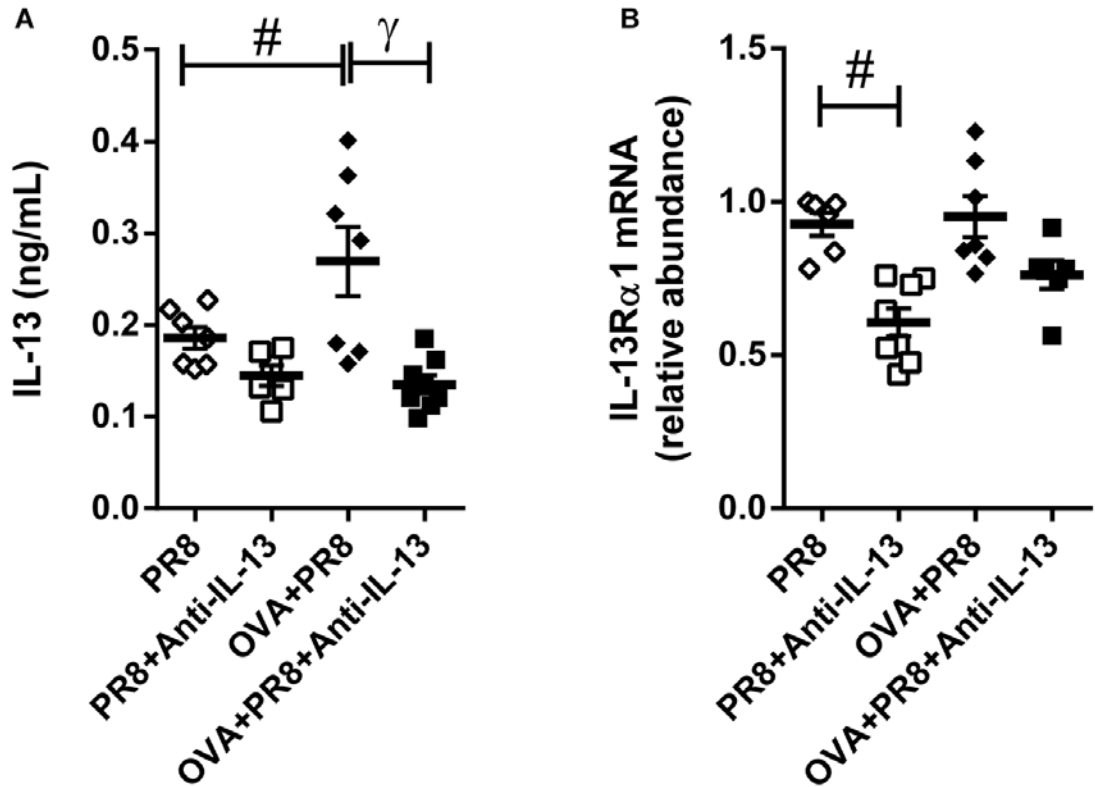


Figure 3.26. Treatment with anti-IL-13 reduces IAV infection and exacerbation of experimental AAD.

BALB/c mice were sensitised with Ova or PBS, challenged with Ova and inoculated with IAV A/PR/8/34 (7.5 pfu) or media on the last day of Ova challenge. Mice were treated with anti-IL-13 antibody or isotype from 0 dpi till 2 dpi. Mice were sacrificed 3 dpi. **(A)** Viral titre at 3 dpi; **(B)** Total inflammatory score in haematoxylin and eosin (H&E) stained lung sections; **(C)** Representative images (10X) of H&E stained lung sections; Scale bar = 200µm; **(D)** Numbers of tissue eosinophils; **(E)** MSCs per 100 µm basement membrane (BM) in periodic acid-Schiff (PAS) stained lung sections; **(F)** Representative images (10X) of PAS stained lung sections; Scale bar = 50µm; **(G)** Transpulmonary resistance and **(H)** dynamic compliance. Data are presented as mean ± SEM (n=4-8); # and γ represents  $P \leq 0.05$  versus PR8 and Ova+PR8 groups, respectively.



**Figure 3.27. IAV infection decreases IL-13 and IL-13R $\alpha$ 1 expression in Ova-induced AAD mice administered with anti-IL-13.**

BALB/c mice were sensitised with Ova or PBS, challenged with Ova and inoculated with IAV A/PR/8/34 (7.5 pfu) or media on the last day of Ova challenge. Mice were treated with anti-IL-13 antibody or isotype from 0 dpi till 2 dpi. Mice were sacrificed 3 dpi. **(A)** IL-13 in lung homogenates and **(B)** IL-13 $\alpha$ 1 mRNA expression in lungs. Data are presented as mean  $\pm$  SEM (n=6-8); # and  $\gamma$  represents  $P \leq 0.05$  versus PR8 and Ova+PR8 groups, respectively.

#### **3.4.14. Treatment with anti-IL-13 reduces miR-21 expression in IAV infection but not in IAV infection in experimental AAD**

Anti-IL13-treated infected non-allergic mice (PR8+Anti-IL-13) had significantly reduced miR-21 expression compared to isotype-treated infected non-allergic controls (PR8). Isotype-treated infected mice with AAD (Ova+PR8) had increased miR-21 expression compared to isotype-treated infected non-allergic controls. Similar levels of miR-21 expression were observed in anti-IL13-treated infected mice with AAD (Ova+PR8+Anti-IL-13) and isotype-treated infected allergic controls (Figure 3.28).

#### **3.4.15. Treatment with intranasal dexamethasone did not reduce viral titre in IAV infection**

To investigate whether steroid (dexamethasone) treatment could protect against infection and reduce the severity of AAD following IAV infection, BALB/c mice were sensitised by i.p. administration of with Ova or PBS and subsequently challenged i.n. with Ova 12-15 days later. On the last day of Ova challenge, mice were infected i.n. with IAV A/PR/8/34 (7.5 pfu) or media. Mice were treated with dexamethasone (Dex) from 0 dpi till 2 dpi. Mice were sacrificed 3 dpi (Figure 3.7).

Viral titre was increased in sham-inoculated infected mice with AAD (Ova+PR8+Veh) and dexamethasone-treated non-allergic infected mice (PBS+PR8+Dex) compared with sham-inoculated non-allergic infected mice (PBS+PR8+Veh). However, dexamethasone-treated non-allergic infected mice (PBS+PR8+Dex) demonstrated significantly increased viral titre when compared with sham-inoculated non-allergic infected mice and sham-inoculated infected mice with AAD (Figure 3.29).

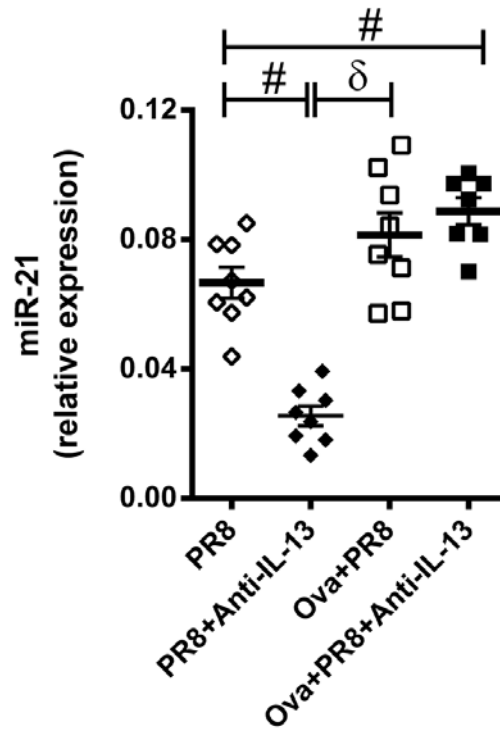


**Figure 3.28. Treatment with anti-IL-13 reduces miR-21 expression in IAV infection but not in IAV infection in experimental AAD.**

BALB/c mice were sensitised with Ova or PBS, challenged with Ova and inoculated with IAV A/PR/8/34 (7.5 pfu) or media on the last day of Ova challenge. Mice were treated with anti-IL-13 antibody or isotype from 0 dpi till 2 dpi. Mice were sacrificed 3 dpi. Data are presented as mean  $\pm$  SEM (n=6-8); # and  $\delta$  represents  $P \leq 0.05$  versus PR8 and PR8+Anti-IL-13 groups, respectively.

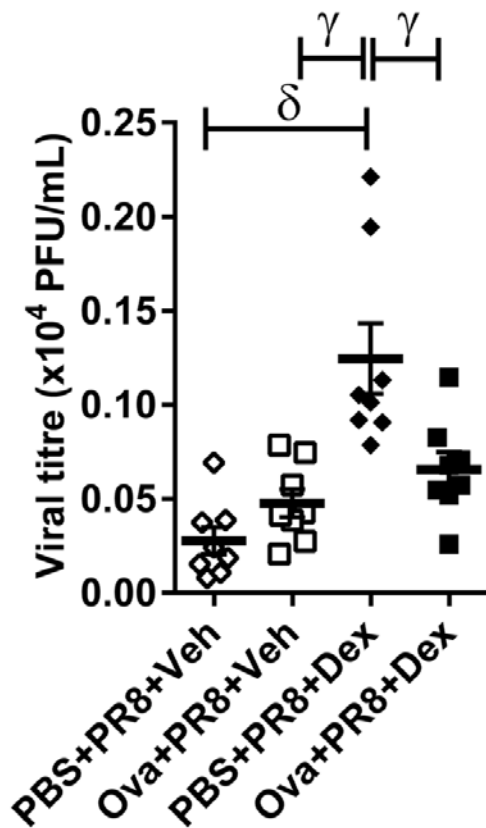


**Figure 3.29. Viral titre at 3 dpi.**

BALB/c mice were sensitised with Ova or PBS, challenged with Ova and inoculated with IAV A/PR/8/34 (7.5 pfu) or media on the last day of Ova challenge. Mice were treated with dexamethasone (Dex) from 0 dpi till 2 dpi. Mice were sacrificed 3 dpi. Data are presented as mean  $\pm$  SEM (n=6-8);  $\delta$  and  $\gamma$  represents  $P \leq 0.05$  versus PBS+PR8+Veh and Ova+PR8+Veh groups respectively.

No change in the viral titre was observed in response to dexamethasone treatment in infected mice with AAD compared with sham-inoculated infected mice with AAD. Dexamethasone-treated infected mice with AAD (Ova+PR8+Dex) showed significantly reduced viral titre compared with dexamethasone-treated non-allergic infected mice (Figure 3.29). This indicates that viral load was dexamethasone-insensitive in IAV infection following Ova-induced AAD.

#### **3.4.16. Treatment with intranasal dexamethasone did not resolve tissue inflammation in IAV infection**

Sham-inoculated allergic non-infected mice (Ova+Sham+Veh) and sham-inoculated non-allergic infected mice (PBS+PR8+Veh) had significantly increased lung tissue inflammation compared with sham-inoculated non-allergic non-infected controls (PBS+Sham+Veh) (Figure 3.30).

Sham-inoculated infected mice with AAD (Ova+PR8+Veh) had significantly increased tissue inflammation compared with sham-inoculated non-allergic non-infected controls and sham-inoculated allergic non-infected mice. However, a non-significant trend towards increase in tissue inflammation was observed between sham-inoculated non-allergic infected mice and sham-inoculated infected mice with AAD (Figure 3.30).

Tissue inflammation did not resolve on treatment with dexamethasone in dexamethasone-treated allergic non-infected mice in contrast to sham-inoculated allergic non-infected mice. Interestingly, significant increase in tissue inflammation was observed in dexamethasone-treated non-allergic infected mice when compared with sham-inoculated non-allergic infected mice. However, dexamethasone-treated infected mice with AAD demonstrated a significant reduction in tissue inflammation compared with sham-inoculated infected mice with AAD (Figure 3.30).

This indicates that tissue inflammation was dexamethasone-insensitive in IAV infection following Ova-induced AAD.

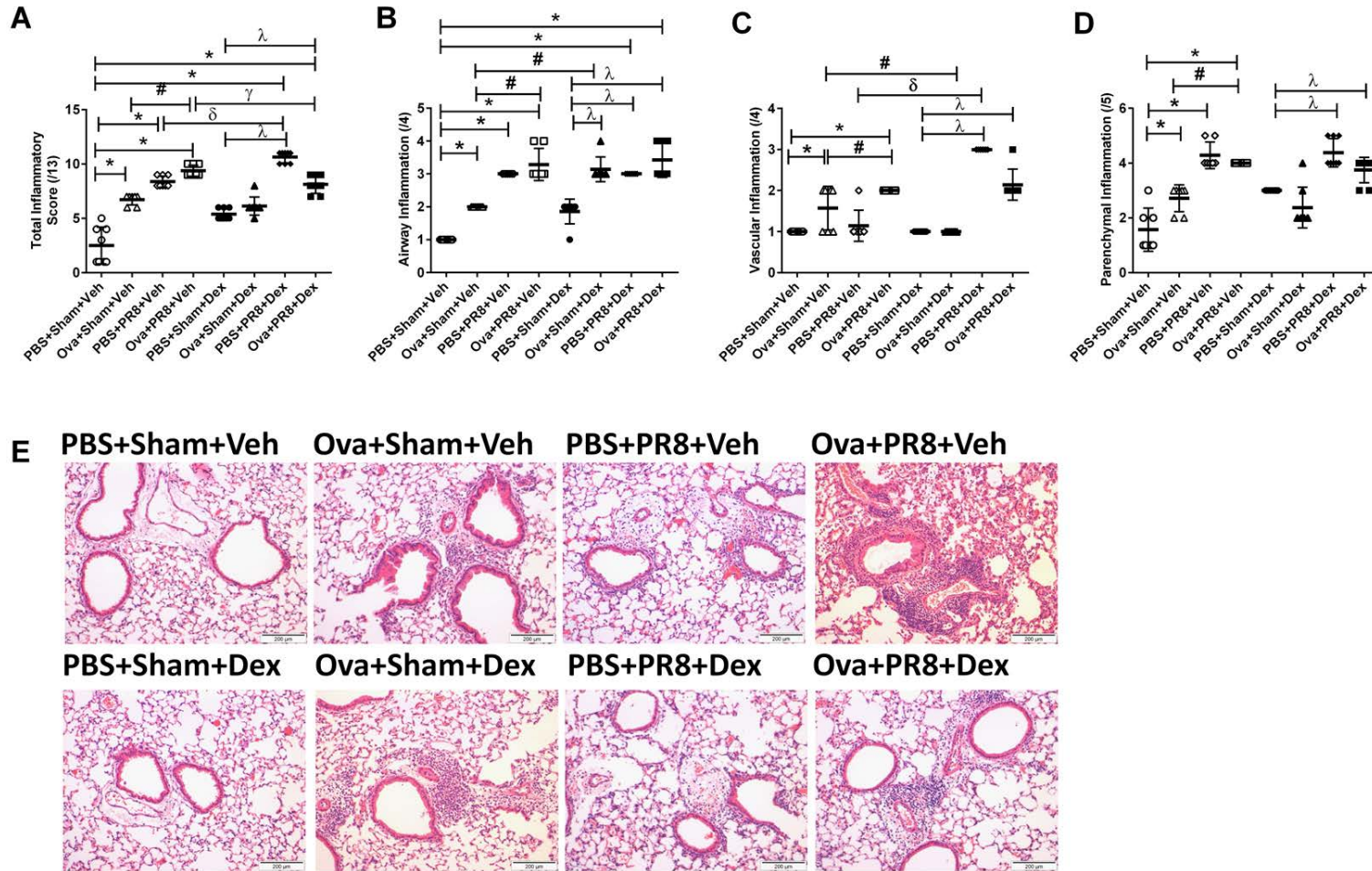


Figure 3.30. Treatment with intranasal dexamethasone did not reduce tissue inflammation in IAV infection.

BALB/c mice were sensitised with Ova or PBS, challenged with Ova and inoculated with IAV A/PR/8/34 (7.5 pfu) or media on the last day of Ova challenge. Mice were treated with dexamethasone (Dex) from 0 dpi till 2 dpi. Mice were sacrificed 3 dpi. **(A)** Total; **(B)** airway; **(C)** vascular and **(D)** parenchymal inflammation score in haematoxylin and eosin (H&E) stained lung sections; **(E)** Representative images (10X) of H&E stained lung sections; Scale bar = 200µm. Data are presented as mean±SEM (n=6-8); \*, #, δ, γ and λ represents  $P \leq 0.05$  versus PBS+Sham+Veh, Ova+Sham+Veh, PBS+PR8+Veh, Ova+PR8+Veh and PBS+Sham+Dex groups respectively.

#### **3.4.17. Treatment with intranasal dexamethasone did not reduce tissue eosinophils in IAV infection following Ova-induced AAD**

Sham-inoculated infected mice with AAD (Ova+PR8+Veh) had significantly increased lung tissue eosinophils compared with sham-inoculated non-allergic non-infected control (PBS+Sham+Veh) and sham-inoculated allergic non-infected mice (Ova+Sham+Veh) (Figure 3.31).

Significant decrease in tissue eosinophils was observed in dexamethasone-treated allergic non-infected mice (Ova+Sham+Dex) when compared with sham-inoculated allergic non-infected mice. Interestingly, the tissue eosinophil counts increased significantly in dexamethasone-treated infected mice with AAD (Ova+PR8+Dex) compared with sham-inoculated infected mice with AAD (Figure 3.31).

This indicates that tissue eosinophils were dexamethasone-insensitive in IAV infection following Ova-induced AAD.

#### **3.4.18. Treatment with intranasal dexamethasone reduces number of MSCs in IAV infection following Ova-induced AAD**

Sham-inoculated infected mice with AAD (Ova+PR8+Veh) had significantly increased number of MSCs compared with sham-inoculated non-allergic non-infected control (PBS+Sham+Veh) and sham-inoculated allergic non-infected mice (Ova+Sham+Veh) (Figure 3.32)

Significant decrease in number of MSCs was observed in dexamethasone-treated allergic non-infected mice (Ova+Sham+Dex) when compared with sham-inoculated allergic non-infected mice. Likewise, number of MSCs was reduced significantly in dexamethasone-treated infected mice with AAD (Ova+PR8+Dex) compared with sham-inoculated infected mice with AAD (Figure 3.32).

This indicates that the number of MSCs was dexamethasone-sensitive in IAV infection following Ova-induced AAD.

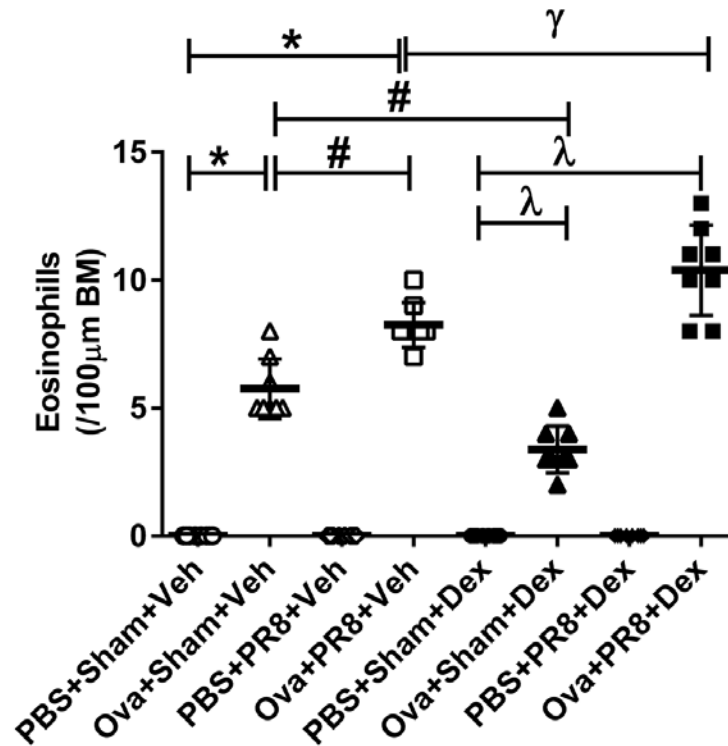


**Figure 3.31. Treatment with intranasal dexamethasone did not reduce tissue eosinophils.**

BALB/c mice were sensitised with Ova or PBS, challenged with Ova and inoculated with IAV A/PR/8/34 (7.5 pfu) or media on the last day of Ova challenge. Mice were treated with dexamethasone (Dex) from 0 dpi till 2 dpi. Mice were sacrificed 3 dpi. Data are presented as mean±SEM (n=6-8); \*, #, γ and λ represents  $P \leq 0.05$  versus PBS+Sham+Veh, Ova+Sham+Veh, Ova+PR8+Veh and PBS+Sham+Dex groups respectively.

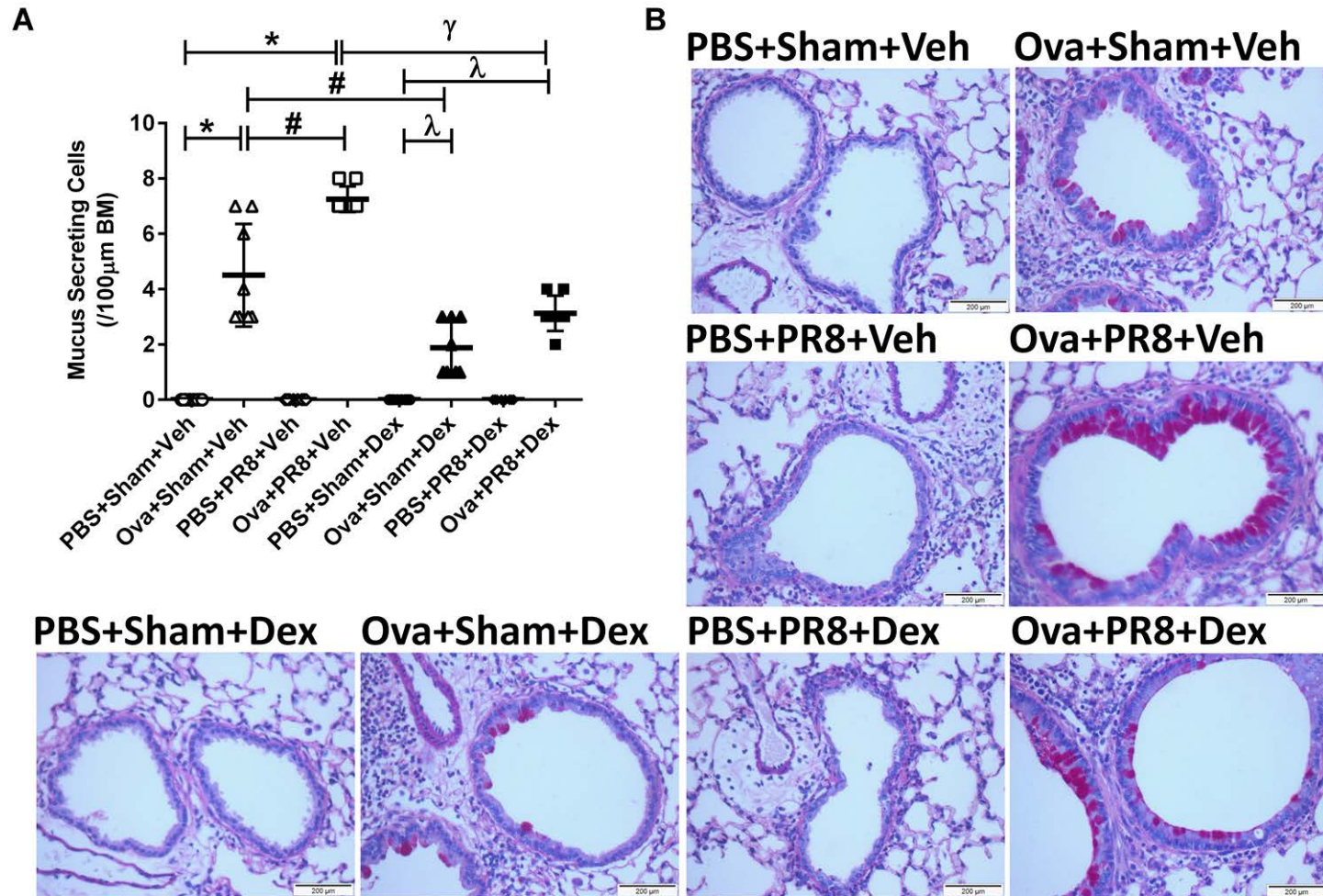


Figure 3.32. Treatment with intranasal dexamethasone reduces the number of MSCs.

BALB/c mice were sensitised with Ova or PBS, challenged with Ova and inoculated with IAV A/PR/8/34 (7.5 pfu) or media on the last day of Ova challenge. Mice were treated with dexamethasone (Dex) from 0 dpi till 2 dpi. Mice were sacrificed 3 dpi. **(A)** MSCs number per 100µm basement membrane in periodic acid-Schiff (PAS) stained lung sections; **(B)** Representative images (20X) of PAS stained lung sections; Scale bar = 200µm. Data are presented as mean±SEM (n=6-8); \*, #, γ and λ represents P≤0.05 versus PBS+Sham+Veh, Ova+Sham+Veh, Ova+PR8+Veh and PBS+Sham+Dex groups respectively

### **3.4.19. Treatment with intranasal dexamethasone worsens AHR substantially in IAV infection following Ova-induced AAD**

Ova and PR8 challenge in sham-inoculated allergic non-infected mice (Ova+Sham+Veh) and sham-inoculated non-allergic infected mice (PBS+PR8+Veh) respectively induced significant increase transpulmonary resistance compared to sham-inoculated non allergic non-infected control (PBS+Sham+Veh) (Figure 3.33 A).

Dexamethasone-treated allergic non-infected mice (Ova+Sham+Dex) demonstrated a significant reduction in transpulmonary resistance in contrast to sham-inoculated allergic non-infected mice (Ova+Sham+Veh). However, dexamethasone administration aggravated transpulmonary resistance in dexamethasone-treated non-allergic infected mice (PBS+PR8+Dex) and dexamethasone-treated infected mice with AAD (Ova+PR8+Dex) when compared with sham-inoculated non-allergic infected mice (PBS+PR8+Veh) and sham-inoculated infected mice with AAD (Ova+PR8+Veh) respectively (Figure 3.33 A). Likewise, dexamethasone treatment suppressed Ova-induced but not IAV infection induced dynamic compliance (Figure 3.33 B).

Consequently, dexamethasone treatment suppressed Ova-induced but not IAV infection induced AHR. Importantly, dexamethasone treatment in IAV infected group further worsened AHR.

### **3.4.20. Treatment with intranasal dexamethasone had no effect on miR-21 expression in IAV infection following Ova-induced AAD**

Sham-inoculated infected mice with AAD (Ova+PR8+Veh) demonstrated a non-significant trend towards increased miR-21 expression compared with sham-inoculated non-allergic non-infected mice (PBS+Sham+Veh), sham-inoculated allergic non-infected mice (Ova+Sham+Veh) and sham-inoculated non-allergic infected mice (PBS+PR8+Veh) (Figure 3.34).

No effect of dexamethasone treatment was observed on miR-21 expression in dexamethasone-treated allergic non-infected mice (Ova+Sham+Dex), sham-

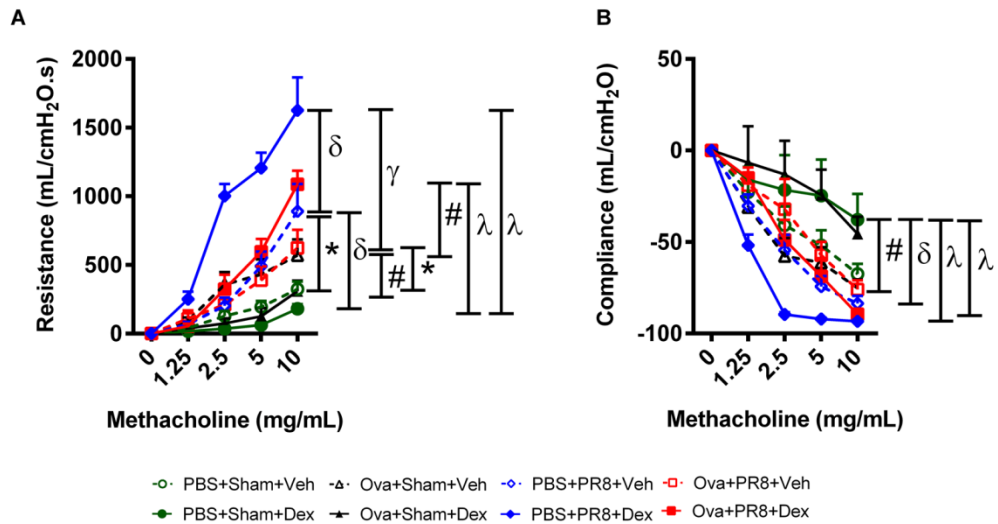


**Figure 3.33. Treatment with intranasal dexamethasone worsens AHR substantially.**

BALB/c mice were sensitised with Ova or PBS, challenged with Ova and inoculated with IAV A/PR/8/34 (7.5 pfu) or media on the last day of Ova challenge. Mice were treated with dexamethasone (Dex) from 0 dpi till 2 dpi. Mice were sacrificed 3 dpi. (A) Transpulmonary resistance and (B) dynamic compliance. Data are presented as mean $\pm$ SEM (n=6); \*, #,  $\gamma$  and  $\lambda$  represents  $P \leq 0.05$  versus PBS+Sham+Veh, Ova+Sham+Veh, Ova+PR8+Veh and PBS+Sham+Dex groups respectively.

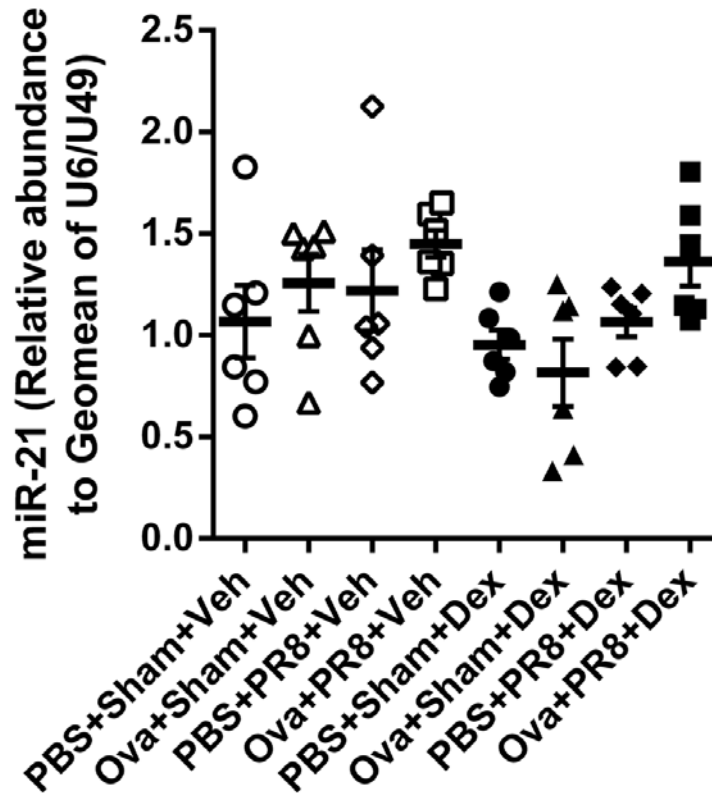


**Figure 3.34. Treatment with intranasal dexamethasone had no effect on miR-21 expression.**

BALB/c mice were sensitised with Ova or PBS, challenged with Ova and inoculated with IAV A/PR/8/34 (7.5 pfu) or media on the last day of Ova challenge. Mice were treated with dexamethasone (Dex) from 0 dpi till 2 dpi. Mice were sacrificed 3 dpi. Data are presented as mean $\pm$ SEM (n=6).

inoculated non-allergic infected mice (PBS+PR8+Dex) and sham-inoculated infected mice with AAD (Ova+PR8+Dex) compared with their respective controls (Figure 3.34) in contrast to previous data shown in Fig. 3.18. This can be attributed to (1) the influence of vehicle (DMSO) on the progression of disease in the model in Figure 3.34 whereas PBS was the vehicle administered to the Sham group in Figure 3.18. Also the basal relative expression of miR-21 was observed to be higher in Figure 3.34 in compared with Figure 3.18, meaning that there was less margin for an increase and (2) the sample size, which was different in two figures where Figure 3.34 had n=6 including outliers while Figure 3.18 had n=8 with no outliers. This indicates that dexamethasone treatment did not suppress miR-21 expression in IAV infection following Ova-induced AAD.

#### **3.4.21. Treatment with intranasal Ant-21 reduces viral titre in IAV infection following Ova-induced AAD**

Our investigations revealed that IAV infection in AAD models (Ova and HDM) not only increased IL-13 protein levels, but also the expression of its receptor, IL-13R $\alpha$ 1 (Figure 2.6 and 3.15). To further identify the mechanism involved downstream of IL-13/IL-13R $\alpha$ 1, we investigated miR-21 as a potential target molecule driving increase susceptibility to IAV infection in experimental AAD. miR-21 expression was observed to be significantly increased in response to IAV infection in AAD (Figure 3.18, 3.19 and 3.21). Furthermore, IAV infection also increased miR-21 expression in mice administered with rIL-13 (Figure 3.20).

To further investigate the functional role of miR-21 in driving susceptibility to IAV infection we targeted miR-21 using specific inhibitor, antagomir 21 (Ant-21). BALB/c mice were sensitised by i.p. administration of Ova or PBS and subsequently challenged i.n. with Ova 12-15 days later. On the last day of Ova challenge, mice were infected with IAV A/PR/8/34 (7.5 pfu) or media. Mice were treated with Ant-21 or scrambled control on 0 dpi. Mice were sacrificed 3 dpi. (Figure 3.8).

Increased viral titre was observed in sham-inoculated infected mice with AAD (Ova+PR8) at 3 dpi compared with sham-inoculated infected non-allergic controls (PR8). Ant-21-treated infected non-allergic mice (PR8+Ant-21) had significantly reduced viral titre compared with Scr-treated infected non-allergic control (PR8+Scr). Importantly, Ant-21-treated infected mice with AAD (Ova+PR8+Ant-21) demonstrated significant reduction in the viral titre compared with Scr-treated infected mice with AAD (Ova+PR8+Scr) (Figure 3.35).

#### **3.4.22. Treatment with intranasal Ant-21 suppresses tissue inflammation in IAV infection following Ova-induced AAD**

Significant increase in tissue inflammation was observed in sham-inoculated infected mice with AAD (Ova+PR8) at 3 dpi compared with sham-inoculated non-allergic non-infected control (Sham) and sham-inoculated infected non-allergic controls (PR8). Ant-21-treated infected non-allergic mice (PR8+Ant-21) demonstrated significantly reduced tissue inflammation compared with both sham-inoculated infected non-allergic controls and Scr-treated infected non-allergic control. Importantly, Ant-21-treated infected mice with AAD (Ova+PR8+Ant-21) demonstrated significant reduction in tissue inflammation compared with sham-inoculated infected mice with AAD and Scr-treated infected mice with AAD (Ova+PR8+Scr) (Figure 3.36).

#### **3.4.23. Treatment with intranasal Ant-21 suppresses number of MSCs in IAV infection following Ova-induced AAD**

Sham-inoculated infected mice with AAD (Ova+PR8) had significantly increased number of MSCs compared with sham-inoculated non-allergic non-infected control (Sham) and sham-inoculated infected non-allergic controls (PR8) (Figure 3.37). Ant-21-treated infected mice with AAD (Ova+PR8+Ant-21) demonstrated significantly reduced number of MSCs compared with sham-inoculated infected mice with AAD (Ova+PR8) and Scr-treated infected mice with AAD (Ova+PR8+Scr) (Figure 3.37).

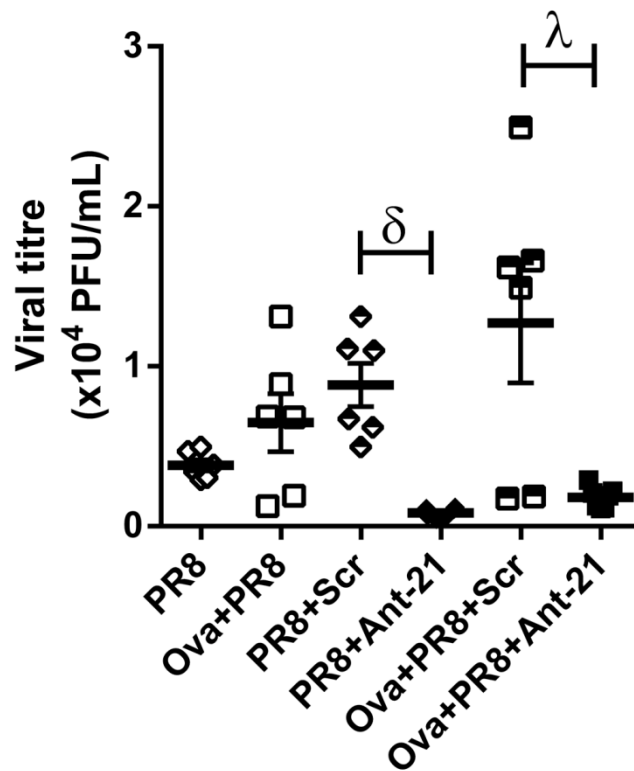


**Figure 3.35. Viral titre at 3 dpi.**

BALB/c mice were sensitised with Ova or PBS, challenged with Ova and inoculated with IAV A/PR/8/34 (7.5 pfu) or media on the last day of Ova challenge. Mice were treated with Ant-21 or scrambled control on 0 dpi. Mice were sacrificed 3 dpi. Data are presented as mean  $\pm$  SEM (n=6-8);  $\delta$  and  $\lambda$  represents  $P \leq 0.05$  versus PR8+Scr and Ova+PR8+Scr groups, respectively.

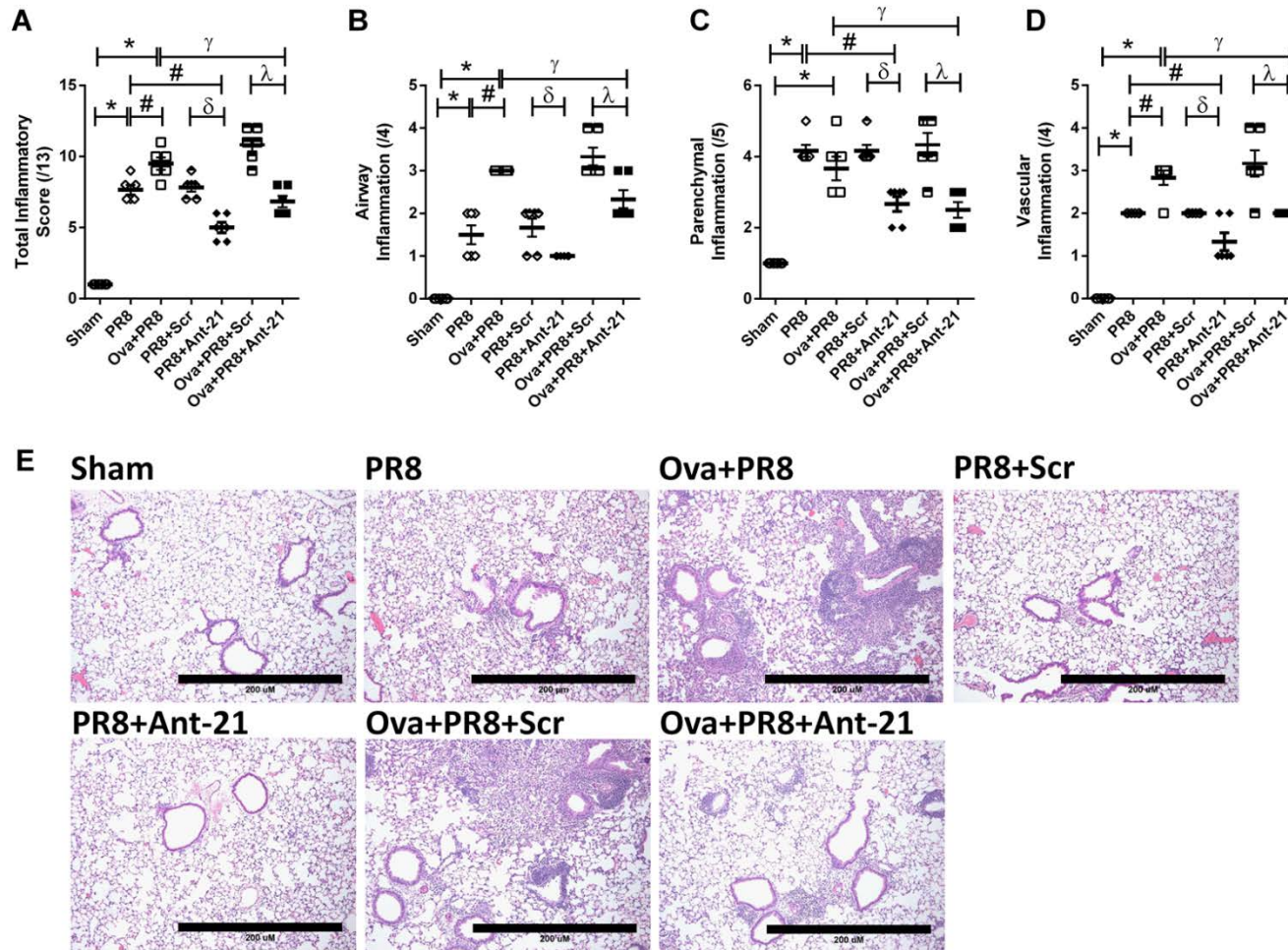
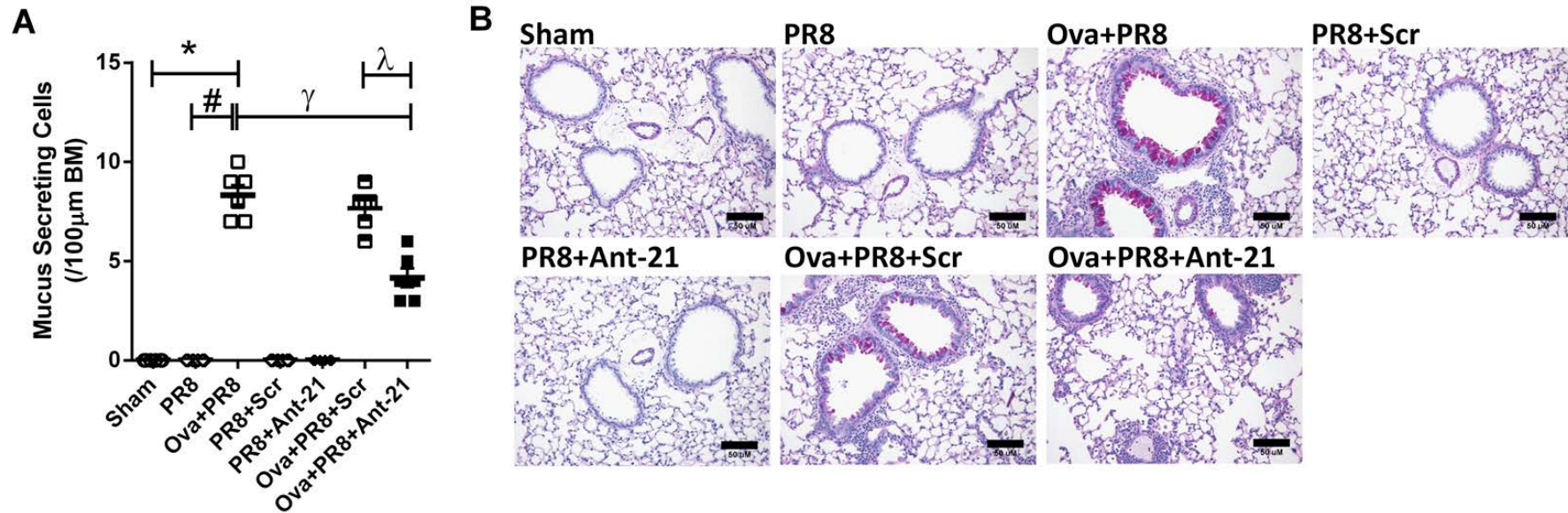


Figure 3.36. Treatment with intranasal Ant-21 suppresses tissue inflammation in IAV infection following Ova-induced AAD.

BALB/c mice were sensitised with Ova or PBS, challenged with Ova and inoculated with IAV A/PR/8/34 (7.5 pfu) or media on the last day of Ova challenge. Mice were treated with Ant-21 or scrambled control on 0 dpi. Mice were sacrificed 3 dpi. **(A)** Total; **(B)** airway; **(C)** parenchymal and **(D)** vascular inflammation score in haematoxylin and eosin (H&E) stained lung sections; **(E)** Representative images (10X) of H&E stained lung sections; Scale bar = 200µm. Data are presented as mean±SEM (n=6-8). \*, #, γ, δ, and λ represents  $P \leq 0.05$  versus Sham, PR8, Ova+PR8, PR8+Scr and Ova+PR8+Scr groups respectively.



**Figure 3.37. Treatment with intranasal Ant-21 suppresses number of MSCs in IAV infection following Ova-induced AAD.**

BALB/c mice were sensitised with Ova or PBS, challenged with Ova and inoculated with IAV A/PR/8/34 (7.5 pfu) or media on the last day of Ova challenge. Mice were treated with Ant-21 or scrambled control on 0 dpi. Mice were sacrificed 3 dpi. **(A)** MSCs per 100 μm basement membrane (BM) in periodic acid-Schiff (PAS) stained lung sections; **(B)** Representative images (20X) of PAS stained lung sections; Scale bar = 50 μm. Data are presented as mean ± SEM (n=6-8); \*, #, γ and λ represents P ≤ 0.05 versus Sham, PR8, Ova+PR8 and Ova+PR8+Scr groups respectively.

#### **3.4.24. Treatment with intranasal Ant-21 suppresses number of tissue eosinophils in IAV infection following Ova-induced AAD**

Sham-inoculated infected mice with AAD (Ova+PR8) had significantly increased number of eosinophils compared with sham-inoculated non-allergic non-infected control (Sham) and sham-inoculated infected non-allergic controls (PR8) (Figure 3.38).

Ant-21-treated infected mice with AAD (Ova+PR8+Ant-21) demonstrated significantly reduced number of eosinophils compared with sham-inoculated infected mice with AAD (Ova+PR8) and Scr-treated infected mice with AAD (Ova+PR8+Scr) (Figure 3.38).

#### **3.4.25. Treatment with intranasal Ant-21 does not suppress AHR in IAV infection following Ova-induced AAD**

Increased transpulmonary resistance was observed in sham-inoculated infected mice with AAD (Ova+PR8) at 3 dpi compared with sham-inoculated non-allergic non-infected control (Sham) and sham-inoculated infected non-allergic controls (PR8). No reduction in transpulmonary resistance was observed in Ant-21-treated infected non-allergic mice (PR8+Ant-21) compared with both sham-inoculated infected non-allergic controls and Scr-treated infected non-allergic control (Figure 3.39A).

Ant-21-treated infected mice with AAD (Ova+PR8+Ant-21) did not show any reduction in the transpulmonary resistance compared with sham-inoculated infected mice with AAD (Ova+PR8) and Scr-treated infected mice with AAD (Ova+PR8+Scr) (Figure 3.39A).

Likewise, decreased dynamic compliance was observed in sham-inoculated infected mice with AAD (Ova+PR8) at 3 dpi compared with sham-inoculated non-allergic non-infected control (Sham) and sham-inoculated infected non-allergic controls (PR8) (Figure 3.39B).

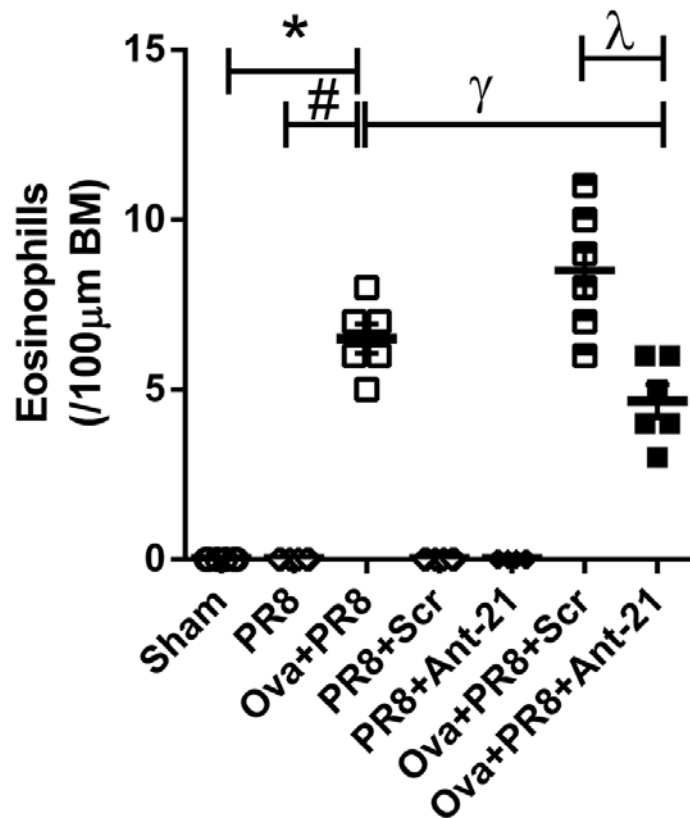


**Figure 3.38. Treatment with intranasal Ant-21 suppresses number of tissue eosinophils in IAV infection following Ova-induced AAD.**

BALB/c mice were sensitised with Ova or PBS, challenged with Ova and inoculated with IAV A/PR/8/34 (7.5 pfu) or media on the last day of Ova challenge. Mice were treated with Ant-21 or scrambled control on 0 dpi. Mice were sacrificed 3 dpi. Data are presented as mean±SEM (n=6-8); \*, #, γ and λ represents  $P \leq 0.05$  versus Sham, PR8, Ova+PR8 and Ova+PR8+Scr groups respectively.

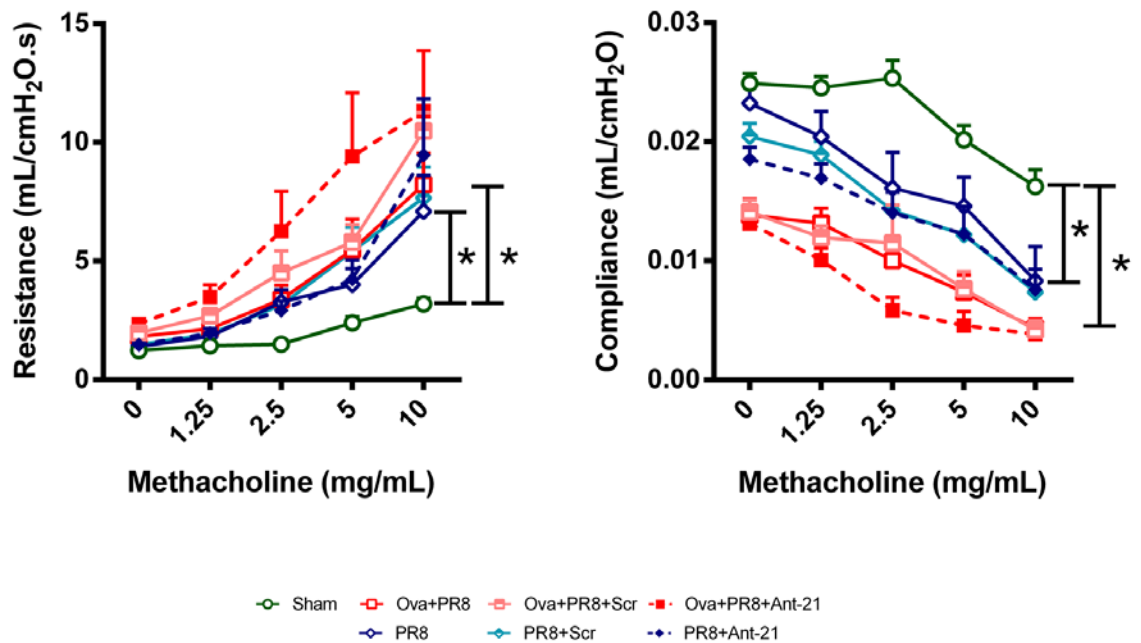


**Figure 3.39. Treatment with intranasal Ant-21 does not suppress AHR in IAV infection following Ova-induced AAD.**

BALB/c mice were sensitised with Ova or PBS, challenged with Ova and inoculated with IAV A/PR/8/34 (7.5 pfu) or media on the last day of Ova challenge. Mice were treated with Ant-21 or scrambled control on 0 dpi. Mice were sacrificed 3 dpi. **(A)** Transpulmonary resistance and **(B)** dynamic compliance. Data are presented as mean±SEM (n=6-8). \* represents P≤0.05 versus Sham.

No increase in dynamic compliance was demonstrated in Ant-21-treated infected non-allergic mice (PR8+Ant-21) compared with both sham-inoculated infected non-allergic controls and Scr-treated infected non-allergic control. Ant-21-treated infected mice with AAD (Ova+PR8+Ant-21) also did not show any increase in dynamic compliance compared with sham-inoculated infected mice with AAD (Ova+PR8) and Scr-treated infected mice with AAD (Ova+PR8+Scr) (Figure 3.39B).

#### **3.4.26. Treatment with intranasal Ant-21 suppresses miR-21 expression in IAV infection following Ova-induced AAD**

miR-21 expression was observed to be significantly increased in sham-inoculated infected mice with AAD (Ova+PR8) at 3 dpi as compared with sham-inoculated non-allergic non-infected control (Sham) and sham-inoculated infected non-allergic controls (PR8). Ant-21-treated infected non-allergic mice (PR8+Ant-21) demonstrated significant reduction in miR-21 expression compared with sham-inoculated infected non-allergic control and Scr-treated infected non-allergic control (Figure 3.40).

Importantly, Ant-21-treated infected mice with AAD (Ova+PR8+Ant-21) demonstrated significant reduction in miR-21 expression compared with sham-inoculated infected mice with AAD and Scr-treated infected mice with AAD (Ova+PR8+Scr) (Figure 3.40).

#### **3.4.27. Treatment with intranasal LY29 reduces viral titre in IAV infection following Ova-induced AAD**

We have already shown that the susceptibility of individuals with COPD to IAV infection is mediated by increased PI3K-p110 $\alpha$  activity. To determine, whether increased PI3K-p110 $\alpha$  activity also regulates susceptibility of AAD to IAV infection, we used PI3K inhibitor (LY294002). BALB/c mice were sensitised by i.p administration of Ova or PBS and subsequently challenged i.n. with Ova 12-15 days later. On the last day of Ova challenge, mice were infected i.n. with IAV A/PR/8/34 (7.5 pfu) or media. Mice were treated with LY29 or vehicle from 0 dpi till 2 dpi. Mice were sacrificed 3 dpi (Figure 3.10).

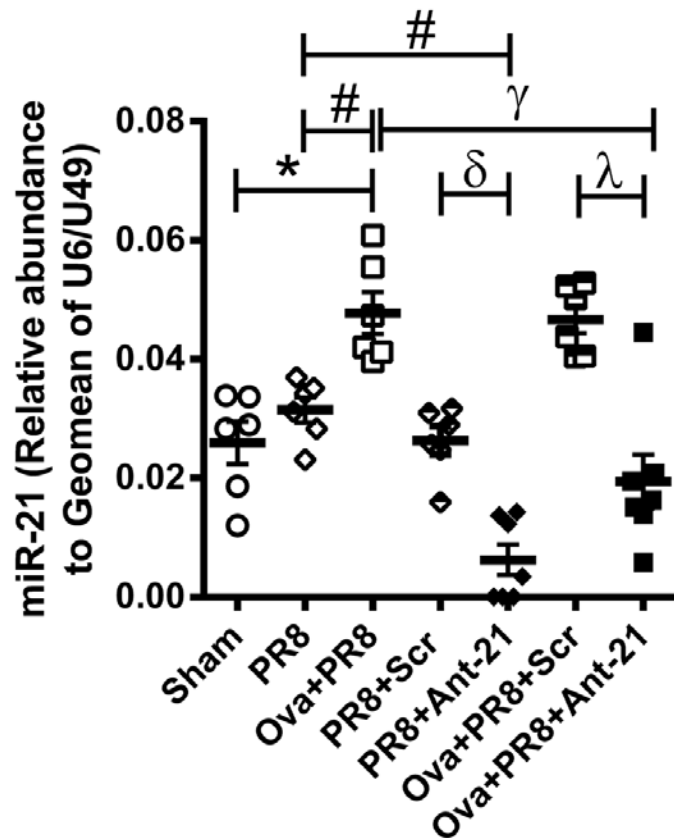


**Figure 3.40. Treatment with intranasal Ant-21 suppresses miR-21 expression in IAV infection following Ova-induced AAD.**

BALB/c mice were sensitised with Ova or PBS, challenged with Ova and inoculated with IAV A/PR/8/34 (7.5 pfu) or media on the last day of Ova challenge. Mice were treated with Ant-21 or scrambled control on 0 dpi. Mice were sacrificed 3 dpi. Data are presented as mean±SEM (n=6-8). \*, #, γ, δ and λ represents  $P \leq 0.05$  versus Sham, PR8, Ova+PR8, PR8+Scr and Ova+PR8+Scr groups respectively.

A non-significant trend towards increased viral titre was observed in sham-inoculated infected mice with AAD (Ova+PR8+Veh) at 3 dpi compared with sham-inoculated infected non-allergic controls (PBS+PR8+Veh). LY29-treated infected non-allergic mice (PBS+PR8+LY29) had significantly reduced viral titre compared with sham-inoculated infected non-allergic control. Importantly, LY29-treated infected mice with AAD (Ova+PR8+LY29) demonstrated significant reduction in the viral titre compared with sham-inoculated infected mice with AAD (Ova+PR8+Veh) (Figure 3.41).

#### **3.4.28. Treatment with intranasal LY29 suppresses tissue inflammation in IAV infection following Ova-induced AAD**

Tissue inflammation was observed to be significantly increased in sham-inoculated infected mice with AAD (Ova+PR8+Veh) at 3 dpi compared with sham-inoculated non-infected non-allergic mice (PBS+Media+Veh), sham-inoculated non-infected allergic (Ova+Media+Veh) and sham-inoculated infected non-allergic controls (PBS+PR8+Veh).

LY29-treated infected non-allergic mice (PBS+PR8+LY29) demonstrated significant reduction in tissue inflammation compared with infected non-allergic controls and sham-inoculated infected mice with AAD. Importantly, LY29-treated infected mice with AAD (Ova+PR8+LY29) demonstrated significant reduction in tissue inflammation compared with sham-inoculated infected mice with AAD (Ova+PR8+Veh) (Figure 3.42).

#### **3.4.29. Treatment with intranasal LY29 suppresses number of MSCs in IAV infection following Ova-induced AAD**

Sham-inoculated allergic non-infected mice (Ova+Media+Veh) demonstrated significantly increased numbers of MSCs around the small airways compared with sham-inoculated non-infected non-allergic controls (PBS+Media+Veh). A non-significant trend towards increased number of MSCs was observed in sham-inoculated infected mice with AAD compared to sham-inoculated allergic non-infected mice. LY29 treatment significantly reduced number of MSCs back to basal in LY29-treated infected mice with AAD (Ova+PR8+LY29) compared

with sham-inoculated infected mice with AAD (Ova+PR8+Veh) and sham-inoculated non-infected allergic mice (Figure 3.43).

#### **3.4.30. Treatment with intranasal LY29 suppresses number of tissue eosinophils in IAV infection following Ova-induced AAD**

Sham-inoculated allergic non-infected mice (Ova+Media+Veh) demonstrated significantly increased numbers of tissue eosinophils around the small airways compared with sham-inoculated non-infected non-allergic controls (PBS+Media+Veh). Number of eosinophils was observed to be significantly increase in sham-inoculated infected mice with AAD compared to sham-inoculated allergic non-infected mice. LY29 treatment significantly reduced number of tissue eosinophils back to basal in LY29-treated infected mice with AAD (Ova+PR8+LY29) compared with sham-inoculated infected mice with AAD (Ova+PR8+Veh) and sham-inoculated non-infected allergic mice (Figure 3.44).

#### **3.4.31. Treatment with intranasal LY29 does not suppress AHR in IAV infection following Ova-induced AAD**

Increased transpulmonary resistance was observed in sham-inoculated non-infected allergic mice (Ova+Media+Veh) at 3 dpi as compared with sham-inoculated non-allergic non-infected controls (PBS+Media+Veh). Reduction in transpulmonary resistance was observed in LY29-treated infected non-allergic mice (PBS+PR8+LY29) compared with sham-inoculated infected non-allergic control (PBS+PR8+Veh). LY29-treated infected mice with AAD (Ova+PR8+LY29) did not show any reduction in the transpulmonary resistance compared with sham-inoculated infected mice with AAD (Ova+PR8+Veh) (Figure 3.45A).

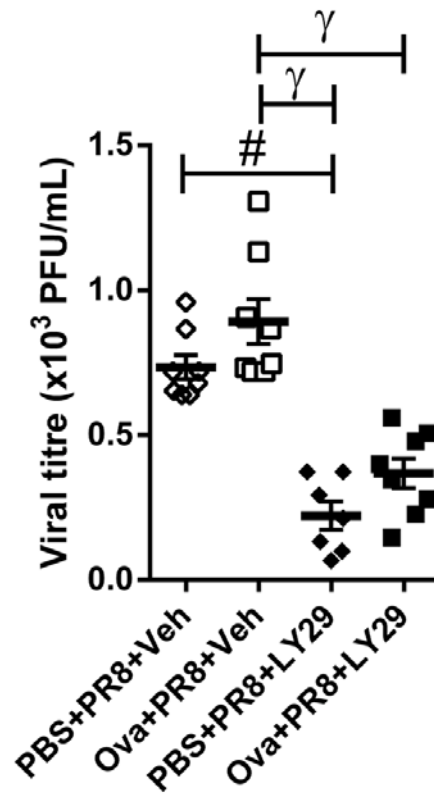


**Figure 3.41. Viral titre at 3 dpi.**

BALB/c mice were sensitised with Ova or PBS, challenged with Ova and inoculated with IAV A/PR/8/34 (7.5 pfu) or media on the last day of Ova challenge. Mice were treated with LY29 or vehicle from 0 dpi till 2 dpi. Mice were sacrificed 3 dpi. Data are presented as mean  $\pm$  SEM (n=6-8); # and  $\gamma$  represents  $P \leq 0.05$  versus PBS+PR8+Veh and Ova+PR8+Veh groups, respectively.

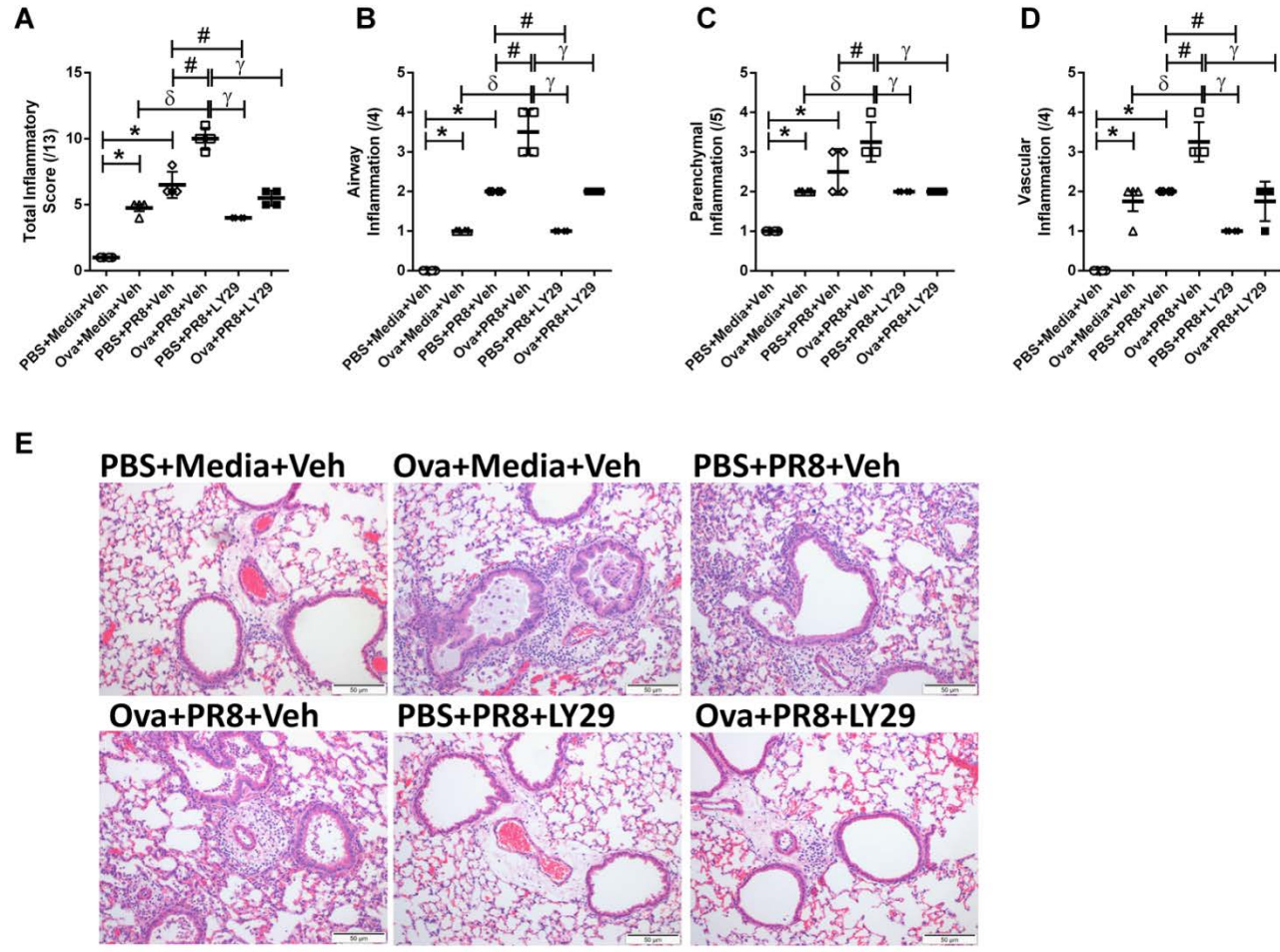
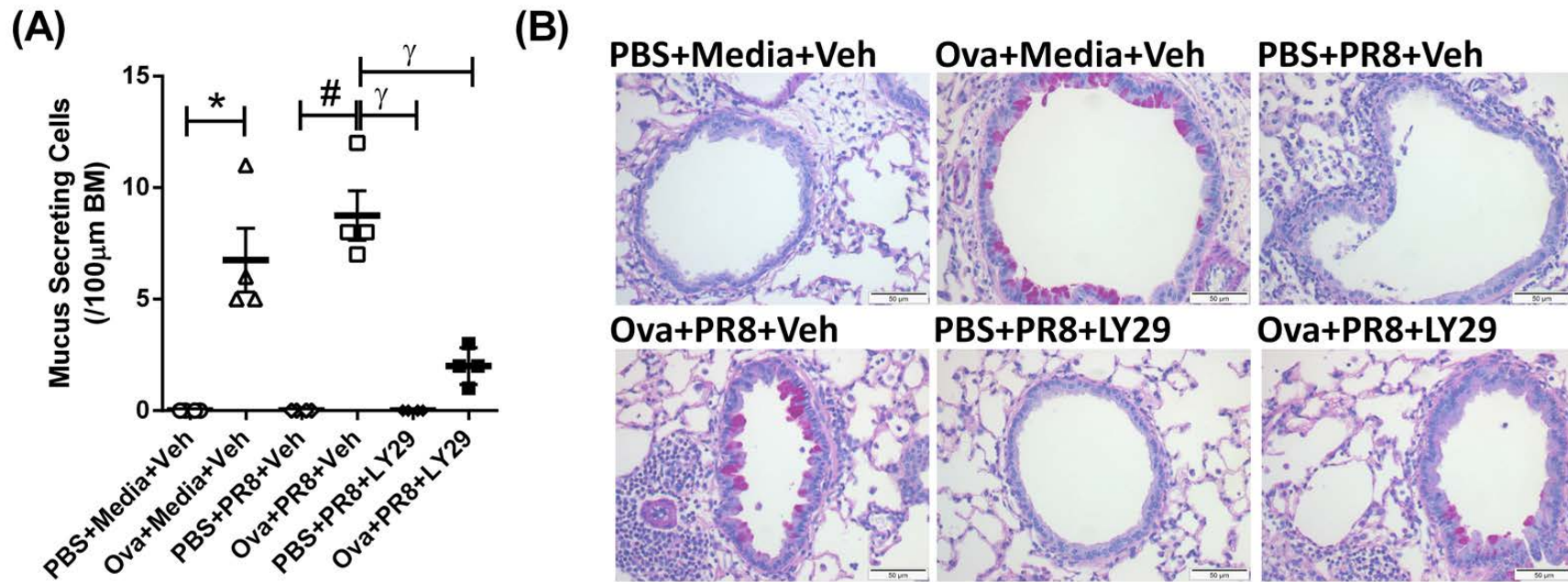


Figure 3.42. Treatment with intranasal LY29 suppresses tissue inflammation in IAV infection following Ova-induced AAD.

BALB/c mice were sensitised with Ova or PBS, challenged with Ova and inoculated with IAV A/PR/8/34 (7.5 pfu) or media on the last day of Ova challenge. Mice were treated with LY29 or vehicle from 0 dpi till 2 dpi. Mice were sacrificed 3 dpi. **(A)** Total; **(B)** airway; **(C)** parenchymal and **(D)** vascular inflammation score in haematoxylin and eosin (H&E) stained lung sections; **(E)** Representative images (10X) of H&E stained lung sections; Scale bar = 200µm. Data are presented as mean±SEM (n=6-8). \*, #, δ and γ represents  $P \leq 0.05$  versus PBS+Media+Veh, PBS+PR8+Veh, Ova+Media+Veh and Ova+PR8+Veh groups respectively.



**Figure 3.43. Treatment with intranasal LY29 suppresses number of MSCs in IAV infection following Ova-induced AAD.**

BALB/c mice were sensitised with Ova or PBS, challenged with Ova and inoculated with IAV A/PR/8/34 (7.5 pfu) or media on the last day of Ova challenge. Mice were treated with LY29 or vehicle from 0 dpi till 2 dpi. Mice were sacrificed 3 dpi. **(A)** MSCs per 100 μm basement membrane in periodic acid-Schiff (PAS) stained lung sections; **(B)** Representative images (20X) of PAS stained lung sections; Scale bar = 200 μm. Data are presented as mean±SEM (n=6-8). \*, # and γ represents P≤0.05 versus PBS+Media+Veh, PBS+PR8+Veh and Ova+PR8+Veh groups respectively.

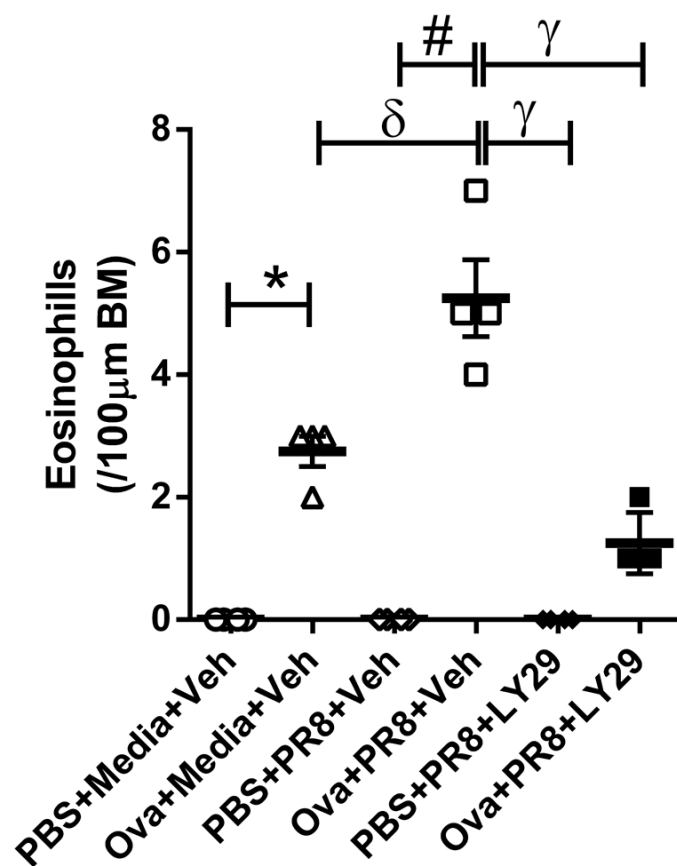


**Figure 3.44. Treatment with intranasal LY29 suppresses number of tissue eosinophils in IAV infection following Ova-induced AAD.**

BALB/c mice were sensitised with Ova or PBS, challenged with Ova and inoculated with IAV A/PR/8/34 (7.5 pfu) or media on the last day of Ova challenge. Mice were treated with LY29 or vehicle from 0 dpi till 2 dpi. Mice were sacrificed 3 dpi. Data are presented as mean±SEM (n=6-8). \*, #, δ and γ represents P≤0.05 versus PBS+Media+Veh, PBS+PR8+Veh, Ova+Media+Veh and Ova+PR8+Veh groups respectively.

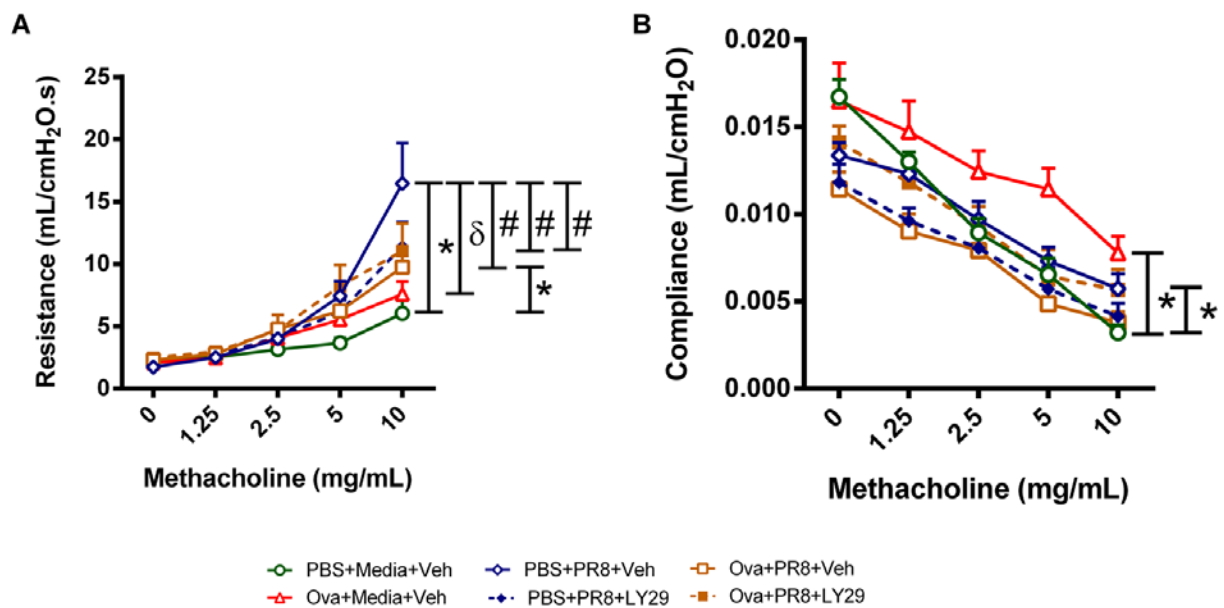


**Figure 3.45. Treatment with intranasal LY29 does not suppress AHR in IAV infection following Ova-induced AAD.**

BALB/c mice were sensitised with Ova or PBS, challenged with Ova and inoculated with IAV A/PR/8/34 (7.5 pfu) or media on the last day of Ova challenge. Mice were treated with LY29 or vehicle from 0 dpi till 2 dpi. Mice were sacrificed 3 dpi. **(A)** Transpulmonary resistance and **(B)** dynamic compliance. Data are presented as mean±SEM (n=6-8). \*, # and δ represents  $P \leq 0.05$  versus PBS+Media+Veh, PBS+PR8+Veh, and Ova+Media+Veh groups respectively.

Likewise, decreased dynamic compliance was observed in sham-inoculated non-infected allergic mice (Ova+Media+Veh) at 3 dpi compared with sham-inoculated non-allergic non-infected controls (PBS+Media+Veh). No increase in dynamic compliance was demonstrated in LY29-treated infected non-allergic mice (PBS+PR8+LY29) compared with sham-inoculated infected non-allergic control (PBS+PR8+Veh). LY29-treated infected mice with AAD (Ova+PR8+LY29) also did not show any increase in the dynamic compliance compared with sham-inoculated infected mice with AAD (Ova+PR8+Veh) (Figure 3.45B).

#### **3.4.32. Treatment with intranasal LY29 does not suppress miR-21 expression in IAV infection following Ova-induced AAD**

miR-21 expression was observed to be significantly increased in sham-inoculated allergic non-infected mice (Ova+Media+Veh) at 3 dpi compared with sham-inoculated non-allergic non-infected controls (PBS+Media+Veh).

A non-significant trend towards increased miR-21 expression was observed in sham-inoculated infected mice with AAD (Ova+PR8+Veh) compared with sham-inoculated allergic non-infected mice (Ova+Media+Veh) and sham-inoculated infected non-allergic mice (PBS+PR8+Veh).

LY29 treatment in infected non-allergic mice (PBS+PR8+LY29) did not reduce miR-21 expression compared with infected non-allergic controls. Similarly, no reduction in miR-21 expression was observed in LY29-treated infected mice with AAD (Ova+PR8+LY29) when compared with sham-inoculated infected mice with AAD (Ova+PR8+Veh) (Figure 3.46)

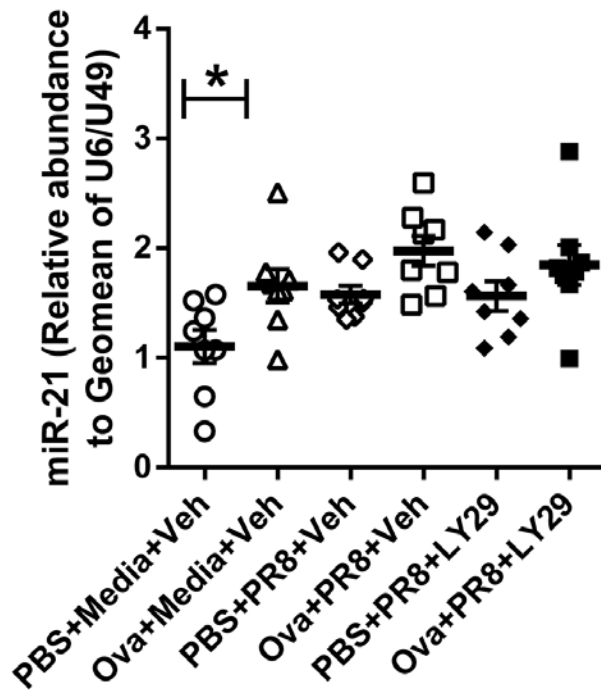


**Figure 3.46. Treatment with intranasal LY29 does not suppress miR-21 expression in IAV infection following Ova-induced AAD.**

BALB/c mice were sensitised with Ova or PBS, challenged with Ova and inoculated with IAV A/PR/8/34 (7.5 pfu) or media on the last day of Ova challenge. Mice were treated with LY29 or vehicle from 0 dpi till 2 dpi. Mice were sacrificed 3 dpi. Data are presented as mean±SEM (n=6-8). \* represents  $P \leq 0.05$  versus PBS+Media+Veh group.

### **3.4.33. IAV infection influences IL-13R $\alpha$ 1 expression in experimental COPD**

Our laboratory has demonstrated that infected mice with experimental COPD had more severe infection characterised by increased viral titre and pulmonary inflammation. To further investigate the mechanism involved in the increased susceptibility of IAV infection in COPD, BALB/c mice were exposed to normal air or CS through the nose only for 8 weeks. The mice were infected i.n. with IAV A/PR/8/34 (7.5 pfu) or media on the last day of smoke exposure. Mice were sacrificed 7 dpi (Figure 3.4).

Localization of IL-13R $\alpha$ 1 in lung tissues was observed using IHC, where IL-13R $\alpha$ 1 expression was observed to be significantly increased in the airway epithelium of non-infected smoke-exposed mice (Smk), infected normal air-exposed mice (PR8) and infected mice with COPD (Smk+PR8) compared with non-infected normal air-exposed mice (control) (Figure 3.47). However, a non-significant trend towards increase in IL-13R $\alpha$ 1 expression was observed in infected mice with COPD compared with non-infected smoke-exposed mice and infected normal air-exposed mice (Figure 3.47).

### **3.4.34. IAV infection increases localization of miR-21 expression in experimental COPD**

To further investigate the mechanism involved in driving susceptibility of COPD to IAV infection downstream of IL-13R $\alpha$ 1, we investigated miR-21 as a potential target molecule. Localization of miR-21 was performed in histological sections of formalin fixed, paraffin embedded lungs using ISH. Representative images of the stained lung sections showed increase in miR-21 localization to the luminal epithelium of small airways of non-infected smoke-exposed mice (Smk) compared to non-infected normal air-exposed mice (control). Also, miR-21 localization was increased to the airway epithelium of infected mice with COPD compared with non-infected smoke-exposed mice and infected normal air-exposed mice (PR8) (Figure 3.48).

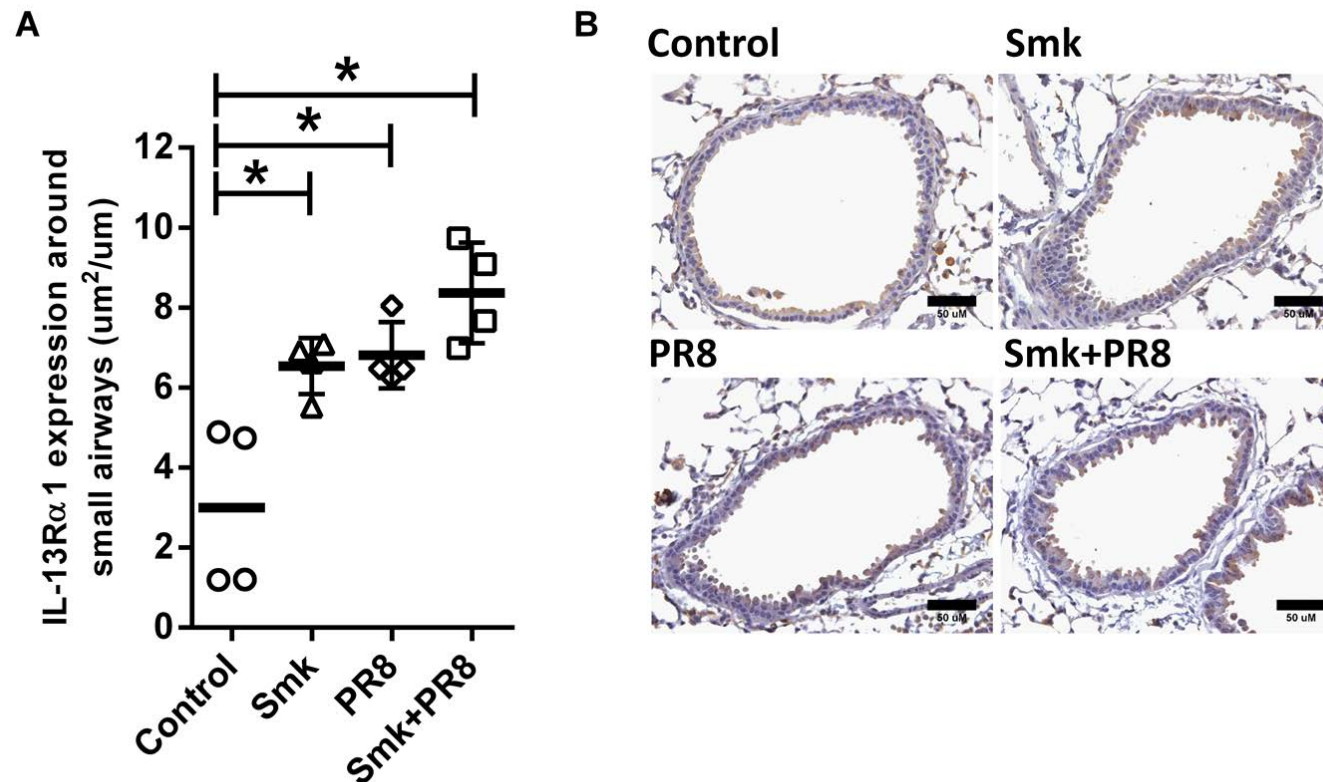


**Figure 3.47. IAV infection influences IL-13R $\alpha$ 1 expression in experimental COPD.**

BALB/c mice were exposed to CS or normal air for 8 weeks and inoculated with IAV A/PR/8/34 (7.5 pfu) or media on the last day of smoke exposure. Mice were sacrificed 7 dpi. **(A)** IL-13R $\alpha$ 1 expression around small airways and **(B)** Representative images (40X) of IL-13R $\alpha$ 1 stained lung tissue sections. Scale bar = 50 $\mu$ m. Data are presented as mean $\pm$ SEM (n=4); \*P $\leq$ 0.05 versus control group.

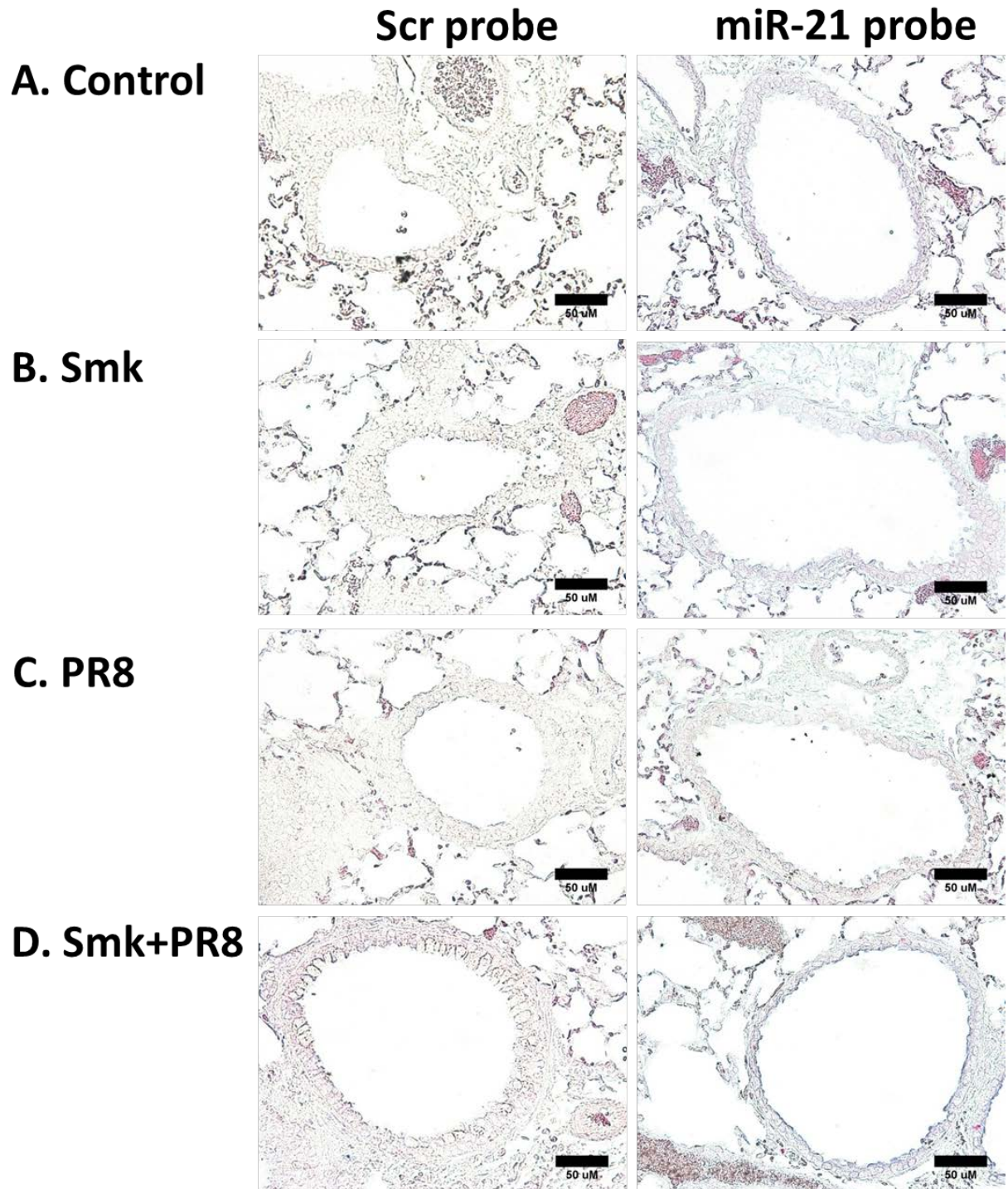


**Figure 3.48. miR-21 is localised to the luminal epithelium associated with small airways in IAV infection in experimental COPD.**

BALB/c mice were exposed to CS or normal air for 8 weeks and inoculated with IAV A/PR/8/34 (7.5 pfu) or media on the last day of smoke exposure. Mice were sacrificed 7 dpi. Representative photomicrographs (40X) showing tissue localization of miR-21 in histological sections of mouse lung collected on 3 dpi of the study protocol. Localisation of miR-21 in lung sections was characterised using in-situ

hybridization analysis with a miR-21-specific locked nucleic acid (LNA<sup>TM</sup>). miR-21-positive signal (blue colour) is visible in epithelial cells associated with small airways. miR-21-positive signal is not evident when a scrambled (Scr) LNA<sup>TM</sup> miR probe was employed. Nuclear Fast Red<sup>TM</sup> was used as counterstain.

### **3.4.35. IAV infection increases number of MSCs in experimental COPD**

At 7 dpi, non-infected smoke-exposed mice (Smk) and infected mice with COPD (Smk+PR8) had significantly increased number of MSCs compared with non-infected normal air-exposed mice (control). Also, infected mice with COPD had significantly higher number of MSCs compared with non-infected smoke-exposed mice and infected normal air-exposed mice. Majority of the MSCs was observed to be present in large airways when compared with small airways (Figure 3.49).

### **3.4.36. Treatment with Anti-IL-13 reduces viral titre in experimental COPD with IAV infection**

We next assessed whether inhibition of IL-13 could protect against infection and reduce the severity of COPD following IAV infection and be a potential human treatment. BALB/c mice were exposed to normal air or CS through the nose only for 8 weeks. The mice were infected i.n. with IAV A/PR/8/34 (7.5 pfu) or media on the last day of smoke exposure. Mice were treated i.p. with IL-13 specific monoclonal antibody (Anti-IL-13) or isotype on day 0, 2, 4 and 6 dpi. Mice were sacrificed 7 dpi (Figure 3.12).

At 7 dpi, a significant increase in viral titre was observed in isotype-treated infected smoke-exposed mice compared with isotype-treated infected normal air-exposed mice. A non-significant trend towards reduced viral titre was observed in Anti-IL-13-treated infected normal air-exposed mice compared with isotype-treated infected normal air-exposed mice. Also, Anti-IL-13-treated infected mice with COPD demonstrated significantly reduced viral titre compared with isotype-treated infected mice with COPD (Figure 3.50).

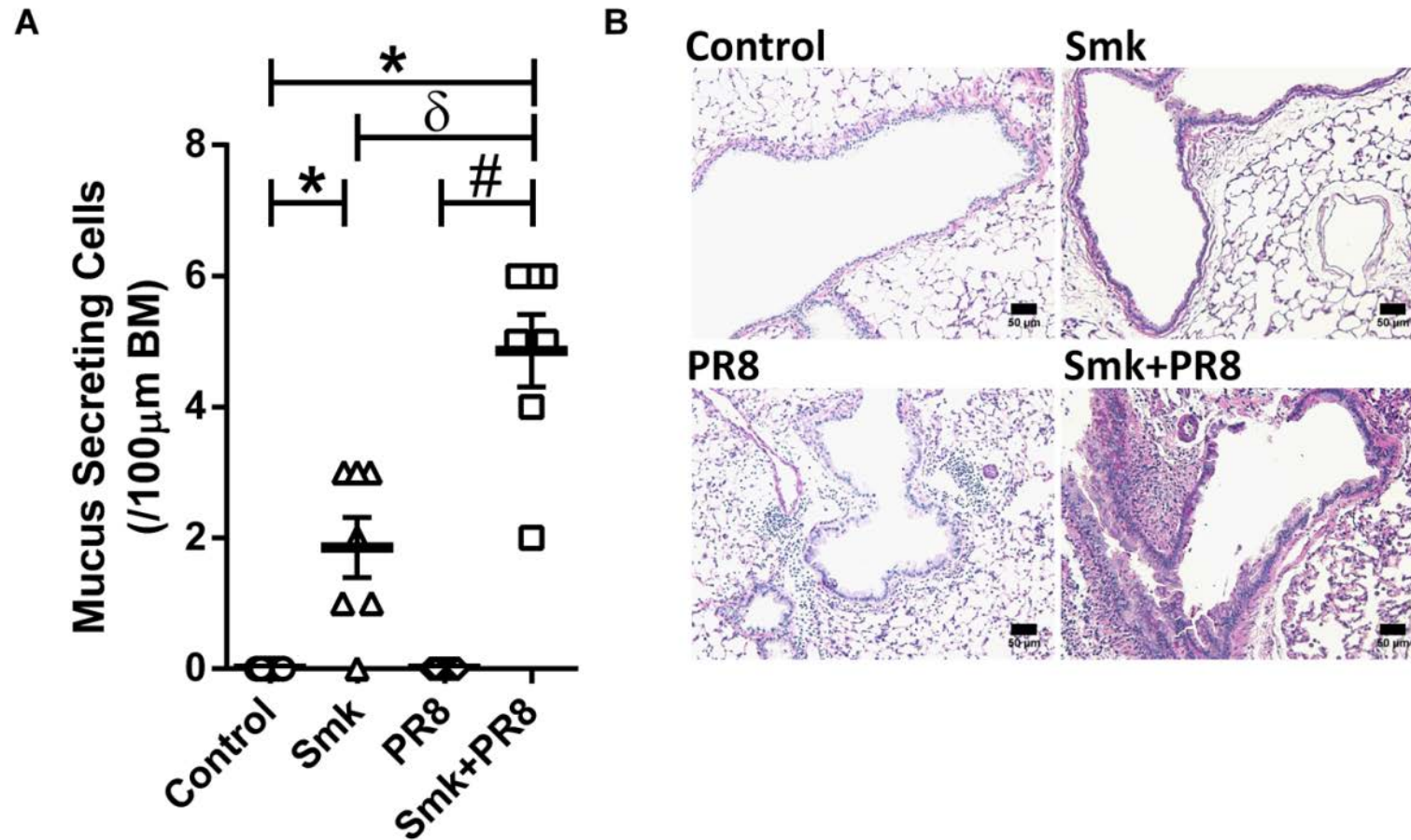
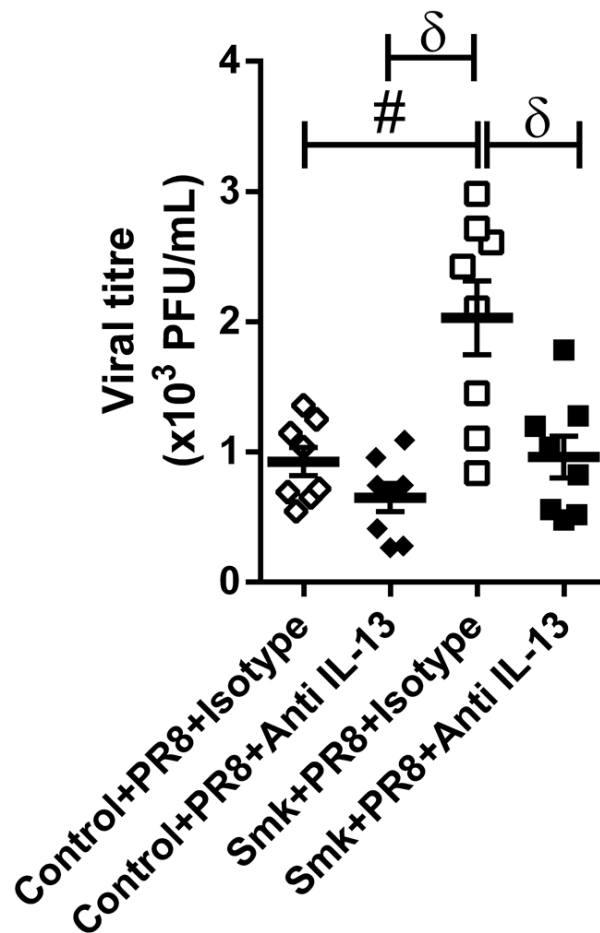


Figure 3.49. IAV infection increases number of MSCs in chronically cigarette smoke-exposed mice.

BALB/c mice were exposed to CS or normal air for 8 weeks and inoculated with IAV A/PR/8/34 (7.5 pfu) or media on the last day of smoke exposure. Mice were sacrificed 7 dpi. **(A)** Mucus secreting cells per 100 $\mu$ m basement membrane (BM) in periodic acid-Schiff (PAS) stained lung sections. **(B)** Representative images (20X) of stained lung tissue sections. Scale bar = 50 $\mu$ m. Data are presented as mean $\pm$ SEM (n=6). \*,  $\delta$ , # represents  $P\leq 0.05$  versus control, Smk and PR8 groups respectively.



**Figure 3.50. Viral titre at 7 dpi.**

BALB/c mice were exposed to CS or normal air for 8 weeks and inoculated with IAV A/PR/8/34 (7.5 pfu) or media on the last day of smoke exposure. Mice were treated anti-IL-13 antibody or isotype on day 0, 2, 4 and 6 dpi. Mice were sacrificed 7 dpi. Data are presented as mean  $\pm$  SEM (n=6-8). # and  $\delta$  represents  $P \leq 0.05$  versus Control+PR8+Isotype and Smk+PR8+Isotype groups, respectively.

#### **3.4.37. Treatment with Anti-IL-13 decreases tissue inflammation in experimental COPD with IAV infection**

At 7 dpi, a significant increase in tissue inflammation was observed in isotype-treated infected smoke-exposed mice compared with isotype-treated infected normal air-exposed mice. Tissue inflammation was significantly decreased in Anti-IL-13-treated infected normal air-exposed mice and Anti-IL-13-treated infected mice with COPD compared with isotype-treated infected normal air-exposed mice and isotype-treated infected mice with COPD respectively (Figure 3.51).

#### **3.4.38. Treatment with Anti-IL-13 reduces number of MSCs in experimental COPD with IAV infection**

At 7 dpi, a significant increase in number of MSCs was observed in isotype-treated infected smoke-exposed mice compared with isotype-treated infected normal air-exposed mice. Anti-IL-13 treatment in infected mice with COPD significantly reduced the number of MSCs compared with isotype-treated infected mice with COPD (Figure 3.52).

#### **3.4.39. Treatment with Anti-IL-13 did not inhibit miR-21 expression in experimental COPD with IAV infection**

miR-21 expression was not reduced in Anti-IL-13-treated infected normal air-exposed mice compared with isotype-treated infected normal air-exposed mice. However, a non-significant trend towards decrease in miR-21 expression was observed in Anti-IL-13 treated infected mice with COPD compared with isotype-treated infected mice with COPD (Figure 3.53).

#### **3.4.40. Inhibition of miR-21 reduces viral titre in experimental COPD with IAV infection**

To further investigate the functional role of miR-21 in driving increased susceptibility of IAV infection in COPD, we targeted miR-21 using specific inhibitor, antagomir 21 (Ant-21). BALB/c mice were exposed to normal air or CS through the nose only for 8 weeks. The mice were infected i.n. with IAV A/PR/8/34 (7.5 pfu) or media on the last day of smoke exposure. Mice were treated with Ant-21 or scrambled control once a week from week 6 till week 8. Mice were sacrificed 7 dpi (Figure 3.9).

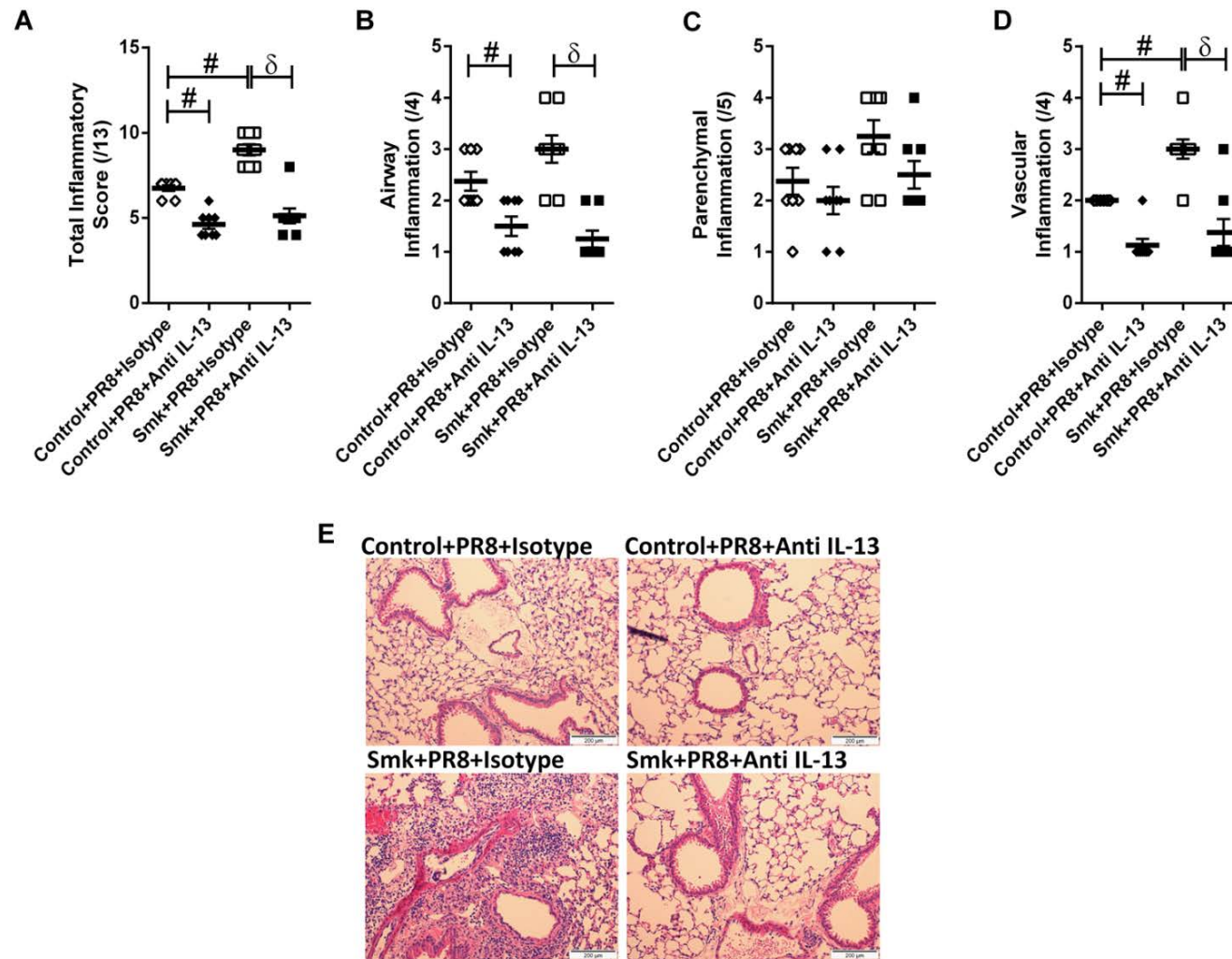
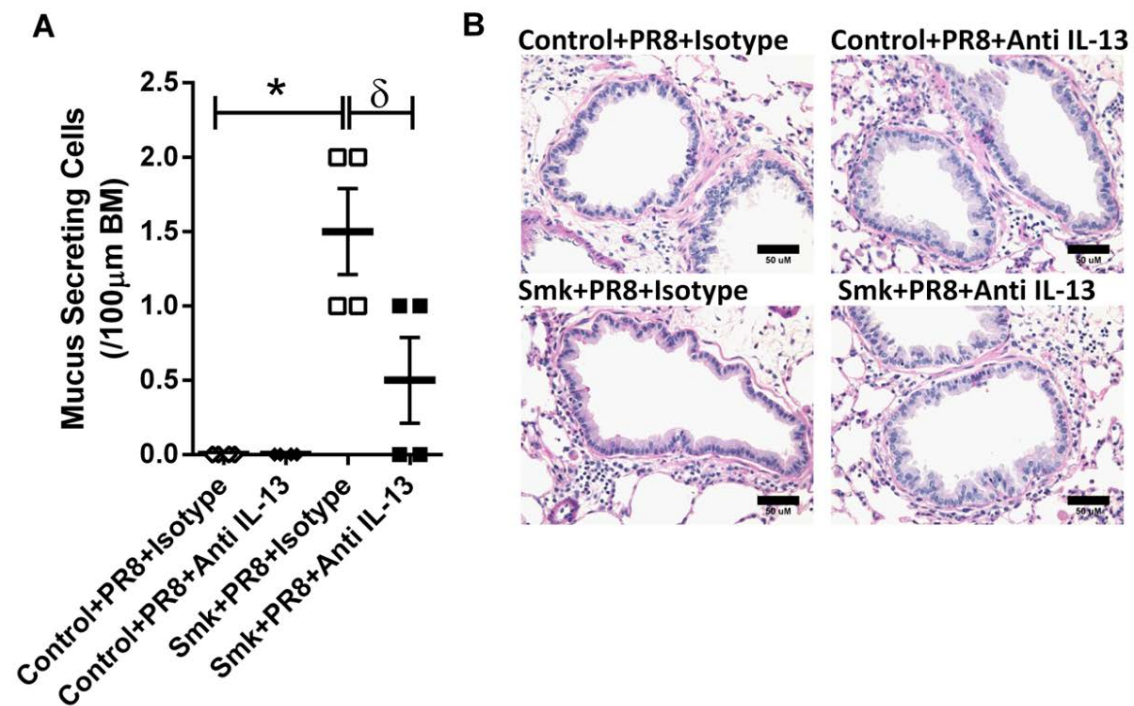


Figure 3.51. Treatment with Anti-IL-13 decreases tissue inflammation in experimental COPD with IAV infection.

BALB/c mice were exposed to CS or normal air for 8 weeks and inoculated with IAV A/PR/8/34 (7.5 pfu) or media on the last day of smoke exposure. Mice were treated anti-IL-13 antibody or isotype on day 0, 2, 4 and 6 dpi. Mice were sacrificed 7 dpi. **(A)** Total; **(B)** airway; **(C)** parenchymal and **(D)** vascular inflammation score in haematoxylin and eosin (H&E) stained lung sections; (E) Representative images (10X) of H&E stained lung sections; Scale bar = 200µm. Data are presented as mean±SEM (n=6-8). # and δ represents  $P \leq 0.05$  versus Control+PR8+Isotype and Smk+PR8+Isotype groups, respectively.



**Figure 3.52. Treatment with Anti-IL-13 reduces number of MSCs in experimental COPD with IAV infection.**

BALB/c mice were exposed to CS or normal air for 8 weeks and inoculated with IAV A/PR/8/34 (7.5 pfu) or media on the last day of smoke exposure. Mice were treated anti-IL-13 antibody or isotype on day 0, 2, 4 and 6 dpi. Mice were sacrificed 7 dpi. **(A)** Mucus secreting cells per 100  $\mu\text{m}$  basement membrane in periodic acid-Schiff (PAS) stained lung sections; **(B)** Representative images (20X) of stained lung tissue sections; Scale bar = 50 $\mu\text{m}$ . Data are presented as mean $\pm$ SEM (n=6). \*,  $\delta$  represents  $P \leq 0.05$  versus Control+PR8+Isotype and Smk+PR8+Isotype group.

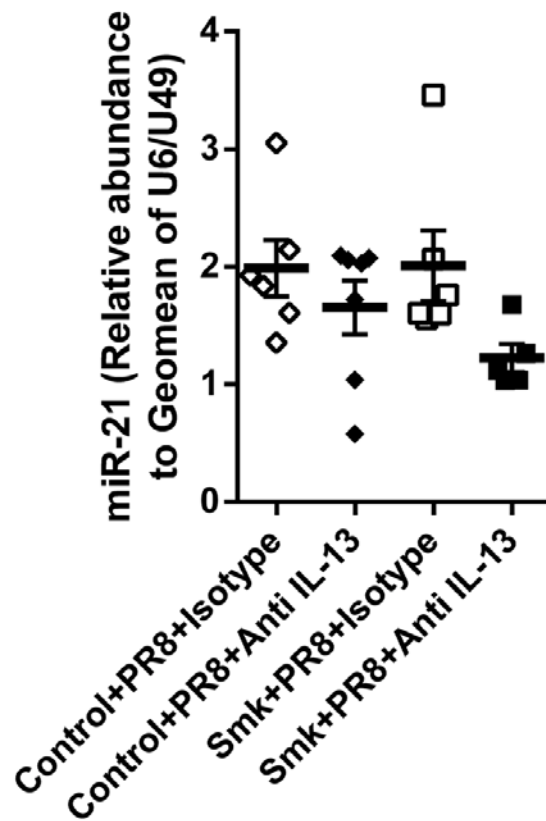


**Figure 3.53. Treatment with Anti-IL-13 did not inhibit miR-21 expression in experimental COPD with IAV infection.**

BALB/c mice were exposed to CS or normal air for 8 weeks and inoculated with IAV A/PR/8/34 (7.5 pfu) or media on the last day of smoke exposure. Mice were treated anti-IL-13 antibody or isotype on day 0, 2, 4 and 6 dpi. Mice were sacrificed 7 dpi. Data are presented as mean±SEM (n=6).

At 7 dpi, viral titre was observed to be significantly increased in infected smoke-exposed mice (Smk+PR8) compared with Scr-treated infected normal air-exposed mice (Scr+PR8). Further, Ant-21 treatment significantly reduced viral titre in infected normal air-exposed mice compared with Scr-treated infected normal air-exposed mice. Also, Ant-21-treated infected mice with COPD demonstrated significantly reduced viral titre in contrast to isotype-treated infected mice with COPD (Figure 3.54).

#### **3.4.41. Treatment with intranasal Ant-21 suppresses tissue inflammation in experimental COPD with IAV infection**

At 7dpi, non-infected smoke-exposed mice exhibited significant increase in lung tissue inflammation compared with non-infected normal air-exposed mice. Infected normal air-exposed mice also had increased histopathological scores compared with non-infected normal air-exposed mice. Infected smoke-exposed mice had increased histopathological scores compared with non-infected normal air-exposed mice, infected normal air-exposed mice and non-infected smoke-exposed mice alone (Figure 3.55).

Ant-21 treatment in non-infected smoke-exposed mice and infected normal air-exposed mice demonstrated a non-significant trend towards reduced tissue inflammation compared with Scr-treated non-infected smoke-exposed mice and Scr-treated infected air-exposed mice respectively. Likewise, Ant-21-treated infected mice with COPD exhibited significantly reduced tissue inflammation compared with Scr-treated infected mice with COPD (Figure 3.55).

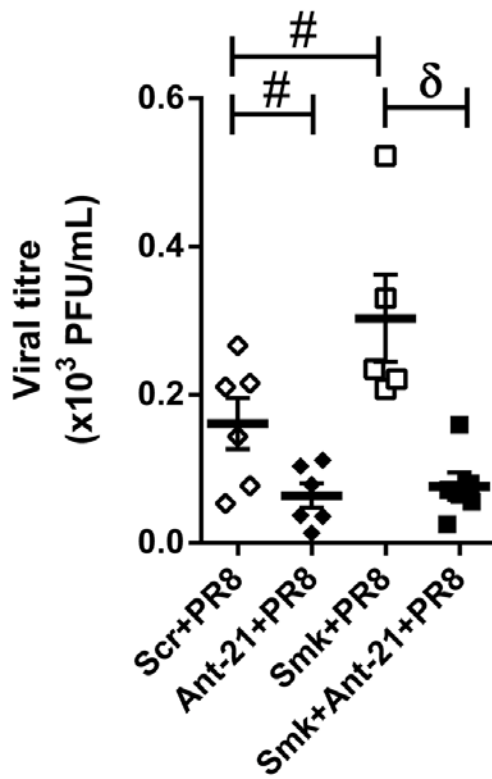


**Figure 3.54. Viral titre at 7 dpi.**

BALB/c mice were exposed to CS or normal air for 8 weeks and inoculated with IAV A/PR/8/34 (7.5 pfu) or media on the last day of smoke exposure. Mice were treated with Ant-21 or scrambled control once a week from week 6 till week 8. Mice were sacrificed 7 dpi. Data are presented as mean  $\pm$  SEM (n=6-8). # and  $\delta$  represents  $P \leq 0.05$  versus Scr+PR8 and Smk+PR8 groups, respectively.

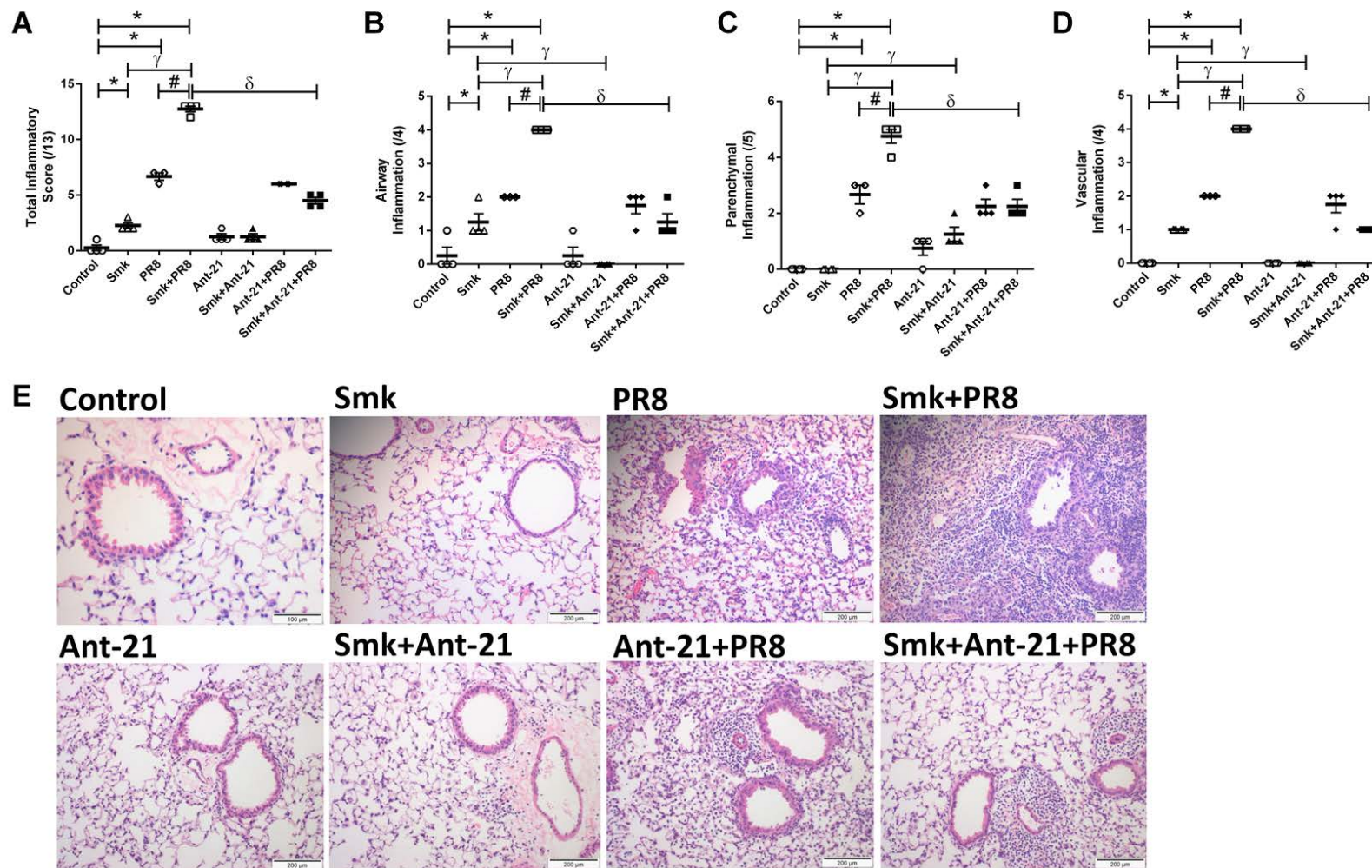


Figure 3.55. Treatment with intranasal Ant-21 suppresses tissue inflammation in experimental COPD with IAV infection.

BALB/c mice were exposed to CS or normal air for 8 weeks and inoculated with IAV A/PR/8/34 (7.5 pfu) or media on the last day of smoke exposure. Mice were treated with Ant-21 or scrambled control once a week from week 6 till week 8. Mice were sacrificed 7 dpi. **(A)** Total; **(B)** airway; **(C)** parenchymal and **(D)** vascular inflammation score in haematoxylin and eosin (H&E) stained lung sections; **(E)** Representative images (10X) of H&E stained lung sections; Scale bar = 200µm. Data are presented as mean±SEM (n=6-8). \*, γ, # and δ represent  $P \leq 0.05$  versus control, Smk, PR8 and Smk+PR8 groups, respectively.

#### **3.4.42. Treatment with intranasal Ant-21 reduces number of MSCs back to base line in experimental COPD with IAV infection**

At 7 dpi, a significant increase in the number of MSCs was observed in infected smoke-exposed mice (Smk+PR8) compared with non-infected normal air-exposed mice (Control) and non-infected smoke-exposed mice (Smk). Furthermore, Ant-21 treatment reduced number of MSCs back to base line in non-infected smoke-exposed mice (Smk+Ant-21), infected normal air-exposed mice (Ant-21+PR8) and infected mice with COPD (Smk+Ant-21+PR8) compared with their respective Scr-treated controls (Figure 3.56).

#### **3.4.43. Treatment with intranasal Ant-21 suppresses miR-21 expression back to base line in experimental COPD with IAV infection**

At 7dpi, non-infected smoke-exposed mice (Smk), infected normal air-exposed mice (PR8) and infected smoke-exposed mice (Smk+PR8) exhibited significant increase in miR-21 expression compared with non-infected normal air-exposed mice (Control). Infected smoke-exposed mice demonstrated a non-significant trend towards an increased miR-21 compared with non-infected smoke-exposed mice (Figure 3.57).

Furthermore, Ant-21 treatment reduced miR-21 expression back to base line in non-infected smoke-exposed mice (Smk+Ant-21), infected normal air-exposed mice (Ant-21+PR8) and infected mice with COPD (Smk+Ant-21+PR8) compared with their respective Scr-treated controls (Figure 3.57).

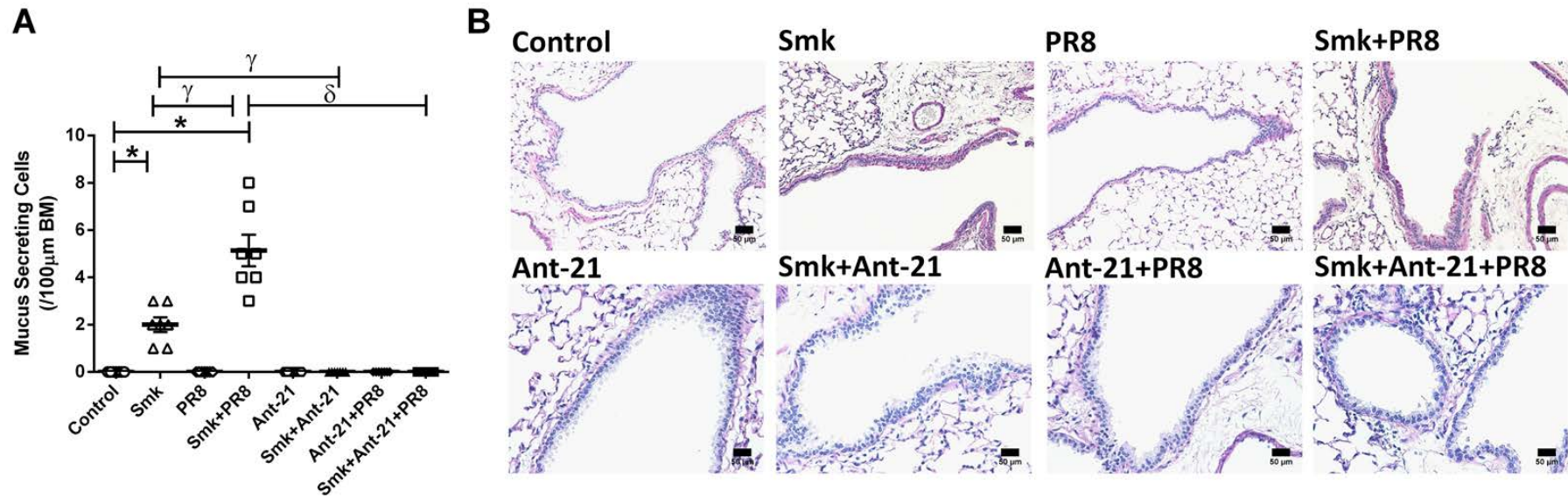


**Figure 3.56. Treatment with intranasal Ant-21 reduces number of MSCs back to base line in experimental COPD with IAV infection.**

BALB/c mice were exposed to CS or normal air for 8 weeks and inoculated with IAV A/PR/8/34 (7.5 pfu) or media on the last day of smoke exposure. Mice were treated with Ant-21 or scrambled control once a week from week 6 till week 8. Mice were sacrificed 7 dpi. **(A)** MSCs per 100 μm basement membrane in periodic acid-Schiff (PAS) stained lung sections; **(B)** Representative images (20X) of PAS stained lung sections; Scale bar = 50 μm. Data are presented as mean±SEM (n=6-8). \*, γ and δ represent P≤0.05 versus control, Smk and Smk+PR8 groups, respectively.

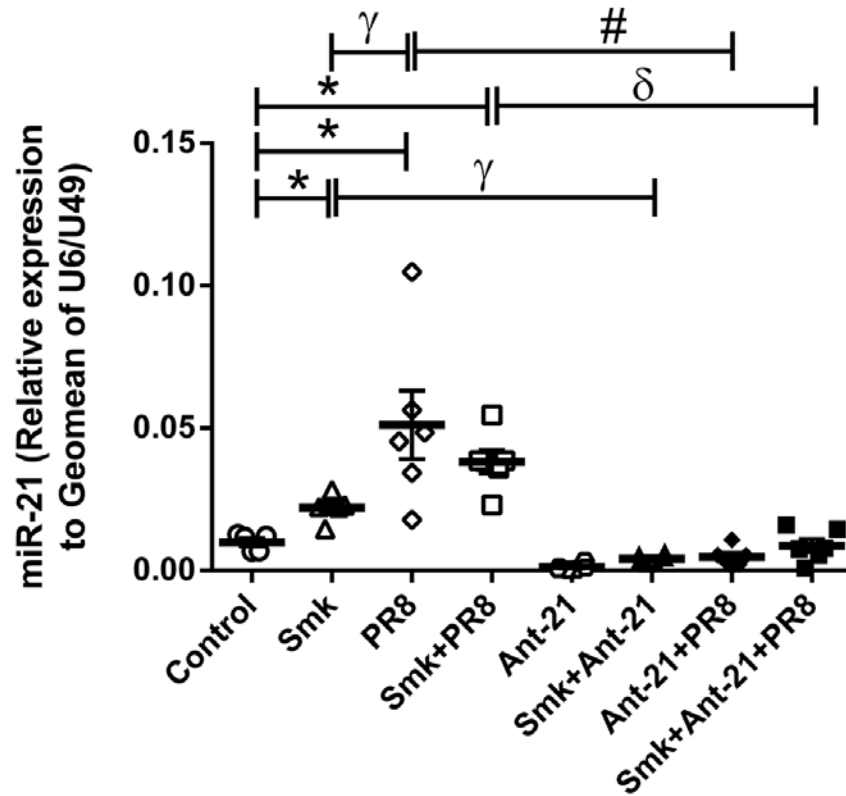


**Figure 3.57. Treatment with intranasal Ant-21 suppresses miR-21 expression back to base line in experimental COPD with IAV infection.**

BALB/c mice were exposed to CS or normal air for 8 weeks and inoculated with IAV A/PR/8/34 (7.5 pfu) or media on the last day of smoke exposure. Mice were treated with Ant-21 or scrambled control once a week from week 6 till week 8. Mice were sacrificed 7 dpi. Data are presented as mean±SEM (n=6-8). \*, γ, # and δ represent P≤0.05 versus control, Smk, PR8 and Smk+PR8 groups, respectively.

### 3.5. DISCUSSION

Asthma is a complex disease caused by multiple genetic and environmental factors and is induced and exacerbated by respiratory virus infections[540]. Clinical and epidemiological data demonstrate that people with asthma and a concomitant IAV infection are at high risk of hospital admission[541, 542]. The most common cause for exacerbation of asthma is the activation of the airways and exacerbation of the underlying disease by viral infections[421, 543, 544]. Our current understanding of the mechanisms that underpin the increased susceptibility to IAV infection in AAD is limited. In our current *in vivo* studies, we utilised an Ova-induced model of AAD to delineate the effects of IAV infection on asthma. This resulted in the establishment of a model of IAV-induced exacerbation of pre-existing AAD with increased allergic airway inflammation and AHR. We used this model to investigate the mechanisms underlying infection-induced exacerbations specifically the roles of IL-13/IL-13R $\alpha$ 1 and miR-21. These studies can be further extended to additional models of AAD including HDM-induced AAD (Chapter 2), to determine if this effect is consistent across different models.

Only a few previous studies have investigated the ability of IAV infection to alter airway function but they only assessed the impacts of infection on the establishment of AAD[545-547]. Yamamoto and colleagues demonstrated that Ova inhalation during the acute phase of IAV infection induced type 2 immune responses, while during the recovery phase type 1 immune responses were generated. Their results indicated that the timing of antigen sensitisation after IAV infection determines the type of immune response [546].

Also, Chang *et al.*, suggested that infection with certain microorganisms can prevent the subsequent development of asthma and allergen-induced AHR in later stages of life by preferential expansion of a CD4<sup>-</sup> and CD8<sup>-</sup> subset of NKT cells[547]. In contrast, we investigated the role of IAV infection in exacerbating pre-existing AAD. We have made important observations that advance our understanding of the mechanisms that underpin the association between IAV infection and asthma.

The existence of established Ova-induced AAD prior to IAV infection resulted in a significant increase in viral titre compared to infected non-allergic controls. Also, an increased lung tissue inflammation, higher numbers of lung eosinophils and MSCs around the airways and increased transpulmonary resistance was observed in infected mice with AAD. These observations are consistent with previously published findings[548-550]. We then used this established model to investigate the underlying mechanisms and to assess the potential of therapeutic interventions.

Very few studies have examined the effects of IL-13 in viral infections. The findings in these studies indicated that IL-13 produced during the IAV infection is one of the main activating factors that mediate the exacerbation of allergic responses. Recent studies have clearly demonstrated that IL-13 plays a prominent role in asthma-type responses[66, 518, 551, 552]. They also showed that RSV infection preferentially induces IL-13 production in the airways and promotes AHR and airway damage[518]. We also observed increased viral titres in rIL-13-treated infected mice as compared with infected controls. The rIL-13-treated IAV infected mice also had higher numbers of lung eosinophils and MSCs around the airways compared to sham-inoculated, infected and rIL-13-treated control groups. These data indicates that IL-13 promotes susceptibility to IAV infection and pro-inflammatory and –remodelling responses relevant to asthma.

Given the role of IL-13 in asthma[52, 553, 554], it is perhaps not surprising to find that inhibition of IL-13 reduces IAV titres. Our observations indicate that hosts with underlying AAD or increased IL-13 responses are more vulnerable to more severe infection. A previous study showed that mice exposed to asthma-exacerbating inducers such as diesel exhaust particles (a potent oxidative air pollutant) had increased IAV titres[555]. Overall, our findings are in agreement with various studies demonstrating an increased susceptibility of asthma patients to various viral infections including IAV[541, 556-559].

To confirm that IL-13 is a likely mechanism driving infection and exacerbating disease features (increased viral titres, MSCs, eosinophils and AHR), we assessed the levels of IL-13 and its receptor, IL-13R $\alpha$ 1, in Ova-induced AAD lung tissues. At 3dpi, in sham-inoculated allergic controls, AAD lead to increased IL-13 compared to sham-inoculated non-allergic controls. Infected mice with AAD also had an increased level of IL-13 in contrast to infected non-allergic controls. Our results highlighted that IAV infection does not induce IL-13 in non-AAD mice, but increased IL-13 levels in AAD. IHC studies further confirmed the localisation of IL-13R $\alpha$ 1 in lung tissues and its increased expression in airway epithelium of infected mice with AAD. Also, sham-inoculated allergic controls had increased IL-13R $\alpha$ 1 expression in the airway epithelium in contrast to sham-inoculated non-allergic controls. Similar findings were observed in our HDM-induced AAD model. Kuperman and colleagues and studies from other groups illustrated IL-13-induced increased responsiveness of epithelial cells where AHR and mucus overproduction was observed as direct effects of IL-13[560-562], which supports our observations. Moreover, increased IL-13 and IL-13R $\alpha$ 1 expression was observed in rIL-13-treated mice with and without IAV infection compared with sham-inoculated and infected non-rIL-13-treated controls. These results clearly demonstrate that IAV infection in established AAD not only increased IL-13 protein levels, but also the expression of its receptor, IL-13R $\alpha$ 1, implicating these responses in the exacerbation of allergen-induced asthma.

Many recent studies widely support the involvement of IL-13 [563-567] and IL-13R $\alpha$ 1[73, 568-570] in the development of various allergic diseases including asthma. Our results raise important clinical questions about the role of IAV infection in the exacerbation of asthma. It appears that IL-13 produced during infection response can significantly increase the AHR that occurs after an allergen rechallenge. There is no doubt that there are numerous pathways that are activated during asthma responses, which can cause disease exacerbation. However, IL-13-induced responses may be one of the more critical pathways that are activated and we suggest that the IL-13/IL-13R $\alpha$ 1/miR-21 axis may be important for determining whether IAV infection induces a severe or mild airway

response. Kaur *et al.*, have shown that human lung mast cell express IL-13Ra1 and activation by IL-13 for 5 days increased proliferation and the expression of the high affinity IgE receptor, Fc-epsilon-RI (FcεRI), suggesting that targeting IL-13 may be beneficial in the treatment of asthma [568]. Similarly Sinha and co-workers found links between of IL13Rα1 1398A/G gene polymorphisms and human asthma subjects using the polymerase chain reaction-restriction fragment length polymorphism method. They demonstrated that 1398A/G polymorphisms in the non-coding region of IL13Ra1 conferred increased risk of asthma in the study population [571]. IL13 is also been shown to have an important role in activating autophagy, which is essential for the formation of airway goblet cells leading to hypersecretion of mucus in the airways in a type 2, IL-13-dependent immune disease process [572]. Some studies also suggest a role for IL-13 in promoting fibrosis by increasing autocrine CTGF signalling in fibroblasts and by inducing the pro-fibrotic cytokine TGF-β1 *via* IL-13Rα2 signalling [573-575].

To investigate the cellular source of IL-13, we performed flow cytometry on cells isolated from the lung homogenates of IL-13<sup>td-tom</sup> mice. Increased numbers of IL-13<sup>+</sup>CD4<sup>+</sup> T-cells were observed in infected mice with AAD compared to sham-inoculated allergic controls. Moreover, infected non-allergic mice and sham-inoculated allergic controls had increased IL-13<sup>+</sup> NKT cells and IL-13<sup>+</sup> ILC2s respectively. These results indicate and confirm the role of IL-13 in promoting IAV infection and exacerbation of AAD. Another recent study showed CD4<sup>+</sup>/CD8<sup>+</sup> T-cell-dependent, HDM-induced AAD has key features of asthma, which supports our findings with Ova-induced AAD model [521]. Akbari *et al.*, showed the relevance and crucial involvement of pulmonary NKT cells in regulating the development of asthma and Th2-biased respiratory immunity against nominal exogenous antigens [576]. Clinically, eosinophilia and asthma severity have been reported to be associated with increased numbers of lymphocytes, which include both CD4<sup>+</sup> and CD8<sup>+</sup> T-cells [577-579]. Specifically, CD4<sup>+</sup> T cells have been identified to be the dominant active T-cell subtype both in clinical subjects with allergic asthma as well as in animal models of asthma [580-583]. On the other hand, the role of CD8<sup>+</sup> T-cells

remains controversial where both protective and deleterious effects have been reported in human subjects with asthma and animal models of allergic diseases [584].

Several miRs have also been reported to be associated with asthma pathogenesis. miR-21 is one of the most well characterised and has been identified to be an important regulator of disease pathology in murine AAD [338, 360, 527, 585]. miR-21 deficient mice have been reported to exhibit reduced eosinophilic inflammation and IL-4 levels with a concomitant increase in IFN- $\gamma$  during Ova-induced AAD [368]. miR-21 has been also demonstrated to down-regulate the expression of various signalling molecules including PTEN that antagonises PI3K activity [586-588]. We identified the involvement of miR-21 as downstream of IL-13/IL-13R $\alpha$ 1 involved in promoting the susceptibility to IAV infection in experimental AAD using qPCR and ISH. Our studies demonstrated significantly increased miR-21 expression in non-infected allergic mice and infected non-allergic mice compared to sham-inoculated non-allergic controls. Also, increased miR-21 expression was observed in infected mice with AAD compared to both sham-inoculated allergic and infected non-allergic controls where, the later group showed only a non-statistical trend towards an increase. ISH studies further confirmed increased localisation of miR-21 in the airway epithelium of infected mice with AAD and sham-inoculated allergic mice. Further, rIL-13-treated mice exhibited increased miR-21 expression compared to sham-treated controls. Infected rIL-13-treated mice demonstrated a further significant increase in miR-21 expression compared to both infected controls and rIL-13-treated mice.

Similar observations were also observed with HDM-induced AAD model where non-infected allergic and infected non-allergic mice had increased miR-21 expression compared to sham-inoculated non-allergic controls. Infected mice with AAD had further significantly increased miR-21 expression compared to sham-inoculated allergic controls. Our group identified a role for a miR-21/PI3K/HDAC2 axis in severe, steroid-insensitive AAD highlighting the importance of miR-21 as a novel therapeutic intervention for the treatment of

this form of asthma [589]. Similarly, various other studies also postulated miR-21 as a novel therapeutic target for the treatment of asthma [327, 364, 365, 367, 590-592].

IL-13 has been shown to be an important regulator of Th2 commitment and may therefore play a central role in atopy and infectious diseases [593]. Other accumulating evidence indicates that antigen-specific Th2 cells and their cytokines such as IL-4, IL-5 and IL-13 orchestrate these pathognomonic features of asthma [564, 594-596]. To further assess the role of IL-13 in susceptibility to IAV in AAD, we used mice deficient in IL-13 (IL-13<sup>-/-</sup> mice). A significant decrease in viral titre and reduced lung tissue inflammation was observed in infected IL-13<sup>-/-</sup> mice at 3 dpi as compared to infected WT mice. Moreover, infected IL-13<sup>-/-</sup> mice had decreased transpulmonary resistance. These observations clearly indicate that the absence of IL-13 during IAV infection leads to decreased viral titres and inflammation in the lung along with reduced AHR.

miR-21 expression was observed to be significantly increased in infected WT mice compared to sham-inoculated WT controls. Infected IL-13<sup>-/-</sup> mice had significantly reduced miR-21 expression compared to sham-inoculated WT mice. An increased expression of miR-21 was detected in infected IL-13<sup>-/-</sup> mice compared to sham-inoculated IL-13<sup>-/-</sup> mice. Lee *et al.*, have also shown that miR-21 is up-regulated during allergic airway inflammation. miR-21 antagomir treatment reduced the levels of Th2 cytokines, including IL-4, IL-5, and IL-13 which reflected an association between the IL-13 and miR-21 in allergic inflammation [365].

All these observations emphasise that IL-13 plays a critical role in driving increased susceptibility to IAV infection and infection-induced exacerbation of AAD. Further, we have validated this and demonstrated the potential for therapeutic targeting of IL-13. We showed that the inhibition of IL-13 with anti-IL-13) protected mice against infection and reduced the severity of IAV infection-induced exacerbations of AAD. This was indicated by reduced viral

titres in anti-IL-13-treated infected non-allergic mice compared to isotype-treated infected non-allergic controls. Also, anti-IL-13-treated groups had reduced tissue inflammation, eosinophil counts, and MSCs and as well as transpulmonary resistance compared to isotype-treated infected allergic controls. Anti-IL13-treated infected non-allergic mice had reduced IL-13 and IL-13R $\alpha$ 1 mRNA expression compared to isotype-treated infected non-allergic controls. These results showed that inhibition of IL-13 also reduced the expression of its receptor, IL-13R $\alpha$ 1. Further, the anti-IL13-treated infected non-allergic mice also had significantly reduced miR-21 expression compared to isotype-treated infected non-allergic controls while the similar levels of expression were observed in anti-IL13-treated infected mice with AAD and isotype-treated infected allergic controls.

The association of IL-13 with asthma pathology and reduced corticosteroid sensitivity suggests a potential benefit of anti-IL-13 therapy in refractory asthma [597]. De Boever *et al.*, investigated GSK679586, a humanized mAb, that inhibited IL-13 binding to both IL-13R $\alpha$ 1 and  $\alpha$ 2 in patients with severe asthma refractory to maximally indicated doses of inhaled corticosteroids. They showed that GSK679586 did not effectively improve asthma control, pulmonary function, or exacerbations in patients with severe asthma [597]. Various humanised anti-IL-13 strategies have been tested (anrukinzumab, lebrikizunab and tralokinumab) and showed clinical improvements in asthma symptoms [598]. All these studies clearly showed that anti-IL-13 is a potential and promising therapeutic intervention for the treatment of AAD and infection-induced exacerbation in AAD. However, this potential requires further in-depth investigation, and appropriate predictive biomarkers are needed to better apply biological treatments and assess treatment responsiveness.

Corticosteroid therapy often fails to control exacerbations in patients with asthma, in particular those with severe disease [599-602]. In our study, we also assessed whether corticosteroid (dexamethasone) treatment could protect against infection and associated exacerbations of AAD. Our results revealed that viral load, tissue inflammation, tissue eosinophils and numbers of MSCs

were steroid insensitive in IAV infection in Ova-induced AAD. No histopathological changes were observed in infection-induced exacerbations in AAD in response to dexamethasone treatment, and interestingly, treatment worsened AHR. Similar features of increased eosinophil numbers following steroid treatment were reported in RSV-induced exacerbation of HDM-driven AAD together with steroid resistant disease exacerbations [603]. Different clinical trials also showed that dexamethasone was ineffective against RSV-induced lung inflammation in children [604, 605]. Taken together, our data clearly indicate that IAV infection-induced AHR is steroid-insensitive and is driven by a steroid-resistant pathway that is linked to innate immune responses such as eosinophil recruitment/activation and neutrophil recruitment mimicking many features of the clinical disease. Our findings are consistent with several studies that report the inability of inhaled steroids to effectively reduce airway inflammation and AHR [606-608]. These studies highlight anti-IL-13 treatment as a potential therapy in this context. Different phenotypes of asthma may explain why current therapies show limited benefits in subgroups of patients [508]. Patients with severe, poorly controlled asthma are insensitive to glucocorticoid treatment and have an urgent need for new treatments. IL-13 signalling may be one pathway involved in the induction of corticosteroid-insensitive airway inflammation and may be targeted therapeutically [609].

Considering the role of miR-21 in the pathogenesis of asthma [338, 360, 585, 610], our laboratory has recently shown for the first time the role of miR-21 in promoting the steroid insensitive inflammation and AHR in respiratory infection-induced severe steroid insensitive AAD. This supports our current findings where we observed that dexamethasone treatment did not suppress miR-21 expression in IAV infection in Ova-induced AAD. These studies clearly define the functional relevance of infection-induced activation and maintenance of a novel miR-21/PI3K/HDAC2 axis in steroid insensitivity [589].

miR-21 has also been indicated as a novel biomarker for human allergic inflammatory diseases [590]. Here we find miR-21 is a potential target molecule that drives increase susceptibility to IAV infection in experimental AAD.

Considering the therapeutic potential of miR-21 and PI3K inhibitors in the treatment of asthma [365, 589, 611-613], we investigated their efficacy in resolving IAV infection-induced AAD pathology. Ant-21-treated infected non-allergic mice had significantly reduced viral titres and tissue inflammation compared with Scr-treated infected non-allergic control. Importantly, Ant-21-treated infected mice with AAD had substantial reductions in viral titre, tissue inflammation, numbers of mucus secreting cells and tissue eosinophils compared with Scr-treated infected allergic control. However, Ant-21 treatment did not suppress AHR in IAV infection in Ova-induced AAD. Interestingly, we did show that Ant-21 treatment suppresses miR-21 expression in IAV infection in Ova-induced AAD. All our findings are supported by a various studies showing the relevance of miR-21 in pathogenesis of asthma and miR-21 antagomir in suppressing the development of allergic airway inflammation and other associated disease features [364-366, 591, 614].

PI3K inhibitor (LY294002; LY29) treated infected non-allergic mice had significantly reduced viral titre, tissue inflammation, numbers of MSCs and tissue eosinophils compared with sham-treated infected non-allergic controls. Importantly, LY29-treated infected mice with AAD also had significant reductions in viral titre, tissue inflammation, numbers of MSCs and tissue eosinophils compared with sham-treated infected allergic control. Huang *et al.*, showed that LY29 attenuated the IL-25-induced AHR, inflammation and remodelling (lung tissue eosinophilia, mucus production, collagen deposition, smooth muscle hypertrophy and angiogenesis) which support our data and highlight the PI3K as a major disease-inducing mechanism in asthma [615]. However, treatment with LY29 did not suppress AHR in IAV infection in Ova-induced AAD in our study. This may be attributed to the different pathophysiological mechanisms involved in the development of AAD between the two mouse models involved. Also, LY29 did not inhibit miR-21 expression in IAV infection in Ova-induced AAD highlighting that miR-21 expression is independent of PI3K. Similarly, Wagh and colleagues also showed that the PI3K and JAK3 inhibitors may be promising alternative therapeutics in asthma, which might counteract the airway inflammation in patients with allergic asthma

[616]. Inflammation/remodelling and AHR have been reported to be two independent processes in airway diseases. AHR is derived from independent factors that are modulated by inflammatory factors but may not be caused by inflammation directly in some situations[617, 618].

Clinically, PI3K- $\gamma$  has been reported to regulate the development of eosinophilic inflammation and attenuated eotaxin-induced eosinophil functions probably via suppression of downstream CCR3 signalling[619]. Our data suggest these inhibitors as novel potential therapeutic interventions for increased susceptibility to IAV infection in AAD.

Though our current study emphasises the involvement of a novel pathogenic IL-13/IL-13R $\alpha$ 1R/miR-21-dependent pathway in pathogenesis and increased susceptibility to IAV infection in AAD, it was limited in attempts to identify specific cell types that expressed miR-21. This would be important to further understand the regulation of the IL-13/IL-13R $\alpha$ 1R/miR-21 pathway and dexamethasone insensitivity. We also lack a molecular understanding as to how miR-21 is driven transcriptionally, and how IL13 affects this induction and under what circumstances. We also demonstrated the functional relevance of IAV infection-induced activation and maintenance of a novel IL-13/IL-13R $\alpha$ 1R/miR-21/ axis in an AAD setting. We also showed that Ant-21 and LY29 treatment suppressed infection (viral titres) and the key features of AAD exacerbated by IAV infection (i. e. tissue inflammation, numbers of MSCs and tissue eosinophils).

Viral infections can also exacerbate COPD leading to increased dyspnea, hospitalisation, and even death. A recent study suggested that the number of virus-induced exacerbations has been grossly underestimated, with up to 60% associated with viral infection [620]. Wark and colleagues reported that virus infection, especially in the presence of chronic bacterial infection was an important determinant of more severe acute exacerbations in both asthma and COPD, and patients with multiple co-infections were more likely to be readmitted to hospital following their exacerbation [621]. However, the

mechanisms leading to increased susceptibility of COPD patients to IAV infection are poorly understood. Moreover, current therapeutic strategies have limited efficacy and novel therapeutic interventions are required. To address this, we investigated and characterized the mechanism (IL-13R $\alpha$ 1/miR-21 axis) involved in the increased susceptibility of COPD to IAV infection. Hsu *et al.*, demonstrated that infected mice with experimental COPD had more severe infection characterised by increased viral titre and pulmonary inflammation. These effects were attributed to exaggerated PI3K (PI3K-p110 $\alpha$ ) activity. Further inhibition of PI3K using pan-PI3K inhibitor, or PI3K-p110 $\alpha$ -specific inhibitors reduced viral titre regardless of IAV subtype. Targeting the PI3K pathway may be a novel therapeutic strategy against IAV infection in COPD [143].

The association of IL-13 with COPD is not well understood. However, in our study, we demonstrated that IAV infection in experimental COPD increased the expression of IL-13R $\alpha$ 1. IL-13R $\alpha$ 1 expression was significantly increased in the airway epithelium in non-infected smoke-exposed compared to non-infected normal air-exposed mice. Surprisingly infected normal air-exposed mice and infected smoke-exposed mice had further substantial increases in IL-13R $\alpha$ 1 levels in airway epithelium. No specific studies have shown the association of IL-13 and IL-13R $\alpha$ 1 and COPD have been reported so far. To further identify the mechanisms involved downstream of IL-13R $\alpha$ 1, we speculate that miR-21 is a potential target molecule driving increase susceptibility to IAV infection in experimental COPD. miR-21 expression was measured in the lung sections and observed to be increased in response to IAV infection in experimental COPD. Xie *et al.*, demonstrated that the upregulation of miR-21 in peripheral blood serum and mononuclear cells of COPD patients may contribute to the pathogenesis and the severity of this disease [369]. They also suggested that the levels of serum miR-21 may be a valuable marker for evaluating the development of COPD in heavy smokers [370].

We also observed a significant increase in the numbers of MSCs in infected smoke-exposed compared to non-infected smoke-exposed mice. It has been

shown that IL-13 drives mucus production in human airway epithelial cells via chloride channel calcium-activated 1 (CLCA1) to MAPK13[622] signalling pathway. This finding supports our data showing increased levels of IL-13R $\alpha$ 1 contributing to the production of MSCs.

As discussed earlier, considering the therapeutic potential of IL-13 specific monoclonal antibody (anti-IL-13), we assessed whether inhibition of IL-13 could protect against infection and reduce the severity of IAV infection in COPD in our experimental models. We observed a decrease in viral titre in anti-IL-13-treated infected normal air-exposed mice at 7 dpi compared to isotype-treatment. Also, anti-IL-13-treated infected smoke-exposed mice at 7 dpi had significantly reduced viral titre compared to isotype-treated infected smoke-exposed mice. Anti-IL-13 treatment also significantly reduced tissue inflammation and number of MSCs in infected smoke-exposed mice compared to isotype-treated infected smoke-exposed mice. Moreover, treatment of infected smoke-exposed mice reduced miR-21 expression compared to isotype-treated infected smoke-exposed mice although statistical significance was not achieved. A recently published review clearly highlighted the importance and implication of monoclonal antibodies against IL-13 (lebrikizumab, tralokinumab) in the treatment of COPD [623]. However, our study is first to demonstrate the therapeutic potential of anti-IL-13 against increased susceptibility to IAV infection in COPD.

Similarly, we also assessed Ant-21 as a novel potential therapeutic to suppress the increased susceptibility to IAV infection in COPD. Viral titre was reduced in Ant-21-treated infected normal air-exposed mice at 7 dpi compared to Scr-treated infected normal air-exposed mice. Also, Ant-21-treated infected smoke-exposed mice at 7 dpi had significantly reduced viral titre in contrast to isotype-treated infected smoke-exposed mice. Ant-21 treatment in non-infected smoke-exposed mice reduced tissue inflammation. Likewise, Ant-21-treated infected smoke-exposed mice had significantly reduced tissue inflammation and reduced numbers of MSCs back to base line. Furthermore, Ant-21 treatment reduced miR-21 expression back to base line in non-infected smoke-exposed mice,

infected normal air-exposed mice as well as in infected smoke-exposed mice when compared to the respective Scr-treated groups.

The role of miR-21 is well reported in asthma, however, very limited investigations has been performed illustrating its involvement in the pathogenesis of COPD. Though various reports defined the association and relevance of miR-21 in COPD [369, 370] and our data revealed a role for miR-21 as regulatory molecule in increased susceptibility to IAV infection in COPD. Our study identified a novel pathogenic IL-13R $\alpha$ 1R/miR-21-dependent pathway in increasing the susceptibility to IAV infection in COPD, however, it did not identify the specific cell types that express miR-21. This would be an important future direction to understand the regulation of the IL-13R $\alpha$ 1R/miR-21 pathway. We also showed that anti-IL-13 and Ant-21 treatment suppressed the key features of IAV infection and exacerbation in COPD (ie viral titre, tissue inflammation and number of MSCs).

The important observations of our study are summarised in Figure 3.58. As a part of our ongoing studies, we intend to identify the specific cell types involved along with the impaired antiviral responses that are mediated by increased IL-13/miR-21 activity that lead to increased susceptibility of individuals with asthma and COPD to IAV infection. Targeting such pathways using various therapeutic interventions, identified in our study (anti-IL-13, Ant-21, LY29) can be used for chronic respiratory diseases like asthma and COPD, or in healthy individuals, during seasonal or pandemic outbreaks to prevent and/or treat IAV infections. Further work is being planned to understand the regulatory mechanisms involved in regulation of miR-21 by IL-13.

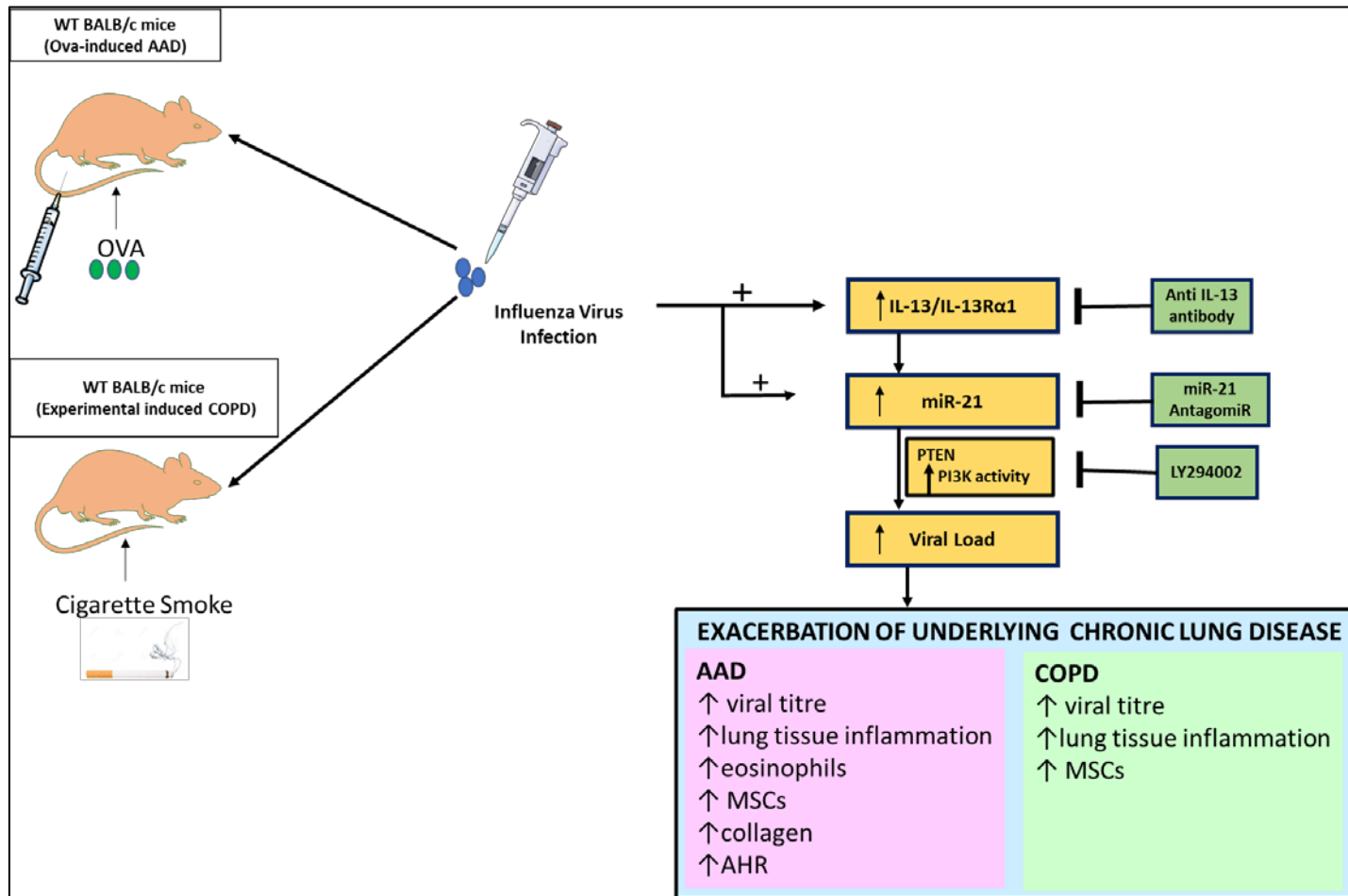


Figure 3.58. Roles of IL-13 and miR-21 in increased susceptibility to IAV in AAD and COPD.

AAD and COPD were induced in mice using sensitisation and challenge with Ova or exposure to cigarette smoke. On the last day of Ova challenge or smoke-exposure, groups of mice were infected with 7.5 plaque forming unit (PFU) of the mouse-adapted IAV H1N1 A/PR/8/34. We have observed increased levels of IL-13/IL-13R $\alpha$ 1, which increase the downstream levels of miR-21 (via increased PI3K activity) leading to increased viral load, disease features and exacerbation of the underlying respective chronic lung disease. Inhibition of augmented IL-13, miR-21 and PI3K using monoclonal anti-IL-13 antibody, Ant-21 and PI3K inhibitor (LY294002), respectively, reduces viral load, associated disease features and exacerbation of the underlying chronic lung disease highlighting these as potential therapeutic interventions. We have shown the effectiveness of all the three therapeutic biological moieties in increased susceptibility to IAV infection in AAD and COPD.

### 3.6. CONCLUSIONS

Viral infections can exacerbate underlying lung diseases such as asthma and COPD and can limit/decrease the efficacy of current medications. Current pharmacological strategies targeting virus-induced lung disease are problematic due to antiviral resistance and the requirement for strain-specific vaccination. Thus, there is a crucial need for new and effective approaches. We generated and characterised murine models of IAV infection in asthma and COPD. We found that AAD increased susceptibility to IAV infection shown by increased viral titre. Also the infection exacerbated AAD with increased lung pathology, pulmonary inflammation, increased number of MSCs and tissue eosinophils and AHR. Likewise, COPD increased susceptibility to IAV infection that exacerbated the underlying disease with increased tissue inflammation, and number of MSCs. These observations were quite consistent with those of clinical and epidemiological studies in asthmatic and COPD patients.

To our knowledge, this is the first study to define the functional relevance of IAV infection-induced activation and maintenance of a novel IL-13/IL-13R $\alpha$ 1/miR-21 and IL-13R $\alpha$ 1/miR-21 axis in the setting of AAD and COPD, respectively. The models developed herein will be valuable for investigating the pathogenesis of IAV infection in asthma and COPD. Moreover, our data identify promising therapeutic interventions for increased susceptibility to IAV infection in AAD (Anti-IL-13, Ant-21 and PI3K inhibitors) and COPD (Anti-IL-13 and Ant-21) which suppresses various key features of the respective airway disease.

# CHAPTER 4

## miR-125a/b INHIBITS A20 AND MAVS TO PROMOTE INFLAMMATION AND IMPAIR ANTIVIRAL RESPONSE IN CHRONIC OBSTRUCTIVE PULMONARY DISEASE

Hsu, A. C., **K. Dua**, M. R. Starkey, T.-J. Haw, P. M. Nair, K. Nichol, N. Zammit, S. T. Grey, K. J. Baines and P. S. Foster (2017). "MicroRNA-125a and-b inhibit A20 and MAVS to promote inflammation and impair antiviral response in COPD." *JCI Insight*, 2(7), e90443. <http://doi.org/10.1172/jci.insight.90443>

## 4.1. ABSTRACT

IAV infections lead to severe inflammation in the airways. Patients with COPD characteristically have exaggerated airway inflammation and are more susceptible to infections with severe symptoms and increased mortality. The mechanisms that control inflammation during IAV infection and the mechanisms of immune dys-regulation in COPD are unclear. We found that IAV infections lead to increased inflammatory and antiviral responses in primary bronchial epithelial cells (pBECs) from healthy non-smoking and smoking subjects. In pBECs from COPD patients, infections resulted in an exaggerated inflammatory but deficient antiviral responses. A20 is an important negative regulator of nuclear factor-kappaB (NF- $\kappa$ B)-mediated inflammatory but not antiviral response, and A20 expression was reduced in COPD. IAV infection increased the expression of micro(miR)-125a/b, which directly reduced the expression of A20 and mitochondrial antiviral signaling (MAVS), and caused exaggerated inflammation and impaired antiviral responses. These events were replicated *in vivo* in a mouse model of experimental COPD. Thus, miR-125a/b and A20 may be targeted therapeutically to inhibit excessive inflammatory responses and enhance antiviral immunity in IAV infections and in COPD.

## 4.2. INTRODUCTION

Influenza A viruses (IAVs) are amongst the most important infectious human pathogens that cause enormous morbidity and mortality worldwide. This largely results from seasonal influenza but an important feature of the biology of IAVs is the frequent emergence of novel pandemic strains/subtypes. Infections cause symptoms ranging from mild to severe viral pneumonia, with uncontrolled inflammation in the airways.

Bronchial epithelial cells (BECs) are the primary site of IAV infection, and innate immune responses produced by these cells are important in the early protection against the viruses[624, 625]. During infection viral RNAs are recognized by toll-like receptor 3 (TLR3) and retinoic acid-inducible gene-I (RIG-I). Upon binding of TLR3 to viral RNAs signalling pathways are initiated that activate receptor

interacting protein 1 (RIP1) by ubiquitination. Activated RIP1 indirectly phosphorylates I $\kappa$ B $\alpha$ , leading to the release of active p65 and p50 subunits of nuclear factor-kappaB (NF- $\kappa$ B) into the nucleus where they induce the transcription of inflammatory genes including of cytokines such as IL-6 (IL-6), TNF- $\alpha$ , and IL-1 $\beta$ , and chemokines such as CXC chemokine ligand-8 (CXCL-8/IL-8)[626-628]. These inflammatory cytokines recruit immune cells, in particular macrophages and neutrophils, to the site of infection that phagocytose pathogens and apoptotic cells[629, 630]. RIG-I interacts with mitochondrial antiviral-signaling protein (MAVS), which activates interferon regulatory factor 3 (IRF3) by phosphorylation. Activated IRF3 then translocates into the nucleus where it initiates the production of type I and III IFNs[461, 462]. These innate cytokines induce the transcription of over 300 IFN-stimulated genes (ISGs) including the Mx1 protein that disrupts virus replication [631].

The control of inflammation is critical to achieving optimal inflammatory responses that clear viruses without excessive damage to host tissues and airways. We have previously shown that A20, also known as TNF- $\alpha$ -inducing protein 3 (TNFAIP3), is a negative regulator of NF- $\kappa$ B-mediated inflammation that functions by targeting RIP1 for degradation, and therefore suppresses NF- $\kappa$ B activation[632-635]. miRs are another important class of immune signaling regulators that silence gene expression by degradation[527]. miR-125a and b have recently been shown to directly inhibit A20, leading to increased NF- $\kappa$ B activation[636]. It is currently unknown if A20 or miR-125a/b regulates type I and III IFNs during IAV infections.

COPD is the 3<sup>rd</sup> leading cause of illness and death globally and is characterized by progressive airway inflammation, emphysema, and reduced lung function [637]. The most important risk factor for COPD in Western societies is cigarette smoking[638]. COPD patients have increased susceptibility to IAV infections that cause acute exacerbations and result in more severe symptoms, disease progression, and increased mortality [639-641]. Current therapeutics remain limited to vaccination and antiviral drugs. These have major issues with the constant need for developing new vaccines, COPD patients respond poorly to

vaccination, IAVs have become drug resistant and all therapeutics have questions surrounding availability and efficacy in future pandemics[642, 643]. There is therefore an urgent need to develop novel therapeutics for influenza, especially for those most susceptible to infection.

Despite inflammatory signalling pathways being well-characterized, the mechanisms underlying the exaggerated inflammatory responses to IAV, including in COPD are unclear. It is known that increased NF- $\kappa$ B activation is elevated in biopsies from COPD patients[644]. We have previously shown that human influenza H3N2 infection induced heightened inflammatory responses[645], and high pathogenic avian H5N1 is known to induce severe cytokine storms in the lung[462, 646]. We also showed that primary BECs (pBECs) from COPD subjects and our established *in vivo* model of experimental COPD have increased inflammatory and impaired antiviral responses to IAV infections, leading to more severe infection[537, 647, 648]. Furthermore, miRs are known to be altered in COPD[362, 649]. However, the molecular mechanisms underpinning the heightened inflammatory response in IAV infections and defective immune responses in COPD remain unclear. In this study, we investigated the mechanisms involved using our established experimental systems[647, 650-652]. We found that COPD pBECs and mice with experimental COPD infected with IAV have higher levels of inflammatory cytokines but reduced antiviral responses[362, 653]. We uncovered that NF- $\kappa$ B-mediated inflammation in IAV infection and in COPD was also exaggerated, which resulted from decreased levels of A20 protein, which in turn was caused by elevated levels of miR-125a/b. Treatment with specific antagomiRs against miR-125a or b reduced NF- $\kappa$ B activation but also increased type I and III IFNs production and suppressed infection. We then found that miR-125a and b directly targets MAVS 3' untranslated region (UTR), thereby suppressing the induction of type I/III IFNs. This study therefore discovers a novel miR-125-mediated pathway that reduces A20 and MAVS and promotes excessive inflammation and increases susceptibility to IAV infection in COPD. It also identifies novel potential therapeutic options that reduce IAV-mediated

inflammation and reverse immune signaling abnormalities in COPD. Some of the data has been previously reported in abstract form[654].

## **4.3. METHODS**

### **4.3.1. Ex vivo methods**

#### **4.3.1.1. Subject recruitment**

Patients with chronic COPD patients (10) and healthy non-smoking (10) and smoking (5) controls were recruited and their characteristics are shown in Table 4.1.

The population was defined by a previous smoking history and fixed airflow limitation on spirometry with an forced expiratory volume in 1 second (FEV<sub>1</sub>) / forced vital capacity (FVC) ratio < 70%, and FEV<sub>1</sub> < 80% predicted and classified by the GOLD criteria [655]. Those with GOLD Stage III (severe COPD) FEV<sub>1</sub> 30 – 50% were included. All COPD subjects were ex-smokers (at least one year abstinent) and none were using inhaled corticosteroids for two weeks before bronchoscopy. Healthy non-smoking controls and current smokers without COPD with no evidence of airflow obstruction, bronchial hyper-responsiveness to hypertonic saline challenge, or chronic respiratory symptoms were also recruited. A clinical history, examination and spirometry were performed on all individuals. At the time of recruitment no subject had symptoms of an acute respiratory tract infection for the preceding four weeks. None were diagnosed with cancer. All subjects gave written informed consent.

#### **4.3.1.2. Viruses**

Human influenza A viruses (IAVs) A/Wellington/43/2006 (H3N2), A/Auckland/1/2009 (H1N1), were obtained from the WHO Collaborating Centre for Reference and Research on Influenza (Victoria, Australia)[656]. Virus stocks were propagated in Madin-Darby canine kidney (MDCK) cells (American Type Culture Collection (ATCC), USA). Virus titers were determined by plaque assay on MDCK cells[462, 645].

**Table 4.1. Subject characteristics**

	<b>Healthy</b>	<b>COPD</b>	<b>Smoker</b>	<b>P – value</b>
<b>Number</b>	15	15	5	NA
<b>Sex (Male:Female ratio)</b>	1.14	1.2	1.5	p = 0.6
<b>Mean Age (SD)</b>	62 (9.9)	68 (4.1)	64.33 (12.82)	p = 0.06
<b>Mean FEV<sub>1</sub> (SD) *</b>	105% (13.5)	40% (7.75)	97.66% (12.66)	p < 0.001
<b>FEV<sub>1</sub>/FVC ratio (SD) *</b>	886x (14.50)	40.20 (13.50)	77.80 (12.28)	p < 0.001
<b>Cigarette (Packs/year; SD)</b>	0	53.70 (15.90)	30 (17.32)	p < 0.001
<b>Years abstinent (SD)</b>	0	13.0 (4.64)	0	NA
<b>ICS (percent treated)</b>	0	Seretide (10%) Spiriva (10%) Tiotropium (10%) Spiriva/Salbutamol (10%) Seretide/Tiotropium (20%) Seretide/Tiotropium/Ventolin (20%) Seretide/Spiriva/Ventolin (20%)	0	NA

FEV<sub>1</sub> and FEV<sub>1</sub>/FVC ratios are % predicted values. FEV<sub>1</sub> is the forced expiratory volume in 1s expressed as a percentage of the predicted value. FVC is forced vital capacity. The statistical analysis used was ANOVA for multiple groups. NA = Not applicable.

#### **4.3.1.3. Cell culture and IAV infection**

Human primary bronchial epithelial cells (pBECs) were obtained by endobronchial brushing during fiber-optic bronchoscopy in accordance with standard guidelines [657]. pBEC were cultured as described previously [462, 645, 649, 658]. Virus was diluted in serum free medium and added to cells at a multiplicity of infection of five. After 1hr incubation, inocula were removed and replaced with serum-free medium.

#### **4.3.1.4. A20 plasmid, siRNA and miR-125a and b antagomiRs and mimetics**

A20 gene was amplified by PCR using the forward primer containing XbaI (5'-aaattctagagccgccaccATGGCTGAACAAGTCCTTCCTC-3') and reverse primer containing EcoRI (5'-gcgcgaattcTTCTGTCAATGTGAACATGTTTCAG -3'). The restriction sites are italic and underlined. The PCR product was cloned into pcDNA3.1 expression vector (pcDNA-A20). The construct was then transfected into pBECs using Lipofectamine 3000 (Life Technologies, USA) according to the manufacturer's instructions. For experiments using short interfering (si)RNAs, A20-specific siRNAs (Applied Biosystems, USA) were transfected into cells using siPORT NeoFX transfection agent (Ambion, USA). AllStars Negative controls (Qiagen, USA) were used as siRNA negative controls. For miR-125a/b antagomiR and mimetic experiments, anti-hsa-miR-125a and anti-hsa-miR-125b antagomiRs (Ambion, USA), and miR-125a and miR-125b mimetics (Ambion, USA) were transfected into cells using siPORT NeoFX transfection agent (Ambion, USA) 24hr before infection according to manufacturer's instructions. Anti-miR inhibitor negative control (Qiagen, USA) was used.

#### **4.3.1.5. Cloning and mutagenesis of miR-125a/b binding site in MAVS 3'UTR**

The fragment spanning the miR-125a/b putative binding site in 3' untranslated region (UTR) of MAVS was generated by PCR and cloned into a pMIR luciferase vector using MluI and HindIII cloning sites (italic; Life Technologies, USA). Next, site-directed mutagenesis was performed to introduce a mutation

(TCA→AGT) into the binding site sequence (shown in bold below). All constructs were sequenced to confirm their identity. The primers used for PCR amplification and mutagenesis are underlined.

MAVS 3`UTR

*ccacgcg*TGTGAACCACAGCTTATCACATGTCTGGAGTTAGGGACCCCACTT  
AAAGTGAGATTTTGGCTGGAGGTGGTGGATCATACTATAATCCCAGCACT  
TTGGGAGACCAAGGCAGAAGGACTGCTTGAGGCCAGGAGTTCAAACCAG  
TGTAGGTAACAGCTAGACCCTATCTCTACAAAAAATTTAAAAATTAGCTGGG  
TGTGGTGGTATGTGCCTCAAGTTCAGCTACTCAGGAGGCTGAGGTGGGA  
GGATCACTTGAGCACAGGAGTTTGAAGTTACAGTGAGCTATGATGGCACC  
ACTGCACTTCAGCCTAGGCAACAGAGGGAGACCCTGTCTTTAAAGTACATA  
GAGGTTTTTTCACACCAACACATCTCTGCCAGTGTGCCAACATCTGCCACC  
TGCTATAATAGTACTATAA  
CACTCAATATGTAATTAATGTAGTCTCAGGGAT  
GTTATGACAATATGATTACA  
ACTATCACGTGTGTGCCCAGCCAGGCTCAAT  
GCCCCAGGCTGGGCGAGGTGGGGCAGGGGACACAGCCTAAAATGCCAG  
GCCTCAGGAAGCCATTTGGTTTAGCAGACATTGTTTATTAAGGAGTTACC  
TATGCCAGATCGAAGGCCTAAGATGATTAAGACACTATGAGTGCCTTCAAG  
TGGTTGGGGACGTTTCATGATTGTGGTACAGACAAATAGGCTTTCACATCAT  
TCTTTTATGTAATCATACAACAGATATTTGCACCTACAT*Gaagcttcg*

#### **4.3.1.6. Luciferase reporter assay**

The constructs described above were co-transfected into HEK293 cells with mimetic pre-miR-125a, pre-miR-125b, or pre-miR scrambled control (Applied Biosystems, USA) using Lipofectamine 3000 (Life Technologies, USA). pRL *Renilla* control vector (Promega, USA) was also used. Cells were harvested 48hr after transfection and luciferase activity was measured using a luminometer (Fluostar Optima, BMG Labtech BMG, Germany). The luciferase reading of pMIR and mimetics was normalized to the *Renilla* control for each sample, and expressed as percentage reduction from miR-scrambled control[636].

#### **4.3.1.7. Immunoblotting and cytometric bead array**

Infected pBECs were lysed in ice-cold RIPA buffer containing protease inhibitor cocktail (Roche, UK). Proteins of lysed pBECs and supernatants (5µg) were resolved by SDS-PAGE and transferred onto polyvinylidene fluoride membranes for detection of A20, and phospho-p65 at Ser536 in the cell lysates using anti-A20 (ab74037, Abcam, UK) and anti-phospho-p65 antibodies (#3031L, Cell Signaling Technology, USA). Glyceraldehyde 3-phosphate dehydrogenase (GAPDH) was detected as a loading control in cell lysates using specific antibody (ab181602, Abcam, UK). IFN-β was detected in the supernatants using specific antibody (ab85803, Abcam, UK). Proteins on membranes were then visualized by chemiluminescence (Bio-Rad ChemiDoc MP System, CA, USA). All blots were probed for proteins of interests and then stripped and re-probed for loading control. The densitometric value of IFN-β was normalized to non-infected media control. For other intracellular proteins, the densitometric values of all lanes in a blot were first normalized to the loading control. Values were then expressed as fold change from healthy media control if comparing between healthy, COPD, and smoker pBECs, or untreated control if cells were treated with siRNAs, pcDNA-A20, antagomiR or mimetics. Blots were run according to the comparisons being made. If comparing between disease groups (healthy vs COPD vs smoker), then samples from one subject from each group were run on the same blot and compared with or without infection and between the disease group (ie fig. S1). The control group was the healthy controls. These were then run for all subjects from each group. If comparing between experimental conditions such as siRNAs or antagomiR treatment, samples from one subject with all experimental controls were run on the same blot (fig. S2B/C/D). The experimental control was non-silenced or non-treated (pcDNA-A20). Some blots were cut at appropriate protein molecular weights so that multiple proteins of interests could be detected at the same time. Blots were stripped and re-probed only once to avoid high backgrounds. Human IL-6, CXCL-8, TNF-α, and IL-1β concentrations were determined by cytometric bead array using a FACSCanto II flow cytometer (BD Biosciences, USA) according to the manufacturer's instructions. IFN-λ1 was measured by ELISA according to the manufacturer's instructions (R&D Systems, USA).

#### **4.3.1.8. Immunoprecipitation**

Ago2 was immunoprecipitated from transfected HEK293 cells using anti-Ago2 antibody (ab32381, Abcam, UK) protein-A conjugated Dynabeads (Life Technologies, USA) according to the manufacturer's instructions.

#### **4.3.1.9. miR extraction and analysis**

Extraction of total RNA from infected pBECs was performed with miRNeasy Mini Kits (Qiagen, USA) according to the manufacturer's instructions. Total RNAs (200ng) were reverse transcribed to cDNA and amplified using miR-125a or b specific primers (Qiagen, USA) and qPCR. RNU6B was used as the reference gene. Expression levels of miRs were calculated relative to RNU6B using the  $2^{-\Delta\Delta Ct}$  method, and were analyzed as fold change induction over media controls.

### **4.3.2. In vivo methods**

#### **4.3.2.1. Experimental mice**

Six to eight-week old female BALB/c mice were used in all the experiments. Animals were obtained from The University of Newcastle Animal Services Unit and were given access to food and water *ad libitum*. Animals were housed in a specific pathogen-free facility with controlled environment of 14h/10h light/dark cycles.

#### **4.3.2.2. Cigarette smoke exposure**

Mice were exposed to the smoke from 12x3R4F reference cigarettes (University of Kentucky, USA) twice per day, five times per week, for eight weeks using a custom-designed and purpose-built specialized nose-only, directed flow inhalation and smoke-exposure system contained in a laminar flow and smoke-extraction unit (CH Technologies)[537, 538, 651, 653, 659-661]. Non-smoking control mice were exposed to normal air for the same period of time.

#### **4.3.2.3. IAV infection and antagomiR treatment**

On the last day of smoke exposure, mice were anesthetized with isoflurane and infected intranasally with eight plaque forming units (PFUs) of the mouse-

adapted A/PR/8/34 in 50µl of media (UltraMDCK, Lonza) [143, 662]. Controls were sham-inoculated with media. The miR-125a and b sequences were downloaded from miRBase University of Manchester, UK (<http://www.mirbase.org/>). miR-125a and b and scrambled antagomiR control (nonspecific RNA VIII, BLAST searched against the mouse genome) were designed and purchased from Sigma-Aldrich. The sequences of the antagomiRs were:

5'mU.\*.mC.\*.mA.mA.mC.mA.mU.mC.mA.mG.mU.mC.mU.mG.mA.mU.mA.mA.mG.\*.mC.\*.mU.\*.mA.\*.3'-Chl, where (m) denotes 2'-O-methyl-modified nucleotides, (\*) denotes phosphorothioate linkages, and (-Chl) denotes hydroxyprolinol-linked cholesterol. Mice were treated with antagomiR (50µg delivered in 50µL sterile saline i.n.) or an equivalent amount of scrambled control as described previously[663, 664]. In each experiment, following IAV inoculation, smoking was discontinued to remove the effects of acute smoke exposure, and mice were sacrificed at 7 dpi.

#### ***4.3.2.4. Histopathology and immunohistochemistry***

Mice lungs were perfused, inflated, formalin-fixed, paraffin-embedded and sectioned (4-6µm). Sections were then stained with haematoxylin and eosin and histopathology score was performed as previously described[392, 535, 665-667]. Sections were also stained with anti-A20 antibody (Abcam, UK) and followed by anti-rabbit horseradish peroxidase-conjugated secondary antibody (R&D Systems). The images were viewed under a light microscope (Olympus, Japan). To assess A20 in mouse lung sections, slides were incubated with Anti-A20 antibody (ab74037, Abcam, UK) at 4°C overnight, followed by anti-rabbit horseradish peroxidase-conjugated secondary antibody (VC002-025, R&D systems, 37°C, 30min). Diaminobenzidine (DAB, DAKO) was applied on slides and haematoxylin was used as a counterstain. Photomicrographs were taken and images evaluated with image J (version 1.47)[668, 669]. Briefly, airways were divided into three categories according to the perimeter of their basement membrane (Pbm): Pbm ≤1 mm (small), Pbm ≤2 mm (medium) and Pbm > 2mm (large)[670]. At least 6 small airways per mouse were blind-selected and

examined with a light microscope (BX41, Olympus). The A20 area and width of Pbm were manually measured using Image J. The A20 area was normalized to the Pbm.

#### **4.3.2.5. Immunoblotting and cytometric bead array**

Whole lung tissues were lysed in RIPA buffer supplemented with protease inhibitor cocktail (Roche). The supernatants containing the protein fraction were collected. Proteins (40µg) were resolved by SDS-PAGE and transferred onto polyvinylidene fluoride membranes for detection of A20, phospho-p65, and IFN-β. β-actin was detected as a loading control. Mouse IL-6, KC, TNF-α, and IL-1β concentrations were determined by cytometric bead array using a FACSCanto II flow cytometer (BD Biosciences, USA) according to the manufacturer's instructions.

#### **4.3.3. Statistical analysis**

When data were normally distributed they were expressed as mean ± standard error of mean (SEM). Data were analyzed using nonparametric equivalents and summarized using the median and inter-quartile range (IQR) when non-normally distributed. Multiple comparisons were first analysed by the Kruskal Wallis test and then by individual testing if significant. A p-value of < 0.05 was considered significant.

#### **4.3.4. Study Approvals**

All procedures were approved by The University of Newcastle Human and Animal Ethics Committees.

## **4.4. RESULTS**

### **4.4.1. IAV infection induces increased inflammatory but reduced antiviral responses *ex vivo* in human COPD pulmonary bronchial epithelial cells (pBECs)**

pBECs from healthy non-smoking control subjects, COPD patients (ex-smoker) or smoking (smoker) controls were infected with IAV H3N2 or H1N1 (MOI 5).

Virus replication was measured 24 h after infection. Virus titers increased at 24 h (Figure 4.1A), and was two-fold greater in COPD pBECs compared to controls. Infection resulted in the production of the pro-inflammatory cytokines/chemokines IL-6, CXCL-8, TNF- $\alpha$ , and IL-1 $\beta$ , and antiviral cytokines type I (IFN- $\beta$ ) and type III IFN- $\lambda$ 1 (Figure 4.1B). In COPD, the induction levels of cytokines were substantially higher (2.5-10 fold) compared with healthy control and smoker pBECs (Figure 4.1B). In contrast, the induction of IFN- $\beta$  and IFN- $\lambda$ 1 proteins were reduced in COPD.

We then measured the levels of activity of NF- $\kappa$ B by assessing the levels of phosphorylated p65 at Ser536 (phospho-p65) [653, 671, 672]. Infection significantly increased the activation of p65 (phospho-p65) in both healthy and smoker pBECs at 6 h, which was further increased at 24 h (Figure 4.1C; Supplementary Figure S4.1A). In COPD pBECs the protein levels of phospho-p65 was elevated at baseline (media controls) at 6 h and significantly increased with infection at 24 h compared to healthy and smoker controls.

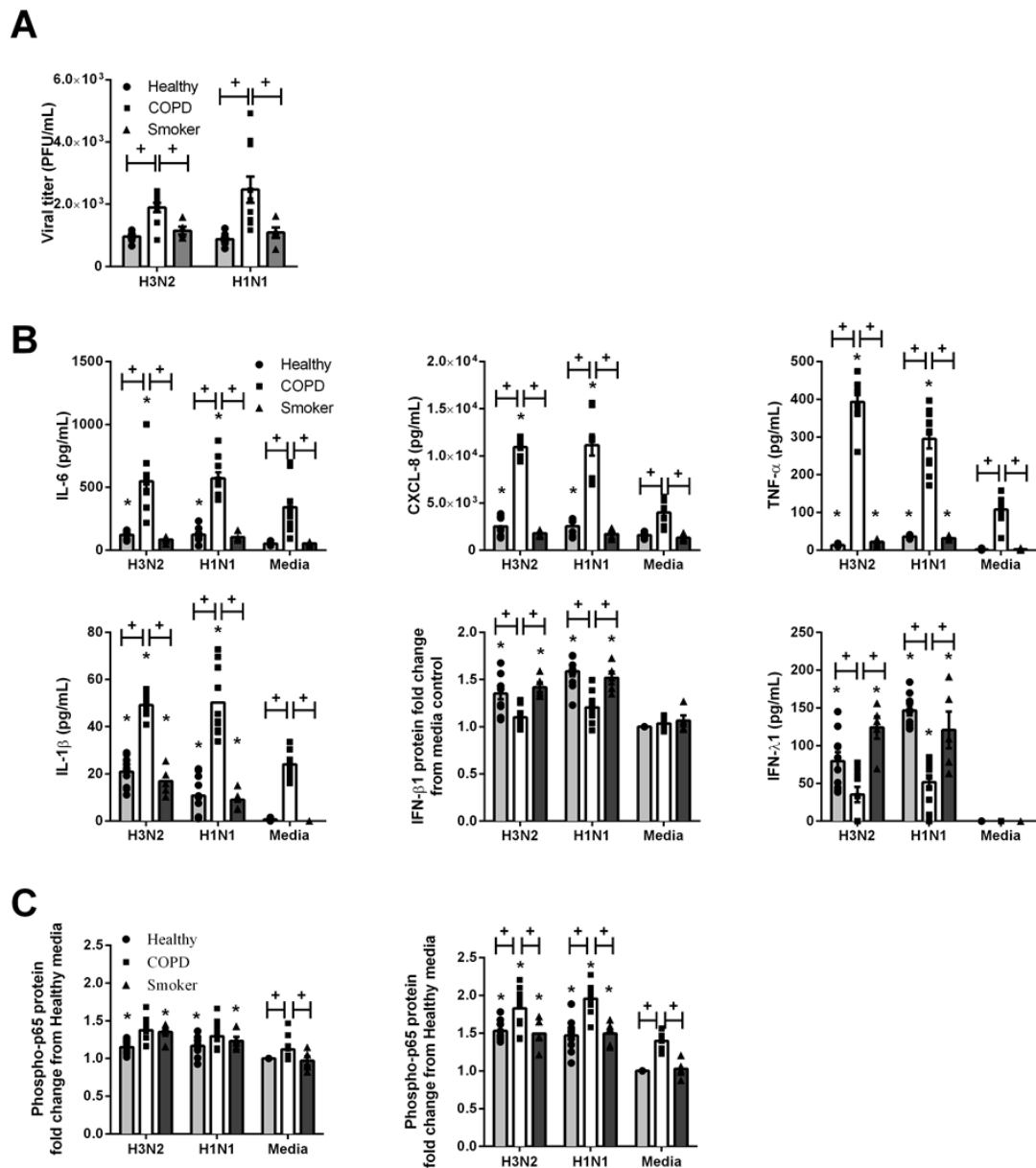


**Figure 4.1. IA virus infection is more severe and results in exaggerated inflammatory but impaired antiviral responses in pBECs from patients with COPD.**

pBECs from healthy controls, COPD patients and healthy smokers were infected with human IA virus H3N2 or H1N1, and **(A)** virus replication was measured at 24 h. **(B)** Pro-inflammatory cytokines/chemokines IL-6, CXCL-8, TNF- $\alpha$ , and IL-1 $\beta$ , and antiviral cytokines IFN- $\beta$  and IFN- $\lambda$ 1 were measured in culture supernatants at 24 h. **(C)** Phospho-p65 was assessed at 6 h and 24 h, densitometry results (from Supplementary Figure S4.1A, representative immunoblot) were calculated as phospho-p65:GAPDH ratios, and expressed as

fold change from healthy media control. Data are mean  $\pm$  SEM,  $n = 15$  (healthy controls and COPD patients) or 5 (healthy smokers). \* $P \leq 0.05$  versus respective non-infected media control, +  $P \leq 0.05$  versus infected or non-infected healthy controls. Statistical differences were determined with one-way ANOVA followed by Bonferroni post-test.

#### **4.4.2. IAV infection also induces increased inflammatory but reduced antiviral responses in vivo in experimental COPD**

We then demonstrated these events also occur *in vivo*. BALB/c mice were exposed to either normal air (air) or CS (Smk) for eight weeks. The Smk group develops hallmark features of COPD as previously described extensively[537, 647, 650-653, 661]. Mice were then infected with IAV A/PR/8/34, and viral titers, airway inflammation (histopathological score), and inflammatory and antiviral cytokines were determined at 7 dpi (Figure 4.2A). Infection in air-exposed controls leads to virus replication (Figure 4.2B) that was accompanied by significant airway inflammation (histopathological score, Supplementary Figure S4.1B). Infection in Smk-exposed mice resulted in a significantly higher virus titers (four-fold) and airway histopathological score (three fold) compared to air-exposed mice. In support of these data, the levels of the pro-inflammatory cytokines/chemokines IL-6, KC (mouse equivalent of CXCL-8), TNF- $\alpha$ , and IL-1 $\beta$  were also increased by infection in air- and to a greater extent in Smk-exposed groups (Figure 4.2C). Antiviral cytokines were increased in infected air-exposed controls but were either not induced (IFN- $\beta$ ) or were induced to a much reduced level (IFN- $\lambda$ 3) in infected Smk-exposed groups (Figure 4.2D). The exaggerated release of pro-inflammatory cytokines was associated with significantly increased levels of phospho-p65 protein in infected Smk-exposed compared to air-exposed controls (Figure 4.2E; Supplementary Figure S4.1C). In all experiments, ultraviolet-inactivated virus did not have any effects compared to media controls (data not shown).

Taken together these human *ex vivo* and experimental *in vivo* data demonstrate that IAV infections result in increased airway inflammation, pro-inflammatory and antiviral responses. However, COPD is associated with exaggerated inflammation and reduced antiviral responses, leading to increased virus replication.

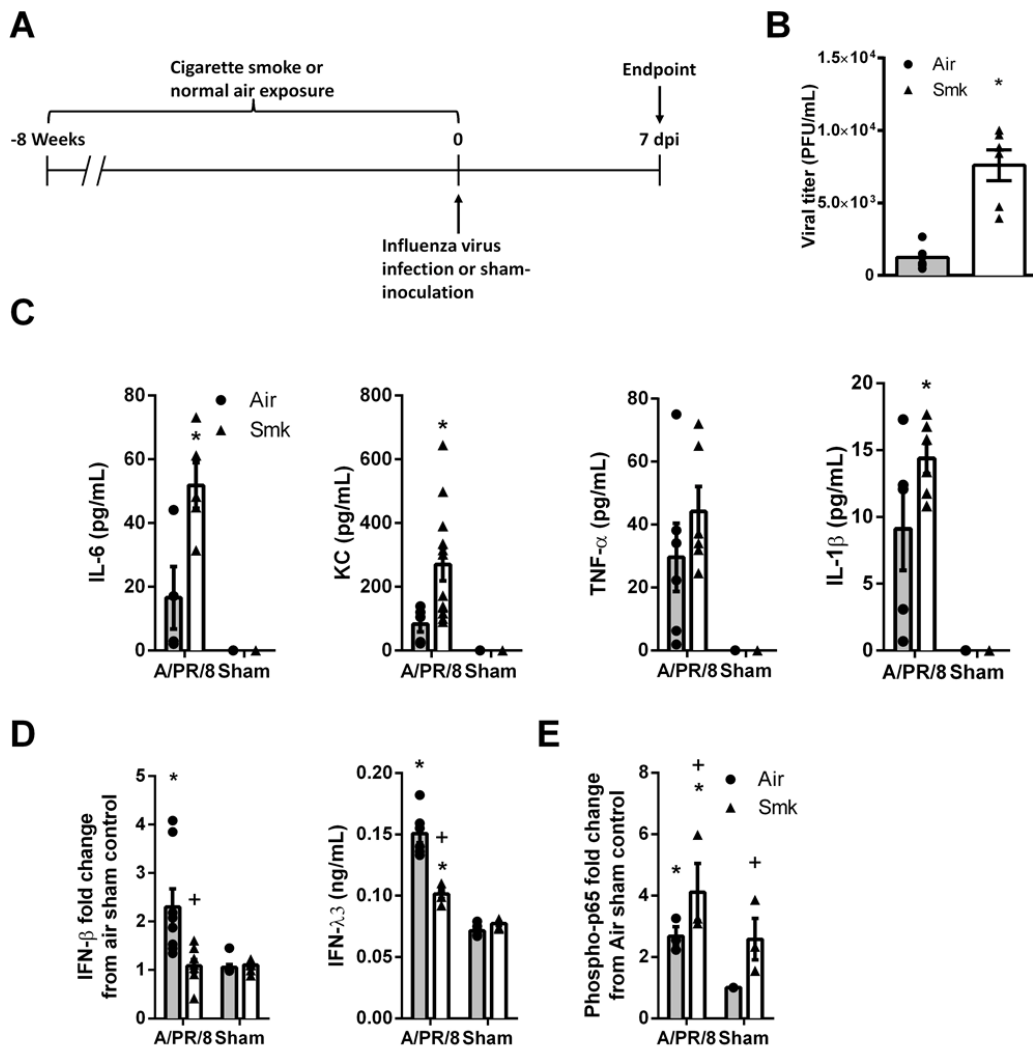


**Figure 4.2. IAV infection is more severe and results in exaggerated inflammatory and impaired antiviral responses in experimental COPD.**

(A) BALB/c mice were exposed to CS (Smk) or normal air (air) for eight weeks, infected with IAV H1N1 (A/PR/8/34, 8pfu) or media (Sham) on the last day of smoke exposure and sacrificed 7 dpi. (B) Virus titers were measured in bronchoalveolar lavage fluid. (C) IL-6, KC, TNF- $\alpha$ , and IL-1 $\beta$ , and (D) IFN- $\beta$  and IFN- $\lambda$ 3 were assessed in lung homogenates. (E) Phospho-p65 protein was determined in lung homogenates, densitometry results (from Supplementary Figure S4.1D, representative immunoblot) were calculated as phospho-p65 or IFN- $\beta$ : $\beta$ -actin ratios, and expressed as fold change from air sham control. Data are mean  $\pm$  SEM,  $n = 6-8$  per group, \* $P \leq 0.05$  versus Sham control, + $P \leq 0.05$  versus air control. Statistical differences were determined with one-way ANOVA followed by Bonferroni post-test.

#### **4.4.3. A20 is an important negative regulatory of NF- $\kappa$ B-mediated inflammatory but not antiviral responses, and its expression is reduced in human COPD and experimental COPD**

We have previously shown that A20 is an important negative regulator of NF- $\kappa$ B activation [632-635], but its roles during IAV infection and whether it also regulates the induction of type I and III IFNs is unclear. We hypothesized that A20 protein expression would be down-regulated and would contribute to the increased activation of NF- $\kappa$ B in response to IAV infection in COPD. IAV infection led to a significant induction of A20 protein at 6 h and 24 h in healthy and smoker controls, but this increase was impaired in COPD pBECs (Figure 4.3A; Supplementary Figure S4.2A). Similarly in Smk-exposed mice, A20 protein expression was reduced in airway epithelial cells compared to air-exposed controls (Supplementary Figure S4.2B).

We then investigated if A20 was important in NF- $\kappa$ B-mediated inflammatory responses, and if exaggerated p65 activation was the direct result of reduced A20 protein levels during infection in COPD pBECs. We inhibited A20 expression using A20-specific siRNA 24 h before infection, and measured the activation of p65 and the production of pro-inflammatory cytokines/chemokines 24 h after infection. Inhibition of A20 expression (Figure 4.3B; Supplementary Figure S4.2C) resulted in significant increases in the protein levels of phospho-p65 (Figure 4.3C; Supplementary Figure S4.2C), and pro-inflammatory cytokines/chemokines IL-6, CXCL-8, TNF- $\alpha$ , and IL-1 $\beta$  (Figure 4.3D) compared to untreated controls, whether pBECs were infected or not. Conversely, ectopic (ecto-) expression using a pcDNA-A20 expression vector reduced the phosphorylation of p65 (Supplementary Figure S4.2D).

Nevertheless, inhibition or ecto-expression of A20 did not affect IFN- $\beta$  and IFN- $\lambda$ 1 induction (Figure 4.3E; Supplementary Figure S4.2D). siRNA negative control or control vector did not affect the induction of A20 or phospho-p65 protein (Supplementary Figure S4.2E-F).

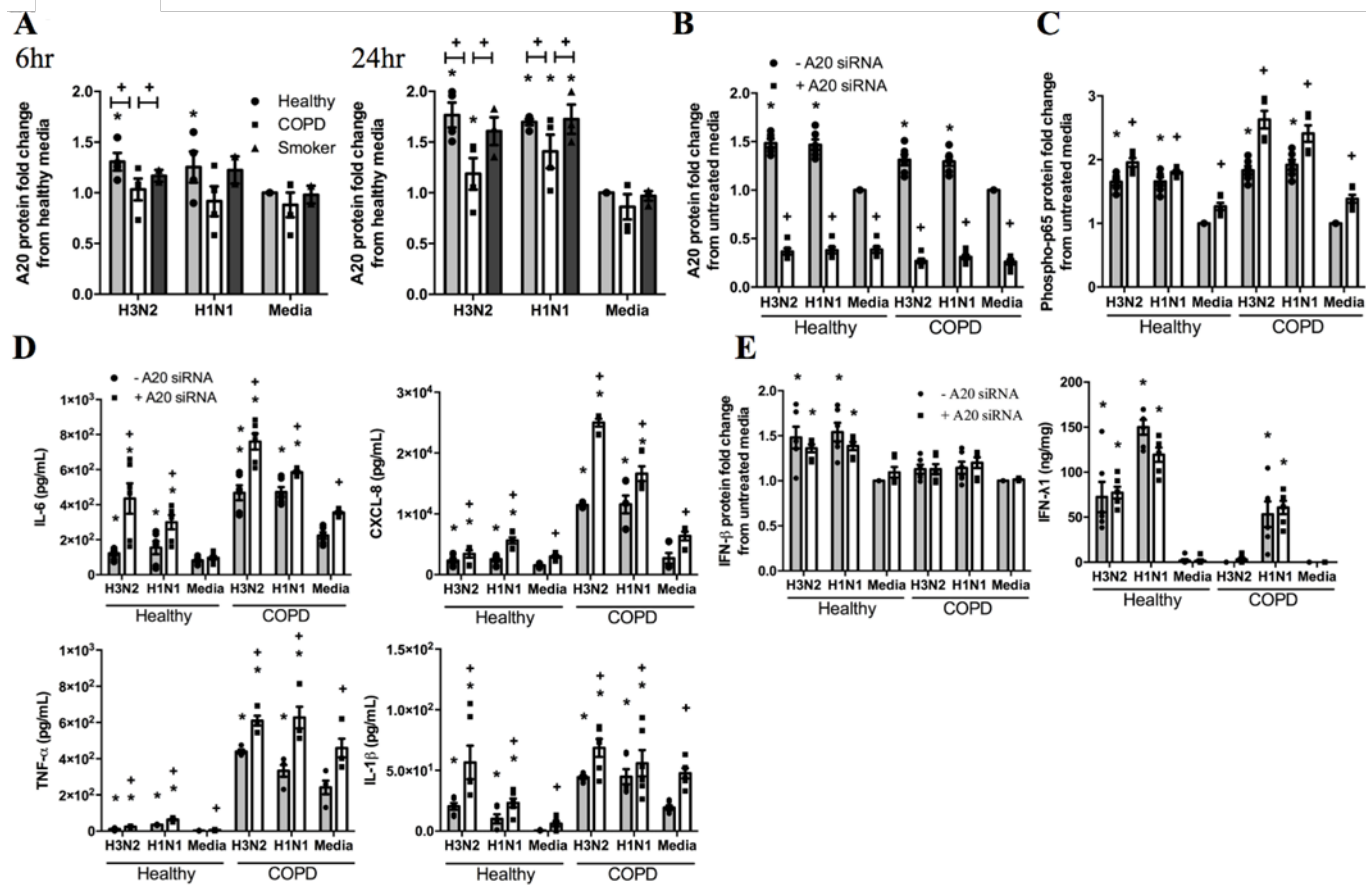


**Figure 4.3. A20 expression is reduced and it negatively regulates inflammatory but not antiviral responses in pBECs from patients with COPD.**

**(A)** pBECs were infected with human IAV H3N2 or H1N1 and the protein levels of A20 were determined at 6 h and 24 h. Densitometry results (from Supplementary Figure S4.2A, representative immunoblot) were calculated as A20 or phospho-p65:GAPDH ratios, and expressed as fold change from healthy media control. Data are mean  $\pm$  SEM,  $n = 15$  per group.  $*P \leq 0.05$  versus respective non-infected media control, +  $P \leq 0.05$  versus healthy control. A20 expression was inhibited with a specific siRNA, pBECs were infected with IAVs and **(B)** protein levels of A20 and **(C)** phospho-p65 and of **(D)** cytokines/chemokines IL-6, CXCL-8, TNF- $\alpha$ , and IL-1 $\beta$ , and antiviral **(E)** IFN- $\beta$  and IFN- $\lambda$ 1 were measured 24 h later. Densitometric ratios (from Supplementary Figure S4.2C, representative immunoblot) were expressed as fold change from untreated media control. Data are mean  $\pm$  SEM,  $n = 3$  per group.  $*P \leq 0.05$  versus untreated, non-infected media control, +  $P \leq 0.05$  versus untreated infected or non-infected control. Statistical differences were determined with one-way ANOVA followed by Bonferroni post-test.

Collectively these data indicate that A20 is an important negative regulator of NF- $\kappa$ B but is dispensable in the induction of type I and III IFNs. A20 protein expression is dysregulated in COPD.

#### **4.4.4. Elevated miR-125a and b levels decrease A20 levels, increase inflammation and impair antiviral responses in COPD pBEC and experimental COPD**

miR-125a and b have recently been shown to directly target and inhibit A20 expression [636], but its roles during IAV infection and in COPD are unknown. Thus, we measured the levels of miR-125a and b induced by IAV infection. H3N2 and H1N1 infections resulted in significant increases in the levels of these miRs at 24 h in pBECs from all groups (Figure 4.4A). However, their levels were substantially greater at baseline and during infection (2-4 fold) in COPD pBECs compared to healthy controls. We then confirmed the direct link between increased miR-125a and b levels and reduced A20 protein induction using specific antagomiRs and mimetics. pBECs were pre-treated with either miR-125a or b specific antagomiRs or mimetics for 24 h before infection, and A20, phospho-p65, inflammatory and antiviral cytokines and were assessed 24 h after infection. AntagomiR treatment inhibited miR-125a or b expression (Supplementary Figure S4.3A), and this resulted in significant increases in A20 protein production, reduced phosphorylation of p65, subsequent induction of pro-inflammatory cytokines/chemokines, and enhanced antiviral IFN- $\beta$  and  $\lambda$ 1 responses (Figure 4.4B and Supplementary Figure S4.3B-E) compared to untreated controls. Conversely miR-125a or b mimetics decreased A20 protein induction, increased phospho-p65 protein levels and reduced IFN- $\beta$  responses (Supplementary Figure S4.3F). Treatment with scrambled miR or mimetic controls did not affect A20, phospho-p65, or IFN- $\beta$  production (Supplementary Figure S4.3G-H).

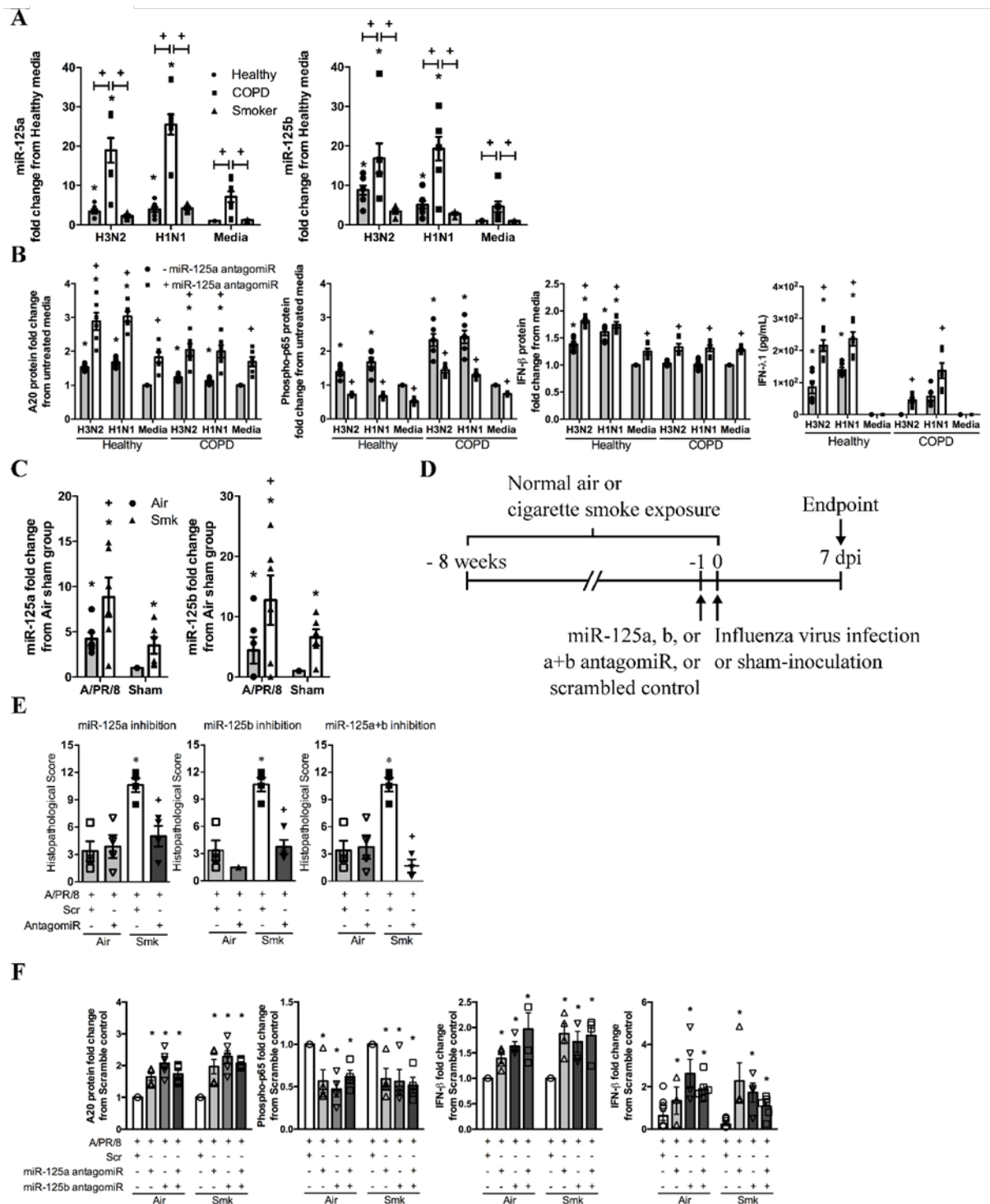


**Figure 4.4. IAV infection increases the levels of miR-125 and b.**

IAV infection increases the levels of miR-125 and b that suppress the production of A20, increase inflammatory and reduce antiviral responses in human COPD pBECs and experimental COPD. pBECs were infected with human IAV H3N2 or H1N1 and **(A)** miR-125a and b levels were assessed 24 h.

Data are mean  $\pm$  SEM,  $n = 15$  per group,  $*P \leq 0.05$  versus non-infected media control.  $+P \leq 0.05$  versus healthy or smoker control. **(B)** pBECs were treated with miR-125a or b antagomiR, infected, and the levels of A20, phospho-p65, IFN- $\beta$  and IFN- $\lambda 1$  were assessed. Densitometry results (Supplementary Figure S4.3B, representative immunoblot) were calculated as A20 or phospho-p65:GAPDH ratios and expressed as fold change from untreated, non-infected control. Data are mean  $\pm$  SEM,  $n = 3$  per group,  $*P \leq 0.05$  versus untreated, non-infected media control,  $+P \leq 0.05$  versus untreated infected or non-infected group. **(C)** BALB/c mice were exposed to CS (Smk) or normal air (air) for eight weeks, inoculated with IAV H1N1 (A/PR/8/34, 8pfu) or media (Sham) on the last day of smoke exposure, sacrificed 7 dpi and the levels of miR-125a and b were measured. Data are mean  $\pm$  SEM,  $n = 6-8$  per group,  $*P \leq 0.05$  versus Sham group,  $+P \leq 0.05$  versus air infected or non-infected group. **(D)** In other groups on the last day of smoke exposure mice were treated with miR-125a or b antagomiR alone or in combination, infected with IAV, and **(E)** airway histological scores were assessed. Data are mean  $\pm$  SEM,  $n = 6-8$  per group,  $*P \leq 0.05$  versus infected and scrambled treated air controls,  $+P \leq 0.05$  versus infected and Scr-treated Smk group. **(F)** The protein levels of A20, phospho-p65, and IFN- $\beta$  in lung homogenates were also measured. Densitometry results (Supplementary Figure S4.4D) were calculated as A20 or phospho-p65: $\beta$ -actin ratios and expressed as fold change from untreated, non-infected control. Data are mean  $\pm$  SEM,  $n = 6-8$  per group,  $*P \leq 0.05$  versus infected Scr-treated air group,  $+P \leq 0.05$  versus infected scrambled Smk group. Statistical differences were determined with one-way ANOVA followed by Bonferroni post-test.

We then assessed whether similar events occurred *in vivo*. IAV infection significantly increased the levels of miR-125a and b in both groups, with the levels in Smk group significantly higher compared to air-exposed controls (Figure 4.4C). We then inhibited miR-125a or b before and during infection (Figure 4.4D). We also extended the *ex vivo* data by inhibiting both miR-125a and b together. Treatment with miR-125a or b antagomiR, alone or in combination, reduced histopathological scores (Figure 4.4E and Supplementary Figure S4.4A) and improved lung function (reduced lung volume determined during a pressure-volume loop manoeuvre) in air and Smk-exposed groups compared to infected scrambled antagomiR-treated controls (Supplementary Figure S4.4B). Inhibition of miR-125a, b, or a and b, also increased A20 protein expression in the airway epithelium and decreased the levels of phospho-p65 compared to the controls (Figure 4.4F; Supplementary Figure S4.4C-D). Importantly while we could only detect reductions in TNF- $\alpha$  and KC with combined treatment (Supplementary Figure S4.4E), antagomiR treatment, either alone or in combination, also significantly increased IFN- $\beta$  and IFN- $\lambda$ 3 protein induction (Figure 4.4F and Supplementary Figure S4.4D).

Collectively, these data show that miR-125a and b are directly involved in the regulation of both inflammatory cytokines, through the control of A20, and antiviral cytokine production through an unknown target.

#### **4.4.5. miR-125a and b target MAVS**

To determine the mechanism of miR-125a and b-mediated regulation of antiviral IFN- $\beta$ / $\lambda$ , we performed miR prediction analysis using TargetScan ([www.targetscan.org](http://www.targetscan.org)). miR-125a and b have a putative binding site in the 3'-UTR of human and mouse MAVS (Figure 4.5A-B). To examine these putative interactions we first assessed the protein levels of MAVS in pBECs. MAVS protein levels were significantly increased 24 h after IAV infection in healthy control and smoker, but notably not in COPD pBECs (Figure 4.5C; Supplementary Figure S4.5A).

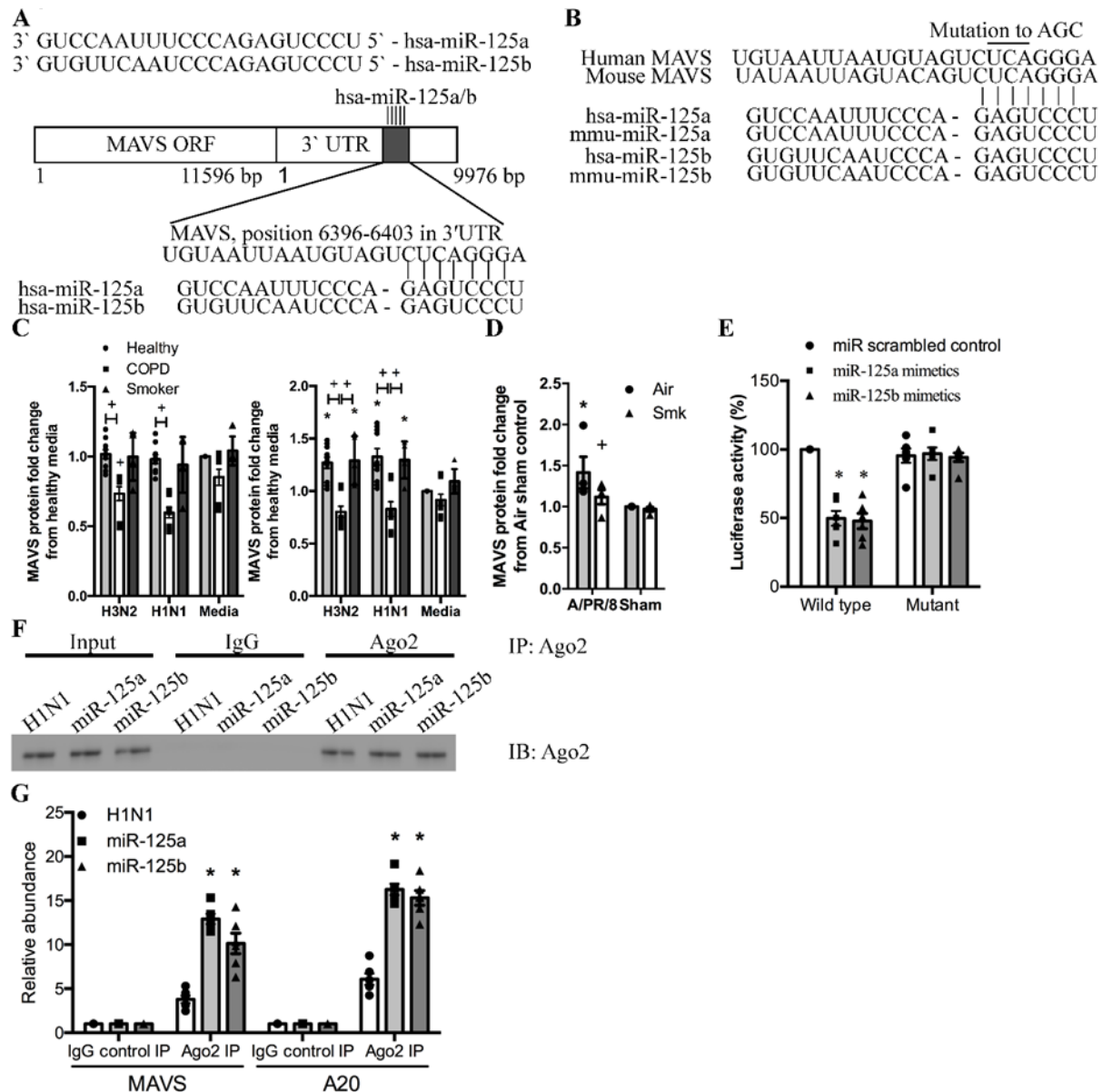


**Figure 4.5. miR-125a and b target a functional binding site of the 3'-UTR of the mRNA of MAVS to suppress its expression.**

(A) Representation of *MAVS* gene structure and location of miR-125a and b binding site. (B) The binding site on 3'-UTR of *MAVS* is 100% conserved between human and mouse *MAVS*. (C) pBECs were infected with H3N2 or H1N1 and MAVS protein was detected at 6 h and 24 h. Densitometry results (Supplementary Figure S4.5A, representative immunoblot) were calculated as MAVS:GAPDH ratios and expressed as fold change from untreated, non-infected controls. Data are mean  $\pm$  SEM,  $n = 15$  per group,  $*P \leq 0.05$  versus non-infected healthy or smoker controls,  $+P \leq 0.05$  versus infected or non-infected healthy controls. (D) BALB/c mice were exposed to CS (Smk) or normal air (air)

for eight weeks, inoculated with IAV H1N1 (A/PR/8/34, 8pfu) or media (Sham) on the last day of smoke exposure, sacrificed 7 days post inoculation (dpi) and the levels of MAVS protein were measured in lung homogenates. Densitometry results (Supplementary Figure S4.5B, representative immunoblot) were calculated as MAVS: $\beta$ -actin ratios in mouse, and expressed as fold change from untreated, non-infected controls. Data are mean  $\pm$  SEM,  $n = 6$  per group,  $*P \leq 0.05$  versus Sham-treated controls. +  $P \leq 0.05$  versus infected air controls. **(E)** The miR-125a and b binding site on 3'-UTR was cloned into a pMIR luciferase reporter construct and transfected into HEK293 cells with miR-125a or b mimetics. The luciferase reporter assay was performed to determine binding. Data are mean  $\pm$  SEM,  $n = 3$  per group,  $*P \leq 0.05$  versus miR scrambled controls. **(F)** Ago2 was immunoprecipitated from miR-125a or b mimetic-transfected HEK293 and **(G)** A20 and MAVS mRNA was detected by qPCR in Ago2-immunoprecipitate. Data are mean  $\pm$  SEM,  $n = 3$  per group,  $*P \leq 0.05$  versus IgG control IP. Statistical differences were determined with one-way ANOVA followed by Bonferroni post-test.

Similarly, infection in Smk-exposed mice was also associated with significantly impaired production of MAVS compared to infected air-exposed controls at 7dpi (Figure 4.5D; Supplementary Figure S4.5B).

To confirm the potential interaction of miR-125a/b and MAVS, we cloned the putative binding region of miR-125a and b in wild-type (MAVS-WT) or mutant (MAVS-MT) *MAVS* 3'-UTR into a luciferase reporter construct. The construct was co-transfected into HEK293 cells along with miR-125a or b mimetics, or scrambled controls, and then luciferase activity was assessed. Co-transfection of miR-125a or miR-125b mimetics with MAVS-WT resulted in a significant decrease in luciferase activity compared to scrambled controls (Figure 4.5E). There was no reduction in activity with co-transfection with MAVS-MT. We then determined if *MAVS* gene is present with the miR-125a or b mimetics in the silencing complex. To do this we immunoprecipitated Argonaute 2 (Ago2), a core component of RNA-induced silencing complex (RISC) that binds to the miRs and their target mRNA, with a specific antibody and detected the presence of both *A20* and *MAVS* by qPCR, which could not be detected with immunoprecipitation with IgG control (Figure 4.5F). This confirmed that miR-125a and b directly bind to the endogenous 3'-UTR of *MAVS*.

#### **4.4.6. miR-125a and b targeting of MAVS regulates antiviral responses in COPD pBEC and experimental COPD**

We then investigated whether inhibition of miR-125 has a functional outcome. We showed that miR-125a and b antagomiR treatment lead to significant increases in MAVS (Figure 4.6A and Supplementary Figure S4.6A-B), IFN- $\beta$  and IFN- $\lambda$ 1 protein induction (Figure 4.4B and Supplementary Figure S4.3C), and reduced viral replication in both healthy and control pBECs (Figure 4.6B). In contrast, mimetics suppressed the induction of antiviral cytokines and increased virus titers (Supplementary Figure S4.3F). Similarly in Smk-exposed mice, inhibition of miR-125a, b, or a+b resulted in increased induction of MAVS (Figure 4.6C and Supplementary Figure S4.6C), IFN- $\beta$  and IFN- $\lambda$ 3 (Figure 4.4F and Supplementary Figure S4.4D-E), and inhibited virus replication (Figure 4.6D).

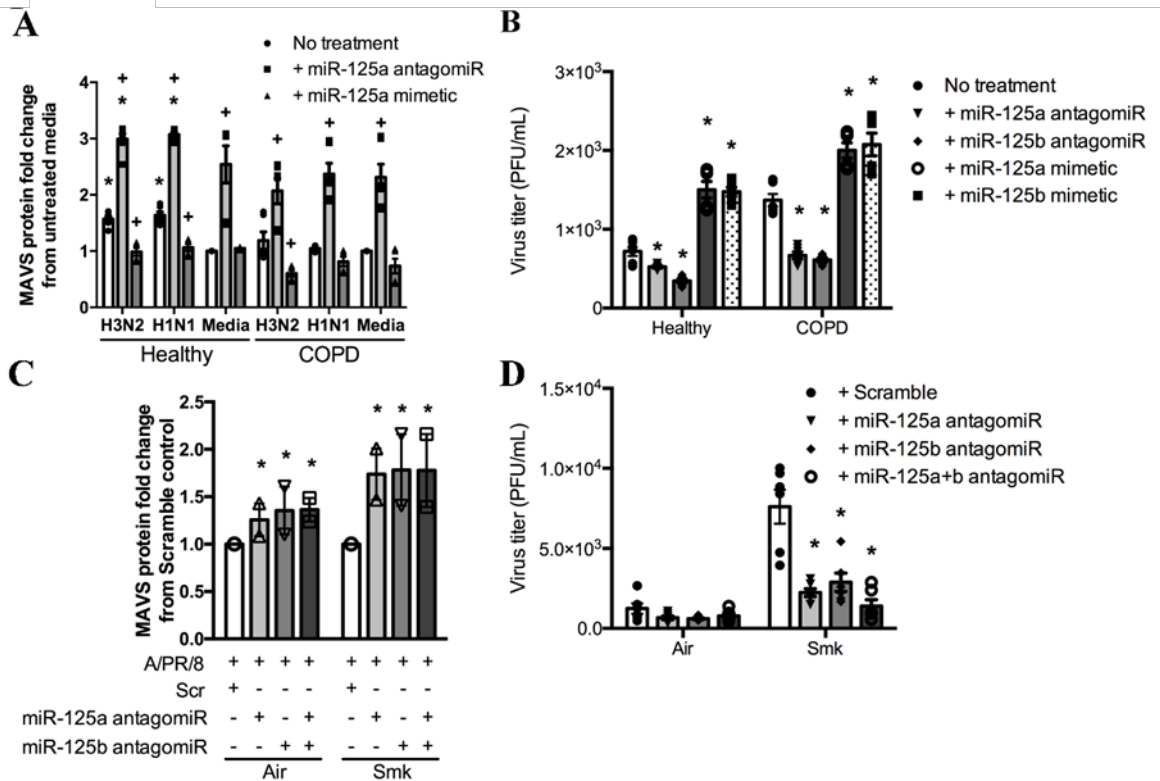


**Figure 4.6. miR-125a and b suppresses the induction of MAVS**

miR-125a and b suppresses the induction of MAVS and promote virus replication in human COPD pBECs and experimental COPD. **(A)** miR-125a and b antagomiR or mimetics were added to pBECs before infection with human IAV H3N2 or H1N1 and mitochondrial antiviral signaling (MAVS) protein were assessed 24 h after infection. Densitometry results (Supplementary Figure S4.6A, representative immunoblot) were calculated as MAVS:GAPDH ratios and expressed as fold change from untreated, non-infected controls. Data are mean  $\pm$  SEM,  $n = 3$ ,  $*P \leq 0.05$  versus untreated, non-infected media controls,  $+P \leq 0.05$  versus untreated, infected or non-infected controls. **(B)** Virus replication was also measured. Data are mean  $\pm$  SEM,  $n = 3$ .  $*P \leq 0.05$  versus untreated, infected controls. **(C)** BALB/c mice were exposed to CS (Smk) or normal air (air) for eight weeks, treated with mir125a and/or b antagomiR, infected with IAV H1N1 (A/PR/8/34, 8pfu) or media (Sham) on the last day of smoke exposure, sacrificed 7 days post inoculation (dpi) and MAVS protein was measured. Densitometry results (Supplementary Figure S4.6C, representative immunoblot) were calculated as MAVS: $\beta$ -actin ratios and expressed as fold change from untreated, non-infected controls. Data are mean  $\pm$  SEM,  $n = 6$ ,

\* $P \leq 0.05$  versus infected, Scr-treated air or Smk controls. **(D)** Virus replication was assessed. Data are mean  $\pm$  SEM,  $n = 6$ , \* $P \leq 0.05$  versus infected, Scr-treated controls. Statistical differences were determined with one-way ANOVA followed by Bonferroni post-test.

Collectively these data demonstrate that miR-125a and b negatively regulate MAVS expression and suppress the induction of IFN- $\beta/\lambda$ , and may potentially be targeted therapeutically in the prevention and/or treatment of IAVs and COPD.

#### 4.5. DISCUSSION

Here we discover that IAV infections induce airway inflammation and antiviral responses, however in COPD pBECs and experimental COPD inflammatory responses and activation of NF- $\kappa$ B are exaggerated but antiviral responses are impaired. We show that A20 is a negative regulator of NF- $\kappa$ B-mediated induction of inflammatory but not antiviral cytokines, and that A20 protein levels were impaired in COPD. The impaired induction of A20 and antiviral responses in COPD was attributed to increased expression of miR-125a and b. Elevated levels of these miRs suppressed A20 expression, leading to heightened NF- $\kappa$ B activity and inflammation and reduced antiviral responses. Inhibition with miR-125a and b antagomiRs increased A20 levels and reduced NF- $\kappa$ B activity, and also promoted IFN production. We then demonstrated that miR-125a and b modulated IFN induction by targeting MAVS translation. MAVS protein levels were reduced in COPD, but could be increased with specific miR-125a and b antagomiR treatment that also induced IFN production. Thus, IAV infection induces the expression of miR-125a/b that suppress A20 and MAVS, in turn promoting NF- $\kappa$ B-induced inflammation and attenuating antiviral IFN production, respectively, increasing viral replication. All these events are exaggerated in COPD (Figure 4.7).

IAV is a major infectious pathogen that poses serious health concerns worldwide. Infections, particularly with highly pathogenic influenza viruses, cause severe airway inflammation and a cytokine storm with high morbidity and mortality. COPD is a major global health problem that is underpinned by exaggerated inflammatory responses in the airways[673]. IAV infections frequently result in acute exacerbations of COPD, leading to accelerated declines in lung function[674, 675] and increased mortality[640]. The mechanisms of exaggerated inflammation and severe outcomes in COPD are poorly understood, and there are no effective therapies for these events.

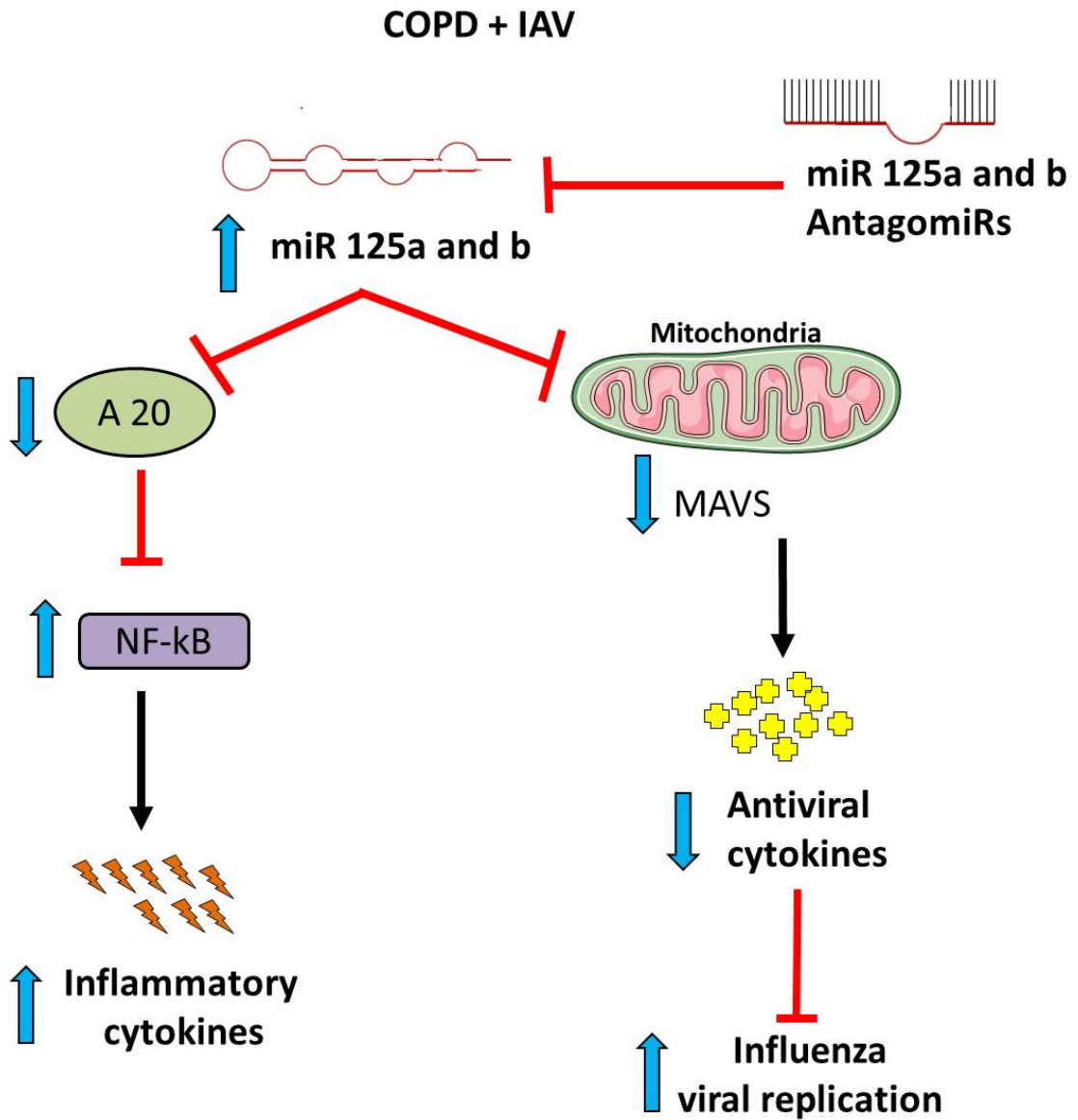


Figure 4.7. Roles of miR-125a and b in the regulation of inflammatory and antiviral responses in IAV infection.

Here we show that IAV-mediated inflammatory response are dampened with ectopic expression of A20 that reduces NF- $\kappa$ B activity and inflammatory responses, without affecting type I and III IFN responses. A20 is a de-ubiquitinating enzyme that degrades RIP1 and inhibits NF- $\kappa$ B activation [634], and has been shown to suppress the induction of IFN- $\beta$ [676]. We found that A20 modulated NF- $\kappa$ B activity and inflammation, but did not affect type I and III IFNs production.

Consistent with our previous findings [647], IAV infections in COPD pBECs and experimental COPD led to heightened inflammation and production of inflammatory cytokines but impaired antiviral responses (IFN- $\beta$  and IFN- $\lambda$ ), which were associated with greater viral replication. Increased inflammation, inflammatory cytokines and activation of NF- $\kappa$ B are well-known in COPD[644, 677]. Here we show that these are the result of reduced induction of A20, leading to uncontrolled activation of NF- $\kappa$ B and subsequent induction of inflammatory cytokines. A20 is a pleiotropic protein involved in various ubiquitin-dependent pathways including NF- $\kappa$ B[636] and mitogen-activated protein (MAP) kinase pathway[678], and has also been shown to negatively regulate type I IFN inductions[676, 679, 680]. Surprisingly inhibition or ectopic expression of A20 did not affect IFN- $\beta$  production. The precise roles of A20 during viral infections therefore require further investigation. We could not rule out that other factors may also contribute to the regulation of A20 expression and of NF- $\kappa$ B activity, including other un-identified miRs, which may also be dys-regulated in COPD.

Forced expression of A20 may be a novel therapeutic option that reduces IAV-mediated inflammation and cytokine storm, particularly from high pathogenic IAVs such as H5N1, or in COPD where airway inflammation is already persistently heightened.

The lack of the induction of A20 protein during IAV infection in COPD was attributed to increased levels of miR-125a and b. These miRs down-regulate A20 expression by directly binding to its 3'-UTR, leading to constitutive activation of NF- $\kappa$ B[636]. We found that heightened levels of miR-125a/b

resulted in increased activation of NF- $\kappa$ B in COPD. Inhibition of miR-125a or b in both healthy and COPD pBECs and in experimental COPD increased A20 protein levels and reduced NF- $\kappa$ B activation during IAV infection.

We also found that miR-125a and b modulated the induction of type I and III antiviral IFNs. This occurred by the direct targeting of MAVS 3'-UTR, therefore down-regulating the subsequent induction of IFN- $\beta$  and IFN- $\lambda$ . MAVS is an important adaptor protein on mitochondria that facilitates the production of IFNs [461], however there was an impaired induction of MAVS by IAV infections in COPD pBECs and in experimental COPD. Inhibition of miR-125a and/or b increased the levels of MAVS and antiviral IFNs, which lead to reduced virus replication both *in vivo* and *in vivo*. Interestingly antagomiRs against miR-125a and/or b (either alone or in combination) in experimental COPD, partially reduced the release of inflammatory cytokines, and substantially suppressed virus replication. This may indicate that miR-125a and b may preferentially target MAVS over A20 during IAV infection in COPD, although such binding preferences of miRs have not been widely investigated. Furthermore, as MAVS is transcriptionally driven by IFN-sensitive response element (ISRE) as part of the IFN-stimulated genes[681], and miR-125a/b have been reported to be induced by NF- $\kappa$ B[682], it is possible that reduced MAVS partly attributed to impaired IFNs in COPD, and with enhanced expression of miR-125a/b (NF- $\kappa$ B-inducible) this then leads to continuous cycle of exaggerated inflammation and impaired antiviral immunity in COPD.

Although miR-125a/b appears to be NF- $\kappa$ B-inducible, the exact molecular mechanisms of enhanced miR-125a/b expression in COPD require further investigation. In colorectal cancer tissues the levels of miR-125a have been shown to be reduced, which is associated with hyper-methylation at the CpG island within the promoter region of miR-125a[683]. Similarly in breast cancer cell line reduced miR-125a has also been shown to be associated with trimethylation at H3K9 and H3K27 at the promoter region of miR-125a[684]. It is therefore possible that the methylation status of miR-125a/b promoter site is altered in COPD, leading to increased expression of miR-125a/b. Nevertheless,

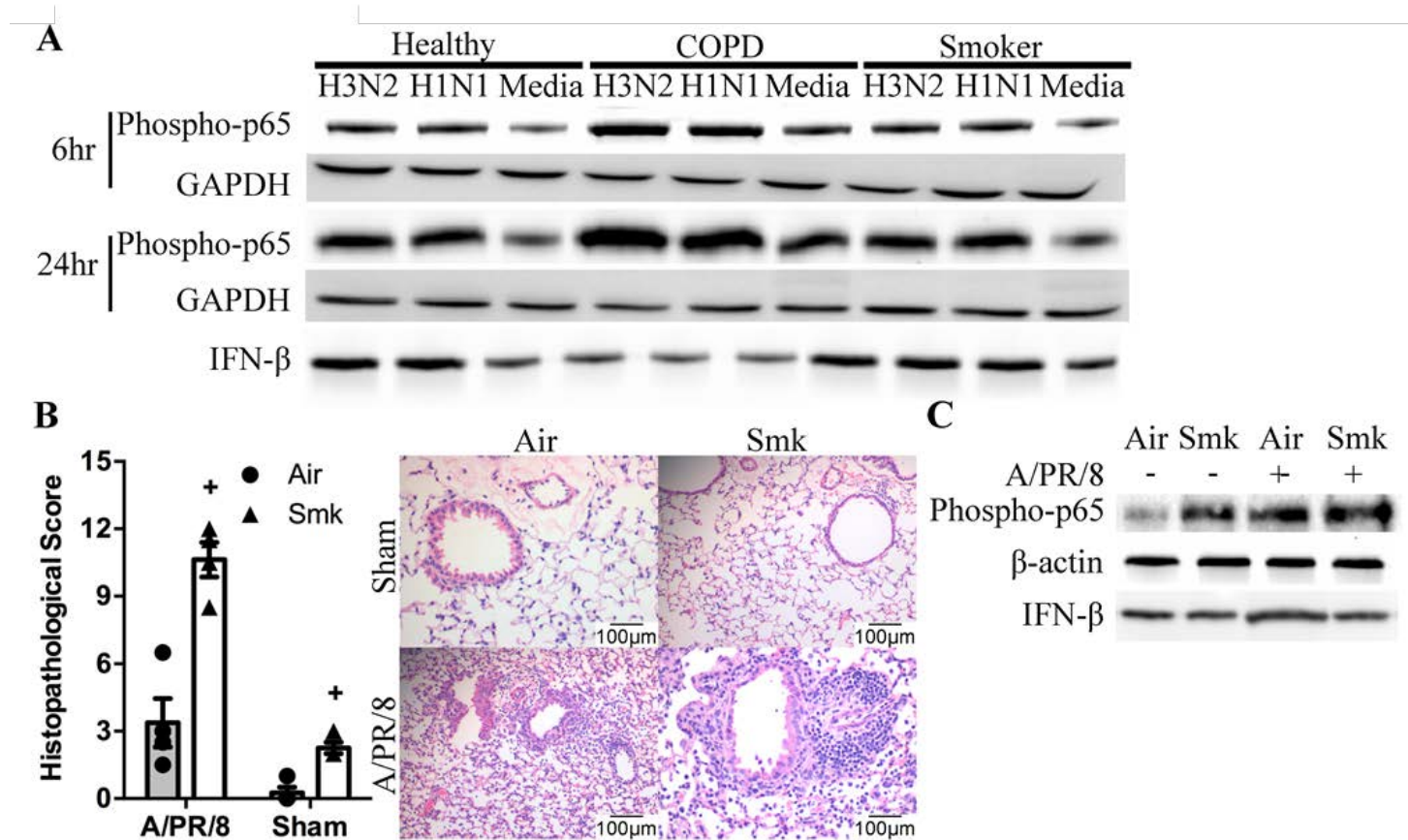
our data also demonstrate that specific inhibition of miR-125a/b may be novel therapeutic options against IAV infections and for those whom are most vulnerable.

CS is the major risk factor for COPD. Acute exposure results in oxidative stress and NF- $\kappa$ B activation[685-687]. However the effects we have observed in COPD appear to be independent of acute exposure to cigarette smoking, as the pBECs obtained from subjects with COPD were all abstinent from smoking for at least 10 years. In support of this, a pooled analysis by Gamble et al., assessed airway mucosal inflammation in COPD smokers and ex-smokers where they demonstrated no significant differences between smokers and ex-smokers in the numbers of any of the inflammatory cell types or markers analysed. The study suggested that in established COPD, the bronchial mucosal inflammatory cell infiltrate is similar in ex-smokers and those that continue to smoke[688]. Also, epigenetic impact of CS exposure and its effect on gene expression of important human innate immune components might have long-term effects that may or may not be reversed[689]. Thus, in the context of our study we consider that it is likely that chronic smoke exposure progressively leads to persistent induction of miR-125a and b and NF- $\kappa$ B activation[690, 691], that then impairs the induction of A20 and MAVS in COPD.

#### **4.6. CONCLUSION**

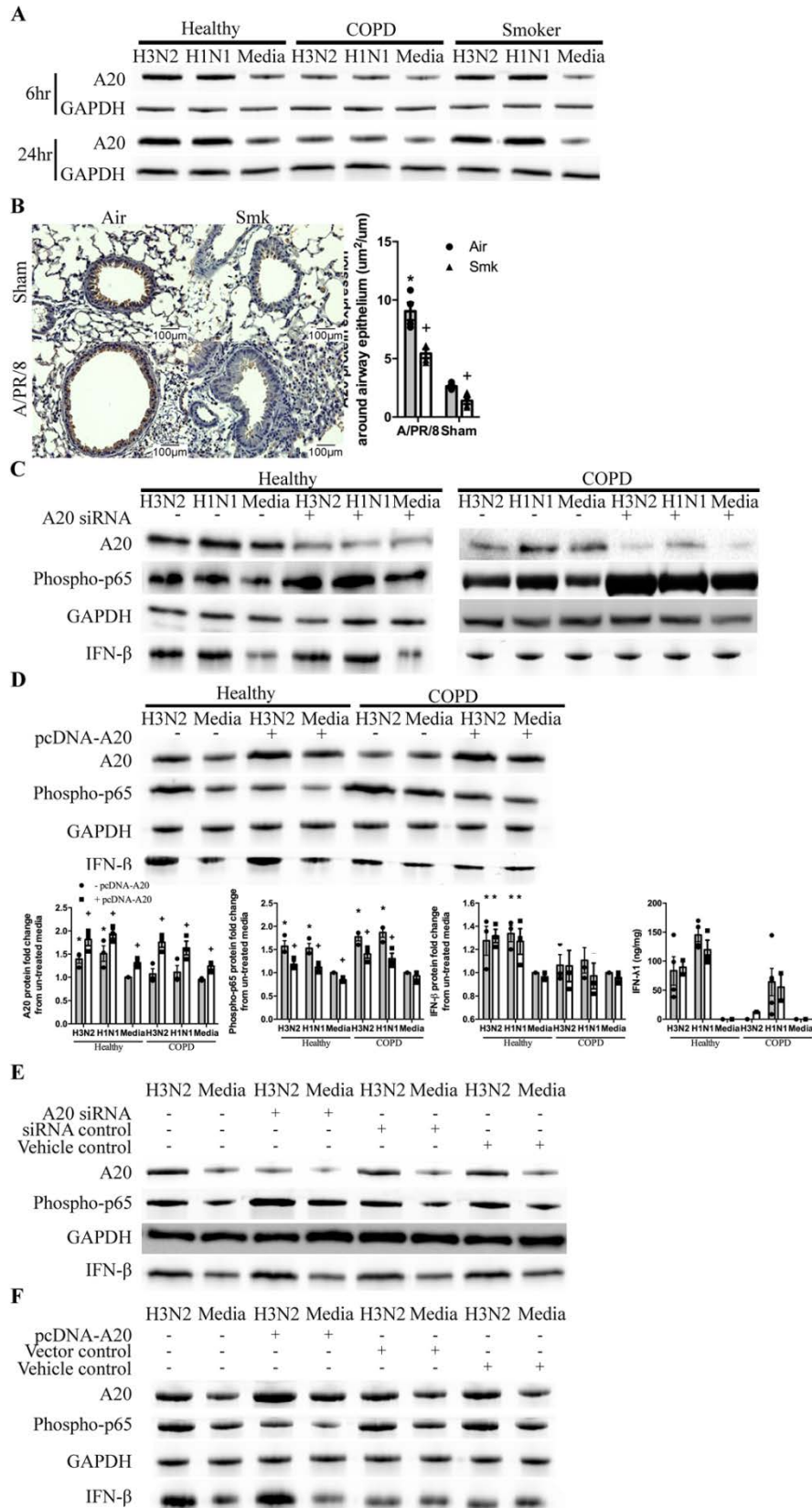
Collectively, our results demonstrate that A20 regulates NF- $\kappa$ B activation and subsequently the production of inflammatory cytokines but not antiviral IFNs. COPD pBECs and mice with experimental COPD responded to IAV infection with an exaggerated inflammatory but impaired antiviral responses. Increased levels of miR-125a and b by IAV and in COPD suppressed protein inductions of A20 and MAVS, leading to heightened airway inflammation and reduced IFN production. Inhibition of miR-125a and b reduced the induction of inflammatory cytokines and enhanced antiviral responses to IAV infection in both healthy and COPD states. This study therefore identifies a novel potential therapeutic target for IAV infection in general and in COPD.

## 4.7. SUPPLEMENTARY FIGURES



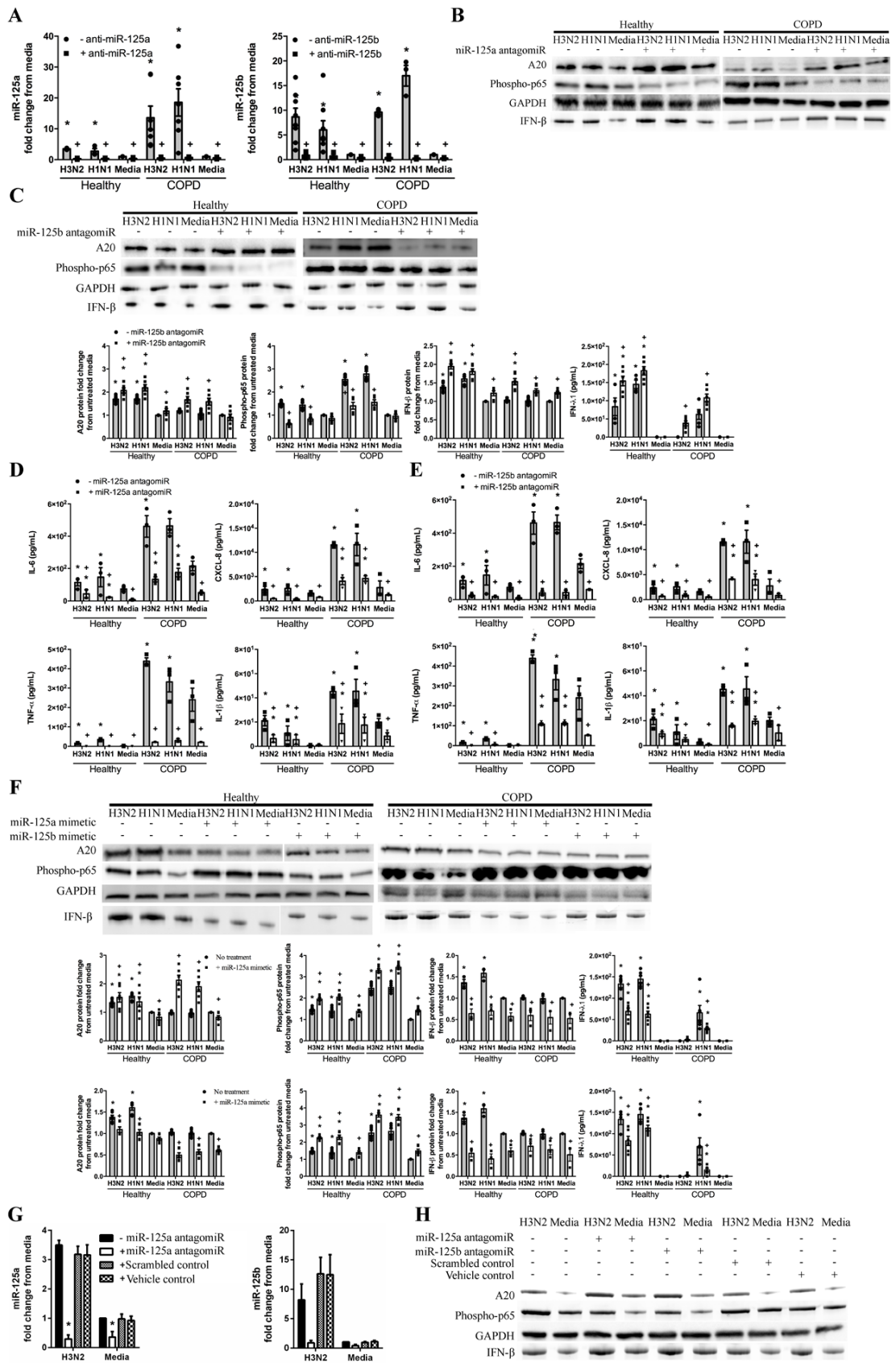
Supplementary Figure S4.1. Protein levels of phospho-p65 in IAV infected pBECs from human COPD patients and histopathology and phospho-p65 and antiviral responses in experimental COPD.

**(A)** pBECs from healthy controls, COPD patients and healthy smokers were infected with human IAV H3N2 or H1N1 and the protein levels of phospho-p65 were measured at 24 h.  $n=10$  (healthy controls and COPD patients) or 5 (healthy 1 smokers). **(B)** BALB/c mice were exposed to CS (Smk) or normal air (air) for eight weeks, infected with IAV H1N1 (A/PR/8/34, 8pfu) or media (Sham) on the last day of smoke exposure and sacrificed 7 days post inoculation (dpi). Lung tissue sections were stained with haematoxylin and eosin stains, and histopathological scores were obtained. Data are mean  $\pm$  SEM,  $n = 6-8$  per group,  $+P\leq 0.05$  versus air control. **(C)** Protein levels of phospho-p65 and IFN- $\beta$  were measured. Statistical differences were determined with one-way ANOVA followed by Bonferroni post-test.



**Supplementary Figure S4.2. Protein levels of A20 in IAV infected human COPD pBECs and experimental COPD, and the effect of A20 inhibition on inflammatory and antiviral responses in pBECs.**

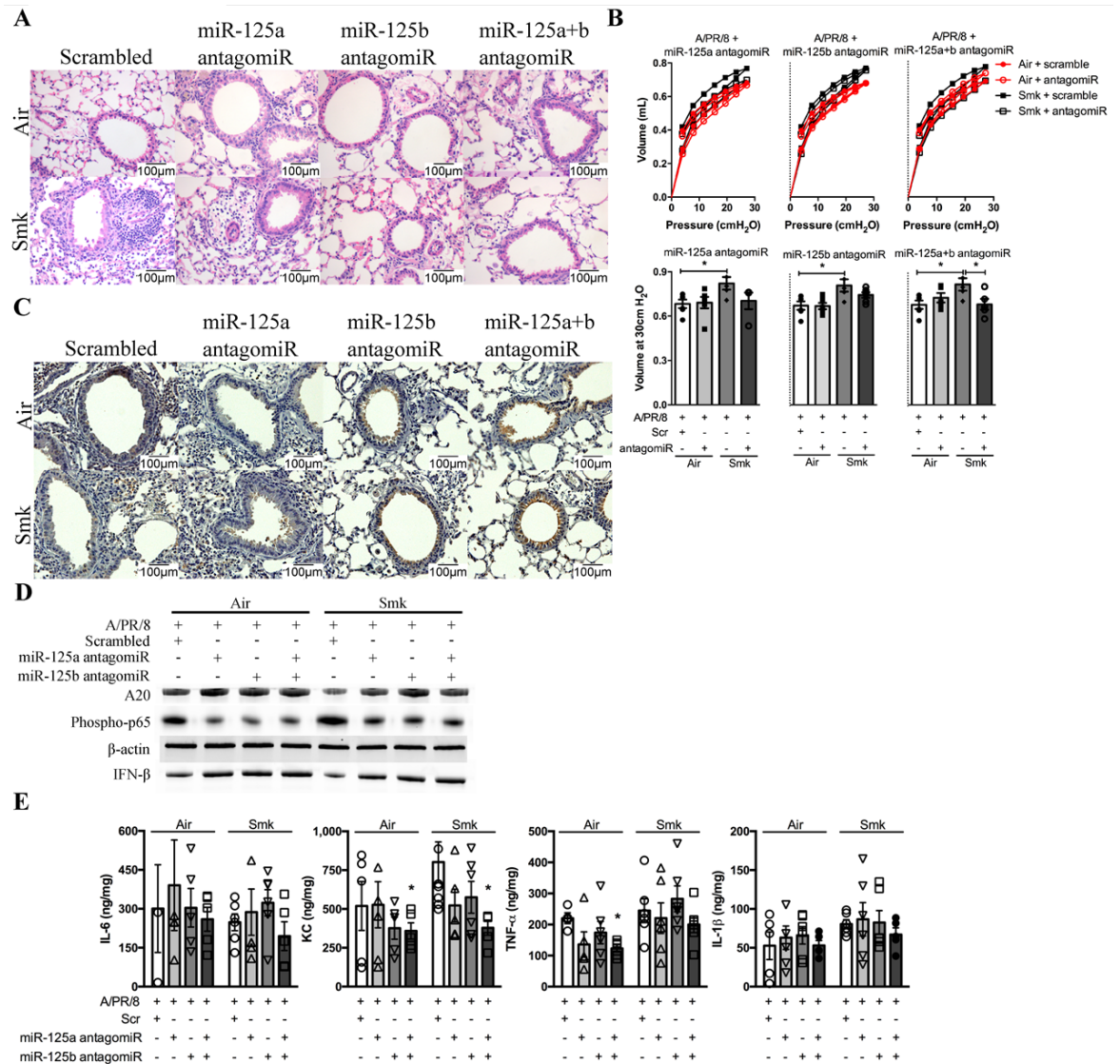
**(A)** pBECs from healthy controls, COPD patients and healthy smokers were infected with human IAV H3N2 or H1N1 and A20 protein levels were measured at 6 h and 24 h. **(B)** BALB/c mice were exposed to CS (Smk) or normal air (air) for eight weeks, infected with IAV H1N1 (A/PR/8/34, 8pfu) or media (Sham) on the last day of smoke exposure and sacrificed 7 days post inoculation (dpi). Mouse lung sections were stained with A20 specific antibody, which was detected by immunohistochemistry, and quantified by normalization to perimeter of basement membrane (pbm). A20 protein expression was quantified. Data are mean  $\pm$  SEM, n = 6-8 per group, \*  $P \leq 0.05$  versus Sham control, +  $P \leq 0.05$  versus air control. **(C)** A20 expression was silenced using specific siRNA or **(D)** increased using a pcDNA-A20 expression plasmid 24 h before infection, and A20, phospho-p65, and IFN- $\beta$  protein levels were determined. Data are mean  $\pm$  SEM, n = 3. \*  $P \leq 0.05$  versus respective non-infected media control, +  $P \leq 0.05$  versus untreated infected or non-infected group. **(E)** pBECs were transfected with siRNA control, siRNA vehicle control, or **(F)** pcDNA vector control or vehicle control and A20, phospho-p65, and IFN- $\beta$  protein levels were detected. Statistical differences were determined with one-way ANOVA followed by Bonferroni post-test.



Supplementary Figure S4.3. miR-125a and b levels and the effects of their inhibition or ectopic-expression on A20, and phospho-p65, inflammatory

**cytokine/chemokine and IFN- $\beta$  production during IAV infection in human COPD pBECs.**

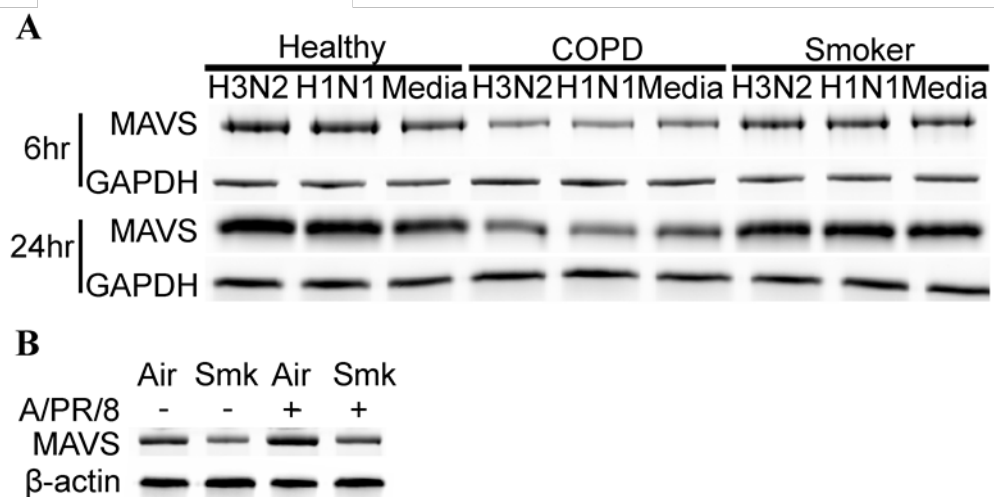
**(A)** pBECs from healthy controls, COPD patients and healthy smokers were infected with human IAV H3N2 or H1N1 and the levels of miR-125a and b were measured 24 h after infection. Data are mean  $\pm$  SEM, n = 3. \*P $\leq$ 0.05 versus respective non-infected media control, + P $\leq$ 0.05 versus untreated infected or non-infected group. **(B)** miR-125a or **(C)** b antagomiR was transfected into pBECs 24 h before infection, and the protein levels of A20, phospho-p65, and IFN- $\beta$  were determined 24 h after infection. Data are mean  $\pm$  SEM, n = 3. \*P $\leq$ 0.05 versus respective non-infected media control, + P $\leq$ 0.05 versus untreated infected or non-infected group. **(D and E)** cytokines/chemokines IL-6, CXCL-8, TNF- $\alpha$ , and IL-1 $\beta$  were also determined 24 h after infection. Data are mean  $\pm$  SEM, n = 3. \*P $\leq$ 0.05 versus respective non-infected media control, + P $\leq$ 0.05 versus untreated infected or non-infected group. **(F)** miR-125a or b mimetics were added to pBECs 24 h before infection, and the protein levels of A20, phospho-p65, and IFN- $\beta$  and IFN- $\lambda$ 1 were detected 24 h after infection. Data are mean  $\pm$  SEM, n = 3. \*P $\leq$ 0.05 versus respective non-infected media control, + P $\leq$ 0.05 versus untreated infected or non-infected group. **(G)** miR scrambled and vehicle controls were added to pBECs before infection and the levels of miR-125a and b, and **(H)** the protein levels of A20, phospho-p65, and IFN- $\beta$  were assessed. Data are mean  $\pm$  SEM, n = 3. \*P $\leq$ 0.05 versus vehicle control. Statistical differences were determined with one-way ANOVA followed by Bonferroni post-test.



**Supplementary Figure S4.4. miR-125a and b levels and the effects of their inhibition on histopathology, lung function, A20, and phospho-p65, inflammatory cytokine/chemokine and IFN- $\beta$  production during IAV infection in experimental COPD.**

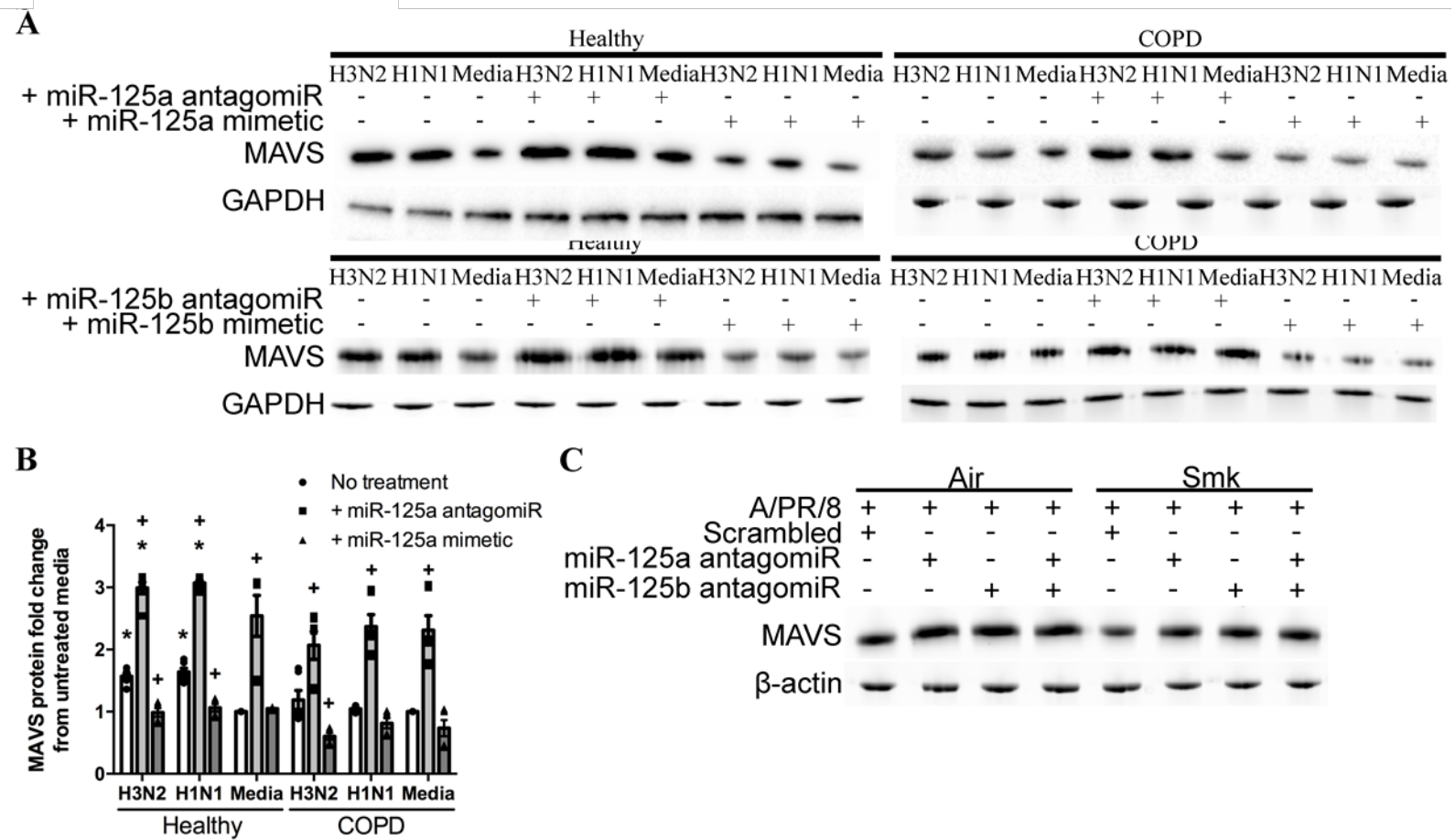
BALB/c mice were exposed to CS (Smk) or normal air (air) for eight weeks, miR-125a or b antagomiR, or both, were administered on the last day of cigarette, before infection with IAV H1N1 (A/PR/8/34, 8pfu) or media (Sham). Mice were sacrificed 7 days post inoculation (dpi). **(A)** Whole lung sections were stained with haematoxylin and eosin, **(B)** lung function was assessed in terms of pressure-volume loops and compliance at 30cmH<sub>2</sub>O. Data are mean  $\pm$  SEM, n = 6-8 per group. \*P $\leq$ 0.05 versus infected scrambled control. **(C)** A20 protein was detected in lung sections. **(D)** protein levels of A20, phospho-p65, and IFN- $\beta$  were detected. **(E)** Cytokines/chemokines IL-6, CXCL-8, TNF- $\alpha$ , and IL-1 $\beta$

were measured 7dpi. Data are mean  $\pm$  SEM, n = 6-8 per group. \*P $\leq$ 0.05 versus infected scrambled control. Statistical differences were determined with one-way ANOVA followed by Bonferroni post-test.



**Supplementary Figure S4.5. Protein levels of MAVS during IAV infection in human COPD pBECs and experimental COPD.**

**(A)** pBECs from healthy controls, COPD patients and healthy smokers were infected with human IAV H3N2 or H1N1 and the protein levels of MAVS were detected 24 h. **(B)** BALB/c mice were exposed to CS (Smk) or normal air (air) for eight weeks, inoculated with IAV H1N1 (A/PR/8/34, 8pfu) or media (Sham) on the last day of smoke exposure and sacrificed 7 days post inoculation (dpi). The protein levels of MAVS were detected in lung homogenates.



Supplementary Figure S4.6. The effect of miR-125a and b inhibition or over-expression on the protein levels of MAVS and IFN- $\beta$  in IAV infection of human COPD pBECs and experimental COPD.

**(A and B)** miR-125a and b antagomiR or mimetics were added to pBECs before infection with human IAV H3N2 or H1N1 and MAVS, IFN- $\beta$ , and IFN- $\lambda$ 1 protein were detected 24 h. Data are mean  $\pm$  SEM, n = 3. \*P $\leq$ 0.05 versus respective non-infected media control, + P $\leq$ 0.05 versus untreated infected or non-infected group. **(C)** BALB/c mice were exposed to CS (Smk) or normal air (air) for eight weeks, treated with mir125a and/or b antagomiR, inoculated with IAV H1N1 (A/PR/8/34, 8pfu) or media (Sham) on the last day of smoke exposure and sacrificed 7 dpi. Statistical differences were determined with one-way ANOVA followed by Bonferroni post-test.

# **CHAPTER 5**

## **GENERAL DISCUSSION AND CONCLUSIONS**

Respiratory diseases such as asthma, COPD and influenza are major causes of mortality and morbidity worldwide[75, 131, 692]. IAV infection is a massive global clinical problem that imposes an enormous socioeconomic burden. People with chronic lung diseases, particularly asthma and COPD are more susceptible to viral infections, including with IAV[141]. Approximately 35% of deaths in asthma patients have been attributed to a concomitant IAV infection[145]. These infections have been identified to be the major causes of exacerbations and worsening of the underlying respiratory diseases[144]. However, the immunological mechanisms that underpin these associations are largely unknown.

Infection-induced exacerbations, often caused by IAV, are the 2<sup>nd</sup> most common cause of hospitalisations in Australia[146] and 2,715 deaths in COPD patients was reported in 2006 due to IAV and its complications[132]. Furthermore, those with COPD are consistently over-represented in those hospitalised or who died during pandemics[147]. Therefore, there is an urgent need to develop novel and effective preventions and treatments for IAV infection, especially for those who are most susceptible. For these reasons, IAV infections have attracted much attention from the pharmaceutical industry. The most effective approach may be to improve host immunity rather than targeting the virus and developing treatments directed against both IAV invasion and proliferation [152].

To understand the biological and molecular mechanisms driving the pathophysiology of chronic respiratory conditions, we utilised mouse models of experimental allergen-induced asthma with Ova[255, 391, 693, 694] and HDM, and experimental COPD[264]. These models mimic the hallmark features of the human diseases within a short time frame and have been recognised as the most relevant animal models. We have also established representative models of IAV infection in healthy mice and those with experimental asthma[693, 695] or COPD[264]. Our studies produced important findings where we have identified the involvement of various regulatory factors such as IL-13 and miR-21 in AAD and IL-13, miR-21, miR-125a and b in COPD respectively. These factors have enhanced our understanding of the molecular mechanisms that

underpin the association between IAV infection and chronic airway diseases. We also observed that targeting these factors protected against IAV infection and disease exacerbations by reducing viral titres and inflammatory responses in both these disease settings.

## **5.1. IAV INFECTION IN EXPERIMENTAL AAD**

We have used HDM, which is a disease-relevant natural antigenic protein and source of indoor allergens in our AAD mice model to understand the mechanisms driving increased susceptibility of AAD to IAV infection. We demonstrated that AAD increased susceptibility to IAV infection as indicated by increased viral titre. We also showed that IAV infection exacerbated HDM-induced AAD by inducing Th2 responses that impaired antiviral responses, exaggerated airway inflammation and IL-13R $\alpha$ 1 expression, increased histopathology, mucus secretion, collagen deposition around small airways, small airways epithelial thickness and induced AHR. This clearly shows the influence of IAV virus infection in exacerbating AAD. The combination of infection and allergen challenge also reduced antiviral responses and levels of IFNs in response to IAV infection. All these characteristic features of IAV infection in HDM-induced AAD could be replicated with Ova- induced AAD.

Our studies also show that infected mice with AAD after rechallenging with an allergen have ongoing remodelling characterised by excessive mucus and collagen production that was unresponsive to dexamethasone. This is supported by numerous published reports where patients with severe asthma responded poorly to the available treatments like corticosteroids and long acting inhaled  $\beta$ 2 agonists[130, 696, 697]. This warrants further in-depth investigation on the mechanisms and kinetics involved in dexamethasone resistance and remodelling events that forms a part of future ongoing studies.

We have also demonstrated that mice with AAD are more susceptible to IAV infection thereby increasing its severity. We have also established a model of IAV infection in healthy mice. Our mouse models of asthma are sensitised and challenged with either Ova or HDM that result in the development of AAD. Ova-

or HDM-induced AAD is characterized by elevated levels of IL-13 and replicated features of the human disease in mice[698]. These observations are supported by previously published findings[548-550]. However, only few studies have examined the effects of IL-13 in viral infections. The findings in this study indicated that IL-13 is probably one of the main activating factors mediating IAV infection-induced exacerbations of AAD.

Corticosteroid therapy often fails to control exacerbations in patients with asthma, particularly those with severe disease[599-602]. We observed that dexamethasone treatment predisposed AAD mice to IAV infection that then induced steroid-resistant allergic inflammation and AHR. Our findings were consistent with several studies that showed poor response to inhaled steroids during disease exacerbation that was assessed as ineffective reductions in airway inflammation and AHR[496, 699-701]. These observations highlight data relevant to the induction of steroid resistance, tissue remodelling and disease exacerbations that have been identified to be regulated by altered glucocorticoid signalling, altered Th cell polarization, innate immune activation and chronic inflammation[496]. They may also indicate that steroids primarily be useful as maintenance therapies to suppress ongoing inflammation but not in acute exacerbations. Steroid treatments need to be considered in the background of multiple undesirable side effects, especially steroid resistance due to long-term use and immune-suppressive effects mediated by this class of drugs.

Many studies have clearly demonstrated that IL-13 plays a prominent role in asthmatic responses[66, 518, 551, 552]. In our study, we demonstrated that the inhibition of IL-13 with anti-IL-13 specific monoclonal antibody protected mice against infection and reduced the severity of AAD following IAV infection. This was indicated by reduced viral titre, tissue inflammation, eosinophil count, mucus-secreting cells and transpulmonary resistance in anti-IL-13-treated infected mice with AAD compared to isotype-treated infected non-allergic controls. Inhibition of IL-13 signalling has been shown to reduce allergic airway responses in patients with asthma[702]. Similarly, the absence of IL-13 or its signalling (either through genetic deletion of IL-13 or blocking of its critical

signalling elements, such as STAT6) has been demonstrated to decrease AHR[703-707]. The genetic overexpression of IL-13 has been linked to increased AAD-related features, including AHR[708]. Also, various anti-IL-13 strategies have been proposed (anrukinzumab, lebrikizumab and tralokinumab). The most relevant clinical results have been reported with lebrikizumab[598] in the treatment of severe asthma and associated exacerbation. A randomized, double-blind, placebo-controlled study of lebrikizumab in asthma patients with uncontrolled disease demonstrated that compared to the control population receiving placebo, patients on lebrikizumab (250 mg monthly for 6 months) had a higher increase in FEV<sub>1</sub> versus at baseline. In particular, greater improvement in lung function and larger reduction in FeNO levels of the patients with higher serum levels of periostin (periostin-high patients) before lebrikizumab treatment was observed compared to patients with low periostin (periostin-low patients)[709]. Another evidence with two randomized, multicentre, double-blind, placebo-controlled studies revealed that treatment with lebrikizumab reduced asthma exacerbations (significant 60% reduction) particularly in periostin-high patients, in contrast to, of periostin-low patients (5% reduction)[710].

Our study highlights anti-IL-13 as a potential and promising therapeutic intervention for the treatment of AAD and infection-induced exacerbations of AAD over corticosteroids treatment. Overall, our findings agree with various clinical studies that demonstrated an increased susceptibility of asthma patients to various viral infections including IAV[541, 556-559].

Further, we have also observed that infections in experimental asthma, including by IAV, increased the expression of miR-21, which we have identified as another potential driver of the pathogenesis of severe asthma. Inhibition of miR-21 or its downstream signalling molecule PI3K potently reduced the severity of experimental asthma. Lee *et al.*, showed that miR-21 is up-regulated during allergic airway inflammation, reflecting a Th2 immune response. miR-21 antagomir treatment reduced the levels of Th2 cytokines, including IL-4, IL-5, and IL-13 thereby showing an association between IL-13 and miR-21 in allergic

inflammation[365]. Moreover our study demonstrated that treatment with the PI3K inhibitor LY294002 (LY29) induced a significant reduction in viral titre, tissue inflammation, number of MSCs and tissue eosinophils in infected mice with AAD compared to infected non-allergic controls. Our results were consistent with the investigation done by Huang and colleagues where they demonstrated that LY29 attenuated AHR, airway inflammation and remodelling (lung tissue eosinophilia, mucus production, collagen deposition, smooth muscle hypertrophy and angiogenesis) in murine model of asthma. However, they observed PI3K as a major downstream messenger for IL-25 mediated signalling while we observed the same for IL-13-mediated mechanism driving the pathogenesis of asthma[615]. Our data also emphasise the potential of PI3K inhibitors as novel therapeutic interventions to manage increased susceptibility of AAD patients to IAV infection. Figure 5.1 represents our consolidated findings observed with IAV infection in experimental asthma.

## **5.2. IAV INFECTION IN EXPERIMENTAL COPD**

Our mouse models of COPD are induced by the chronic inhalation of CS and recapitulate the hallmark features of the human disease. The features in our model induced by nose-only exposure develop in eight weeks compared to 4-6 months that is typically required. Our model represents exposure in a pack a day smoker[711], and the same gene signatures occur as those observed in human emphysema[712]. Our group has recently published that mice with experimental COPD are more susceptible to IAV infection with increased viral titres and impaired anti-viral responses[371]. In turn the exaggerated infection exacerbated the chronic disease with increased airway inflammation and impaired lung function. This model was subsequently used to demonstrate that an increase in the levels of PI3K protein is involved in increased susceptibility to infection. Similar observations were reported by Hsu and colleagues in human cultured primary bronchial epithelial cells (pBECs) from COPD patients infected with seasonal influenza (H1N1)[371]. To further explore the mechanisms of increased susceptibility to IAV infection in COPD, we investigated and identified various critical factors.

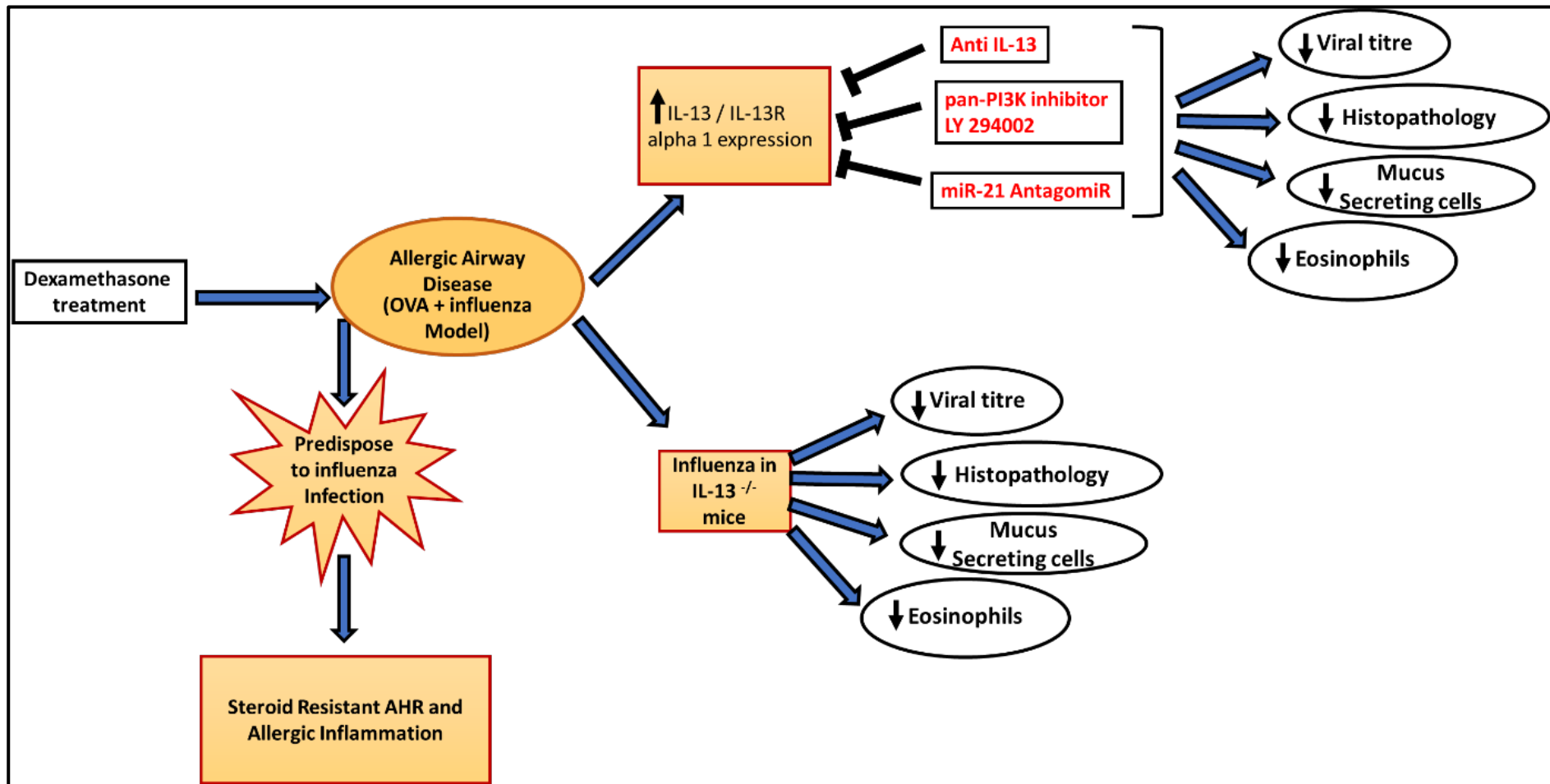


Figure 5.1. Roles of IL-13, IL-13R $\alpha$ 1 and miR-21 in increased susceptibility to IAV infection in AAD.

AAD was induced in mice by sensitisation and challenge with Ova. On the last day of Ova challenge, some mice were infected with 7.5 plaque forming unit (PFU) of the mouse-adapted IAV H1N1 A/PR/8/34. We observed an association between increased levels of IL-13/IL-13R $\alpha$ 1 and miR-21 (via increased PI3K activity). This in turn led to increased viral load, worsening of disease features and exacerbation of the underlying chronic lung disease. Inhibition of augmented IL-13, miR-21 and PI3K using monoclonal anti-IL-13 antibody, Ant-21 and PI3K inhibitor (LY294002), respectively, reduced viral load, and improved disease features and exacerbation of the underlying chronic lung disease. This highlights their potential to be used as novel therapeutic interventions. We demonstrated the effectiveness of all the three therapeutic biological/chemical moieties in managing increased susceptibility of AAD patients to influenza infection.

IL-13 is generally not associated with COPD but in our study, we showed using IHC that IAV infection in experimental COPD increased the expression of IL-13R $\alpha$ 1. IL-13R $\alpha$ 1 expression was significantly increased in the airway epithelium of non-infected smoke-exposed mice compared to non-infected normal air-exposed mice. Both infected normal air-exposed mice and infected smoke-exposed mice had further increases in IL-13R $\alpha$ 1 levels in the airway epithelium, which is a novel finding in itself. To date there have been few investigations of the association between IL-13 and COPD. Also, we demonstrated an increased expression of miR-21 in response to IAV infection in COPD using ISH.

Xie and colleagues demonstrated that the upregulation of miR-21 in peripheral blood serum and mononuclear cells of COPD patients may contribute to the pathogenesis and increased severity of COPD[369]. They also suggested that levels of serum miR-21 may be a valuable marker for evaluating the development of COPD in heavy smokers[370], although this miR-21 is unlikely to be used solely as biomarker because numerous diseases have increased miR-21, not only smoking and COPD. We also observed a significant increase in the numbers of MSCs in infected smoke-exposed mice compared to non-infected smoke-exposed mice. This is in agreement with a study by Alevy and colleagues where IL-13 was demonstrated to drive mucus production in human airway epithelial cells probably via signalling from chloride channel calcium-activated 1 (CLCA1) to MAPK13[622].

To further assess the therapeutic potential of targeting IL-13 using anti-IL-13 specific monoclonal antibody, we again used our experimental smoking model. We observed that anti-IL-13 treatment significantly reduced tissue inflammation, numbers of MSCs and miR-21 expression in infected smoke-exposed mice compared to isotype-treated infected smoke-exposed mice. A recently published review highlighted the potential of monoclonal antibodies against IL-13 (lebrikizumab, tralokinumab) in the treatment of COPD[623]. However, ours is the first laboratory-based work that demonstrates the therapeutic potential of

anti-IL-13 to manage the increased susceptibility of COPD patients to IAV infection.

miR-21 is postulated to play a pathogenic role in various chronic respiratory diseases particularly, asthma more so than COPD[713]. So far various reports have defined the associations of miR-21 with COPD[369, 370], but our data defined the links between miR-21 and increased susceptibility to IAV infection in COPD. To further understand and assess the clinical potential of targeting miR-21 in COPD patients who are highly susceptible to IAV infection, we used Ant-21. Ant-21 treatment reduced viral titres in infected normal air-exposed mice compared to Scr-treated infected normal air-exposed mice. Also, Ant-21-treated infected smoke-exposed mice had significantly reduced viral titre and numbers of MSCs (back to base line) compared to isotype-treated infected smoke-exposed mice. Figure 5.2 summarises our important observations that show the mechanisms of increased susceptibility to IAV infection in COPD.

We also identified a novel signalling pathway that is mediated by miR-125a and b that regulates susceptibility to IAV infection in experimental COPD. We demonstrated that miR-125a/b reduce the expression of A20 (a negative regulator of NF- $\kappa$ B activation) and mitochondrial antiviral signalling (MAVS) and subsequently worsens inflammation and increases susceptibility to IAV infection in COPD. We observed that IAV infections lead to increased inflammatory and reduced antiviral responses in pBECs from healthy non-smoking and smoking subjects. However, infection resulted in exaggerated inflammatory and impaired antiviral response in pBECs from COPD patients. We again observed increased expression of miR-125a/b, reduced expression of both A20 and MAVS and exaggerated inflammatory responses and impaired antiviral immunity to IAV infection in experimental COPD. These observations were replicated in *in vivo* mouse model of experimental COPD. Inhibition of miR-125a and b reduced the induction of inflammatory cytokines and enhanced antiviral responses to IAV infection in both healthy and COPD states. This study therefore identified a novel potential therapeutic target to suppress IAV infection in general and in COPD.

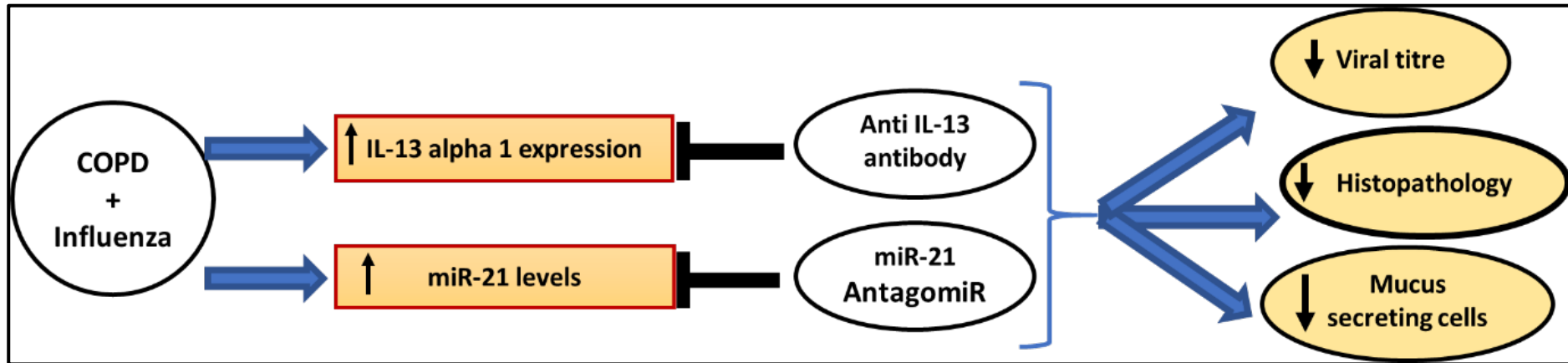


**Figure 5.2. Roles of IL-13R $\alpha$ 1 and miR-21 in increased susceptibility to IAV infection in COPD.**

COPD was induced in mice by nose-only exposure to CS for eight weeks. On the last day of smoke-exposure, some mice were infected with 7.5 plaque forming unit (PFU) of the mouse-adapted IAV H1N1 A/PR/8/34. We observed increased levels of IL-13R $\alpha$ 1 and miR-21 that were associated with increased viral load, worsening disease features and exacerbation of the underlying chronic lung disease. Inhibition of IL-13 and miR-21 levels using monoclonal anti-IL-13 antibody and Ant-21, respectively, reduced the viral load and improved the associated disease features and exacerbation of the underlying chronic lung disease. Thus, we identified the potential effectiveness of anti-IL-13 antibody and Ant-21 as potential therapeutic interventions to target increased susceptibility to IAV infection in COPD.

Thus, miR-125a/b and A20 and may be targeted therapeutically to inhibit excessive inflammatory responses and enhance antiviral immunity in IAV infections, particularly in COPD (Figure 5.3).

Collectively, our studies provide new evidence for IL-13, miR-21, miR125a and b as promising targets of IAV infection management and therapy, particularly in patients with asthma and COPD. At the same time, our observations provide a platform for the expansion of ongoing studies in our laboratory. The results from our *in vivo* study are being used to translate into *ex-vivo* influenza studies on cells obtained from human donors by our clinical collaborators. Moreover, extensions of this study are planned to further investigate the molecular interactions between the identified biological targets including IL-13 and miR-21 and host immune responses. Further, translation of these findings in the clinical settings would also be valuable. Figure 5.4 represents the overall findings of this research.

### **5.3. FUTURE DIRECTIONS**

In these studies we have elucidated the mechanisms underlying increased susceptibility of IAV infection in AAD and COPD. Our studies uncovered findings that can act as a scaffold to expand our research.

#### **5.3.1. IAV infection in AAD**

Our studies identified a novel IL-13/IL-13R $\alpha$ 1R/miR-21-dependent signalling pathway that drives the pathogenesis/increased susceptibility to IAV infection in AAD. However, it still warrants further investigations to address the biological complexity at molecular and cellular levels. All our mechanistic studies were performed using the Ova-induced AAD model. It would also be valuable to further confirm and validate the findings of this study in other established AAD models such as with HDM-induced AAD to validate our observations in different settings.

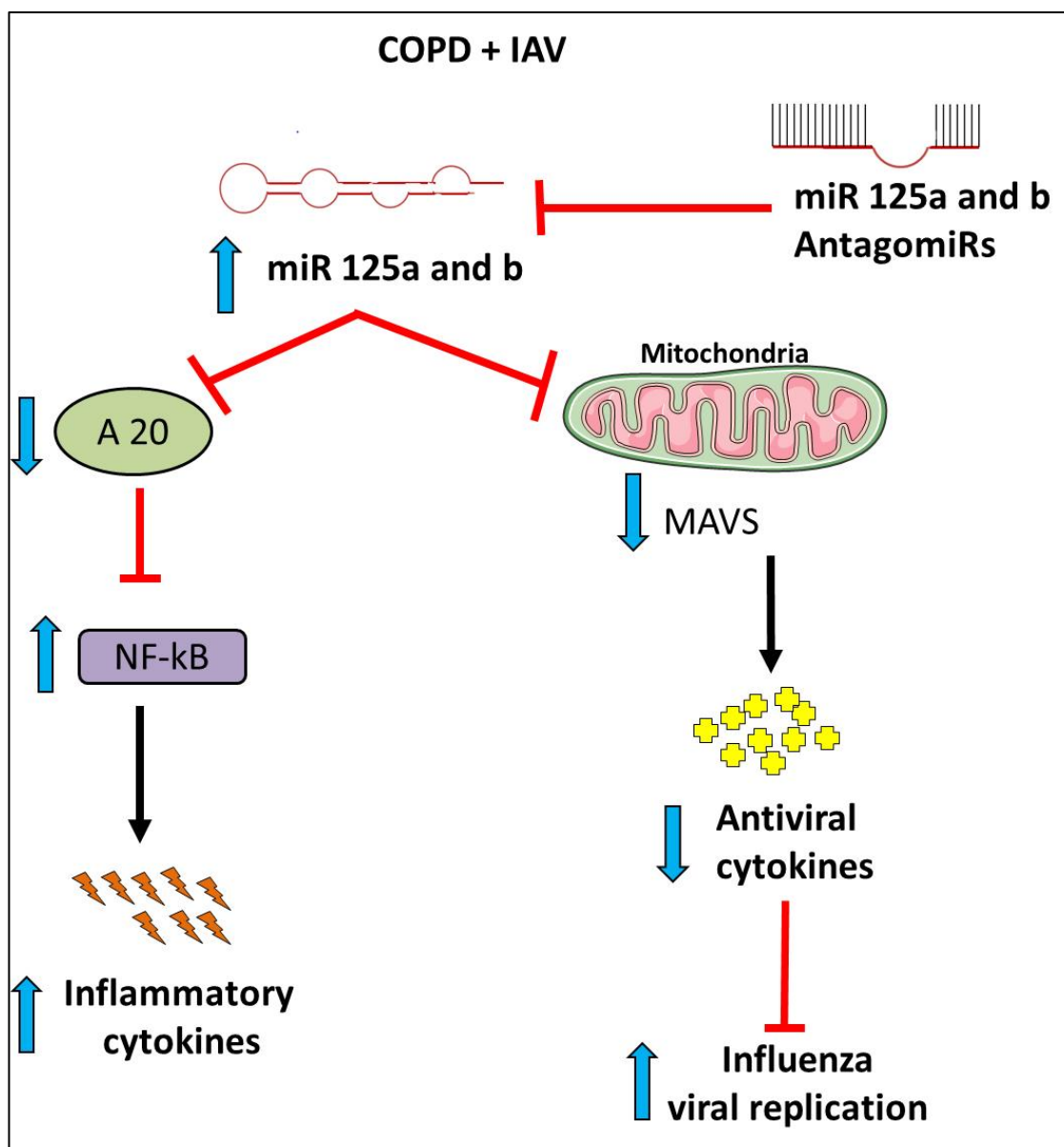


**Figure 5.3. Roles of miR-125a and b in the regulation of inflammatory and antiviral responses in IAV infection.**

IAV infection in experimental COPD demonstrated increased levels of miR-125a and b, subsequently, reducing the protein expression of A20 resulting in uncontrolled NF- $\kappa$ B activation and thus exaggerated induction of pro-inflammatory cytokines. miR-125a and b also targets and reduces MAVS and antiviral type I and III IFN production. Inhibition of miR-125a and b enhances MAVS and antiviral responses and suppresses viral infection[714].

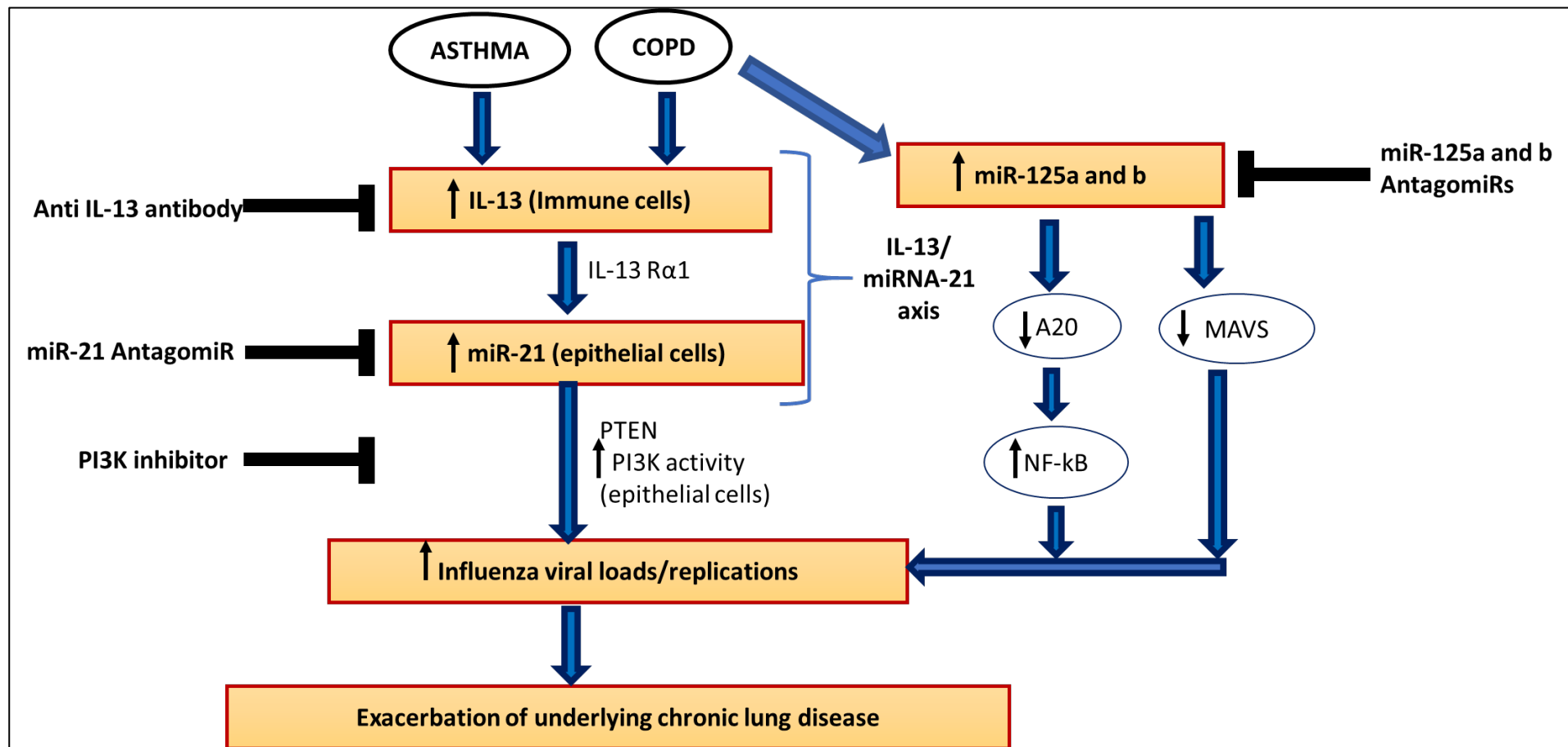


Figure 5.4. Roles of IL-13, IL-13R $\alpha$ 1 and miR-21, miR-125 and b in increased susceptibility to IAV infection in AAD and COPD.

AAD and experimental COPD were induced using Ova sensitisation and challenge or chronic CS exposure. On the last day of Ova challenge or smoke exposure, some mice were infected with 7.5 plaque forming unit (PFU) of the mouse-adapted IAV H1N1 A/PR/8/34. We observed increased levels of IL-13/IL-13R $\alpha$ 1, miR-21 (via increased PI3K activity) that were associated with increases in viral load, worsening of disease features and exacerbation of the underlying respective chronic lung disease. Also, increased levels of miR-125a and b in COPD, reduced the protein expression of A20 that consequently induced uncontrolled NF- $\kappa$ B activation leading to the exaggerated induction of pro-inflammatory cytokines. miR-125a and b also targeted and reduced levels of MAVS and the production of antiviral type I and III IFNs. Inhibition of miR-125a and b enhanced MAVS and antiviral responses and suppressed viral infection and replication probably by reducing inflammatory cytokines. Inhibition of augmented IL-13, miR-21, PI3K, miR-125a and b using monoclonal anti-IL-13 antibody, Ant-21, PI3K inhibitor (LY294002), Ant-125a and b, respectively, reduced the viral load, and improved associated disease features and exacerbation of the underlying chronic lung disease. We assessed and demonstrated the effectiveness and therapeutic potential of targeting these various biological/regulatory signalling molecules identified in our study to manage increased susceptibility to IAV infection in AAD and COPD.

We also performed a study that demonstrated ongoing remodelling in response to an allergen rechallenge in infected mice with AAD. This remodelling was characterised by excessive mucus and collagen production together with dexamethasone insensitivity.

These observations are in agreement with previously published literature that report the poor control of asthma symptoms in patients with severe asthma prescribed long acting inhaled  $\beta_2$  agonists and high dose corticosteroids[399, 400, 492-495]. Further in depth investigations are required to elucidate the detailed mechanisms and kinetics involved in the dexamethasone resistance and remodelling events. Epithelial-mesenchymal transition (EMT) has been proposed to be one of the potential mechanisms contributing to the airway remodelling[715, 716]. We have recently shown that EMT occurs in our model of COPD (unpublished data). Our mechanistic studies lack an extensive investigation involving various antiviral responses and their direct or indirect interactions with various regulatory targets identified in the present study. For instance, it would be worth investigating interactions between various IFNs and increased IL-13 levels in AAD and how they regulate susceptibility of AAD patients to IAV infection. This would open avenues to understand the mechanisms contributing to the impairment of IFNs responses during the IAV infection in AAD. It has been reported that miR-21 regulates the expression of PI3K by associating with PTEN[586, 717, 718], which subsequently negatively regulates Akt signalling[719]. Our laboratory has demonstrated that the negative regulation of PI3K/Akt signalling can significantly improve the infection outcomes of IAV infection in COPD[143]. This mechanistic understanding could be extended on in our AAD models where we have shown roles for increased miR-21 expression in promoting susceptibility to IAV infection in COPD. This may provide alternative targets for managing this disease. Also, proteomics approaches could be pursued to assess the targets of miR-21 in these situations, and to further validate our observations obtained at transcription level. As we demonstrated increases in the levels of IL-33 in sham-inoculated and infected mice with AAD together with increased fibronectin and collagen it

would be valuable to pursue the effects dexamethasone and miR-21 antagomirs on IL-33 levels in the AAD animal models.

As many viral-induced exacerbations of asthma occur in children[539, 720-722], our study identifies therapeutic approaches that could be beneficial in the paediatric population. We can investigate this by extending our study from adult mice to also include neonatal and infant AAD mouse models. This would also examine whether there are different mechanisms of susceptibility at different stages of life.

### **5.3.2. IAV infection in COPD**

Our findings suggest that elevated miR-21 expression in COPD, may contribute to the impairment of host antiviral responses. Therefore, further studies need to be performed that investigate various host antiviral responses and their interactions with elevated miRs identified in our studies. This may help in defining the possible epigenetic alterations in miR-21 or IFN pathways. Novel findings from our studies may further expand our understanding of how underlying COPD increases susceptibility to IAV infection. Also, it would be interesting to assess IL-33 as a potential target in COPD and investigate the effect of dexamethasone, miR-21 and miR-125a and b antagomirs on IL-33 levels in the COPD animal models.

All these studies will further strengthen our *in vivo* work and highlight the importance of IL-13, IL-13R $\alpha$ 1, miR-21, 125a and b as potential therapeutic targets.

While we show promising findings experimentally, we have yet to explore some of these in human tissues. This will be the next critical step to take these promising findings to and translating them to human disease.

## **5.4. CONCLUSIONS**

Our studies have furthered the understanding of the effects of IAV infection in chronic lung diseases (AAD and COPD). Our HDM model of virus-induced

asthma exacerbation has translational value as it replicates aspects of HDM-induced exacerbations of asthma in humans. Also, using experimental *in-vivo* mouse models, we have identified various specific factors such as miRs and IL-13 that are involved in increasing the susceptibility to IAV infection and exacerbation of the respective underlying chronic respiratory disease. This is the first study that defines functional relevance of IAV infection-induced activation and maintenance of a novel IL-13/IL-13R $\alpha$ 1/miR-21 and IL-13R $\alpha$ 1/miR-21 axis in AAD and COPD, respectively. However, to understand whether IAV, OVA and smoke exposure induce miR-21 expression independently of IL-13/IL-13R $\alpha$ 1, it would require further investigations using transgenic and knock-out mice. All these factors (IL-13, miR-21, miR-125a and b) promote increases in viral titre and inflammation in the respective diseases. Inhibition of these factors subsequently suppressed IAV infection and disease pathology and exacerbation. These approaches possess the potential of being novel and effective therapeutic interventions to manage chronic respiratory diseases. These outcomes of our study suggest an association between IAV infection and airway inflammation that might be one of the mechanisms driving susceptibility of IAV infection in asthma and COPD.

# BIBLIOGRAPHY

1. Lemanske, R.F. and W.W. Busse, 6. *Asthma*. Journal of allergy and clinical immunology, 2003. **111**(2): p. S502-S519.
2. Boulet, L.P., et al., *The allergen bronchoprovocation model: an important tool for the investigation of new asthma anti-inflammatory therapies*. Allergy, 2007. **62**(10): p. 1101-1110.
3. Masoli, M., et al., *The global burden of asthma: executive summary of the GINA Dissemination Committee report*. Allergy, 2004. **59**(5): p. 469-478.
4. Akinbami, O.J., J.E. Moorman, and X. Liu, *Asthma prevalence, health care use, and mortality: United States, 2005-2009*. 2011: US Department of Health and Human Services, Centers for Disease Control and Prevention, National Center for Health Statistics Washington, DC.
5. Chapman, K., et al., *Suboptimal asthma control: prevalence, detection and consequences in general practice*. European Respiratory Journal, 2008. **31**(2): p. 320-325.
6. Jaakkola, M.S., A. Ieromnimon, and J.J. Jaakkola, *Are atopy and specific IgE to mites and molds important for adult asthma?* Journal of allergy and clinical immunology, 2006. **117**(3): p. 642-648.
7. Jian, Y.R., et al., *Inactivated influenza virus vaccine is efficient and reduces IL-4 and IL-6 in allergic asthma mice*. Influenza and other respiratory viruses, 2013. **7**(6): p. 1210-1217.
8. Health, N.I.o., *Global Initiative for Asthma. Global strategy for asthma management and prevention*. NHLBI/WHO work shop report, 1995.
9. STATISTICS, A.B.O., *National Health Survey*. Two thirds of Australian women aged, 2005. **18**.
10. AIHW. *Asthma, chronic obstructive pulmonary disease and other respiratory diseases in Australia*. Asthma 2010.
11. Smith, D.H., et al., *A national estimate of the economic costs of asthma*. American journal of respiratory and critical care medicine, 1997. **156**(3): p. 787-793.
12. Control, C.f.D. and Prevention, *Asthma in the US: CDC Vital Signs, May 2011*.
13. Woolcock, A.J., et al., *The burden of asthma in Australia*. The Medical Journal of Australia, 2001. **175**(3): p. 141-145.
14. Strachan, D.P., *Family size, infection and atopy: the first decade of the 'hygiene hypothesis'*. Thorax, 2000. **55**(Suppl 1): p. S2.
15. Strachan, D.P., *Hay fever, hygiene, and household size*. BMJ: British Medical Journal, 1989. **299**(6710): p. 1259.
16. Simpson, J.L., et al., *Inflammatory subtypes in asthma: assessment and identification using induced sputum*. Respirology, 2006. **11**(1): p. 54-61.
17. Shin, B., et al., *The transition of sputum inflammatory cell profiles is variable in stable asthma patients*. Asia Pacific Allergy, 2017. **7**(1): p. 19.

18. Mattes, J. and W. Karmaus, *The use of antibiotics in the first year of life and development of asthma: which comes first?* Clinical and experimental allergy: journal of the British Society for Allergy and Clinical Immunology, 1999. **29**(6): p. 729-732.
19. Xiao, C., et al., *Defective epithelial barrier function in asthma.* Journal of Allergy and Clinical Immunology, 2011. **128**(3): p. 549-556. e12.
20. Holgate, S.T., *The sentinel role of the airway epithelium in asthma pathogenesis.* Immunological reviews, 2011. **242**(1): p. 205-219.
21. Wills-Karp, M., J. Santeliz, and C.L. Karp, *The germless theory of allergic disease: revisiting the hygiene hypothesis.* Nature Reviews Immunology, 2001. **1**(1): p. 69-75.
22. Ten Hacken, N.H., D.S. Postma, and W. Timens, *Airway remodeling and long-term decline in lung function in asthma.* Current opinion in pulmonary medicine, 2003. **9**(1): p. 9-14.
23. Tan, W.C., et al., *Epidemiology of respiratory viruses in patients hospitalized with near-fatal asthma, acute exacerbations of asthma, or chronic obstructive pulmonary disease.* The American journal of medicine, 2003. **115**(4): p. 272-277.
24. Cohn, L., J.A. Elias, and G.L. Chupp, *Asthma: mechanisms of disease persistence and progression.* Annu. Rev. Immunol., 2004. **22**: p. 789-815.
25. Maddox, L. and D.A. Schwartz, *The pathophysiology of asthma.* Annual review of medicine, 2002. **53**(1): p. 477-498.
26. Agrawal, D.K. and Z. Shao, *Pathogenesis of allergic airway inflammation.* Current allergy and asthma reports, 2010. **10**(1): p. 39-48.
27. Van Eerdewegh, P., et al., *Association of the ADAM33 gene with asthma and bronchial hyperresponsiveness.* Nature, 2002. **418**(6896): p. 426-430.
28. Laitinen, T., et al., *Characterization of a common susceptibility locus for asthma-related traits.* Science, 2004. **304**(5668): p. 300-304.
29. Marks, G.B., *Environmental factors and gene–environment interactions in the aetiology of asthma.* Clinical and experimental pharmacology and physiology, 2006. **33**(3): p. 285-289.
30. Hansbro, P.M., G.E. Kaiko, and P.S. Foster, *Cytokine/anti-cytokine therapy—novel treatments for asthma?* British journal of pharmacology, 2011. **163**(1): p. 81-95.
31. Kaiko, G.E., et al., *Immunological decision-making: how does the immune system decide to mount a helper T-cell response?* Immunology, 2008. **123**(3): p. 326-338.
32. Fahy, J.V., *Eosinophilic and neutrophilic inflammation in asthma: insights from clinical studies.* Proceedings of the American Thoracic Society, 2009. **6**(3): p. 256-259.

33. Lloyd, C.M. and E.M. Hessel, *Functions of T cells in asthma: more than just TH2 cells*. Nature Reviews Immunology, 2010. **10**(12): p. 838-848.
34. Ohshima, Y., et al., *Dysregulation of IL-13 production by cord blood CD4+ T cells is associated with the subsequent development of atopic disease in infants*. Pediatric research, 2002. **51**(2): p. 195-200.
35. Mitchell, P.D. and P.M. O'byrne, *Epithelial-derived cytokines in asthma*. Chest, 2017. **151**(6): p. 1338-1344.
36. *Global Initiative for Chronic Obstructive Lung Disease strategy for the diagnosis, management and prevention of chronic obstructive pulmonary disease: an Asia-Pacific perspective*. Respiriology, 2005. **10**(1): p. 9-17.
37. MacNee, W., *Pathophysiology of cor pulmonale in chronic obstructive pulmonary disease. Part One*. American journal of respiratory and critical care medicine, 1994. **150**(3): p. 833-852.
38. Thompson, A.B., et al., *Aerosolized beclomethasone in chronic bronchitis: improved pulmonary function and diminished airway inflammation*. American Review of Respiratory Disease, 1992. **146**(2): p. 389-395.
39. Lambrecht, B.N., et al., *Dendritic cells are required for the development of chronic eosinophilic airway inflammation in response to inhaled antigen in sensitized mice*. The Journal of Immunology, 1998. **160**(8): p. 4090-4097.
40. van Rijt, L.S., et al., *In vivo depletion of lung CD11c+ dendritic cells during allergen challenge abrogates the characteristic features of asthma*. Journal of Experimental Medicine, 2005. **201**(6): p. 981-991.
41. van Rijt, L.S., et al., *Respiratory viral infections and asthma pathogenesis: a critical role for dendritic cells?* Journal of Clinical Virology, 2005. **34**(3): p. 161-169.
42. Hansbro, P.M., et al., *Th2 cytokine antagonists: potential treatments for severe asthma*. Expert opinion on investigational drugs, 2013. **22**(1): p. 49-69.
43. Monticelli, L.A., et al., *Innate lymphoid cells promote lung-tissue homeostasis after infection with influenza virus*. Nature immunology, 2011. **12**(11): p. 1045-1054.
44. Mjösberg, J.M., et al., *Human IL-25-and IL-33-responsive type 2 innate lymphoid cells are defined by expression of CCR4 and CD161*. Nature immunology, 2011. **12**(11): p. 1055-1062.
45. van der Pouw Kraan, T.v., et al., *An IL-13 promoter polymorphism associated with increased risk of allergic asthma*. Genes and immunity, 1999. **1**(1): p. 61-65.
46. Graves, P.E., et al., *A cluster of seven tightly linked polymorphisms in the IL-13 gene is associated with total serum IgE levels in three populations of white children*. Journal of Allergy and Clinical Immunology, 2000. **105**(3): p. 506-513.

47. Balzano, G., et al., *Eosinophilic inflammation in stable chronic obstructive pulmonary disease: relationship with neutrophils and airway function*. American journal of respiratory and critical care medicine, 1999. **160**(5): p. 1486-1492.
48. O'byrne, P. and D. Postma, *The many faces of airway inflammation: asthma and chronic obstructive pulmonary disease*. American journal of respiratory and critical care medicine, 1999. **159**(supplement\_2): p. S1-S63.
49. Sluiter, H., et al., *The Dutch hypothesis (chronic non-specific lung disease) revisited*. European Respiratory Journal, 1991. **4**(4): p. 479-489.
50. Kaplan, M.H., et al., *Stat6 is required for mediating responses to IL-4 and for the development of Th2 cells*. Immunity, 1996. **4**(3): p. 313-319.
51. Baumann, R., et al., *The release of IL-31 and IL-13 after nasal allergen challenge and their relation to nasal symptoms*. Clinical and translational allergy, 2012. **2**(1): p. 13.
52. Huang, S.-K., et al., *IL-13 expression at the sites of allergen challenge in patients with asthma*. The Journal of Immunology, 1995. **155**(5): p. 2688-2694.
53. Kroegel, C., et al., *Endobronchial secretion of interleukin-13 following local allergen challenge in atopic asthma: relationship to interleukin-4 and eosinophil counts*. European Respiratory Journal, 1996. **9**(5): p. 899-904.
54. Konstantinidis, A., et al., *Genetic association studies of interleukin-13 receptor  $\alpha 1$  subunit gene polymorphisms in asthma and atopy*. European Respiratory Journal, 2007. **30**(1): p. 40-47.
55. Miloux, B., et al., *Cloning of the human IL-13R $\alpha 1$  chain and reconstitution with the IL-4R $\alpha$  of a functional IL-4/IL-13 receptor complex*. FEBS letters, 1997. **401**(2-3): p. 163-166.
56. Takeda, K., et al., *Impaired IL-13-mediated functions of macrophages in STAT6-deficient mice*. The Journal of Immunology, 1996. **157**(8): p. 3220-3222.
57. Donaldson, D.D., et al., *The murine IL-13 receptor  $\alpha 2$ : molecular cloning, characterization, and comparison with murine IL-13 receptor  $\alpha 1$* . The Journal of Immunology, 1998. **161**(5): p. 2317-2324.
58. Tabata, Y. and G.K.K. Hershey, *IL-13 receptor isoforms: breaking through the complexity*. Current allergy and asthma reports, 2007. **7**(5): p. 338-345.
59. Chen, W., et al., *IL-13 receptor  $\alpha 2$  contributes to development of experimental allergic asthma*. Journal of Allergy and Clinical Immunology, 2013. **132**(4): p. 951-958. e6.
60. Boulet, L.-P. and E. Franssen, *Influence of obesity on response to fluticasone with or without salmeterol in moderate asthma*. Respiratory medicine, 2007. **101**(11): p. 2240-2247.

61. Starkey, M., et al., *Constitutive production of IL-13 promotes early-life Chlamydia respiratory infection and allergic airway disease*. *Mucosal immunology*, 2013. **6**(3): p. 569.
62. Hilton, D.J., et al., *Cloning and characterization of a binding subunit of the interleukin 13 receptor that is also a component of the interleukin 4 receptor*. *Proceedings of the National Academy of Sciences*, 1996. **93**(1): p. 497-501.
63. Aman, M.J., et al., *cDNA cloning and characterization of the human interleukin 13 receptor  $\alpha$  chain*. *Journal of Biological Chemistry*, 1996. **271**(46): p. 29265-29270.
64. Caput, D., et al., *Cloning and characterization of a specific interleukin (IL)-13 binding protein structurally related to the IL-5 receptor  $\alpha$  chain*. *Journal of Biological Chemistry*, 1996. **271**(28): p. 16921-16926.
65. Zhang, J.-G., et al., *Identification, Purification, and Characterization of a Soluble Interleukin (IL)-13-binding Protein EVIDENCE THAT IT IS DISTINCT FROM THE CLONED IL-13 RECEPTOR AND IL-4 RECEPTOR  $\alpha$ -CHAINS*. *Journal of Biological Chemistry*, 1997. **272**(14): p. 9474-9480.
66. Wills-Karp, M., et al., *Interleukin-13: central mediator of allergic asthma*. *science*, 1998. **282**(5397): p. 2258-2261.
67. Munitz, A., et al., *Distinct roles for IL-13 and IL-4 via IL-13 receptor  $\alpha 1$  and the type II IL-4 receptor in asthma pathogenesis*. *Proceedings of the National Academy of Sciences*, 2008. **105**(20): p. 7240-7245.
68. Myrtek, D., et al., *Expression of interleukin-13 receptor  $\alpha 1$ -subunit on peripheral blood eosinophils is regulated by cytokines*. *Immunology*, 2004. **112**(4): p. 597-604.
69. Rothenberg, M.E., et al., *IL-13 receptor  $\alpha 1$  differentially regulates aeroallergen-induced lung responses*. *The Journal of Immunology*, 2011. **187**(9): p. 4873-4880.
70. Karo-Atar, D., et al., *A protective role for IL-13 receptor  $\alpha 1$  in bleomycin-induced pulmonary injury and repair*. *Mucosal immunology*, 2016. **9**(1): p. 240.
71. Ramalingam, T.R., et al., *Unique functions of the type II interleukin 4 receptor revealed in mice lacking the interleukin 13 receptor  $\alpha 1$  chain*. *The FASEB Journal*, 2008. **22**(1 Supplement): p. 674.9-674.9.
72. Newcomb, D.C., et al., *Human T H 17 cells express a functional IL-13 receptor and IL-13 attenuates IL-17A production*. *Journal of Allergy and Clinical Immunology*, 2011. **127**(4): p. 1006-1013. e4.
73. Sinha, S., et al., *Association of IL13R alpha 1+ 1398A/G polymorphism in a North Indian population with asthma: A case-control study*. *Allergy & Rhinology*, 2015. **6**(2): p. e111.
74. Global Strategy for the Diagnosis, M.a.P.o.C., *Global Initiative for Chronic Obstructive Lung Disease (GOLD)*. *News & events from around the world*. 2015.

75. Lozano, R., et al., *Global and regional mortality from 235 causes of death for 20 age groups in 1990 and 2010: a systematic analysis for the Global Burden of Disease Study 2010*. The Lancet, 2013. **380**(9859): p. 2095-2128.
76. *Chronic Obstructive Pulmonary Disease (COPD)*. World Health Organisation. Available from: <http://www.who.int/mediacentre/factsheets/fs315/en/>. Date accessed: 3rd March 2016.
77. Welfare AloHa. *Chronic respiratory diseases in Australia: their prevalence, consequences and prevention*. Report no. AIHW Cat. No. PHE 63. Canberra: AIHW., 2005.
78. *How much is spent on COPD? (AIHW)*. Available from: <http://www.aihw.gov.au/copd/expenditure>. Date accessed: 3rd March 2016.
79. AIHW, *Australia's health 2012*. Australia's health no. 13. Cat. no. AUS 156. Canberra: AIHW, 2012.
80. Banks, E., et al., *Tobacco smoking and all-cause mortality in a large Australian cohort study: findings from a mature epidemic with current low smoking prevalence*. BMC Medicine, 2015. **13**(1): p. 1-10.
81. Buist, A.S., et al., *The Burden of Obstructive Lung Disease Initiative (BOLD): rationale and design*. Copd, 2005. **2**(2): p. 277-83.
82. Toelle, B.G., et al., *Respiratory symptoms and illness in older Australians: the Burden of Obstructive Lung Disease (BOLD) study*. Med J Aust, 2013. **198**(3): p. 144-8.
83. Buist, A.S., et al., *International variation in the prevalence of COPD (the BOLD Study): a population-based prevalence study*. Lancet, 2007. **370**(9589): p. 741-50.
84. Mannino, D.M., *Chronic obstructive pulmonary disease: definition and epidemiology*. Respiratory care, 2003. **48**(12): p. 1185-1193.
85. Lebowitz, M.D., R. Knudson, and B. Burrows, *Family Aggregation of Pulmonary Function Measurements 1–3*. American Review of Respiratory Disease, 1984. **129**(1): p. 8-11.
86. Lomas, D.A. and E.K. Silverman, *The genetics of chronic obstructive pulmonary disease*. Respiratory research, 2001. **2**(1): p. 20.
87. Rycroft, C.E., et al., *Epidemiology of chronic obstructive pulmonary disease: a literature review*. Int J Chron Obstruct Pulmon Dis, 2012. **7**: p. 457-94.
88. WHO, *The top 10 causes of death*. 2014.
89. Vos, T., et al., *Years lived with disability (YLDs) for 1160 sequelae of 289 diseases and injuries 1990-2010: a systematic analysis for the Global Burden of Disease Study 2010*. Lancet, 2012. **380**(9859): p. 2163-96.
90. *Global, regional, and national age-sex specific all-cause and cause-specific mortality for 240 causes of death, 1990-2013: a systematic*

- analysis for the Global Burden of Disease Study 2013*. Lancet, 2015. **385**(9963): p. 117-71.
91. Lomborg, B., *Global problems, local solutions : costs and benefits*. 2013.
  92. Bloom, D., *The Global Economic Burden of Noncommunicable Diseases*. World Economic Forum, 2011: p. p.24.
  93. GOLD., *Global strategy for the diagnosis, management, and prevention of chronic obstructive pulmonary disease 2016*. Available from: <http://www.goldcopd.org/>.
  94. Mapel, D.W., et al., *Application of the new GOLD COPD staging system to a US primary care cohort, with comparison to physician and patient impressions of severity*. Int J Chron Obstruct Pulmon Dis, 2015. **10**: p. 1477-86.
  95. MacNee, W., *Pathophysiology of cor pulmonale in chronic obstructive pulmonary disease. Part two*. American journal of respiratory and critical care medicine, 1994. **150**(4): p. 1158-1168.
  96. Fujita, J., et al., *Evaluation of elastase and antielastase balance in patients with chronic bronchitis and pulmonary emphysema*. Am Rev Respir Dis, 1990. **142**(1): p. 57-62.
  97. Shapiro, S.D., et al., *Neutrophil elastase contributes to cigarette smoke-induced emphysema in mice*. The American journal of pathology, 2003. **163**(6): p. 2329-2335.
  98. Hubbard, R., et al., *Oxidants spontaneously released by alveolar macrophages of cigarette smokers can inactivate the active site of alpha 1-antitrypsin, rendering it ineffective as an inhibitor of neutrophil elastase*. Journal of Clinical Investigation, 1987. **80**(5): p. 1289.
  99. Gadek, J.E., G.A. Fells, and R.G. Crystal, *Cigarette smoking induces functional antiprotease deficiency in the lower respiratory tract of humans*. Science, 1979. **206**(4424): p. 1315-1316.
  100. Barnes, P.J., *Cellular and molecular mechanisms of chronic obstructive pulmonary disease*. Clin Chest Med, 2014. **35**(1): p. 71-86.
  101. Shao, M.X., T. Nakanaga, and J.A. Nadel, *Cigarette smoke induces MUC5AC mucin overproduction via tumor necrosis factor- $\alpha$ -converting enzyme in human airway epithelial (NCI-H292) cells*. American Journal of Physiology-Lung Cellular and Molecular Physiology, 2004. **287**(2): p. L420-L427.
  102. Toossi, Z., et al., *Decreased production of TGF-beta 1 by human alveolar macrophages compared with blood monocytes*. The Journal of Immunology, 1996. **156**(9): p. 3461-3468.
  103. Burgel, P. and J. Nadel, *Roles of epidermal growth factor receptor activation in epithelial cell repair and mucin production in airway epithelium*. Thorax, 2004. **59**(11): p. 992-996.
  104. DE CREMOUX, H. and J. BIGNON, *Ciliary abnormalities in bronchial epithelium of smokers, ex-smokers, and nonsmokers*. Am J Respir Crit Care Med, 1995. **151**: p. 630-634.

105. Lee, H.-M., et al., *Agarose plug instillation causes goblet cell metaplasia by activating EGF receptors in rat airways*. American Journal of Physiology-Lung Cellular and Molecular Physiology, 2000. **278**(1): p. L185-L192.
106. Bialas, A.J., et al., *The Role of Mitochondria and Oxidative/Antioxidative Imbalance in Pathobiology of Chronic Obstructive Pulmonary Disease*. Oxid Med Cell Longev, 2016. **2016**: p. 7808576.
107. Hanta, I., et al., *Oxidant-antioxidant balance in patients with COPD*. Lung, 2006. **184**(2): p. 51-5.
108. Kanaji, N., et al., *Fibroblasts that resist cigarette smoke-induced senescence acquire profibrotic phenotypes*. American Journal of Physiology-Lung Cellular and Molecular Physiology, 2014. **307**(5): p. L364-L373.
109. Perng, D.-W., K.-C. Su, and L.-Y. Liu, *Airway Inflammation and Airflow Limitation in COPD*. Current Respiratory Medicine Reviews, 2006. **2**(4): p. 419-426.
110. Sarir, H., et al., *Cells, mediators and Toll-like receptors in COPD*. European journal of pharmacology, 2008. **585**(2): p. 346-353.
111. Pettersen, C.A. and K.B. Adler, *Airways inflammation and COPD: epithelial-neutrophil interactions*. CHEST Journal, 2002. **121**(5\_suppl): p. 142S-150S.
112. Barnes, P.J., *New concepts in chronic obstructive pulmonary disease*. Annual review of medicine, 2003. **54**(1): p. 113-129.
113. Barnes, P.J., *Immunology of asthma and chronic obstructive pulmonary disease*. Nature Reviews Immunology, 2008. **8**(3): p. 183-192.
114. Pouwels, S., et al., *DAMPs activating innate and adaptive immune responses in COPD*. Mucosal immunology, 2014. **7**(2): p. 215-226.
115. Pillai, S.G., et al., *A genome-wide association study in chronic obstructive pulmonary disease (COPD): identification of two major susceptibility loci*. PLoS Genet, 2009. **5**(3): p. e1000421.
116. Wilk, J.B., et al., *A genome-wide association study of pulmonary function measures in the Framingham Heart Study*. PLoS Genet, 2009. **5**(3): p. e1000429.
117. Hunninghake, G.M., et al., *MMP12, lung function, and COPD in high-risk populations*. New England Journal of Medicine, 2009. **361**(27): p. 2599-2608.
118. Holt, P.G., et al., *Regulation of immunological homeostasis in the respiratory tract*. Nat Rev Immunol, 2008. **8**(2): p. 142-52.
119. Luft, T., et al., *Type I IFNs enhance the terminal differentiation of dendritic cells*. J Immunol, 1998. **161**(4): p. 1947-53.
120. Zinselmeyer, B.H., et al., *In situ characterization of CD4+ T cell behavior in mucosal and systemic lymphoid tissues during the induction of oral priming and tolerance*. J Exp Med, 2005. **201**(11): p. 1815-23.

121. Turner, S.J., et al., *Characterization of CD8+ T cell repertoire diversity and persistence in the influenza A virus model of localized, transient infection*. Semin Immunol, 2004. **16**(3): p. 179-84.
122. Graham, M.B. and T.J. Braciale, *Resistance to and recovery from lethal influenza virus infection in B lymphocyte-deficient mice*. J Exp Med, 1997. **186**(12): p. 2063-8.
123. Shope, R.E., *Swine influenza: III. Filtration experiments and etiology*. The Journal of experimental medicine, 1931. **54**(3): p. 373.
124. Smith, W., C. Andrewes, and P. Laidlaw, *A virus obtained from influenza patients*. Lancet, 1933: p. 66-8.
125. Francis Jr, T., *A new type of virus from epidemic influenza*. Science (Washington), 1940. **92**: p. 405-8.
126. FRANCIS Jr, T., J. Quilligan Jr, and E. Minuse, *Identification of another epidemic respiratory disease*. Science (Washington), 1950: p. 495-7.
127. Wright, P.F. and R.G. Webster, *Orthomyxoviruses*. Fields virology, 2001. **1**: p. 1533-1579.
128. Lamb, R. and R. Krug, *Orthomyxoviridae: the viruses and their replication, p 1487–1531*. Fields virology, 2001. **1**.
129. Potter, C.W., *A history of influenza*. Journal of applied microbiology, 2001. **91**(4): p. 572-579.
130. Loconsole, D. and M. Chironna, *Epidemiological aspects of seasonal and pandemic influenza in recent years and emerging viruses*. Clinical Immunology, Endocrine & Metabolic Drugs, 2016. **3**(1): p. 15-24.
131. Tumpey, T.M. and J.A. Belser, *Resurrected pandemic influenza viruses*. Annual review of microbiology, 2009. **63**: p. 79-98.
132. Gall, M., K. Krysiak, and V. Prescott, *Asthma, Chronic Obstructive Pulmonary Disease, and Other Respiratory Diseases in Australia*. 2010: Australian Institute of Health and Welfare.
133. Broor, S., et al., *Dynamic patterns of circulating seasonal and pandemic A(H1N1)pdm09 influenza viruses from 2007-2010 in and around Delhi, India*. PLoS One, 2012. **7**(1): p. e29129.
134. Chadha, M.S., et al., *Multisite virological influenza surveillance in India: 2004-2008*. Influenza Other Respir Viruses, 2012. **6**(3): p. 196-203.
135. Ramamurty, N., et al., *Influenza activity among the paediatric age group in Chennai*. Indian J Med Res, 2005. **121**(6): p. 776-9.
136. Rao, B.L. and K. Banerjee, *Influenza surveillance in Pune, India, 1978-90*. Bull World Health Organ, 1993. **71**(2): p. 177-81.
137. Guan, Y., et al., *The emergence of pandemic influenza viruses*. Protein Cell, 2010. **1**(1): p. 9-13.
138. Khanna, M., et al., *Influenza pandemics of 1918 and 2009: a comparative account*. Future Virology, 2013. **8**(4): p. 335-342.

139. Watanabe, Y., et al., *The changing nature of avian influenza A virus (H5N1)*. Trends in microbiology, 2012. **20**(1): p. 11-20.
140. Sander, B., et al., *Economic evaluation of influenza pandemic mitigation strategies in the United States using a stochastic microsimulation transmission model*. Value in Health, 2009. **12**(2): p. 226-233.
141. Wesseling, G., *Occasional review: influenza in COPD: pathogenesis, prevention, and treatment*. International journal of chronic obstructive pulmonary disease, 2007. **2**(1): p. 5.
142. Matsumoto, K. and H. Inoue, *Viral infections in asthma and COPD*. Respir Investig, 2014. **52**(2): p. 92-100.
143. Hsu, A.C., et al., *Targeting PI3K-p110alpha Suppresses Influenza Virus Infection in Chronic Obstructive Pulmonary Disease*. Am J Respir Crit Care Med, 2015. **191**(9): p. 1012-23.
144. De Serres, G., et al., *Importance of viral and bacterial infections in chronic obstructive pulmonary disease exacerbations*. Journal of Clinical Virology, 2009. **46**(2): p. 129-133.
145. AIHW disease expenditure data base, Nov 2014.
146. ABS, *Australian Health Survey: First Results, 2011-12*. ABS Cat. no. 4364.0.55.001. Canberra: ABS. 2012. .
147. Van Kerkhove, M.D., et al., *Risk factors for severe outcomes following 2009 influenza A (H1N1) infection: a global pooled analysis*. PLoS Med, 2011. **8**(7): p. e1001053.
148. Chambers, B.S., et al., *Identification of Hemagglutinin Residues Responsible for H3N2 Antigenic Drift during the 2014-2015 Influenza Season*. Cell Rep, 2015. **12**(1): p. 1-6.
149. Poole, P., et al., *Influenza vaccine for patients with chronic obstructive pulmonary disease*. Cochrane Database Syst Rev, 2006. **1**.
150. Jefferson, T., et al., *Neuraminidase inhibitors for preventing and treating influenza in healthy adults and children*. Sao Paulo Medical Journal, 2014. **132**(4): p. 256-257.
151. Hurt, A.C., et al., *Community transmission of oseltamivir-resistant A (H1N1) pdm09 influenza*. New England Journal of Medicine, 2011. **365**(26): p. 2541-2542.
152. Hayden, F., *Developing new antiviral agents for influenza treatment: what does the future hold?* Clinical Infectious Diseases, 2009. **48**(Supplement 1): p. S3-S13.
153. Hilleman, M.R., *Realities and enigmas of human viral influenza: pathogenesis, epidemiology and control*. Vaccine, 2002. **20**(25): p. 3068-3087.
154. Memorandum, W., *A revision of the system of nomenclature for influenza viruses: a WHO memorandum*. Bull World Health Organ, 1980. **58**: p. 585-91.

155. Webster, R.G., et al., *Evolution and ecology of influenza A viruses*. Microbiological reviews, 1992. **56**(1): p. 152-179.
156. Treanor, J., *Influenza vaccine—outmaneuvering antigenic shift and drift*. New England Journal of Medicine, 2004. **350**(3): p. 218-220.
157. Wiley, D.C. and J.J. Skehel, *The structure and function of the hemagglutinin membrane glycoprotein of influenza virus*. Annual review of biochemistry, 1987. **56**(1): p. 365-394.
158. Lamb, R.A., S.L. Zebedee, and C.D. Richardson, *Influenza virus M2 protein is an integral membrane protein expressed on the infected-cell surface*. Cell, 1985. **40**(3): p. 627-633.
159. Wang, C., R.A. Lamb, and L.H. Pinto, *Direct measurement of the influenza A virus M2 protein ion channel activity in mammalian cells*. Virology, 1994. **205**(1): p. 133-140.
160. Iwatsuki-Horimoto, K., et al., *The cytoplasmic tail of the influenza A virus M2 protein plays a role in viral assembly*. Journal of virology, 2006. **80**(11): p. 5233-5240.
161. Julkunen, I., et al., *Molecular pathogenesis of influenza A virus infection and virus-induced regulation of cytokine gene expression*. Cytokine Growth Factor Rev, 2001. **12**(2-3): p. 171-80.
162. Jin, H., et al., *Two residues in the hemagglutinin of A/Fujian/411/02-like influenza viruses are responsible for antigenic drift from A/Panama/2007/99*. Virology, 2005. **336**(1): p. 113-9.
163. Pinto, L.H., L.J. Holsinger, and R.A. Lamb, *Influenza virus M2 protein has ion channel activity*. Cell, 1992. **69**(3): p. 517-28.
164. Skehel, J.J., et al., *Changes in the conformation of influenza virus hemagglutinin at the pH optimum of virus-mediated membrane fusion*. Proc Natl Acad Sci U S A, 1982. **79**(4): p. 968-72.
165. Plotch, S.J., et al., *A unique cap(m7GpppXm)-dependent influenza virion endonuclease cleaves capped RNAs to generate the primers that initiate viral RNA transcription*. Cell, 1981. **23**(3): p. 847-58.
166. Lamb, R.A. and M. Takeda, *Death by influenza virus protein*. Nat Med, 2001. **7**(12): p. 1286-8.
167. Katz, J.M., et al., *Antibody response in individuals infected with avian influenza A (H5N1) viruses and detection of anti-H5 antibody among household and social contacts*. Journal of Infectious Diseases, 1999. **180**(6): p. 1763-1770.
168. Katze, M.G., D. DeCorato, and R.M. Krug, *Cellular mRNA translation is blocked at both initiation and elongation after infection by influenza virus or adenovirus*. Journal of virology, 1986. **60**(3): p. 1027-1039.
169. Kondo, S. and K. Abe, *The effects of influenza virus infection on FEV 1 in asthmatic children: the time-course study*. Chest, 1991. **100**(5): p. 1235-1238.

170. Lawrence, C.W. and T.J. Braciale, *Activation, differentiation, and migration of naive virus-specific CD8<sup>+</sup> T cells during pulmonary influenza virus infection*. The Journal of Immunology, 2004. **173**(2): p. 1209-1218.
171. Lipatov, A.S., et al., *Pathogenesis of Hong Kong H5N1 influenza virus NS gene reassortants in mice: the role of cytokines and B-and T-cell responses*. Journal of General Virology, 2005. **86**(4): p. 1121-1130.
172. Huang, K.J., et al., *An interferon- $\gamma$ -related cytokine storm in SARS patients*. Journal of medical virology, 2005. **75**(2): p. 185-194.
173. Osterholm, M.T., *Preparing for the next pandemic*. New England Journal of Medicine, 2005. **352**(18): p. 1839-1842.
174. Daniels, R., et al., *Antigenic analyses of influenza virus haemagglutinins with different receptor-binding specificities*. Virology, 1984. **138**(1): p. 174-177.
175. Hemmes, J., K. Winkler, and S. Kool, *Virus survival as a seasonal factor in influenza and poliomyelitis*. Nature, 1960. **188**(4748): p. 430-431.
176. Folkerts, G., et al., *Virus-induced airway hyperresponsiveness and asthma*. American journal of respiratory and critical care medicine, 1998. **157**(6): p. 1708-1720.
177. van der Sluijs, K.F., et al., *Bench-to-bedside review: bacterial pneumonia with influenza-pathogenesis and clinical implications*. Critical care, 2010. **14**(2): p. 219.
178. Hulse, D.J., et al., *Molecular determinants within the surface proteins involved in the pathogenicity of H5N1 influenza viruses in chickens*. Journal of virology, 2004. **78**(18): p. 9954-9964.
179. Ishikawa, E., et al., *Role of tumor necrosis factor-related apoptosis-inducing ligand in immune response to influenza virus infection in mice*. Journal of virology, 2005. **79**(12): p. 7658-7663.
180. Acosta-Rodriguez, E.V., et al., *Interleukins 1 $\beta$  and 6 but not transforming growth factor- $\beta$  are essential for the differentiation of interleukin 17-producing human T helper cells*. Nature immunology, 2007. **8**(9): p. 942-949.
181. Alexopoulou, L., et al., *Recognition of double-stranded RNA and activation of NF- $\kappa$ B by Toll-like receptor 3*. Nature, 2001. **413**(6857): p. 732-738.
182. Yewdell, J.W., et al., *Influenza A virus nucleoprotein is a major target antigen for cross-reactive anti-influenza A virus cytotoxic T lymphocytes*. Proceedings of the National Academy of Sciences, 1985. **82**(6): p. 1785-1789.
183. Weinstein, R.A., et al., *Transmission of influenza: implications for control in health care settings*. Clinical infectious diseases, 2003. **37**(8): p. 1094-1101.
184. Hsu, A.C., et al., *Innate immunity to influenza in chronic airways diseases*. Respiriology, 2012. **17**(8): p. 1166-75.

185. Hennessy, B.T., et al., *Exploiting the PI3K/AKT pathway for cancer drug discovery*. Nat Rev Drug Discov, 2005. **4**(12): p. 988-1004.
186. Yoneyama, M., et al., *The RNA helicase RIG-I has an essential function in double-stranded RNA-induced innate antiviral responses*. Nat Immunol, 2004. **5**(7): p. 730-7.
187. Hornung, V., et al., *5'-Triphosphate RNA is the ligand for RIG-I*. Science, 2006. **314**(5801): p. 994-7.
188. Pichlmair, A., et al., *RIG-I-mediated antiviral responses to single-stranded RNA bearing 5'-phosphates*. Science, 2006. **314**(5801): p. 997-1001.
189. Kawai, T., et al., *IPS-1, an adaptor triggering RIG-I- and Mda5-mediated type I interferon induction*. Nat Immunol, 2005. **6**(10): p. 981-8.
190. Hsu, A.C., et al., *Critical role of constitutive type I interferon response in bronchial epithelial cell to influenza infection*. PloS one, 2012. **7**(3): p. e32947.
191. Weiss, I.D., et al., *IFN-gamma treatment at early stages of influenza virus infection protects mice from death in a NK cell-dependent manner*. J Interferon Cytokine Res, 2010. **30**(6): p. 439-49.
192. Cook, D.N., et al., *Requirement of MIP-1 alpha for an inflammatory response to viral infection*. Science, 1995. **269**(5230): p. 1583-5.
193. Dufour, J.H., et al., *IFN-gamma-inducible protein 10 (IP-10; CXCL10)-deficient mice reveal a role for IP-10 in effector T cell generation and trafficking*. J Immunol, 2002. **168**(7): p. 3195-204.
194. Organization, W.H., *Standardization of terminology of the pandemic A (H1N1) 2009 virus= Normalisation de la terminologie pour le virus de la grippe pandémique A (H1N1) 2009*. Wkly Epidemiol Rec, 2011. **86**(43): p. 480-480.
195. Fairbrother, G., et al., *High costs of influenza: Direct medical costs of influenza disease in young children*. Vaccine, 2010. **28**(31): p. 4913-4919.
196. Chowell, G., et al., *Severe respiratory disease concurrent with the circulation of H1N1 influenza*. New England Journal of Medicine, 2009. **361**(7): p. 674-679.
197. Neuzil, K.M., et al., *The effect of influenza on hospitalizations, outpatient visits, and courses of antibiotics in children*. New England Journal of Medicine, 2000. **342**(4): p. 225-231.
198. Louie, J.K., et al., *Children hospitalized with 2009 novel influenza A (H1N1) in California*. Archives of pediatrics & adolescent medicine, 2010. **164**(11): p. 1023-1031.
199. Schanzer, D., J. Vachon, and L. Pelletier, *Age-specific differences in influenza A epidemic curves: do children drive the spread of influenza epidemics?* American journal of epidemiology, 2011. **174**(1): p. 109-117.

200. Schulz, O., et al., *Toll-like receptor 3 promotes cross-priming to virus-infected cells*. *Nature*, 2005. **433**(7028): p. 887-892.
201. Iwasaki, A. and P.S. Pillai, *Innate immunity to influenza virus infection*. *Nature Reviews Immunology*, 2014. **14**(5): p. 315-328.
202. Martinon, F., A. Mayor, and J. Tschopp, *The inflammasomes: guardians of the body*. *Annual review of immunology*, 2009. **27**: p. 229-265.
203. Zinselmeyer, B.H., et al., *In situ characterization of CD4+ T cell behavior in mucosal and systemic lymphoid tissues during the induction of oral priming and tolerance*. *Journal of Experimental Medicine*, 2005. **201**(11): p. 1815-1823.
204. Turner, S.J., et al. *Characterization of CD8+ T cell repertoire diversity and persistence in the influenza A virus model of localized, transient infection*. in *Seminars in immunology*. 2004. Elsevier.
205. Graham, M.B. and T.J. Braciale, *Resistance to and recovery from lethal influenza virus infection in B lymphocyte-deficient mice*. *Journal of Experimental Medicine*, 1997. **186**(12): p. 2063-2068.
206. Saturni, S., et al., *Models of respiratory infections: virus-induced asthma exacerbations and beyond*. *Allergy, asthma & immunology research*, 2015. **7**(6): p. 525-533.
207. Busse, W.W., R.F. Lemanske, and J.E. Gern, *Role of viral respiratory infections in asthma and asthma exacerbations*. *The Lancet*, 2010. **376**(9743): p. 826-834.
208. Sigurs, N., et al., *Respiratory syncytial virus bronchiolitis in infancy is an important risk factor for asthma and allergy at age 7*. *American journal of respiratory and critical care medicine*, 2000. **161**(5): p. 1501-1507.
209. Hansbro, P.M., et al., *Pulmonary immunity during respiratory infections in early life and the development of severe asthma*. *Annals of the American Thoracic Society*, 2014. **11**(Supplement 5): p. S297-S302.
210. Starkey, M., et al., *Constitutive production of IL-13 promotes early-life Chlamydia respiratory infection and allergic airway disease*. *Mucosal immunology*, 2013. **6**(3): p. 569-579.
211. Starkey, M., et al., *Tumor necrosis factor-related apoptosis-inducing ligand translates neonatal respiratory infection into chronic lung disease*. *Mucosal immunology*, 2014. **7**(3): p. 478-488.
212. Nguyen, T.H., et al., *TNF- $\alpha$  and Macrophages Are Critical for Respiratory Syncytial Virus-Induced Exacerbations in a Mouse Model of Allergic Airways Disease*. *The Journal of Immunology*, 2016. **196**(9): p. 3547-3558.
213. Arikatt, J., et al., *RAGE deficiency predisposes mice to virus-induced paucigranulocytic asthma*. *eLife*, 2017. **6**: p. e21199.
214. Durham, A., I. Adcock, and O. Tliba, *Steroid resistance in severe asthma: current mechanisms and future treatment*. *Current pharmaceutical design*, 2011. **17**(7): p. 674-684.

215. Kim, R.Y., et al., *MicroRNA-21 drives severe, steroid-insensitive experimental asthma by amplifying phosphoinositide 3-kinase-mediated suppression of histone deacetylase 2*. Journal of Allergy and Clinical Immunology, 2016.
216. Manni, M.L., et al., *Molecular Mechanisms of Airway Hyperresponsiveness in a Murine Model of Steroid-Resistant Airway Inflammation*. J Immunol, 2016. **196**(3): p. 963-77.
217. Chambers, E.S., et al., *Distinct endotypes of steroid-resistant asthma characterized by IL-17A high and IFN- $\gamma$  high immunophenotypes: potential benefits of calcitriol*. Journal of Allergy and Clinical Immunology, 2015. **136**(3): p. 628-637. e4.
218. Onions, S.T., et al., *Discovery of narrow spectrum kinase inhibitors: new therapeutic agents for the treatment of COPD and steroid-resistant asthma*. Journal of medicinal chemistry, 2016. **59**(5): p. 1727-1746.
219. Li, J.J., et al., *MicroRNA-9 regulates steroid-resistant airway hyperresponsiveness by reducing protein phosphatase 2A activity*. J Allergy Clin Immunol, 2015. **136**(2): p. 462-73.
220. Tian, B.P., et al., *Bcl-2 Inhibitors Reduce Steroid-insensitive Airway Inflammation*. J Allergy Clin Immunol, 2016.
221. Mejías, A., et al., *Anti-respiratory syncytial virus (RSV) neutralizing antibody decreases lung inflammation, airway obstruction, and airway hyperresponsiveness in a murine RSV model*. Antimicrobial agents and chemotherapy, 2004. **48**(5): p. 1811-1822.
222. Group, I.-R.S., *Palivizumab, a humanized respiratory syncytial virus monoclonal antibody, reduces hospitalization from respiratory syncytial virus infection in high-risk infants*. Pediatrics, 1998. **102**(3): p. 531-537.
223. Carbonell-Estrany, X. and J.J. Quero, *Guidelines for respiratory syncytial virus prophylaxis. An update*. Anales espanoles de pediatria, 2002. **56**(4): p. 334-336.
224. Hines, E.A., et al., *Comparison of temporal transcriptomic profiles from immature lungs of two rat strains reveals a viral response signature associated with chronic lung dysfunction*. PloS one, 2014. **9**(12): p. e112997.
225. High, M., et al., *Determinants of host susceptibility to murine respiratory syncytial virus (RSV) disease identify a role for the innate immunity scavenger receptor MARCO gene in human infants*. EBioMedicine, 2016. **11**: p. 73-84.
226. Odajima, H., et al., *Long-term safety, efficacy, pharmacokinetics and pharmacodynamics of omalizumab in children with severe uncontrolled asthma*. Allergology International, 2017. **66**(1): p. 106-115.
227. LaForce, C., et al., *Efficacy and safety of inhaled zanamivir in the prevention of influenza in community-dwelling, high-risk adult and adolescent subjects: a 28-day, multicenter, randomized, double-blind, placebo-controlled trial*. Clinical therapeutics, 2007. **29**(8): p. 1579-1590.

228. Colombo, R.E., et al., *A phase 1 randomized, double-blind, placebo-controlled, crossover trial of DAS181 (Fludase®) in adult subjects with well-controlled asthma*. BMC infectious diseases, 2016. **16**(1): p. 54.
229. Zenilman, J.M., et al., *Phase 1 clinical trials of DAS181, an inhaled sialidase, in healthy adults*. Antiviral research, 2015. **123**: p. 114-119.
230. Moss, R.B., et al., *A phase II study of DAS181, a novel host directed antiviral for the treatment of influenza infection*. Journal of Infectious Diseases, 2012: p. jis622.
231. Miravittles, M., et al., *Relationship between bacterial flora in sputum and functional impairment in patients with acute exacerbations of COPD*. CHEST Journal, 1999. **116**(1): p. 40-46.
232. Rosell, A., et al., *Microbiologic determinants of exacerbation in chronic obstructive pulmonary disease*. Archives of Internal Medicine, 2005. **165**(8): p. 891-897.
233. Sapey, E. and R. Stockley, *COPD exacerbations· 2: Aetiology*. Thorax, 2006. **61**(3): p. 250-258.
234. Soler-Cataluna, J., et al., *Severe acute exacerbations and mortality in patients with chronic obstructive pulmonary disease*. Thorax, 2005. **60**(11): p. 925-931.
235. Patel, I., et al., *Relationship between bacterial colonisation and the frequency, character, and severity of COPD exacerbations*. Thorax, 2002. **57**(9): p. 759-764.
236. Donaldson, G., et al., *Relationship between exacerbation frequency and lung function decline in chronic obstructive pulmonary disease*. Thorax, 2002. **57**(10): p. 847-852.
237. Papi, A., et al., *Infections and airway inflammation in chronic obstructive pulmonary disease severe exacerbations*. American journal of respiratory and critical care medicine, 2006. **173**(10): p. 1114-1121.
238. Sethi, S. and T.F. Murphy, *Bacterial infection in chronic obstructive pulmonary disease in 2000: a state-of-the-art review*. Clinical microbiology reviews, 2001. **14**(2): p. 336-363.
239. Silverman, E.K., A. Spira, and P.D. Paré, *Genetics and genomics of chronic obstructive pulmonary disease*. Proceedings of the American Thoracic Society, 2009. **6**(6): p. 539-542.
240. van der Strate, B.W., et al., *Cigarette smoke–induced emphysema: a role for the B cell?* American journal of respiratory and critical care medicine, 2006. **173**(7): p. 751-758.
241. Lee, S.-H., et al., *Anti-elastin autoimmunity in tobacco smoking–induced emphysema*. Nature medicine, 2007. **13**(5): p. 567-569.
242. López-de-Andrés, A., et al., *Coverages and factors associated with influenza vaccination among subjects with chronic respiratory diseases in Spain*. The European Journal of Public Health, 2008. **18**(2): p. 173-177.

243. Mohan, A., et al., *Prevalence of viral infection detected by PCR and RT-PCR in patients with acute exacerbation of COPD: A systematic review*. *Respirology*, 2010. **15**(3): p. 536-542.
244. Hershenson, M.B., *Rhinovirus-induced exacerbations of asthma and COPD*. *Scientifica*, 2013. **2013**.
245. Fagon, J.Y., et al., *Characterization of distal bronchial microflora during acute exacerbation of chronic bronchitis*. *Am Rev Respir Dis*, 1990. **142**(5): p. 1004-1008.
246. Soler, N., et al., *Bronchial microbial patterns in severe exacerbations of chronic obstructive pulmonary disease (COPD) requiring mechanical ventilation*. *American journal of respiratory and critical care medicine*, 1998. **157**(5): p. 1498-1505.
247. Shukla, S.D., et al., *Platelet activating factor receptor: gateway for bacterial chronic airway infection in chronic obstructive pulmonary disease and potential therapeutic target*. *Expert review of respiratory medicine*, 2015. **9**(4): p. 473-485.
248. Almansa, R., et al., *Host response cytokine signatures in viral and nonviral acute exacerbations of chronic obstructive pulmonary disease*. *Journal of Interferon & Cytokine Research*, 2011. **31**(5): p. 409-413.
249. He, J.-Q., et al., *Polymorphisms in the IL13, IL13RA1, and IL4RA genes and rate of decline in lung function in smokers*. *American journal of respiratory cell and molecular biology*, 2003. **28**(3): p. 379-385.
250. Chen, L., et al., *Interleukin-13- 1112 C/T Promoter Polymorphism Confers Risk for COPD: A Meta-Analysis*. *PloS one*, 2013. **8**(7): p. e68222.
251. Ezzeldin, N., et al., *Association of TNF- $\alpha$ -308G/A, SP-B 1580 C/T, IL-13-1055 C/T gene polymorphisms and latent adenoviral infection with chronic obstructive pulmonary disease in an Egyptian population*. *Archives of medical science: AMS*, 2012. **8**(2): p. 286.
252. Zheng, T., et al., *Inducible targeting of IL-13 to the adult lung causes matrix metalloproteinase- and cathepsin-dependent emphysema*. *Journal of Clinical Investigation*, 2000. **106**(9): p. 1081.
253. Holtzman, M.J., et al., *Immune pathways for translating viral infection into chronic airway disease*. *Advances in immunology*, 2009. **102**: p. 245-276.
254. Chung, S.I., et al., *IL-13 is a therapeutic target in radiation lung injury*. *Scientific reports*, 2016. **6**.
255. Preston, J.A., et al., *Inhibition of allergic airways disease by immunomodulatory therapy with whole killed *Streptococcus pneumoniae**. *Vaccine*, 2007. **25**(48): p. 8154-8162.
256. Thorburn, A.N., et al., *Components of *Streptococcus pneumoniae* suppress allergic airways disease and NKT cells by inducing regulatory T cells*. *The Journal of Immunology*, 2012. **188**(9): p. 4611-4620.

257. Thorburn, A.N., et al., *Pneumococcal conjugate vaccine-induced regulatory T cells suppress the development of allergic airways disease*. Thorax, 2010. **65**(12): p. 1053-1060.
258. Finkelman, F.D. and M. Wills-Karp, *Usefulness and optimization of mouse models of allergic airway disease*. The Journal of allergy and clinical immunology, 2008. **121**(3).
259. Nials, A.T. and S. Uddin, *Mouse models of allergic asthma: acute and chronic allergen challenge*. Disease models & mechanisms, 2008. **1**(4-5): p. 213-220.
260. Koerner-Rettberg, C., et al., *Reduced lung function in a chronic asthma model is associated with prolonged inflammation, but independent of peribronchial fibrosis*. PLoS one, 2008. **3**(2): p. e1575.
261. Kumar, R.K. and P.S. Foster, *Are mouse models of asthma appropriate for investigating the pathogenesis of airway hyper-responsiveness?* Frontiers in physiology, 2012. **3**: p. 312.
262. Vlahos, R., et al., *Modelling COPD in mice*. Pulmonary pharmacology & therapeutics, 2006. **19**(1): p. 12-17.
263. Wright, J.L., M. Cosio, and A. Churg, *Animal models of chronic obstructive pulmonary disease*. american journal of physiology-lung cellular and molecular physiology, 2008. **295**(1): p. L1-L15.
264. Beckett, E.L., et al., *A new short-term mouse model of chronic obstructive pulmonary disease identifies a role for mast cell tryptase in pathogenesis*. Journal of Allergy and Clinical Immunology, 2013. **131**(3): p. 752-762. e7.
265. Margine, I. and F. Krammer, *Animal models for influenza viruses: implications for universal vaccine development*. Pathogens, 2014. **3**(4): p. 845-874.
266. Bouvier, N.M. and A.C. Lowen, *Animal Models for Influenza Virus Pathogenesis and Transmission*. Viruses, 2010. **2**(8): p. 1530-1563.
267. Belser, J.A., J.M. Katz, and T.M. Tumpey, *The ferret as a model organism to study influenza A virus infection*. Disease models & mechanisms, 2011. **4**(5): p. 575-579.
268. DiLillo, D.J., et al., *Broadly neutralizing hemagglutinin stalk-specific antibodies require Fc [gamma] R interactions for protection against influenza virus in vivo*. Nature medicine, 2014. **20**(2): p. 143-151.
269. Carey, M.A., et al., *Pharmacologic inhibition of COX-1 and COX-2 in influenza A viral infection in mice*. PLoS One, 2010. **5**(7): p. e11610.
270. Ishikawa, H., et al., *Mice with asthma are more resistant to influenza virus infection and NK cells activated by the induction of asthma have potentially protective effects*. Journal of clinical immunology, 2012. **32**(2): p. 256-267.
271. Ishikawa, H., et al., *IFN- $\gamma$  production downstream of NKT cell activation in mice infected with influenza virus enhances the cytolytic activities of*

- both NK cells and viral antigen-specific CD8+ T cells.* Virology, 2010. **407**(2): p. 325-332.
272. Thomas, B.J., et al., *Glucocorticosteroids enhance replication of respiratory viruses: effect of adjuvant interferon.* Scientific reports, 2014. **4**: p. 7176.
273. Wortham, B.W., et al., *NKG2D mediates NK cell hyperresponsiveness and influenza-induced pathologies in a mouse model of chronic obstructive pulmonary disease.* The Journal of Immunology, 2012. **188**(9): p. 4468-4475.
274. Haw, T., et al., *A pathogenic role for tumor necrosis factor-related apoptosis-inducing ligand in chronic obstructive pulmonary disease.* Mucosal immunology, 2015.
275. Pei, Z., et al., *Oral delivery of a novel attenuated Salmonella vaccine expressing influenza A virus proteins protects mice against H5N1 and H1N1 viral infection.* PloS one, 2015. **10**(6): p. e0129276.
276. Greene, C.M. and K.P. Gaughan, *microRNAs in asthma: potential therapeutic targets.* Current opinion in pulmonary medicine, 2013. **19**(1): p. 66-72.
277. Winter, J., et al., *Many roads to maturity: microRNA biogenesis pathways and their regulation.* Nat Cell Biol, 2009. **11**(3): p. 228-34.
278. Schickel, R., et al., *MicroRNAs: key players in the immune system, differentiation, tumorigenesis and cell death.* Oncogene, 2008. **27**(45): p. 5959-5974.
279. Griffiths-Jones, S., *The microRNA registry.* Nucleic acids research, 2004. **32**(suppl 1): p. D109-D111.
280. Griffiths-Jones, S., et al., *miRBase: microRNA sequences, targets and gene nomenclature.* Nucleic acids research, 2006. **34**(suppl 1): p. D140-D144.
281. Weiland, M., et al., *Small RNAs have a large impact: circulating microRNAs as biomarkers for human diseases.* RNA biology, 2012. **9**(6): p. 850-859.
282. Dua, K., et al., *MicroRNAs as therapeutics for future drug delivery systems in treatment of lung diseases.* Drug Delivery and Translational Research, 2016: p. 1-11.
283. Szymczak, I., J. Wieczfinska, and R. Pawliczak, *Molecular Background of miRNA Role in Asthma and COPD: An Updated Insight.* Biomed Res Int, 2016. **2016**: p. 7802521.
284. Bader, A.G., D. Brown, and M. Winkler, *The promise of microRNA replacement therapy.* Cancer Res, 2010. **70**(18): p. 7027-30.
285. Krutzfeldt, J., et al., *Silencing of microRNAs in vivo with 'antagomirs'.* Nature, 2005. **438**(7068): p. 685-9.
286. Elmen, J., et al., *LNA-mediated microRNA silencing in non-human primates.* Nature, 2008. **452**(7189): p. 896-9.

287. Borchert, G.M., W. Lanier, and B.L. Davidson, *RNA polymerase III transcribes human microRNAs*. Nature structural & molecular biology, 2006. **13**(12): p. 1097-1101.
288. Chen, C.-Z., et al., *MicroRNAs modulate hematopoietic lineage differentiation*. science, 2004. **303**(5654): p. 83-86.
289. Cullen, B.R., *Transcription and processing of human microRNA precursors*. Molecular cell, 2004. **16**(6): p. 861-865.
290. Lee, Y., et al., *The nuclear RNase III Drosha initiates microRNA processing*. Nature, 2003. **425**(6956): p. 415-419.
291. Landthaler, M., A. Yalcin, and T. Tuschl, *The human DiGeorge syndrome critical region gene 8 and its D. melanogaster homolog are required for miRNA biogenesis*. Current biology, 2004. **14**(23): p. 2162-2167.
292. Yi, R., et al., *Exportin-5 mediates the nuclear export of pre-microRNAs and short hairpin RNAs*. Genes & development, 2003. **17**(24): p. 3011-3016.
293. Bohnsack, M.T., K. Czaplinski, and D. GÖRLICH, *Exportin 5 is a RanGTP-dependent dsRNA-binding protein that mediates nuclear export of pre-miRNAs*. Rna, 2004. **10**(2): p. 185-191.
294. Lund, E., et al., *Nuclear export of microRNA precursors*. Science, 2004. **303**(5654): p. 95-98.
295. Grishok, A., et al., *Genes and mechanisms related to RNA interference regulate expression of the small temporal RNAs that control C. elegans developmental timing*. Cell, 2001. **106**(1): p. 23-34.
296. Hutvagner, G., et al., *A cellular function for the RNA-interference enzyme Dicer in the maturation of the let-7 small temporal RNA*. Science, 2001. **293**(5531): p. 834-838.
297. Zhang, H., et al., *Human Dicer preferentially cleaves dsRNAs at their termini without a requirement for ATP*. The EMBO journal, 2002. **21**(21): p. 5875-5885.
298. Plank, M., et al., *Targeting translational control as a novel way to treat inflammatory disease: the emerging role of microRNAs*. Clinical & Experimental Allergy, 2013. **43**(9): p. 981-999.
299. Kumar, M., et al., *Let-7 microRNA-mediated regulation of IL-13 and allergic airway inflammation*. Journal of Allergy and Clinical Immunology, 2011. **128**(5): p. 1077-1085. e10.
300. Lu, T.X., A. Munitz, and M.E. Rothenberg, *MicroRNA-21 is up-regulated in allergic airway inflammation and regulates IL-12p35 expression*. The Journal of Immunology, 2009. **182**(8): p. 4994-5002.
301. Lu, T.X., et al., *MicroRNA-21 limits in vivo immune response-mediated activation of the IL-12/IFN- $\gamma$  pathway, Th1 polarization, and the severity of delayed-type hypersensitivity*. The Journal of Immunology, 2011. **187**(6): p. 3362-3373.

302. Liu, G., et al., *miR-21 mediates fibrogenic activation of pulmonary fibroblasts and lung fibrosis*. Journal of Experimental Medicine, 2010. **207**(8): p. 1589-1597.
303. Kuhn, A.R., et al., *MicroRNA expression in human airway smooth muscle cells: role of miR-25 in regulation of airway smooth muscle phenotype*. American journal of respiratory cell and molecular biology, 2010. **42**(4): p. 506-513.
304. Mohamed, J.S., M.A. Lopez, and A.M. Boriek, *Mechanical stretch up-regulates microRNA-26a and induces human airway smooth muscle hypertrophy by suppressing glycogen synthase kinase-3 $\beta$* . Journal of Biological Chemistry, 2010. **285**(38): p. 29336-29347.
305. Sharma, A., et al., *Antagonism of mmu-mir-106a attenuates asthma features in allergic murine model*. Journal of applied physiology, 2012. **113**(3): p. 459-464.
306. Mattes, J., et al., *Antagonism of microRNA-126 suppresses the effector function of TH2 cells and the development of allergic airways disease*. Proceedings of the National Academy of Sciences, 2009. **106**(44): p. 18704-18709.
307. Collison, A., et al., *Altered expression of microRNA in the airway wall in chronic asthma: miR-126 as a potential therapeutic target*. BMC pulmonary medicine, 2011. **11**(1): p. 29.
308. Oglesby, I.K., et al., *miR-126 is downregulated in cystic fibrosis airway epithelial cells and regulates TOM1 expression*. The journal of immunology, 2010. **184**(4): p. 1702-1709.
309. Xie, T., et al., *MicroRNA-127 inhibits lung inflammation by targeting IgG Fc $\gamma$  receptor I*. The Journal of Immunology, 2012. **188**(5): p. 2437-2444.
310. Chiba, Y., et al., *Down-regulation of miR-133a contributes to up-regulation of Rhoa in bronchial smooth muscle cells*. American journal of respiratory and critical care medicine, 2009. **180**(8): p. 713-719.
311. Collison, A., et al., *Inhibition of house dust mite-induced allergic airways disease by antagonism of microRNA-145 is comparable to glucocorticoid treatment*. Journal of Allergy and Clinical Immunology, 2011. **128**(1): p. 160-167. e4.
312. Sato, T., et al., *Reduced miR-146a increases prostaglandin E2 in chronic obstructive pulmonary disease fibroblasts*. American journal of respiratory and critical care medicine, 2010. **182**(8): p. 1020-1029.
313. Larner-Svensson, H.M., et al., *Pharmacological studies of the mechanism and function of interleukin-1 $\beta$ -induced miRNA-146a expression in primary human airway smooth muscle*. Respiratory research, 2010. **11**(1): p. 68.
314. Yamamoto, M., et al., *Decreased miR-192 expression in peripheral blood of asthmatic individuals undergoing an allergen inhalation challenge*. BMC genomics, 2012. **13**(1): p. 655.

315. Mizuno, S., et al., *MicroRNA-199a-5p is associated with hypoxia-inducible factor-1 $\alpha$  expression in lungs from patients with COPD*. CHEST Journal, 2012. **142**(3): p. 663-672.
316. Liu, F., et al., *Profiling of miRNAs in pediatric asthma: upregulation of miRNA-221 and miRNA-485-3p*. Molecular medicine reports, 2012. **6**(5): p. 1178-1182.
317. Qin, H.-b., et al., *Inhibition of miRNA-221 suppresses the airway inflammation in asthma*. Inflammation, 2012. **35**(4): p. 1595-1599.
318. Chen, M., et al., *MiR-23b controls TGF-beta1 induced airway smooth muscle cell proliferation via direct targeting of Smad3*. Pulm Pharmacol Ther, 2017.
319. Rodriguez, A., et al., *Requirement of bic/microRNA-155 for normal immune function*. Science, 2007. **316**(5824): p. 608-11.
320. Zhou, H., et al., *miR-155: A Novel Target in Allergic Asthma*. Int J Mol Sci, 2016. **17**(10).
321. Matsukura, S., et al., *Overexpression of microRNA-155 suppresses chemokine expression induced by Interleukin-13 in BEAS-2B human bronchial epithelial cells*. Allergol Int, 2016. **65 Suppl**: p. S17-23.
322. Huo, X., et al., *Decreased epithelial and plasma miR-181b-5p expression associates with airway eosinophilic inflammation in asthma*. Clin Exp Allergy, 2016. **46**(10): p. 1281-90.
323. Wang, Y., et al., *MicroRNA-181b stimulates inflammation via the nuclear factor-kappaB signaling pathway in vitro*. Exp Ther Med, 2015. **10**(4): p. 1584-1590.
324. Fan, L., et al., *MicroRNA-145 influences the balance of Th1/Th2 via regulating RUNX3 in asthma patients*. Exp Lung Res, 2016: p. 1-8.
325. Hussein, M.H., et al., *A passenger strand variant in miR-196a2 contributes to asthma severity in children and adolescents: A preliminary study*. Biochem Cell Biol, 2016. **94**(4): p. 347-57.
326. Tang, G.N., et al., *MicroRNAs Involved in Asthma After Mesenchymal Stem Cells Treatment*. Stem Cells Dev, 2016. **25**(12): p. 883-96.
327. Elbehidy, R.M., et al., *MicroRNA-21 as a novel biomarker in diagnosis and response to therapy in asthmatic children*. Mol Immunol, 2016. **71**: p. 107-14.
328. Hu, R., et al., *MicroRNA-10a controls airway smooth muscle cell proliferation via direct targeting of the PI3 kinase pathway*. Faseb j, 2014. **28**(5): p. 2347-57.
329. Chiba, Y., et al., *Down-regulation of miR-133a contributes to up-regulation of Rhoa in bronchial smooth muscle cells*. Am J Respir Crit Care Med, 2009. **180**(8): p. 713-9.
330. Liu, Y., et al., *Effects of miRNA-145 on airway smooth muscle cells function*. Mol Cell Biochem, 2015. **409**(1-2): p. 135-43.

331. Collison, A., et al., *Altered expression of microRNA in the airway wall in chronic asthma: miR-126 as a potential therapeutic target*. BMC Pulm Med, 2011. **11**: p. 29.
332. Ho, C.Y., et al., *Protective Effects of Diallyl Sulfide on Ovalbumin-Induced Pulmonary Inflammation of Allergic Asthma Mice by MicroRNA-144, -34a, and -34b/c-Modulated Nrf2 Activation*. J Agric Food Chem, 2016. **64**(1): p. 151-60.
333. Haj-Salem, I., et al., *MicroRNA-19a enhances proliferation of bronchial epithelial cells by targeting TGFbetaR2 gene in severe asthma*. Allergy, 2015. **70**(2): p. 212-9.
334. Veremeyko, T., et al., *IL-4/IL-13-dependent and independent expression of miR-124 and its contribution to M2 phenotype of monocytic cells in normal conditions and during allergic inflammation*. PLoS One, 2013. **8**(12): p. e81774.
335. Sharma, A., et al., *Antagonism of mmu-mir-106a attenuates asthma features in allergic murine model*. J Appl Physiol (1985), 2012. **113**(3): p. 459-64.
336. Zhang, X.Y., et al., *LncRNAs BCYRN1 promoted the proliferation and migration of rat airway smooth muscle cells in asthma via upregulating the expression of transient receptor potential 1*. Am J Transl Res, 2016. **8**(8): p. 3409-18.
337. Wang, S.Y., et al., *The lncRNAs involved in mouse airway allergic inflammation following induced pluripotent stem cell-mesenchymal stem cell treatment*. Stem Cell Res Ther, 2017. **8**(1): p. 2.
338. Mattes, J., et al., *Antagonism of microRNA-126 suppresses the effector function of TH2 cells and the development of allergic airways disease*. Proc Natl Acad Sci U S A, 2009. **106**(44): p. 18704-9.
339. Edwards, M.R., et al., *Targeting the NF-kappaB pathway in asthma and chronic obstructive pulmonary disease*. Pharmacol Ther, 2009. **121**(1): p. 1-13.
340. Shapiro, S.D., et al., *Neutrophil elastase contributes to cigarette smoke-induced emphysema in mice*. Am J Pathol, 2003. **163**(6): p. 2329-35.
341. Huang, S.L., C.H. Su, and S.C. Chang, *Tumor necrosis factor-alpha gene polymorphism in chronic bronchitis*. Am J Respir Crit Care Med, 1997. **156**(5): p. 1436-9.
342. Stevenson, C.S., et al., *Characterization of cigarette smoke-induced inflammatory and mucus hypersecretory changes in rat lung and the role of CXCR2 ligands in mediating this effect*. Am J Physiol Lung Cell Mol Physiol, 2005. **288**(3): p. L514-22.
343. Stevenson, C.S., et al., *Comprehensive gene expression profiling of rat lung reveals distinct acute and chronic responses to cigarette smoke inhalation*. Am J Physiol Lung Cell Mol Physiol, 2007. **293**(5): p. L1183-93.

344. Aoshiba, K., N. Yokohori, and A. Nagai, *Alveolar wall apoptosis causes lung destruction and emphysematous changes*. Am J Respir Cell Mol Biol, 2003. **28**(5): p. 555-62.
345. Kasahara, Y., et al., *Inhibition of VEGF receptors causes lung cell apoptosis and emphysema*. J Clin Invest, 2000. **106**(11): p. 1311-9.
346. Izzotti, A., et al., *Downregulation of microRNA expression in the lungs of rats exposed to cigarette smoke*. The FASEB Journal, 2009. **23**(3): p. 806-812.
347. Davidson, M.R., et al., *MicroRNA-218 is deleted and downregulated in lung squamous cell carcinoma*. PLoS One, 2010. **5**(9): p. e12560.
348. Schembri, F., et al., *MicroRNAs as modulators of smoking-induced gene expression changes in human airway epithelium*. Proceedings of the National Academy of Sciences, 2009. **106**(7): p. 2319-2324.
349. Conickx, G., et al., *MicroRNA profiling reveals a role for microRNA-218-5p in the pathogenesis of chronic obstructive pulmonary disease*. American journal of respiratory and critical care medicine, 2017. **195**(1): p. 43-56.
350. Rusca, N. and S. Monticelli, *MiR-146a in Immunity and Disease*. Mol Biol Int, 2011. **2011**: p. 437301.
351. Perry, M.M., et al., *Divergent intracellular pathways regulate interleukin-1beta-induced miR-146a and miR-146b expression and chemokine release in human alveolar epithelial cells*. FEBS Lett, 2009. **583**(20): p. 3349-55.
352. Trang, P., et al., *Regression of murine lung tumors by the let-7 microRNA*. Oncogene, 2010. **29**(11): p. 1580-1587.
353. Wiggins, J.F., et al., *Development of a lung cancer therapeutic based on the tumor suppressor microRNA-34*. Cancer research, 2010. **70**(14): p. 5923-5930.
354. Liu, C., et al., *The microRNA miR-34a inhibits prostate cancer stem cells and metastasis by directly repressing CD44*. Nature medicine, 2011. **17**(2): p. 211-215.
355. Van Rooij, E., et al., *Dysregulation of microRNAs after myocardial infarction reveals a role of miR-29 in cardiac fibrosis*. Proceedings of the National Academy of Sciences, 2008. **105**(35): p. 13027-13032.
356. Lanford, R.E., et al., *Therapeutic silencing of microRNA-122 in primates with chronic hepatitis C virus infection*. Science, 2010. **327**(5962): p. 198-201.
357. Bader, A.G. and P. Lammers, *The therapeutic potential of microRNAs*. Innovations in Pharmaceutical Technology, 2011: p. 52-55.
358. Van Rooij, E. and E.N. Olson, *MicroRNA therapeutics for cardiovascular disease: opportunities and obstacles*. Nature reviews. Drug discovery, 2012. **11**(11): p. 860.

359. Wang, H., et al., *Recent progress in microRNA delivery for cancer therapy by non-viral synthetic vectors*. *Advanced drug delivery reviews*, 2015. **81**: p. 142-160.
360. Lu, T.X., A. Munitz, and M.E. Rothenberg, *MicroRNA-21 is up-regulated in allergic airway inflammation and regulates IL-12p35 expression*. *J Immunol*, 2009. **182**(8): p. 4994-5002.
361. Foster, P.S., et al., *The emerging role of microRNAs in regulating immune and inflammatory responses in the lung*. *Immunological reviews*, 2013. **253**(1): p. 198-215.
362. Tay, H.L., et al., *Antagonism of miR-328 increases the antimicrobial function of macrophages and neutrophils and rapid clearance of non-typeable Haemophilus influenzae (NTHi) from infected lung*. *PLoS Pathog*, 2015. **11**(4): p. e1004549.
363. Kim, R.Y., et al., *MicroRNA-21 drives severe, steroid-insensitive experimental asthma by amplifying phosphoinositide 3-kinase-mediated suppression of histone deacetylase 2*. *J Allergy Clin Immunol*, 2016.
364. Li, C.L., et al., *microRNA-21 Mediates the Protective Effects of Mesenchymal Stem Cells Derived from iPSCs to Human Bronchial Epithelial Cell Injury Under Hypoxia*. *Cell Transplant*, 2017.
365. Lee, H.Y., et al., *Inhibition of MicroRNA-21 by an antagomir ameliorates allergic inflammation in a mouse model of asthma*. *Exp Lung Res*, 2017. **43**(3): p. 109-119.
366. Liu, Y., et al., *MiR-21 modulates human airway smooth muscle cell proliferation and migration in asthma through regulation of PTEN expression*. *Exp Lung Res*, 2015. **41**(10): p. 535-45.
367. Jiang, C., et al., *Extracellular microRNA-21 and microRNA-26a increase in body fluids from rats with antigen induced pulmonary inflammation and children with recurrent wheezing*. *BMC Pulm Med*, 2016. **16**: p. 50.
368. Lu, T.X., et al., *MicroRNA-21 limits in vivo immune response-mediated activation of the IL-12/IFN-gamma pathway, Th1 polarization, and the severity of delayed-type hypersensitivity*. *J Immunol*, 2011. **187**(6): p. 3362-73.
369. Xie, L., F. Yang, and S. Sun, *[Expression of miR-21 in peripheral blood serum and mononuclear cells in patients with chronic obstructive pulmonary disease and its clinical significance]*. *Zhong Nan Da Xue Xue Bao Yi Xue Ban*, 2016. **41**(3): p. 238-43.
370. Xie, L., et al., *An increased ratio of serum miR-21 to miR-181a levels is associated with the early pathogenic process of chronic obstructive pulmonary disease in asymptomatic heavy smokers*. *Mol Biosyst*, 2014. **10**(5): p. 1072-81.
371. Chen-Yu Hsu, A., et al., *Targeting PI3K-p110 $\alpha$  suppresses influenza virus infection in chronic obstructive pulmonary disease*. *American journal of respiratory and critical care medicine*, 2015. **191**(9): p. 1012-1023.

372. Murphy, S.T., et al., *Discovery of novel, potent, and selective inhibitors of 3-phosphoinositide-dependent kinase (PDK1)*. J Med Chem, 2011. **54**(24): p. 8490-500.
373. Liu, Z., et al., *miR-125b inhibits goblet cell differentiation in allergic airway inflammation by targeting SPDEF*. European journal of pharmacology, 2016. **782**: p. 14-20.
374. Li, D., et al., *MiR-125a-5p Decreases the Sensitivity of Treg cells Toward IL-6-Mediated Conversion by Inhibiting IL-6R and STAT3 Expression*. Sci Rep, 2015. **5**: p. 14615.
375. Inchley, C.S., et al., *Nasal mucosal microRNA expression in children with respiratory syncytial virus infection*. BMC Infect Dis, 2015. **15**: p. 150.
376. Panganiban, R.P., et al., *Circulating microRNAs as biomarkers in patients with allergic rhinitis and asthma*. J Allergy Clin Immunol, 2016. **137**(5): p. 1423-32.
377. Vender R, T.K., Kraft M, Ingram JL, Ishmael FT, *Differential microRNA expression in airway fibroblasts of asthmatic and non-asthmatic subjects identify putative therapeutic targets*. Transl Genet Genom, 2017. **1**: p. 36-45.
378. Zhang, X.H., et al., *Overexpression of miR-125b, a novel regulator of innate immunity, in eosinophilic chronic rhinosinusitis with nasal polyps*. Am J Respir Crit Care Med, 2012. **185**(2): p. 140-51.
379. Wang, R., et al., *Peripheral leukocyte micrornas as novel biomarkers for COPD*. International journal of chronic obstructive pulmonary disease, 2017. **12**: p. 1101.
380. Li, D., et al., *Mir-125a-5p decreases the sensitivity of treg cells toward il-6-mediated conversion by inhibiting il-6r and stat3 expression*. Scientific reports, 2015. **5**.
381. Tassano, E., et al., *MicroRNA-125b-1 and BLID upregulation resulting from a novel IGH translocation in childhood B-Cell precursor acute lymphoblastic leukemia*. Genes, Chromosomes and Cancer, 2010. **49**(8): p. 682-687.
382. Bousquet, M., et al., *MicroRNA-125b transforms myeloid cell lines by repressing multiple mRNA*. Haematologica, 2012. **97**(11): p. 1713-1721.
383. Xu, N., et al., *MicroRNA-125b down-regulates matrix metalloproteinase 13 and inhibits cutaneous squamous cell carcinoma cell proliferation, migration, and invasion*. Journal of Biological Chemistry, 2012. **287**(35): p. 29899-29908.
384. Ge, Y., Y. Sun, and J. Chen, *IGF-II is regulated by microRNA-125b in skeletal myogenesis*. The Journal of cell biology, 2011: p. jcb.201007165.
385. Pottelberge, G.R.V., et al., *MicroRNA expression in induced sputum of smokers and patients with chronic obstructive pulmonary disease*. American journal of respiratory and critical care medicine, 2011. **183**(7): p. 898-906.

386. Yuxia, M., T. Zhennan, and Z. Wei, *Circulating miR-125b is a novel biomarker for screening non-small-cell lung cancer and predicts poor prognosis*. Journal of cancer research and clinical oncology, 2012. **138**(12): p. 2045-2050.
387. Kim, S.-W., et al., *MicroRNAs miR-125a and miR-125b constitutively activate the NF- $\kappa$ B pathway by targeting the tumor necrosis factor alpha-induced protein 3 (TNFAIP3, A20)*. Proceedings of the National Academy of Sciences, 2012. **109**(20): p. 7865-7870.
388. Haemmig, S., et al., *miR-125b controls apoptosis and temozolomide resistance by targeting TNFAIP3 and NKIRAS2 in glioblastomas*. Cell death & disease, 2014. **5**(6): p. e1279.
389. Kilbourne, E.D., *Influenza Pandemics of the 20th Century-Volume 12, Number 1—January 2006-Emerging Infectious Disease journal-CDC*. 2006.
390. Arcavi, L. and N.L. Benowitz, *Cigarette smoking and infection*. Archives of internal medicine, 2004. **164**(20): p. 2206-2216.
391. Essilfie, A.-T., et al., *Haemophilus influenzae infection drives IL-17-mediated neutrophilic allergic airways disease*. PLoS Pathog, 2011. **7**(10): p. e1002244.
392. Asquith, K.L., et al., *Interleukin-13 promotes susceptibility to chlamydial infection of the respiratory and genital tracts*. PLoS Pathog, 2011. **7**(5): p. e1001339.
393. Essilfie, A.-T., et al., *Macrolide therapy suppresses key features of experimental steroid-sensitive and steroid-insensitive asthma*. Thorax, 2015: p. thoraxjnl-2014-206067.
394. Cockcroft, D.W. and B.E. Davis, *Mechanisms of airway hyperresponsiveness*. Journal of Allergy and Clinical Immunology, 2006. **118**(3): p. 551-559.
395. Graham, L.M. and N. Eid, *The impact of asthma exacerbations and preventive strategies*. Current medical research and opinion, 2015. **31**(4): p. 825-835.
396. Moore, W.C., et al., *Characterization of the severe asthma phenotype by the national heart, lung, and blood institute's severe asthma research program*. Journal of Allergy and Clinical Immunology, 2007. **119**(2): p. 405-413.
397. O'Byrne, P.M., *Therapeutic strategies to reduce asthma exacerbations*. Journal of Allergy and Clinical Immunology, 2011. **128**(2): p. 257-263.
398. Bai, T., et al., *Severe exacerbations predict excess lung function decline in asthma*. European Respiratory Journal, 2007. **30**(3): p. 452-456.
399. Tattersfield, A.E., et al., *Exacerbations of asthma: a descriptive study of 425 severe exacerbations*. American journal of respiratory and critical care medicine, 1999. **160**(2): p. 594-599.

400. Harrison, T., et al., *Doubling the dose of inhaled corticosteroid to prevent asthma exacerbations: randomised controlled trial*. The Lancet, 2004. **363**(9405): p. 271-275.
401. Influenza, W., *Fact sheet no. 211*. World Health Organization, 2014.
402. Poole, P., et al., *Influenza vaccine for patients with chronic obstructive pulmonary disease*. The Cochrane Library, 2006.
403. Monto, A.S., et al., *Comparative efficacy of inactivated and live attenuated influenza vaccines*. New England Journal of Medicine, 2009. **361**(13): p. 1260-1267.
404. Jefferson, T., et al., *Neuraminidase inhibitors for preventing and treating influenza in healthy adults: systematic review and meta-analysis*. Bmj, 2009. **339**: p. b5106.
405. Chirkova, T., et al., *Immunization with live influenza viruses in an experimental model of allergic bronchial asthma: infection and vaccination*. Influenza Other Respir Viruses, 2008. **2**(5): p. 165-74.
406. Marsland, B.J., et al., *Allergic airway inflammation is exacerbated during acute influenza infection and correlates with increased allergen presentation and recruitment of allergen-specific T-helper type 2 cells*. Clin Exp Allergy, 2004. **34**(8): p. 1299-306.
407. Ravanetti, L., et al., *An early innate response underlies severe influenza-induced exacerbations of asthma in a novel steroid-insensitive and anti-IL-5-responsive mouse model*. Allergy, 2016.
408. Hasegawa, S., et al., *Cytokine profile of bronchoalveolar lavage fluid from a mouse model of bronchial asthma during seasonal H1N1 infection*. Cytokine, 2014. **69**(2): p. 206-10.
409. Kim, R.Y., et al., *Elucidating novel disease mechanisms in severe asthma*. Clin Transl Immunology, 2016. **5**(7): p. e91.
410. Buday, T. and J. Plevkova, *House Dust Mite Allergy Models—Reliability for Research of Airway Defensive Mechanisms*. Open Journal of Molecular and Integrative Physiology, 2014. **2014**.
411. Thomas, W. and W. Smith, *House-dust-mite allergens*. Allergy, 1998. **53**(9): p. 821-832.
412. An, S., et al., *Dermatophagoides farinae allergens diversity identification by proteomics*. Molecular & Cellular Proteomics, 2013. **12**(7): p. 1818-1828.
413. Phillips, J.E., et al., *House dust mite models: will they translate clinically as a superior model of asthma?* Journal of Allergy and Clinical Immunology, 2013. **132**(1): p. 242-244.
414. Huprikar, J. and S. Rabinowitz, *A simplified plaque assay for influenza viruses in Madin-Darby kidney (MDCK) cells*. Journal of virological methods, 1980. **1**(2): p. 117-120.

415. Hsu, A.C.-Y., et al., *Human influenza is more effective than avian influenza at antiviral suppression in airway cells*. American journal of respiratory cell and molecular biology, 2011. **44**(6): p. 906-913.
416. Horvat, J.C., et al., *Neonatal chlamydial infection induces mixed T-cell responses that drive allergic airway disease*. American journal of respiratory and critical care medicine, 2007. **176**(6): p. 556-564.
417. Chomczynski, P. and N. Sacchi, *Single-step method of RNA isolation by acid guanidinium thiocyanate-phenol-chloroform extraction*. Anal Biochem, 1987. **162**(1): p. 156-9.
418. Hansbro, P.M., et al., *Importance of mast cell Prss31/transmembrane tryptase/tryptase- $\gamma$  in lung function and experimental chronic obstructive pulmonary disease and colitis*. Journal of Biological Chemistry, 2014. **289**(26): p. 18214-18227.
419. Liu, G., et al., *Fibulin-1 regulates the pathogenesis of tissue remodeling in respiratory diseases*. JCI insight, 2016. **1**(9).
420. Krishnaswamy, G. and D.S. Chi, *Mast cells: methods and protocols*. Vol. 315. 2006: Springer Science & Business Media.
421. Johnston, S.L., et al., *Community study of role of viral infections in exacerbations of asthma in 9-11 year old children*. Bmj, 1995. **310**(6989): p. 1225-1229.
422. Jackson, D.J. and S.L. Johnston, *The role of viruses in acute exacerbations of asthma*. Journal of Allergy and Clinical Immunology, 2010. **125**(6): p. 1178-1187.
423. Morgan, D.W. and L.A. Marshall, *In vivo models of inflammation*. Vol. 9. 1999: Springer Science & Business Media.
424. Ashino, S., et al., *Janus kinase 1/3 signaling pathways are key initiators of T H 2 differentiation and lung allergic responses*. Journal of Allergy and Clinical Immunology, 2014. **133**(4): p. 1162-1174. e4.
425. Larcombe, A.N., et al., *Acute diesel exhaust particle exposure increases viral titre and inflammation associated with existing influenza infection, but does not exacerbate deficits in lung function*. Influenza Other Respir Viruses, 2013. **7**(5): p. 701-9.
426. Papadopoulos, N.G., et al., *Viruses and bacteria in acute asthma exacerbations--a GA(2) LEN-DARE systematic review*. Allergy, 2011. **66**(4): p. 458-68.
427. Jain, S., et al., *Hospitalized patients with 2009 H1N1 influenza in the United States, April-June 2009*. N Engl J Med, 2009. **361**(20): p. 1935-44.
428. Miller, E.K., et al., *Influenza burden for children with asthma*. Pediatrics, 2008. **121**(1): p. 1-8.
429. Samransamruajkit, R., et al., *Prevalence, clinical presentations and complications among hospitalized children with influenza pneumonia*. Jpn J Infect Dis, 2008. **61**(6): p. 446-9.

430. Narain, J.P., R. Kumar, and R. Bhatia, *Pandemic (H1N1) 2009: epidemiological, clinical and prevention aspects*. Natl Med J India, 2009. **22**(5): p. 242-7.
431. Levandowski, R.A., C.W. Weaver, and G.G. Jackson, *Nasal-Secretion leukocyte populations determined by flow cytometry during acute rhinovirus infection*. Journal of medical virology, 1988. **25**(4): p. 423-432.
432. Fraenkel, D.J., et al., *Lower airways inflammation during rhinovirus colds in normal and in asthmatic subjects*. American journal of respiratory and critical care medicine, 1995. **151**(3): p. 879-886.
433. Fireman, P., *Understanding asthma pathophysiology*. Allergy Asthma Proc, 2003. **24**(2): p. 79-83.
434. Cohn, L., J.A. Elias, and G.L. Chupp, *Asthma: mechanisms of disease persistence and progression*. Annu Rev Immunol, 2004. **22**: p. 789-815.
435. Maddox, L. and D.A. Schwartz, *The pathophysiology of asthma*. Annu Rev Med, 2002. **53**: p. 477-98.
436. Rogers, D.F., *Airway mucus hypersecretion in asthma: an undervalued pathology?* Curr Opin Pharmacol, 2004. **4**(3): p. 241-50.
437. Yuta, A., et al., *Rhinovirus infection induces mucus hypersecretion*. Am J Physiol, 1998. **274**(6 Pt 1): p. L1017-23.
438. Hewson, C.A., et al., *Rhinovirus induces MUC5AC in a human infection model and in vitro via NF-kappaB and EGFR pathways*. Eur Respir J, 2010. **36**(6): p. 1425-35.
439. Tamura, S.-i. and T. Kurata, *Defense mechanisms against influenza virus infection in the respiratory tract mucosa*. Jpn J Infect Dis, 2004. **57**(6): p. 236-47.
440. Zhu, L., et al., *Rhinovirus-induced major airway mucin production involves a novel TLR3-EGFR-dependent pathway*. American journal of respiratory cell and molecular biology, 2009. **40**(5): p. 610-619.
441. Rose, M.C. and J.A. Voynow, *Respiratory tract mucin genes and mucin glycoproteins in health and disease*. Physiological reviews, 2006. **86**(1): p. 245-278.
442. Voynow, J.A., S.J. Gendler, and M.C. Rose, *Regulation of mucin genes in chronic inflammatory airway diseases*. American journal of respiratory cell and molecular biology, 2006. **34**(6): p. 661-665.
443. Lee, N.A., E.W. Gelfand, and J.J. Lee, *Pulmonary T cells and eosinophils: coconspirators or independent triggers of allergic respiratory pathology?* Journal of Allergy and Clinical Immunology, 2001. **107**(6): p. 945-957.
444. Foster, P.S., et al., *Targeting eosinophils in asthma*. Current molecular medicine, 2008. **8**(6): p. 585-590.
445. Nissim Ben Efraim, A. and F. Levi-Schaffer, *Review: Tissue remodeling and angiogenesis in asthma: the role of the eosinophil*. Therapeutic advances in respiratory disease, 2008. **2**(3): p. 163-171.

446. KIM, H.W., et al., *Respiratory syncytial virus disease in infants despite prior administration of antigenic inactivated vaccine*. American journal of epidemiology, 1969. **89**(4): p. 422-434.
447. Williams, C.M., et al., *Cytokine pathways in allergic disease*. Toxicologic pathology, 2012. **40**(2): p. 205-215.
448. Hamid, Q. and M. Tulic, *Immunobiology of asthma*. Annual review of physiology, 2009. **71**: p. 489-507.
449. Finkelman, F.D., et al., *Importance of cytokines in murine allergic airway disease and human asthma*. The Journal of Immunology, 2010. **184**(4): p. 1663-1674.
450. Wu, W., et al., *Innate immune response to H3N2 and H1N1 influenza virus infection in a human lung organ culture model*. Virology, 2010. **396**(2): p. 178-188.
451. Xing, Z., et al., *Regulation of proinflammatory cytokine Interleukin-6 (IL-6) induction by NF-kappaB signaling in pandemic H1N1 influenza A virus-infected human bronchial epithelial cells (45.29)*. The Journal of Immunology, 2010. **184**(1 Supplement): p. 45.29-45.29.
452. Hammad, H., et al., *House dust mite allergen induces asthma via Toll-like receptor 4 triggering of airway structural cells*. Nature medicine, 2009. **15**(4): p. 410-416.
453. Wong, C., et al., *Proinflammatory cytokines (IL-17, IL-6, IL-18 and IL-12) and Th cytokines (IFN- $\gamma$ , IL-4, IL-10 and IL-13) in patients with allergic asthma*. Clinical & Experimental Immunology, 2001. **125**(2): p. 177-183.
454. Ying, S., et al., *Eosinophil chemotactic chemokines (eotaxin, eotaxin-2, RANTES, monocyte chemoattractant protein-3 (MCP-3), and MCP-4), and CC chemokine receptor 3 expression in bronchial biopsies from atopic and nonatopic (Intrinsic) asthmatics*. The Journal of Immunology, 1999. **163**(11): p. 6321-6329.
455. Rothenberg, M.E., et al., *Targeted disruption of the chemokine eotaxin partially reduces antigen-induced tissue eosinophilia*. Journal of Experimental Medicine, 1997. **185**(4): p. 785-790.
456. Teran, L.M., et al., *Eosinophil recruitment following allergen challenge is associated with the release of the chemokine RANTES into asthmatic airways*. The Journal of Immunology, 1996. **157**(4): p. 1806-1812.
457. Persson, I.M., et al., *Increased expression of upstream TH 2-cytokines in a mouse model of viral-induced asthma exacerbation*. Journal of translational medicine, 2016. **14**(1): p. 52.
458. Byers, D.E., *Defining the roles of IL-33, thymic stromal lymphopoietin, and IL-25 in human asthma*. 2014, Am Thoracic Soc.
459. Fajt, M.L. and S.E. Wenzel, *Asthma phenotypes and the use of biologic medications in asthma and allergic disease: the next steps toward personalized care*. Journal of Allergy and Clinical Immunology, 2015. **135**(2): p. 299-310.

460. Kawai, T., et al., *IPS-1, an adaptor triggering RIG-I-and Mda5-mediated type I interferon induction*. Nature immunology, 2005. **6**(10): p. 981-988.
461. Seth, R.B., et al., *Identification and characterization of MAVS, a mitochondrial antiviral signaling protein that activates NF-kappaB and IRF 3*. Cell, 2005. **122**(5): p. 669-82.
462. Hsu, A.C., et al., *Critical role of type I interferon response in bronchial epithelial cell to influenza infection*. PLoS ONE, 2012. **7**(3): p. e32947.
463. Contoli, M., et al., *Role of deficient type III interferon-λ production in asthma exacerbations*. Nature medicine, 2006. **12**(9): p. 1023-1026.
464. Wark, P.A., et al., *Diversity in the bronchial epithelial cell response to infection with different rhinovirus strains*. Respirology, 2009. **14**(2): p. 180-186.
465. Brod, S.A., *Ingested type I interferon: a potential treatment for autoimmunity*. Journal of interferon & cytokine research, 2002. **22**(12): p. 1153-1166.
466. Djukanović, R., et al., *The effect of inhaled IFN-β on worsening of asthma symptoms caused by viral infections. A randomized trial*. American journal of respiratory and critical care medicine, 2014. **190**(2): p. 145-154.
467. Kikkawa, Y., et al., *Interferon-alpha inhibits airway eosinophila and hyperresponsiveness in an animal asthma model*. Asia Pacific Allergy, 2012. **2**(4): p. 256-263.
468. Simon, H.U., et al., *Clinical and immunological effects of low-dose IFN-α treatment in patients with corticosteroid-resistant asthma*. Allergy, 2003. **58**(12): p. 1250-1255.
469. Jackson, D.J., *Inhaled interferon: a novel treatment for virus-induced asthma?* 2014, Am Thoracic Soc.
470. Bergeron, C., M.K. Tulic, and Q. Hamid, *Airway remodelling in asthma: from benchside to clinical practice*. Canadian respiratory journal, 2010. **17**(4): p. e85-e93.
471. Aikawa, T., et al., *Marked goblet cell hyperplasia with mucus accumulation in the airways of patients who died of severe acute asthma attack*. Chest, 1992. **101**(4): p. 916-921.
472. Beasley, R., et al., *Cellular events in the bronchi in mild asthma and after bronchial provocation*. American Review of Respiratory Disease, 1989. **139**(3): p. 806-817.
473. Lambert, R., et al., *Functional significance of increased airway smooth muscle in asthma and COPD*. Journal of Applied Physiology, 1993. **74**(6): p. 2771-2781.
474. Pascual, R.M. and S.P. Peters, *Airway remodeling contributes to the progressive loss of lung function in asthma: an overview*. Journal of Allergy and Clinical Immunology, 2005. **116**(3): p. 477-486.

475. Elias, J.A., et al., *Airway remodeling in asthma*. The Journal of clinical investigation, 1999. **104**(8): p. 1001-1006.
476. Zhu, Z., et al., *IL-13-induced chemokine responses in the lung: role of CCR2 in the pathogenesis of IL-13-induced inflammation and remodeling*. The Journal of Immunology, 2002. **168**(6): p. 2953-2962.
477. Kumar, R.K., et al., *Role of interleukin-13 in eosinophil accumulation and airway remodelling in a mouse model of chronic asthma*. Clinical & Experimental Allergy, 2002. **32**(7): p. 1104-1111.
478. Cohn, L., J.S. Tepper, and K. Bottomly, *Cutting edge: IL-4-independent induction of airway hyperresponsiveness by Th2, but not Th1, cells*. The Journal of Immunology, 1998. **161**(8): p. 3813-3816.
479. Kuperman, D.A., et al., *Direct effects of interleukin-13 on epithelial cells cause airway hyperreactivity and mucus overproduction in asthma*. Nature medicine, 2002. **8**(8): p. 885-889.
480. Guo, Z., et al., *IL-33/ST2 promotes airway remodeling in asthma by activating the expression of fibronectin 1 and type 1 collagen in human lung fibroblasts*. Xi bao yu fen zi mian yi xue za zhi= Chinese journal of cellular and molecular immunology, 2014. **30**(9): p. 975-979.
481. Saglani, S., et al., *IL-33 promotes airway remodeling in pediatric patients with severe steroid-resistant asthma*. Journal of Allergy and Clinical Immunology, 2013. **132**(3): p. 676-685. e13.
482. Tagaya, E. and J. Tamaoki, *Mechanisms of airway remodeling in asthma*. Allergology International, 2007. **56**(4): p. 331-340.
483. Homer, R.J. and J.A. Elias, *Airway remodeling in asthma: therapeutic implications of mechanisms*. Physiology, 2005. **20**(1): p. 28-35.
484. Kang, H.-R., et al., *Transforming growth factor (TGF)- $\beta$ 1 stimulates pulmonary fibrosis and inflammation via a Bax-dependent, Bid-activated pathway that involves matrix metalloproteinase-12*. Journal of Biological Chemistry, 2007. **282**(10): p. 7723-7732.
485. Kelly, E.A. and N.N. Jarjour, *Role of matrix metalloproteinases in asthma*. Current opinion in pulmonary medicine, 2003. **9**(1): p. 28-33.
486. Zhiguang, X., et al., *Over-expression of IL-33 leads to spontaneous pulmonary inflammation in mIL-33 transgenic mice*. Immunology letters, 2010. **131**(2): p. 159-165.
487. Schmitz, J., et al., *IL-33, an interleukin-1-like cytokine that signals via the IL-1 receptor-related protein ST2 and induces T helper type 2-associated cytokines*. Immunity, 2005. **23**(5): p. 479-490.
488. Stolarski, B., et al., *IL-33 exacerbates eosinophil-mediated airway inflammation*. The Journal of Immunology, 2010. **185**(6): p. 3472-3480.
489. Donovan, C., J.E. Bourke, and R. Vlahos, *Targeting the IL-33/IL-13 Axis for Respiratory Viral Infections*. Trends Pharmacol Sci, 2016. **37**(4): p. 252-61.

490. Snibson, K., et al., *Airway remodelling and inflammation in sheep lungs after chronic airway challenge with house dust mite*. *Clinical & Experimental Allergy*, 2005. **35**(2): p. 146-152.
491. Van Scott, M.R., et al., *Dust mite-induced asthma in cynomolgus monkeys*. *Journal of Applied Physiology*, 2004. **96**(4): p. 1433-1444.
492. Wenzel, S.E., et al., *Bronchoscopic evaluation of severe asthma: persistent inflammation associated with high dose glucocorticoids*. *American journal of respiratory and critical care medicine*, 1997. **156**(3): p. 737-743.
493. Ädelroth, E., et al., *Inflammatory cells and eosinophilic activity in asthmatics investigated by bronchoalveolar lavage: the effects of antiasthmatic treatment with budesonide or terbutaline*. *American review of respiratory disease*, 1990. **142**(1): p. 91-99.
494. Crimi, E., et al., *Dissociation between airway inflammation and airway hyperresponsiveness in allergic asthma*. *American Journal of Respiratory and Critical Care Medicine*, 1998. **157**(1): p. 4-9.
495. Lundgren, R., et al., *Morphological studies of bronchial mucosal biopsies from asthmatics before and after ten years of treatment with inhaled steroids*. *European Respiratory Journal*, 1988. **1**(10): p. 883-889.
496. Maltby, S., et al., *Mouse models of severe asthma: Understanding the mechanisms of steroid resistance, tissue remodelling and disease exacerbation*. *Respirology*, 2017. **22**(5): p. 874-885.
497. Bel, E., et al., *Difficult/therapy-resistant asthma*. *Eur Respir J*, 1999. **13**(5): p. 1198-1208.
498. Barnes, P. and A. Woolcock, *Difficult asthma*. *European Respiratory Journal*, 1998. **12**(5): p. 1209-1218.
499. Adcock, I. and S. Lane, *Corticosteroid-insensitive asthma: molecular mechanisms*. *Journal of Endocrinology*, 2003. **178**(3): p. 347-355.
500. Nelson, H.S., D.Y. Leung, and J.W. Bloom, *Update on glucocorticoid action and resistance*. *Journal of allergy and Clinical Immunology*, 2003. **111**(1): p. 3-22.
501. Hawrylowicz, C., et al., *A defect in corticosteroid-induced IL-10 production in T lymphocytes from corticosteroid-resistant asthmatic patients*. *Journal of allergy and clinical immunology*, 2002. **109**(2): p. 369.
502. Xystrakis, E., et al., *Reversing the defective induction of IL-10-secreting regulatory T cells in glucocorticoid-resistant asthma patients*. *The Journal of clinical investigation*, 2006. **116**(1): p. 146-155.
503. Weiss, S.T. and B.A. Raby, *Asthma genetics 2003*. *Human molecular genetics*, 2004. **13**(suppl 1): p. R83-R89.
504. Cookson, W. and M. Moffatt, *Making sense of asthma genes*. 2004, Mass Medical Soc.
505. Busse, P.J., J.J. Wang, and E.A. Halm, *Allergen sensitization evaluation and allergen avoidance education in an inner-city adult cohort with*

- persistent asthma*. Journal of allergy and clinical immunology, 2005. **116**(1): p. 146-152.
506. Bourke, J.E., et al., *Collagen remodelling by airway smooth muscle is resistant to steroids and  $\beta$ 2-agonists*. European Respiratory Journal, 2011. **37**(1): p. 173-182.
  507. Goleva, E., et al., *Airway remodeling and lack of bronchodilator response in steroid-resistant asthma*. Journal of Allergy and Clinical Immunology, 2007. **120**(5): p. 1065-1072.
  508. Wenzel, S.E., *Asthma: defining of the persistent adult phenotypes*. The Lancet, 2006. **368**(9537): p. 804-813.
  509. Holgate, S.T. and R. Polosa, *The mechanisms, diagnosis, and management of severe asthma in adults*. The Lancet, 2006. **368**(9537): p. 780-793.
  510. Holgate, S.T., et al., *Understanding the pathophysiology of severe asthma to generate new therapeutic opportunities*. Journal of Allergy and Clinical Immunology, 2006. **117**(3): p. 496-506.
  511. Hsu, C.I. and H.H. Shih, *Transmission and control of an emerging influenza pandemic in a small-world airline network*. Accid Anal Prev, 2010. **42**(1): p. 93-100.
  512. Edinger, T.O., M.O. Pohl, and S. Stertz, *Entry of influenza A virus: host factors and antiviral targets*. Journal of General Virology, 2014. **95**(2): p. 263-277.
  513. de Vries, E., et al., *Influenza A virus entry into cells lacking sialylated N-glycans*. Proceedings of the National Academy of Sciences, 2012. **109**(19): p. 7457-7462.
  514. Kumar, R.K., P.S. Foster, and H.F. Rosenberg, *Respiratory viral infection, epithelial cytokines, and innate lymphoid cells in asthma exacerbations*. Journal of leukocyte biology, 2014. **96**(3): p. 391-396.
  515. Saito, T., et al., *Respiratory syncytial virus induces selective production of the chemokine RANTES by upper airway epithelial cells*. Journal of Infectious Diseases, 1997. **175**(3): p. 497-504.
  516. Herold, S., et al., *Alveolar epithelial cells direct monocyte transepithelial migration upon influenza virus infection: impact of chemokines and adhesion molecules*. The Journal of Immunology, 2006. **177**(3): p. 1817-1824.
  517. Sprenger, H., et al., *Selective induction of monocyte and not neutrophil-attracting chemokines after influenza A virus infection*. Journal of Experimental Medicine, 1996. **184**(3): p. 1191-1196.
  518. Tekkanat, K.K., et al., *IL-13-induced airway hyperreactivity during respiratory syncytial virus infection is STAT6 dependent*. The Journal of Immunology, 2001. **166**(5): p. 3542-3548.
  519. Lukacs, N.W., et al., *Respiratory syncytial virus predisposes mice to augmented allergic airway responses via IL-13-mediated mechanisms*. The Journal of Immunology, 2001. **167**(2): p. 1060-1065.

520. Liew, F.Y., N.I. Pitman, and I.B. McInnes, *Disease-associated functions of IL-33: the new kid in the IL-1 family*. *Nature Reviews Immunology*, 2010. **10**(2): p. 103-110.
521. Raemdonck, K., et al., *CD4(+) and CD8(+) T cells play a central role in a HDM driven model of allergic asthma*. *Respir Res*, 2016. **17**: p. 45.
522. Barlow, J.L., et al., *IL-33 is more potent than IL-25 in provoking IL-13-producing nuocytes (type 2 innate lymphoid cells) and airway contraction*. *Journal of Allergy and Clinical Immunology*, 2013. **132**(4): p. 933-941.
523. Akbari, O., et al., *Essential role of NKT cells producing IL-4 and IL-13 in the development of allergen-induced airway hyperreactivity*. *Nature medicine*, 2003. **9**(5): p. 582-588.
524. Walter, D.M., et al., *Critical role for IL-13 in the development of allergen-induced airway hyperreactivity*. *The Journal of Immunology*, 2001. **167**(8): p. 4668-4675.
525. Alevy, Y.G., et al., *IL-13-induced airway mucus production is attenuated by MAPK13 inhibition*. *The Journal of clinical investigation*, 2012. **122**(12): p. 4555-4568.
526. Saha, S.K., et al., *Increased sputum and bronchial biopsy IL-13 expression in severe asthma*. *Journal of Allergy and Clinical Immunology*, 2008. **121**(3): p. 685-691.
527. Foster, P.S., et al., *The emerging role of microRNAs in regulating immune and inflammatory responses in the lung*. *Immunol Rev*, 2013. **253**(1): p. 198-215.
528. Asangani, I.A., et al., *MicroRNA-21 (miR-21) post-transcriptionally downregulates tumor suppressor Pcdcd4 and stimulates invasion, intravasation and metastasis in colorectal cancer*. *Oncogene*, 2008. **27**(15): p. 2128-36.
529. Tay, H.L., et al., *Antagonism of miR-328 increases the antimicrobial function of macrophages and neutrophils and rapid clearance of non-typeable *Haemophilus influenzae* (NTHi) from infected lung*. *PLoS Pathog*, 2015. **11**(4): p. e1004549.
530. Kim, R.Y., J.C. Horvat, J.W. Pinkerton, M.R. Starkey, A.T. Essilfie, J.R. Mayall, P.M. Nair, N.G. Hansbro, B. Jones, T.J. Haw, K.P. Sunkara, T.H. Nguyen, A.G. Jarnicki, S. Keely, J. Mattes, I.M. Adcock, P.S. Foster, and P.M. Hansbro, *MicroRNA-21 drives severe, steroid-insensitive experimental asthma by amplifying PI3K-mediated suppression of HDAC2*. *J Allergy Clin Immunol* 2016, in Press.
531. Meng, F., et al., *MicroRNA-21 regulates expression of the PTEN tumor suppressor gene in human hepatocellular cancer*. *Gastroenterology*, 2007. **133**(2): p. 647-658.
532. Carracedo, A. and P. Pandolfi, *The PTEN-PI3K pathway: of feedbacks and cross-talks*. *Oncogene*, 2008. **27**(41): p. 5527-5541.

533. Roy, S., et al., *MicroRNA expression in response to murine myocardial infarction: miR-21 regulates fibroblast metalloprotease-2 via phosphatase and tensin homologue*. Cardiovascular research, 2009.
534. Essilfie, A.T., et al., *Haemophilus influenzae infection drives IL-17-mediated neutrophilic allergic airways disease*. PLoS Pathog, 2011. **7**(10): p. e1002244.
535. Preston, J.A., et al., *Inhibition of allergic airways disease by immunomodulatory therapy with whole killed Streptococcus pneumoniae*. Vaccine, 2007. **25**(48): p. 8154-62.
536. Essilfie, A.T., et al., *Combined Haemophilus influenzae respiratory infection and allergic airways disease drives chronic infection and features of neutrophilic asthma*. Thorax, 2012. **67**(7): p. 588-99.
537. Beckett, E.L., et al., *A new short-term mouse model of chronic obstructive pulmonary disease identifies a role for mast cell tryptase in pathogenesis*. J Allergy Clin Immunol, 2013. **131**(3): p. 752-62.
538. Essilfie, A.T., et al., *Macrolide therapy suppresses key features of experimental steroid-sensitive and steroid-insensitive asthma*. Thorax, 2015. **70**(5): p. 458-67.
539. Tekkanat, K.K., et al., *IL-13-induced airway hyperreactivity during respiratory syncytial virus infection is STAT6 dependent*. J Immunol, 2001. **166**(5): p. 3542-8.
540. Jacoby, D.B., *Virus-induced asthma attacks*. Jama, 2002. **287**(6): p. 755-761.
541. Jain, S., et al., *Hospitalized patients with 2009 H1N1 influenza in the United States, April–June 2009*. New England journal of medicine, 2009. **361**(20): p. 1935-1944.
542. Van Kerkhove, M.D., et al., *Risk factors for severe outcomes following 2009 influenza A (H1N1) infection: a global pooled analysis*. PLoS medicine, 2011. **8**(7): p. e1001053.
543. Busse, W., J.E. Gern, and E.C. Dick. *The role of respiratory viruses in asthma*. in *The rising trends in asthma*. Ciba Foundation Symposium. 1997.
544. Jackson, D.J., et al., *Asthma exacerbations: origin, effect, and prevention*. Journal of Allergy and Clinical Immunology, 2011. **128**(6): p. 1165-1174.
545. Kawaguchi, A., et al., *Impacts of allergic airway inflammation on lung pathology in a mouse model of influenza A virus infection*. PloS one, 2017. **12**(2): p. e0173008.
546. Yamamoto, N., et al., *Immune response induced by airway sensitization after influenza A virus infection depends on timing of antigen exposure in mice*. Journal of virology, 2001. **75**(1): p. 499-505.
547. Chang, Y.-J., et al., *Influenza infection in suckling mice expands an NKT cell subset that protects against airway hyperreactivity*. The Journal of clinical investigation, 2011. **121**(1): p. 57.

548. Hazlewood, L.C., et al., *Dietary lycopene supplementation suppresses Th2 responses and lung eosinophilia in a mouse model of allergic asthma*. J Nutr Biochem, 2011. **22**(1): p. 95-100.
549. Daubeuf, F. and N. Frossard, *Eosinophils and the ovalbumin mouse model of asthma*. Methods Mol Biol, 2014. **1178**: p. 283-93.
550. Kung, T.T., et al., *Mechanisms of allergic pulmonary eosinophilia in the mouse*. Journal of allergy and clinical immunology, 1994. **94**(6): p. 1217-1224.
551. Grünig, G., et al., *Requirement for IL-13 independently of IL-4 in experimental asthma*. Science, 1998. **282**(5397): p. 2261-2263.
552. Zhu, Z., et al., *Pulmonary expression of interleukin-13 causes inflammation, mucus hypersecretion, subepithelial fibrosis, physiologic abnormalities, and eotaxin production*. Journal of Clinical Investigation, 1999. **103**(6): p. 779.
553. Ingram, J.L. and M. Kraft, *IL-13 in asthma and allergic disease: asthma phenotypes and targeted therapies*. Journal of Allergy and Clinical Immunology, 2012. **130**(4): p. 829-842.
554. Humbert, M., et al., *Elevated expression of messenger ribonucleic acid encoding IL-13 in the bronchial mucosa of atopic and nonatopic subjects with asthma*. Journal of Allergy and Clinical Immunology, 1997. **99**(5): p. 657-665.
555. Larcombe, A.N., et al., *Acute diesel exhaust particle exposure increases viral titre and inflammation associated with existing influenza infection, but does not exacerbate deficits in lung function*. Influenza and other respiratory viruses, 2013. **7**(5): p. 701-709.
556. Papadopoulos, N., et al., *Viruses and bacteria in acute asthma exacerbations—A GA2LEN-DARE systematic review*. Allergy, 2011. **66**(4): p. 458-468.
557. Miller, E.K., et al., *Influenza burden for children with asthma*. Pediatrics, 2008. **121**(1): p. 1-8.
558. Narain, J.P., R. Kumar, and R. Bhatia, *Pandemic (H1N1) 2009: epidemiological, clinical and prevention aspects*. 2009.
559. Deerojanawong, J., N. Prapphal, and Y. Poovorawan, *Prevalence, clinical presentations and complications among hospitalized children with influenza pneumonia*. Jpn. J. Infect. Dis, 2008. **61**: p. 446-449.
560. Kuperman, D.A., et al., *Direct effects of interleukin-13 on epithelial cells cause airway hyperreactivity and mucus overproduction in asthma*. Nature medicine, 2002. **8**(8): p. 885.
561. Woodruff, P.G., et al., *Genome-wide profiling identifies epithelial cell genes associated with asthma and with treatment response to corticosteroids*. Proceedings of the National Academy of Sciences, 2007. **104**(40): p. 15858-15863.
562. Atherton, H.C., G. Jones, and H. Danahay, *IL-13-induced changes in the goblet cell density of human bronchial epithelial cell cultures: MAP kinase*

- and phosphatidylinositol 3-kinase regulation*. American Journal of Physiology-Lung Cellular and Molecular Physiology, 2003. **285**(3): p. L730-L739.
563. Ptaschinski, C., et al., *Hox5 Paralogous Genes Modulate Th2 Cell Function during Chronic Allergic Inflammation via Regulation of Gata3*. J Immunol, 2017.
564. Hirose, K., et al., *Allergic airway inflammation: key players beyond the Th2 cell pathway*. Immunol Rev, 2017. **278**(1): p. 145-161.
565. Nair, P.M., et al., *Targeting PP2A and proteasome activity ameliorates features of allergic airway disease in mice*. Allergy, 2017.
566. Ye, P., et al., *Hyperoside attenuates OVA-induced allergic airway inflammation by activating Nrf2*. Int Immunopharmacol, 2017. **44**: p. 168-173.
567. Gour, N. and M. Wills-Karp, *IL-4 and IL-13 signaling in allergic airway disease*. Cytokine, 2015. **75**(1): p. 68-78.
568. Kaur, D., et al., *Mast cells express IL-13R alpha 1: IL-13 promotes human lung mast cell proliferation and Fc epsilon RI expression*. Allergy, 2006. **61**(9): p. 1047-53.
569. Karo-Atar, D., et al., *A protective role for IL-13 receptor alpha 1 in bleomycin-induced pulmonary injury and repair*. Mucosal immunology, 2016. **9**(1): p. 240-253.
570. Coyle, A.J., C.M. Lloyd, and J.C. Gutierrez-Ramos, *Biotherapeutic targets for the treatment of allergic airway disease*. Am J Respir Crit Care Med, 2000. **162**(4 Pt 2): p. S179-84.
571. Sinha, S., et al., *Association of IL13R alpha 1 +1398A/G polymorphism in a North Indian population with asthma: A case-control study*. Allergy Rhinol (Providence), 2015. **6**(2): p. 111-7.
572. Dickinson, J.D., et al., *IL13 activates autophagy to regulate secretion in airway epithelial cells*. Autophagy, 2016. **12**(2): p. 397-409.
573. Liu, Y., et al., *IL-13 induces connective tissue growth factor in rat hepatic stellate cells via TGF-beta-independent Smad signaling*. J Immunol, 2011. **187**(5): p. 2814-23.
574. Shimamura, T., et al., *Novel role of IL-13 in fibrosis induced by nonalcoholic steatohepatitis and its amelioration by IL-13R-directed cytotoxin in a rat model*. J Immunol, 2008. **181**(7): p. 4656-65.
575. Sugimoto, R., et al., *Effect of IL-4 and IL-13 on collagen production in cultured LI90 human hepatic stellate cells*. Liver Int, 2005. **25**(2): p. 420-8.
576. Akbari, O., et al., *Essential role of NKT cells producing IL-4 and IL-13 in the development of allergen-induced airway hyperreactivity*. Nat Med, 2003. **9**(5): p. 582-8.

577. Walker, C., et al., *Activated T cells and eosinophilia in bronchoalveolar lavages from subjects with asthma correlated with disease severity*. J Allergy Clin Immunol, 1991. **88**(6): p. 935-42.
578. Robinson, D.S., et al., *Activated memory T helper cells in bronchoalveolar lavage fluid from patients with atopic asthma: relation to asthma symptoms, lung function, and bronchial responsiveness*. Thorax, 1993. **48**(1): p. 26-32.
579. Ying, S., et al., *Expression of IL-4 and IL-5 mRNA and protein product by CD4+ and CD8+ T cells, eosinophils, and mast cells in bronchial biopsies obtained from atopic and nonatopic (intrinsic) asthmatics*. J Immunol, 1997. **158**(7): p. 3539-44.
580. Corry, D.B., et al., *Requirements for allergen-induced airway hyperreactivity in T and B cell-deficient mice*. Mol Med, 1998. **4**(5): p. 344-55.
581. Gavett, S.H., et al., *Depletion of murine CD4+ T lymphocytes prevents antigen-induced airway hyperreactivity and pulmonary eosinophilia*. Am J Respir Cell Mol Biol, 1994. **10**(6): p. 587-93.
582. Robinson, D., et al., *Activation of CD4+ T cells, increased TH2-type cytokine mRNA expression, and eosinophil recruitment in bronchoalveolar lavage after allergen inhalation challenge in patients with atopic asthma*. J Allergy Clin Immunol, 1993. **92**(2): p. 313-24.
583. Kon, O.M., et al., *Randomised, dose-ranging, placebo-controlled study of chimeric antibody to CD4 (keliximab) in chronic severe asthma*. Lancet, 1998. **352**(9134): p. 1109-13.
584. Betts, R.J. and D.M. Kemeny, *CD8+ T cells in asthma: friend or foe?* Pharmacology & therapeutics, 2009. **121**(2): p. 123-131.
585. Tay, H.L., et al., *Correction: Antagonism of miR-328 Increases the Antimicrobial Function of Macrophages and Neutrophils and Rapid Clearance of Non-typeable Haemophilus Influenzae (NTHi) from Infected Lung*. PLoS Pathog, 2015. **11**(6): p. e1004956.
586. Meng, F., et al., *MicroRNA-21 regulates expression of the PTEN tumor suppressor gene in human hepatocellular cancer*. Gastroenterology, 2007. **133**(2): p. 647-58.
587. Carracedo, A. and P.P. Pandolfi, *The PTEN-PI3K pathway: of feedbacks and cross-talks*. Oncogene, 2008. **27**(41): p. 5527-41.
588. Roy, S., et al., *MicroRNA expression in response to murine myocardial infarction: miR-21 regulates fibroblast metalloprotease-2 via phosphatase and tensin homologue*. Cardiovasc Res, 2009. **82**(1): p. 21-9.
589. Kim, R.Y., et al., *MicroRNA-21 drives severe, steroid-insensitive experimental asthma by amplifying phosphoinositide 3-kinase-mediated suppression of histone deacetylase 2*. J Allergy Clin Immunol, 2017. **139**(2): p. 519-532.
590. Sawant, D.V., et al., *Serum MicroRNA-21 as a Biomarker for Allergic Inflammatory Disease in Children*. Microna, 2015. **4**(1): p. 36-40.

591. Wu, X.B., et al., *Overexpression of microRNA-21 and microRNA-126 in the patients of bronchial asthma*. Int J Clin Exp Med, 2014. **7**(5): p. 1307-12.
592. Wu, S.Q., et al., *Effects of microRNA-21 on the interleukin 12/signal transducer and activator of transcription 4 signaling pathway in asthmatic mice*. Cent Eur J Immunol, 2014. **39**(1): p. 40-5.
593. McKenzie, G.J., et al., *Impaired development of Th2 cells in IL-13-deficient mice*. Immunity, 1998. **9**(3): p. 423-32.
594. Alvarez-Simon, D., et al., *Effects of diesel exhaust particle exposure on a murine model of asthma due to soybean*. PLoS One, 2017. **12**(6): p. e0179569.
595. He, J., et al., *Pulvis Fellis Suis extract attenuates ovalbumin-induced airway inflammation in murine model of asthma*. J Ethnopharmacol, 2017.
596. Lee, A.J., et al., *Lipopolysaccharide/TLR4 Stimulates IL-13 Production through a MyD88-BLT2-Linked Cascade in Mast Cells, Potentially Contributing to the Allergic Response*. J Immunol, 2017.
597. De Boever, E.H., et al., *Efficacy and safety of an anti-IL-13 mAb in patients with severe asthma: a randomized trial*. J Allergy Clin Immunol, 2014. **133**(4): p. 989-96.
598. Bagnasco, D., et al., *A Critical Evaluation of Anti-IL-13 and Anti-IL-4 Strategies in Severe Asthma*. Int Arch Allergy Immunol, 2016. **170**(2): p. 122-31.
599. Tattersfield, A.E., et al., *Exacerbations of asthma: a descriptive study of 425 severe exacerbations. The FACET International Study Group*. Am J Respir Crit Care Med, 1999. **160**(2): p. 594-9.
600. FitzGerald, J.M., et al., *Doubling the dose of budesonide versus maintenance treatment in asthma exacerbations*. Thorax, 2004. **59**(7): p. 550-6.
601. Wenzel, S.E., et al., *Bronchoscopic evaluation of severe asthma. Persistent inflammation associated with high dose glucocorticoids*. Am J Respir Crit Care Med, 1997. **156**(3 Pt 1): p. 737-43.
602. Green, R.H., et al., *Analysis of induced sputum in adults with asthma: identification of subgroup with isolated sputum neutrophilia and poor response to inhaled corticosteroids*. Thorax, 2002. **57**(10): p. 875-9.
603. Mori, H., et al., *Differences in respiratory syncytial virus and influenza infection in a house-dust-mite-induced asthma mouse model: consequences for steroid sensitivity*. Clin Sci (Lond), 2013. **125**(12): p. 565-74.
604. Somers, C.C., et al., *Effect of dexamethasone on respiratory syncytial virus-induced lung inflammation in children: results of a randomized, placebo controlled clinical trial*. Pediatr Allergy Immunol, 2009. **20**(5): p. 477-85.

605. van Woensel, J.B. and H. Vyas, *Dexamethasone in children mechanically ventilated for lower respiratory tract infection caused by respiratory syncytial virus: a randomized controlled trial*. Crit Care Med, 2011. **39**(7): p. 1779-83.
606. Adelroth, E., et al., *Inflammatory cells and eosinophilic activity in asthmatics investigated by bronchoalveolar lavage. The effects of antiasthmatic treatment with budesonide or terbutaline*. Am Rev Respir Dis, 1990. **142**(1): p. 91-9.
607. Crimi, E., et al., *Dissociation between airway inflammation and airway hyperresponsiveness in allergic asthma*. Am J Respir Crit Care Med, 1998. **157**(1): p. 4-9.
608. Lundgren, R., et al., *Morphological studies of bronchial mucosal biopsies from asthmatics before and after ten years of treatment with inhaled steroids*. Eur Respir J, 1988. **1**(10): p. 883-9.
609. Barnes, P.J., *Corticosteroid resistance in patients with asthma and chronic obstructive pulmonary disease*. J Allergy Clin Immunol, 2013. **131**(3): p. 636-45.
610. Plank, M., et al., *Targeting translational control as a novel way to treat inflammatory disease: the emerging role of microRNAs*. Clin Exp Allergy, 2013. **43**(9): p. 981-99.
611. Koziol-White, C.J., et al., *Inhibition of PI3K promotes dilation of human small airways in a rho kinase-dependent manner*. Br J Pharmacol, 2016. **173**(18): p. 2726-38.
612. Oikawa, Y., et al., *A phosphatidylinositol 3-kinase inhibitor strongly suppressed pulmonary vascular remodeling of allergic vasculitis in a murine model*. Exp Lung Res, 2016. **42**(3): p. 111-20.
613. Yao, L., et al., *Phosphatidylinositol 3-Kinase Mediates beta-Catenin Dysfunction of Airway Epithelium in a Toluene Diisocyanate-Induced Murine Asthma Model*. Toxicol Sci, 2015. **147**(1): p. 168-77.
614. Bartel, S., et al., *Pulmonary microRNA profiles identify involvement of Creb1 and Sec14l3 in bronchial epithelial changes in allergic asthma*. Sci Rep, 2017. **7**: p. 46026.
615. Huang, P., et al., *Comprehensive attenuation of IL-25-induced airway hyperresponsiveness, inflammation and remodelling by the PI3K inhibitor LY294002*. Respirology, 2017. **22**(1): p. 78-85.
616. Wagh, A.D., et al., *Investigation into the Role of PI3K and JAK3 Kinase Inhibitors in Murine Models of Asthma*. Front Pharmacol, 2017. **8**: p. 82.
617. Rao, V., *Airway Hyperresponsiveness: An Unsung Clinical Manifestation*. Journal of Allergy & Therapy 2016.
618. Scichilone, N., et al., *Clinical implications of airway hyperresponsiveness in COPD*. International journal of chronic obstructive pulmonary disease, 2006. **1**(1): p. 49.

619. Saito, Y., et al., *The effect of pharmacological PI3Kgamma inhibitor on eotaxin-induced human eosinophil functions*. *Pulm Pharmacol Ther*, 2014. **27**(2): p. 164-9.
620. Varkey, J.B. and B. Varkey, *Viral infections in patients with chronic obstructive pulmonary disease*. *Curr Opin Pulm Med*, 2008. **14**(2): p. 89-94.
621. Wark, P.A., et al., *Viral and bacterial infection in acute asthma and chronic obstructive pulmonary disease increases the risk of readmission*. *Respirology*, 2013. **18**(6): p. 996-1002.
622. Alevy, Y.G., et al., *IL-13-induced airway mucus production is attenuated by MAPK13 inhibition*. *J Clin Invest*, 2012. **122**(12): p. 4555-68.
623. Bel, E.H. and A. Ten Brinke, *New Anti-Eosinophil Drugs for asthma and COPD: targeting the trait!* *Chest*, 2017.
624. Hallstrand, T.S., et al., *Airway epithelial regulation of pulmonary immune homeostasis and inflammation*. *Clin Immunol*, 2014. **151**(1): p. 1-15.
625. Hsu, A.C., H.V. See, and P.A. Wark, *Innate immunity to influenza in chronic airways diseases*. *Respirology*, 2012.
626. Chaouat, A., et al., *Role for interleukin-6 in COPD-related pulmonary hypertension*. *Chest*, 2009. **136**(3): p. 678-87.
627. Meylan, E., et al., *RIP1 is an essential mediator of Toll-like receptor 3-induced NF-kappa B activation*. *Nat Immunol*, 2004. **5**(5): p. 503-7.
628. Monks, B.G., et al., *An upstream protein interacts with a distinct protein that binds to the cap site of the human interleukin 1 beta gene*. *Mol Immunol*, 1994. **31**(2): p. 139-51.
629. Tate, M.D., et al., *The role of neutrophils during mild and severe influenza virus infections of mice*. *PLoS ONE*, 2011. **6**(3): p. e17618.
630. Hashimoto, Y., et al., *Evidence for phagocytosis of influenza virus-infected, apoptotic cells by neutrophils and macrophages in mice*. *J Immunol*, 2007. **178**(4): p. 2448-57.
631. Verhelst, J., et al., *Interferon-inducible protein Mx1 inhibits influenza virus by interfering with functional viral ribonucleoprotein complex assembly*. *J Virol*, 2012. **86**(24): p. 13445-55.
632. Heyninck, K., et al., *The zinc finger protein A20 inhibits TNF-induced NF-kappaB-dependent gene expression by interfering with an RIP- or TRAF2-mediated transactivation signal and directly binds to a novel NF-kappaB-inhibiting protein ABIN*. *J Cell Biol*, 1999. **145**(7): p. 1471-82.
633. Heyninck, K. and R. Beyaert, *The cytokine-inducible zinc finger protein A20 inhibits IL-1-induced NF-kappaB activation at the level of TRAF6*. *FEBS Lett*, 1999. **442**(2-3): p. 147-50.
634. Grey, S.T., et al., *A20 inhibits cytokine-induced apoptosis and nuclear factor kappaB-dependent gene activation in islets*. *J Exp Med*, 1999. **190**(8): p. 1135-46.

635. Ferran, C., et al., *A20 inhibits NF-kappaB activation in endothelial cells without sensitizing to tumor necrosis factor-mediated apoptosis*. *Blood*, 1998. **91**(7): p. 2249-58.
636. Kim, S.W., et al., *MicroRNAs miR-125a and miR-125b constitutively activate the NF-kappaB pathway by targeting the tumor necrosis factor alpha-induced protein 3 (TNFAIP3, A20)*. *Proc Natl Acad Sci U S A*, 2012. **109**(20): p. 7865-70.
637. WHO, *Chronic Obstructive Pulmonary Disease (COPD)*. Fact Sheet No. 315, 2012. **accessed November 2012**.
638. Lopez, A.D., et al., *Global and regional burden of disease and risk factors, 2001: systematic analysis of population health data*. *Lancet*, 2006. **367**(9524): p. 1747-1757.
639. Hurst, J.R., et al., *Susceptibility to Exacerbation in Chronic Obstructive Pulmonary Disease*. *New England Journal of Medicine*, 2010. **363**(12): p. 1128-1138.
640. Soler-Cataluna, J.J., et al., *Severe acute exacerbations and mortality in patients with chronic obstructive pulmonary disease*. *Thorax*, 2005. **60**(11): p. 925-31.
641. Seemungal, T., et al., *Respiratory viruses, symptoms, and inflammatory markers in acute exacerbations and stable chronic obstructive pulmonary disease*. *Am J Respir Crit Care Med*, 2001. **164**(9): p. 1618-23.
642. Nath, K.D., et al., *Clinical factors associated with the humoral immune response to influenza vaccination in chronic obstructive pulmonary disease*. *Int J Chron Obstruct Pulmon Dis*, 2014. **9**: p. 51-6.
643. Hurt, A.C., et al., *Community transmission of oseltamivir-resistant A(H1N1)pdm09 influenza*. *N Engl J Med*, 2011. **365**(26): p. 2541-2.
644. Di Stefano, A., et al., *Increased expression of nuclear factor-kappaB in bronchial biopsies from smokers and patients with COPD*. *Eur Respir J*, 2002. **20**(3): p. 556-63.
645. Hsu, A.C., et al., *Human influenza is more effective than avian influenza at antiviral suppression in airway cells*. *American Journal of Respiratory Cell and Molecular Biology*, 2011. **44**(6): p. 906-13.
646. Chan, M.C., et al., *Proinflammatory cytokine responses induced by influenza A (H5N1) viruses in primary human alveolar and bronchial epithelial cells*. *Respir Res*, 2005. **6**: p. 135.
647. Hsu, A., et al., *Targeting PI3K-p110alpha Suppresses Influenza Virus Infection in Chronic Obstructive Pulmonary Disease*. *Am J Respir Crit Care Med*, 2015. **191**(9): p. 1012-23.
648. Hsu, A.C., et al., *Impaired Antiviral Stress Granule and IFN-beta Enhanceosome Formation Enhances Susceptibility to Influenza Infection in Chronic Obstructive Pulmonary Disease Epithelium*. *Am J Respir Cell Mol Biol*, 2016. **55**(1): p. 117-27.

649. Conickx, G., et al., *MicroRNA profiling reveals a role for microRNA-218-5p in the pathogenesis of chronic obstructive pulmonary disease*. Am J Respir Crit Care Med, 2016. **In Press**.
650. Fricker, M., A. Deane, and P.M. Hansbro, *Animal models of chronic obstructive pulmonary disease*. Expert Opin Drug Discov, 2014. **9**(6): p. 629-45.
651. Franklin, B.S., et al., *The adaptor ASC has extracellular and 'prionoid' activities that propagate inflammation*. Nat Immunol, 2014. **15**(8): p. 727-37.
652. Hansbro, P.M., et al., *Importance of mast cell Prss31/transmembrane tryptase/tryptase-gamma in lung function and experimental chronic obstructive pulmonary disease and colitis*. J Biol Chem, 2014. **289**(26): p. 18214-27.
653. Haw, T.J., et al., *A pathogenic role for tumor necrosis factor-related apoptosis-inducing ligand in chronic obstructive pulmonary disease*. Mucosal Immunol, 2015. **Advance online publication. 10.1038/mi.2015.111**.
654. Hsu, A.C., et al. *Enhanced levels of micro-RNA (miR)-125a/b increase inflammatory and impair antiviral responses to influenza infection in chronic obstructive pulmonary disease*. in *Federation of Immunological Societies of Asia-Oceania*. 2015. Singapore.
655. Pauwels, R.A., A.S. Buist, P.M. Calverley, C.R. Jenkins, and S.S. Hurd., *NHLBI/WHO Global initiative for chronic obstructive lung disease (GOLD) Workshop summary*. Am J Respir Crit Care Med 2001. **163**: p. 1256-1276.
656. Hurt, A.C., et al., *Isolation of avian influenza viruses from two different transhemispheric migratory shorebird species in Australia*. Arch Virol, 2006. **151**(11): p. 2301-9.
657. Hurd, S.Z., *Workshop summary and guidelines: investigative use of bronchoscopy*. J Allergy Clin Immunol 1991. **88**: p. 808-814.
658. Baines, K.J., et al., *Novel immune genes associated with excessive inflammatory and antiviral responses to rhinovirus in COPD*. Respir Res, 2013. **14**: p. 15.
659. Horvat, J.C., et al., *Chlamydial respiratory infection during allergen sensitization drives neutrophilic allergic airways disease*. J Immunol, 2010. **184**(8): p. 4159-69.
660. Thorburn, A.N., et al., *Components of Streptococcus pneumoniae suppress allergic airways disease and NKT cells by inducing regulatory T cells*. J Immunol, 2012. **188**(9): p. 4611-20.
661. Liu, G., et al., *Fibulin-1 regulates the pathogenesis of tissue remodeling in respiratory diseases*. JCI Insight, 2016. **1**(9):e86380.
662. Beckett, E., et al., *A short-term model of COPD identifies a role for mast cell tryptase*. J Allergy Clin Immunol, 2013. **Accepted 28.11.12**.

663. Plank, M.W., et al., *MicroRNA Expression Is Altered in an Ovalbumin-Induced Asthma Model and Targeting miR-155 with Antagomirs Reveals Cellular Specificity*. PLoS One, 2015. **10**(12): p. e0144810.
664. Kim, R.Y., et al., *MicroRNA-21 drives severe, steroid-insensitive experimental asthma by amplifying PI3K-mediated suppression of HDAC2*. Journal of Allergy and Clinical Immunology. **Accepted 30 Apr 2016**.
665. Horvat, J.C., et al., *Neonatal chlamydial infection induces mixed T-cell responses that drive allergic airway disease*. Am J Respir Crit Care Med, 2007. **176**(6): p. 556-64.
666. Starkey, M.R., et al., *Constitutive production of IL-13 promotes early-life Chlamydia respiratory infection and allergic airway disease*. Mucosal Immunol, 2013. **6**(3): p. 569-79.
667. Starkey, M.R., et al., *Tumor necrosis factor-related apoptosis-inducing ligand translates neonatal respiratory infection into chronic lung disease*. Mucosal Immunol, 2014. **7**(3): p. 478-88.
668. Liu, G., et al., *Fibulin-1 regulates the pathogenesis of tissue remodeling in respiratory diseases*. JCI Insight, 2016. **1**(9).
669. Haw, T.J., et al., *A pathogenic role for tumor necrosis factor-related apoptosis-inducing ligand in chronic obstructive pulmonary disease*. Mucosal Immunol, 2015.
670. Palmans, E., J.C. Kips, and R.A. Pauwels, *Prolonged allergen exposure induces structural airway changes in sensitized rats*. Am J Respir Crit Care Med, 2000. **161**(2 Pt 1): p. 627-35.
671. Hussain, S., et al., *Inflammasome activation in airway epithelial cells after multi-walled carbon nanotube exposure mediates a profibrotic response in lung fibroblasts*. Part Fibre Toxicol, 2014. **11**: p. 28.
672. Higham, A., et al., *Corticosteroid effects on COPD alveolar macrophages: dependency on cell culture methodology*. J Immunol Methods, 2014. **405**: p. 144-53.
673. Asher MI, et al., *Worldwide time trends in the prevalence of symptoms of asthma, allergic rhinoconjunctivitis, and eczema in childhood: ISAAC Phases One and Three repeat multicountry cross sectional surveys*. Lancet, 2006. **368**(9537): p. 733-43.
674. Kanner, R.E., et al., *Lower respiratory illnesses promote FEV(1) decline in current smokers but not ex-smokers with mild chronic obstructive pulmonary disease: results from the lung health study*. Am J Respir Crit Care Med, 2001. **164**(3): p. 358-64.
675. Seemungal, T.A., et al., *Effect of exacerbation on quality of life in patients with chronic obstructive pulmonary disease*. Am J Respir Crit Care Med, 1998. **157**(5 Pt 1): p. 1418-22.
676. Wang, Y.Y., et al., *A20 is a potent inhibitor of TLR3- and Sendai virus-induced activation of NF-kappaB and ISRE and IFN-beta promoter*. FEBS Lett, 2004. **576**(1-2): p. 86-90.

677. Barnes, P.J., *The cytokine network in asthma and chronic obstructive pulmonary disease*. J Clin Invest, 2008. **118**(11): p. 3546-56.
678. Jung, S.M., et al., *Smad6 inhibits non-canonical TGF-beta1 signalling by recruiting the deubiquitinase A20 to TRAF6*. Nat Commun, 2013. **4**: p. 2562.
679. Saitoh, T., et al., *A20 is a negative regulator of IFN regulatory factor 3 signaling*. J Immunol, 2005. **174**(3): p. 1507-12.
680. Maelfait, J., et al., *A20 (Tnfrsf3) deficiency in myeloid cells protects against influenza A virus infection*. PLoS Pathog, 2012. **8**(3): p. e1002570.
681. Rusinova, I., et al., *Interferome v2.0: an updated database of annotated interferon-regulated genes*. Nucleic Acids Res, 2013. **41**(Database issue): p. D1040-6.
682. Lee, H.M., T.S. Kim, and E.K. Jo, *MiR-146 and miR-125 in the regulation of innate immunity and inflammation*. BMB Rep, 2016. **49**(6): p. 311-8.
683. Chen, H. and Z. Xu, *Hypermethylation-Associated Silencing of miR-125a and miR-125b: A Potential Marker in Colorectal Cancer*. Dis Markers, 2015. **2015**: p. 345080.
684. Cisneros-Soberanis, F., M.A. Andonegui, and L.A. Herrera, *miR-125b-1 is repressed by histone modifications in breast cancer cell lines*. Springerplus, 2016. **5**(1): p. 959.
685. Kirkham, P.A. and P.J. Barnes, *Oxidative stress in COPD*. Chest, 2013. **144**(1): p. 266-73.
686. Fischer, B.M., E. Pavlisko, and J.A. Voynow, *Pathogenic triad in COPD: oxidative stress, protease-antiprotease imbalance, and inflammation*. Int J Chron Obstruct Pulmon Dis, 2011. **6**: p. 413-21.
687. Kratsovnik, E., et al., *Oxidative stress activates transcription factor NF-kB-mediated protective signaling in primary rat neuronal cultures*. J Mol Neurosci, 2005. **26**(1): p. 27-32.
688. Gamble, E., et al., *Airway mucosal inflammation in COPD is similar in smokers and ex-smokers: a pooled analysis*. European Respiratory Journal, 2007. **30**(3): p. 467-471.
689. Wu, W., et al., *Human primary airway epithelial cells isolated from active smokers have epigenetically impaired antiviral responses*. Respiratory research, 2016. **17**(1): p. 111.
690. Tan, G., et al., *NF-kappaB-dependent microRNA-125b up-regulation promotes cell survival by targeting p38alpha upon ultraviolet radiation*. J Biol Chem, 2012. **287**(39): p. 33036-47.
691. Werner, S.L., et al., *Encoding NF-kappaB temporal control in response to TNF: distinct roles for the negative regulators IkappaBalpha and A20*. Genes Dev, 2008. **22**(15): p. 2093-101.
692. Asher, M.I., et al., *Worldwide time trends in the prevalence of symptoms of asthma, allergic rhinoconjunctivitis, and eczema in childhood: ISAAC*

*Phases One and Three repeat multicountry cross-sectional surveys.* The Lancet, 2006. **368**(9537): p. 733-743.

693. Kim, R.Y., et al., *Infection-Induced MicroRNA-21 Drives Severe, Steroid-Insensitve Experimental Asthma By Amplifying Phosphoinositide-3-Kinase (PI3K)-Mediated Suppression Of Histone Deacetylase (HDAC) 2*, in *D14. EPIGENETIC REGULATION OF INFLAMMATION*. 2015, Am Thoracic Soc. p. A5384-A5384.
694. Hansbro, P., et al., *MicroRNA-21 drives severe, steroid-insensitive experimental asthma by amplifying PI3K-mediated suppression of HDAC2 (HYP7P. 262)*. The Journal of Immunology, 2015. **194**(1 Supplement): p. 191.10-191.10.
695. Kim, R.Y., et al., *MicroRNA-21 drives severe, steroid-insensitive experimental asthma by amplifying PI3K-mediated suppression of HDAC2*. Journal of Allergy and Clinical Immunology, 2016.
696. Simpson, J.L., et al., *Reduced antiviral interferon production in poorly controlled asthma is associated with neutrophilic inflammation and high-dose inhaled corticosteroids*. Chest, 2016. **149**(3): p. 704-713.
697. Pavord, I.D., et al., *The impact of poor asthma control among asthma patients treated with inhaled corticosteroids plus long-acting  $\beta$  2-agonists in the United Kingdom: a cross-sectional analysis*. NPJ primary care respiratory medicine, 2017. **27**(1): p. 17.
698. Horvat, J.C., et al., *Early-life chlamydial lung infection enhances allergic airways disease through age-dependent differences in immunopathology*. Journal of Allergy and Clinical Immunology, 2010. **125**(3): p. 617-625. e6.
699. Siegle, J.S., et al., *Airway hyperreactivity in exacerbation of chronic asthma is independent of eosinophilic inflammation*. Am J Respir Cell Mol Biol, 2006. **35**(5): p. 565-70.
700. Ito, K., et al., *Steroid-resistant neutrophilic inflammation in a mouse model of an acute exacerbation of asthma*. Am J Respir Cell Mol Biol, 2008. **39**(5): p. 543-50.
701. Herbert, C., et al., *Alveolar macrophages stimulate enhanced cytokine production by pulmonary CD4+ T-lymphocytes in an exacerbation of murine chronic asthma*. Am J Pathol, 2010. **177**(4): p. 1657-64.
702. Gauvreau, G.M., et al., *Effects of interleukin-13 blockade on allergen-induced airway responses in mild atopic asthma*. Am J Respir Crit Care Med, 2011. **183**(8): p. 1007-14.
703. Walter, D.M., et al., *Critical role for IL-13 in the development of allergen-induced airway hyperreactivity*. J Immunol, 2001. **167**(8): p. 4668-75.
704. Grunig, G., et al., *Requirement for IL-13 independently of IL-4 in experimental asthma*. Science, 1998. **282**(5397): p. 2261-3.
705. Wills-Karp, M., et al., *Interleukin-13: central mediator of allergic asthma*. Science, 1998. **282**(5397): p. 2258-61.

706. Kuperman, D., et al., *Signal transducer and activator of transcription factor 6 (Stat6)-deficient mice are protected from antigen-induced airway hyperresponsiveness and mucus production*. J Exp Med, 1998. **187**(6): p. 939-48.
707. Kuperman, D.A., et al., *Direct effects of interleukin-13 on epithelial cells cause airway hyperreactivity and mucus overproduction in asthma*. Nat Med, 2002. **8**(8): p. 885-9.
708. Zhu, Z., et al., *Pulmonary expression of interleukin-13 causes inflammation, mucus hypersecretion, subepithelial fibrosis, physiologic abnormalities, and eotaxin production*. J Clin Invest, 1999. **103**(6): p. 779-88.
709. Corren, J., et al., *Lebrikizumab treatment in adults with asthma*. N Engl J Med, 2011. **365**(12): p. 1088-98.
710. Hanania, N.A., et al., *Lebrikizumab in moderate-to-severe asthma: pooled data from two randomised placebo-controlled studies*. Thorax, 2015. **70**(8): p. 748-56.
711. Fricker, M., A. Deane, and P.M. Hansbro, *Animal models of chronic obstructive pulmonary disease*. Expert opinion on drug discovery, 2014. **9**(6): p. 629-645.
712. Jarnicki AG, D.A., Campbell JD, Kim RY, Beckett EL, Hsu AC, Wark PA, Foster PS, Spira A, Stevens RL, Hansbro PM., *Identification of a mRNA transcript signature in the lungs of mice with experimental COPD that is comparable to human disease*. PLoS One (Under revision), 2016.
713. Kupczyk, M. and P. Kuna, *[MicroRNAs--new biomarkers of respiratory tract diseases]*. Pneumonol Alergol Pol, 2014. **82**(2): p. 183-90.
714. Hsu, A.C., et al., *MicroRNA-125a and -b inhibit A20 and MAVS to promote inflammation and impair antiviral response in COPD*. JCI Insight, 2017. **2**(7): p. e90443.
715. Hackett, T.L., *Epithelial-mesenchymal transition in the pathophysiology of airway remodelling in asthma*. Curr Opin Allergy Clin Immunol, 2012. **12**(1): p. 53-9.
716. Johnson, J.R., et al., *Chronic respiratory aeroallergen exposure in mice induces epithelial-mesenchymal transition in the large airways*. PLoS One, 2011. **6**(1): p. e16175.
717. Zhang, J.G., et al., *MicroRNA-21 (miR-21) represses tumor suppressor PTEN and promotes growth and invasion in non-small cell lung cancer (NSCLC)*. Clin Chim Acta, 2010. **411**(11-12): p. 846-52.
718. Zhang, B.G., et al., *microRNA-21 promotes tumor proliferation and invasion in gastric cancer by targeting PTEN*. Oncol Rep, 2012. **27**(4): p. 1019-26.
719. Leslie, N.R. and C.P. Downes, *PTEN: The down side of PI 3-kinase signalling*. Cell Signal, 2002. **14**(4): p. 285-95.

720. Tan, W.C., *Viruses in asthma exacerbations*. *Curr Opin Pulm Med*, 2005. **11**(1): p. 21-6.
721. Johnston, S.L., et al., *The relationship between upper respiratory infections and hospital admissions for asthma: a time-trend analysis*. *Am J Respir Crit Care Med*, 1996. **154**(3 Pt 1): p. 654-60.
722. Kloefer, K.M., et al., *Increased H1N1 infection rate in children with asthma*. *Am J Respir Crit Care Med*, 2012. **185**(12): p. 1275-9.

# APPENDIX: PUBLICATIONS

# MicroRNA-125a and -b inhibit A20 and MAVS to promote inflammation and impair antiviral response in COPD

Alan C-Y. Hsu,<sup>1</sup> Kamal Dua,<sup>1</sup> Malcolm R. Starkey,<sup>1</sup> Tatt-Jhong Haw,<sup>1</sup> Prema M. Nair,<sup>1</sup> Kristy Nichol,<sup>1</sup> Nathan Zammit,<sup>2</sup> Shane T. Grey,<sup>2</sup> Katherine J. Baines,<sup>1</sup> Paul S. Foster,<sup>1</sup> Philip M. Hansbro,<sup>1</sup> and Peter A. Wark<sup>1,3</sup>

<sup>1</sup>Priority Research Centre for Healthy Lungs, Hunter Medical Research Institute and The University of Newcastle, New South Wales, Australia. <sup>2</sup>Transplantation Immunology Group, Immunology Division, Garvan Institute of Medical Research, Sydney, New South Wales, Australia. <sup>3</sup>Department of Respiratory and Sleep Medicine, John Hunter Hospital, Newcastle, New South Wales, Australia.

Influenza A virus (IAV) infections lead to severe inflammation in the airways. Patients with chronic obstructive pulmonary disease (COPD) characteristically have exaggerated airway inflammation and are more susceptible to infections with severe symptoms and increased mortality. The mechanisms that control inflammation during IAV infection and the mechanisms of immune dysregulation in COPD are unclear. We found that IAV infections lead to increased inflammatory and antiviral responses in primary bronchial epithelial cells (pBECs) from healthy nonsmoking and smoking subjects. In pBECs from COPD patients, infections resulted in exaggerated inflammatory but deficient antiviral responses. A20 is an important negative regulator of NF- $\kappa$ B-mediated inflammatory but not antiviral responses, and A20 expression was reduced in COPD. IAV infection increased the expression of miR-125a or -b, which directly reduced the expression of A20 and mitochondrial antiviral signaling (MAVS), and caused exaggerated inflammation and impaired antiviral responses. These events were replicated *in vivo* in a mouse model of experimental COPD. Thus, miR-125a or -b and A20 may be targeted therapeutically to inhibit excessive inflammatory responses and enhance antiviral immunity in IAV infections and in COPD.

## Introduction

Influenza A viruses (IAVs) are among the most important infectious human pathogens that cause enormous morbidity and mortality worldwide. This largely results from seasonal influenza, but an important feature of the biology of IAVs is the frequent emergence of novel pandemic strains/subtypes. Infections cause symptoms ranging from mild to severe viral pneumonia, with uncontrolled inflammation in the airways.

Bronchial epithelial cells (BECs) are the primary site of IAV infection, and innate immune responses produced by these cells are important in the early protection against the viruses (1, 2). During infection, viral RNAs are recognized by TLR3 and retinoic acid-inducible gene-I (RIG-I). Upon binding of TLR3 to viral RNAs, signalling pathways are initiated that activate receptor interacting protein 1 (RIP1) by ubiquitination. Activated RIP1 indirectly phosphorylates I $\kappa$ B $\alpha$ , leading to the release of active p65 and p50 subunits of NF- $\kappa$ B into the nucleus, where they induce the transcription of inflammatory genes including cytokines such as IL-6, TNF- $\alpha$ , and IL-1 $\beta$  and chemokines such as CXC chemokine ligand-8 (CXCL-8/IL-8) (3–5). These inflammatory cytokines recruit immune cells, in particular macrophages and neutrophils, to the site of infection that phagocytose pathogens and apoptotic cells (6, 7). RIG-I interacts with mitochondrial antiviral-signaling protein (MAVS), which activates interferon regulatory factor 3 (IRF3) by phosphorylation. Activated IRF3 then translocates into the nucleus, where it initiates the production of type I and III IFNs (8, 9). These innate cytokines induce the transcription of over 300 IFN-stimulated genes (ISGs), including the Mx1 protein that disrupts virus replication (10).

The control of inflammation is critical to achieving optimal inflammatory responses that clear viruses without excessive damage to host tissues and airways. We have previously shown that A20, also known as TNF- $\alpha$ -inducing protein 3 (TNFAIP3), is a negative regulator of NF- $\kappa$ B-mediated inflammation that

**Authorship note:** PMH and PAW are co-senior authors.

**Conflict of interest:** The authors have declared that no conflict of interest exists.

**Submitted:** October 24, 2016

**Accepted:** February 9, 2017

**Published:** April 6, 2017

**Reference information:**

JCI Insight. 2017;2(7):e90443. <https://doi.org/10.1172/jci.insight.90443>.

functions by targeting RIP1 for degradation, and therefore suppresses NF- $\kappa$ B activation (11–14). MicroRNAs (miRNAs) are another important class of immune signaling regulators that silence gene expression by degradation (15). miR-125a and -b have recently been shown to directly inhibit A20, leading to increased NF- $\kappa$ B activation (16). It is currently unknown if A20 or miR-125a or -b regulates type I and III IFNs during IAV infections.

Chronic obstructive pulmonary disease (COPD) is the third leading cause of illness and death globally and is characterized by progressive airway inflammation, emphysema, and reduced lung function (17). The most important risk factor for COPD in Western societies is cigarette smoking (18). COPD patients have increased susceptibility to IAV infections that cause acute exacerbations and result in more severe symptoms, disease progression, and increased mortality (19–21). Current therapeutics remain limited to vaccination and antiviral drugs. These have major issues with the constant need for developing new vaccines. COPD patients respond poorly to vaccination, as IAVs have become drug resistant and all therapeutics have questions surrounding availability and efficacy in future pandemics (22, 23). There is therefore an urgent need to develop novel therapeutics for influenza, especially for those most susceptible to infection.

Despite inflammatory signalling pathways being well characterized, the mechanisms underlying the exaggerated inflammatory responses to IAV, including in COPD, are unclear. It is known that increased NF- $\kappa$ B activation is elevated in biopsies from COPD patients (24). We have previously shown that human influenza H3N2 infection induced heightened inflammatory responses (25), and high pathogenic avian H5N1 is known to induce severe cytokine storms in the lung (9, 26). We also showed that primary BECs (pBECs) from COPD subjects and our established *in vivo* model of experimental COPD have increased inflammatory and impaired antiviral responses to IAV infections, leading to more severe infection (27–29). Furthermore, miRNAs are known to be altered in COPD (30, 31). However, the molecular mechanisms underpinning the heightened inflammatory response in IAV infections and defective immune responses in COPD remain unclear. In this study, we investigated the mechanisms involved using our established experimental systems (27, 32–34). We found that COPD pBECs and mice with experimental COPD infected with IAV have higher levels of inflammatory cytokines but reduced antiviral responses (30, 35). We uncovered that NF- $\kappa$ B-mediated inflammation in IAV infection and in COPD was also exaggerated and resulted from decreased levels of A20 protein, which in turn was caused by elevated levels of miR-125a or -b. Treatment with specific antagomirs against miR-125a or -b reduced NF- $\kappa$ B activation but also increased type I and III IFN production and suppressed infection. We then found that miR-125a and -b directly target MAVS 3'-UTR, thereby suppressing the induction of type I and III IFNs. This study therefore discovers an miR-125-mediated pathway that reduces A20 and MAVS, promotes excessive inflammation, and increases susceptibility to IAV infection in COPD. It also identifies potential therapeutic options that reduce IAV-mediated inflammation and reverse immune signaling abnormalities in COPD.

Some of the data has been previously reported in abstract form (36).

## Results

*IAV infection induces increased inflammatory but reduced antiviral responses ex vivo in human COPD pBECs.* pBECs from healthy nonsmoking control subjects, COPD patients (ex-smoker), or smoking (smoker) controls were infected with IAV H3N2 or H1N1 (MOI 5). Virus replication was measured 24 hours after infection. Virus titers increased at 24 hours (Figure 1A) and were 2-fold greater in COPD pBECs compared with controls. Infection resulted in the production of the proinflammatory cytokines/chemokines IL-6, CXCL-8, TNF- $\alpha$ , and IL-1 $\beta$  and antiviral cytokines type I (IFN- $\beta$ ) and type III interferons (IFN- $\lambda$ 1) (Figure 1B). In COPD, the induction levels of cytokines were substantially higher (2.5–10 fold) compared with healthy control and smoker pBECs (Figure 1B). In contrast, the induction of IFN- $\beta$  and IFN- $\lambda$ 1 proteins were reduced in COPD.

We then measured the levels of activity of NF- $\kappa$ B by assessing the levels of phosphorylated p65 (phospho-p65) at Ser536 (35, 37, 38). Infection significantly increased the activation of phospho-p65 in both healthy and smoker pBECs at 6 hours, which was further increased at 24 hours (Figure 1C and Supplemental Figure 1A; supplemental material available online with this article; <https://doi.org/10.1172/jci.insight.90443DS1>). In COPD pBECs, the protein levels of phospho-p65 was elevated at baseline (media controls) at 6 hours and significantly increased with infection at 24 hours compared with healthy and smoker controls.

*IAV infection also induces increased inflammatory but reduced antiviral responses in vivo in experimental COPD.* We then demonstrated these events also occur *in vivo*. BALB/c mice were exposed to either normal air (Air) or cigarette smoke (Smk) for 8 weeks. The Smk group develops hallmark features of

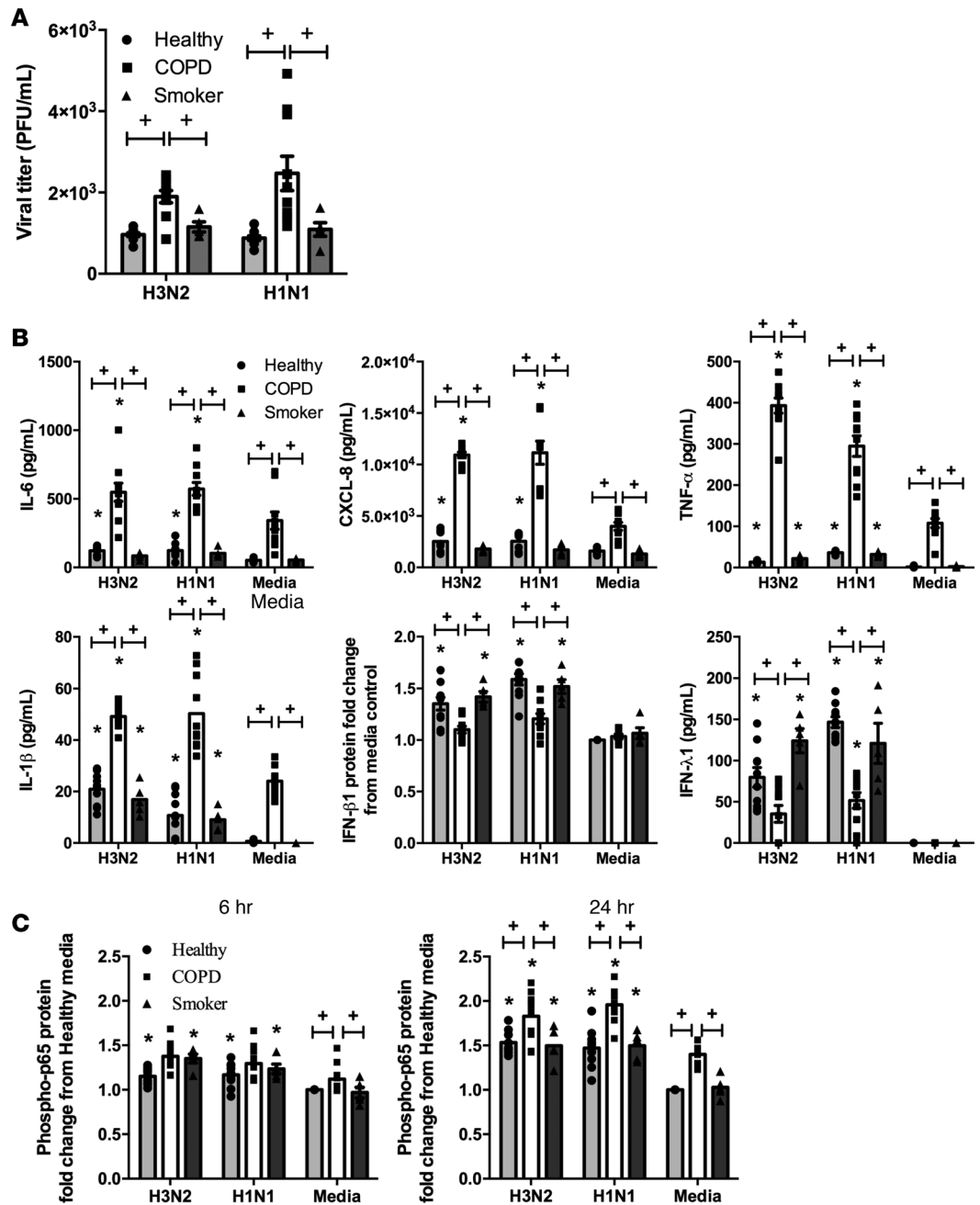


**Figure 1. IAV infection is more severe and results in exaggerated inflammatory but impaired antiviral responses in pBECs from patients with COPD.** pBECs from healthy controls, COPD patients, and healthy smokers were infected with human IAV H3N2 or H1N1, and (A) virus replication was measured at 24 hours. (B) Proinflammatory cytokines/chemokines IL-6, CXCL-8, TNF- $\alpha$ , and IL-1 $\beta$  and antiviral cytokines IFN- $\beta$  and IFN- $\lambda$ 1 were measured in culture supernatants at 24 hours. (C) Phospho-p65 was assessed at 6 hours and 24 hours, and densitometry results (from Supplemental Figure 1A, representative immunoblot) were calculated as phospho-p65/GAPDH ratios and expressed as fold change from healthy media control. Data are mean  $\pm$  SEM,  $n = 15$  (healthy controls and COPD patients) or 5 (healthy smokers). \* $P \leq 0.05$  versus respective uninfected media control, \* $P \leq 0.05$  versus infected or uninfected healthy controls. Statistical differences were determined with one-way ANOVA followed by Bonferroni post-test.

COPD as previously described (27, 28, 32–35, 39). Mice were then infected with IAV A/PR/8/34, and viral titers, airway inflammation (histopathological score), and inflammatory and antiviral cytokines were determined at 7 days postinfection (dpi) (Figure 2A). Infection in Air-exposed controls leads to virus replication (Figure 2B) that was accompanied by significant airway inflammation (histopathological score, Supplemental Figure 1B). Infection in Smk-exposed mice resulted in a significantly higher

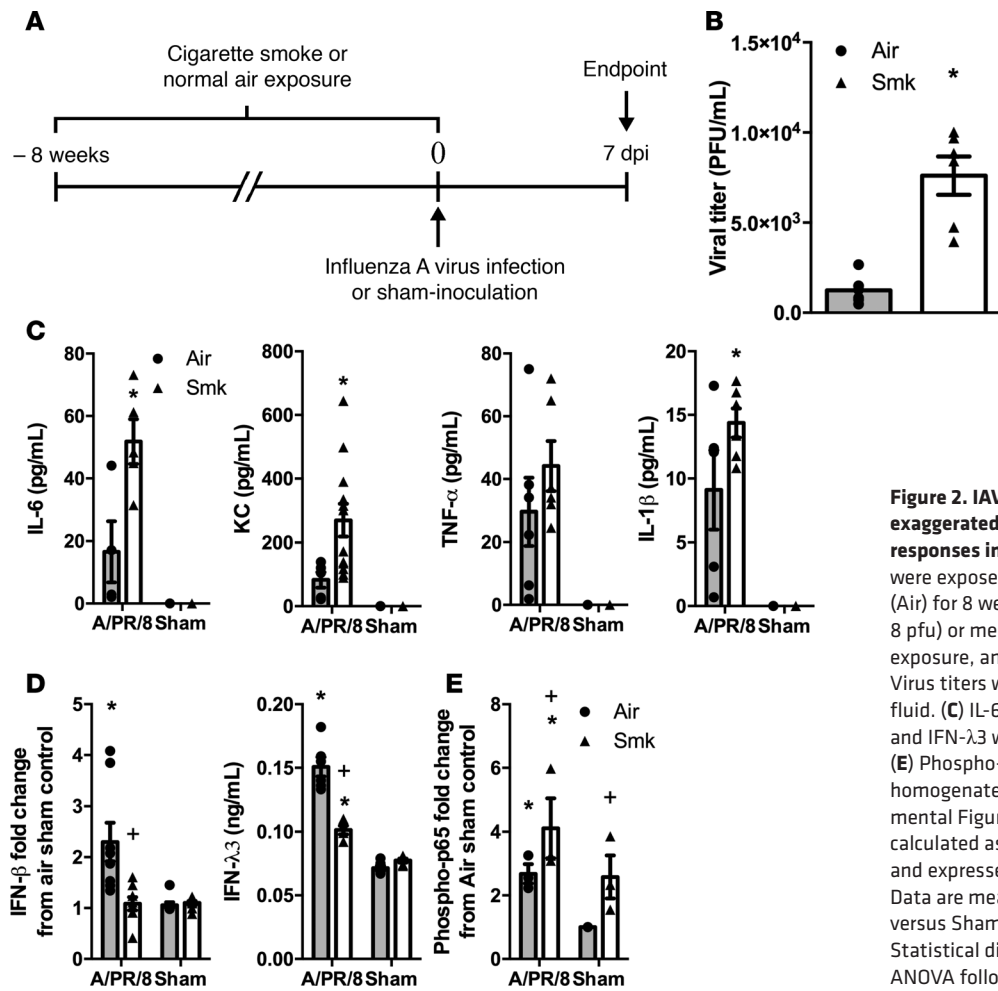


**Figure 2. IAV infection is more severe and results in exaggerated inflammatory and impaired antiviral responses in experimental COPD.** (A) BALB/c mice were exposed to cigarette smoke (Smk) or normal air (Air) for 8 weeks, infected with IAV H1N1 (A/PR/8/34, 8 pfu) or media (Sham) on the last day of smoke exposure, and sacrificed 7 days postinfection (dpi). (B) Virus titers were measured in bronchoalveolar lavage fluid. (C) IL-6, KC, TNF- $\alpha$ , and IL-1 $\beta$  and (D) IFN- $\beta$  and IFN- $\lambda$ 3 were assessed in lung homogenates. (E) Phospho-p65 protein was determined in lung homogenates. Densitometry results (from Supplemental Figure 1D, representative immunoblot) were calculated as phospho-p65 or IFN- $\beta$ / $\beta$ -actin ratios and expressed as fold change from Air sham control. Data are mean  $\pm$  SEM,  $n = 6-8$  per group. \* $P \leq 0.05$  versus Sham control, \* $P \leq 0.05$  versus Air control. Statistical differences were determined with one-way ANOVA followed by Bonferroni post-test.

virus titer (4-fold) and airway histopathological score (3-fold) compared with Air-exposed mice. In support of these data, the levels of the proinflammatory cytokines/chemokines IL-6, KC (mouse equivalent of CXCL-8), TNF- $\alpha$ , and IL-1 $\beta$  were also increased by infection in Air-exposed groups and to a greater extent in Smk-exposed groups (Figure 2C). Antiviral cytokines were increased in infected Air-exposed controls but were either not induced (IFN- $\beta$ ) or were induced to a much reduced level (IFN- $\lambda$ 3) in infected Smk-exposed groups (Figure 2D). The exaggerated release of proinflammatory cytokines was associated with significantly increased levels of phospho-p65 protein in infected Smk-exposed compared with Air-exposed controls (Figure 2E and Supplemental Figure 1C). In all experiments, ultraviolet-inactivated virus did not have any effects compared with media controls (data not shown).

Taken together, these human ex vivo and experimental in vivo data demonstrate that IAV infections result in increased airway inflammation and proinflammatory and antiviral responses. However, COPD is associated with exaggerated inflammation and reduced antiviral responses, leading to increased virus replication.

*A20 is an important negative regulatory of NF- $\kappa$ B-mediated inflammatory but not antiviral responses, and its expression is reduced in human COPD and experimental COPD.* We have previously shown that A20 is an important negative regulator of NF- $\kappa$ B activation (11–14), but its roles during IAV infection and whether it also regulates the induction of type I and III IFNs is unclear. We hypothesized that A20 protein expression would be downregulated and would contribute to the increased activation of NF- $\kappa$ B in response to IAV infection in COPD. IAV infection led to a significant induction of A20 protein at 6 hours and 24 hours in healthy and smoker controls, but this increase was impaired in COPD pBECs (Figure 3A and Supplemental Figure 2A). Similarly in Smk-exposed mice, A20 protein expression was reduced in airway epithelial cells compared with Air-exposed controls (Supplemental Figure 2B).

We then investigated if A20 was important in NF- $\kappa$ B-mediated inflammatory responses and if exaggerated p65 activation was the direct result of reduced A20 protein levels during infection in COPD pBECs.

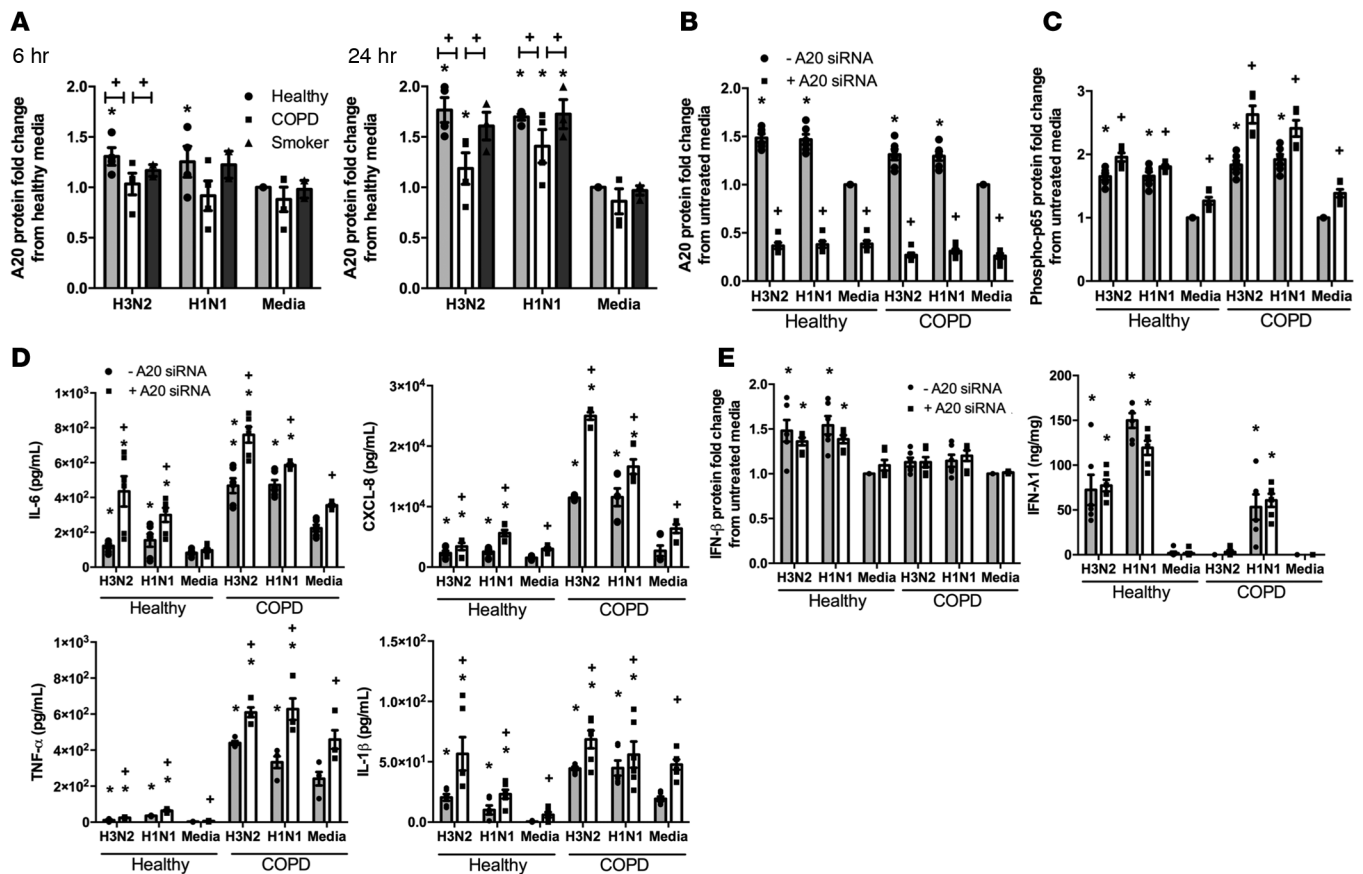


**Figure 3. A20 expression is reduced and negatively regulates inflammatory but not antiviral responses in pBECs from patients with COPD.** (A) pBECs were infected with human IAV H3N2 or H1N1, and the protein levels of A20 were determined at 6 hours and 24 hours. Densitometry results (from Supplemental Figure 2A, representative immunoblot) were calculated as A20 or phospho-p65/GAPDH ratios and expressed as fold change from healthy media control. Data are mean  $\pm$  SEM,  $n = 15$  per group. \* $P \leq 0.05$  versus respective uninfected media control,  $^{\dagger}P \leq 0.05$  versus healthy control. A20 expression was inhibited with a specific siRNA, pBECs were infected with IAVs, and protein levels of (B) A20; (C) phospho-p65; (D) cytokines/chemokines IL-6, CXCL-8, TNF- $\alpha$ , and IL-1 $\beta$ ; and antiviral (E) IFN- $\beta$  and IFN- $\lambda$ 1 were measured 24 hours later. Densitometric ratios (from Supplemental Figure 2C, representative immunoblot) were expressed as fold change from untreated media control. Data are mean  $\pm$  SEM,  $n = 3$  per group. \* $P \leq 0.05$  versus untreated, uninfected media control,  $^{\dagger}P \leq 0.05$  versus untreated infected or uninfected control. Statistical differences were determined with one-way ANOVA followed by Bonferroni post-test.

We inhibited A20 expression using A20-specific siRNA 24 hours before infection and measured the activation of p65 and the production of proinflammatory cytokines/chemokines 24 hours after infection. Inhibition of A20 expression (Figure 3B and Supplemental Figure 2C) resulted in significant increases in the protein levels of phospho-p65 (Figure 3C and Supplemental Figure 2C) and proinflammatory cytokines/chemokines IL-6, CXCL-8, TNF- $\alpha$ , and IL-1 $\beta$  (Figure 3D) compared with untreated controls, whether pBECs were infected or not. Conversely, ectopic expression (ecto-expression) using a pcDNA-A20 expression vector reduced the phosphorylation of p65 (Supplemental Figure 2D). Nevertheless, inhibition or ecto-expression of A20 did not affect IFN- $\beta$  and IFN- $\lambda$ 1 induction (Figure 3E and Supplemental Figure 2D). siRNA negative control or control vector did not affect the induction of A20 or phospho-p65 protein (Supplemental Figure 2, E and F).

Collectively, these data indicate that A20 is an important negative regulator of NF- $\kappa$ B but is dispensable in the induction of type I and III IFNs. A20 protein expression is dysregulated in COPD.

*Elevated miR-125a and -b levels decrease A20 levels, increase inflammation and impair antiviral responses in COPD pBEC and experimental COPD.* miR-125a and -b have recently been shown to directly target and inhibit A20 expression (16), but their roles during IAV infection and in COPD are unknown. Thus, we measured the levels of miR-125a and -b induced by IAV infection. H3N2 and H1N1 infections resulted in significant increases in the levels of these miRNAs at 24 hours in pBECs from all groups (Figure 4A). However, their levels were substantially greater at baseline and during infection (2- to 4-fold) in COPD pBECs compared with healthy controls. We then confirmed the direct link between increased miR-125a and -b levels and



Densitometry results (Supplemental Figure 3B, representative immunoblot) were calculated as A20 or phospho-p65/GAPDH ratios and expressed as fold change from untreated, uninfected control. Data are mean  $\pm$  SEM,  $n = 3$  per group. \* $P \leq 0.05$  versus untreated, uninfected media control; \* $P \leq 0.05$  versus untreated infected or uninfected group. (C) BALB/c mice were exposed to cigarette smoke (Smk) or normal air (Air) for 8 weeks, inoculated with IAV H1N1 (A/PR/8/34, 8 pfu) or media (Sham) on the last day of smoke exposure, and sacrificed 7 days postinfection (dpi). The levels of miR-125a and -b were measured. Data are mean  $\pm$  SEM,  $n = 6-8$  per group. \* $P \leq 0.05$  versus Sham group, \* $P \leq 0.05$  versus Air-infected or uninfected group. (D) In other groups, on the last day of smoke exposure, mice were treated with miR-125a or -b antagomir alone or in combination and infected with IAV, and (E) airway histological scores were assessed. Data are mean  $\pm$  SEM,  $n = 6-8$  per group. \* $P \leq 0.05$  versus infected and scrambled treated Air controls, \* $P \leq 0.05$  versus infected and scramble-treated Smk group. (F) The protein levels of A20, phospho-p65, and IFN- $\beta$  in lung homogenates were also measured. Densitometry results (Supplemental Figure 4D) were calculated as A20 or phospho-p65/ $\beta$ -actin ratios and expressed as fold change from untreated, uninfected control. Data are mean  $\pm$  SEM,  $n = 6-8$  per group. \* $P \leq 0.05$  versus infected scrambled-treated Air group, \* $P \leq 0.05$  versus infected scrambled Smk group. Statistical differences were determined with one-way ANOVA followed by Bonferroni post-test.

reduced A20 protein induction using specific antagomirs and mimetics. pBECs were pretreated with either miR-125a or -b specific antagomirs or mimetics for 24 hours before infection, and A20, phospho-p65, inflammatory, and antiviral cytokines were assessed 24 hours after infection. Antagomir treatment inhibited miR-125a or -b expression (Supplemental Figure 3A), and this resulted in significant increases in A20 protein production, reduced phosphorylation of p65, subsequent induction of proinflammatory cytokines/chemokines, and enhanced antiviral IFN- $\beta$  and  $\lambda 1$  responses (Figure 4B and Supplemental Figure 3, B–E) compared with untreated controls. Conversely, miR-125a or -b mimetics decreased A20 protein induction, increased phospho-p65 protein levels, and reduced IFN- $\beta$  responses (Supplemental Figure 3F). Treatment with scrambled miRNA or mimetic controls did not affect A20, phospho-p65, or IFN- $\beta$  production (Supplemental Figure 3, G and H).

We then assessed whether similar events occurred in vivo. IAV infection significantly increased the levels of miR-125a and -b in both groups, with the levels in Smk group significantly higher compared with Air-exposed controls (Figure 4C). We then inhibited miR-125a or -b before and during infection (Figure 4D). We also extended the ex vivo data by inhibiting both miR-125a and -b together. Treatment with miR-125a or -b antagomir, alone or in combination, reduced histopathological scores (Figure 4E and Supplemental Figure 4A) and improved lung function (reduced lung volume determined during a pressure-volume loop maneuver) in Air- and Smk-exposed groups compared with infected scrambled antagomir-treated controls (Supplemental Figure 4B). Inhibition of miR-125a, -b, or -a and -b, also increased A20 protein expression in the airway epithelium and decreased the levels of phospho-p65 compared with the controls (Figure 4F and Supplemental Figure 4, C and D). Importantly, while we could only detect reductions in TNF- $\alpha$  and KC with combined treatment (Supplemental Figure 4E), antagomir treatment, either alone or in combination, also significantly increased IFN- $\beta$  and IFN- $\lambda 3$  protein induction (Figure 4F and Supplemental Figure 4D).

Collectively, these data show that miR-125a and -b are directly involved in the regulation of both inflammatory cytokines — through the control of A20 — and antiviral cytokine production through an unknown target.

*miR-125a and -b target MAVS.* To determine the mechanism of miR-125a- and -b-mediated regulation of antiviral IFN- $\beta/\lambda$ , we performed miRNA prediction analysis using TargetScan ([www.targetscan.org](http://www.targetscan.org)). miR-125a and -b have a putative binding site in the 3'-UTR of human and mouse *MAVS* (Figure 5, A and B). To examine these putative interactions, we first assessed the protein levels of MAVS in pBECs. MAVS protein levels were significantly increased 24 hours after IAV infection in healthy control and smoker pBECs, but notably not in COPD pBECs (Figure 5C and Supplemental Figure 5A). Similarly, infection in Smk-exposed mice was also associated with significantly impaired production of MAVS compared with infected Air-exposed controls at 7 dpi (Figure 5D and Supplemental Figure 5B).

To confirm the potential interaction of miR-125a or -b and MAVS, we cloned the putative binding region of miR-125a and -b in WT (*MAVS-WT*) or mutant (*MAVS-MT*) *MAVS* 3'-UTR into a luciferase reporter construct. The construct was cotransfected into HEK293 cells along with miR-125a or -b mimetics, or scrambled controls, and then luciferase activity was assessed. Cotransfection of miR-125a or miR-125b mimetics with *MAVS-WT* resulted in a significant decrease in luciferase activity compared with scrambled controls (Figure 5E). There was no reduction in activity with cotransfection with *MAVS-MT*. We then determined if *MAVS* gene is present with the miR-125a or -b mimetics in the silencing complex. To do this, we immunoprecipitated Argonaute 2 (Ago2), a core component of RNA-induced silencing complex (RISC) that binds to the miRNAs and their target mRNA, with a specific antibody and detected the presence of both

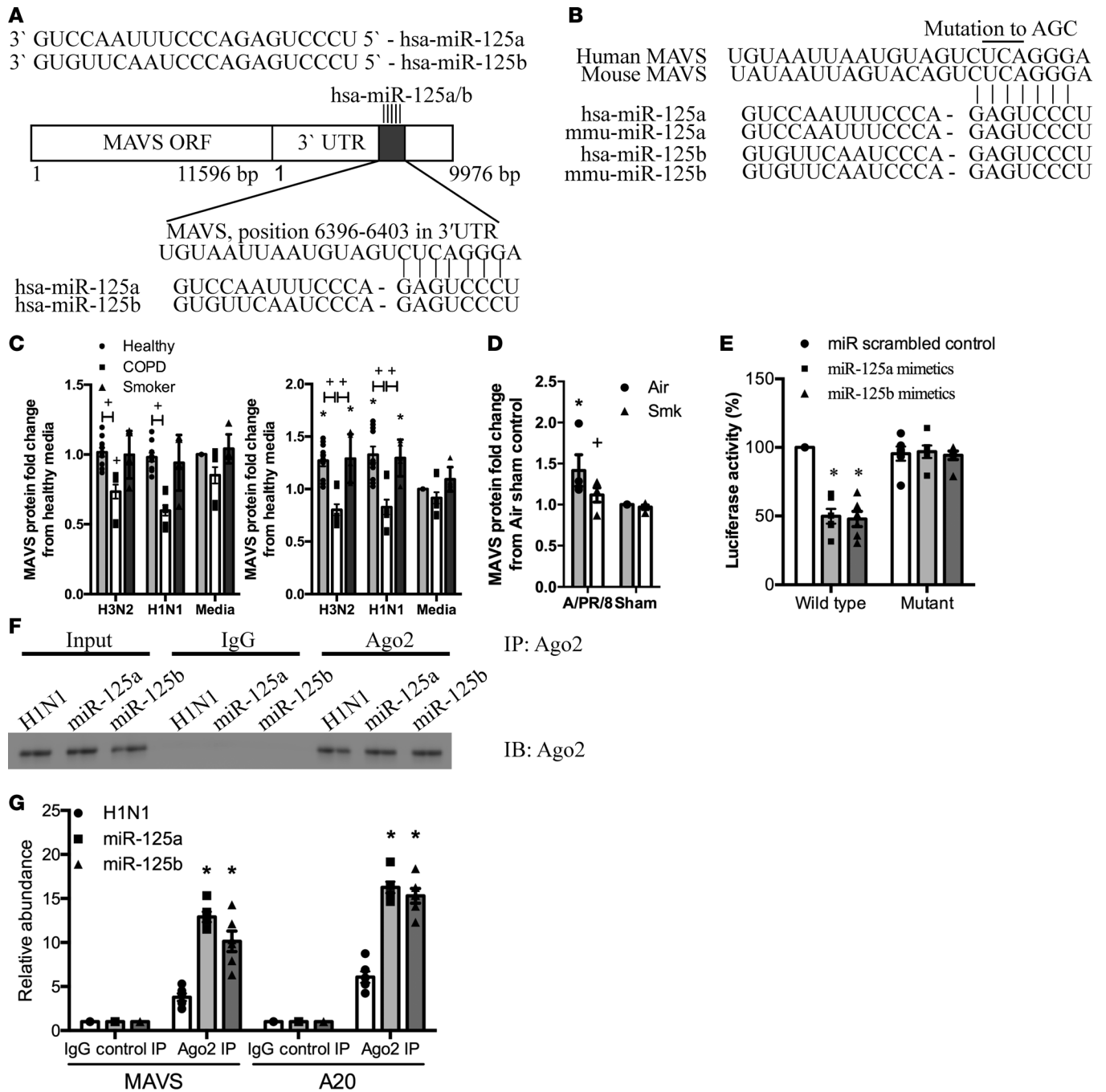


**Figure 5. miR-125a and -b target a functional binding site of the 3'-UTR of the mRNA of MAVS to suppress its expression.** (A) Representation of MAVS gene structure and location of miR-125a and -b binding site. (B) The binding site on 3'-UTR of MAVS is 100% conserved between human and mouse MAVS. (C) pBECs were infected with H3N2 or H1N1, and MAVS protein was detected at 6 hours (left) and 24 hours (right). Densitometry results (Supplemental Figure 5A, representative immunoblot) were calculated as MAVS/GAPDH ratios and expressed as fold change from untreated, uninfected controls. Data are mean  $\pm$  SEM,  $n = 15$  per group.  $*P \leq 0.05$  versus uninfected healthy or smoker controls,  $*P \leq 0.05$  versus infected or uninfected healthy controls. (D) BALB/c mice were exposed to cigarette smoke (Smk) or normal air (Air) for 8 weeks, inoculated with IAV H1N1 (A/PR/8/34, 8 pfu) or media (Sham) on the last day of smoke exposure, and sacrificed 7 days postinoculation (dpi). The levels of MAVS protein were measured in lung homogenates. Densitometry results (Supplemental Figure 5B, representative immunoblot) were calculated as MAVS/ $\beta$ -actin ratios in mouse and expressed as fold change from untreated, uninfected controls. Data are mean  $\pm$  SEM,  $n = 6$  per group.  $*P \leq 0.05$  versus Sham-treated controls,  $*P \leq 0.05$  versus infected Air controls. (E) The miR-125a and -b binding site on 3'-UTR was cloned into a pMIR luciferase reporter construct and transfected into HEK293 cells with miR-125a or -b mimetics. The luciferase reporter assay was performed to determine binding. Data are mean  $\pm$  SEM,  $n = 3$  per group.  $*P \leq 0.05$  versus miRNA scrambled controls. (F) Ago2 was immunoprecipitated from miR-125a or -b mimetic-transfected HEK293, and (G) A20 and MAVS mRNA was detected by qPCR in Ago2-immunoprecipitate. Data are mean  $\pm$  SEM,  $n = 3$  per group.  $*P \leq 0.05$  versus IgG control IP. Statistical differences were determined with one-way ANOVA followed by Bonferroni post-test.

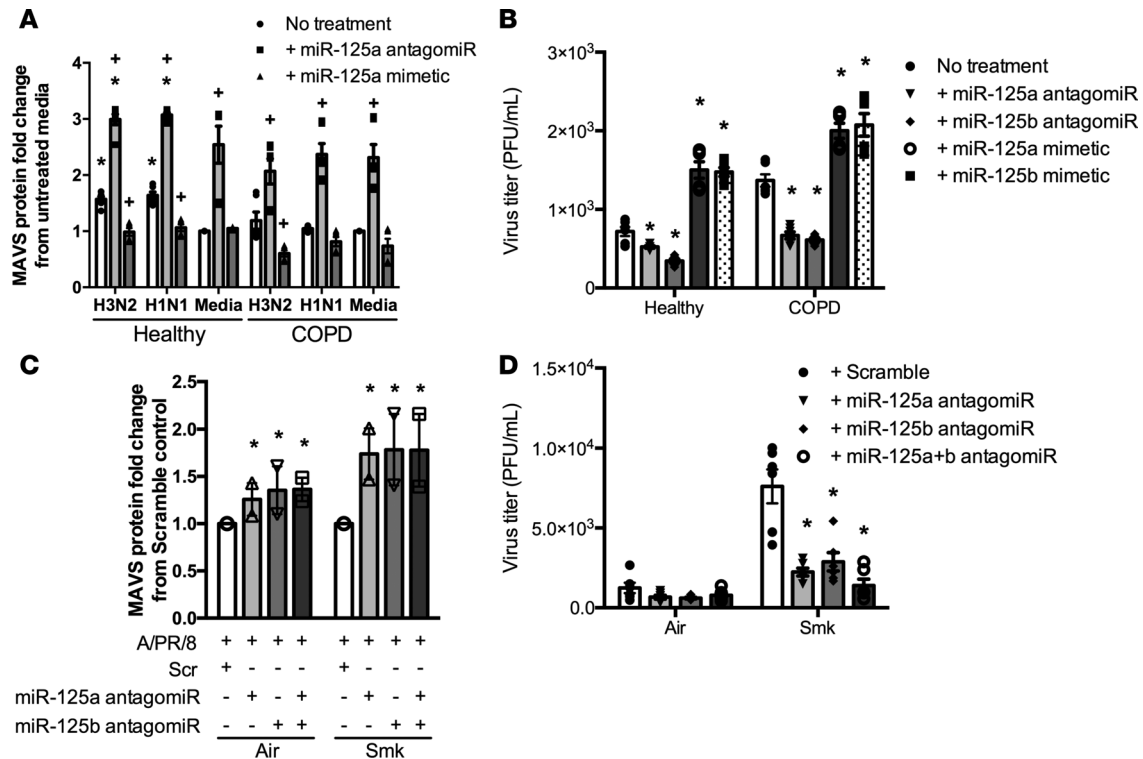


**Figure 6. miR-125a and -b suppress the induction of MAVS and promote virus replication in human COPD pBECs and experimental COPD.** (A) miR-125a and -b antagomiR or mimetics were added to pBECs before infection with human IAV H3N2 or H1N1, and mitochondrial antiviral signaling (MAVS) protein were assessed 24 hours after infection. Densitometry results (Supplemental Figure 6A, representative immunoblot) were calculated as MAVS/GAPDH ratios and expressed as fold change from untreated, uninfected controls. Data are mean  $\pm$  SEM,  $n = 3$ . \* $P \leq 0.05$  versus untreated, uninfected media controls; \* $P \leq 0.05$  versus untreated, infected or uninfected controls. (B) Virus replication was also measured. Data are mean  $\pm$  SEM,  $n = 3$ . \* $P \leq 0.05$  versus untreated, infected controls. (C) BALB/c mice were exposed to cigarette smoke (Smk) or normal air (Air) for 8 weeks, treated with miR-125a and/or -b antagomiR, infected with IAV H1N1 (A/PR/8/34, 8 pfu) or media (Sham) on the last day of smoke exposure, and sacrificed 7 days postinoculation (dpi). MAVS protein was measured. Densitometry results (Supplemental Figure 6C, representative immunoblot) were calculated as MAVS/ $\beta$ -actin ratios and expressed as fold change from untreated, uninfected controls. Data are mean  $\pm$  SEM,  $n = 6$ . \* $P \leq 0.05$  versus infected, scramble treated Air or Smk controls. (D) Virus replication was assessed. Data are mean  $\pm$  SEM,  $n = 6$ . \* $P \leq 0.05$  versus infected, scramble-treated controls. Statistical differences were determined with one-way ANOVA followed by Bonferroni post-test.

A20 and MAVS by qPCR, which could not be detected with immunoprecipitation with IgG control (Figure 5, F and G). This confirmed that miR-125a and -b directly bind to the endogenous 3'-UTR of MAVS.

*miR-125a and -b targeting of MAVS regulates antiviral responses in COPD pBEC and experimental COPD.* We then investigated whether inhibition of miR-125 has a functional outcome. We showed that miR-125a and -b antagomiR treatment led to significant increases in MAVS (Figure 6A and Supplemental Figure 6, A and B), IFN- $\beta$ , and IFN- $\lambda 1$  protein induction (Figure 4B and Supplemental Figure 3C) and reduced viral replication in both healthy and control pBECs (Figure 6B). In contrast, mimetics suppressed the induction of antiviral cytokines and increased virus titers (Supplemental Figure 3F). Similarly in Smk-exposed mice, inhibition of miR-125a, -b, or -a and -b resulted in increased induction of MAVS (Figure 6C and Supplemental Figure 6C), IFN- $\beta$ , and IFN- $\lambda 3$  (Figure 4F and Supplemental Figure 4, D and E) and inhibited virus replication (Figure 6D).

Collectively, these data demonstrate that miR-125a and -b negatively regulate MAVS expression, suppress the induction of IFN- $\beta/\lambda$ , and may potentially be targeted therapeutically in the prevention and/or treatment of IAVs and COPD.

## Discussion

Here, we discovered that IAV infections induce airway inflammation and antiviral responses; however, in COPD, pBECs and experimental COPD inflammatory responses and activation of NF- $\kappa$ B are exaggerated, but antiviral responses are impaired. We show that A20 is a negative regulator of NF- $\kappa$ B-mediated induction of inflammatory but not antiviral cytokines and that A20 protein levels were impaired in

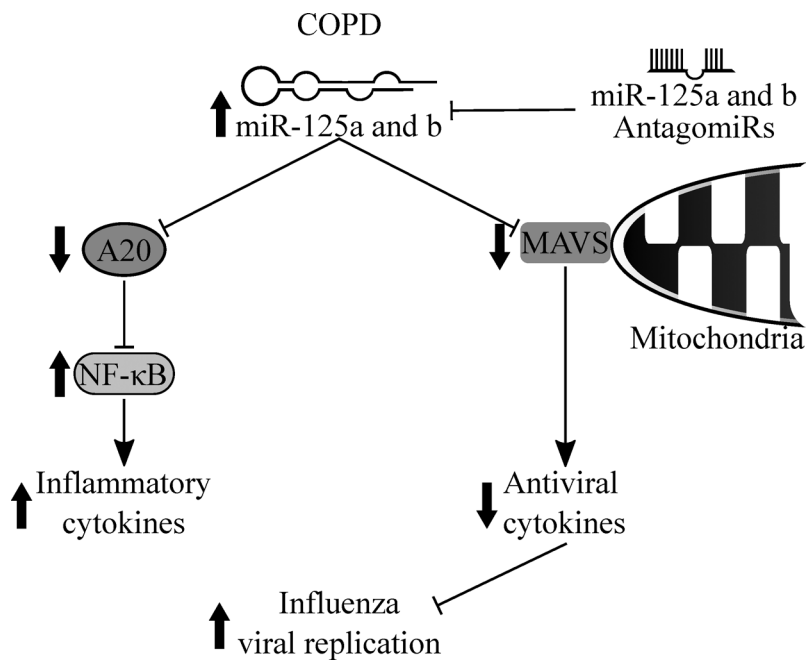


**Figure 7. Roles of miR-125a and -b in the regulation of inflammatory and antiviral responses in IAV infection.**

Increased levels of miR-125a and -b, for example in COPD, reduce the protein expression of A20 that results in uncontrolled NF- $\kappa$ B activation, leading to exaggerated induction of proinflammatory cytokines. miR-125a and -b also target and reduce MAVS and antiviral type I and III IFN production. Inhibition of miR-125a and -b enhances MAVS and antiviral responses, and it suppresses viral infection.

COPD. The impaired induction of A20 and antiviral responses in COPD were attributed to increased expression of miR-125a and -b. Elevated levels of these miRNAs suppressed A20 expression, leading to heightened NF- $\kappa$ B activity and inflammation and reduced antiviral responses. Inhibition with miR-125a and -b antagomirs increased A20 levels and reduced NF- $\kappa$ B activity, and also promoted IFN production. We then demonstrated that miR-125a and -b modulated IFN induction by targeting MAVS translation. MAVS protein levels were reduced in COPD but could be increased with specific miR-

125a and -b antagomir treatment that also induced IFN production. Thus, IAV infection induces the expression of miR-125a or -b that suppresses A20 and MAVS, in turn promoting NF- $\kappa$ B-induced inflammation and attenuating antiviral IFN production, respectively, increasing viral replication. All these events are exaggerated in COPD (Figure 7).

IAV is a major infectious pathogen that poses serious health concerns worldwide. Infections, particularly with highly pathogenic influenza viruses, cause severe airway inflammation and a cytokine storm with high morbidity and mortality. COPD is a major global health problem that is underpinned by exaggerated inflammatory responses in the airways (40). IAV infections frequently result in acute exacerbations of COPD, leading to accelerated declines in lung function (41, 42) and increased mortality (20). The mechanisms of exaggerated inflammation and severe outcomes in COPD are poorly understood, and there are no effective therapies for these events.

Here, we show that IAV-mediated inflammatory response are dampened with ectopic expression of A20 that reduces NF- $\kappa$ B activity and inflammatory responses, without affecting type I and III IFN responses. A20 is a deubiquitinating enzyme that degrades RIP1, inhibits NF- $\kappa$ B activation (13), and has been shown to suppress the induction of IFN- $\beta$  (43). We found that A20 modulated NF- $\kappa$ B activity and inflammation, but it did not affect type I and III IFNs production.

Consistent with our previous findings (27), IAV infections in COPD pBECs and experimental COPD led to heightened inflammation and production of inflammatory cytokines but impaired antiviral responses (IFN- $\beta$  and IFN- $\lambda$ ), which were associated with greater viral replication. Increased inflammation, inflammatory cytokines, and activation of NF- $\kappa$ B are well known in COPD (24, 44). Here, we show that these are the result of reduced induction of A20, leading to uncontrolled activation of NF- $\kappa$ B and subsequent induction of inflammatory cytokines. A20 is a pleiotropic protein involved in various ubiquitin-dependent pathways, including NF- $\kappa$ B (16) and MAPK pathway (45), and has also been shown to negatively regulate type I IFN inductions (43, 46, 47). Surprisingly, inhibition or ectopic expression of A20 did not affect IFN- $\beta$  production. The precise roles of A20 during viral infections, therefore, require further investigation. We could not rule out that other factors may also contribute to the regulation of A20 expression and of NF- $\kappa$ B activity, including other unidentified miRNAs, which may also be dysregulated in COPD.

Forced expression of A20 may be a novel therapeutic option that reduces IAV-mediated inflammation and cytokine storm, particularly from high pathogenic IAVs, such as H5N1, or in COPD where airway inflammation is already persistently heightened.

The lack of the induction of A20 protein during IAV infection in COPD was attributed to increased levels of miR-125a and -b. These miRNAs downregulate A20 expression by directly binding to its 3'-UTR,

Table 1. Subject characteristics

	Healthy	COPD	Smoker	P value
<i>n</i>	15	15	5	NA
Sex (male/female ratio)	1.14	1.2	1.5	<i>P</i> = 0.6
Mean age (SD)	62 (9.9)	68 (4.1)	64.33 (12.82)	<i>P</i> = 0.06
Mean FEV <sub>1</sub> (SD) <sup>a</sup>	105% (13.5)	40% (7.75)	97.66% (12.66)	<i>P</i> < 0.001
FEV <sub>1</sub> /FVC ratio (SD) <sup>a</sup>	886 (14.50)	40.20 (13.50)	77.80 (12.28)	<i>P</i> < 0.001
Cigarette (packs/year; SD)	0	53.70 (15.90)	30 (17.32)	<i>P</i> < 0.001
Years abstinent (SD)	0	13.0 (4.64)	0	NA
ICS (percent treated)	0	Seretide (10%) Spiriva (10%) Tiotropium (10%) Spiriva/Salbutamol (10%) Seretide/Tiotropium (20%) Seretide/Tiotropium/Ventolin (20%) Seretide/Spiriva/Ventolin (20%)	0	NA

<sup>a</sup>FEV<sub>1</sub> and FEV<sub>1</sub>/FVC ratios are % predicted values. FEV<sub>1</sub> is the forced expiratory volume in 1s expressed as a percentage of the predicted value. FVC is forced vital capacity. The statistical analysis used was ANOVA for multiple groups. NA, not applicable.

leading to constitutive activation of NF- $\kappa$ B (16). We found that heightened levels of miR-125a or -b resulted in increased activation of NF- $\kappa$ B in COPD. Inhibition of miR-125a or -b in both healthy and COPD pBECs and in experimental COPD increased A20 protein levels and reduced NF- $\kappa$ B activation during IAV infection.

We also found that miR-125a and -b modulated the induction of type I and III antiviral IFNs. This occurred by the direct targeting of MAVS 3'-UTR, therefore downregulating the subsequent induction of IFN- $\beta$  and IFN- $\lambda$ . MAVS is an important adaptor protein on mitochondria that facilitates the production of IFNs (8); however, there was an impaired induction of MAVS by IAV infections in COPD pBECs and in experimental COPD. Inhibition of miR-125a and/or -b increased the levels of MAVS and antiviral IFNs, which led to reduced virus replication both in vivo and in vitro. Interestingly, antagomirs against miR-125a and/or -b in experimental COPD partially reduced the release of inflammatory cytokines and substantially suppressed virus replication. This may indicate that miR-125a and -b may preferentially target MAVS over A20 during IAV infection in COPD, although such binding preferences of miRNAs have not been widely investigated. Furthermore, as MAVS is transcriptionally driven by IFN-sensitive response element (ISRE) as part of the ISGs (48), and miR-125a or -b have been reported to be induced by NF- $\kappa$ B (49), it is possible that reduced MAVS partly attributed to impaired IFNs in COPD; with enhanced expression of miR-125a or -b (NF- $\kappa$ B-inducible), this then leads to a continuous cycle of exaggerated inflammation and impaired antiviral immunity in COPD.

Although miR-125a or -b appear to be NF- $\kappa$ B inducible, the exact molecular mechanisms of enhanced miR-125a or -b expression in COPD require further investigation. In colorectal cancer tissues, the levels of miR-125a have been shown to be reduced, which is associated with hypermethylation at the CpG island within the promoter region of miR-125a (50). Similarly, in breast cancer cell lines, reduced miR-125a has also been shown to be associated with trimethylation at H3K9 and H3K27 at the promoter region of miR-125a (51). It is therefore possible that the methylation status of miR-125a or -b promoter site is altered in COPD, leading to increased expression of miR-125a or -b. Nevertheless, our data also demonstrate that specific inhibition of miR-125a or -b may be a novel therapeutic option against IAV infections and for those most vulnerable.

Cigarette smoke is the major risk factor for COPD. Acute exposure results in oxidative stress and NF- $\kappa$ B activation (52–54). However, the effects we have observed in COPD appear to be independent of acute exposure to cigarette smoking, as the pBECs obtained from subjects with COPD were all abstinent from smoking for at least 10 years. It is likely that chronic exposure progressively leads to persistent induction of miR-125a and -b and NF- $\kappa$ B activation (55, 56), which then reduces the induction of A20 and MAVS in COPD.

Collectively, our results demonstrate that A20 regulates NF- $\kappa$ B activation and, subsequently, the production of inflammatory cytokines, but not antiviral IFNs. COPD pBECs and mice with experimental COPD responded to IAV infection with an exaggerated inflammatory but impaired antiviral responses. Increased levels of miR-125a and -b by IAV and in COPD suppressed protein inductions of A20 and

MAVS, leading to heightened airway inflammation and reduced IFN production. Inhibition of miR-125a and -b reduced the induction of inflammatory cytokines and enhanced antiviral responses to IAV infection in both healthy and COPD states. This study therefore identifies a potential therapeutic target for IAV infection in general and in COPD.

## Methods

*Ex vivo.* COPD patients (10) and healthy nonsmoking (10) and smoking (5) controls were recruited, and their characteristics are shown in Table 1. Subject recruitment, viruses, cell culture and viral infection, A20 plasmid, siRNA, miR-125a and -b antagomir/mimetic treatment, cloning and mutagenesis of miR-125a and -b binding sites in MAVS 3'-UTR, reporter assays, immunoblotting, cytometric bead array, immunoprecipitation, miRNA extraction and analysis, and statistical tests were performed as previously described and/or as in Supplemental Methods (27, 31, 57, 58).

*In vivo.* Experimental COPD and influenza infection were induced; miR-125a and -b were inhibited using specific antagomirs; and histopathology, IHC, immunoblotting, and cytometric bead array and data analyses were performed as previously described and/or as in Supplemental Methods (33, 35, 39, 59–67).

*Statistics.* When data were normally distributed, they were expressed as mean  $\pm$  SEM. Data were analyzed using nonparametric equivalents and summarized using the median and interquartile range (IQR) when non-normally distributed. Multiple comparisons were first analyzed by the Kruskal Wallis test and then by individual testing, if significant.  $P < 0.05$  was considered significant.

*Study Approval.* All procedures were approved by The University of Newcastle Human and Animal Ethics Committees.

## Author contributions

ACYH conceived and designed the study. ACYH and KN performed all in vitro experiments. KD, TJH, and PMN performed all in vivo experiments. ACYH, KD, MRS, TJH, PMN, KN, NZ, STG, KJB, PSF, PMH, and PAW participated in the completion of the manuscript.

## Acknowledgments

This study is funded by National Health and Medical Research Council of Australia (grant no. 1045762) and University of Newcastle (grant no. 1300661). The authors thank Kristy Wheeldon and Nathalie Kiaos for technical assistance with in vivo protocols.

Address correspondence to: Alan Hsu or Phil Hansbro, Priority Research Centre for Healthy Lungs, Hunter Medical Research Institute, Lot 1 Kookaburra Circuit, New Lambton Heights, Newcastle, NSW 2305, Australia. Phone: 61.2.4042.0109; E-mail: Alan.Hsu@newcastle.edu.au (A. Hsu); Philip.Hansbro@newcastle.edu.au (P. Hansbro).

- Hallstrand TS, Hackett TL, Altemeier WA, Matute-Bello G, Hansbro PM, Knight DA. Airway epithelial regulation of pulmonary immune homeostasis and inflammation. *Clin Immunol.* 2014;151(1):1–15.
- Hsu AC, See HV, Hansbro PM, Wark PA. Innate immunity to influenza in chronic airways diseases. *Respirology.* 2012;17(8):1166–1175.
- Chaouat A, et al. Role for interleukin-6 in COPD-related pulmonary hypertension. *Chest.* 2009;136(3):678–687.
- Meylan E, et al. RIP1 is an essential mediator of Toll-like receptor 3-induced NF-kappa B activation. *Nat Immunol.* 2004;5(5):503–507.
- Monks BG, Martell BA, Buras JA, Fenton MJ. An upstream protein interacts with a distinct protein that binds to the cap site of the human interleukin 1 beta gene. *Mol Immunol.* 1994;31(2):139–151.
- Tate MD, Ioannidis LJ, Croker B, Brown LE, Brooks AG, Reading PC. The role of neutrophils during mild and severe influenza virus infections of mice. *PLoS ONE.* 2011;6(3):e17618.
- Hashimoto Y, Moki T, Takizawa T, Shiratsuchi A, Nakanishi Y. Evidence for phagocytosis of influenza virus-infected, apoptotic cells by neutrophils and macrophages in mice. *J Immunol.* 2007;178(4):2448–2457.
- Seth RB, Sun L, Ea CK, Chen ZJ. Identification and characterization of MAVS, a mitochondrial antiviral signaling protein that activates NF-kappaB and IRF 3. *Cell.* 2005;122(5):669–682.
- Hsu AC, et al. Critical role of constitutive type I interferon response in bronchial epithelial cell to influenza infection. *PLoS ONE.* 2012;7(3):e32947.
- Verhelst J, Parthoens E, Schepens B, Fiers W, Saelens X. Interferon-inducible protein Mx1 inhibits influenza virus by interfering with functional viral ribonucleoprotein complex assembly. *J Virol.* 2012;86(24):13445–13455.

11. Heynink K, et al. The zinc finger protein A20 inhibits TNF-induced NF-kappaB-dependent gene expression by interfering with an RIP- or TRAF2-mediated transactivation signal and directly binds to a novel NF-kappaB-inhibiting protein ABIN. *J Cell Biol.* 1999;145(7):1471–1482.
12. Heynink K, Beyaert R. The cytokine-inducible zinc finger protein A20 inhibits IL-1-induced NF-kappaB activation at the level of TRAF6. *FEBS Lett.* 1999;442(2-3):147–150.
13. Grey ST, Arvelo MB, Hasenkamp W, Bach FH, Ferran C. A20 inhibits cytokine-induced apoptosis and nuclear factor kappaB-dependent gene activation in islets. *J Exp Med.* 1999;190(8):1135–1146.
14. Ferran C, et al. A20 inhibits NF-kappaB activation in endothelial cells without sensitizing to tumor necrosis factor-mediated apoptosis. *Blood.* 1998;91(7):2249–2258.
15. Foster PS, et al. The emerging role of microRNAs in regulating immune and inflammatory responses in the lung. *Immunol Rev.* 2013;253(1):198–215.
16. Kim SW, Ramasamy K, Bouamar H, Lin AP, Jiang D, Aguiar RC. MicroRNAs miR-125a and miR-125b constitutively activate the NF-kB pathway by targeting the tumor necrosis factor alpha-induced protein 3 (TNFAIP3, A20). *Proc Natl Acad Sci USA.* 2012;109(20):7865–7870.
17. World Health Organization. Chronic Obstructive Pulmonary Disease (COPD) Fact Sheet. <http://www.who.int/mediacentre/factsheets/fs315/en/>. Published November 2016. Accessed February 20, 2017.
18. Lopez AD, Mathers CD, Ezzati M, Jamison DT, Murray CJ. Global and regional burden of disease and risk factors, 2001: systematic analysis of population health data. *Lancet.* 2006;367(9524):1747–1757.
19. Hurst JR, et al. Susceptibility to exacerbation in chronic obstructive pulmonary disease. *N Engl J Med.* 2010;363(12):1128–1138.
20. Soler-Cataluña JJ, Martínez-García MA, Román Sánchez P, Salcedo E, Navarro M, Ochando R. Severe acute exacerbations and mortality in patients with chronic obstructive pulmonary disease. *Thorax.* 2005;60(11):925–931.
21. Seemungal T, et al. Respiratory viruses, symptoms, and inflammatory markers in acute exacerbations and stable chronic obstructive pulmonary disease. *Am J Respir Crit Care Med.* 2001;164(9):1618–1623.
22. Nath KD, et al. Clinical factors associated with the humoral immune response to influenza vaccination in chronic obstructive pulmonary disease. *Int J Chron Obstruct Pulmon Dis.* 2014;9:51–56.
23. Hurt AC, et al. Community transmission of oseltamivir-resistant A(H1N1)pdm09 influenza. *N Engl J Med.* 2011;365(26):2541–2542.
24. Di Stefano A, et al. Increased expression of nuclear factor-kappaB in bronchial biopsies from smokers and patients with COPD. *Eur Respir J.* 2002;20(3):556–563.
25. Hsu AC, Barr I, Hansbro PM, Wark PA. Human influenza is more effective than avian influenza at antiviral suppression in airway cells. *Am J Respir Cell Mol Biol.* 2011;44(6):906–913.
26. Chan MC, et al. Proinflammatory cytokine responses induced by influenza A (H5N1) viruses in primary human alveolar and bronchial epithelial cells. *Respir Res.* 2005;6:135.
27. Hsu AC, et al. Targeting PI3K-p110 $\alpha$  Suppresses Influenza Virus Infection in Chronic Obstructive Pulmonary Disease. *Am J Respir Crit Care Med.* 2015;191(9):1012–1023.
28. Beckett EL, et al. A new short-term mouse model of chronic obstructive pulmonary disease identifies a role for mast cell tryptase in pathogenesis. *J Allergy Clin Immunol.* 2013;131(3):752–762.
29. Hsu AC, et al. Impaired Antiviral Stress Granule and IFN- $\beta$  Enhanceosome Formation Enhances Susceptibility to Influenza Infection in Chronic Obstructive Pulmonary Disease Epithelium. *Am J Respir Cell Mol Biol.* 2016;55(1):117–127.
30. Tay HL, et al. Antagonism of miR-328 increases the antimicrobial function of macrophages and neutrophils and rapid clearance of non-typeable Haemophilus influenzae (NTHi) from infected lung. *PLoS Pathog.* 2015;11(4):e1004549.
31. Conicx G, et al. MicroRNA Profiling Reveals a Role for MicroRNA-218-5p in the Pathogenesis of Chronic Obstructive Pulmonary Disease. *Am J Respir Crit Care Med.* 2017;195(1):43–56.
32. Fricker M, Deane A, Hansbro PM. Animal models of chronic obstructive pulmonary disease. *Expert Opin Drug Discov.* 2014;9(6):629–645.
33. Franklin BS, et al. The adaptor ASC has extracellular and ‘prionoid’ activities that propagate inflammation. *Nat Immunol.* 2014;15(8):727–737.
34. Hansbro PM, et al. Importance of mast cell Prss31/transmembrane tryptase/tryptase- $\gamma$  in lung function and experimental chronic obstructive pulmonary disease and colitis. *J Biol Chem.* 2014;289(26):18214–18227.
35. Haw TJ, et al. A pathogenic role for tumor necrosis factor-related apoptosis-inducing ligand in chronic obstructive pulmonary disease. *Mucosal Immunol.* 2016;9(4):859–872.
36. Mehra NK. A brief history of the Federation of Immunological Societies of Asia-Oceania (FIMSA). *Ann N Y Acad Sci.* 2013;1283:v–x.
37. Hussain S, et al. Inflammasome activation in airway epithelial cells after multi-walled carbon nanotube exposure mediates a profibrotic response in lung fibroblasts. *Part Fibre Toxicol.* 2014;11:28.
38. Higham A, Lea S, Ray D, Singh D. Corticosteroid effects on COPD alveolar macrophages: dependency on cell culture methodology. *J Immunol Methods.* 2014;405:144–153.
39. Liu G, et al. Fibulin-1 regulates the pathogenesis of tissue remodeling in respiratory diseases. *JCI Insight.* 2016;1(9):e86380.
40. Asher MI, et al. Worldwide time trends in the prevalence of symptoms of asthma, allergic rhinoconjunctivitis, and eczema in childhood: ISAAC Phases One and Three repeat multicountry cross-sectional surveys. *Lancet.* 2006;368(9537):733–743.
41. Kanner RE, Anthonisen NR, Connett JE, Lung Health Study Research Group. Lower respiratory illnesses promote FEV(1) decline in current smokers but not ex-smokers with mild chronic obstructive pulmonary disease: results from the lung health study. *Am J Respir Crit Care Med.* 2001;164(3):358–364.
42. Seemungal TA, Donaldson GC, Paul EA, Bestall JC, Jeffries DJ, Wedzicha JA. Effect of exacerbation on quality of life in patients with chronic obstructive pulmonary disease. *Am J Respir Crit Care Med.* 1998;157(5 Pt 1):1418–1422.
43. Wang YY, Li L, Han KJ, Zhai Z, Shu HB. A20 is a potent inhibitor of TLR3- and Sendai virus-induced activation of NF-kappaB and ISRE and IFN-beta promoter. *FEBS Lett.* 2004;576(1-2):86–90.
44. Barnes PJ. The cytokine network in asthma and chronic obstructive pulmonary disease. *J Clin Invest.* 2008;118(11):3546–3556.
45. Jung SM, et al. Smad6 inhibits non-canonical TGF- $\beta$ 1 signalling by recruiting the deubiquitinase A20 to TRAF6. *Nat Commun.*

- 2013;4:2562.
46. Saitoh T, et al. A20 is a negative regulator of IFN regulatory factor 3 signaling. *J Immunol.* 2005;174(3):1507–1512.
47. Maelfait J, et al. A20 (Tnfrif3) deficiency in myeloid cells protects against influenza A virus infection. *PLoS Pathog.* 2012;8(3):e1002570.
48. Rusinova I, et al. Interferome v2.0: an updated database of annotated interferon-regulated genes. *Nucleic Acids Res.* 2013;41(Database issue):D1040–D1046.
49. Lee HM, Kim TS, Jo EK. MiR-146 and miR-125 in the regulation of innate immunity and inflammation. *BMB Rep.* 2016;49(6):311–318.
50. Chen H, Xu Z. Hypermethylation-Associated Silencing of miR-125a and miR-125b: A Potential Marker in Colorectal Cancer. *Dis Markers.* 2015;2015:345080.
51. Cisneros-Soberanis F, Andonegui MA, Herrera LA. miR-125b-1 is repressed by histone modifications in breast cancer cell lines. *Springerplus.* 2016;5(1):959.
52. Kirkham PA, Barnes PJ. Oxidative stress in COPD. *Chest.* 2013;144(1):266–273.
53. Fischer BM, Pavlisko E, Voynow JA. Pathogenic triad in COPD: oxidative stress, protease-antiprotease imbalance, and inflammation. *Int J Chron Obstruct Pulmon Dis.* 2011;6:413–421.
54. Kratsovnik E, Bromberg Y, Sperling O, Zoref-Shani E. Oxidative stress activates transcription factor NF- $\kappa$ B-mediated protective signaling in primary rat neuronal cultures. *J Mol Neurosci.* 2005;26(1):27–32.
55. Tan G, Niu J, Shi Y, Ouyang H, Wu ZH. NF- $\kappa$ B-dependent microRNA-125b up-regulation promotes cell survival by targeting p38 $\alpha$  upon ultraviolet radiation. *J Biol Chem.* 2012;287(39):33036–33047.
56. Werner SL, et al. Encoding NF-kappaB temporal control in response to TNF: distinct roles for the negative regulators Ikappa-Balpha and A20. *Genes Dev.* 2008;22(15):2093–2101.
57. Gómez FP, Rodriguez-Roisin R. Global Initiative for Chronic Obstructive Lung Disease (GOLD) guidelines for chronic obstructive pulmonary disease. *Curr Opin Pulm Med.* 2002;8(2):81–86.
58. . Workshop summary guidelines: investigative use of bronchoscopy, lavage, bronchial biopsies in asthma other airway diseases. *J Allergy Clin Immunol.* 1991;88(5):808–814.
59. Horvat JC, et al. Chlamydial respiratory infection during allergen sensitization drives neutrophilic allergic airways disease. *J Immunol.* 2010;184(8):4159–4169.
60. Thorburn AN, Foster PS, Gibson PG, Hansbro PM. Components of Streptococcus pneumoniae suppress allergic airways disease and NKT cells by inducing regulatory T cells. *J Immunol.* 2012;188(9):4611–4620.
61. Essilfie AT, et al. Macrolide therapy suppresses key features of experimental steroid-sensitive and steroid-insensitive asthma. *Thorax.* 2015;70(5):458–467.
62. Plank MW, et al. MicroRNA Expression Is Altered in an Ovalbumin-Induced Asthma Model and Targeting miR-155 with Antagomirs Reveals Cellular Specificity. *PLoS ONE.* 2015;10(12):e0144810.
63. Preston JA, et al. Inhibition of allergic airways disease by immunomodulatory therapy with whole killed Streptococcus pneumoniae. *Vaccine.* 2007;25(48):8154–8162.
64. Asquith KL, et al. Interleukin-13 promotes susceptibility to chlamydial infection of the respiratory and genital tracts. *PLoS Pathog.* 2011;7(5):e1001339.
65. Starkey MR, et al. Constitutive production of IL-13 promotes early-life Chlamydia respiratory infection and allergic airway disease. *Mucosal Immunol.* 2013;6(3):569–579.
66. Starkey MR, et al. Tumor necrosis factor-related apoptosis-inducing ligand translates neonatal respiratory infection into chronic lung disease. *Mucosal Immunol.* 2014;7(3):478–488.
67. Kim RY, et al. MicroRNA-21 drives severe, steroid-insensitive experimental asthma by amplifying phosphoinositide 3-kinase-mediated suppression of histone deacetylase 2. *J Allergy Clin Immunol.* 2017;139(2):519–532.

## Letter to the editor:

# STEROID RESISTANCE AND CONCOMITANT RESPIRATORY INFECTIONS: A CHALLENGING BATTLE IN PULMONARY CLINIC

Kamal Dua<sup>1,2,3\*</sup>, Nicole G. Hansbro<sup>2,3</sup>, Philip M. Hansbro<sup>2,3\*</sup>

- 1 Discipline of Pharmacy, Graduate School of Health, University of Technology, Sydney, Ultimo NSW 2007, Australia
- 2 School of Biomedical Sciences and Pharmacy, The University of Newcastle, Callaghan, NSW2308, Australia
- 3 Priority Research Centre for Healthy Lungs, Hunter Medical Research Institute, J Lot 1 Kookaburra Circuit, New Lambton Heights, Newcastle, NSW 2305, Australia

\* Corresponding authors: Dr. Kamal Dua & Prof. Philip M. Hansbro, Priority Research Centre for Healthy Lungs, Hunter Medical Research Institute, J Lot 1 Kookaburra Circuit, New Lambton Heights, Newcastle, NSW 2305, Australia, Tel: +61 2 4042 20203; Fax: +61 2 4042 0024; e-mail: [kamalpharmacist@gmail.com](mailto:kamalpharmacist@gmail.com), [philip.hansbro@newcastle.edu.au](mailto:philip.hansbro@newcastle.edu.au)

<http://dx.doi.org/10.17179/excli2017-425>

This is an Open Access article distributed under the terms of the Creative Commons Attribution License (<http://creativecommons.org/licenses/by/4.0/>).

Dear Editor,

Globally, the viral respiratory infections are one of the major health problems. The investigations in this area are becoming more challenging because of the complexity of relationship between the host's defences and microbial virulence (Saturni et al., 2015). Particularly, the role of infections in asthma can cause wheezing as an "inducer" and can also act as a "protector" against allergic airway disease (Busse et al., 2010). According to the "hygiene" hypothesis, early life infection may protect against asthma. If the parents of the offspring have asthma or allergies, the chances of exacerbations with viral respiratory infections particularly provoke wheezing in the early life and lead to the development of asthma in later stages (Budden et al., 2017; Okada et al., 2010). Sigurs et al. (2000) have shown that the family history of asthma along with severe respiratory syncytial virus (RSV) infections increases the development of asthma in children at the age of seven. Nowadays, increasing number of asthma patients with steroid-resistance and coexisting respiratory viral infections has severely affected the cost of treating asthma patients (Durham et al., 2011). Moreover, viral respiratory infections are also one of the major causes of exacerbations further deteriorating the quality of life for these patients.

Various studies have provided mechanistic insights showing an association of respiratory viral (RSV, rhinovirus) and bacterial (Chlamydia, Mycoplasma) infections with asthma (Hansbro et al., 2014). Using the mouse model, it has been well demonstrated that chlamydia respiratory infections during early life modify lung physiology where it increases the severity of allergic airway disease by targeting factor like interleukin-13 (IL-13) (Starkey et al., 2013) and

tumor necrosis factor-related apoptosis-inducing ligand (TRAIL) (Starkey et al., 2014a, b). Various other factors that have been investigated to play a role in the susceptibility to respiratory viral infections in allergic airway diseases include monocyte chemoattractant protein-1 (MCP-1), keratinocyte-derived protein chemokine (KC) (Nguyen et al., 2016b) and receptor for advanced glycation end-products (RAGE) (Arikkatt et al., 2017).

It has been demonstrated in mice models that IL-13 impaired antiviral immune responses in various respiratory diseases including asthma and chronic obstructive pulmonary disease (COPD). These impaired responses predisposed these mice to severe influenza infection that exacerbated the underlying disease via increased expression of micro-RNA-21 (miRNA-21) and phosphoinositide 3-kinase (PI3K). This indicates the potential of PI3K inhibitors, anti-IL-13 and miRNA-21 antagonists as novel therapeutic interventions in management of allergic airways diseases (Dua et al., 2017; Starkey et al., 2014a, b). Furthermore, miR-21/PI3K/histone deacetylase (HDAC) 2 axis has recently been reported to drive severe, steroid-insensitive experimental asthma (Kim et al., 2017). In a dual T-helper 2/T-helper 17 (Th2/Th17) model of steroid-resistant asthma, IL-13-mediated and signal transducer and activator of transcription 6 (STAT6)-dependent airway hyper-responsiveness (AHR) and mucus metaplasia was observed, however, IL-13 was not identified to be directly contributing to airway/tissue inflammation. Similarly, in the same mixed model, interleukin-17A (IL-17A) was identified as an independent contributor to AHR with only partial mediation of inflammation and mucus metaplasia (Manni et al., 2016).

Specifically with PI3K, increased PI3K catalytic subunit p110 $\alpha$  (PI3K-p110 $\alpha$ ) activity has been demonstrated to increase susceptibility of individuals with COPD to influenza infections (Chen-Yu Hsu et al., 2015). This was evident with the increased viral entry and replication (increased viral titre) in COPD primary bronchial epithelial cells (pBECs) and pulmonary inflammation along with compromised lung function in infected mice with experimental COPD (Beckett et al., 2013; Chen-Yu Hsu et al., 2015). Long et al. (2016) have shown the involvement of natural killer (NK) cells in persistent airway inflammation and AHR during later stages of RSV infection in mice, where targeting NK cells therapeutically may be a novel approach to improve recurrent wheezing following to RSV infection.

One of the recent studies emphasized on the involvement of bromodomain and extra terminal (BET) proteins in regulation of AHR and airway inflammation in interferon- $\gamma$  (IFN $\gamma$ )/lipopolysaccharide (LPS, an endotoxin) and RSV-induced steroid-resistant exacerbations models. They presented the therapeutic potential of BET inhibitor in suppressing macrophage-driven steroid-resistant exacerbations (Nguyen et al., 2016a). In COPD, combination of roflumilast N-oxide and dexamethasone was demonstrated to produce additive anti-inflammatory effects in COPD pBECs by increasing the expression of mitogen-activated protein kinase phosphatase 1 (MKP1; also known as dual specificity protein phosphatase 1, (DUSP1) and enhancing inhibitory effects on phospho-p38 and nuclear factor- $\kappa$ B (NF $\kappa$ B) (Milara et al., 2015).

The investigation of Chambers et al. (2015) into identifying immunological differences between steroid-sensitive and steroid-resistant asthma demonstrated patients with steroid resistance asthma to produce significantly high levels of IL-17A and IFN- $\gamma$ . Calcitriol treatment in both an *in-vitro* (peripheral blood mononuclear cell, PBMCs) and *in-vivo* (steroid resistance asthma patients) settings demonstrated an improvement in clinical response to oral glucocorticoids probably by directing the cytokine profile of steroid-resistance asthma patients towards the steroid-sensitive immune phenotype. With an aim of increasing patient compliance in COPD and steroid-refractory asthma, Onions and his co-workers designed and optimized various chemical compounds that could produce sustained action post-inhalation (Onions et al.,

2016). Further, microRNA-9 (miRNA-9) was investigated as another potential therapeutic target by Li et al. (2015), where it was hypothesised to regulate glucocorticoid receptor (GR) signalling and steroid-resistant AHR in steroid-resistant asthma.

Tian et al. (2016) emphasised on the apoptosis of inflammatory cells which is an important prerequisite feature in clearing airway inflammation induced by insults such as allergens. They demonstrated the potential of Bcl-2 inhibitors ABT-737 or ABT-199 as promising therapeutic tools in the treatment of corticosteroid-insensitive neutrophilic airway inflammation (Tian et al., 2016). Another potential therapeutic intervention included an anti-RSV neutralizing antibody (palivizumab) which has recently been approved for the prevention of severe RSV infection in high-risk patients. This antibody was tested in mice model where the antibody was administered once either (a) 24 hours prior to infection as prophylaxis or (b) 48 hours post-infection (inoculation with RSV). They showed attenuated RSV replication in the lower respiratory tract as well as significant reduction in the cytopathic effect of virus particularly in the respiratory epithelial cells and in the immune response elicited by RSV in response to the treatment (Carbonell-Estrany and Quero, 2002; Group, 1998; Mejías et al., 2004).

Hines and colleagues investigated molecular processes involved in structural remodelling as a consequence of repeated respiratory viral infections during early childhood. They demonstrated distinct responses from the macrophages and mast cells along with abnormal re-epithelization resulting in various structural defects using Sendai virus infection model in weanling rats (an atopic asthma susceptible strain, Brown Norway, and a non-atopic asthma resistant strain, Fischer 344) (Hines et al., 2014). A translational investigation using a blend of genetic animal model and *in-vitro* human studies identified an innate immunity scavenger receptor MARCO gene to be associated with increased susceptibility of children to RSV infection (High et al., 2016). Also a clinical trial investigating the efficacy and safety of long-term treatment with anti-IgE antibody, omalizumab, in children with uncontrolled severe allergic asthma demonstrated it to be well tolerated with improvements in asthma control (Odajima et al., 2017).

A multicenter, randomized, double-blind, placebo-controlled, parallel-group study assessed the safety and efficacy of inhaled Zanamivir in preventing infection in adult and adolescent subjects susceptible to influenza infection particularly against the circulating strains of the 2000-2001 influenza season in the Northern Hemisphere (influenza A/New Calendonia/20/99-like and influenza B/ Sichuan/379/99-like). Zanamivir was demonstrated to be well-tolerated with a placebo comparable safety profile (LaForce et al., 2007). Likewise, a randomized, double-blind, placebo-controlled, crossover phase 1 study evaluated the safety of an inhaled anti-viral DAS181 (Fludase®) in adult subjects with well-controlled asthma (Colombo et al., 2016; Zenilman et al., 2015) which was a part of clinical trial where DAS181 was shown to reduce viral load (Moss et al., 2012).

Though, there are number of translational and clinical studies performed worldwide to investigate molecular mechanisms interlinking influenza infection and allergic airway diseases along with the ongoing search for potential therapeutic interventions, there are still many questions that remain unaddressed. Some of these impediments include patterns of inflammation involved due to various respiratory viruses and multiple genes and their products, which underpin the regulatory mechanisms driving the disease pathology.

## REFERENCES

- Arikkatt J, Ullah MA, Short KR, Zhang V, Gan WJ, Loh Z, et al. RAGE deficiency predisposes mice to virus-induced paucigranulocytic asthma. *eLife*. 2017;6:e21199.
- Beckett EL, Stevens RL, Jarnicki AG, Kim RY, Hanish I, Hansbro NG, et al. A new short-term mouse model of chronic obstructive pulmonary disease identifies a role for mast cell tryptase in pathogenesis. *J Allergy Clin Immunol*. 2013;131:752-62. e7.
- Budden KF, Gellatly SL, Wood DL, Cooper MA, Morrison M, Hugenholtz P, et al. Emerging pathogenic links between microbiota and the gut-lung axis. *Nat Rev Microbiol*. 2017;15:55-63.
- Busse WW, Lemanske RF, Gern JE. Role of viral respiratory infections in asthma and asthma exacerbations. *The Lancet*. 2010;376(9743):826-34.
- Carbonell-Estrany X, Quero JJ. Guidelines for respiratory syncytial virus prophylaxis. An update. *Anales Espanoles de Pediatria*. 2002;56:334-6.
- Chambers ES, Nanzer AM, Pfeffer PE, Richards DF, Timms PM, Martineau AR, et al. Distinct endotypes of steroid-resistant asthma characterized by IL-17A high and IFN- $\gamma$  high immunophenotypes: potential benefits of calcitriol. *J Allergy Clin Immunol*. 2015;136:628-37. e4.
- Chen-Yu Hsu A, Starkey MR, Hanish I, Parsons K, Haw TJ, Howland LJ, et al. Targeting PI3K-p110 $\alpha$  suppresses influenza virus infection in chronic obstructive pulmonary disease. *Am J Respirat Crit Care Med*. 2015;191:1012-23.
- Colombo RE, Fiorentino C, Dodd LE, Hunsberger S, Haney C, Barrett K, et al. A phase 1 randomized, double-blind, placebo-controlled, crossover trial of DAS181 (Fludase®) in adult subjects with well-controlled asthma. *BMC Infect Dis*. 2016;16(1):54.
- Dua K, Hansbro NG, Foster PS, Hansbro PM. MicroRNAs as therapeutics for future drug delivery systems in treatment of lung diseases. *Drug Deliv Translat Res*. 2017;7:168-78.
- Durham A, Adcock I, Tliba O. Steroid resistance in severe asthma: current mechanisms and future treatment. *Curr Pharm Design*. 2011;17:674-84.
- Group IRS. Palivizumab, a humanized respiratory syncytial virus monoclonal antibody, reduces hospitalization from respiratory syncytial virus infection in high-risk infants. *Pediatrics*. 1998;102:531-7.
- Hansbro PM, Starkey MR, Mattes J, Horvat JC. Pulmonary immunity during respiratory infections in early life and the development of severe asthma. *Ann Am Thoracic Soc*. 2014;11(Suppl 5):S297-S302.
- High M, Cho H-Y, Marzec J, Wiltshire T, Verhein KC, Caballero MT, et al. Determinants of host susceptibility to murine respiratory syncytial virus (RSV) disease identify a role for the innate immunity scavenger receptor MARCO gene in human infants. *EBioMedicine*. 2016;11:73-84.
- Hines EA, Szakaly RJ, Leng N, Webster AT, Verheyden JM, Lashua AJ, et al. Comparison of temporal transcriptomic profiles from immature lungs of two rat strains reveals a viral response signature associated with chronic lung dysfunction. *PloS One*. 2014;9(12):e112997.
- Kim RY, Horvat JC, Pinkerton JW, Starkey MR, Essilfie AT, Mayall JR, et al. MicroRNA-21 drives severe, steroid-insensitive experimental asthma by amplifying phosphoinositide 3-kinase-mediated suppression of histone deacetylase 2. *J Allergy Clin Immunol*. 2017;139:519-32.
- LaForce C, Man CY, Henderson FW, McElhaney JE, Hampel FC, Bettis R, et al. Efficacy and safety of inhaled zanamivir in the prevention of influenza in community-dwelling, high-risk adult and adolescent subjects: a 28-day, multicenter, randomized, double-blind, placebo-controlled trial. *Clin Therap*. 2007;29:1579-90.
- Li JJ, Tay HL, Maltby S, Xiang Y, Evers F, Hatchwell L, et al. MicroRNA-9 regulates steroid-resistant airway hyperresponsiveness by reducing protein phosphatase 2A activity. *J Allergy Clin Immunol*. 2015;136:462-73.
- Long X, Xie J, Zhao K, Li W, Tang W, Chen S, et al. NK cells contribute to persistent airway inflammation and AHR during the later stage of RSV infection in mice. *Med Microbiol Immunol*. 2016;205:459-70.
- Manni ML, Mandalapu S, McHugh KJ, Elloso MM, Dudas PL, Alcorn JF. Molecular mechanisms of airway hyperresponsiveness in a murine model of steroid-resistant airway inflammation. *J Immunol*. 2016;196:963-77.
- Mejías A, Chávez-Bueno S, Ríos AM, Saavedra-Lozano J, Aten MF, Hatfield J, et al. Anti-respiratory syncytial virus (RSV) neutralizing antibody decreases lung inflammation, airway obstruction, and airway hyperresponsiveness in a murine RSV model. *Antimicrobial Agents Chemother*. 2004;48:1811-22.

- Milara J, Morell A, Ballester B, Sanz C, Freire J, Qian X, et al. Roflumilast improves corticosteroid resistance COPD bronchial epithelial cells stimulated with toll like receptor 3 agonist. *Respir Res.* 2015;16(1):12.
- Moss RB, Hansen C, Sanders RL, Hawley S, Li T, Steigbigel RT. A phase II study of DAS181, a novel host directed antiviral for the treatment of influenza infection. *J Infect Dis.* 2012;206:1844-51.
- Nguyen TH, Maltby S, Evers F, Foster PS, Yang M. Bromodomain and extra terminal (BET) inhibitor suppresses macrophage-driven steroid-resistant exacerbations of airway hyper-responsiveness and inflammation. *PloS One.* 2016a;11(9):e0163392.
- Nguyen TH, Maltby S, Simpson JL, Evers F, Baines KJ, Gibson PG, et al. TNF- $\alpha$  and macrophages are critical for respiratory syncytial virus-induced exacerbations in a mouse model of allergic airways disease. *J Immunol.* 2016b;196:3547-58.
- Odajima H, Ebisawa M, Nagakura T, Fujisawa T, Akasawa A, Ito K, et al. Long-term safety, efficacy, pharmacokinetics and pharmacodynamics of omalizumab in children with severe uncontrolled asthma. *Allergol Int.* 2017;66:106-15.
- Okada H, Kuhn C, Feillet H, Bach JF. The 'hygiene hypothesis' for autoimmune and allergic diseases: an update. *Clin Exp Immunol.* 2010;160:1-9.
- Onions ST, Ito K, Charron CE, Brown RJ, Colucci M, Frickel F, et al. Discovery of narrow spectrum kinase inhibitors: new therapeutic agents for the treatment of COPD and steroid-resistant asthma. *J Med Chem.* 2016;59:1727-46.
- Saturni S, Contoli M, Spanevello A, Papi A. Models of respiratory infections: virus-induced asthma exacerbations and beyond. *Allergy Asthma Immunol Res.* 2015;7:525-33.
- Sigurs N, Bjarnason R, Sigurbergsson F, Kjellman B. Respiratory syncytial virus bronchiolitis in infancy is an important risk factor for asthma and allergy at age 7. *Am J Respir Crit Care Med.* 2000;161:1501-7.
- Starkey M, Essilfie A, Horvat J, Kim R, Nguyen D, Beagley K, et al. Constitutive production of IL-13 promotes early-life Chlamydia respiratory infection and allergic airway disease. *Mucosal Immunol.* 2013;6:569-79.
- Starkey M, Nguyen D, Essilfie A, Kim R, Hatchwell L, Collison A, et al. Tumor necrosis factor-related apoptosis-inducing ligand translates neonatal respiratory infection into chronic lung disease. *Mucosal Immunol.* 2014a;7:478-88.
- Starkey M, Hanish I, Dua K, Nair P, Haw T, Hsu A, et al. Interleukin-13 predisposes mice to more severe influenza infection by suppressing interferon responses and activating microRNA-21/PI3K. *Cytokine.* 2014b;70(1):70.
- Tian BP, Xia LX, Bao ZQ, Zhang H, Xu ZW, Mao YY, et al. Bcl-2 inhibitors reduce steroid-insensitive airway inflammation. *J Allergy Clin Immunol.* 2016; Epub ahead of print. doi: 10.1016/j.jaci.2016.11.027.
- Zenilman JM, Fuchs EJ, Hendrix CW, Radebaugh C, Jurao R, Nayak SU, et al. Phase 1 clinical trials of DAS181, an inhaled sialidase, in healthy adults. *Antiviral Res.* 2015;123:114-9.

This article was removed for copyright purposes and is available online:

Dua, K., Hansbro, N.G., Foster, P.S. et al. MicroRNAs as therapeutics for future drug delivery systems in treatment of lung disease (2017) *Drug Deliv. and Transl. Res.* 7: 168.  
<https://doi.org/10.1007/s13346-016-0343-6>

This article was removed for copyright purposes and is available online:

Philip M. Hansbro Richard Y. Kim Malcolm R. Starkey Chantal Donovan Kamal Dua Jemma R. Mayall Gang Liu Nicole G. Hansbro Jodie L. Simpson Lisa G. Wood Jeremy A. Hirota Darryl A. Knight Paul S. Foster Jay C. Horvat. (2017) Mechanisms and treatments for severe, steroid-resistant allergic airway disease and asthma, *Immunological Reviews* Vol. 278, Issue 1, 41-62.  
<https://doi.org/10.1111/imr.12543>